REPORT DOCUMENTATION PAGE

READ INSTRUCTIONS BEFORE COMPLETING FORM

1. REPORT NUMBER: NAVENVPREDRSCHFAC Technical Report 83-01
2. GOVT ACCESSION NO.:
3. RECIPIENT'S CATALOG NUMBER:

4. TITLE *(and Subtitle)*:
Navy Tactical Applications Guide. Volume 4. Part 1
Eastern North Pacific
Weather Analysis and Forecast Applications

5. TYPE OF REPORT & PERIOD COVERED:

6. PERFORMING ORG. REPORT NUMBER:

7. AUTHOR(s):
Robert W. Fett
Walter A. Bohan
Jay Rosenthal

8. CONTRACT OR GRANT NUMBER(s):
The Walter A. Bohan Company
N00228-82-C-6222

9. PERFORMING ORGANIZATION NAME AND ADDRESS:
The Walter A. Bohan Company
2026 Oakton Street
Park Ridge, IL 60068

10. PROGRAM ELEMENT, PROJECT, TASK AREA & WORK UNIT NUMBERS:
62759N. WF 59-553.
NEPRF WU: 6.2-9

11. CONTROLLING OFFICE NAME AND ADDRESS:
Naval Air Systems Command
Department of the Navy
Washington, D.C. 20361

12. REPORT DATE:
June 1984

13. NUMBER OF PAGES:
180

14. MONITORING AGENCY NAME & ADDRESS *(if different from Controlling Office)*:
Naval Environmental Prediction Research Facility
Monterey, California 93943

15. SECURITY CLASS. *(of this report)*:
Unclassified

15a. DECLASSIFICATION/DOWNGRADING SCHEDULE:

16. DISTRIBUTION STATEMENT *(of this Report)*:
Approved for Public Release
Distribution Unlimited

17. DISTRIBUTION STATEMENT *(of the abstract entered in Block 20, if different from Report)*:

18. SUPPLEMENTARY NOTES:

19. KEY WORDS *(Continue on reverse side if necessary and identify by block number)*:
Satellites
Remote Sensing
Blocking
Cut-off Low
Cyclogenesis
Coastal Zone Phenomena
Catalina Eddy

20. ABSTRACT *(Continue on reverse side if necessary and identify by block number)*:
A detailed presentation on the subject of Blocking over the eastern North Pacific is provided combining geostationary satellite evidence with conventional charts, analyses, and forecasts. Every stage in the life cycle of the block from the initiation through development and dissipation is clearly depicted. The effects of steering of cyclonic disturbances by a block and the formation of cut-off lows downstream of blocking highs are also presented.

20.

The subject of Cyclogenesis in the eastern North Pacific is additionally described in which three separate types of cyclogenesis based on satellite analysis are clearly defined. These types differ considerably from classical models but are readily identifiable in sequences of geostationary satellite imagery.

The usefulness of water vapor imagery in synoptic analysis and in defining the location of the Tropical Upper-Tropospheric Trough (TUTT) is shown.

Finally, a section devoted to selected Coastal Zone Phenomena is presented, illustrating diurnal effects in the dissipation of coastal stratus and important observations concerning the formation of the Catalina Eddy.

AN (1) AD-A150 097
FG (2) 040200
CI (3) (U)
CA (5) BOHAN (WALTER A) CO PARK RIDGE IL
TI (6) Navy Tactical Applications Guide. Volume 4. Part 1. Eastern North Pacific Weather Analysis and Forecast Applications.
TC (8) (U)
DN (9) Technical rept.,
AU (10) Fett,R. W.
AU (10) Bohan,W. A.
AU (10) Rosenthal,J.
RD (11) Jun 1984
PG (12) 211p
CT (15) N00228-82-C-6222
PJ (16) F59553
TN (17) WF59553
RN (18) NEPRF-TR-83-01
RC (20) Unclassified report
NO (21) See also Volume 5, Part 1, AD-A134 412.
DE (23) *Meteorological phenomena, *Weather forecasting, North Pacific Ocean, East(Direction), Atmospheric motion, Cyclones, Coastal regions, Blocking
DC (24) (U)
ID (25) Cyclogenesis, TUTT(Tropical upper tropospheric trough), WU629, PE62759N
IC (26) (U)
AB (27) A detailed presentation on the subject of Blocking over the eastern North Pacific is provided combining geostationary satellite evidence with conventional charts, analyses, and forecasts. Every stage in the life cycle of the block from the initiation through development and dissipation is clearly depicted. The effects of steering of cyclonic disturbances by a block and the formation of cut-off lows downstream of blocking highs are also presented. The subject of Cyclogenesis in the eastern North Pacific is additionally described in which three separate types of cyclogenesis based on satellite analysis are clearly defined. These types differ considerably from classic models but are readily identifiable in sequences of geostationary satellite imagery. The usefulness of water vapor imagery in synoptic analysis and in defining the location of the Tropical Upper-Tropospheric Trough (TUTT) is shown. Finally, a section devoted to selected Coastal Zone Phenomena is presented, illustrating diurnal effects in the dissipation of coastal stratus and important observations concerning the formation of the Catalina Eddy. (Author).
AC (28) (U)
DL (33) 01

** MAY CONTAIN EXPORT CONTROL DATA **
ADAxxxxxx MICROFICHE ARE HOUSED IN THE GENERAL MICROFORMS RM

SE (34) 4
CC (35) 059910

#

NEPRF TECHNICAL REPORT TR 83-01

NAVY TACTICAL APPLICATIONS GUIDE

VOLUME 4
PART 1

EASTERN NORTH PACIFIC
WEATHER ANALYSIS and FORECAST APPLICATIONS

METEOROLOGICAL
SATELLITE
SYSTEMS

TACTICAL APPLICATIONS DEPARTMENT
NAVAL ENVIRONMENTAL PREDICTION RESEARCH FACILITY
MONTEREY, CALIFORNIA 93940

NAVY TACTICAL APPLICATIONS GUIDE

VOLUME 4

PART 1

EASTERN NORTH PACIFIC

WEATHER ANALYSIS AND FORECAST APPLICATIONS

METEOROLOGICAL SATELLITE SYSTEMS

Prepared under the direction of
Robert W. Fett
Tactical Applications Department
Naval Environmental Prediction Research Facility

Scientific Coordinator
Walter A. Bohan
The Walter A. Bohan Company

1984

THE WALTER A. BOHAN COMPANY

2026 OAKTON STREET, PARK RIDGE, ILLINOIS 60068
APPLIED RESEARCH IN SATELLITE METEOROLOGY AND OCEANOGRAPHY

List of Contributors

Robert W. Fett, Head
Tactical Applications Department
Naval Environmental Prediction Research Facility
Monterey, California 93943

Walter A. Bohan, Certified Consulting Meteorologist
The Walter A. Bohan Company
Park Ridge, Illinois 60068

Jay Rosenthal, Head
Geophysics Sciences Branch
Geophysics Division
Pacific Missile Test Center
Point Mugu, California 93042

Ronald J. Englebretson, Research Meteorologist
Science Applications, Inc.
Monterey, California 93943

Sherree L. Tipton, Remote Sensing Specialist
The Walter A. Bohan Company
Park Ridge, Illinois 60068

Martin Lee
Geophysics Division
Pacific Missile Test Center
Point Mugu, California 93042

Thomas F. Lee
Geophysics Division
Pacific Missile Test Center
Point Mugu, California 93042

Foreword

This volume of the Navy Tactical Applications Guide series supplements previous volumes with the focus on regional weather analysis and forecast applications in the eastern North Pacific. Part 2 of this guide, originally intended to cover the western North Pacific, will be incorporated in Forecaster's Handbooks for that region and in NTAG Vol. 6, which will be devoted to tropical weather phenomena.

The approach to forecasting presented here is unique in that actual case studies of regional weather are described by combining satellite imagery with conventional analyses and prognoses. This case study technique, incorporating satellite data along with numerical guidance products, permits the description of weather events that occur over several days and thus can help in longer range forecasting applications. The studies so-presented can then provide useful insights into similar weather developments as they may occur in the future.

This is intended as an evolving volume which will be supplemented on a case study basis. The initial material is being distributed to the fleet to expedite access of completed work for operational use. These initial case studies include topics on blocking, cyclogenesis, and coastal zone phenomena.

Although the principles derived are developed from case studies in the eastern North Pacific region, it should be noted that many of the rules are general in nature and equally applicable to similar weather events in other areas of the world.

It is anticipated that these guides will provide a routine basis for supplementing the operational forecaster's ability to more effectively support Naval operations.

Kenneth L. Van Sickle

KENNETH L. VAN SICKLE
Captain, U.S. Navy
Commanding Officer, NEPRF

Acknowledgments

This volume could not have been published without the devoted effort of the NEPRF Meteorological Laboratory personnel who obtained required documentation, and who spent many hours on the computer terminal entering information for the analyses utilized in the studies. Directed by AGCM D.M. Ales, the following personnel: AG2 J.V. Klimas, AG2 R.J. Bonaly, AG3 J.L. Benvick, AG3 B.H. Kenthack and AGAN J.M. Roy, did an outstanding job in supporting the work effort required for this volume.

PH1 A. Matthews and PH2 W.A. Anderson processed many of the original photos utilized. The correlative meteorological data were provided by the Fleet Numerical Oceanography Center, Monterey, CA, and the U.S. Naval Oceanographic Detachment, Asheville, NC.

Additional satellite imagery was supplied by the National Environmental Satellite, Data, and Information Service (NESDIS) of the National Ocean and Atmospheric Administration (NOAA).

The assistance of the staff of the Walter A. Bohan Company is again acknowledged; in particular, Lido A. Andreoni for design of the format of the publication and layout of the case studies. Gregory E. Terhune assisted in the preparation of case study graphics and in the editing and formatting of the text. The high quality of the reproduction of the satellite imagery used in the case studies and the excellent printing of the publication are due to the combined efforts of Peter M. Samorez and Michael E. Brock.

Printing of this volume was funded under OM & N-1, Fleet Applications Work Unit, sponsored by the Naval Oceangraphic Command, NSTL Station, Bay St. Louis, MS.

Contents

Introduction

Volume 4 is a continuation of the Navy Tactical Applications Guide (NTAG) series, devoted to regional satellite analysis and forecast applications.

The eastern North Pacific is an especially challenging region for the Navy forecaster due to sparcity of data and the frequent rapid evolution of storm systems within this area. Numerical prognoses in this region are often excellent in predicting the longer wave features, but the important short-wave developments within the long-wave structure that precede major storm evolution are often missed. This volume shows how a careful analysis of satellite imagery combined with correlative synoptic charts and data can aid in the identification of such short-wave features for improved analysis and forecast skill.

The topics of blocking and cyclogenesis are treated in a non-classical fashion primarily based on weather satellite evidence which reveal details on initiation, development, and dissipation of winter storms. Much of the background rationale for this work is based on the work of Roger B. Weldon, Satellite Applications Laboratory, National Environmental Satellite, Data, and Information Service/NOAA, for which we are deeply indepted.

As in preceding volumes, suggestions and/or comments from Fleet users for improving or for supplementing the material enclosed are welcomed.

Address comments and suggestions to the Tactical Applications Department, Naval Environmental Prediction Research Facility.

Section 1

Blocking

1A Introduction

1B Case Studies

Blocking

1A Introduction

A Blocking Event over the Eastern North Pacific

The 22-day blocking event described in the following case study is not a unique or necessarily a typical blocking event observed over the eastern Pacific during the winter months. Every blocking event over the eastern Pacific has similarities and differences. The similarities allow a list to be made of common characteristics—the large synoptic-scale features that can be identified. The differences arise from the variety of ways that flow patterns can evolve and disturbances on various time and space scales can interact. In addition, only a selection of all of the available weather charts, numerical guidance products, and satellite imagery are presented. The selection is limited to that required to provide continuity on the blocking event from its formation to its dissipation. To make the presentation more dynamic, jet streak analyses based on the 300-mb isotachs are superimposed on the 300-mb charts.

The main features of the blocking event can be obtained from a casual examination of the series of weather analyses and satellite pictures. A careful reading of the accompanying text will provide not only insight into characteristic features common to blocking events, but details on the evolution of the flow patterns and disturbances that characterize this blocking event. In particular, the value of numerical prognoses in providing guidance on major flow pattern changes during the blocking event is demonstrated; the use of the 300-mb jet streaks in relation to the flow patterns to determine the most probable areas of cyclogenesis or enhancement of convection is emphasized; and the usefulness of satellite imagery to pinpoint the location of short-wave features within the overall blocking pattern is firmly established.

Index to Characteristic Features

Case 1 Blocking

Large-scale Circulation Features of a Blocking Event over the Eastern North Pacific December 1978 to January 1979

The following case concerns a blocking event that occurred over a 22-day period from late December 1978 to early January 1979. It is an interesting case because each stage in the life cycle of the block—the initiation, development, and dissipation—is clearly depicted and can be readily followed in the upper-air and surface analyses. The FNOC 500-mb, 36- and 72-hour prognoses provide the clues to each stage of development: the 36-hour prognoses for the initiation phase and combination of the 36- and 72-hour prognoses for evidence on the persistence and finally the dissipation of the block. Every major storm development in the vicinity of the block can be followed in the satellite pictures and, in particular, the dissipation of these storms as they move against the block. In order to show the characteristics and evolution of the synoptic features preceding the onset of the block, the case begins several days prior to the initiation of the blocking episode.

The mean 700-mb contours for December 1978 (1B-1a) and January 1979 (1B-1b) show the change in the flow pattern over the eastern Pacific from non-blocking to blocked conditions. During December, strong polar westerlies (band of closely-spaced height contour lines) predominate across the Pacific and North America. This is typical of non-blocked flow. In contrast, the mean 700-mb contours for January 1979 show a pronounced ridge along 135° W, extending from low latitudes to the arctic—unmistakable evidence of a persistent block. The deviation of the westerly flow northward upstream of the block is clearly evident, and the diffluent contour pattern along 150° W indicates a pronounced reduction in the speed of the westerlies across the eastern Pacific by the block, when compared to December 1978.

References

Taubensee, R.E., 1979: Weather and circulation of December 1978. *Mon. Wea. Rev.*, **107**, 354–360.

Wagner, A.J., 1979: Weather and circulation of January 1979. *Mon. Wea. Rev.*, **107**, 354–360.

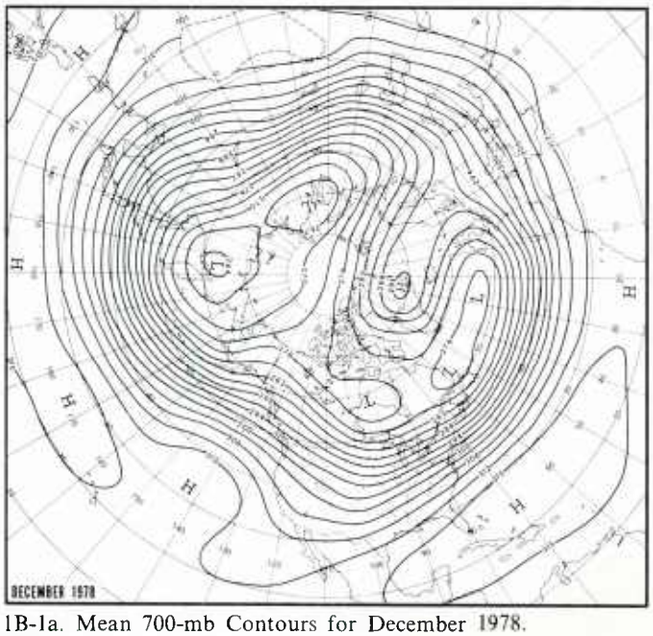

1B-1a. Mean 700-mb Contours for December 1978. (After Taubensee, 1979.)

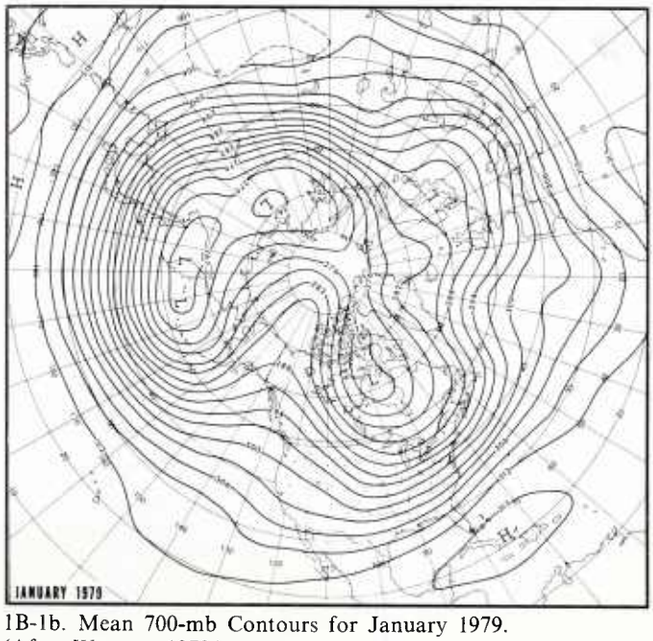

1B-1b. Mean 700-mb Contours for January 1979. (After Wagner, 1979.)

Pre-Blocking Situation

Pre-Blocking Situation

Characteristic Features

1. *Strong upper-level zonal polar westerlies at mid and high latitudes over the Pacific.*
2. *Presence of a cut-off low over the eastern Pacific and a strong polar jet stream at mid latitudes upstream of the cut-off low.*
3. *Unobstructed eastward progress of cyclonic disturbances in the zonal westerlies across the eastern Pacific.*

22 December

The 300-mb analysis for 0000 GMT (1B-2a) shows strong zonal polar westerlies at mid and high latitudes over the Pacific. The main polar westerlies extend in a nearly continuous band from the western Pacific to North America. Axes of maximum wind (jet streams) are depicted by thin black line segments of varying length; isotach maxima (jet streaks) along the jet are shown by thicker black line segments. This presentation technique emphasizes the observation that the polar jet stream is not a continuous belt of strong upper-level winds encircling the globe, but consists of high-speed wind segments (jet streaks) connected by regions of lower wind speeds.

On the 300-mb analysis, note that the regions of strong jet streaks over the Pacific are reflected at the 500-mb level (1B-2b) by bands of very closely-spaced height contour lines. This relationship is especially useful for identifying the location of strong polar jets on NMC 500-mb analyses over oceanic areas where few wind observations are available and on FNOC 500-mb prognoses, which do not show plotted winds.

The cut-off low **A** at 300 mb, has two jet streaks in its cyclonic circulation. This is typical of cut-off lows recently separated from the main polar westerlies. The presence of the cut-off low over the eastern Pacific and a strong polar jet **B** (130-kt jet streak) at mid latitudes upstream of the cut-off low are often observed prior to the initiation of blocking over the eastern Pacific.

The cut-off low **A** decreases in intensity to the surface (1B-3b), where only a weak low **A′** is observed. In the satellite picture (1B-3a), convection cells **A″** are located in the thermally unstable central region of the cut-off low. This is characteristic of vertically deep, cold core lows in this region during the winter. Note that there are two distinct cirrus cloud decks **C″** and **D″** to the west and east of the cut-off low, respectively. In both cases, the cirrus decks are located in a ridge aloft (300 mb) and the narrow cirrus bands and streaks outline the anticyclonic flow. The dense cirrus **D″** in the pronounced ridge to the east of the cut-off low is associated with a strong jet at 300 mb, which accounts for the enhanced convection in this ridge.

The location of cyclonic centers on the surface analysis over the Pacific and North America shows a train of nearly equally spaced centers **E′**, **F′**, and **G′** at high latitudes along the 55°N parallel. These disturbances are migratory cyclones in the main belt of the westerlies (300 mb). The regular spacing along 55°N indicates that the eastward progress of storms across the Pacific is not obstructed at this time. Note that the surface high centers across the Pacific are also oriented west-east, along the 35°N parallel, which also reflects the absence of strong meridional flow aloft.

In the satellite picture, spiral cloud bands are associated with the surface cyclones at high latitudes. In particular, note the short frontal cloud bands associated with storms **F″** and **G″**. The presence of these short frontal cloud bands provides confirming evidence that these disturbances are located in strong zonal flow. If large north-south amplitude systems were present, there would be prominent meridional frontal cloud bands instead. The frontal cloud band **E″** is considerably longer than **F″** and **G″** since it is associated with a new major disturbance that has recently moved off the Asiatic mainland. This frontal band has merged with the older, broad frontal system **H″** which trails from storm **F″** over the Gulf of Alaska. At the surface, there is a potential wave development along the trailing front **H′**.

In the DMSP picture (1B-5a), portions of the cloud patterns of the high-latitude storms are observed along the western and southern edge of the picture. Note the clear view of northern Siberia, the Chukchi Sea, and Alaska. These regions are generally cloud-free during the winter due to insufficient local surface heating and the lack of open water areas. Strong zonal flow at latitudes south of this region generally restricts storm tracks from passing over this area.

An examination of the initial 500-mb analysis (1B-4a) and the 36-hour 500-mb prognosis (1B-4b) reveals the following events: The strong zonal westerlies (band of closely-spaced height contour lines) across the Pacific and North America are forecast to persist: however, the westerlies between 140°W and 170°W are forecast to shift southward in response to the movement of the upper low from Siberia to the Bering Sea (60°N, 170°W). This action depresses the ridge to the west of the cut-off low **A**. The cut-off low remains essentially stationary and fills slightly.

continued on page 1B-6

300 mb

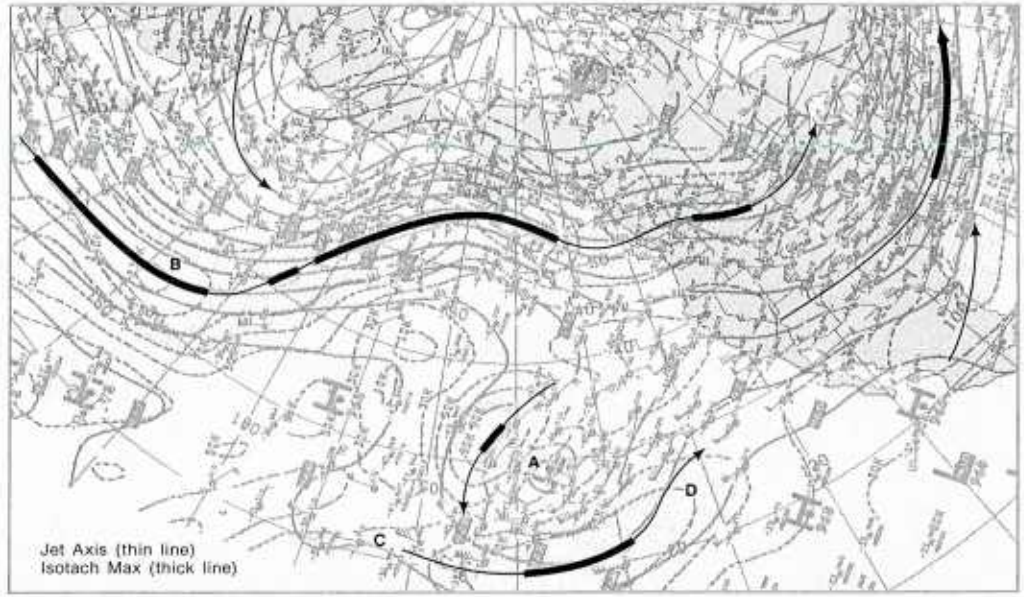

1B-2a. NMC 300-mb Analysis. 0000 GMT 22 December 1978.

500 mb

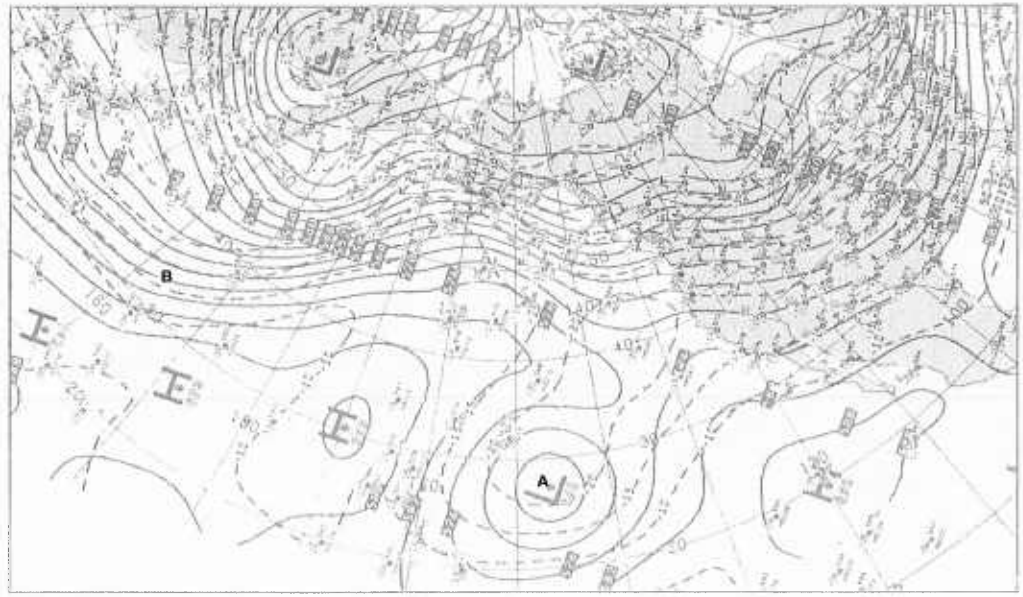

1B-2b. NMC 500-mb Analysis. 0000 GMT 22 December 1978.

Pre-Blocking Situation

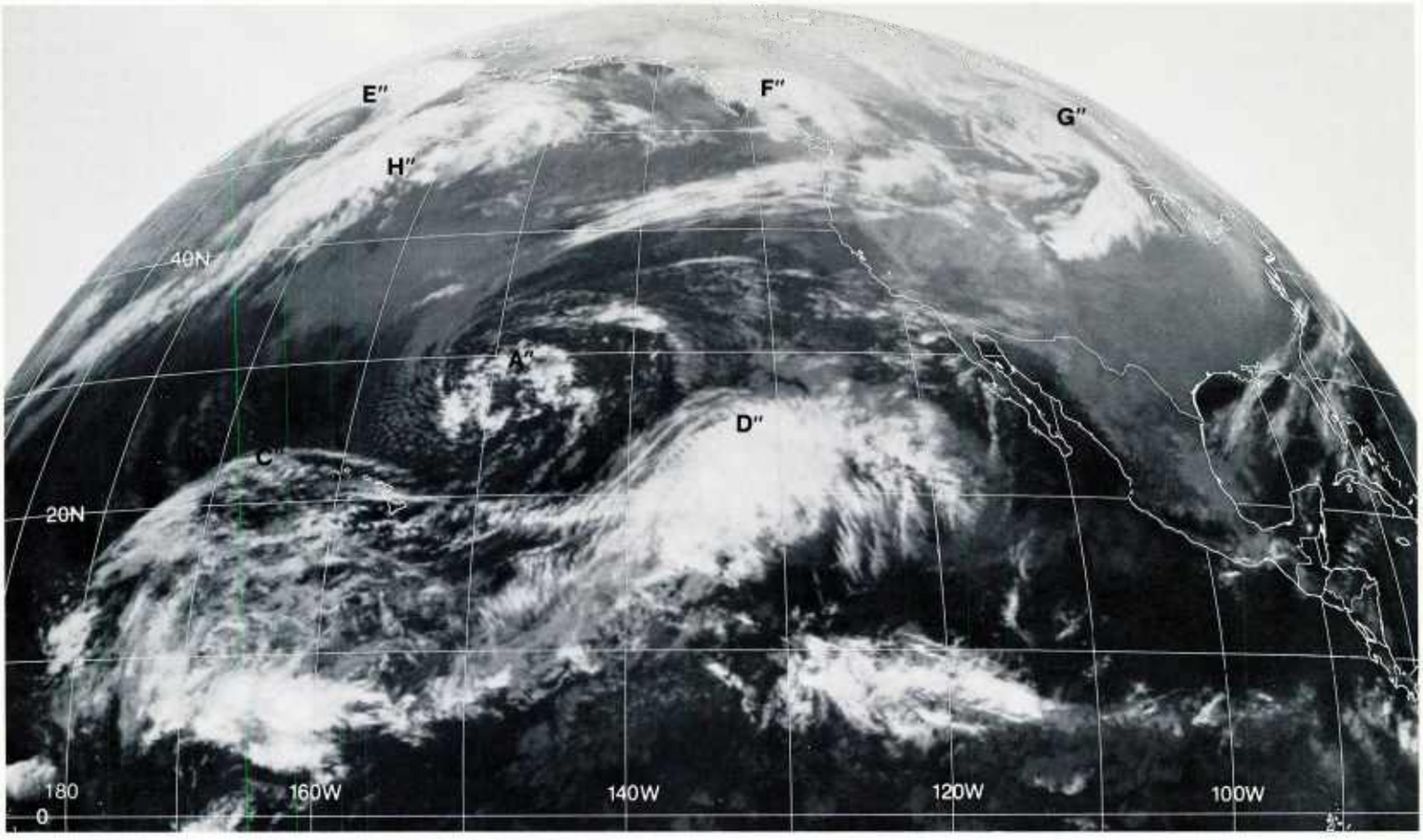

1B-3a. GOES-W. Infrared Picture. 0015 GMT 22 December 1978.

surface

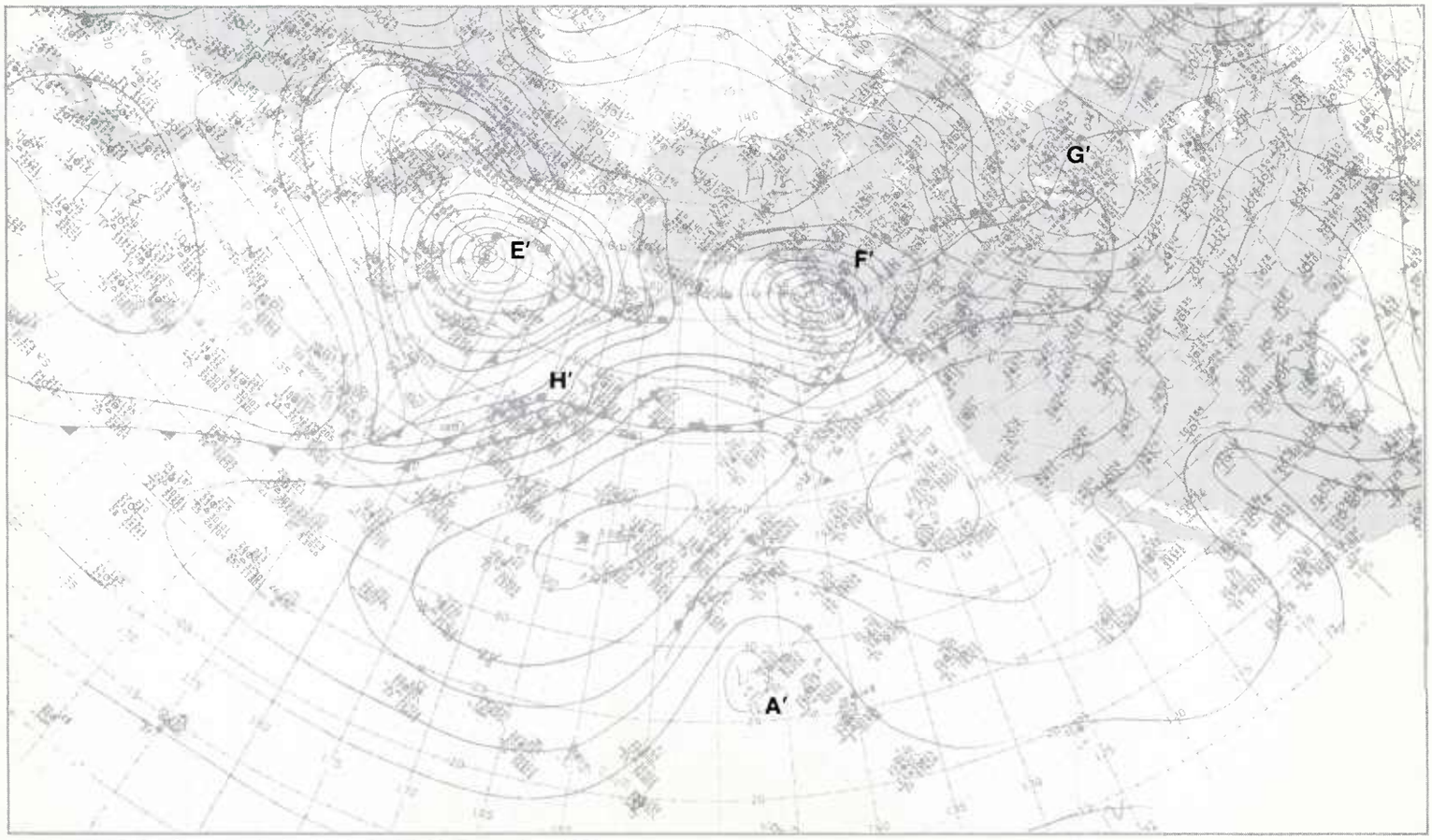

1B-3b. NMC Surface Analysis. 0000 GMT 22 December 1978.

500 mb

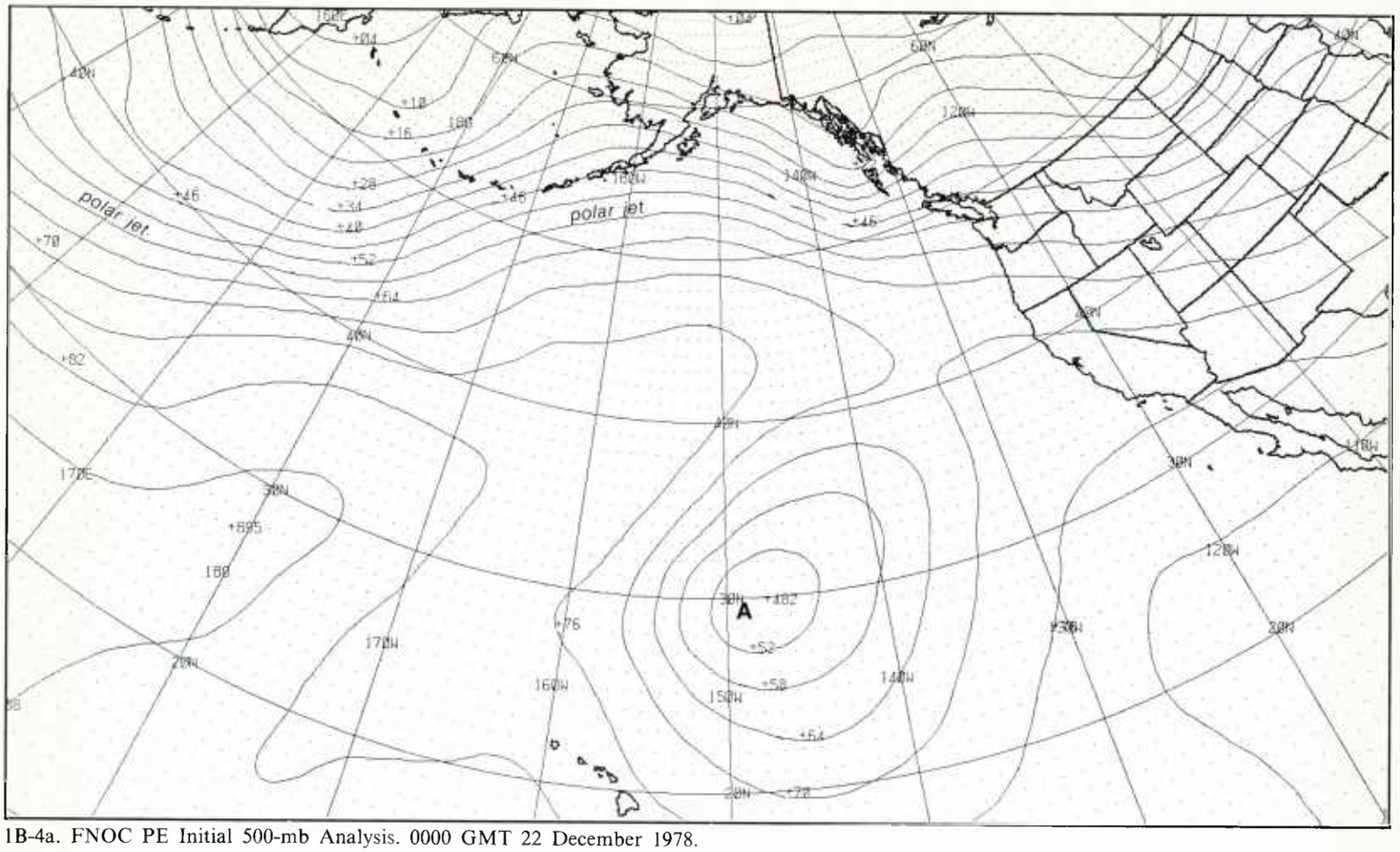

1B-4a. FNOC PE Initial 500-mb Analysis. 0000 GMT 22 December 1978.

500 mb

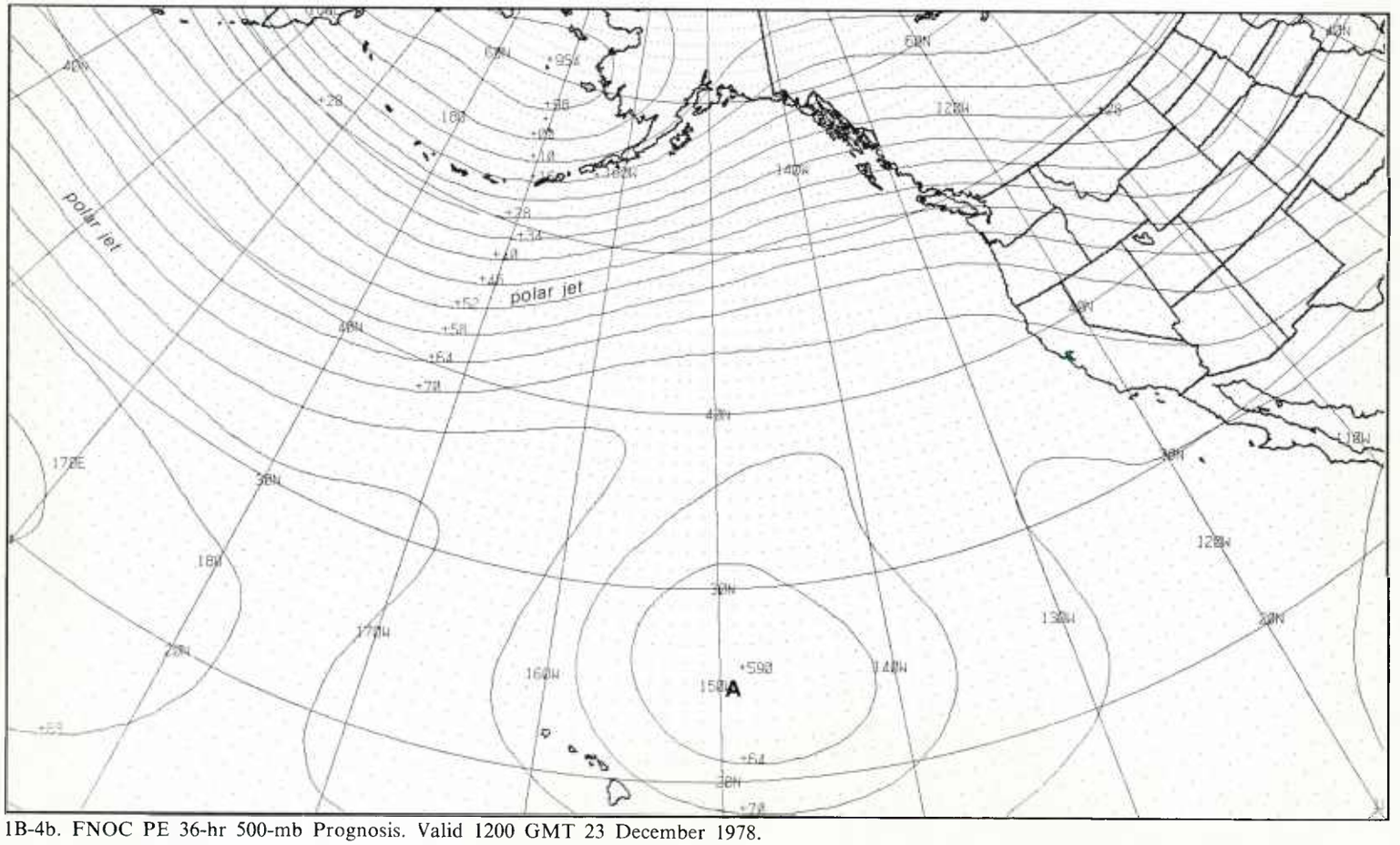

1B-4b. FNOC PE 36-hr 500-mb Prognosis. Valid 1200 GMT 23 December 1978.

Pre-Blocking Situation

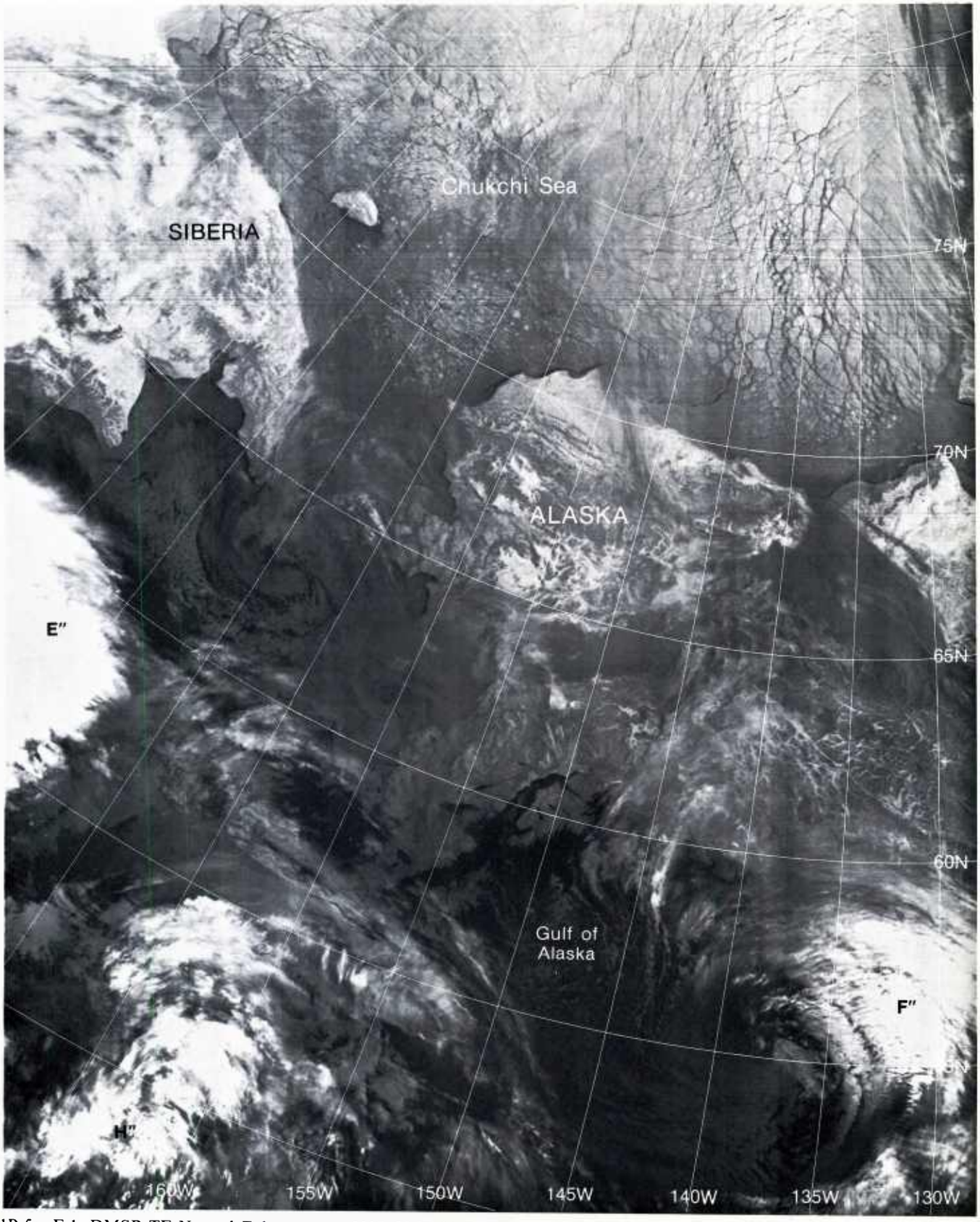

1B-5a. F-1. DMSP TF Normal Enhancement. 2007 GMT 21 December 1978.

23 December

As forecast, the 500-mb analysis at 1200 GMT (1B-6b) shows that strong zonal westerlies continue at high latitudes across the eastern Pacific. The cut-off low **A** has not changed position significantly; however, at 300 mb (1B-6a), a decrease in wind speed in the cyclonic circulation (note the absence of a jet streak in the upstream portion, as compared to 36 hours earlier) indicates that the cut-off low is weaker aloft. A weak surface low **A'** (1B-7b) and the convective activity **A"** in the satellite picture (1B-7a) indicate that this system continues to be synoptically active. Note that a long cirrus cloud band has developed in response to the nearly continuous jet at 300 mb at low latitudes over the eastern Pacific.

A significant change in the upper-level synoptic-scale flow pattern has occurred aloft over the Pacific and North America. At 500 mb, a short-wave trough **I** has developed over the central Pacific. The flow pattern upstream of this trough shows that the mid-latitude jet (closely-spaced height contour lines) no longer merges with the jet at high latitudes due to the presence of the short-wave disturbance. At 300 mb, a split at **I** is evident in the jet axis connecting the mid- and high-latitude jet streams. For comparison, see the 300-mb (1B-2a) and the 500-mb (1B-2b) analyses 36 hours earlier. The presence of a surface low **I'** (1B-7b) indicates that the 500-mb short-wave disturbance has developed through a deep vertical layer of the atmosphere. The distinct comma cloud **I"** (1B-7a) further identifies this system as an incipient storm. The development of the low at mid latitudes and the split in the jet at 300 mb are preliminary indications of the breakdown of the zonal flow regime over the Pacific.

Over North America, the upper-level zonal flow has been interrupted by the development of a ridge over northwest Canada and a deep trough downstream over North America. The surface storm **E'** has moved rapidly eastward; however, the satellite picture (1B-7a) shows only a faint, west-east elongated frontal cloud band extending from the cloud vortex **E"**, which indicates that this storm is in the dissipating stage as it moves under the influence of the ridge aloft. The storm **F'** (1B-7b) has been forced to the southeast by the development of the deep trough aloft. This has resulted in the disruption of the pattern of equally-spaced cyclones along 55°N. Storms **F'** and **G'** have weakened significantly due to the change in the flow pattern aloft over North America.

A comparison of the initial 500-mb analysis (1B-8a) and the 36-hour 500-mb prognosis (1B-9a) shows that the short-wave trough **I** will intensify as it moves into the eastern Pacific. To the east of this trough, the polar jet (closely-spaced contours) remains strong over the Gulf of Alaska. To the west, however, the height contour lines indicate that the jet is not swinging around the base of the trough **I**—which would maintain the zonal westerlies across the Pacific—but is beginning to dig to the southeast toward the cut-off low **A**. The surface prognosis (1B-9b) reveals that the surface highs will tend to assume a meridional orientation, in contrast to the zonal orientation observed on the initial analysis (1B-8b). Note that the 500-mb ridge to the east of the cut-off low also shows a significant building to the north. All of these factors favor the development of a blocking event over the eastern Pacific. *continued on page 1B-10*

300 mb

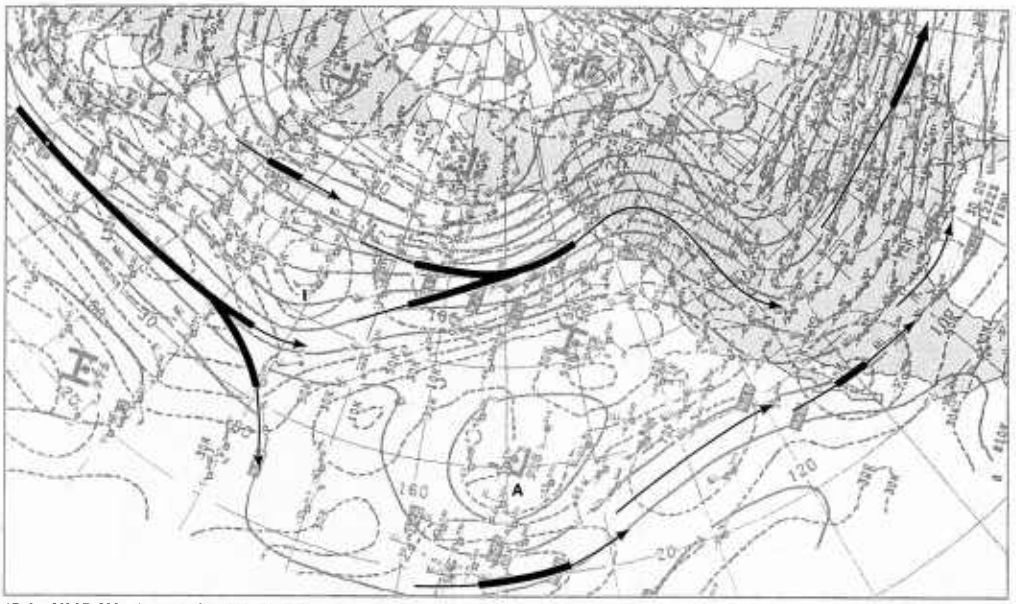

1B-6a. NMC 300-mb Analysis. 1200 GMT 23 December 1978.

500 mb

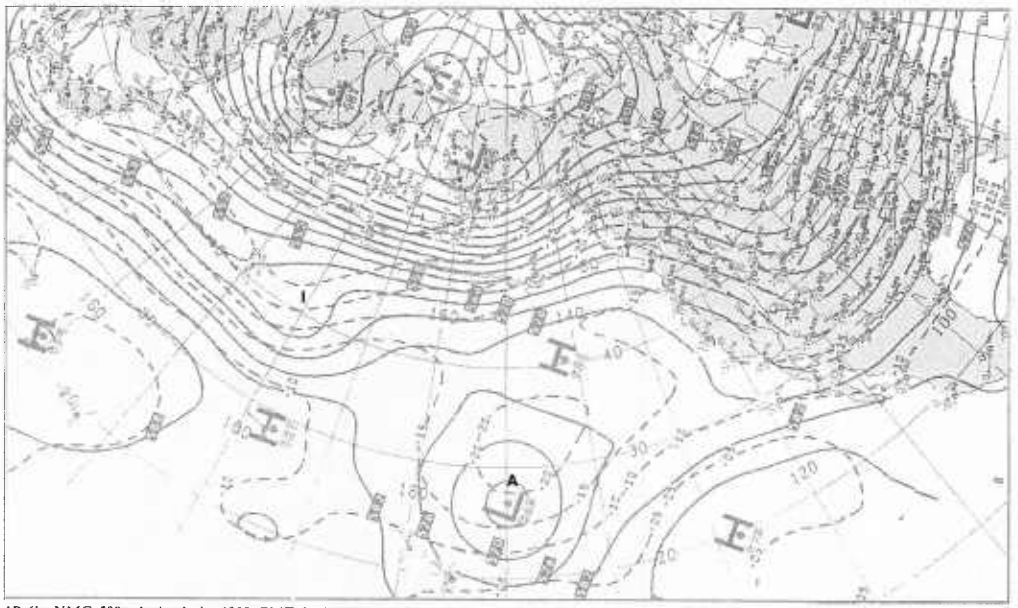

1B-6b. NMC 500-mb Analysis. 1200 GMT 23 December 1978.

Pre-Blocking Situation

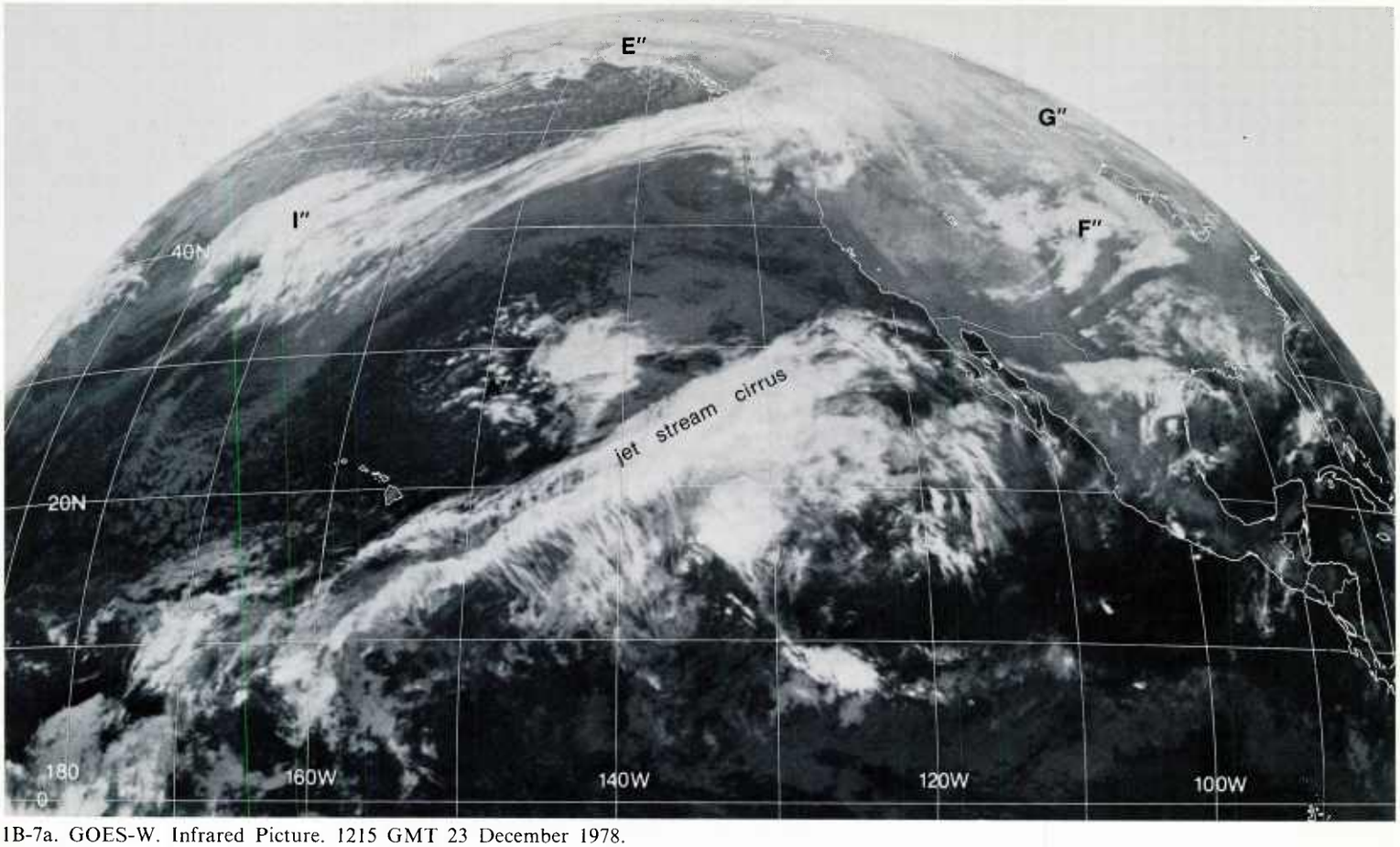

1B-7a. GOES-W. Infrared Picture. 1215 GMT 23 December 1978.

surface

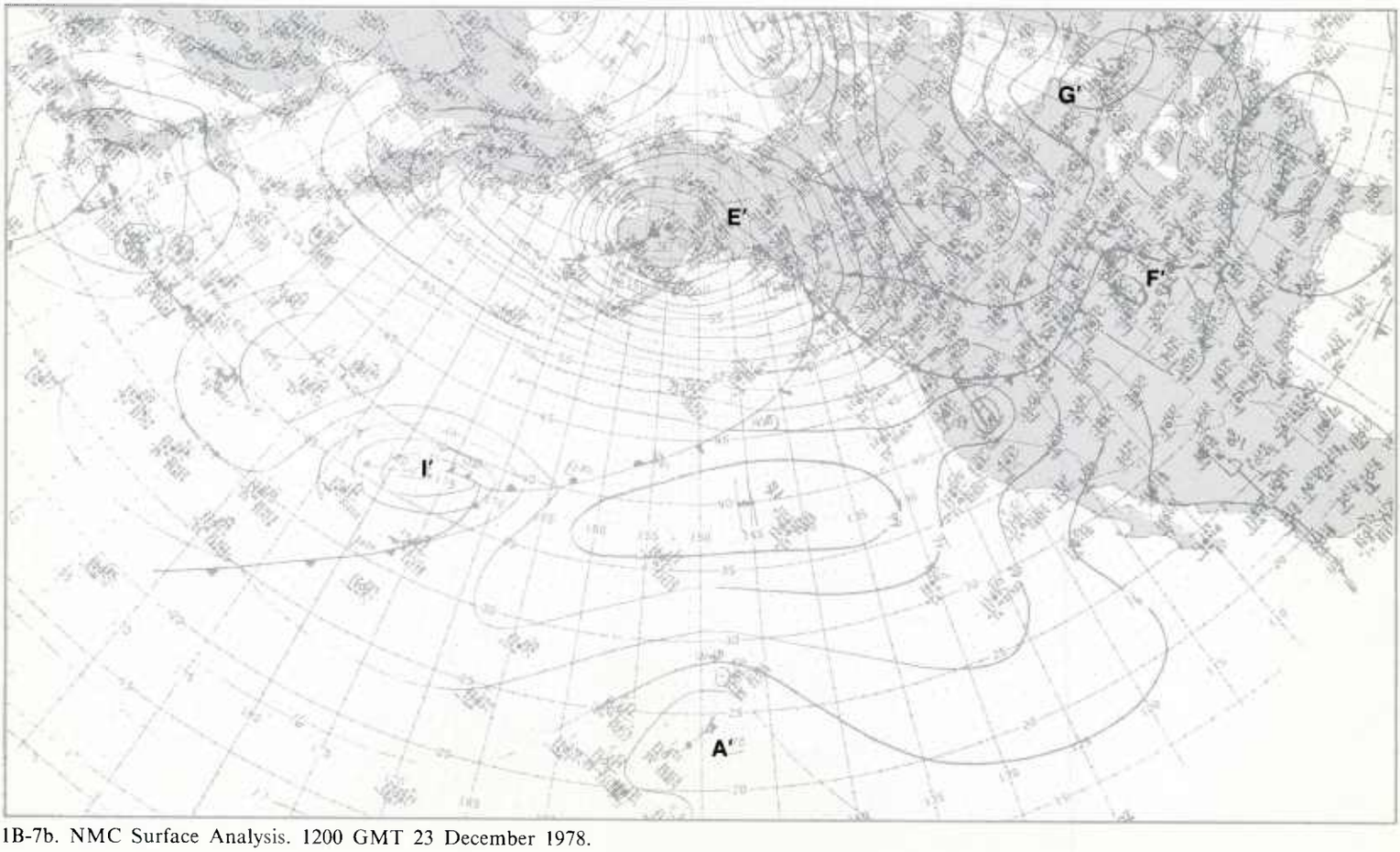

1B-7b. NMC Surface Analysis. 1200 GMT 23 December 1978.

500 mb

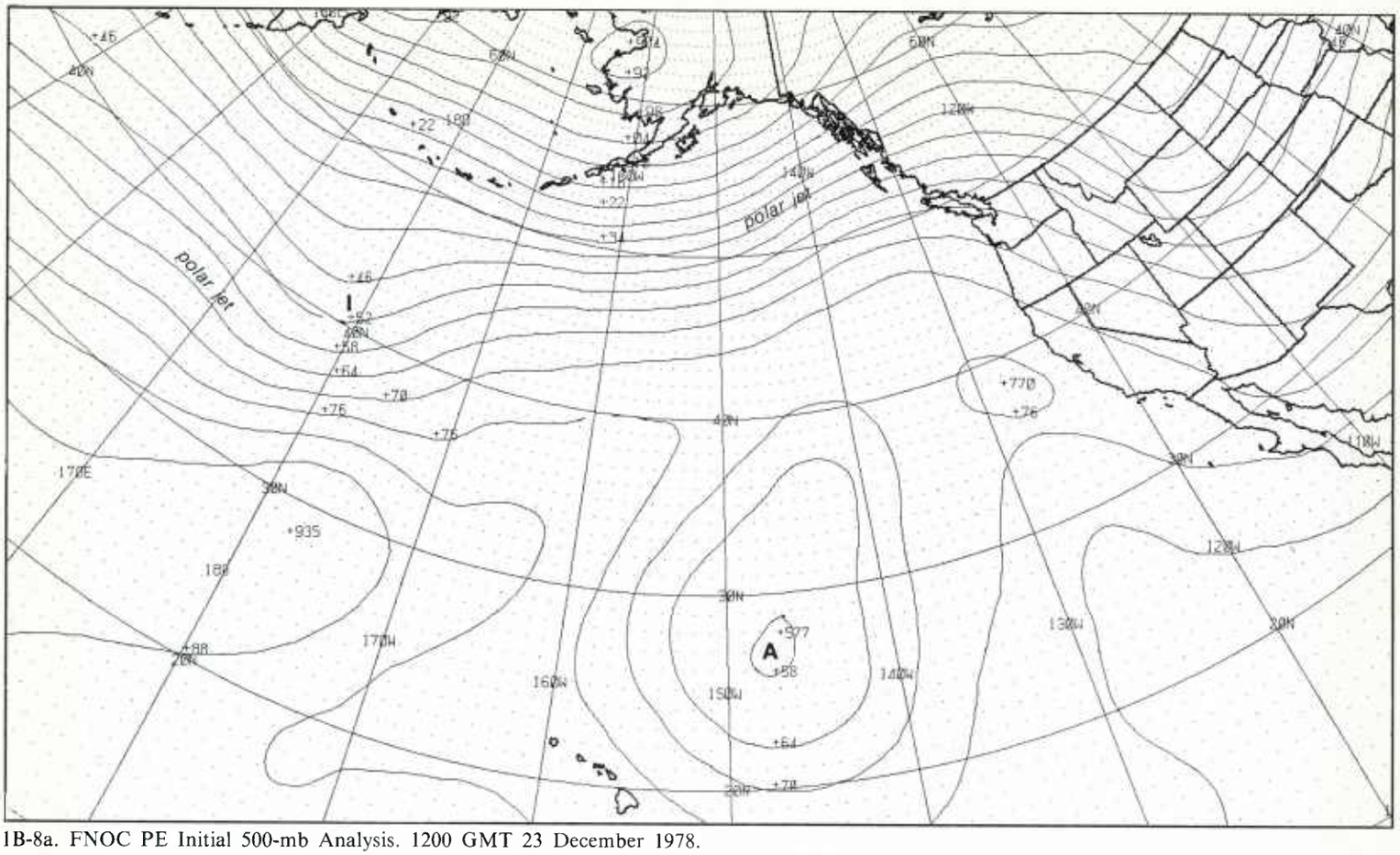

1B-8a. FNOC PE Initial 500-mb Analysis. 1200 GMT 23 December 1978.

surface

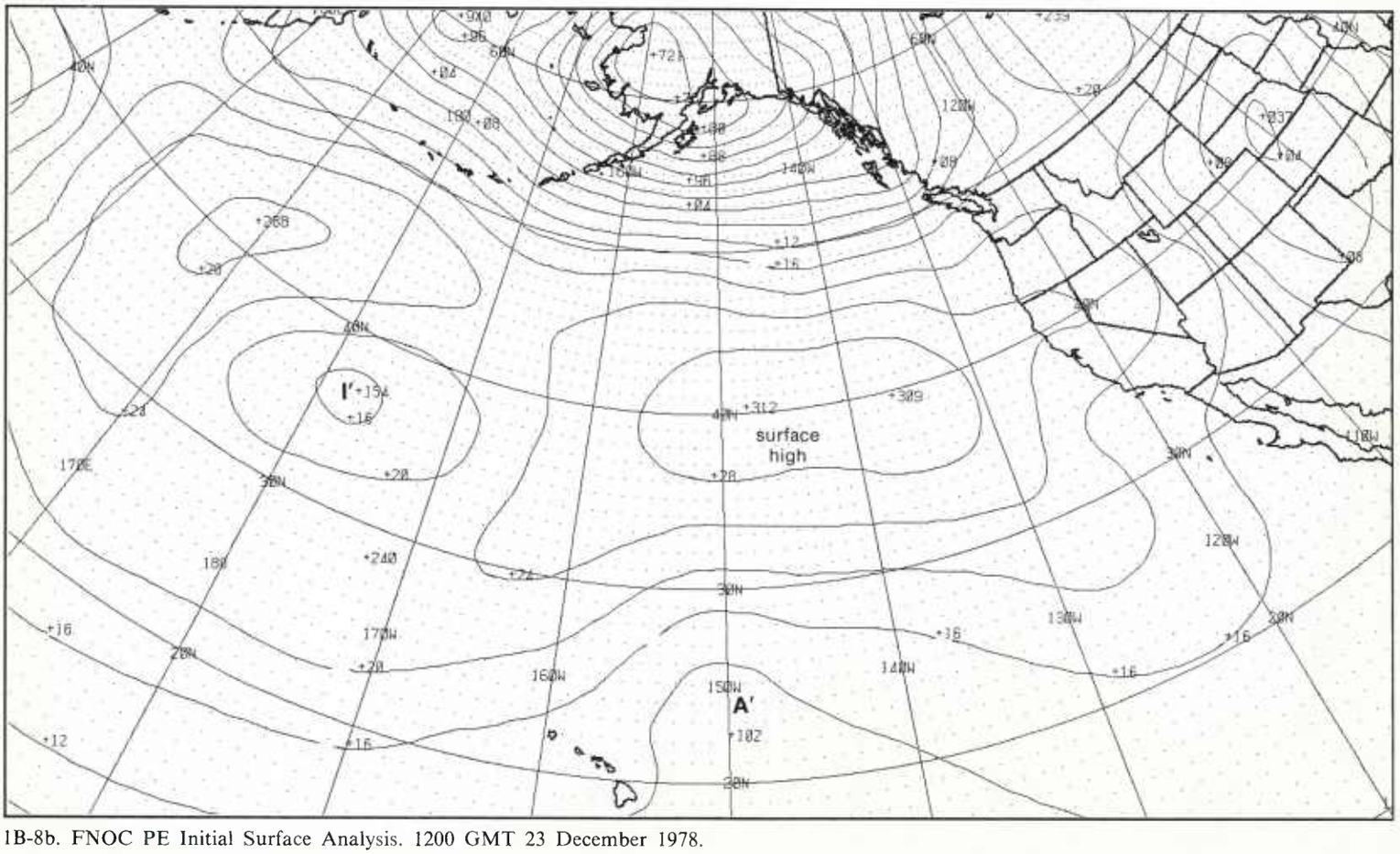

1B-8b. FNOC PE Initial Surface Analysis. 1200 GMT 23 December 1978.

500 mb

Pre-Blocking Situation

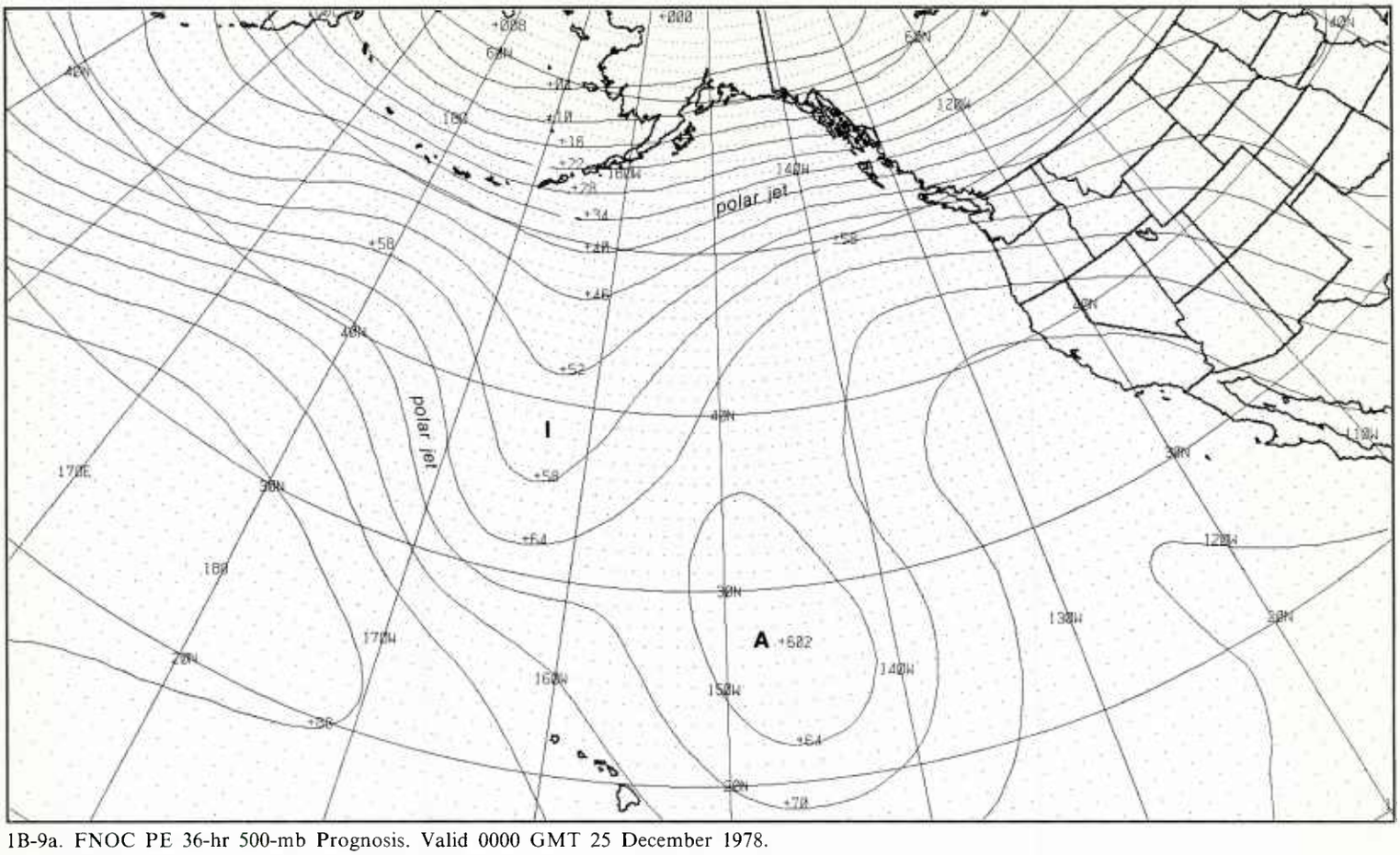

1B-9a. FNOC PE 36-hr 500-mb Prognosis. Valid 0000 GMT 25 December 1978.

surface

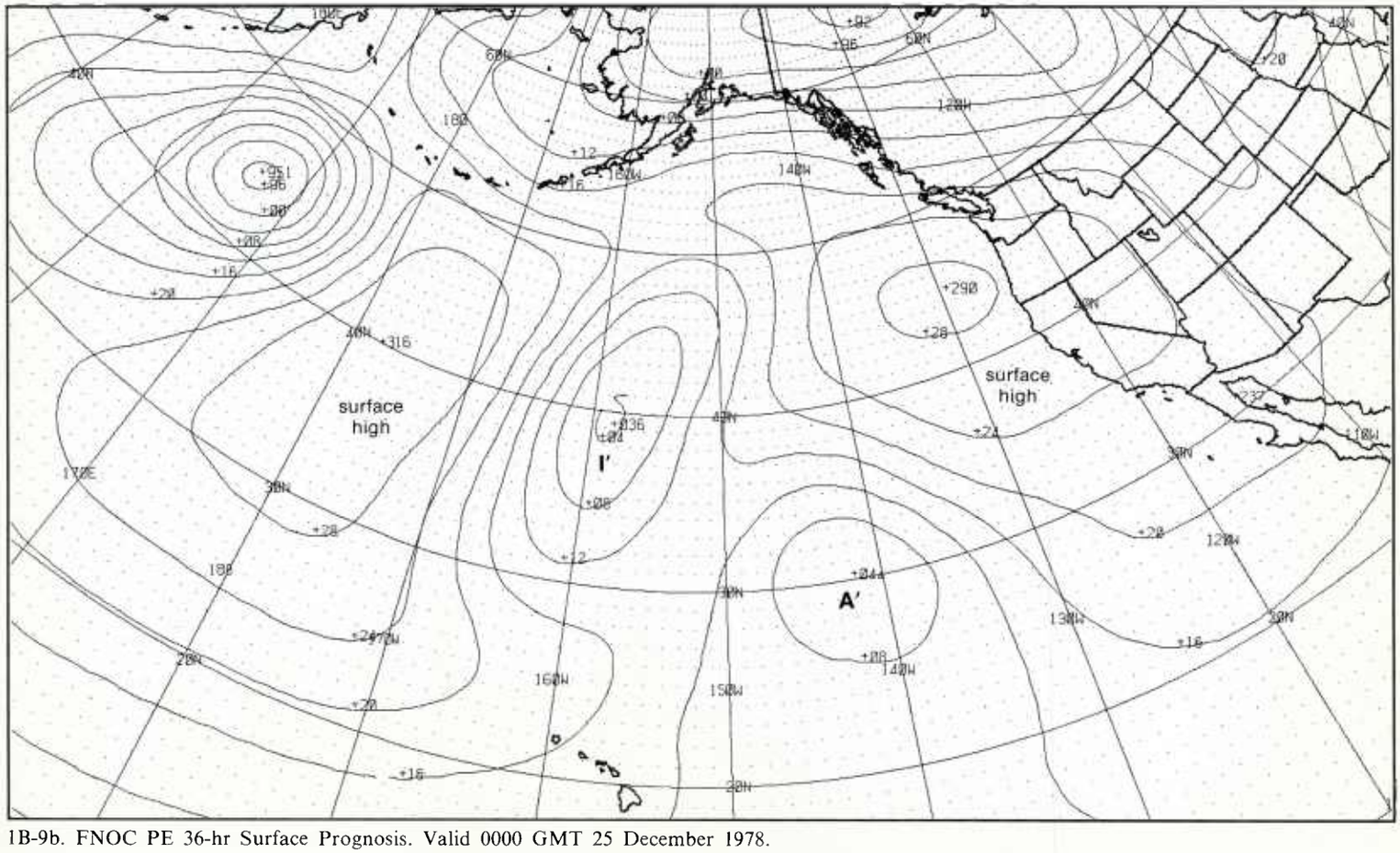

1B-9b. FNOC PE 36-hr Surface Prognosis. Valid 0000 GMT 25 December 1978.

Onset of Blocking

Onset of Blocking

Characteristic Features

1. *Development of a meridional trough at mid latitudes which disrupts the zonal flow regime over the Pacific.*
2. *Building of a ridge downstream of the developing meridional trough.*
3. *Movement of an intense low aloft, accompanied by a strong polar jet, into the west-central Pacific upstream of the meridional trough.*

25 December

As forecast: (1) the sharp meridional trough **I** has intensified over the central Pacific at 500 mb (1B-10b), (2) the isotach analysis at 300 mb (1B-10a) shows a strong polar jet over the Gulf of Alaska, and (3) a southward digging jet is located west of the meridional trough. These jet features are reflected by the closely-spaced height contour lines upstream and downstream of the meridional trough **I** at 500 mb, the FNOC forecast level. A wedge of high pressure **N** has developed over the eastern Pacific, from the surface to 300 mb, with the cut-off low **A** at 500 mb trapped between the ridge and the trough **I** to the west. Upstream, a new major trough **J**, with strong cold air advection to the rear, has moved into the central Pacific. Note the strong 300-mb jet associated with this disturbance.

The surface analysis (1B-11b) shows two mature cyclones **I′** and **J′** at mid latitudes over the central Pacific and no major storms at high latitudes over the eastern Pacific—the train of storms at high latitudes over the eastern Pacific and North America has dissipated. In the satellite picture (1B-11a), the faint vortex cloud pattern at **I″** and the weak frontal cloud bands extending to the south from the vortex, indicate that this storm is dissipating. In contrast, the distinct cloud vortex and frontal cloud band associated with the disturbance **J″** is characteristic of a storm that is in the developing stage. In the eastern Pacific, convection clouds around **A″** in the 500-mb cut-off low **A** reveals that this low continues to behave as an active, deep, cold core system. To the south of the cut-off low, note how readily the jet-associated cirrus cloud decks and streaks can be used to trace the subtropical jet from the central Pacific to the Gulf of Mexico. (Compare with the 300-mb jet analysis.)

During the next 36 hours, the trough **I** at 500 mb over the east-central Pacific (1B-12a) is forecast to move southeast (1B-13a). The continued development of this trough completes the disruption of the zonal flow regime over the Pacific. Downstream of the trough, the ridge **N** is forecast to develop into a sharp wedge of high pressure. The most significant feature, insofar as the onset of blocking is concerned, is the rapid deepening of the low **J** at 500 mb as it moves eastward. The diffluence of the closely-spaced height contour lines downstream of this low indicates a continued split in the polar jet: a northerly branch moving up and over the ridge at high latitudes and a southerly branch swinging around the base of the trough over the east-central Pacific. The above features are characteristic of the onset of blocking over the eastern Pacific.

At the surface, a comparison of the initial analysis (1B-12b) with the 36-hour prognosis (1B-13b) shows that the closed low **I′** and the surface reflection of the upper cold low **A′** over the east-central Pacific will continue to weaken, as they move under the influence of the building 500-mb ridge to the north. The storm **J′** over the west-central Pacific, however, will continue to deepen, as it advances on a northeasterly track.

continued on page 1B-14

300 mb

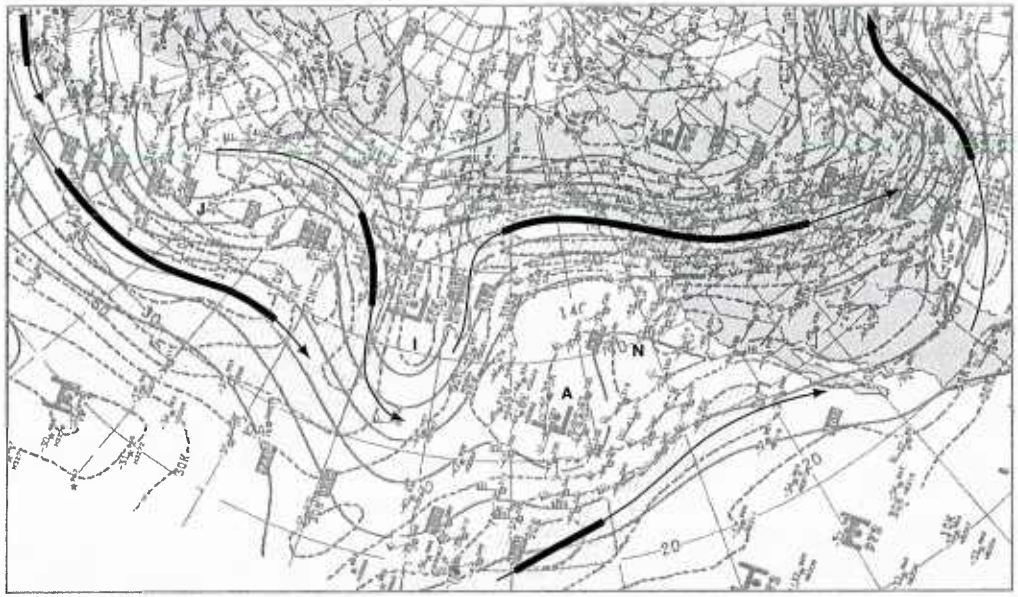

1B-10a. NMC 300-mb Analysis. 0000 GMT 25 December 1978.

500 mb

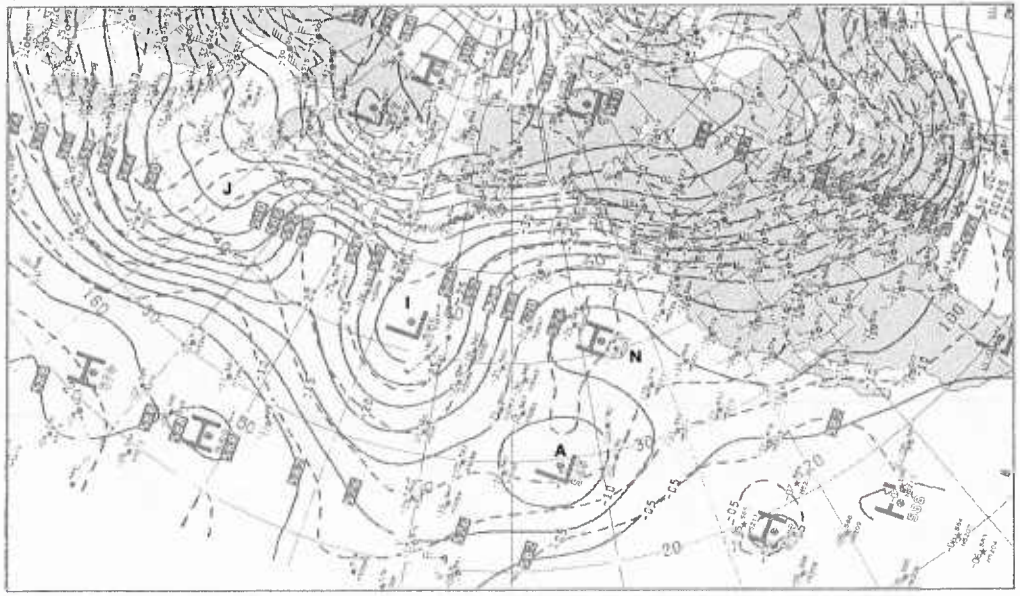

1B-10b. NMC 500-mb Analysis. 0000 GMT 25 December 1978.

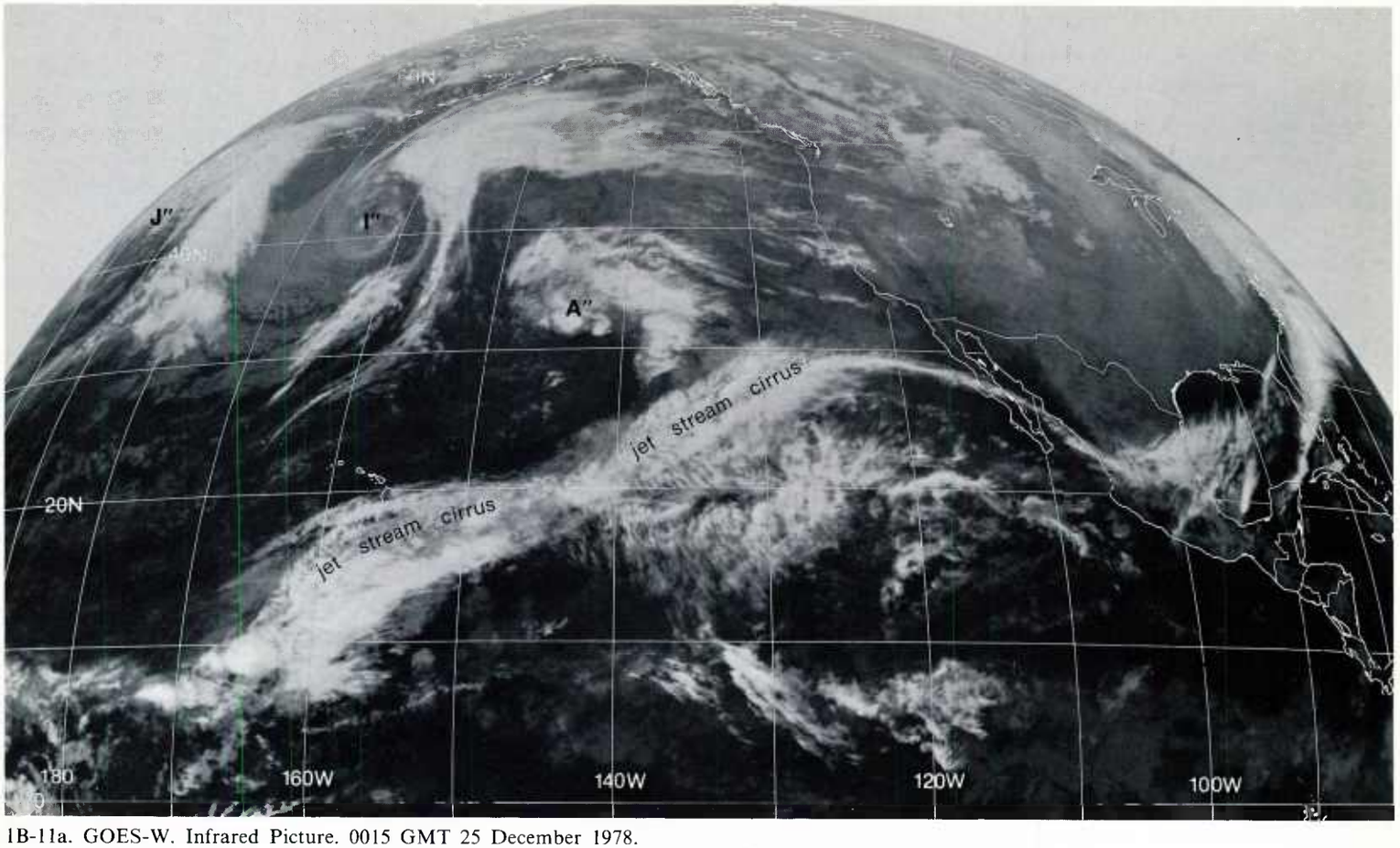

1B-11a. GOES-W. Infrared Picture. 0015 GMT 25 December 1978.

surface

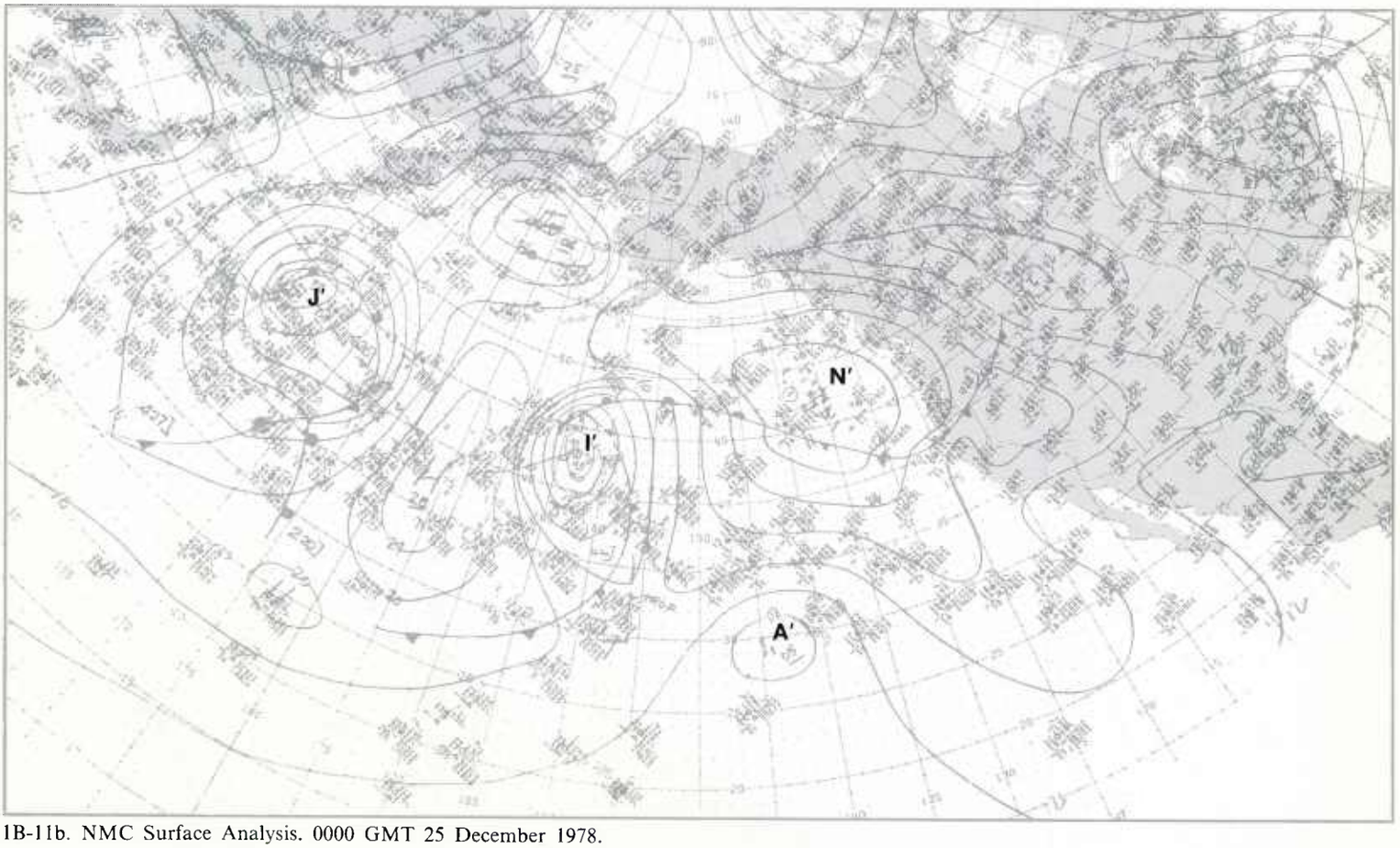

1B-11b. NMC Surface Analysis. 0000 GMT 25 December 1978.

500 mb

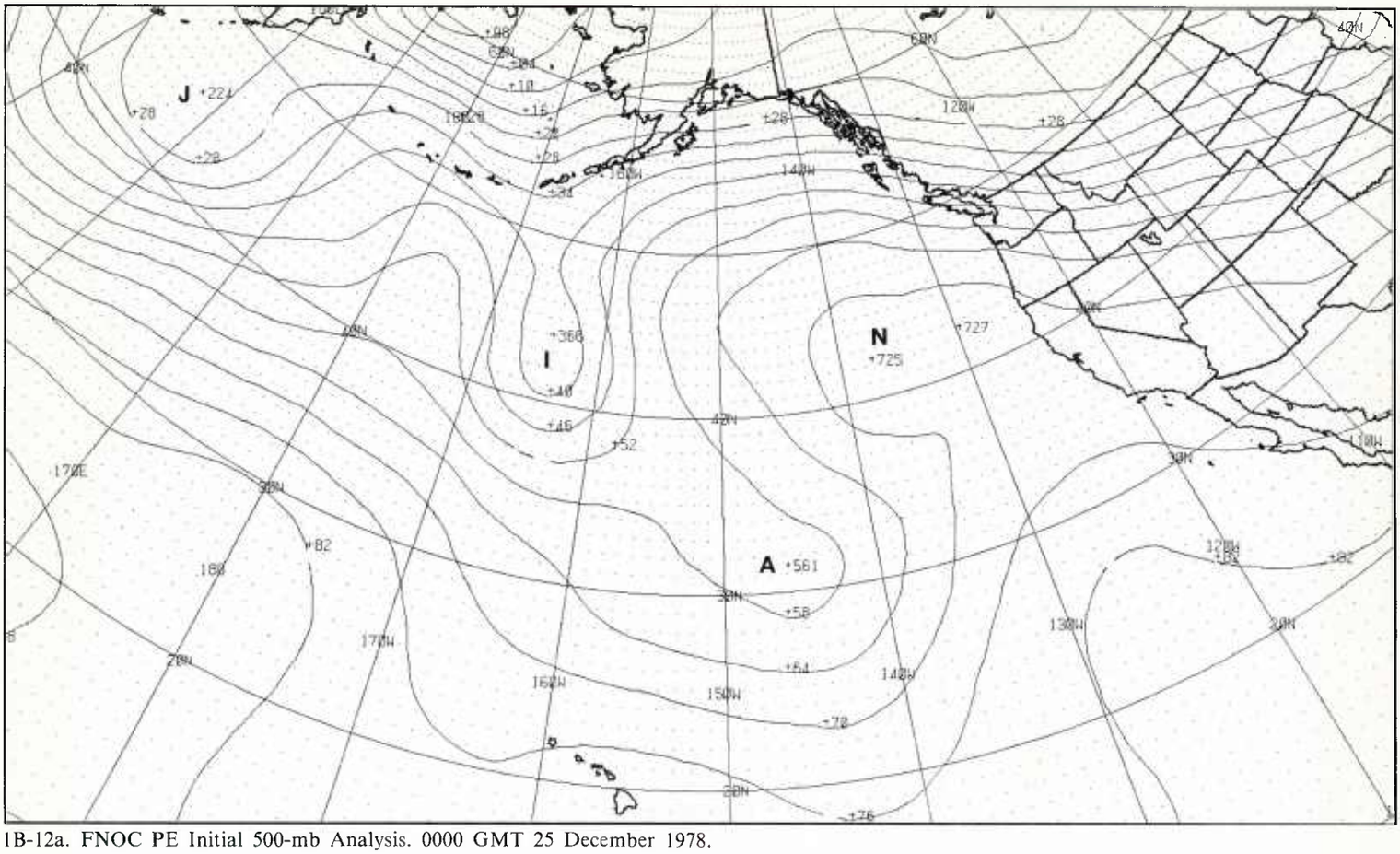

1B-12a. FNOC PE Initial 500-mb Analysis. 0000 GMT 25 December 1978.

surface

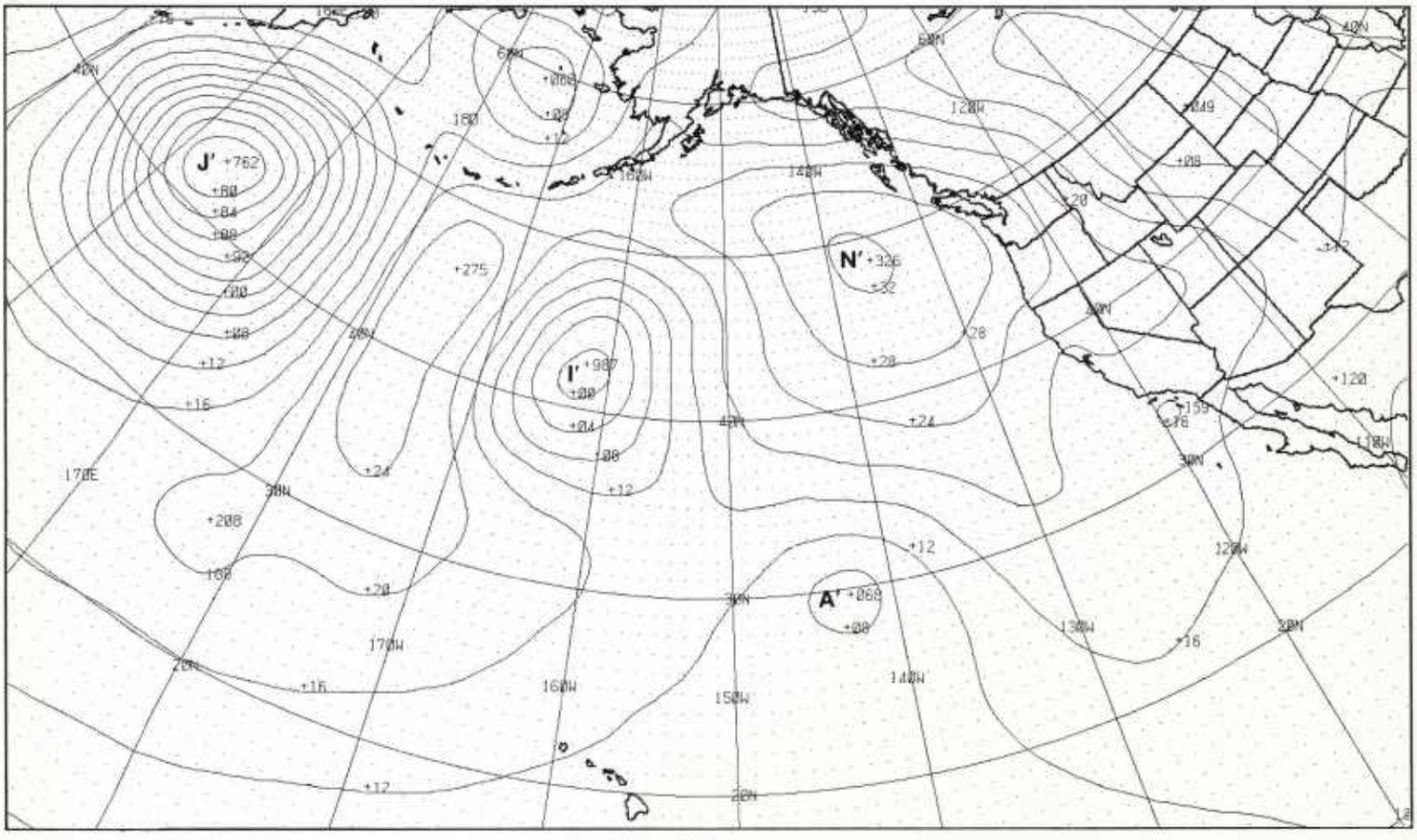

1B-12b. FNOC PE Initial Surface Analysis. 0000 GMT 25 December 1978.

500 mb

Onset of Blocking

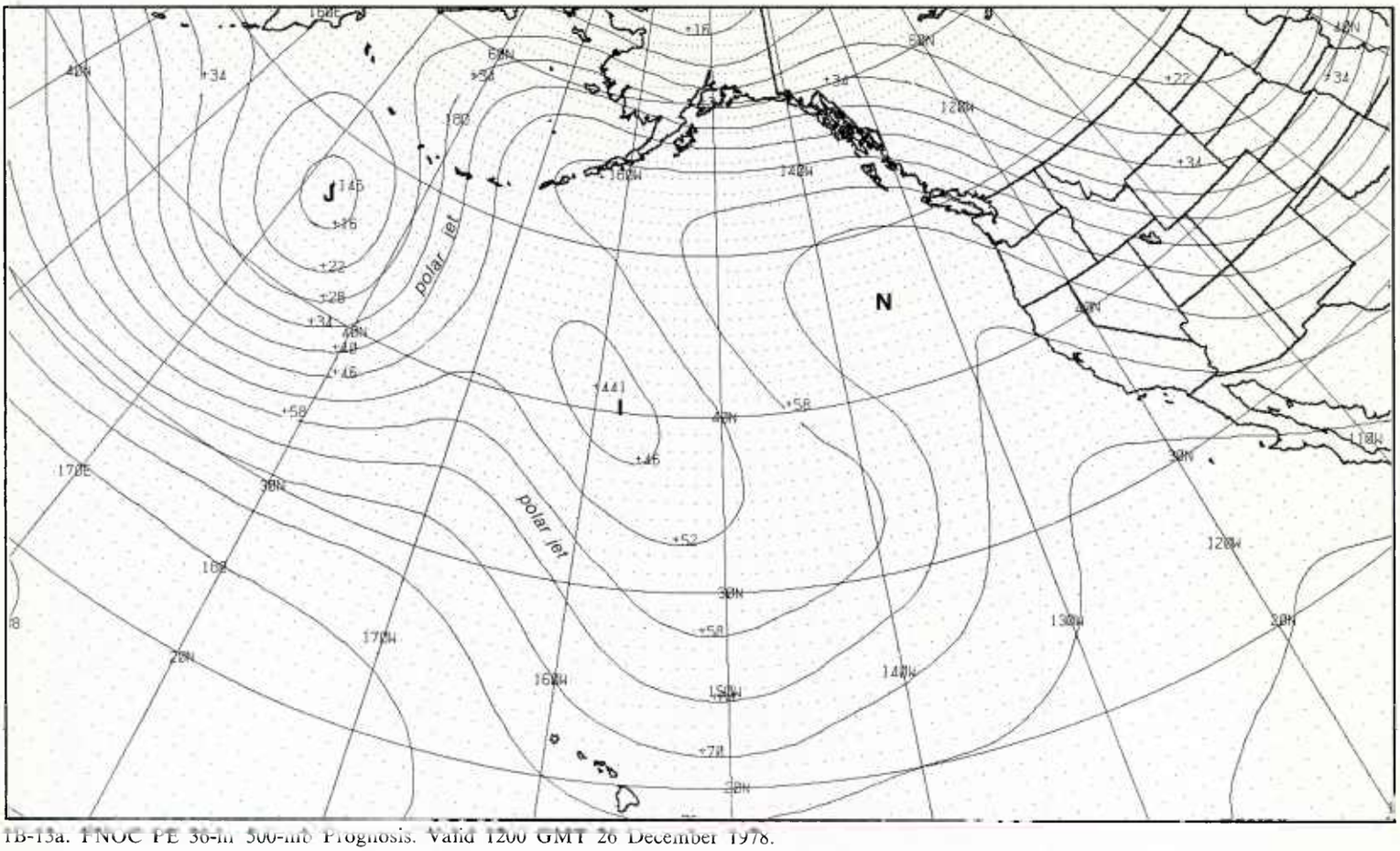

1B-13a. FNOC PE 36-hr 500-mb Prognosis. Valid 1200 GMT 26 December 1978.

surface

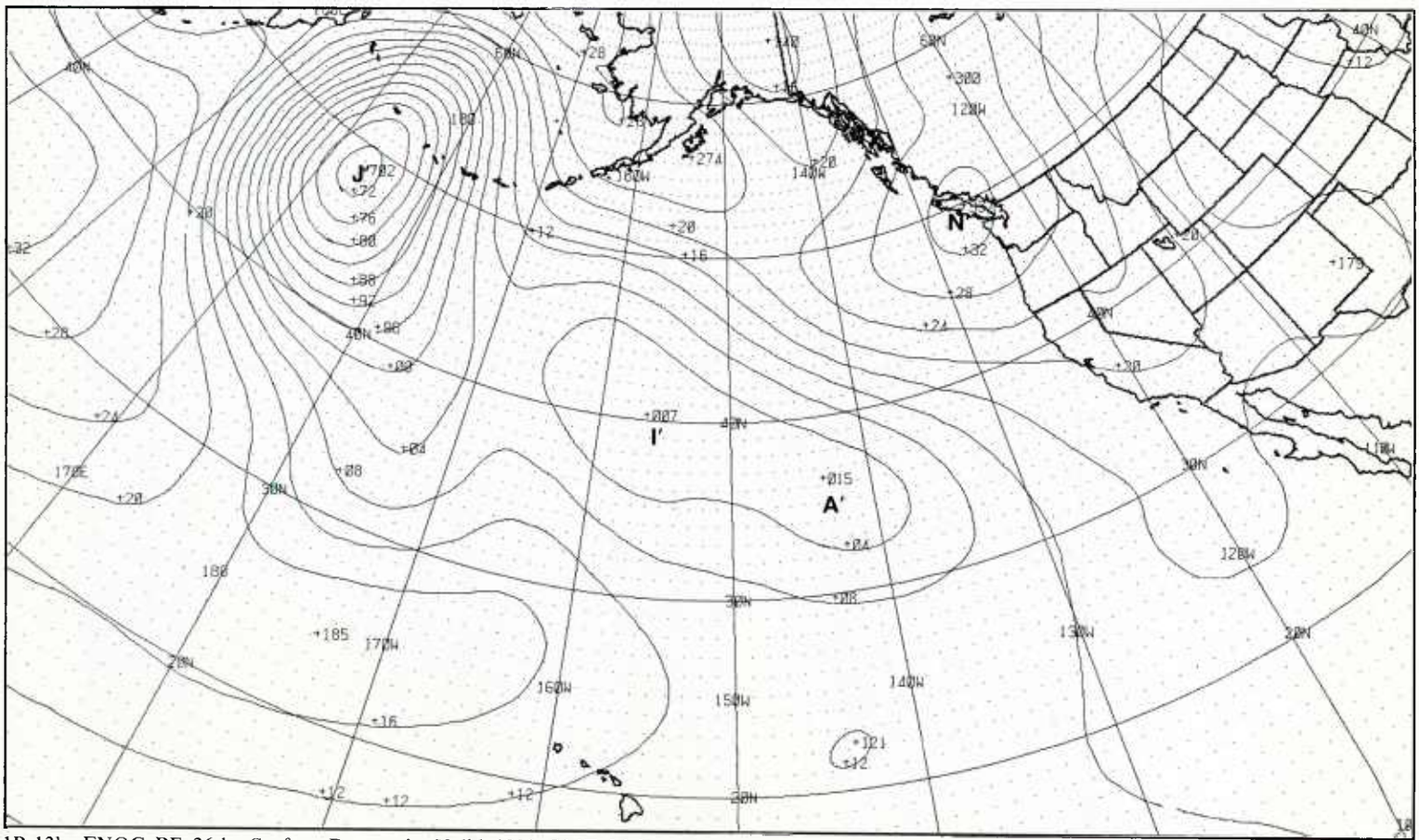

1B-13b. FNOC PE 36-hr Surface Prognosis. Valid 1200 GMT 26 December 1978.

26 December

At 500 mb (1B-14b), the large-scale circulation systems over the Pacific are developing in general as forecast. A deep low **J** dominates the west-central Pacific, and a sharp wedge of high pressure **N** extending to high latitudes has developed over the eastern Pacific. The meridional trough **I** along 155° W, however, has not developed as forecast and is being squeezed between the amplifying ridge to the east and the ridge **M** developing ahead of the intense low moving in from the west. There is a definite split in the mid-latitude jet near 40° N, 170° W—this confirms that the zonal flow over the eastern Pacific has been disrupted. The split of the mid-latitude jet upstream of the building ridge **N** continues to signal the onset of blocking over the eastern Pacific.

The jet stream analysis at 300 mb (1B-14a) also shows that the zonal flow regime over the Pacific has been disrupted (see for comparison 1B-2a). There is a long polar jet stream segment extending from Alaska to the central U.S., a subtropical jet segment at low latitudes over the eastern Pacific, and a very strong polar jet segment at mid latitudes over the west-central Pacific. A new polar jet over the northwest Pacific upstream of low **J** is moving on a merging course with the strong jet at mid latitudes.

In the satellite picture (1B-15a), the two cloudy areas **A″** and **I″** identify the merged lows **A′** and **I′** passing under the 500-mb ridge **N**. The cloudy area **K″** is located in a short-wave trough on the north side of the ridge. At the surface (1B-15b), the lows **A′** and **I′** have merged in a single elongated trough. As forecast, the surface cyclone **J′** has deepened and moved on a northeasterly track. It is a major oceanic winter storm. The satellite picture shows the typical, large spiral cloud vortex **J″** characteristic of a mature winter storm with an active frontal cloud band extending to the southwest across the Pacific. At the surface, the pronounced southerly meridional flow to the east and the corresponding strong northerly meridional flow to the west of the surface low **J′** are additional evidence that the zonal flow regime over the Pacific has also disappeared at lower levels. The broad anticyclonically-curved cirrus band in the satellite picture has formed in response to the sharply-curved subtropical jet streak **PJS** at 300 mb.

A comparison of the initial 500-mb analysis (1B-16a) and the 36-hour 500-mb prognosis (1B-17a) reveals that the characteristic features of a typical high-latitude block will develop over the eastern Pacific. The elongated ridge over the eastern Pacific on the initial analysis is forecast to consolidate into a high-amplitude closed (blocking) anticyclone **N**, and the eastern portion of the narrow meridional trough **I** upstream of the ridge evolves into a trapped low **P** below the block. The polar jet (closely-spaced height contour lines) associated with the intense low **J** over the west-central Pacific on the initial analysis is forecast to split into two distinct branches: the northern branch curves over the blocking anticyclone and the southern branch passes to the south around the trapped low below the block. The main surface circulation feature is the transformation of the high **N′** on the initial surface analysis (1B-16b) into a strong, blocking surface high **N′** over the eastern Pacific (1B-17b). Note also that the surface lows **A′** and **I′** merge into a single low center **P′**.

continued on page 1B-18

300 mb

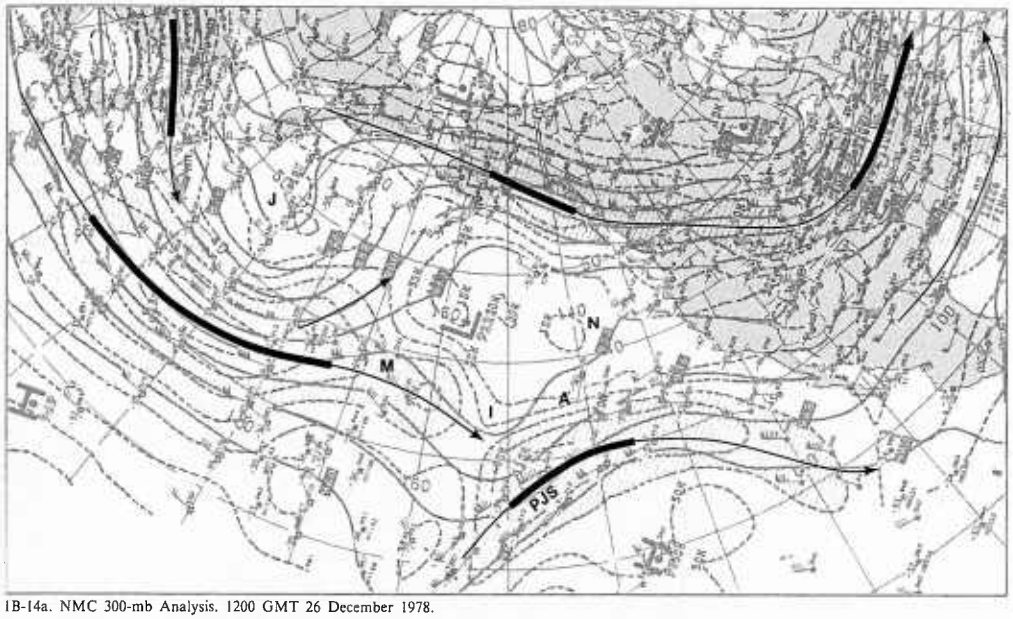

1B-14a. NMC 300-mb Analysis. 1200 GMT 26 December 1978.

500 mb

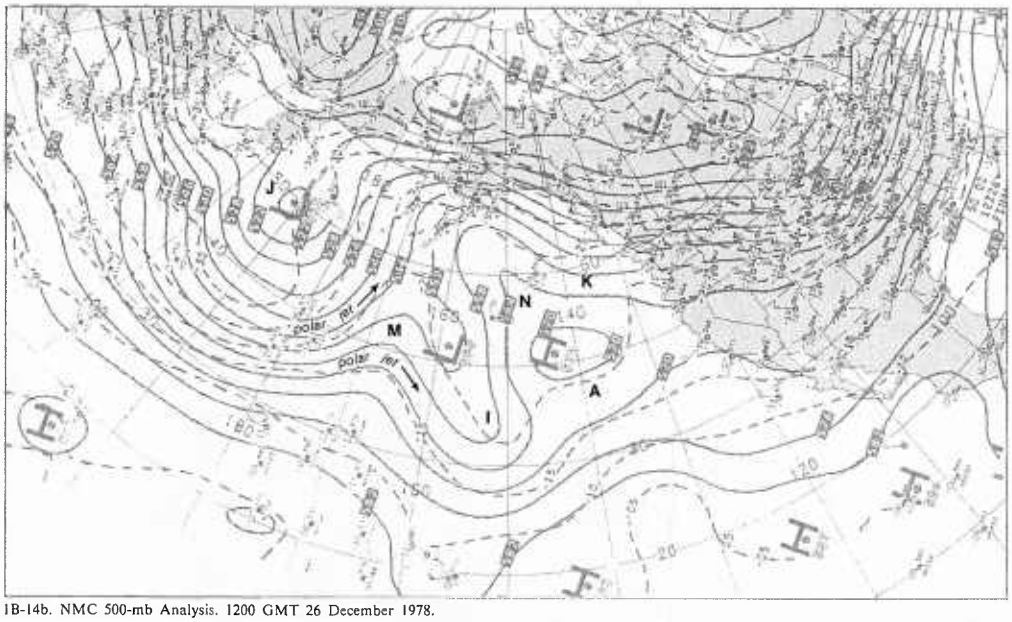

1B-14b. NMC 500-mb Analysis. 1200 GMT 26 December 1978.

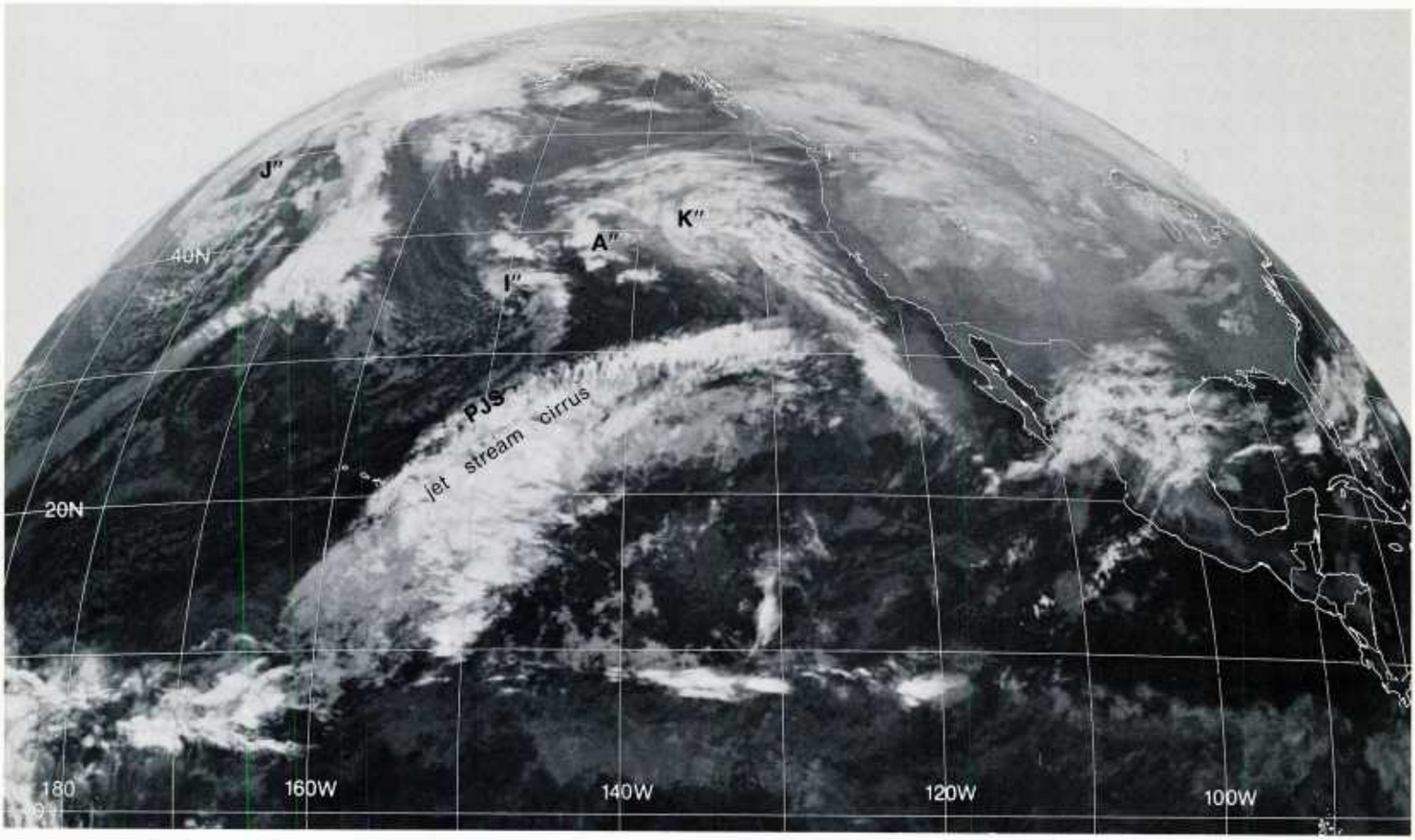

1B-15a. GOES-W. Infrared Picture. 1215 GMT 26 December 1978.

surface

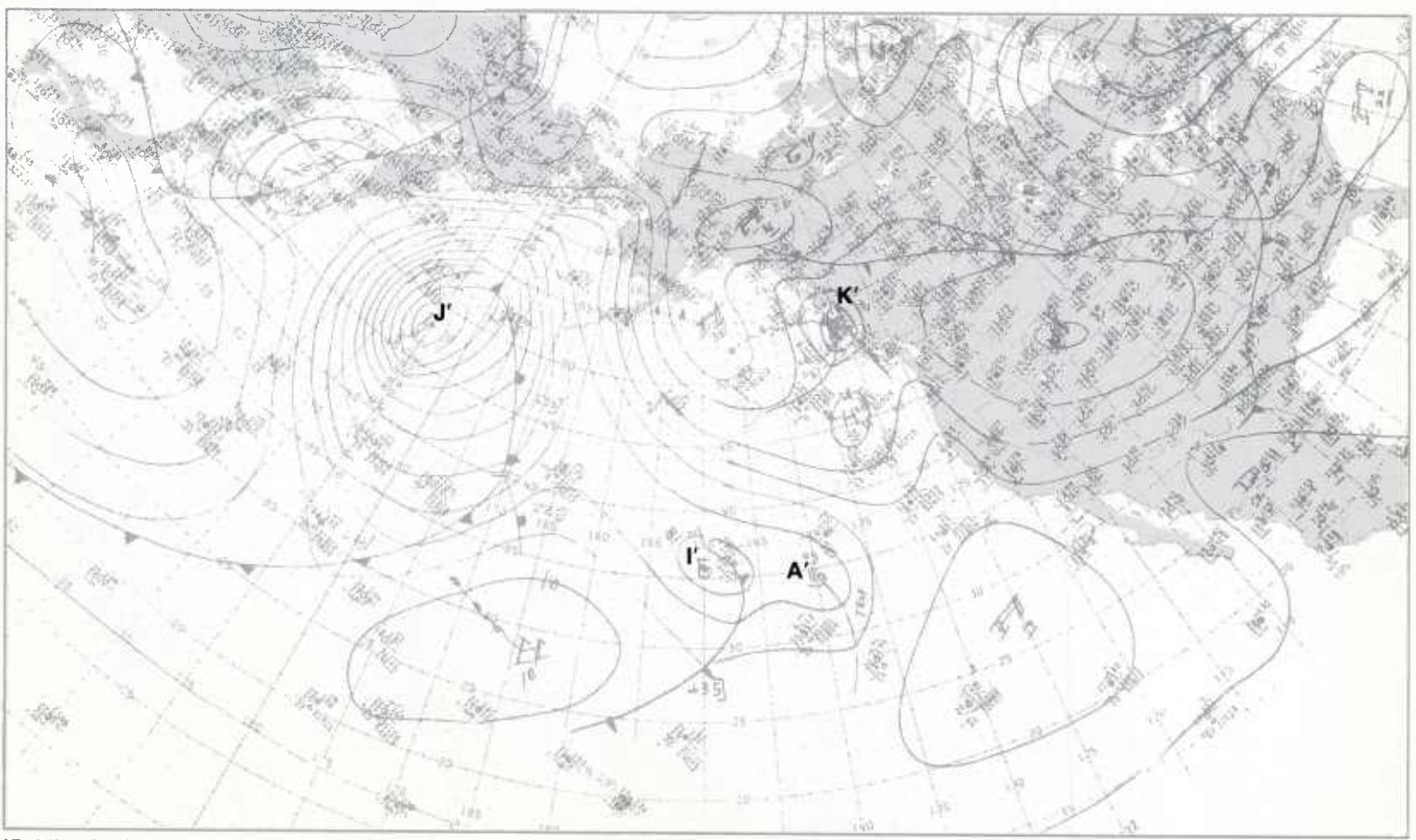

1B-15b. NMC Surface Analysis. 1200 GMT 26 December 1978.

500 mb

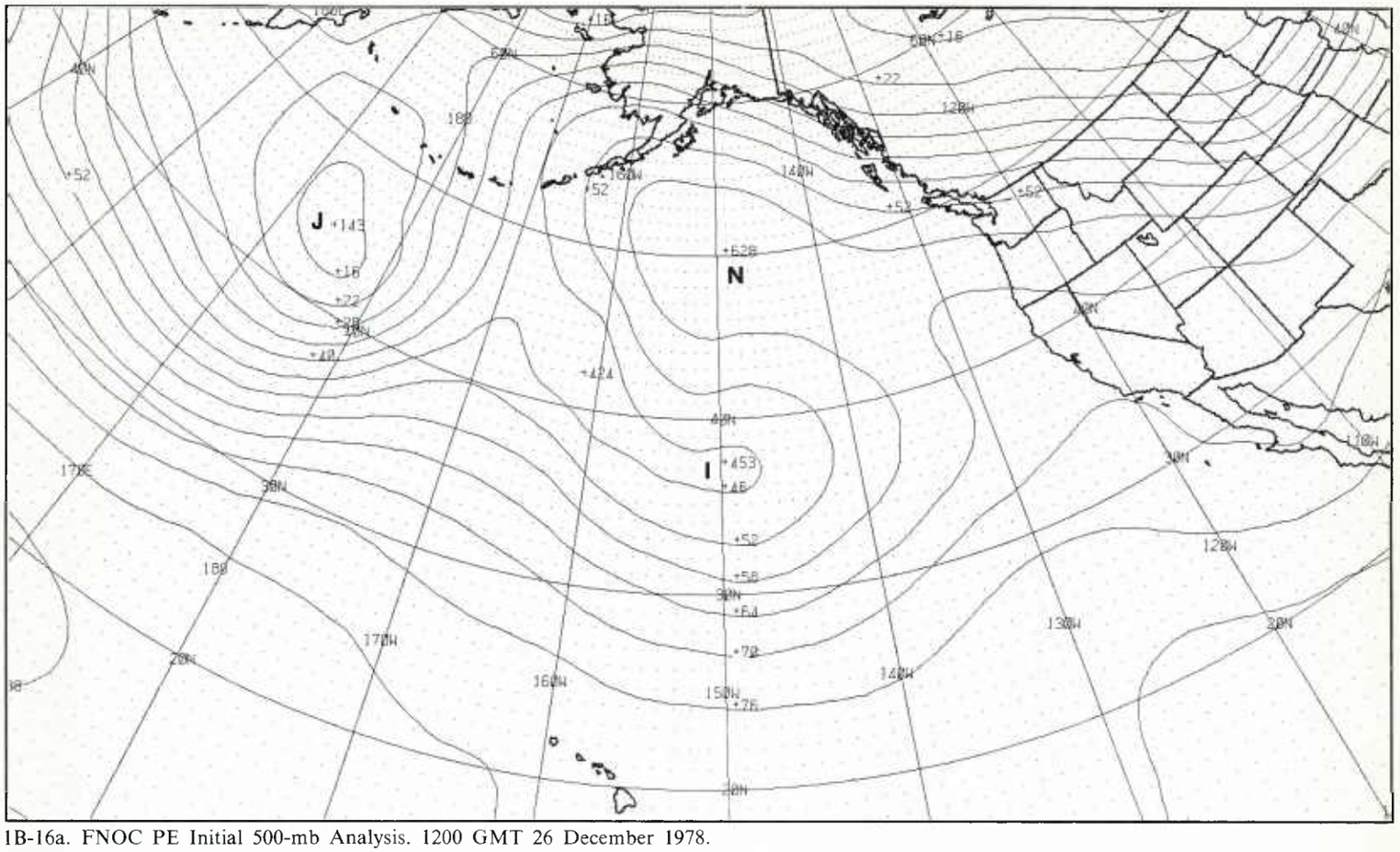

1B-16a. FNOC PE Initial 500-mb Analysis. 1200 GMT 26 December 1978.

surface

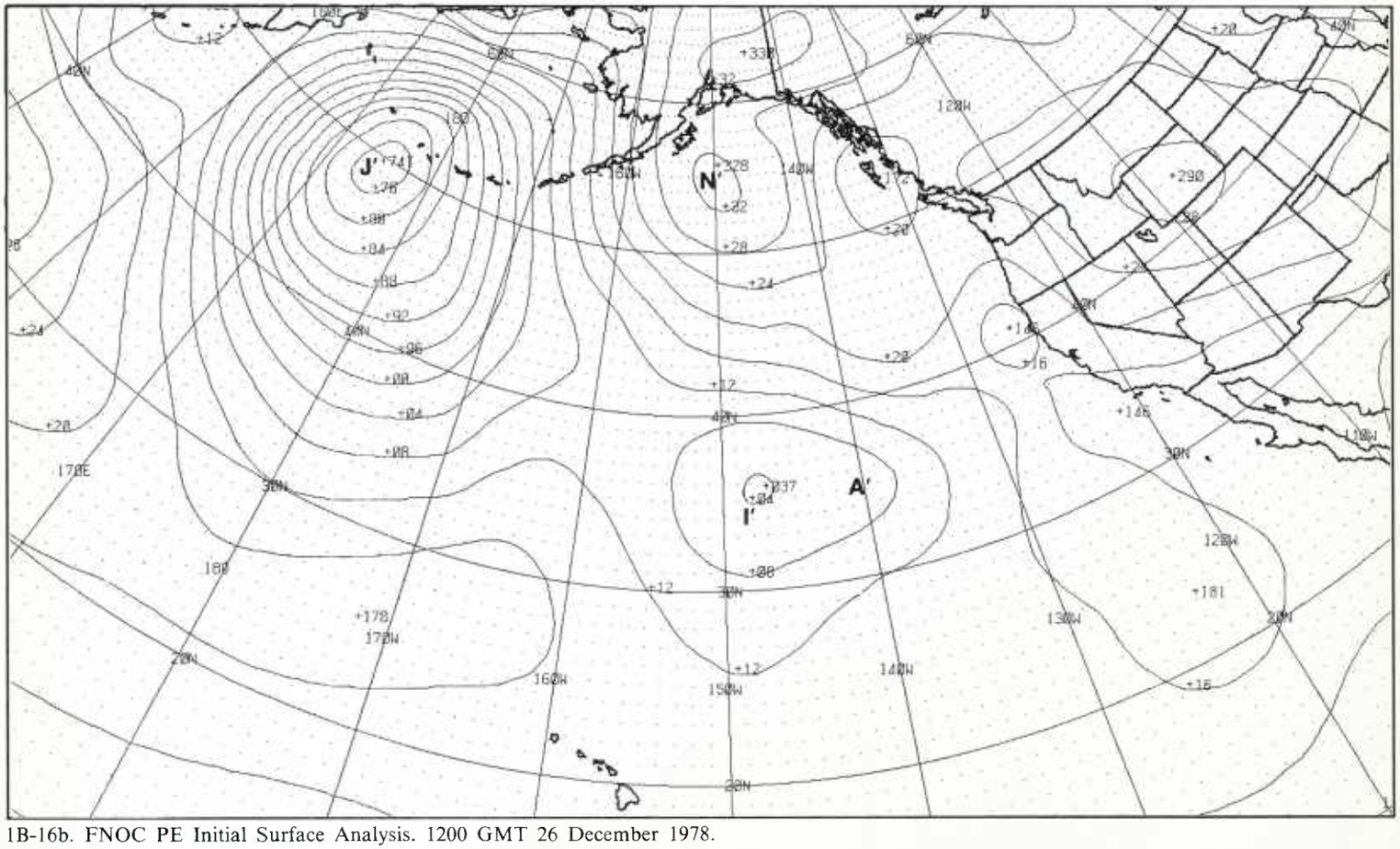

1B-16b. FNOC PE Initial Surface Analysis. 1200 GMT 26 December 1978.

500 mb

Onset of Blocking

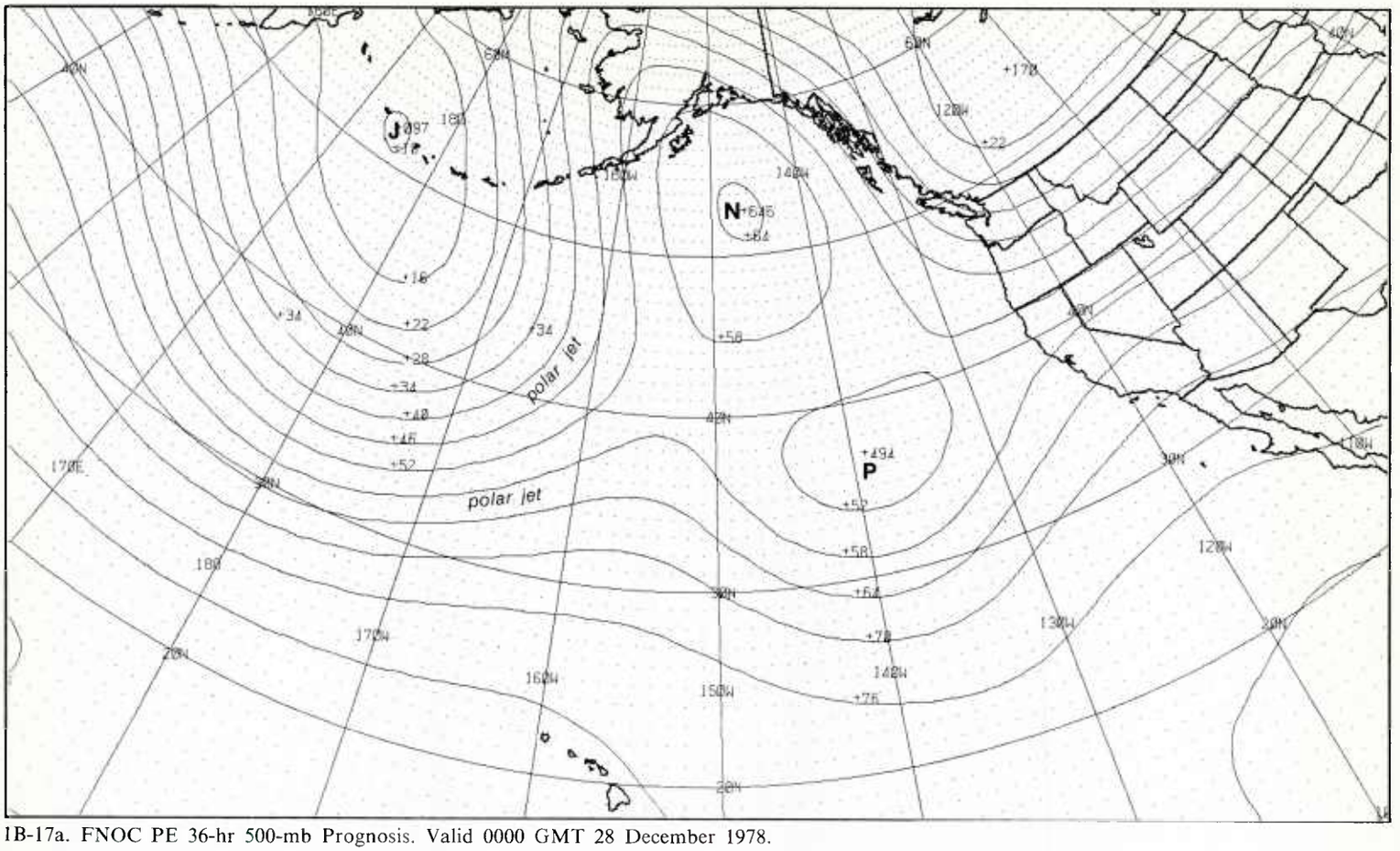

1B-17a. FNOC PE 36-hr 500-mb Prognosis. Valid 0000 GMT 28 December 1978.

surface

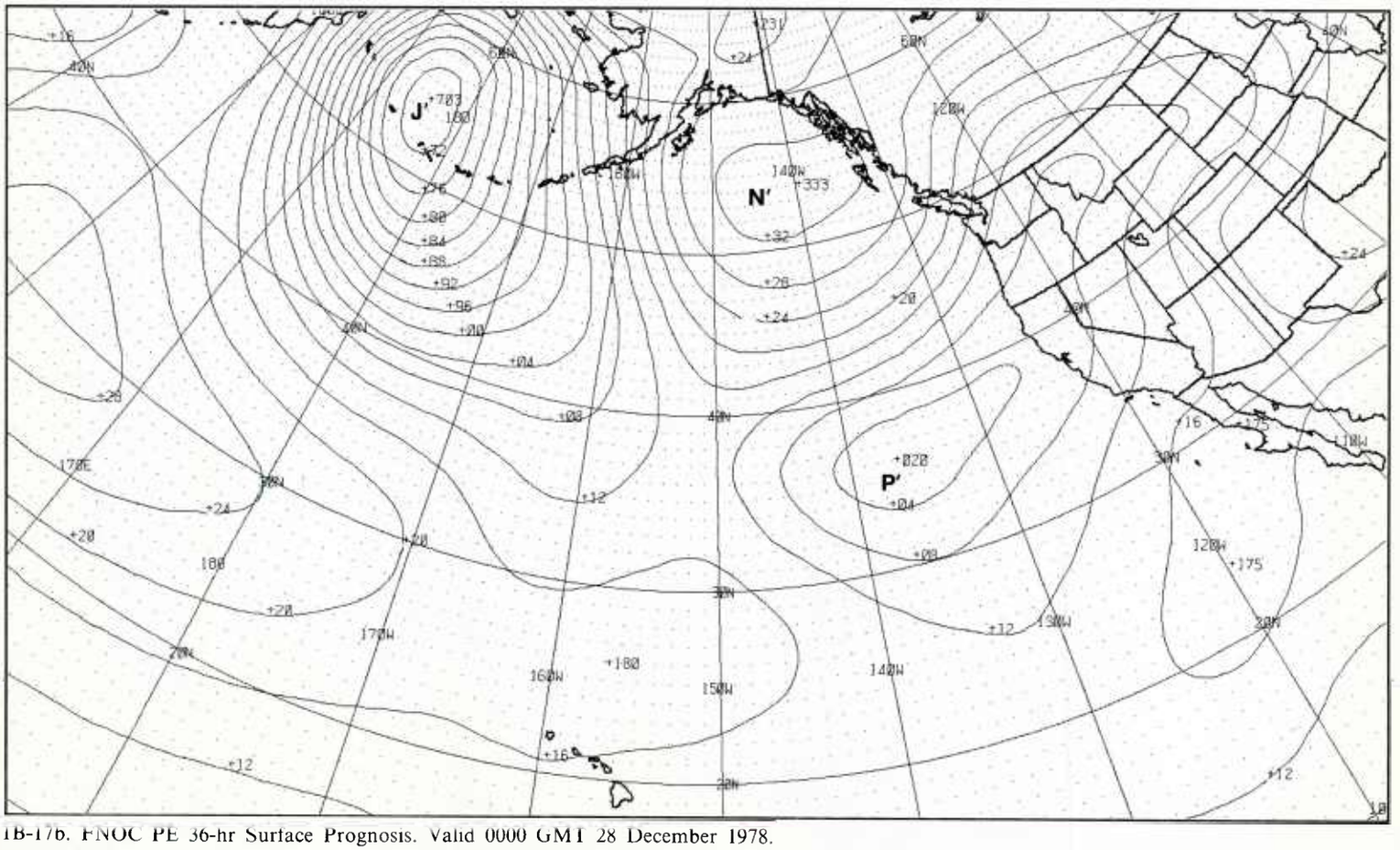

1B-17b. FNOC PE 36-hr Surface Prognosis. Valid 0000 GMT 28 December 1978.

Blocking is Established over the Eastern Pacific

Blocking is Established over the Eastern Pacific

Characteristic Features

1. *Development of a high-amplitude warm ridge over the eastern Pacific.*
2. *Deep cold lows upstream and downstream of the ridge.*
3. *A split in the mid-latitude polar jet upstream of the ridge: one branch passing poleward of the ridge and the other passing equatorward.*

28 December

At 500 mb (1B-18b), strong warm air advection in advance of the intense low **J** has resulted in the development of a broad, high-amplitude blocking ridge **M–N** over the eastern Pacific. Deep cold lows **J** and **O** are observed upstream and downstream of the ridge. At 300 mb (1B-18a), a distinct split in the mid-latitude polar jet is maintained near 40° N, 160° W. The northern branch curves sharply around the blocking ridge, and the southern branch swings to the south where it merges with the subtropical jet.

Note that the blocking pattern of a closed 500-mb anticyclone at high latitudes over the eastern Pacific with a cut-off low to the south did not develop as forecast. The reason for the observed difference is that the strong warm air advection in advance of the intense low **J** has caused the ridge **M** to build northward and to merge with the ridge **N** to form a blocking ridge **M–N** from mid latitudes to the arctic (compare 500-mb analyses 1B-14b and 1B-18b). As the blocking ridge **M–N** develops, the two lows **A** and **I** observed on the previous 500-mb analysis (1B-14b) are forced eastward by the ridge and merge into a single low. The result is the low **P** on the east side of the blocking ridge (1B-18b) instead of the cut-off low trapped to the south of the block, as forecast (1B-17a). At the surface (1B-19b), the merged storms **A′** and **I′** appear as a single low center **P′** in which an "instant occlusion" is depicted.

In the satellite picture (1B-19a), the distinct comma cloud **P″** over the eastern Pacific has developed in the new low on the east side of the blocking ridge and is the basis for the surface analysis showing an "instant occlusion" at the surface. This system is located in the vicinity of the left front quadrant of a jet streak **PJS** at 300 mb (1B-18a), a very favorable cyclogenetic region. There is a sharp, anticyclonically-curved, subtropical jet cirrus deck just to the south of the comma cloud **P″** on the satellite picture, which identifies the location of the axis of the subtropical jet in this area (just to the north of the sharp boundary of the cirrus deck).

Large-scale meridional (south to north) flow is now observed at 500 mb (1B-18b) along the western border of the blocking ridge **M–N**. In response to this flow aloft, the surface frontal system **J′I** associated with the low **J′** extends from low latitudes to high latitudes in a meridional orientation, as it moves against the blocking ridge. The widely-spaced contour lines at the center of the low indicates that it is in the mature stage. In such cases over oceanic regions, numerous vorticity commas, which indicate cyclogenetic regions, are frequently observed in the polar air stream circulating around the cyclone. Two prominent vorticity centers **Q″** and **R″** are observed on the satellite picture that are reflected in the surface analysis. The vorticity comma **Q″** is carried as a trough line on the surface analysis because of its mature stage of development; the vorticity center **R″** does not show a distinct comma so that there is only a cyclonic curvature in the contours.

Another prominent feature on the surface analysis is the development of the blocking surface high **N′**, as forecast, off the west coast of Canada. This development confirms that the block extends through a deep vertical layer of the atmosphere. In the satellite picture, the presence of the clear area **N″** off the west coast of Canada and the stratiform cloudiness (medium gray shades) over the Gulf of Alaska reveals the lateral extent of this prominent surface high.

An examination of the 500-mb prognosis (1B-20b), based on the initial analysis (1B-20a), shows that the high-amplitude ridge **M–N** over the eastern Pacific is forecast to persist, with no major changes in the associated synoptic circulation features (lows upstream and downstream and a split in the polar jet upstream of the ridge). The persistence of these synoptic features confirms that a high-latitude block has been established over the eastern Pacific. Additional evidence is provided by the DMSP picture (1B-21a) obtained later in the day. Note the sharp meridional orientation of the cloud bands associated with storms that have been forced against the blocking ridge at high latitudes.

continued on page 1B-22

300 mb

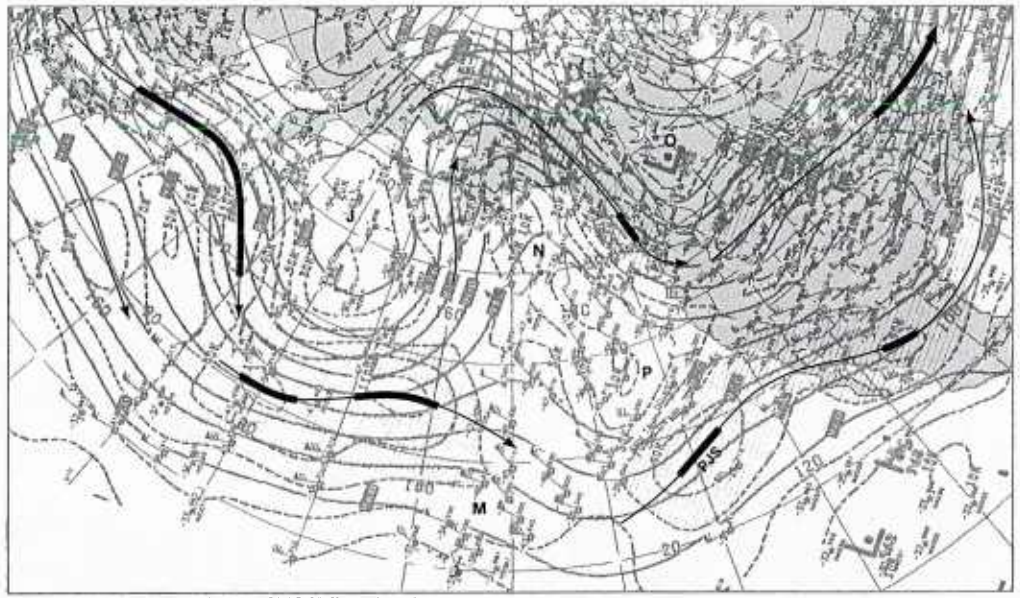

1B-18a. NMC 300-mb Analysis. 0000 GMT 28 December 1978.

500 mb

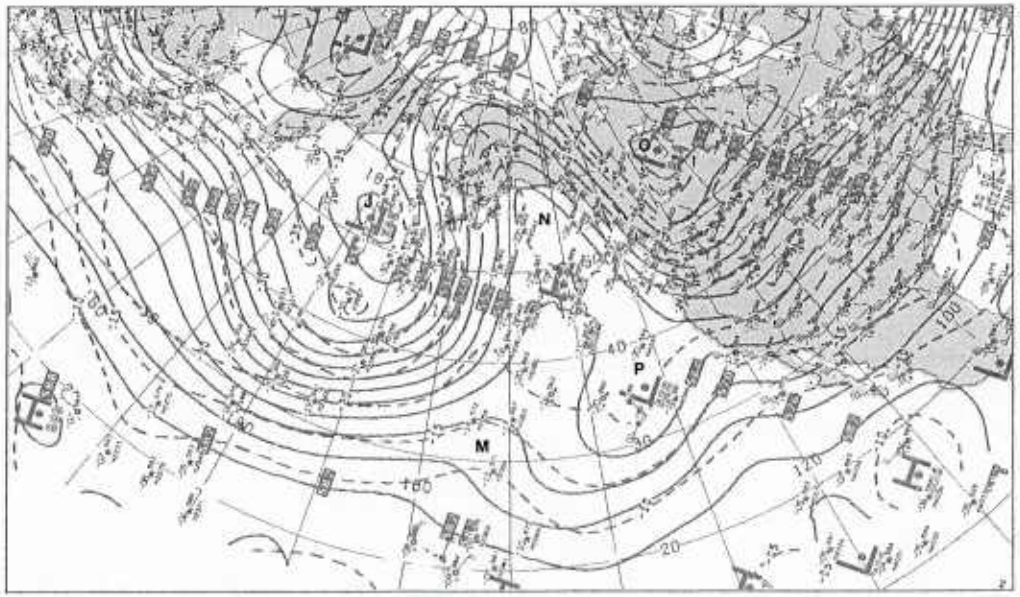

1B-18b. NMC 500-mb Analysis. 0000 GMT 28 December 1978.

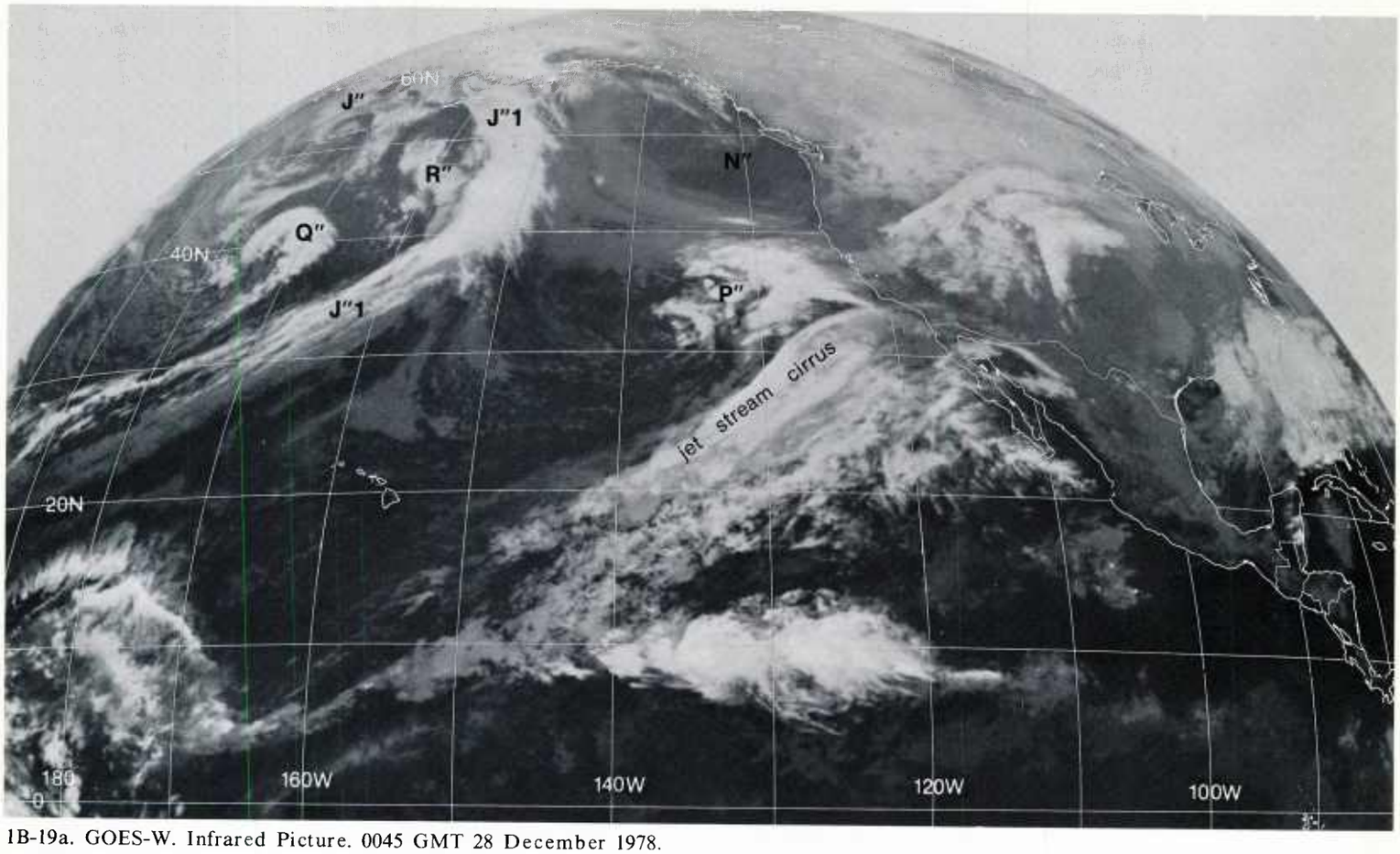

1B-19a. GOES-W. Infrared Picture. 0045 GMT 28 December 1978.

surface

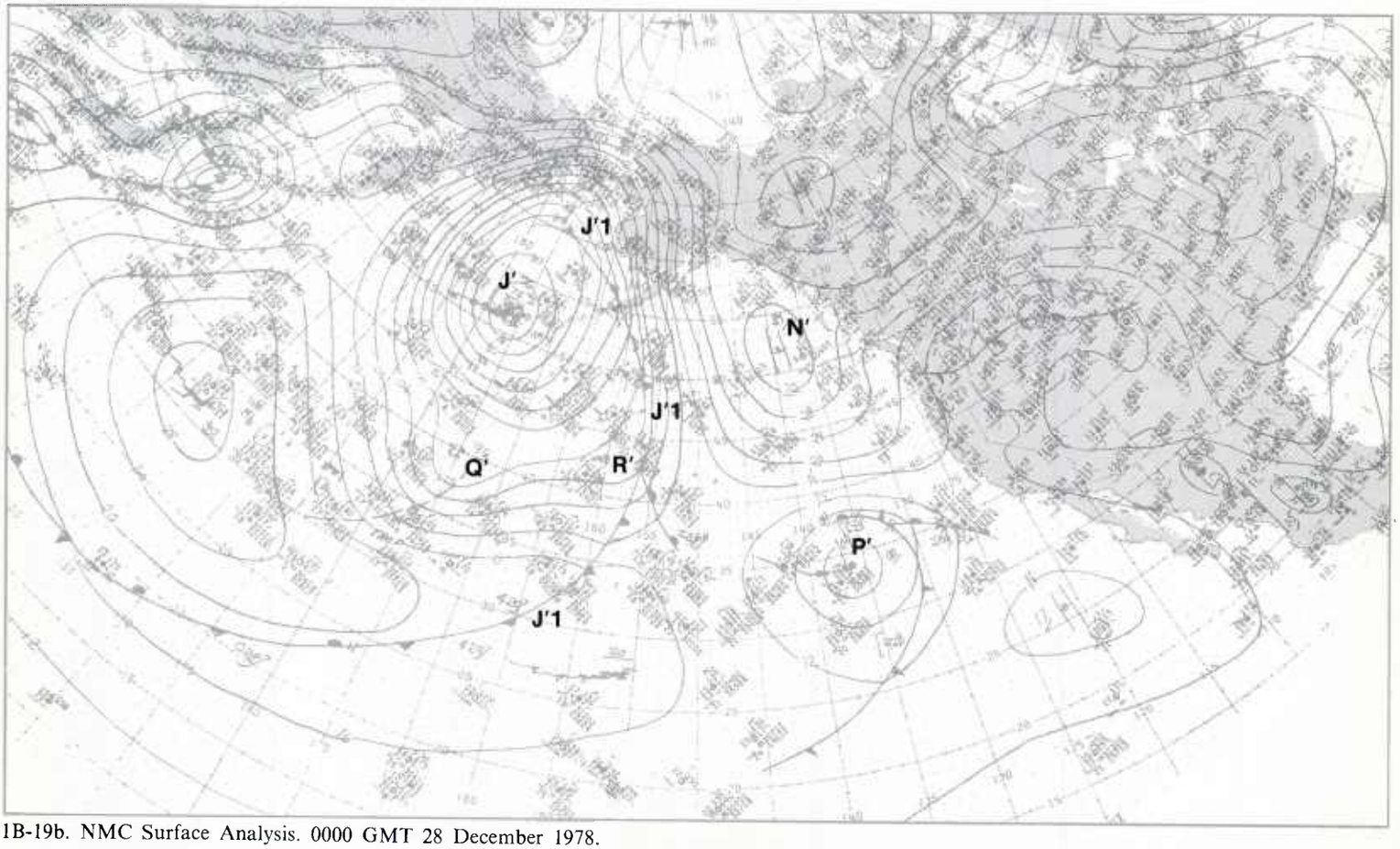

1B-19b. NMC Surface Analysis. 0000 GMT 28 December 1978.

500 mb

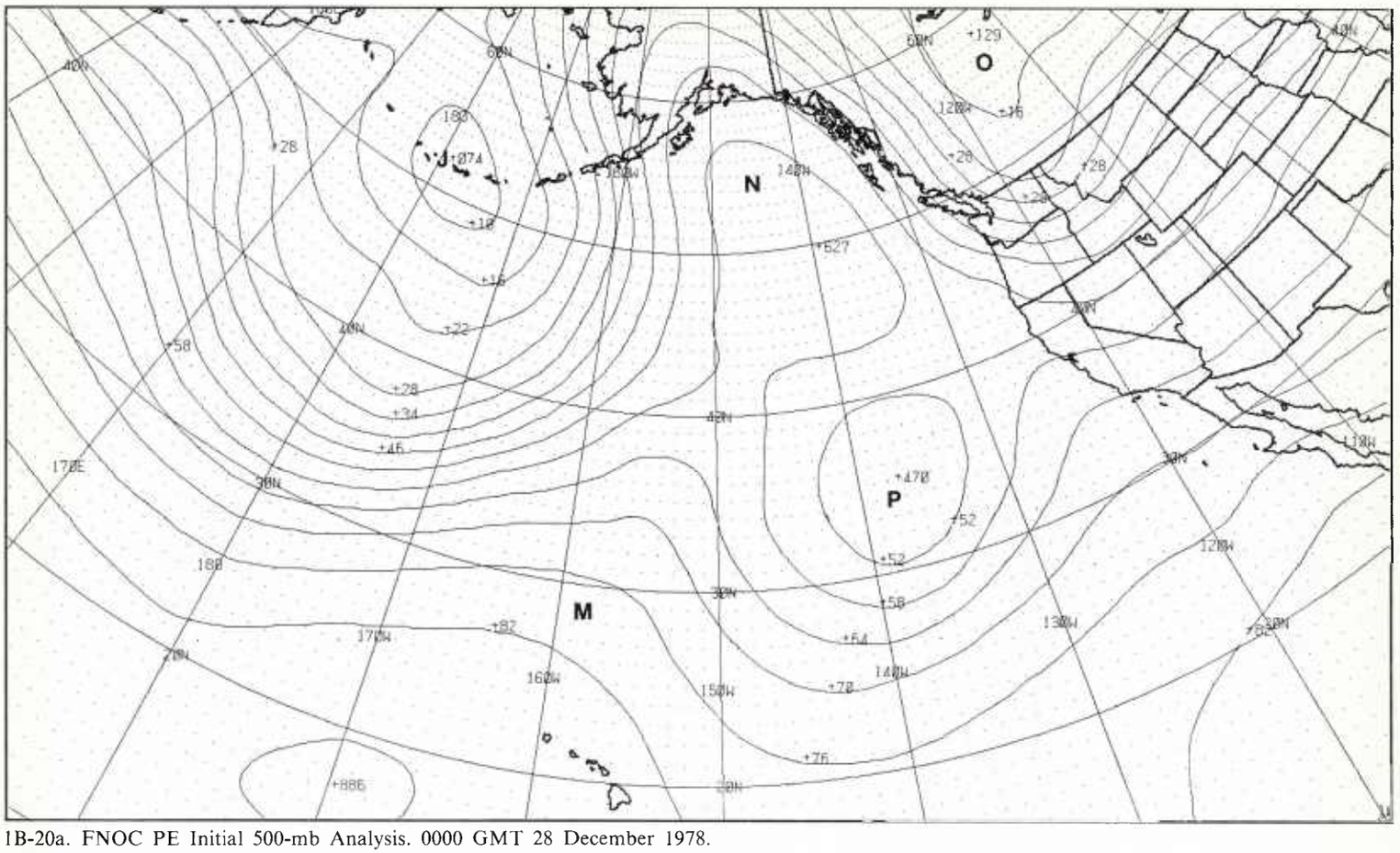

1B-20a. FNOC PE Initial 500-mb Analysis. 0000 GMT 28 December 1978.

500 mb

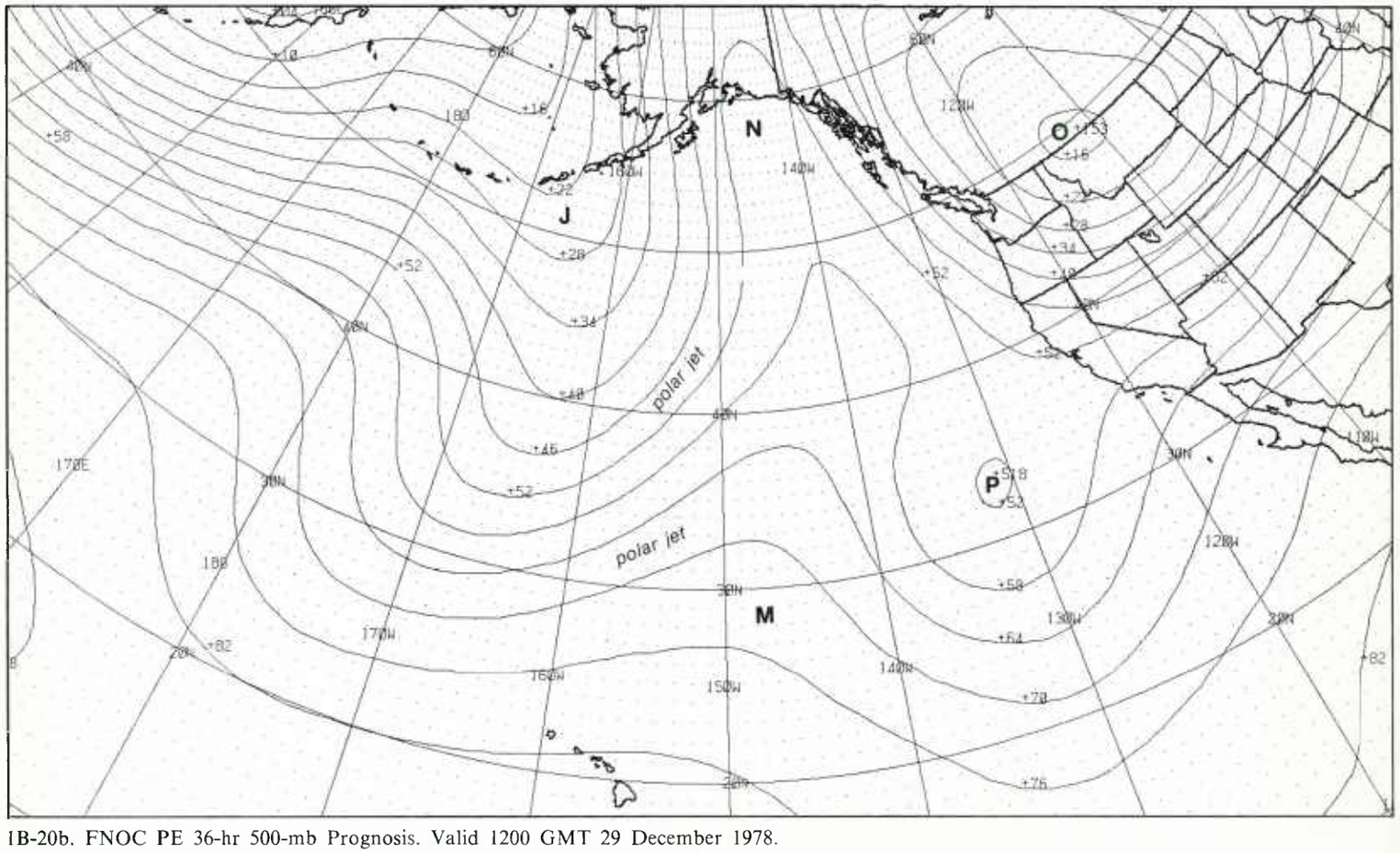

1B-20b. FNOC PE 36-hr 500-mb Prognosis. Valid 1200 GMT 29 December 1978.

Blocking is Established over the Eastern Pacific

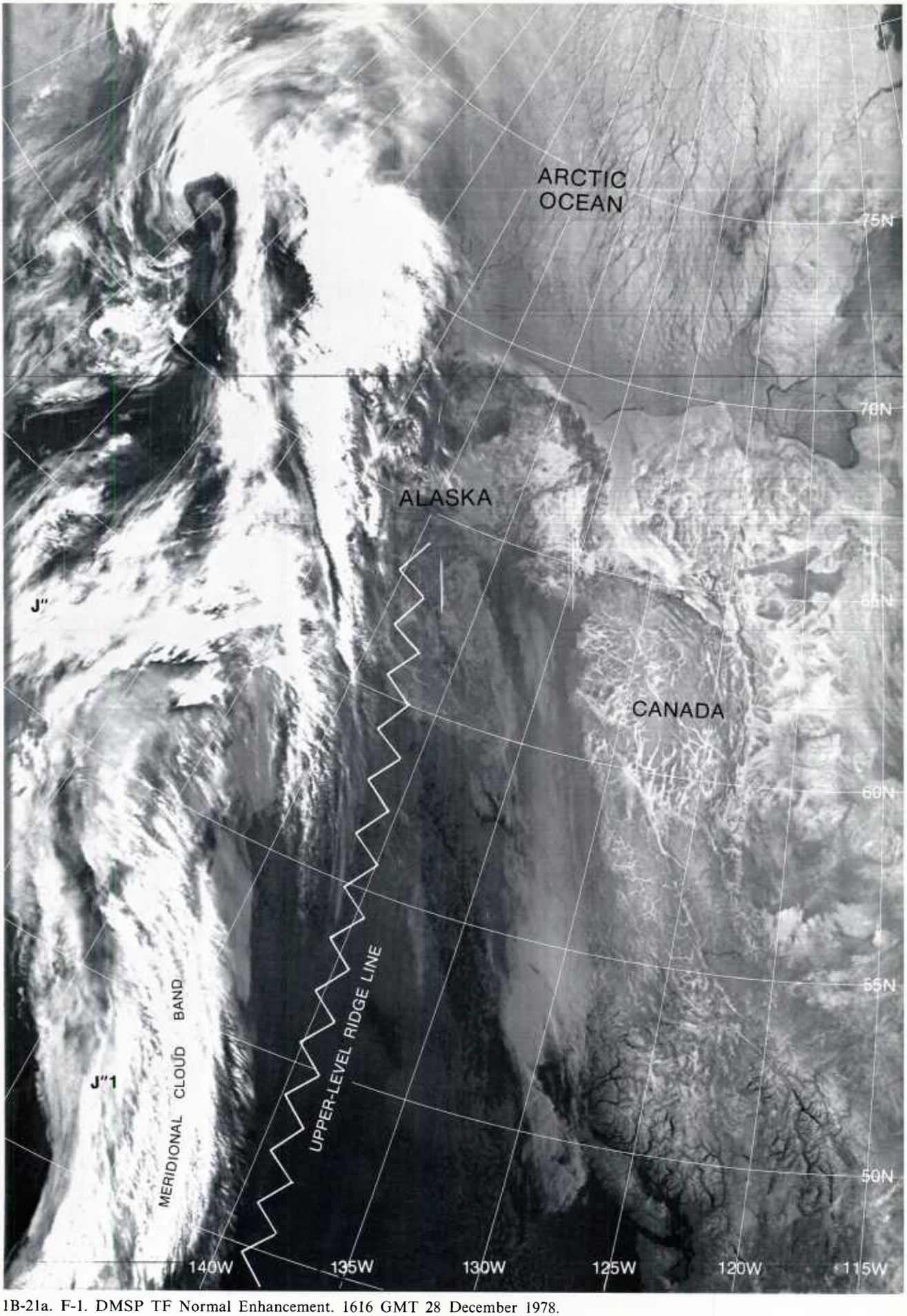

1B-21a. F-1. DMSP TF Normal Enhancement. 1616 GMT 28 December 1978.

Blocking Action: Early Phase

Blocking Action: Early Phase

Characteristic Features

1. *Blocking ridge persists from mid to high latitudes over the eastern Pacific.*
2. *Eastward moving cyclonic disturbances in the westerlies at mid latitudes dissipate against the blocking ridge.*
3. *As cyclones move into the blocking zone, the associated frontal cloud bands become meridionally oriented along the western boundary of the blocking ridge.*

29 December

The contour pattern on the 500-mb analysis (1B-22b) shows a pronounced blocking ridge **M–N** along 140° W. The low **O** has intensified downstream of the block, and the deep low **J** observed upstream of the block 36 hours earlier (1B-18b) has become a sharp, elongated cold trough as it moves against the blocking ridge. The jet stream analysis at 300 mb (1B-22a) shows a split in the polar jet in the vicinity of 35° N, 155° W; however, the jet streaks are weak. The strongest jet streak appears at mid latitudes over the west-central Pacific accompanying a new vigorous low **R**.

A most obvious effect of blocking over the eastern Pacific is the dissipation of eastward moving cyclones as they move against the block. In the satellite picture (1B-23a), the cloudy area **J″1** just off the U.S. west coast was a vigorous frontal system 36 hours earlier (1B-19a and 19b). It has a fragmented appearance and is dissipating as it advances into the block at 500 mb—a very graphic example of blocking action. The following vortex **Q″** and frontal system **Q″1** has developed from a vorticity comma cloud observed 36 hours before at 40° N, 175° W (1B-19a). As the cyclone advances into the blocking zone, the associated frontal cloud band **Q″1** has become meridionally oriented against the western boundary of the blocking ridge at 500 mb. Although the satellite picture shows distinct convective activity along the frontal band, this system has weakened significantly as shown on the surface analysis (1B-23b). Note that the two dissipating frontal systems **J′1** and **Q′1** have become meridionally elongated against the western boundary of the blocking high at the surface. This is characteristic of blocking action at that level.

On the east side of the block the 500-mb low **P** remains active as it advances toward the West Coast. There is a closed surface low **P′** (1B-23b), and the satellite picture (1B-23a) shows a distinct comma pattern **P″** with sharp edges—an indication that an active frontal band is approaching the Lower California coastline.

A new, vigorous surface low **R′** has developed upstream of the blocked surface lows over the eastern Pacific. Only a broad meridional frontal cloud band **R″1** is observed in the satellite picture due to the angle of view from the GOES-West satellite. This low has strong upper-level support—a sharp cold trough aloft **R** at 500 mb and an intense jet streak (150 kt) at 300 mb.

During the next 36 hours, the low **J** on the initial 500-mb analysis (1B-24a) weakens as it is forced against the blocking ridge **M–N** over the eastern Pacific (1B-25a), and a deep meridional trough is forecast along the western boundary of the block, extending from Hawaii to the Gulf of Alaska. Upstream of the meridional trough, the low **R** is forecast to deepen significantly as it advances over the eastern Bering Sea.

The most significant circulation feature at the surface is the persistence of the blocking high **M′–N′** along the west coast of the U.S. and Canada. This high will preclude the advance into the U.S. of any surface storms at mid latitudes over the eastern Pacific. A comparison of the initial surface analysis (1B-24b) and the 36-hour prognosis (1B-25b) shows that the eastward moving low pressure system **Q′** over the east-central Pacific will weaken as it becomes trapped against the blocking high. Note that surface low **P′** weakens as it moves inland. Over the northwest Pacific, cyclone **R′** will continue to deepen as it moves on a northeasterly track.

continued on page 1B-26

300 mb

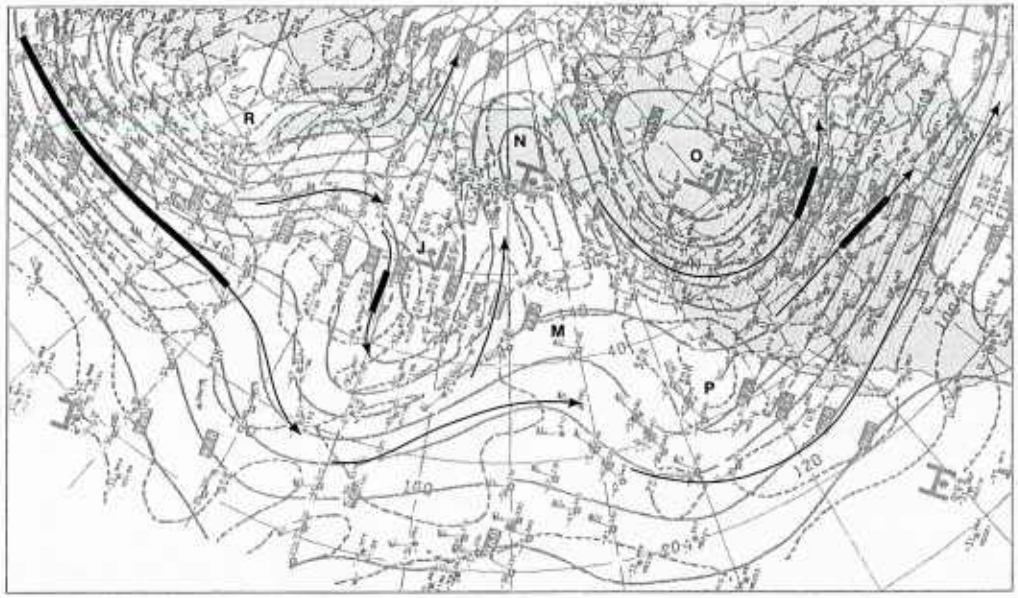

1B-22a. NMC 300-mb Analysis. 1200 GMT 29 December 1978.

500 mb

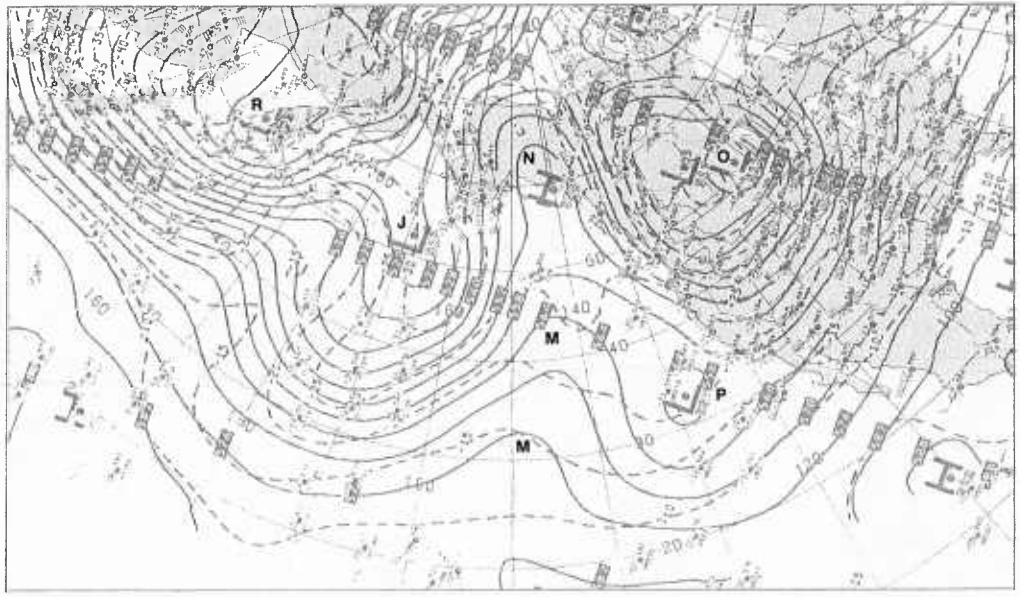

1B-22b. NMC 500-mb Analysis. 1200 GMT 29 December 1978.

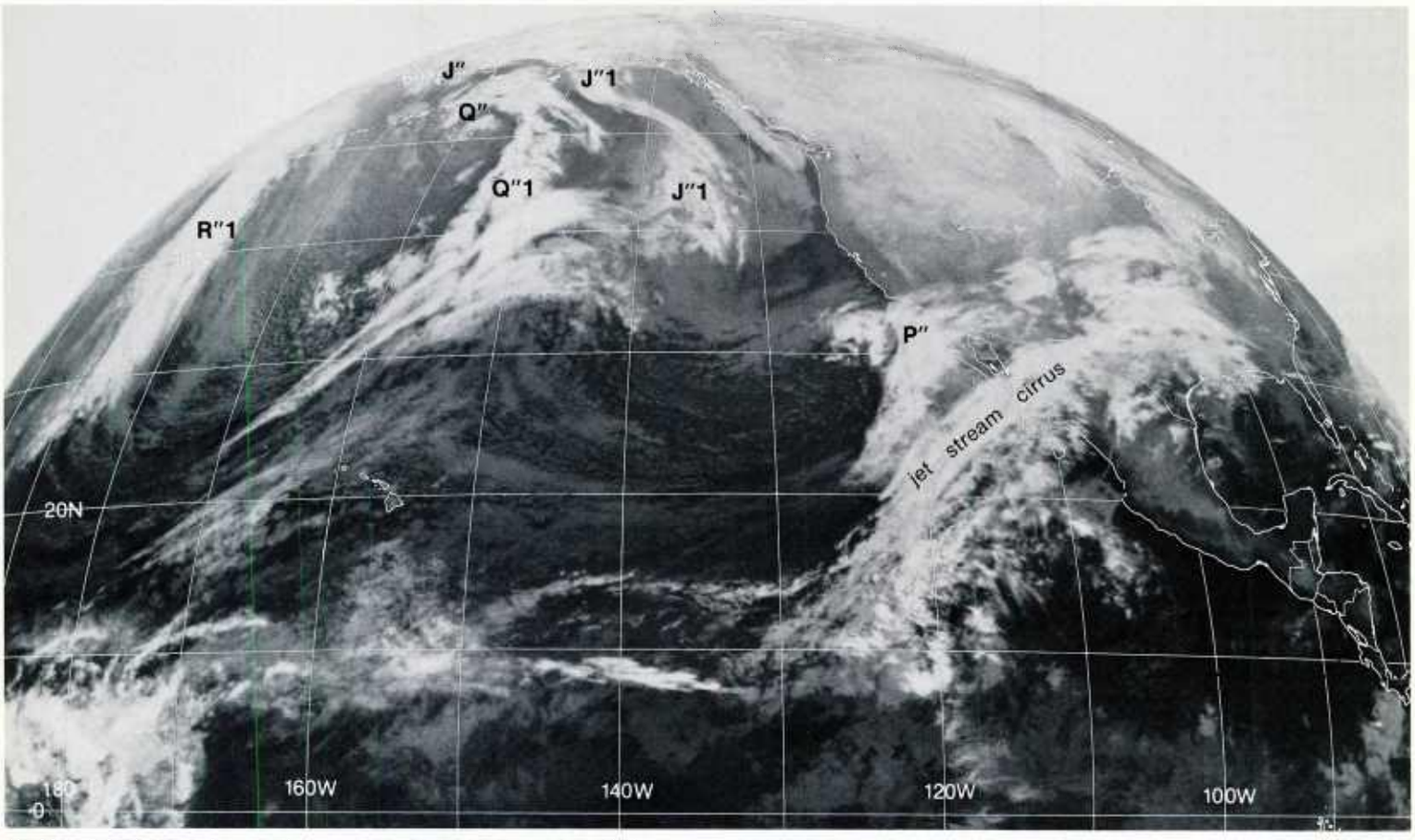

1B-23a. GOES-W. Infrared Picture. 1215 GMT 29 December 1978.

surface

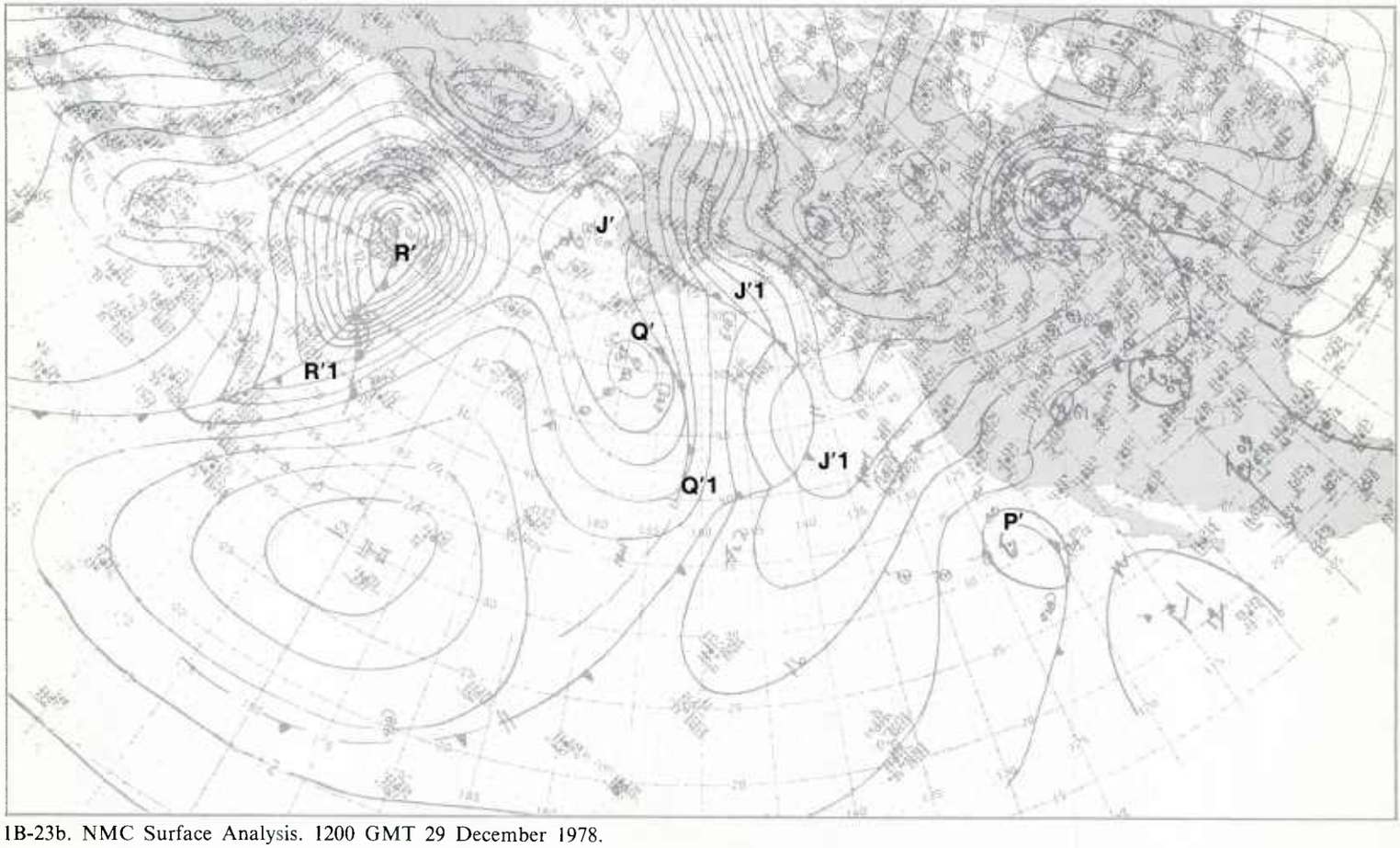

1B-23b. NMC Surface Analysis. 1200 GMT 29 December 1978.

500 mb

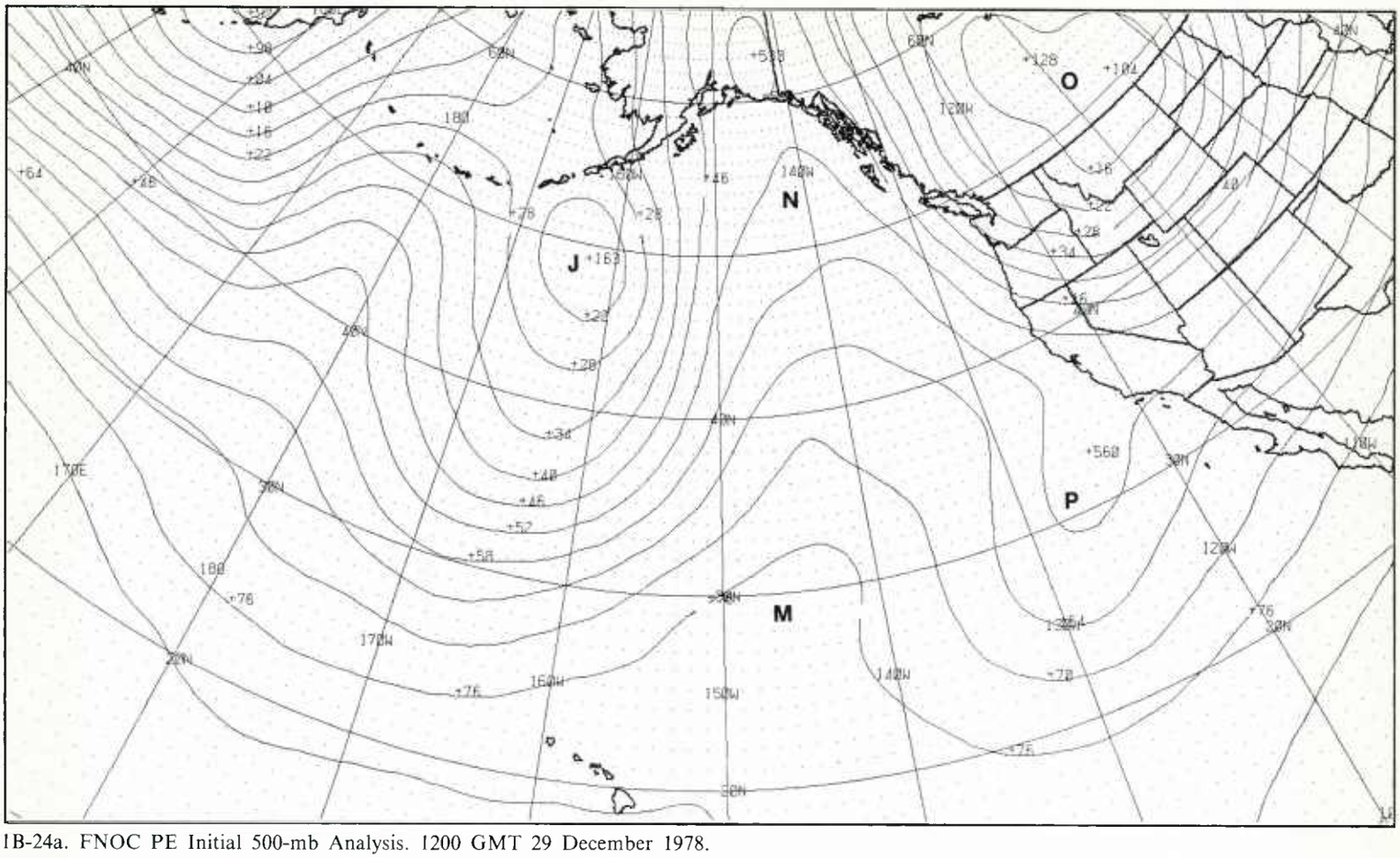

1B-24a. FNOC PE Initial 500-mb Analysis. 1200 GMT 29 December 1978.

surface

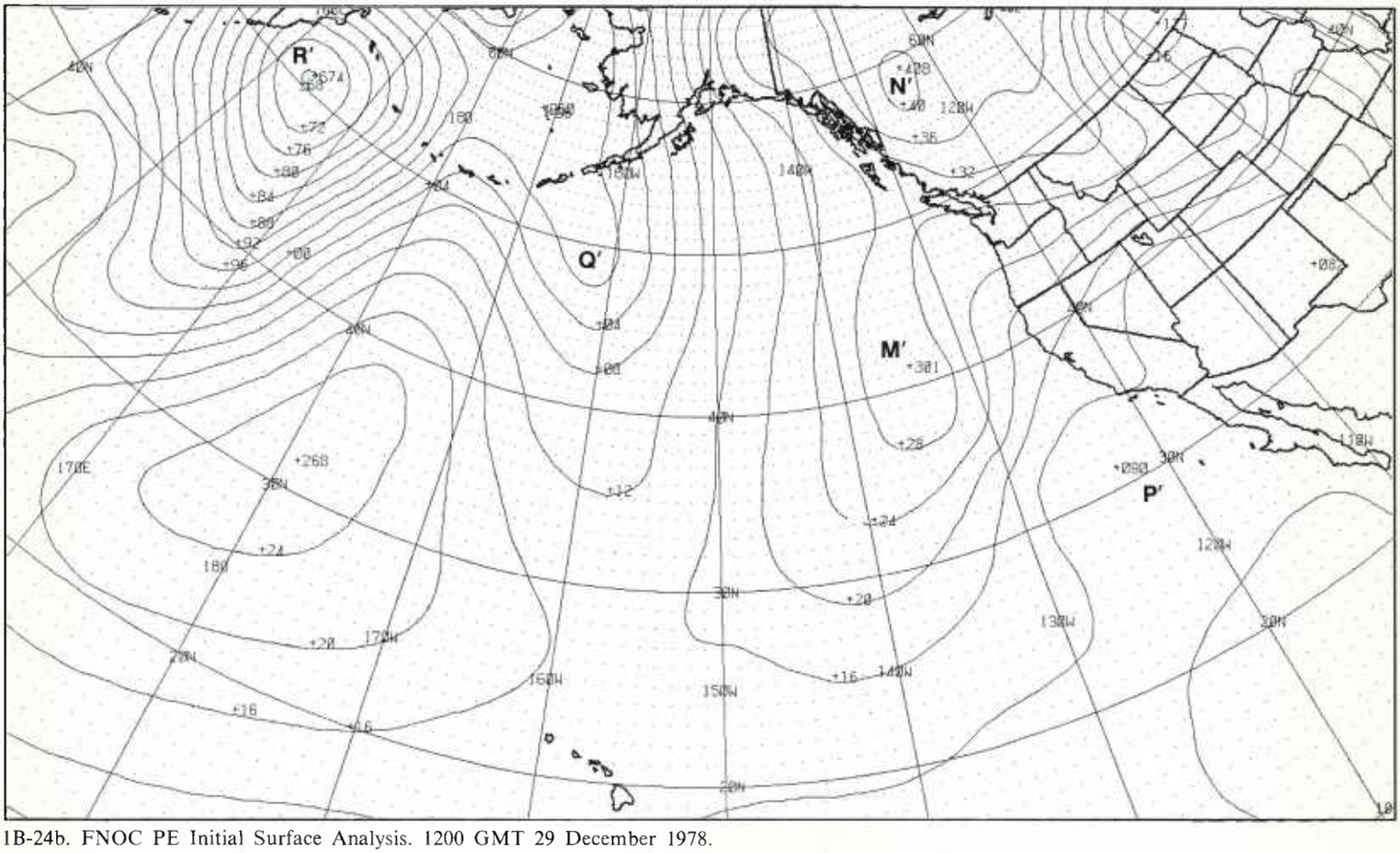

1B-24b. FNOC PE Initial Surface Analysis. 1200 GMT 29 December 1978.

500 mb

Blocking Action: Early Phase

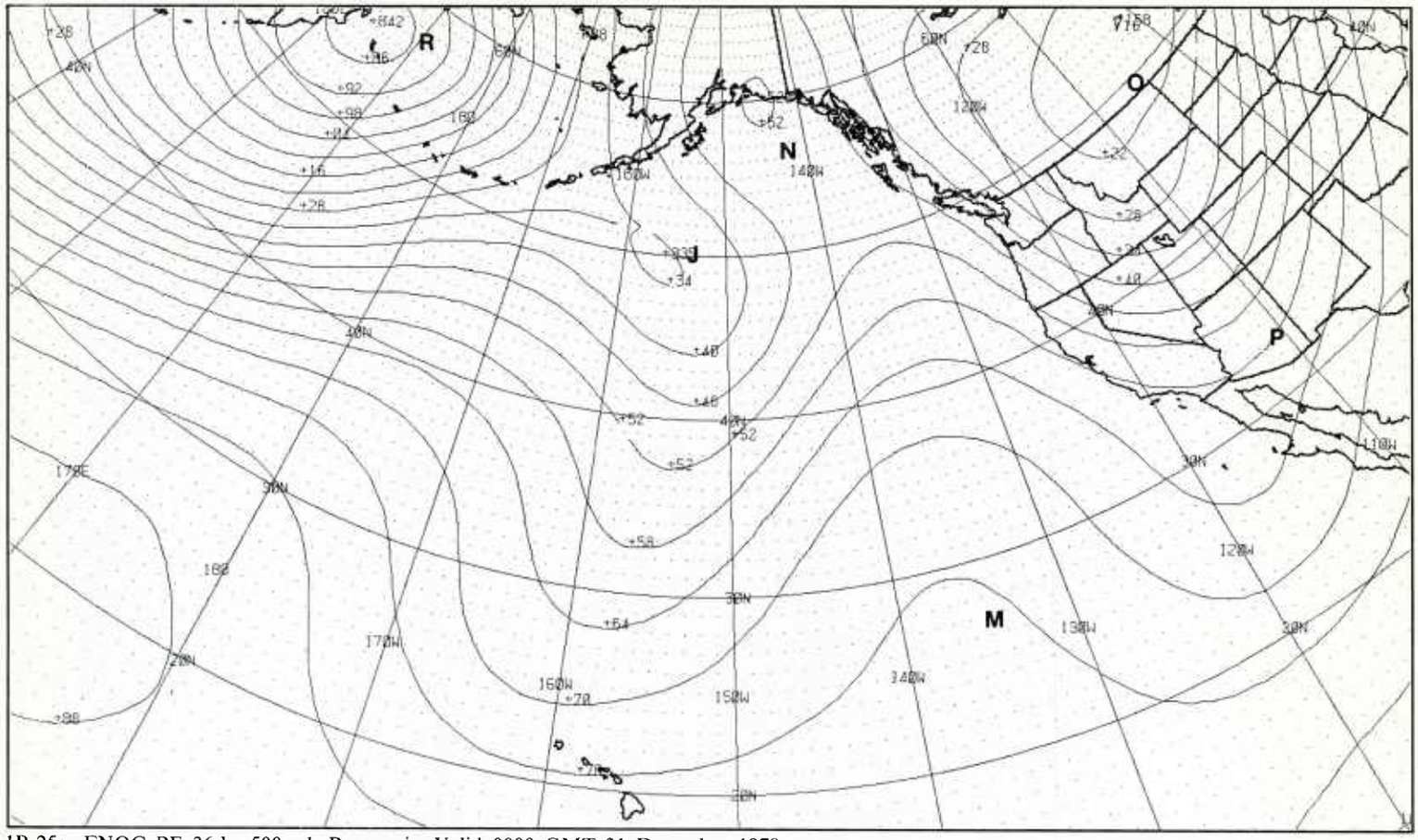

1B-25a. FNOC PE 36-hr 500-mb Prognosis. Valid 0000 GMT 31 December 1978.

surface

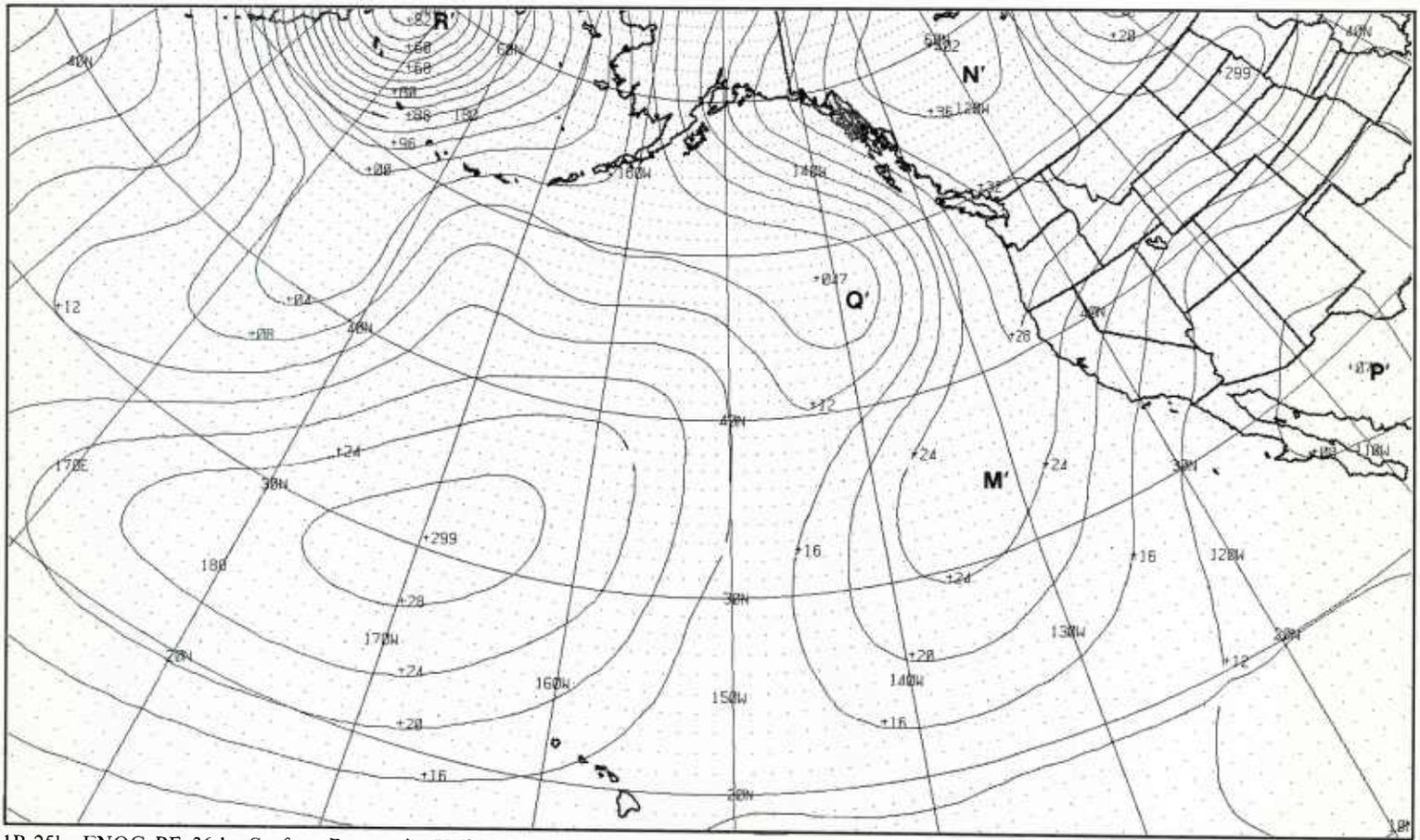

1B-25b. FNOC PE 36-hr Surface Prognosis. Valid 0000 GMT 31 December 1978.

31 December

The jet stream analysis at 300 mb (1B-26a) clearly reveals the extent of the disruption of the zonal westerlies at mid latitudes by the blocking ridge over the eastern Pacific. Within the blocking zone at mid latitudes there is no regular pattern to the jet streak segments: jet streak **PJS-1** is oriented south-north, jet streak **PJS-2** is oriented northwest-southeast, and jet streak **PJS-3** is oriented southwest-northeast. Upstream of the block, a multiple jet structure is observed. Similarly, downstream of the block, over North America, a multiple jet structure can be identified. There is no continuous zonal westerly band across the Pacific and North America—only a series of discontinuous jet stream segments.

At 500 mb (1B-26b), the blocking ridge **M–N** extends from a closed anticyclone at low latitudes to the arctic. The cold lows **R** and **O** upstream and downstream of the block have deepened and show strong jet streak circulations—evidence of pronounced baroclinic zones for cyclogenetic developments. A new low **S** has developed at the base of the trough of the low **J** due to strong cold air advection to the rear of the trough.

At the surface (1B-27b), a storm **S′** has developed under the new low **S** aloft; the presence of jet streaks **PJS-2** and **PJS-3** at 300 mb indicates strong upper-level support for this system. This storm is forced against the blocking ridge **M–N**, as have the previous surface storms **J′** and **Q′**. The storm **J′** has dissipated against the block and storm **Q′** shows only a weak front at the surface. To the east of the block, storm **P′** remains active as it advances across the southern U.S. and northern Mexico.

The satellite picture (1B-27a) shows the classic meridional orientation of the vortex cloud systems **Q″** and **S″** of the two surface storms **Q′** and **S′** whose eastward progress has been blocked. The frontal cloud bands associated with these storms assume a meridional orientation as the cyclones are forced against the western boundary of the blocking ridge. Note the bright, anticyclonically-curved, jet-associated cirrus cloud deck to the south of cloud vortex **S″**. The bright vortex cloud pattern **P″** (1B-27a) to the east of the block is associated with the surface cyclone **P′**. Convective activity has increased in this system as the 500-mb low **P** merges with the flow along the eastern boundary of the blocking ridge.

Upstream of the block the weak frontal cloud band **R″1** is the remnants of the front **R′1** moving into the blocking zone at the surface. The two vorticity comma clouds **T″** and **U″** are incipient storms developing over the west-central Pacific. These disturbances are being steered by the mid-latitude westerlies (500 mb) toward the blocking zone over the eastern Pacific.

The 36-hour 500-mb prognoses have been very useful for forecasting the overall large synoptic-scale patterns associated with the onset and the development of the blocking event over the eastern Pacific. Now that the block is in place, useful estimates of the duration of the blocking event can be obtained from a consideration of the 36- and 72-hour 500-mb prognoses.

31 December continued on page 1B-29

300 mb **31 December**

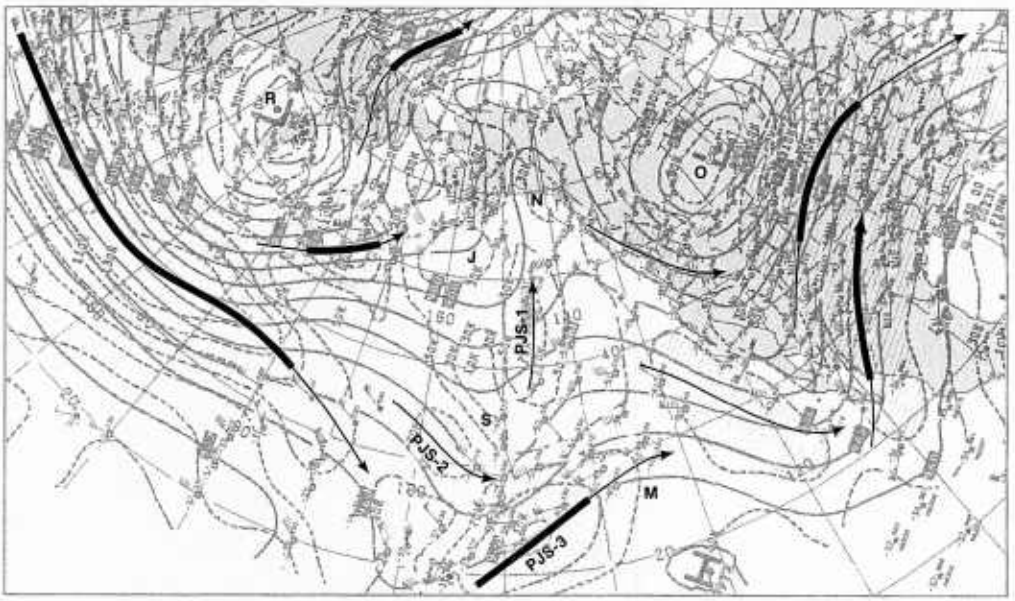

1B-26a. NMC 300-mb Analysis. 0000 GMT 31 December 1978.

500 mb

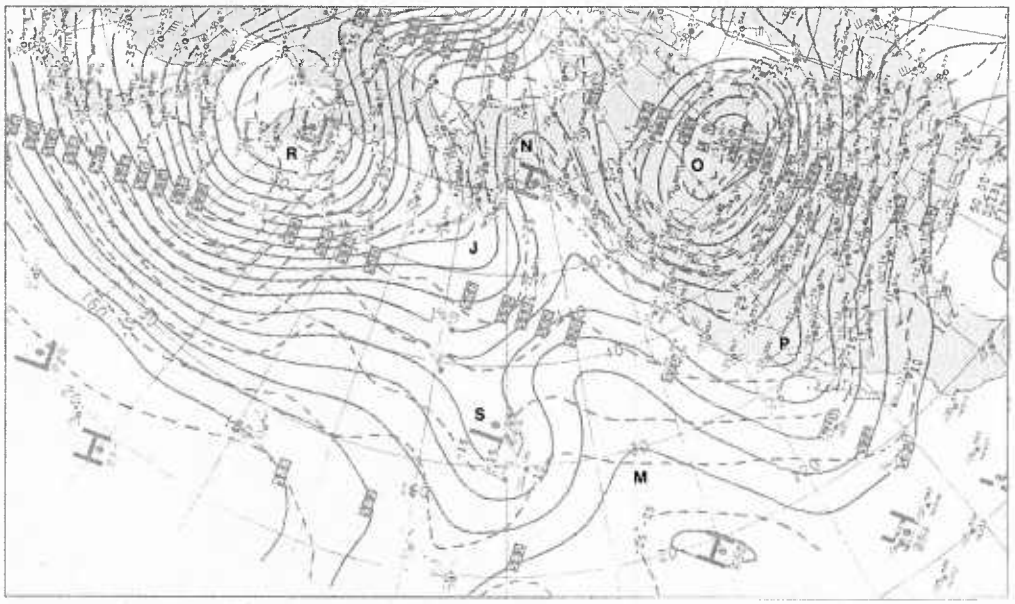

1B-26b. NMC 500-mb Analysis. 0000 GMT 31 December 1978.

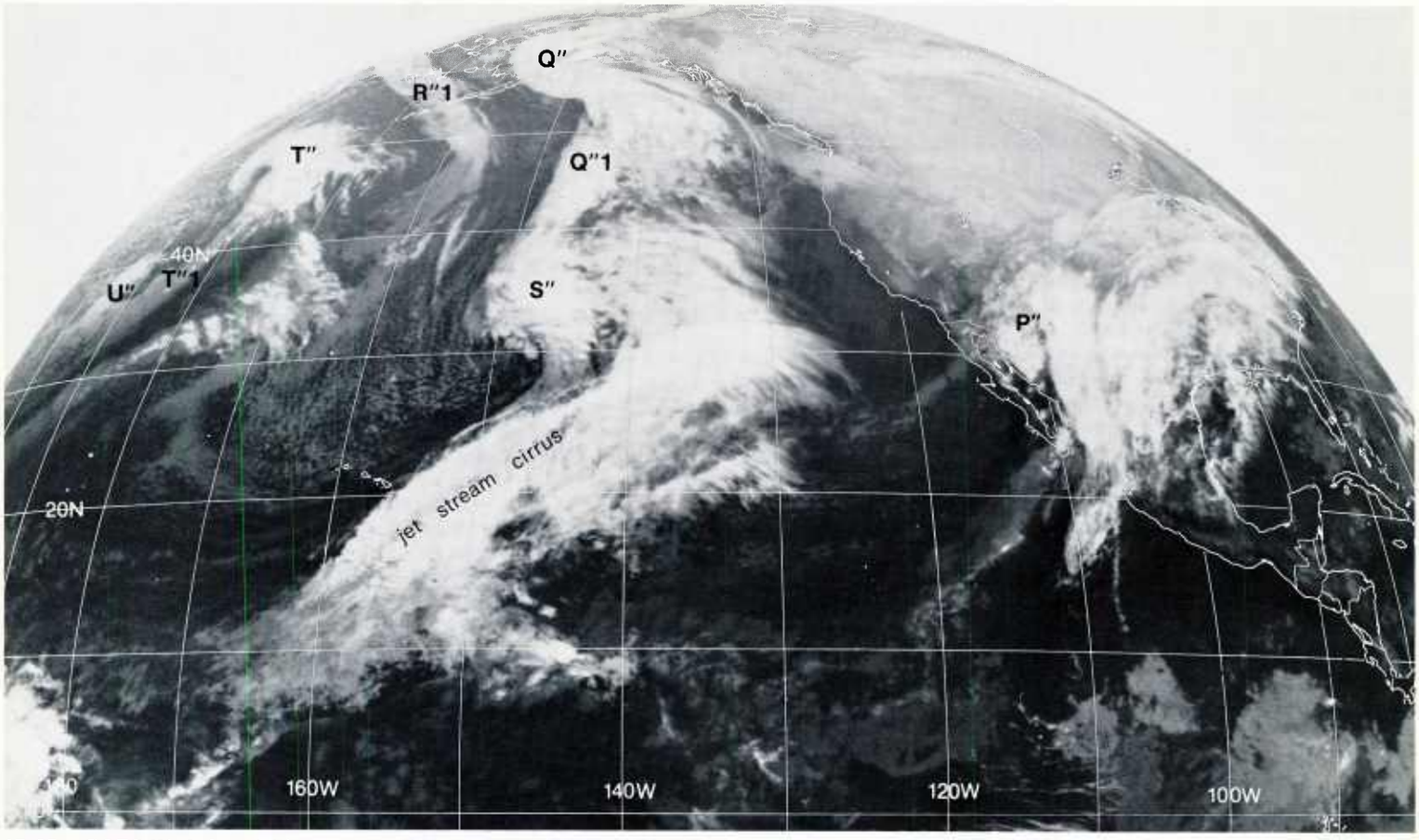

1B-27a. GOES-W. Infrared Picture. 0015 GMT 31 December 1978.

surface

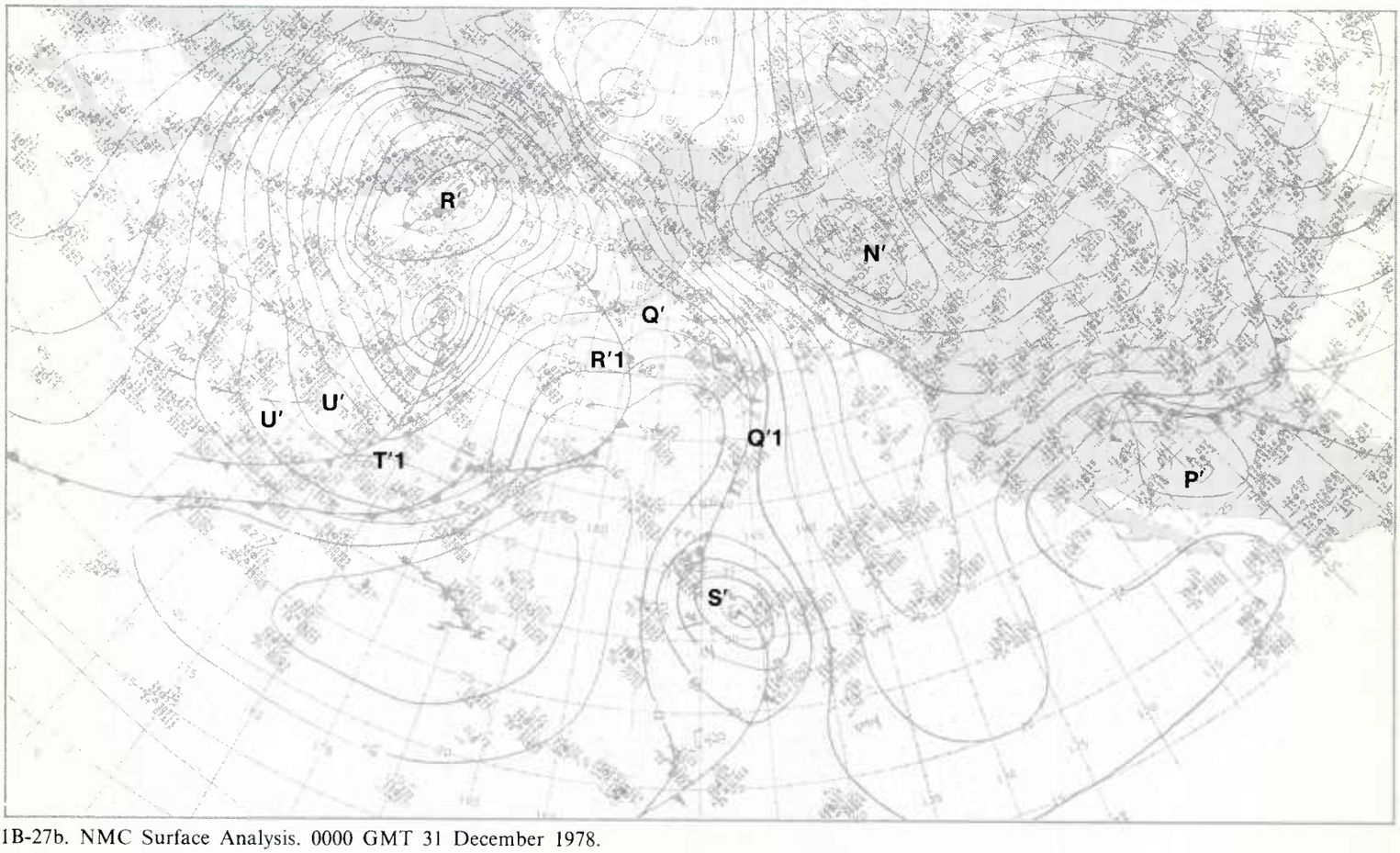

1B-27b. NMC Surface Analysis. 0000 GMT 31 December 1978.

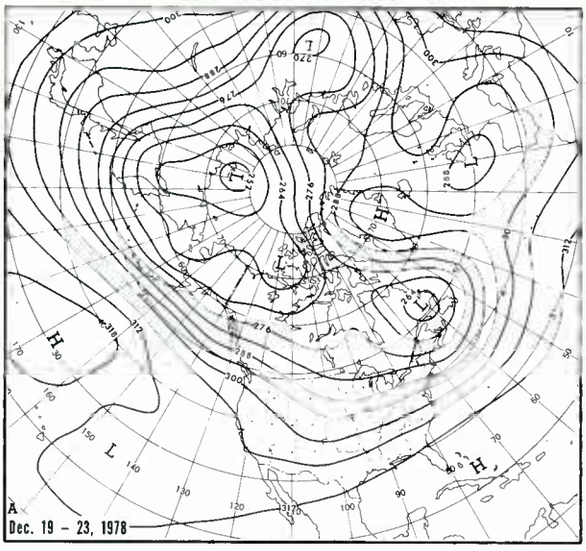

1B-28a. Mean 700-mb Contours for 19–23 December 1978. (After Taubensee, 1979.)

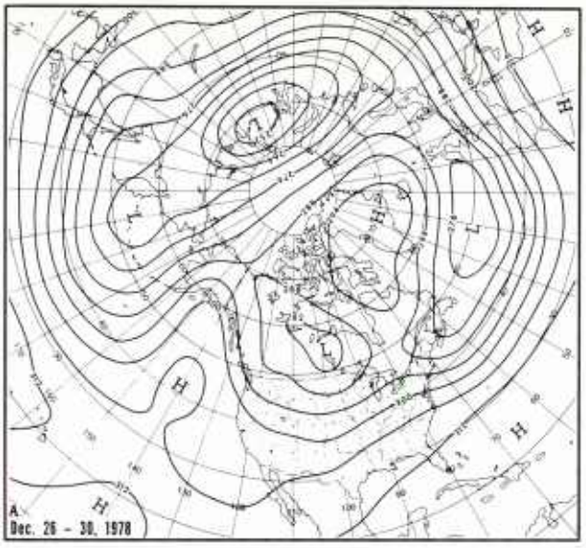

1B-28b. Mean 700-mb Contours for 26–30 December 1978. (After Taubensee, 1979.)

500 mb

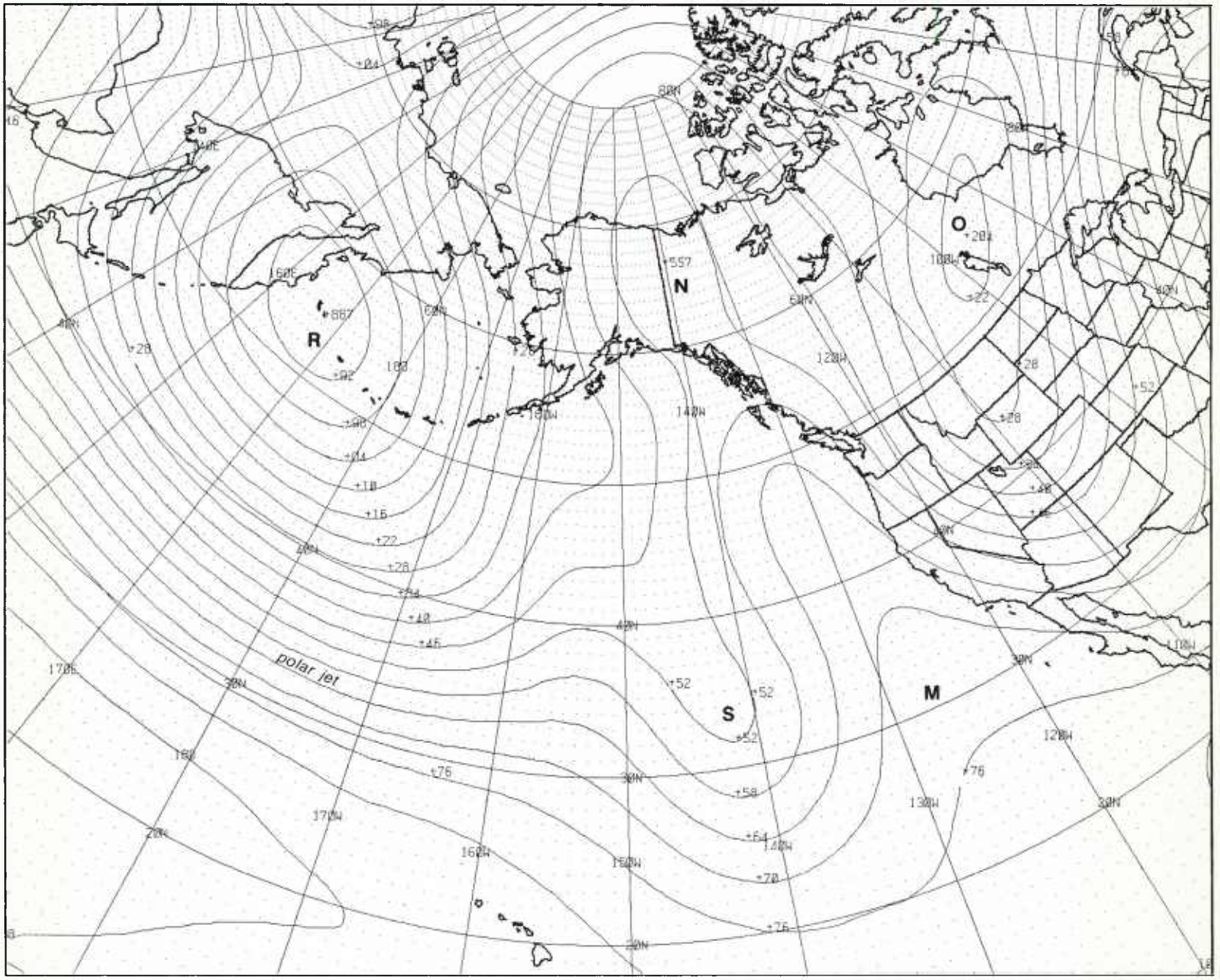

1B-28c. FNOC PE 36-hr 500-mb Prognosis. Valid 1200 GMT 1 January 1979.

Blocking Action: Early Phase

The 500-mb prognoses (1B-28c and 29a) show that the block over the eastern Pacific will persist for an additional 72 hours—a very formidable block to eastward moving disturbances in the westerlies. During the early forecast period, strong polar westerlies (tight contour gradient) are observed upstream from the block. By the end of the forecast period (1B-29a), the polar westerlies have penetrated into low latitudes over the eastern Pacific, which forces a southeast-northwest tilt in the blocking pattern.

continued on page 1B-30

A comparison of the mean 700-mb contours over the eastern Pacific for the week prior to the block (1B-28a), with the mean 700-mb contours for the week of the development of the block (1B-28b), provides graphic evidence of the significant change in the flow pattern over the eastern Pacific. Prior to the block, disturbances in the westerlies could advance rapidly across the eastern Pacific in the zonal flow. During the blocking period, however, this open channel is no longer available for the disturbances.

Reference

Taubensee, R.E., 1979: Weather and circulation of December 1978. *Mon. Wea. Rev.*, **107**, 354–360.

500 mb

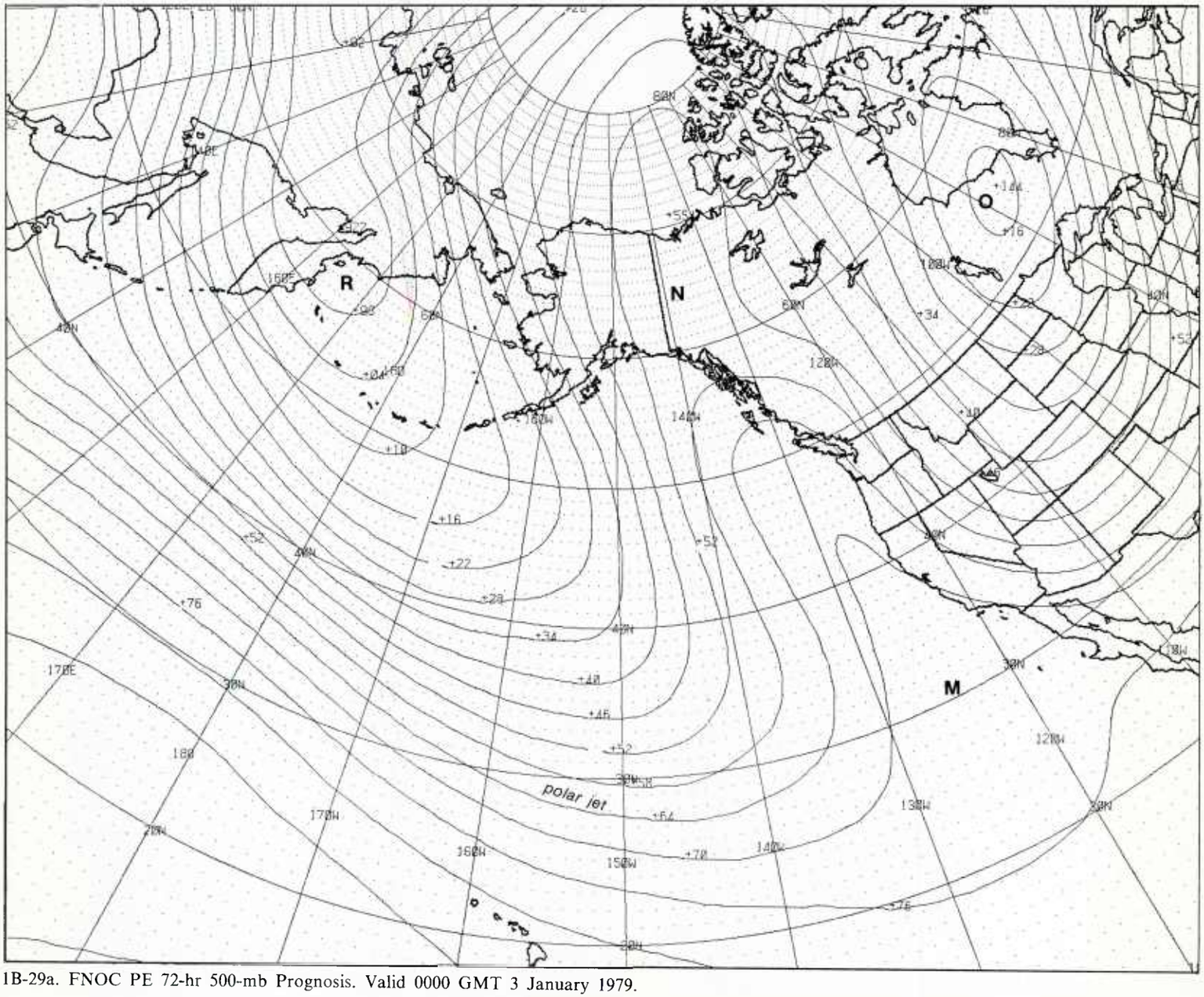

1B-29a. FNOC PE 72-hr 500-mb Prognosis. Valid 0000 GMT 3 January 1979.

1-2 January 1979

On the following four pages, a series of satellite pictures and corresponding 500-mb analyses are presented for a two-day period, at 12-hour intervals. This series illustrates how effectively the blocking ridge over the eastern Pacific obstructs the normal eastward progress of migratory cyclones. In the first satellite picture (1B-30a), the very distinct cloud vortex **S″** over the east-central Pacific is a major oceanic winter storm that has developed rapidly from the vorticity comma **S″** 12 hours earlier (1B-27a).

On the 500-mb analysis (1B-30b), the closed cold low aloft **S** associated with this system indicates that the storm extends through a deep vertical layer of the atmosphere. During the next 24 hours (1B-31b and 31d), this 500-mb low is steered on an almost due north track by the blocking ridge over the eastern Pacific. The storm **S″** is forced against the blocking ridge and dissipates, as shown by the break-up of the cloud vortex in the corresponding satellite pictures (1B-31a and 31c). A broad, meridional cloud band has developed in the deep baroclinic zone along the western boundary of the blocking ridge **M-N**. The convex cloud protrusions into the cold air along this cloud band are short-wave disturbances moving northward in the strong meridional flow between the 500-mb low and the blocking ridge.

The 500-mb low **S** continues to advance on a northerly track during the following 24 hours (1B-32b and 33b), where this system is identified by a minor waving of the contour lines. Only broken cloud remnants of the primary cloud vortex **S** are observed on the satellite pictures (1B-32a and 33a). The storm has dissipated against the block. This example demonstrates how readily the initiation, development, and dissipation of storms can be followed in the satellite pictures.

A characteristic feature of the block is the split in the polar jet into a northern and a southern branch upstream of the blocking ridge. Cyclonic disturbances developing along the polar jet will therefore take one of two tracks—a northern route or a southern route. In the satellite picture (1B-30a), storms **Q″** and **R″** (1B-30a) are located in the northern branch of the split in the polar westerlies, and they dissipate (1B-31c) against the high-latitude portion **N** of the block (1B-31d). These storms are followed by disturbance **T″** (1B-30a) which also follows the northern route against the block where it also dissipates. Cyclonic disturbance **U″** (1B-30a), however, follows the southern branch of the split polar westerlies. Near the end of this two-day period (1B-33b), a major 500-mb low **U** develops, as the disturbance **U″** moves to the southeast in the strong southern branch of the split in the polar westerlies. Short black line segments on the 500-mb analysis (1B-33b) indicate the northern and southern branches, respectively, of the polar jet stream.

continued on page 1B-34

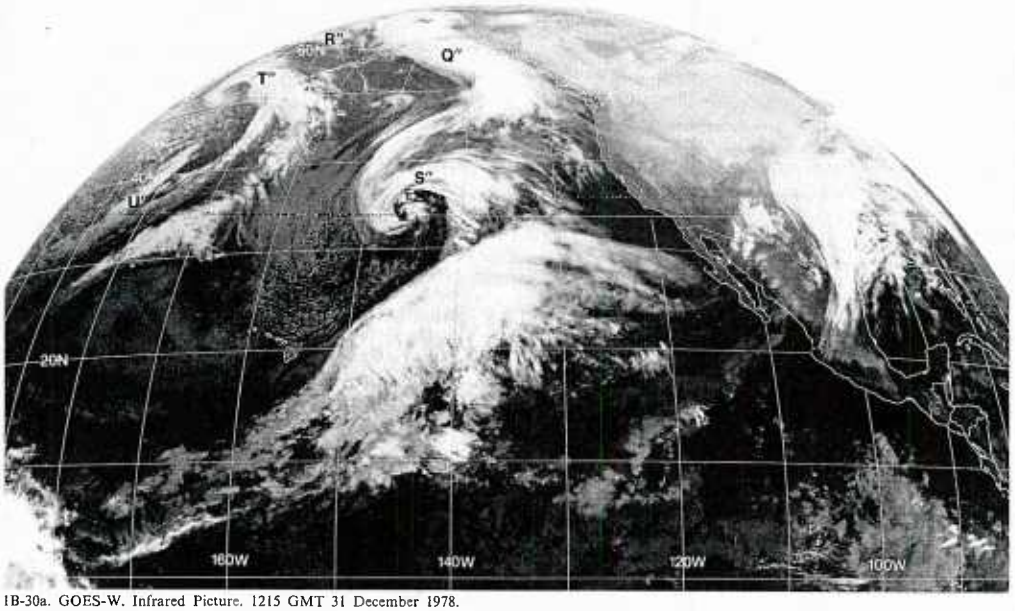

1B-30a. GOES-W. Infrared Picture. 1215 GMT 31 December 1978.

500 mb

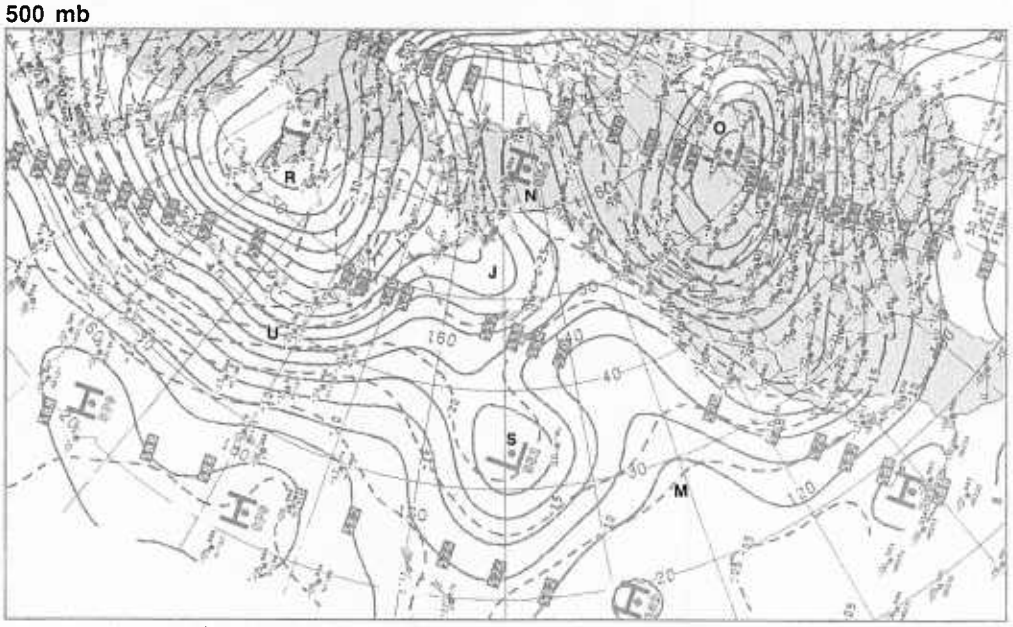

1B-30b. NMC 500-mb Analysis. 1200 GMT 31 December 1978.

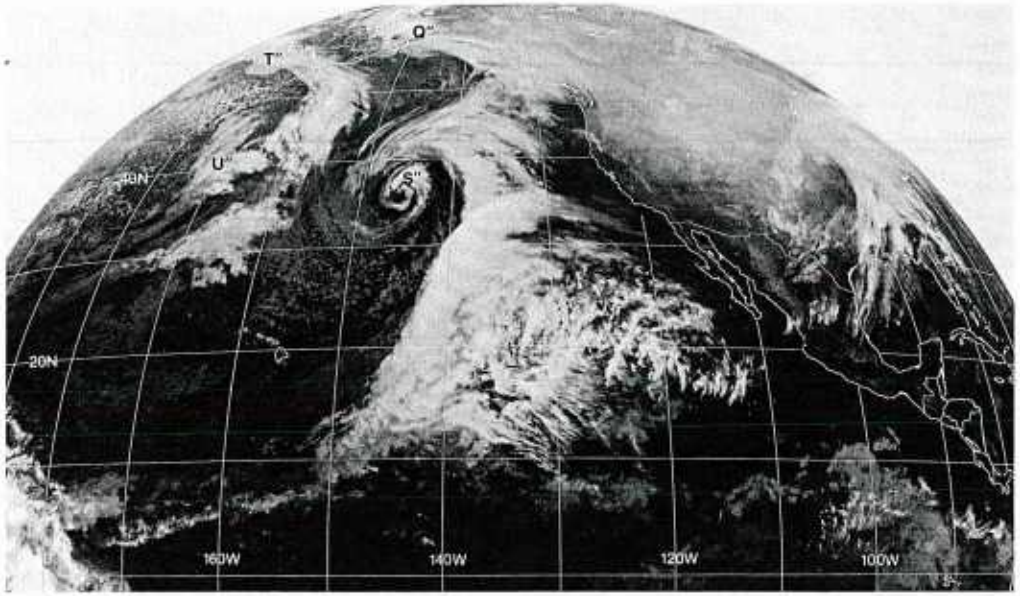

1B-31a. GOES-W. Infrared Picture. 0015 GMT 1 January 1979.

500 mb

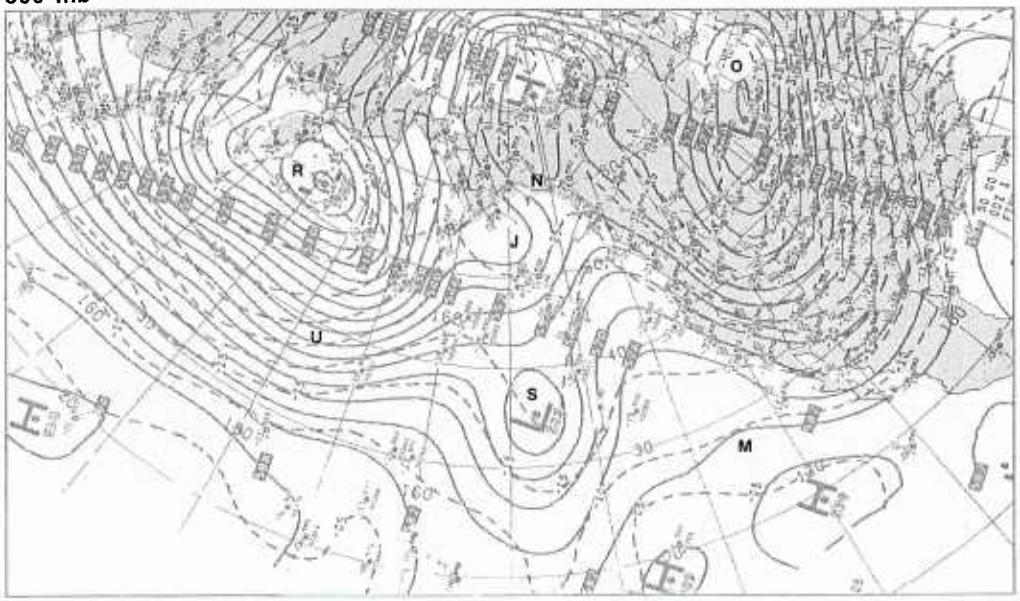

1B-31b. NMC 500-mb Analysis. 0000 GMT 1 January 1979.

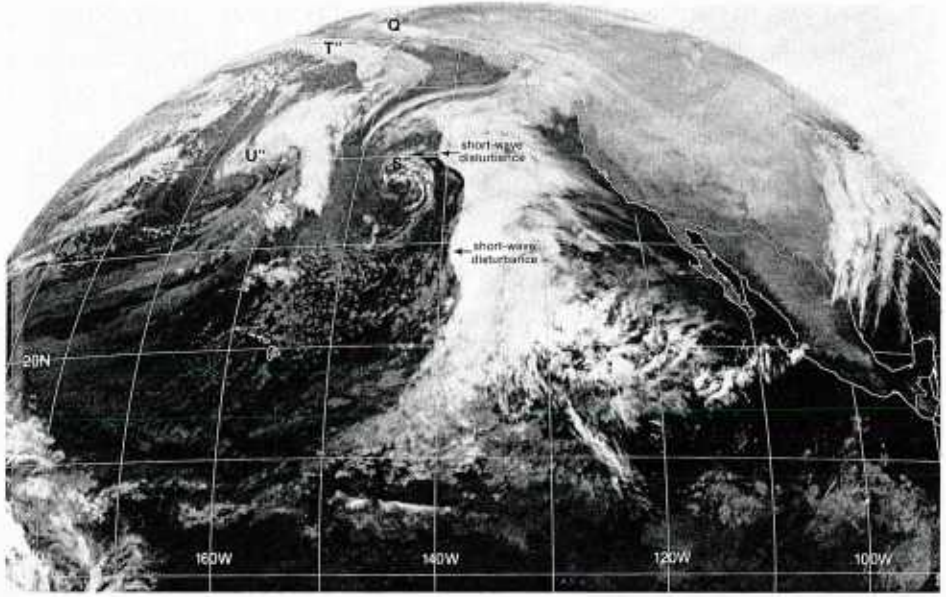

1B-31c. GOES-W. Infrared Picture. 1215 GMT 1 January 1979.

500 mb

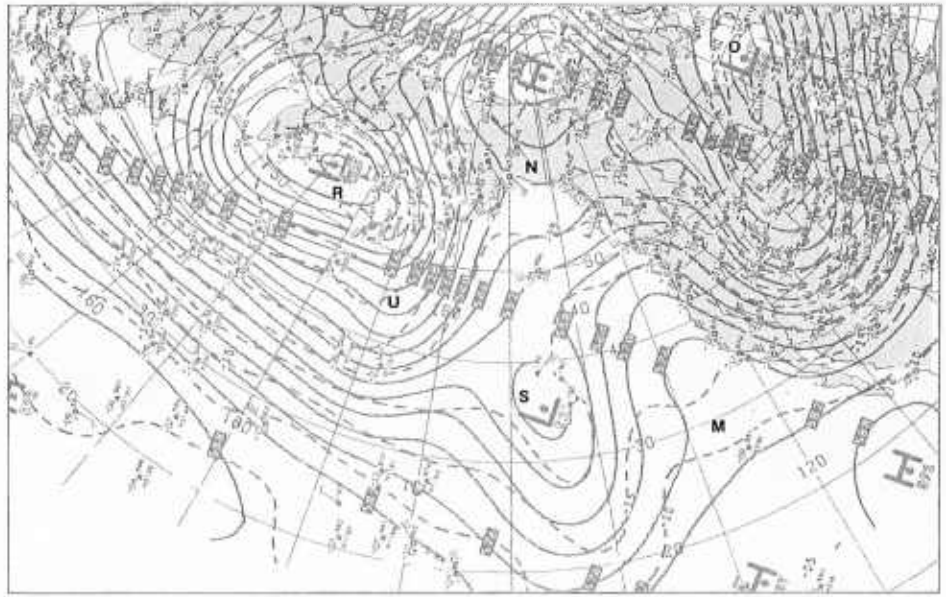

1B-31d. NMC 500-mb Analysis. 1200 GMT 1 January 1979.

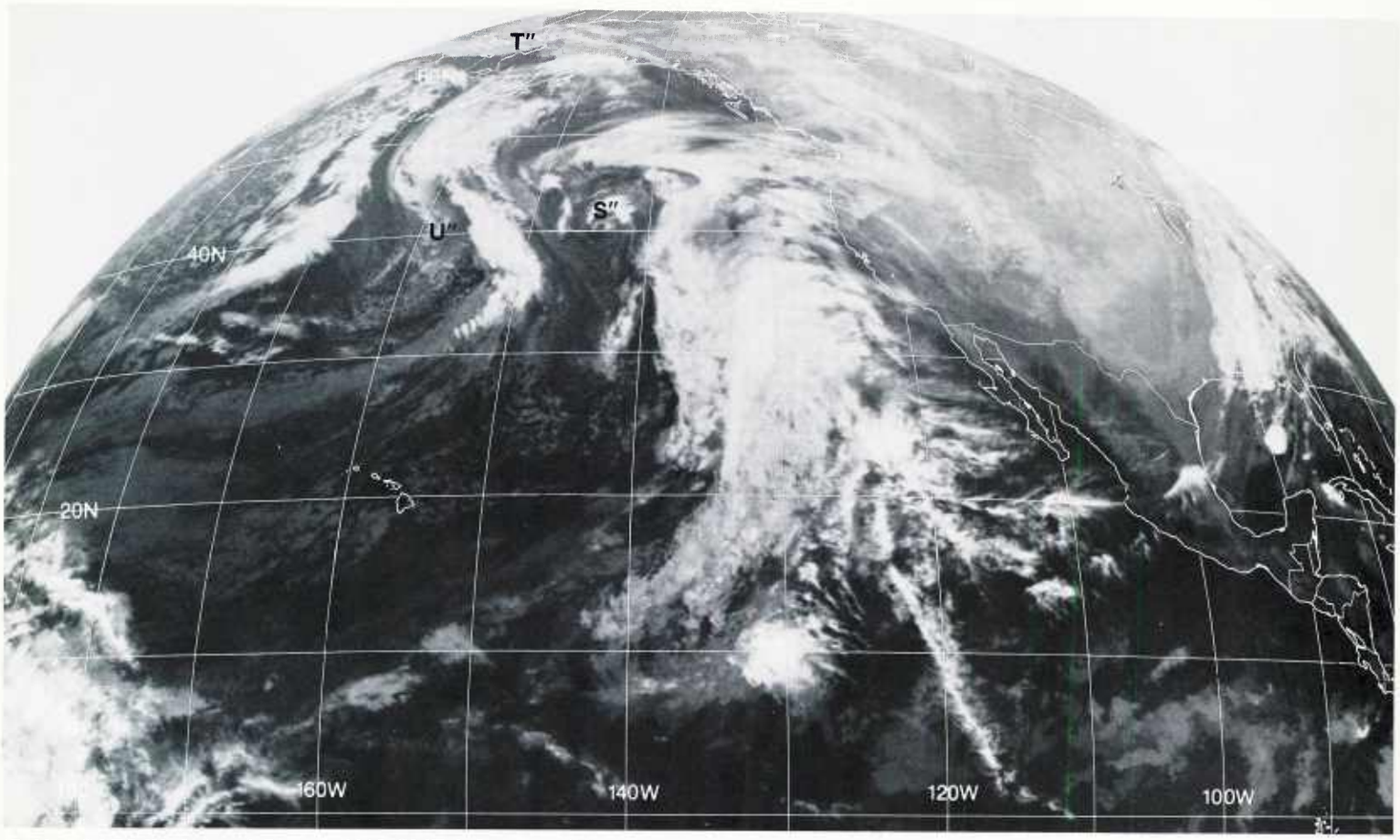

1B-32a. GOES-W. Infrared Picture. 0015 GMT 2 January 1979.

500 mb

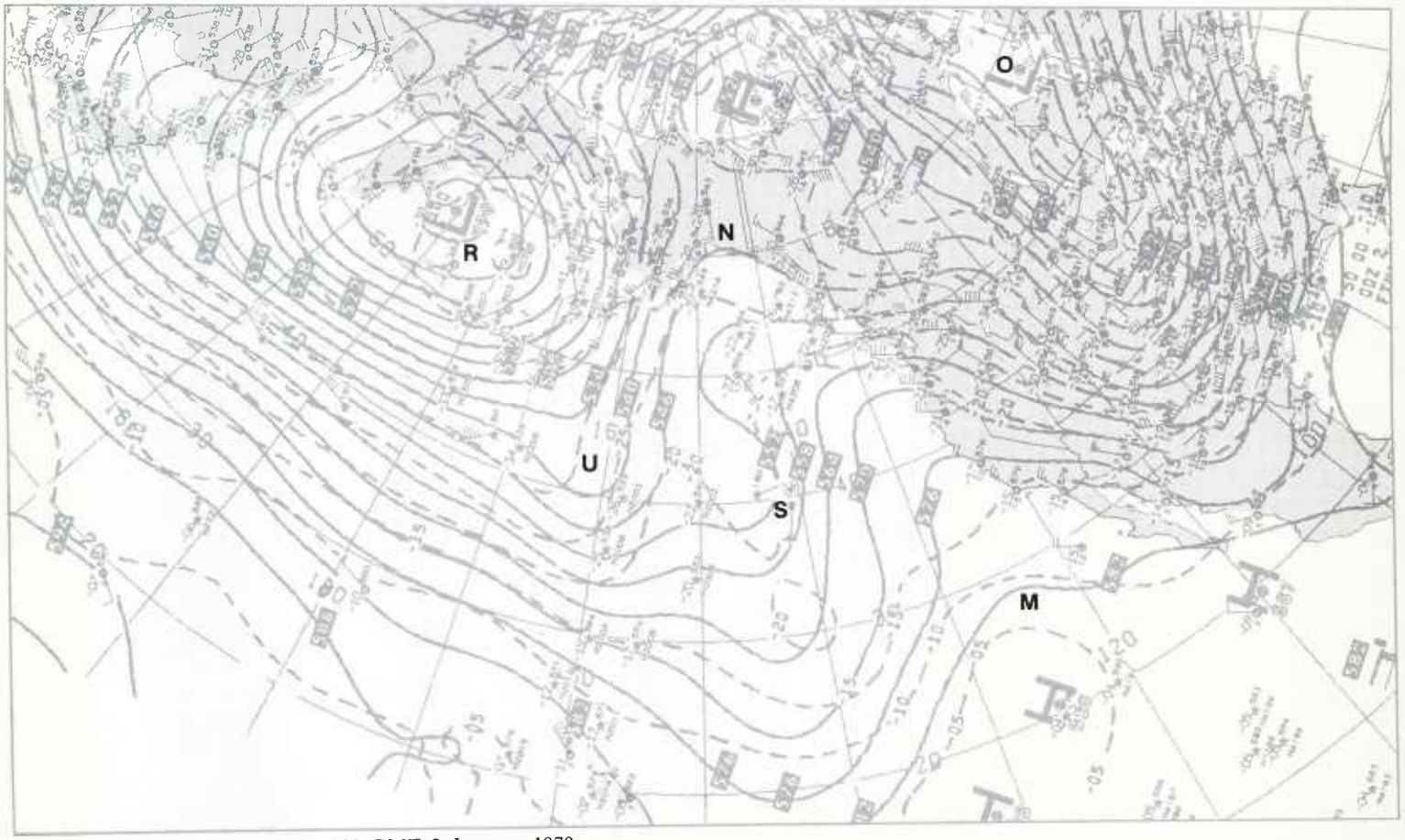

1B-32b. NMC 500-mb Analysis. 0000 GMT 2 January 1979.

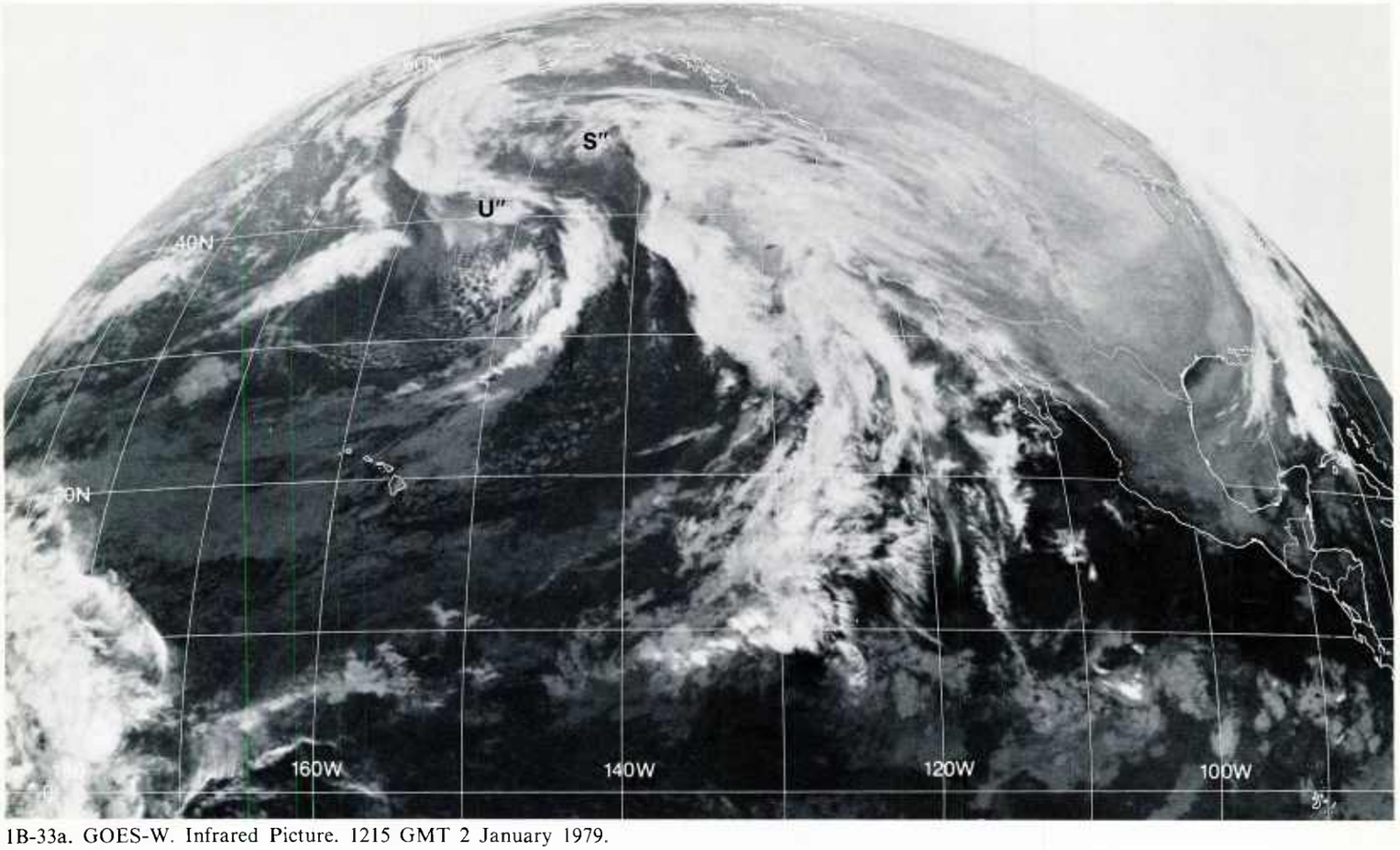

1B-33a. GOES-W. Infrared Picture. 1215 GMT 2 January 1979.

500 mb

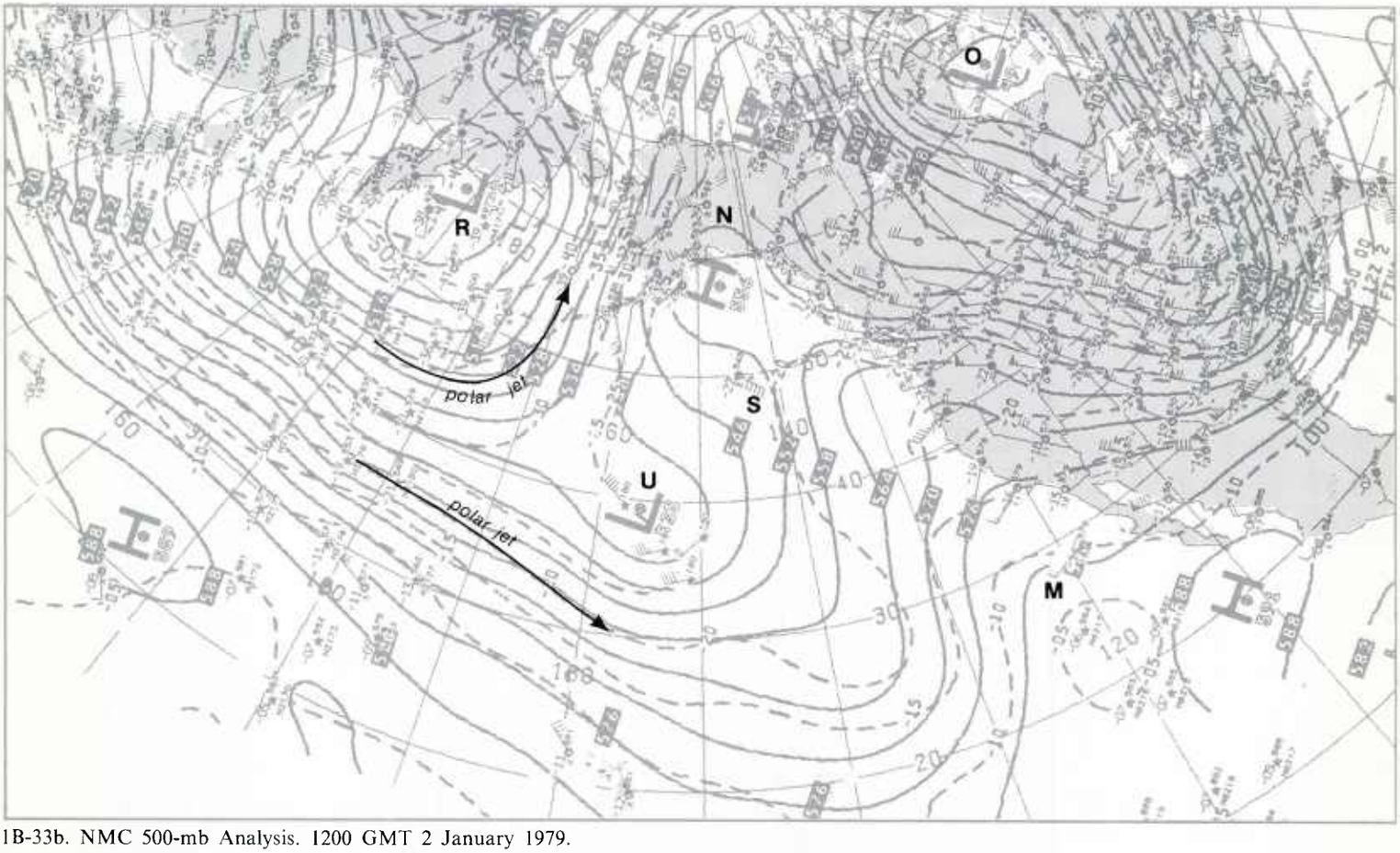

1B-33b. NMC 500-mb Analysis. 1200 GMT 2 January 1979.

Blocking Action: Mature Phase

Blocking Action: Mature Phase

Characteristic Features

1. *Blocking pattern continues over the eastern Pacific. A blocking ridge extends from low latitudes to the arctic and deep upper-air lows are located upstream and downstream of the block.*
2. *The development of an intense surface anticyclone over western North America produces strong southerly flow along the west coast from southern California to Alaska.*
3. *The eastward progress of cyclonic disturbances in the mid-latitude westerlies is slowed as they move against the block.*

3 January

The 500-mb analysis (1B-34b) shows that the blocking ridge **M–N** is persisting over the eastern Pacific, as forecast (1B-28c and 29a). There is a closed high-pressure cell at 62°N, 144°W, and the axis of the blocking ridge at mid latitudes has a pronounced southeast to northwest tilt, as indicated on the 72-hour prognosis (1B-29a). Deep cold lows **R** and **O** are located upstream and downstream of the block. At 300 mb (1B-34a), the northern branch of the split in the polar westerlies **PJS-1** shows a strong jet streak (125 kt) moving around the northern boundary of the block. The southern branch in the polar westerlies **PJS-2** has intensified considerably and extends from mid latitudes over the western Pacific to low latitudes over the eastern Pacific. This jet identifies the location of the main belt of the polar westerlies over the Pacific.

In the satellite picture (1B-35a), the minimum cloud cover zone stretching from Texas into western Canada confirms that the blocking extends through a vertically deep layer of the atmosphere. On the surface analysis (1B-35b), the blocking anticyclone **M′–N′** over western North America is very strong (1056-mb high at **N′**). The surface anticyclone contour lines along the west coast of North America reflect the southeast to northwest tilt of the upper-level ridge **M–N** at 500 mb, and strong southerly flow is observed offshore from southern California to the Gulf of Alaska. This strong southerly flow is typical of the mature stage of blocking action over the eastern Pacific.

At 500 mb, the eastward progress of storm **U** at mid latitudes over the eastern Pacific has been arrested by the blocking ridge **M–N**. There is a closed low **U′** at the surface. The eastward progress of this low is blocked by the surface anticyclone **M′–N′**. **U′1**, **U′2**, and **U′3** are cold frontal systems circulating around the **U′** center. The frontal cloud bands **U″1**, **U″2**, and **U″3** identify these disturbances in the satellite picture. The frontal cloud band **U″1** broadens into a large cloud mass off the West Coast and consists of the remnants of previous frontal systems that have dissipated against the block.

A large, dissipating, closed surface low **R′** is observed over the west-central Pacific. This low is located below the 500-mb low **R** aloft. An incipient frontal wave **V′** is developing in a trough line extending to the south from the surface low center **R′**. The typical incipient frontal wave cloud band **V″** identifies the location of this disturbance in the satellite picture.

At 300 mb (1B-34a), the polar jet **PJS-2** appears as a nearly continous band at low latitudes across the east-central Pacific. In the satellite picture (1B-35a), there is a break in the jet-associated cirrus decks along the jet axis between 140°W and 160°W. This clear zone coincides precisely with the base of the 500-mb trough (1B-34b). Vertical motions are suppressed along the base of 500-mb troughs, which accounts for the dissipation of the cirrus (high-level cloudiness) along the jet. The suppression of vertical motions is primarily an upper-level event so that lower-level cloudiness is often observed in the same area (note the dark gray shades in the satellite picture which identify low-level cloudiness).

During the next 72-hour period, the blocking pattern at high latitudes is forecast to persist (1B-36a and 37a). A large, closed anticyclone **N** will remain over Alaska throughout the period. The deep cold lows **R** and **O** upstream and downstream of the block, however, are forecast to advance rapidly eastward, in contrast to their slow eastward progression during the previous periods. In particular, low **R** moves southeastward and begins to intrude under the western boundary of the high-latitude blocking anticyclone **N**. At mid latitudes the blocking ridge **M** along the West Coast (1B-36a) is replaced by the low **U** at the end of the forecast period (1B-37a). This low has been carried eastward rapidly by the main branch of the polar westerlies (closely-spaced height contour lines) which extend across the central and eastern Pacific along approximately 30°N. The ridge **W** develops in response to the strong warm air advection in the southerly flow in advance of the deep low **R**.

continued on page 1B-38

300 mb

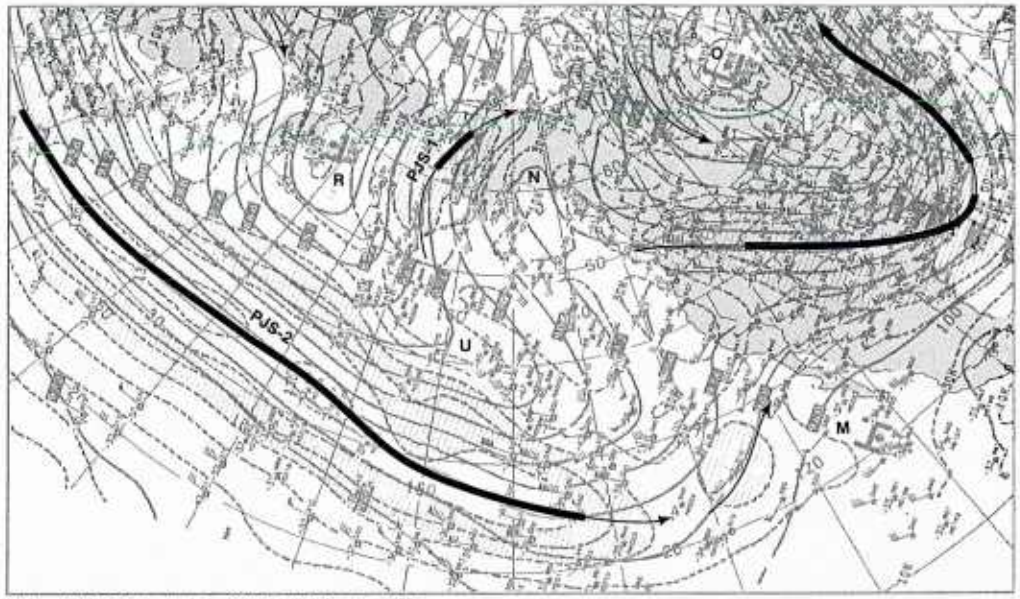

1B-34a. NMC 300-mb Analysis. 0000 GMT 3 January 1979.

500 mb

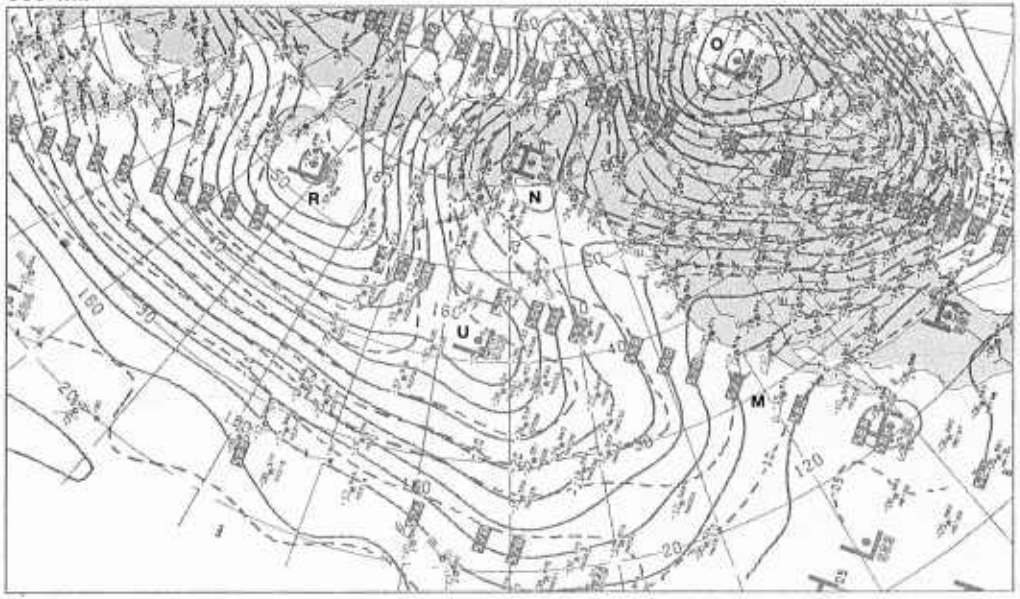

1B-34b. NMC 500-mb Analysis. 0000 GMT 3 January 1979.

Blocking Action: Mature Phase

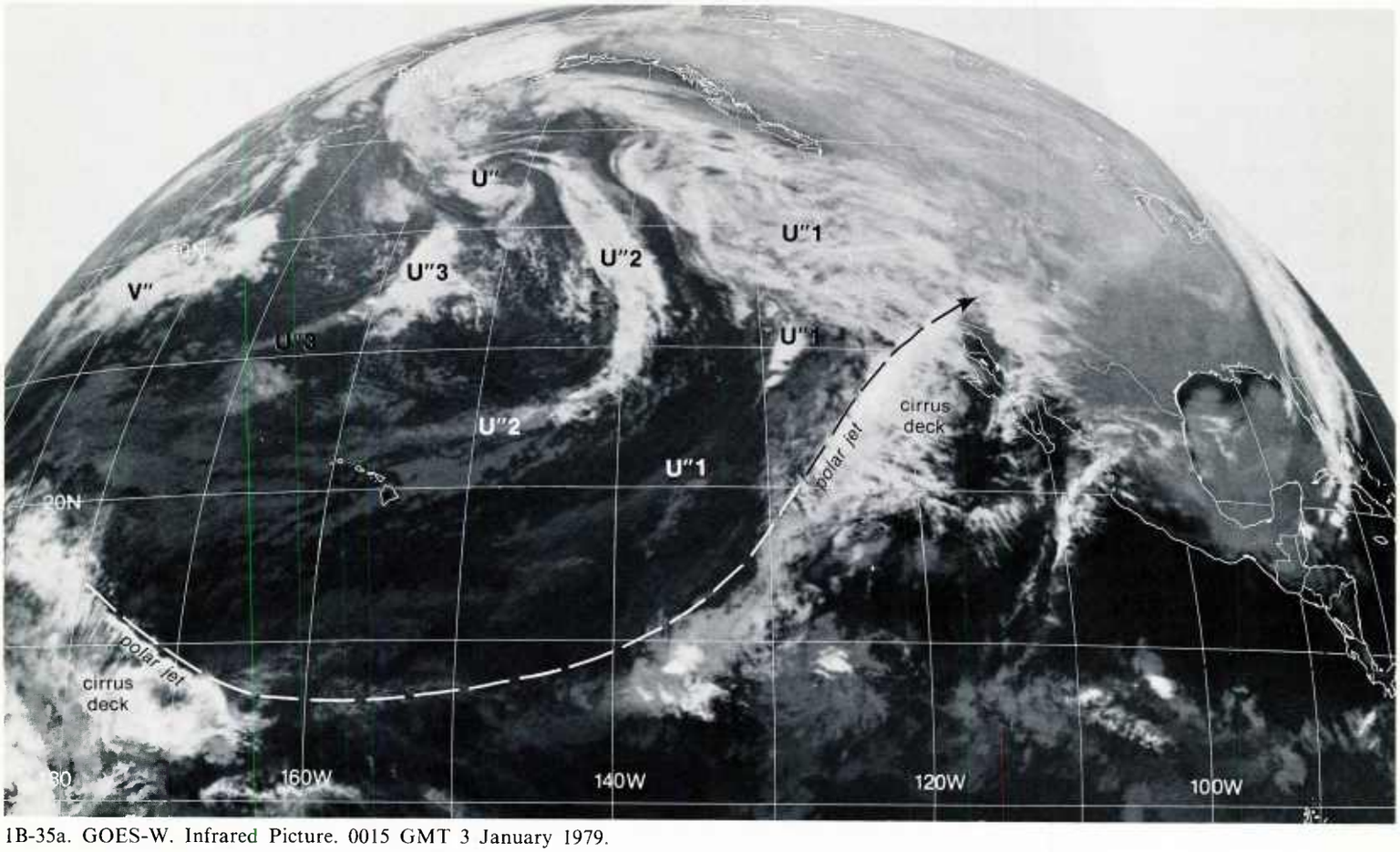

1B-35a. GOES-W. Infrared Picture. 0015 GMT 3 January 1979.

surface

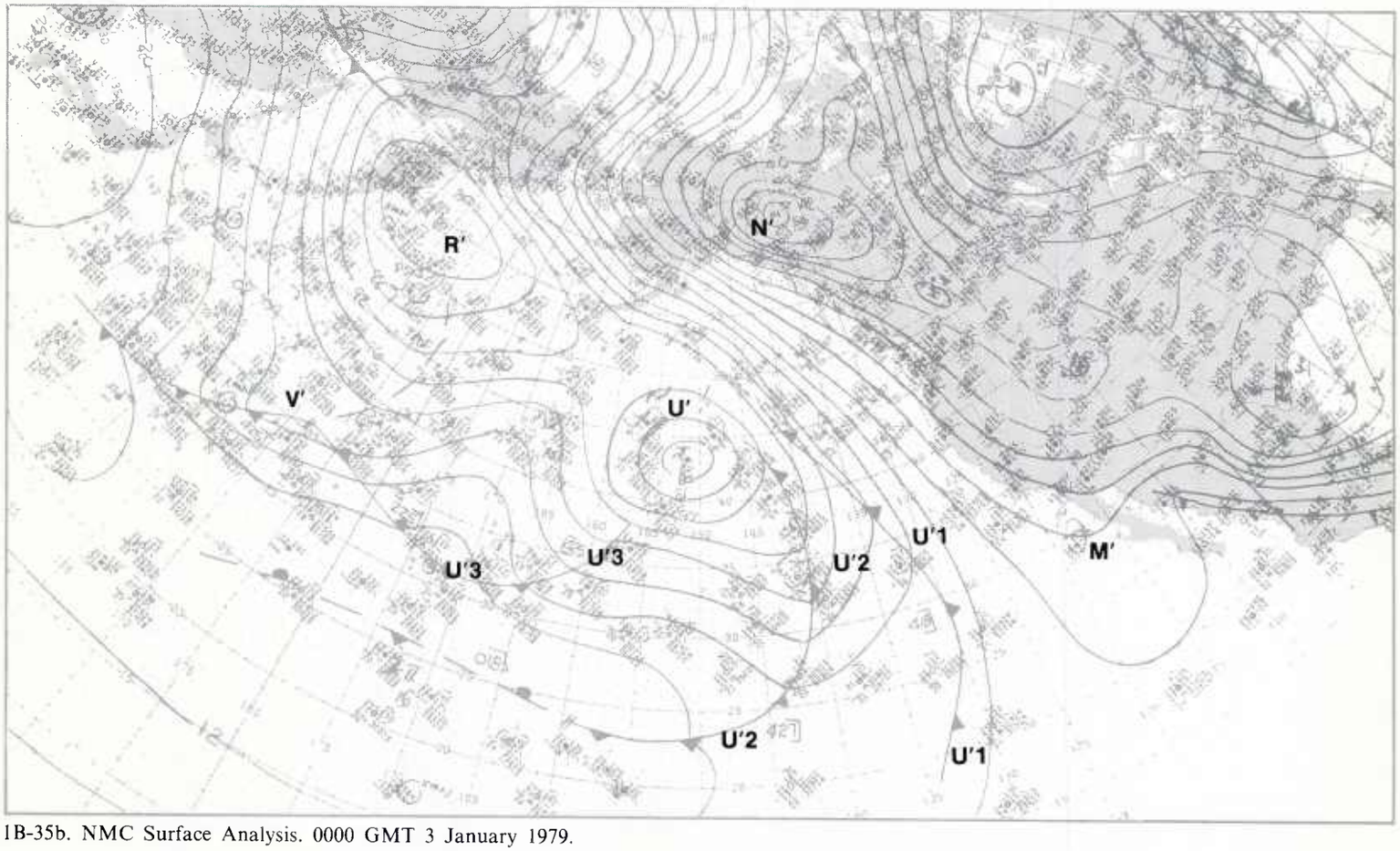

1B-35b. NMC Surface Analysis. 0000 GMT 3 January 1979.

500 mb

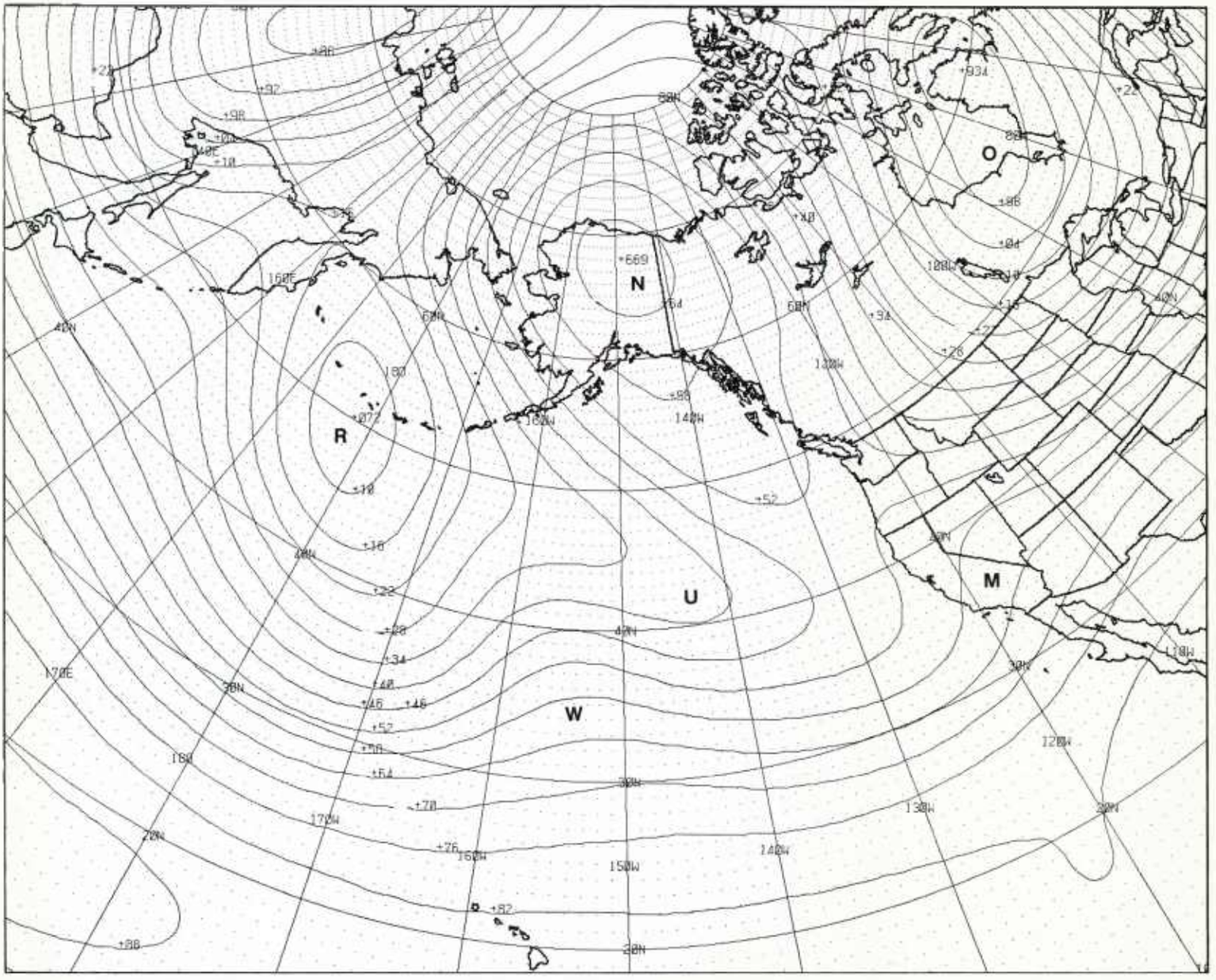

1B-36a. FNOC PE 36-hr 500-mb Prognosis. Valid 1200 GMT 4 January 1979.

500 mb

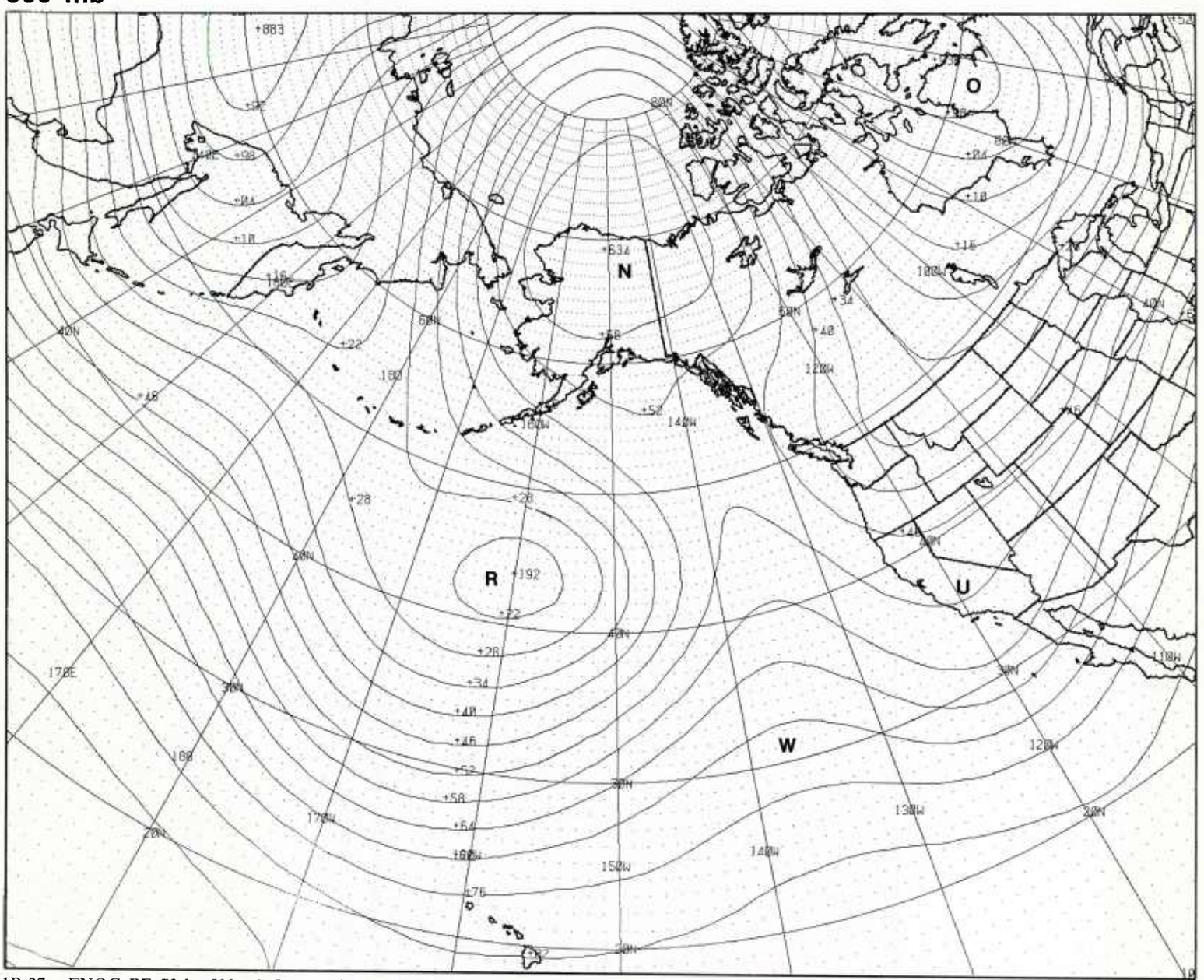

1B-37a. FNOC PE 72-hr 500-mb Prognosis. Valid 0000 GMT 6 January 1979.

4–5 January

In the following series of 500-mb analyses and satellite pictures, the changing pattern of the blocking action on disturbances moving eastward in the polar westerlies is presented at 12-hour intervals. At 500 mb (1B-38b), the low **U** at mid latitudes advances to the east on a track that takes it under the high-latitude block **N** (1B-39d). The blocking ridge **M** downstream decreases in amplitude as the low **U** moves eastward and, during the same period, a new ridge **W** develops upstream. In the corresponding satellite pictures, the cloud vortex **U″** (1B-38a) is caught in the strong southerly flow ahead of the 500-mb low and moves rapidly to the north, where it dissipates against the high-latitude block **N** (1B-39c). The frontal cloud bands **U″1** and **U″2** (1B-38a) are also observed to dissipate as they move against the block (1B-39c).

The comma cloud **U″3** (1B-38a), on the other hand, initially shows a rapid development into a distinct comma pattern (1B-39a) which dissipates just as rapidly (1B-39c), as a new development **X″** occurs in the southeast quadrant of the 500-mb low (1B-39d).

The cloud vortex **V″** (1B-38a) is located in the northern branch of the polar westerlies. This storm develops rapidly (1B-39a) and reaches the mature stage (1B-39c). Note that the storm shows a tight spiral cloud vortex near 45° N, 170° W. During this same period, the 500-mb low **R** (1B-38b), in which the storm **V″** is embedded, advances eastward (1B-39b and 39d), where previously this low had been quasi-stationary in the vicinity of 55° N, 170° W (see 1B-31b).

The effect of the high-latitude block **N** on the disturbance **V″** is depicted in the satellite pictures (1B-40a and 41a) on the following pages. The eastward progress of the storm is blocked—the position of the spiral cloud vortex remains fixed near 45° N, 170° W—while the frontal cloud band **V″1** is forced against the western boundary of the block and becomes fragmented as it weakens. The 500-mb low **R** (1B-40b) moves directly over this disturbance (1B-41b), which is not favorable for continued development of the storm.

The 500-mb analyses (1B-40b and 41b) show that the low **U** develops a closed center as it approaches the West Coast. The rapid eastward advance of this low results in an elongated trough extending to the low **R** upstream, which has not moved appreciably to the east during this period. With the blocking ridge **M–N** still in place, the satellite pictures (1B-40a and 41a) show that the eastward progress of the cloud vortex **X″** is blocked. With the eastward progress of this system blocked, the following comma cloud **X″1** merges with the trailing cloud band of cloud vortex **X″**, and an elongated frontal cloud band is formed against the western boundary of the block.

continued on page 1B-42

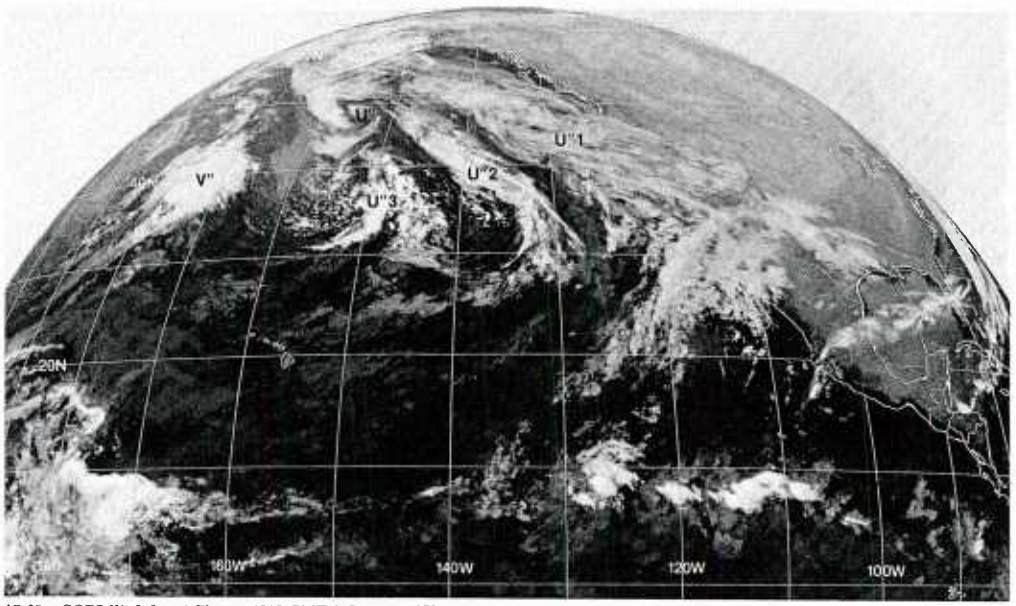

1B-38a. GOES-W. Infrared Picture. 1215 GMT 3 January 1979.

500 mb

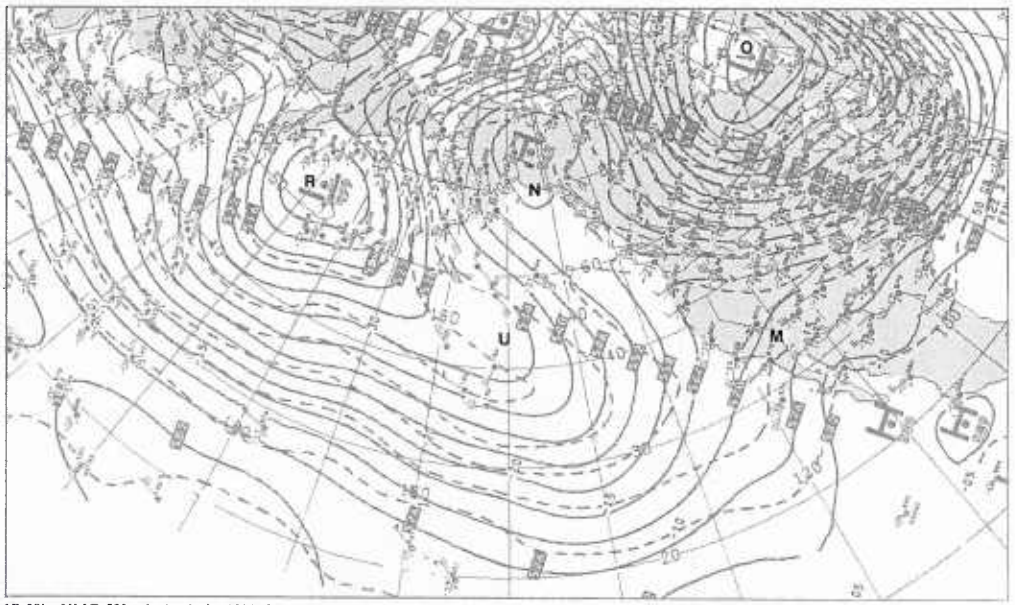

1B-38b. NMC 500-mb Analysis. 1200 GMT 3 January 1979.

Blocking Action: Mature Phase

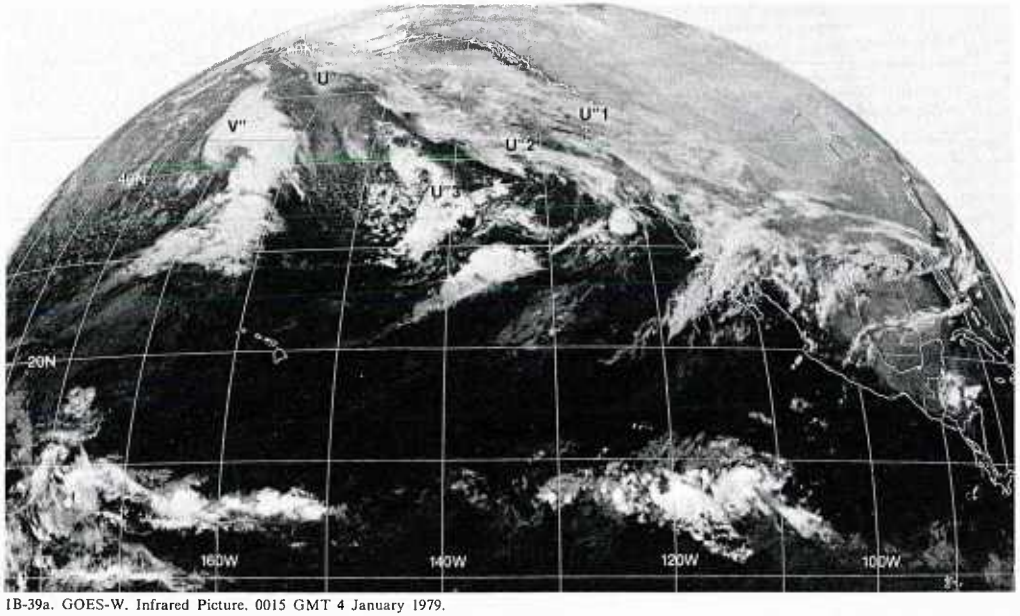

1B-39a. GOES-W. Infrared Picture. 0015 GMT 4 January 1979.

500 mb

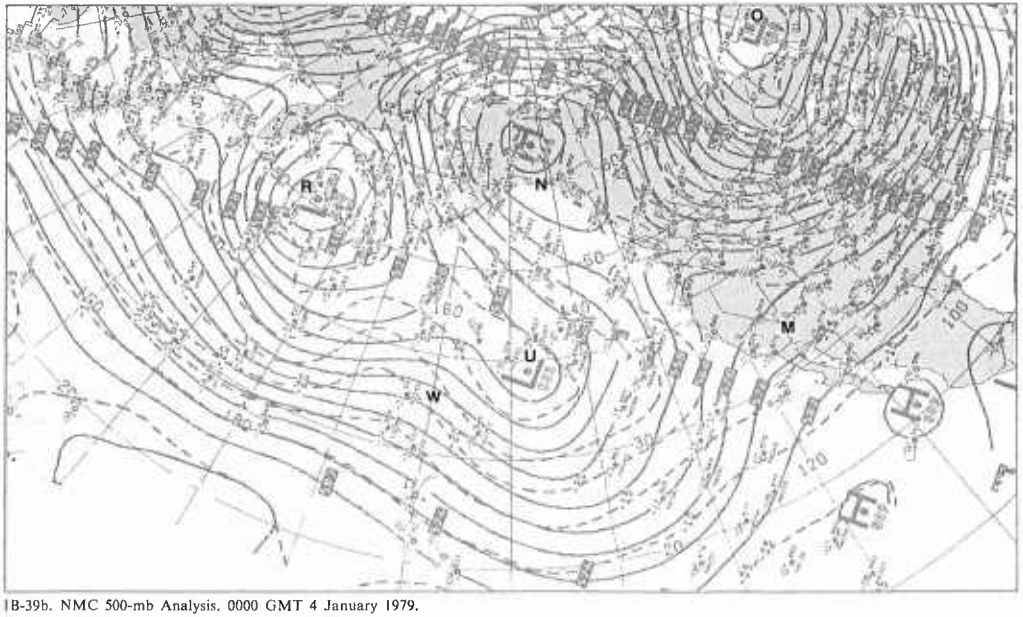

1B-39b. NMC 500-mb Analysis. 0000 GMT 4 January 1979.

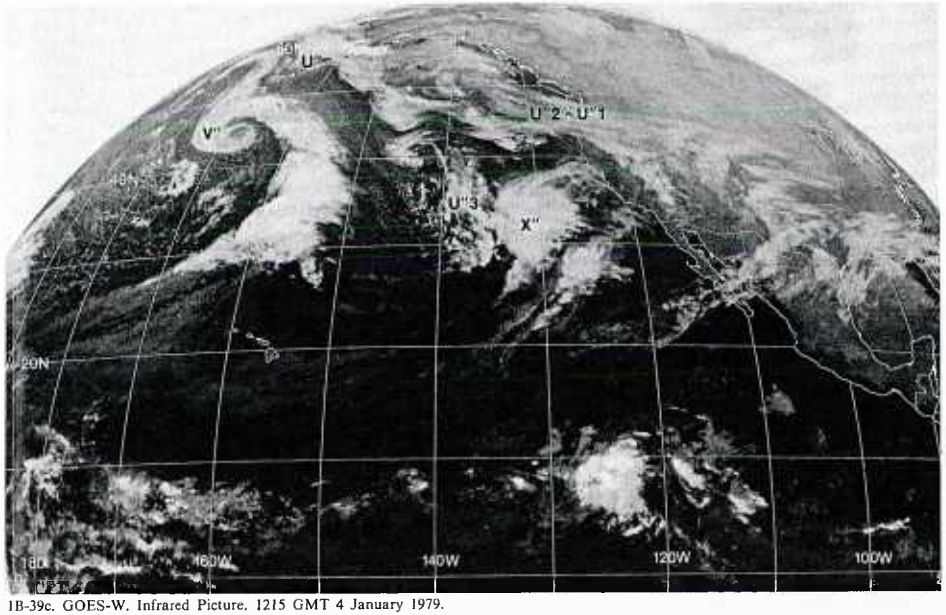

1B-39c. GOES-W. Infrared Picture. 1215 GMT 4 January 1979.

500 mb

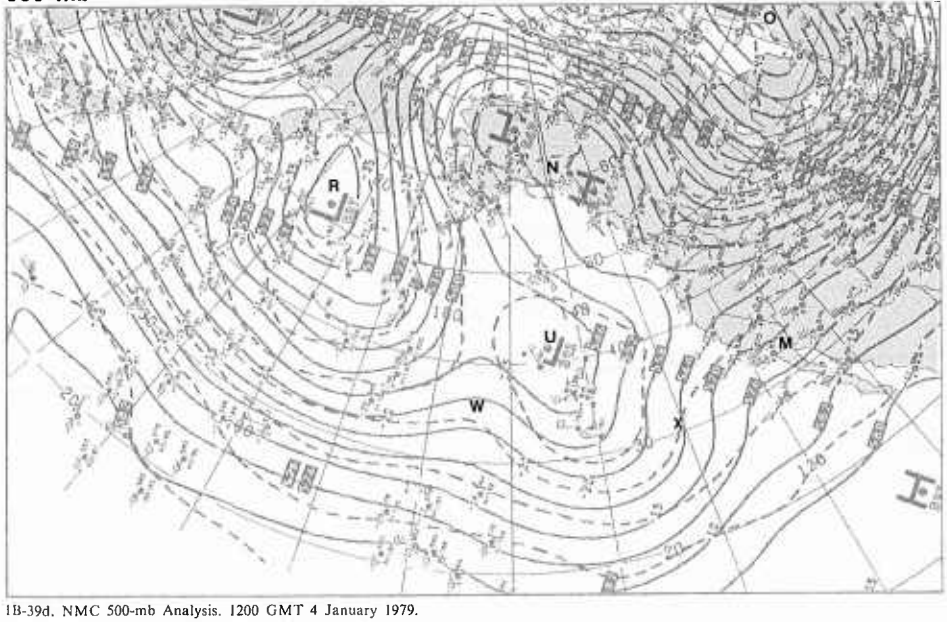

1B-39d. NMC 500-mb Analysis. 1200 GMT 4 January 1979.

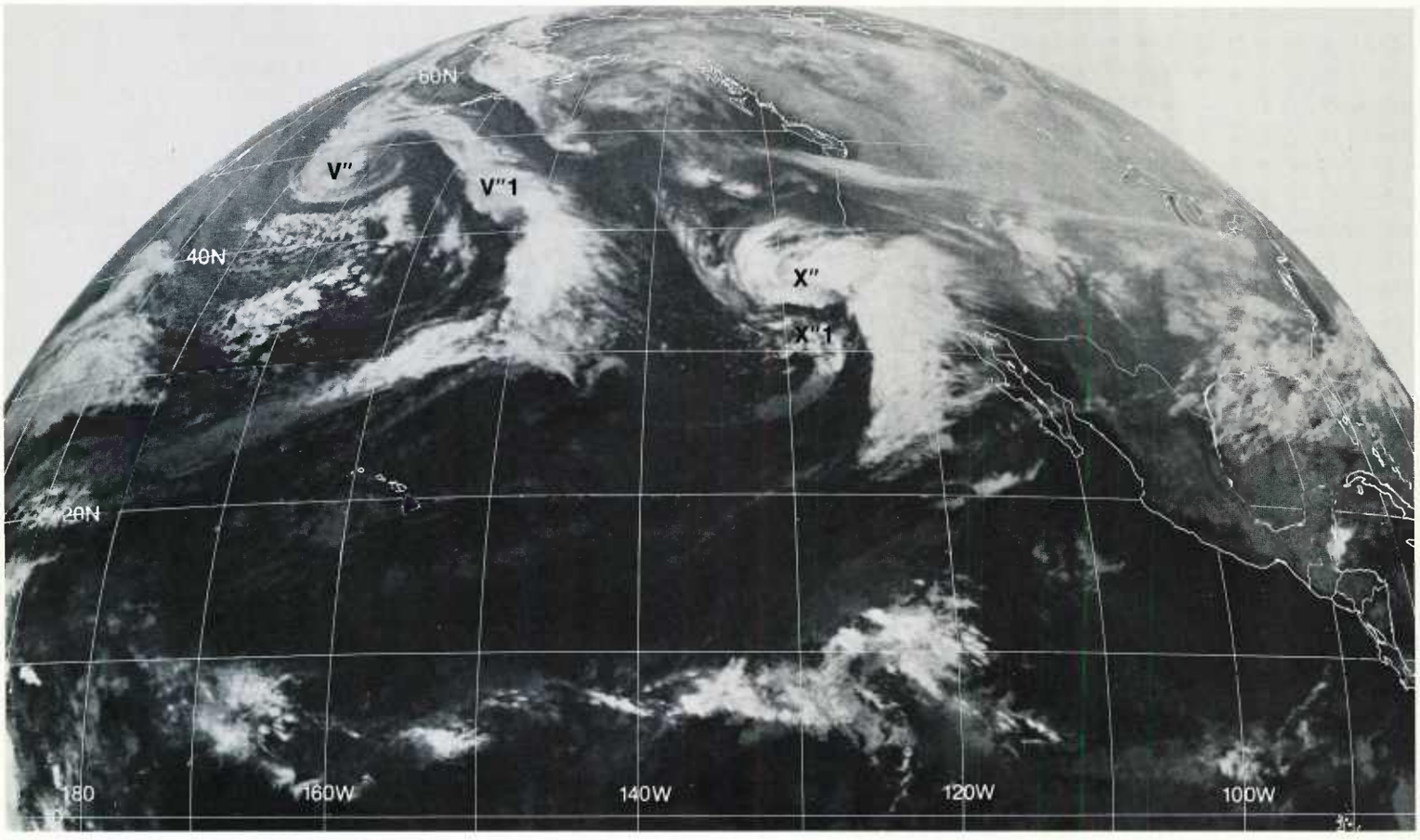

1B-40a. GOES-W. Infrared Picture. 0015 GMT 5 January 1979.

500 mb

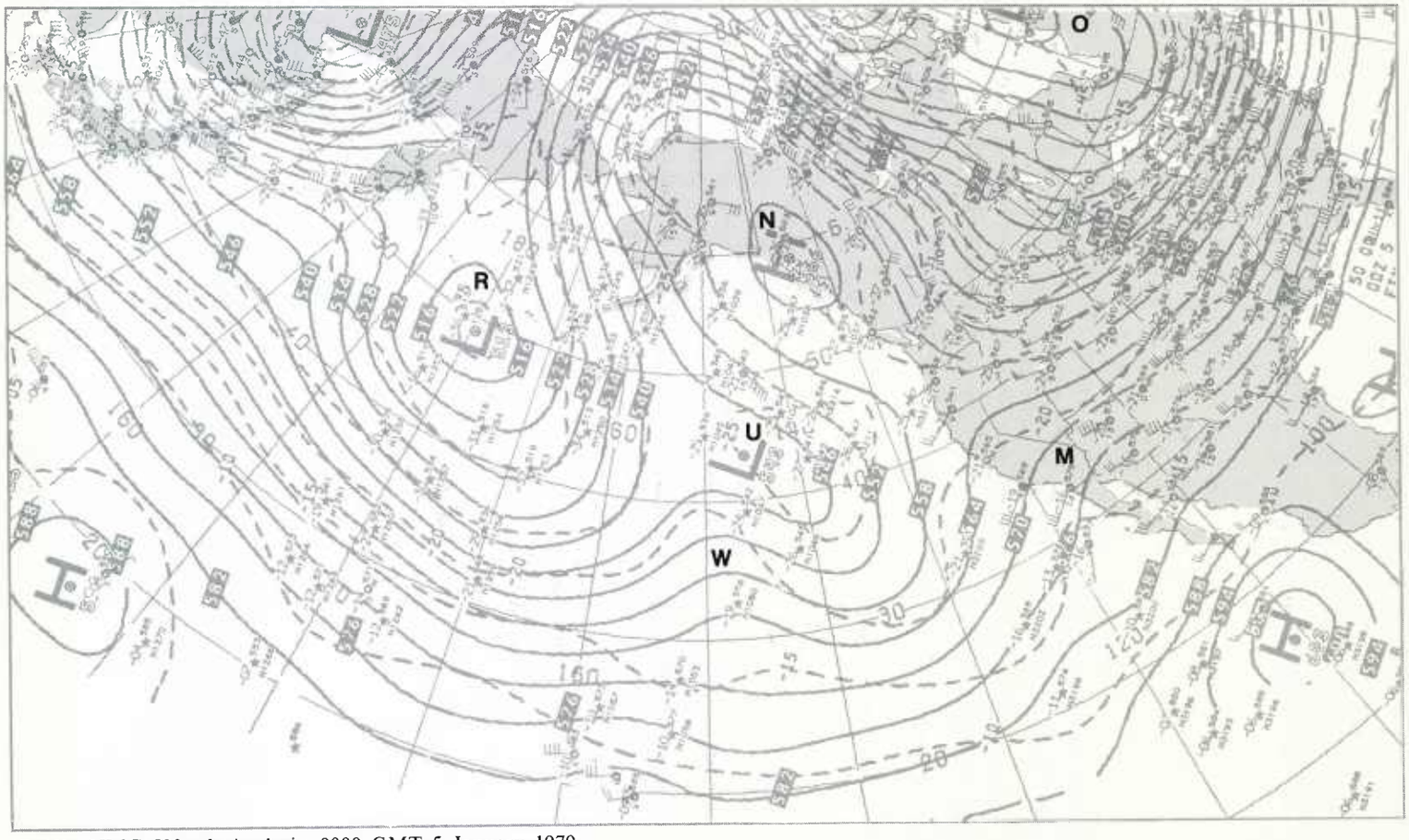

1B-40b. NMC 500-mb Analysis. 0000 GMT 5 January 1979.

Blocking Action: Mature Phase

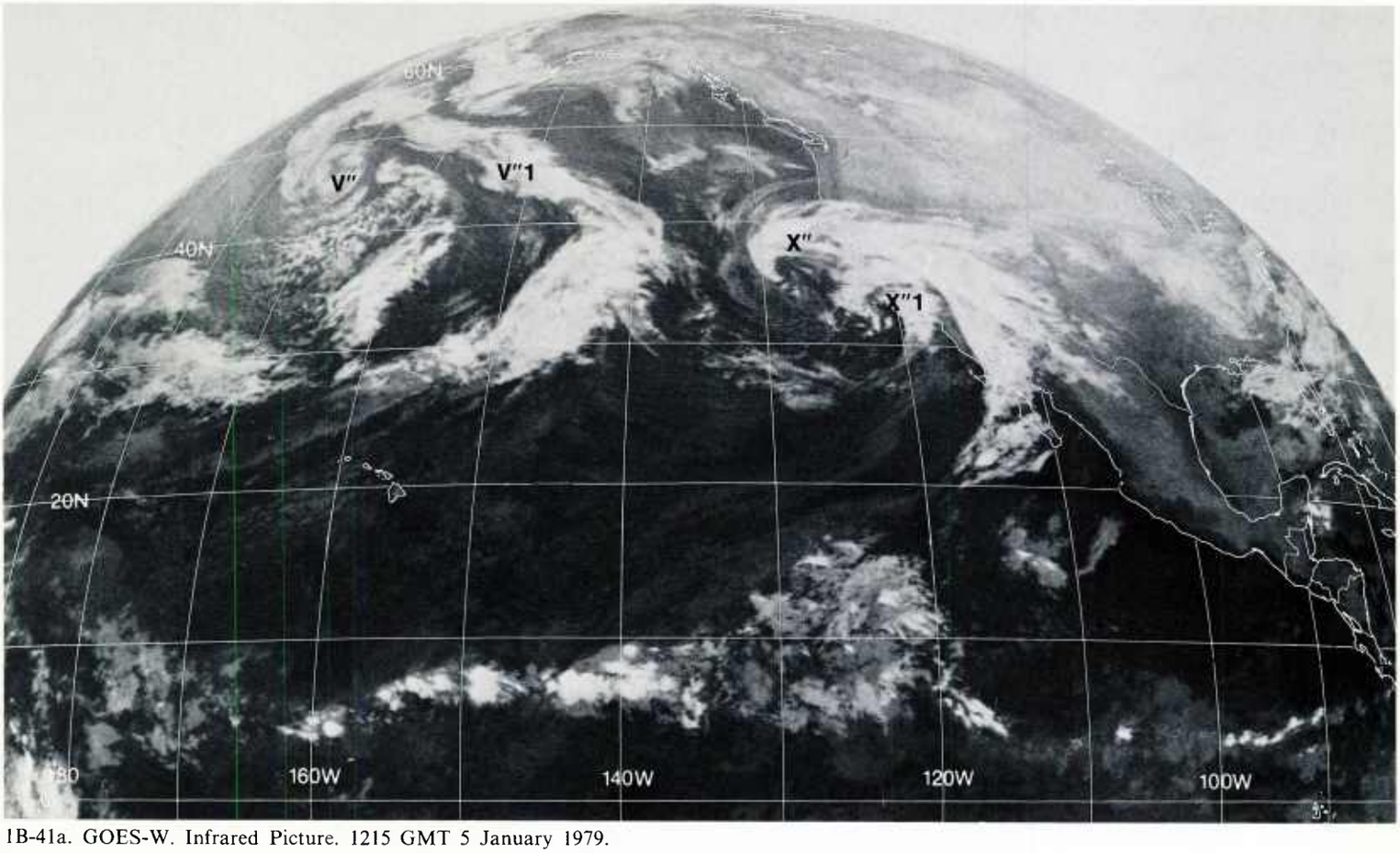

1B-41a. GOES-W. Infrared Picture. 1215 GMT 5 January 1979.

500 mb

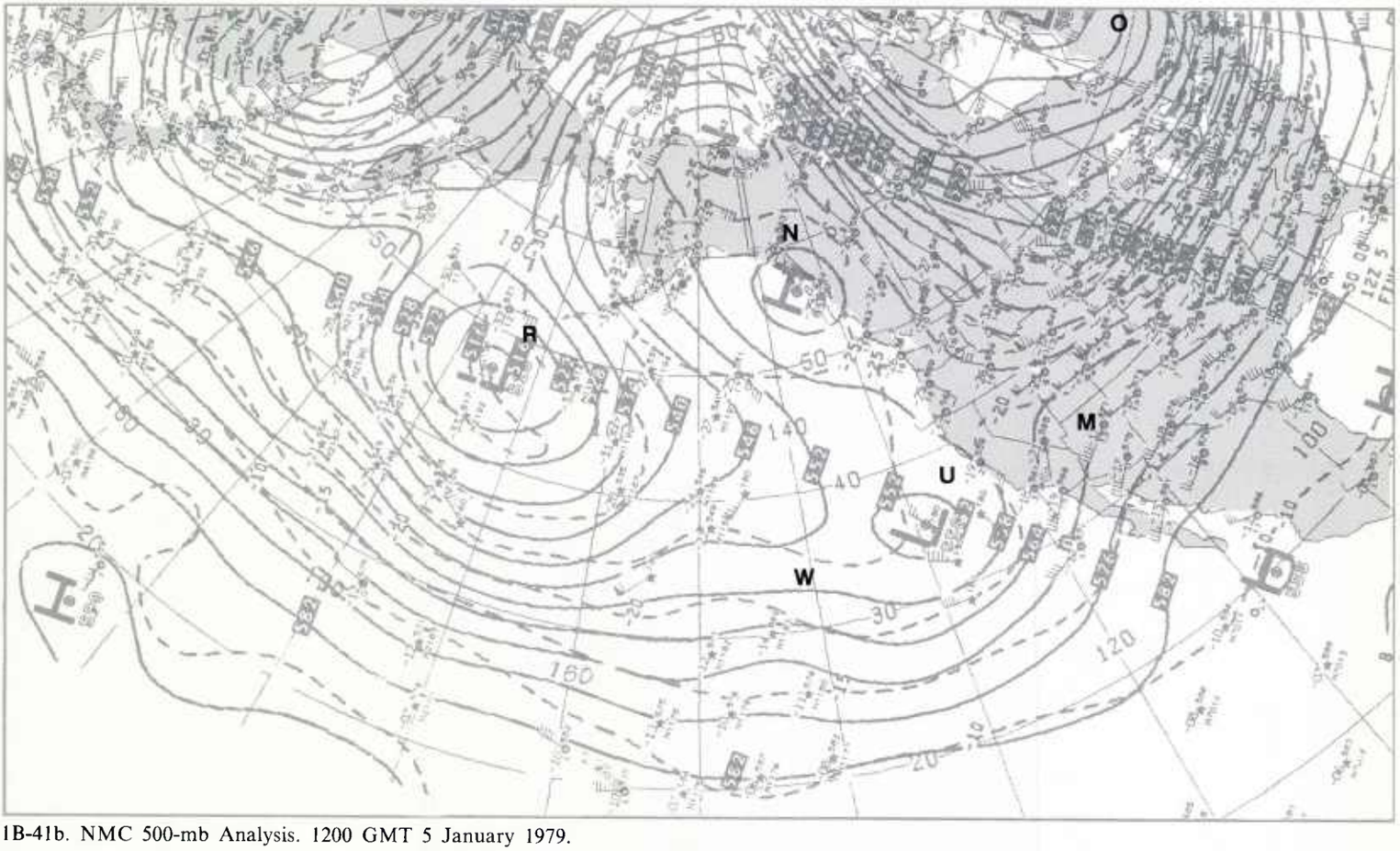

1B-41b. NMC 500-mb Analysis. 1200 GMT 5 January 1979.

Blocking Action: Late Phase

Characteristic Features

1. *The high-latitude block is maintained over northwest Canada and Alaska.*
2. *Polar westerlies at low latitudes strengthen across the eastern Pacific and advance under the high-latitude block into the U.S.*
3. *Penetration of the polar westerlies into the U.S. forces the mid-latitude block over the western U.S. to collapse.*
4. *Eastward moving disturbances in the polar westerlies at low latitudes progress inland over the U.S., as the mid-latitude block breaks down.*
5. *Strong southerly flow offshore along the west coast of the U.S. and Canada also diminishes rapidly as the mid-latitude block weakens.*

6 January

At 500 mb (1B-42b), the closed high **N** confirms the persistence of the high-latitude blocking, as forecast (1B-36a and 37a). Low **R** has become a mobile system and is moving on a southeasterly track under the block. This forces the mid-latitude polar jet **PJS-2** over the eastern Pacific to very low latitudes, as shown on the 300-mb analysis (1B-42a).

The mid-latitude jet streaks **PJS-1**, **2**, and **3** form an almost continuous line across the Pacific with the result that zonal flow is observed from the western Pacific to Mexico. This strong zonal jet has replaced the southern branch of the split in the westerlies observed earlier (see 1B-18a). The northern branch of the split in the polar westerlies **PJS-4** has weakened and is no longer significant (compare with 1B-34a). A polar jet **PJS-5**, however, has developed upstream of the low **R** which passes around the block **N** into northern Canada and to the rear of the new low **BB** (the original low **O** has moved eastward over the Atlantic), so that a polar jet is maintained at high latitudes. Thus, during this late phase of blocking, the storm tracks will be either along the high-latitude polar jet moving against the block **N** and dissipating, or the storm tracks will be along the mid-latitude jet advancing across the eastern Pacific and into the U.S.

The 500-mb analysis (1B-42b) shows that low **U**, which is caught up in the strong mid-latitude polar jet, has passed under the high-latitude block **N** and is now located over the West Coast. The penetration of the mid-latitude jet **PJS-1** and this disturbance into the U.S. has forced the breakdown of the blocking ridge **M**. The ridge **W** did not increase in amplitude as much as forecast because the deep low **R** did not move as far east, and the pattern of strong cold air advection to the rear and warm air advection in advance of this low did not develop. Thus only a weak ridging ahead of low **R** is observed. At the surface (1B-43b), the frontal system **X′** associated with the disturbance **U′** has advanced well inland, and the frontal cloud band **X″1**, in the satellite picture (1B-43a), confirms that this system is progressing inland undisturbed, due to the collapse of the blocking ridge **M**. With the collapse of the blocking ridge **M**, the strong offshore surface flow along the U.S. and Canadian west coast has also diminished (compare with 1B-35a).

The eastward advance of the surface low **V′** over the central Pacific (1B-43b) has slowed, and it has the typical characteristics of a decaying cyclone—the front **V′1** to the east is weak (it is located between contour lines and not in a sharp trough) and does not extend into the low center. In the satellite picture (1B-43a), the cloud vortex **V″** is very weak and shows only slight banding (compare with 1B-41a). The frontal cloudiness **V″1** extending to the east from the cloud vortex is dissipating; however, deep convection (bright white cloud clusters) is observed along the portion of the frontal cloud band **V″2-3** curving to the southwest from 40°N, 140°W. Note that this portion of the front is located in the left front quadrant of a broad jet max **PJS-2** at 300 mb (1B-42a)—a favorable area for deep vertical convection. The bright, meridional, cloudy area **Y″** is an area of deep vertical convection in the southwesterly flow around the 500-mb low **R**, and the convection extends to lower levels, as indicated by the presence of a trough line (TROF) **Y′** on the surface analysis.

The surface low **Z′** is a developing disturbance in the zonal westerlies at mid latitudes over the western Pacific. Note that the disturbance has support aloft—a short-wave trough **Z** at 500 mb—and it is located in the left front quadrant of a 300-mb jet max **PJS-3**. A distinct comma cloud **Z″** is also observed on the satellite picture.

The 36-hour (1B-44a) and 72-hour (1B-45a) 500-mb prognoses show a closed high-pressure cell **N** over Alaska. This indicates that the high-latitude block is forecast to continue for an additional three days. In addition, the major low **R** over the central Pacific and low **BB** over Hudson Bay are forecast to remain almost stationary during the same period. The increase in the amplitude of the ridge **W** (1B-44a) acts to reinforce the blocking action along the West Coast. This ridge does not intensify further (1B-45a) so that the blocking action is temporary. Strong, zonal westerlies (closely-spaced height contour lines) are forecast to persist at mid latitudes across the Pacific.

continued on page 1B-46

300 mb

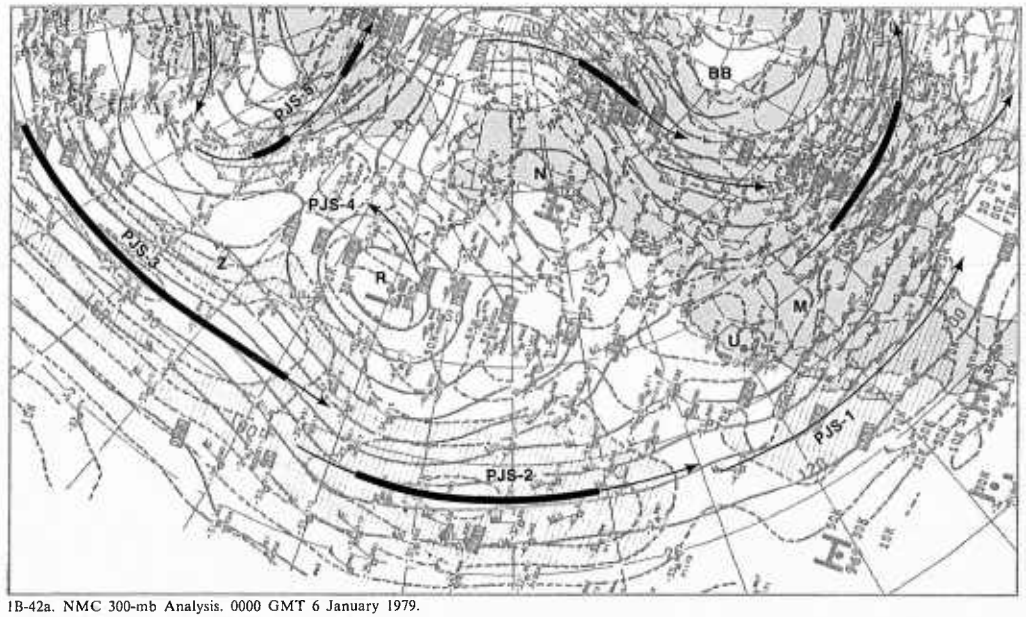

1B-42a. NMC 300-mb Analysis. 0000 GMT 6 January 1979.

500 mb

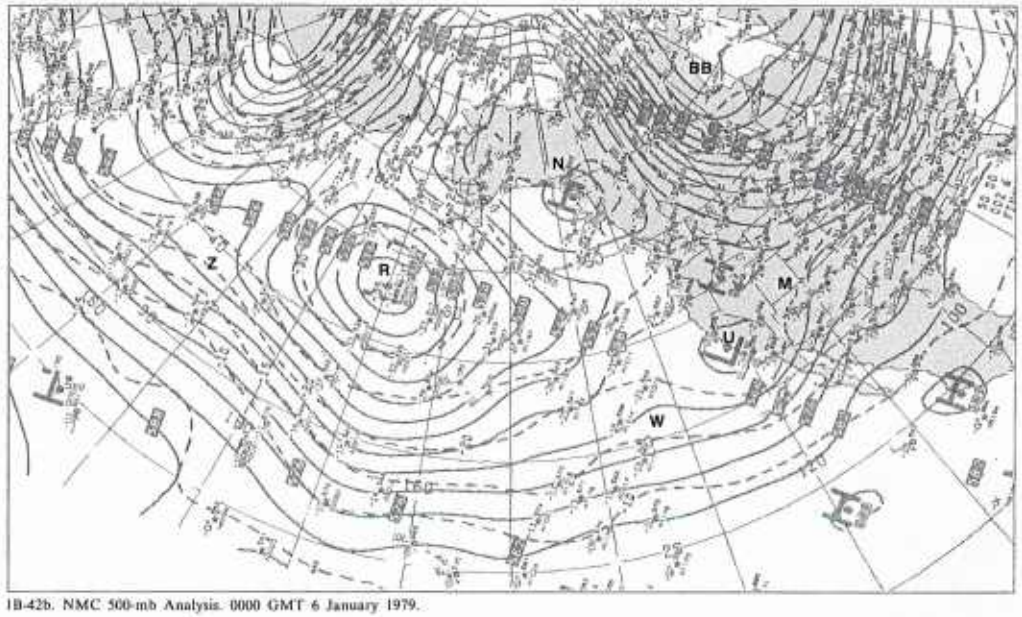

1B-42b. NMC 500-mb Analysis. 0000 GMT 6 January 1979.

Blocking Action: Late Phase

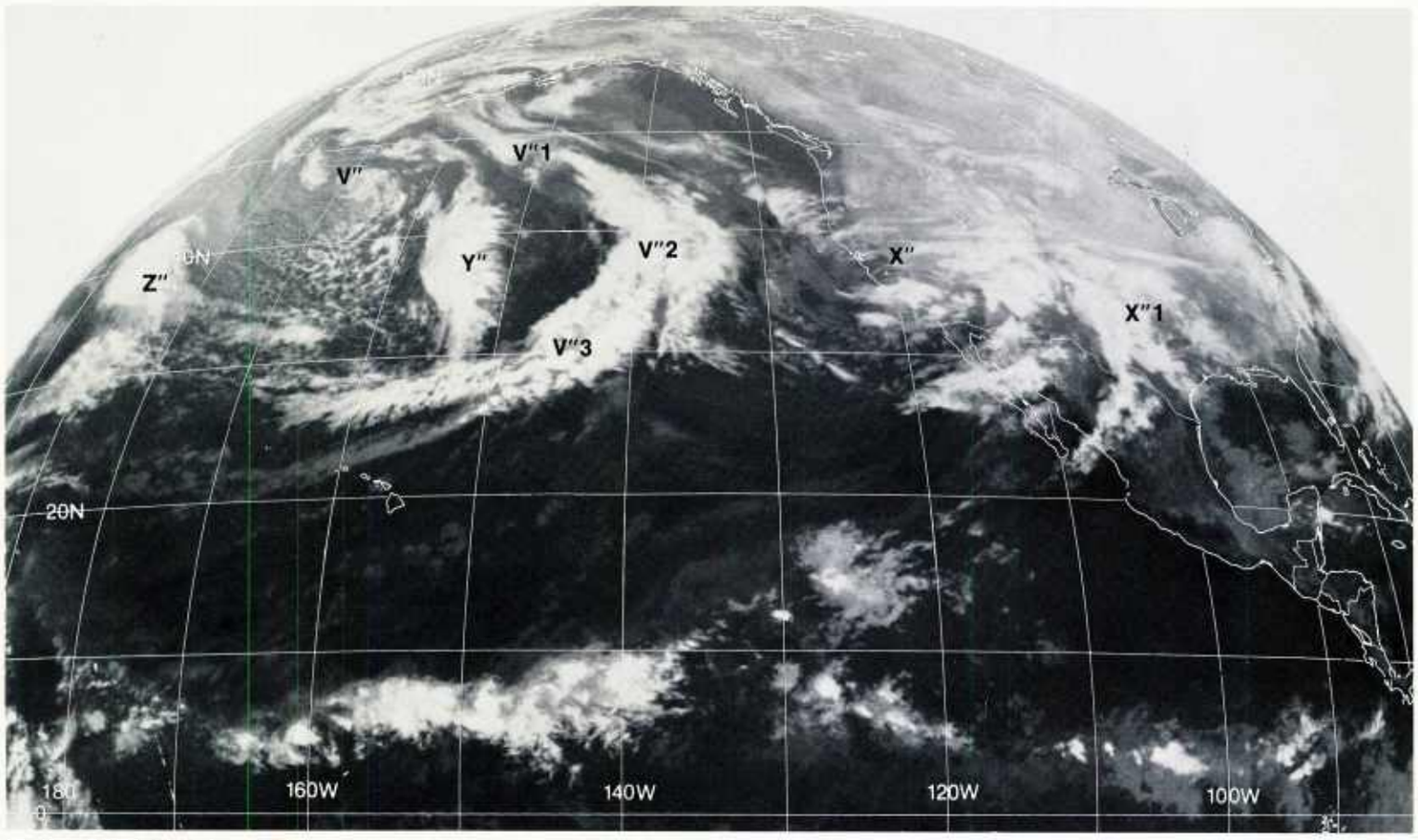

1B-43a. GOES-W. Infrared Picture. 0015 GMT 6 January 1979.

surface

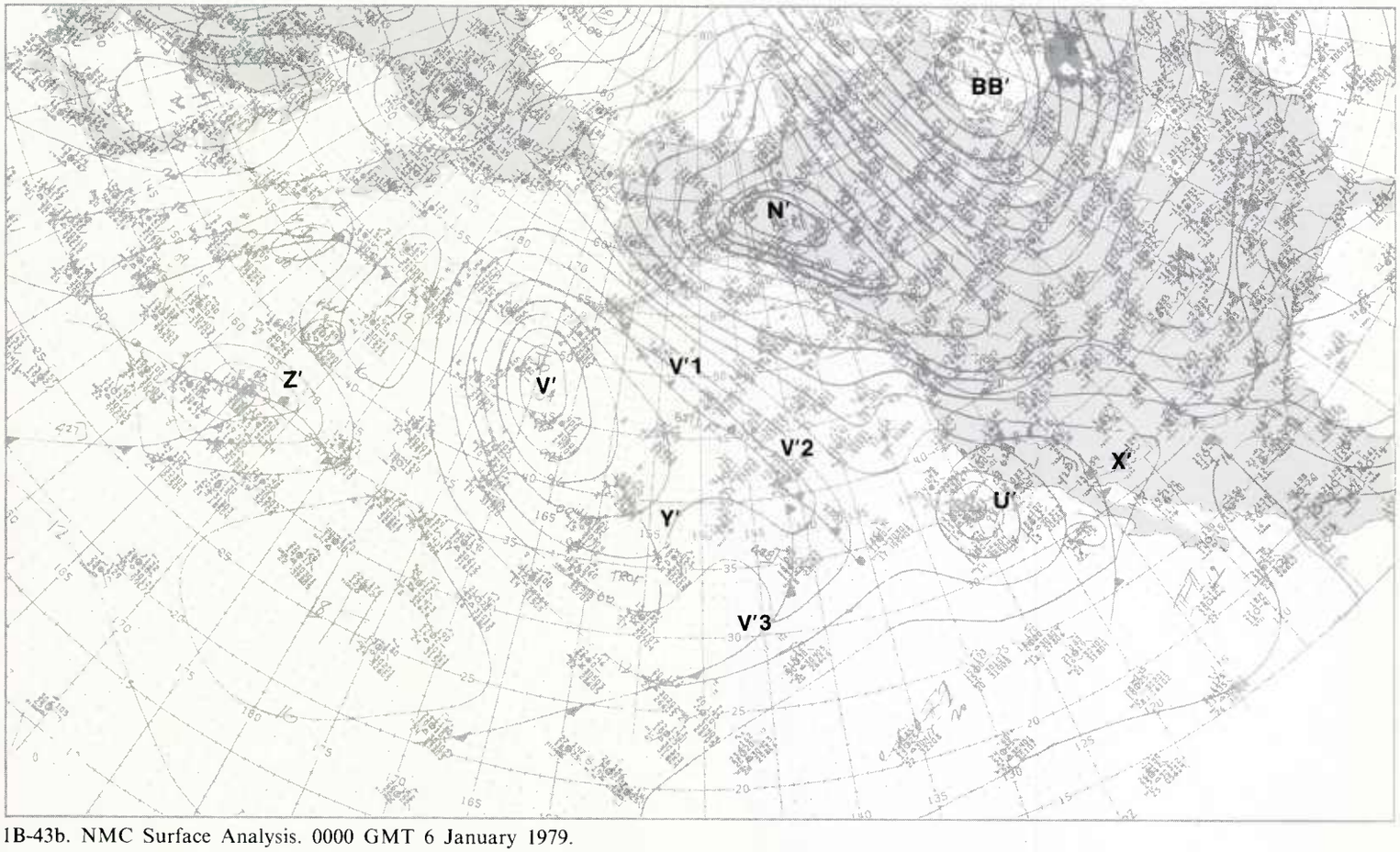

1B-43b. NMC Surface Analysis. 0000 GMT 6 January 1979.

500 mb

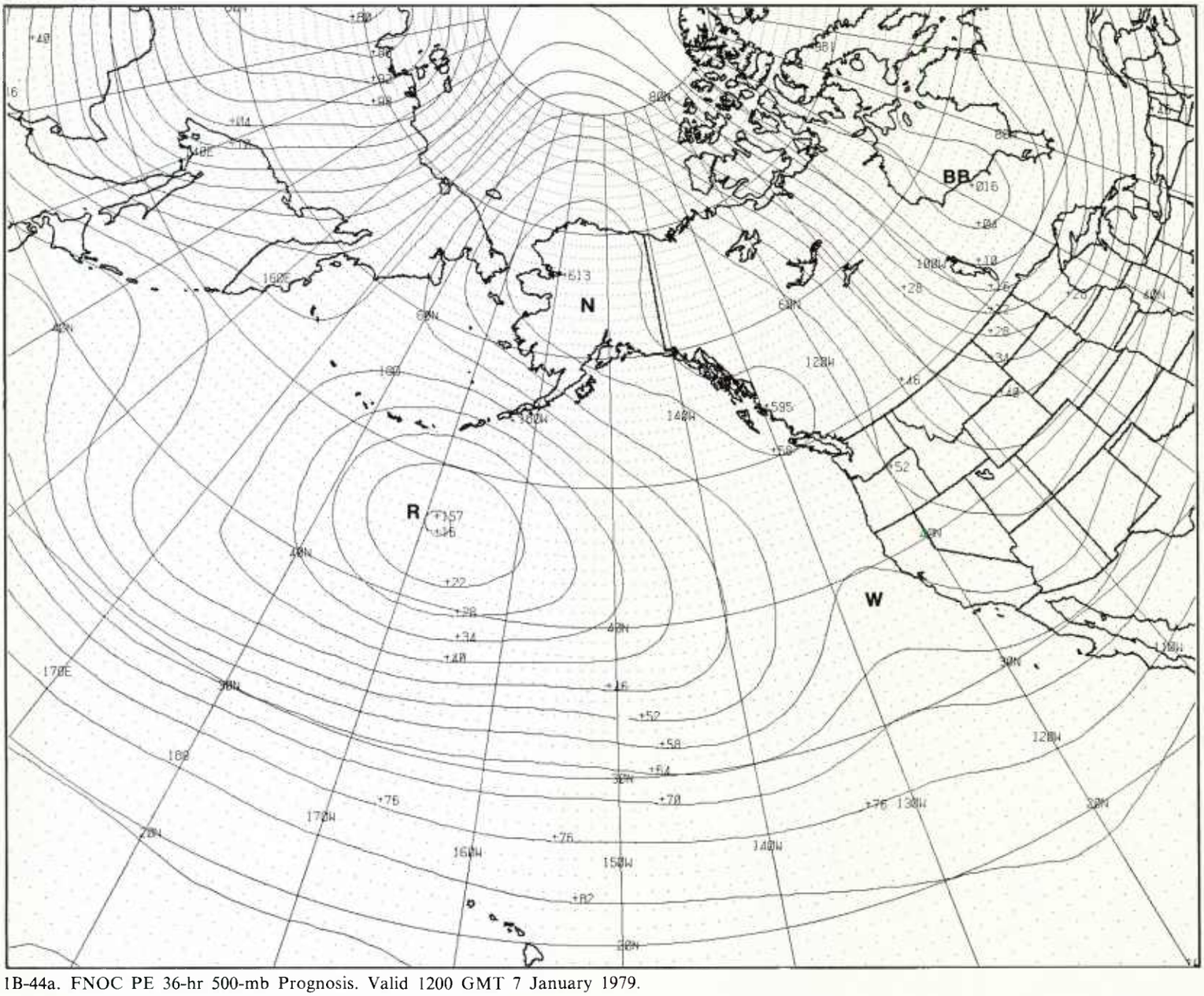

1B-44a. FNOC PE 36-hr 500-mb Prognosis. Valid 1200 GMT 7 January 1979.

500 mb

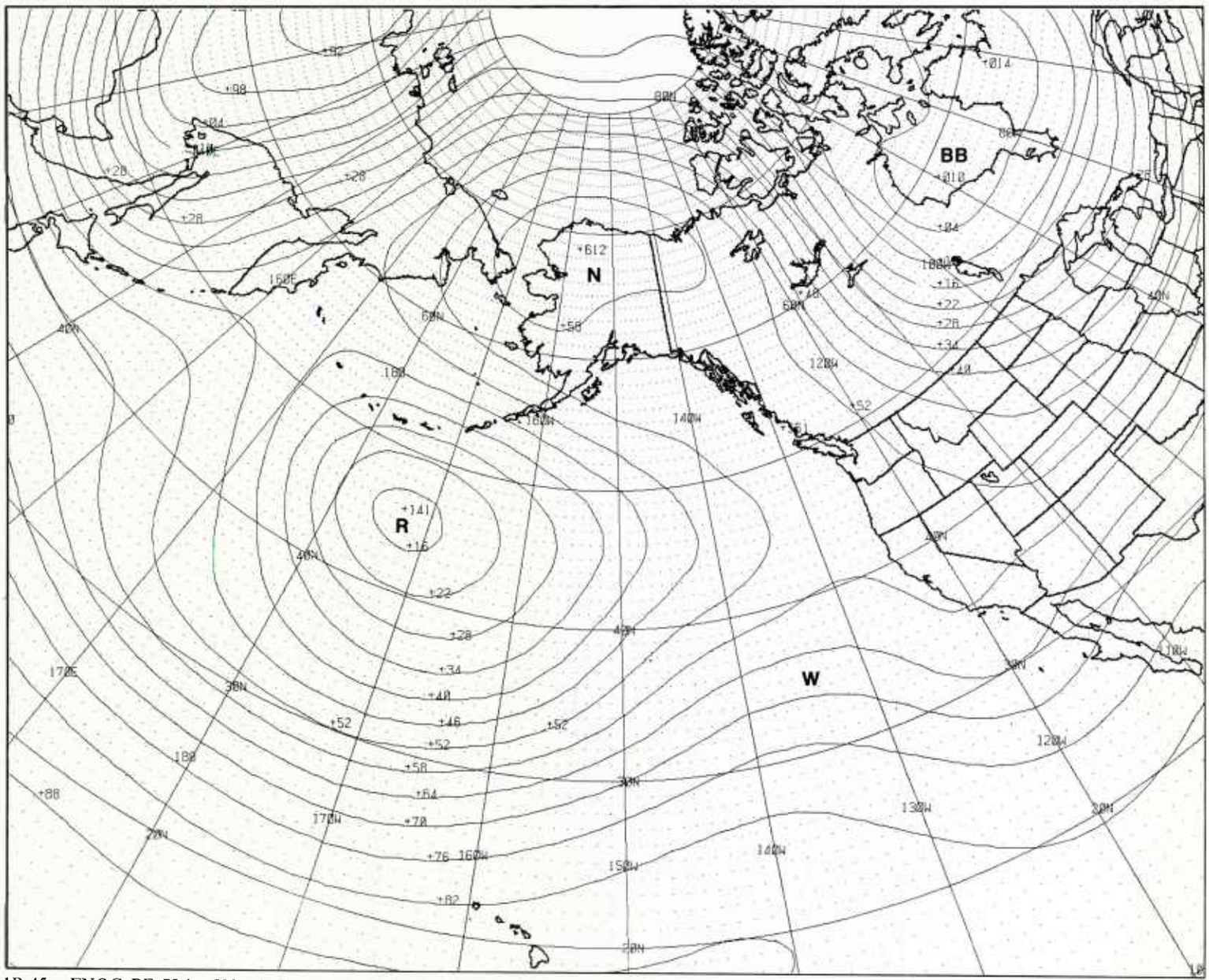

1B-45a. FNOC PE 72-hr 500-mb Prognosis. Valid 0000 GMT 9 January 1979.

7–8 January

During the first 36 hours of the forecast period, the 500-mb analyses (1B-46b, 47b, and 47d), show that the large synoptic-scale circulation features behave as forecast: a closed high-pressure system N is maintained over Alaska so that blocking persists at high latitudes; the major low **R** over the central Pacific is blocked and holds near 35°N, 170°W; the ridge **W** develops downstream, and strong zonal westerlies (closely-spaced height contours) are observed across the Pacific at mid latitudes. The pronounced waving of the westerlies over the central Pacific indicates that intense disturbances are present in the zonal flow.

With the major low **R** at 500 mb stalled over the central Pacific, the associated cloud vortex **V″** remains essentially stationary as shown in the satellite pictures, while short-wave disturbances **Z″** and **AA″** develop along the southern boundary of the low. The cloud vortex **Z″** advances slowly eastward in the weaker circulation around the center of the low **R** at 500 mb; however, the frontal cloudiness **Z″1** moves rapidly eastward because it is caught in the stronger zonal westerlies to the south. This difference in motion results in the elongated frontal band **Z″–Z″1**, which shows signs of dissipating. The enhanced cumulus area **AA″** (1B-46a) develops into the intense, small comma cloud **AA″** (1B-47a). This storm is located in the deepening low **AA** at 500 mb. As this low advances eastward it slows as it moves against the blocking ridge **W–N**, and the comma cloud pattern does not develop the clear-cut banding features of a major winter storm (1B-47c). The cloud vortex **X″** associated with the 500-mb trough **U** (1B-46b) over the western U.S., tends to dissipate as **U** merges with the long-wave trough along the eastern boundary of the block (1B-47d), while frontal cloudiness **X″1** moves rapidly eastward.

The effects of the re-established 500-mb blocking ridge **W–N** along the Pacific coast of North America on eastward moving disturbances is clearly evident in the satellite pictures. The frontal cloud bands **V″1** and **Y″1** (1B-46a) move eastward in the flow around the eastern periphery of the low **R** and shear-out, in succession, as they are forced against the blocking ridge (1B-47c). Note that the cloud vortex **V″** persists long after the connections with the frontal clouds to the east dissipate.

Toward the end of the 72-hour forecast period (1B-48a and 49a), the storm over the central Pacific intensifies dramatically, as evidenced by the development of a spiral cloud vortex **Z″** and a distinct frontal cloud band **Z″1** extending to the southwest. The rapid development of this storm occurred as the 500-mb short-wave low **Z** (1B-48b) passed south of the major low **R** and intensified in the southerly flow on the eastern side (1B-49b). A similar deepening of the storm **AA″** occurs (1B-48a and 49a) in the southerly flow along the western boundary of the blocking ridge along the West Coast, as the low **AA** (1B-48b and 49b) moves against the block. This system is most intense aloft, however, since there is no prominent trailing frontal cloud band emerging from the tail of the comma cloud **AA″** (1B-49a). The remnants of the frontal band **V″2** also dissipate against the block **W**.

continued on page 1B-50

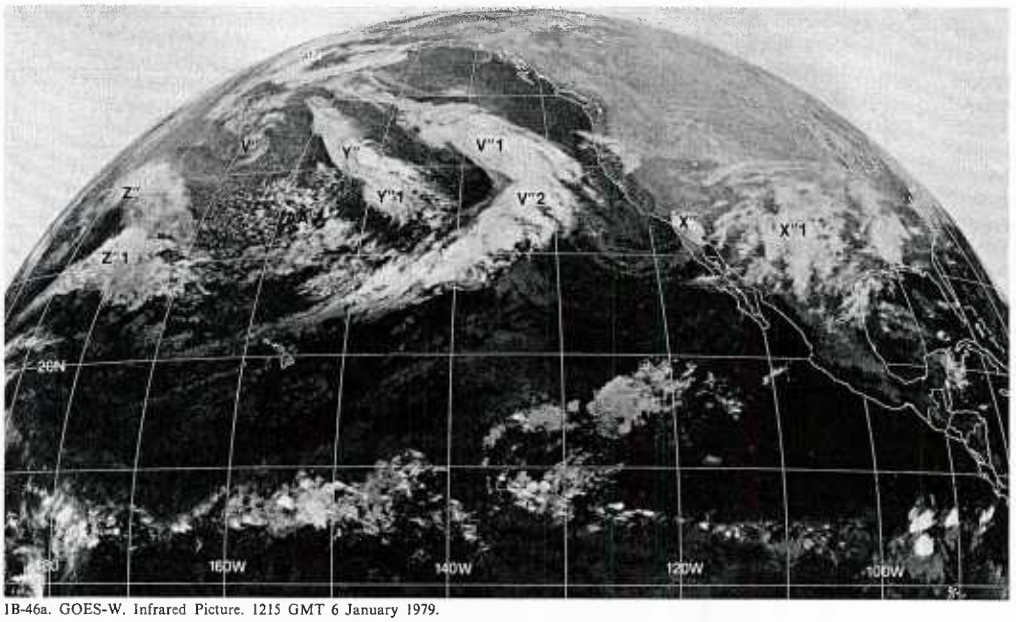

1B-46a. GOES-W. Infrared Picture. 1215 GMT 6 January 1979.

500 mb

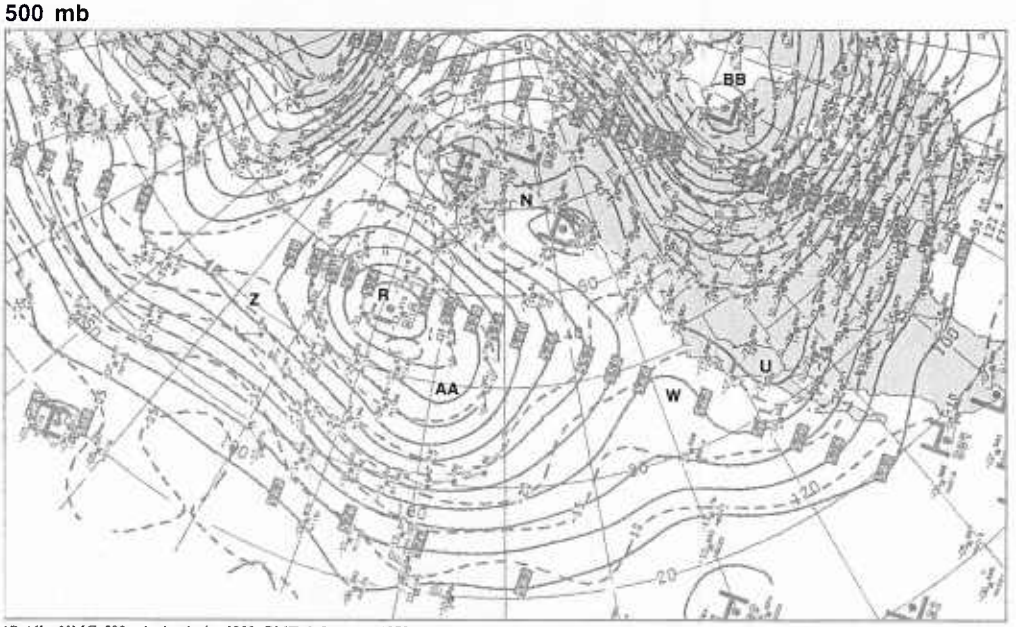

1B-46b. NMC 500-mb Analysis. 1200 GMT 6 January 1979.

Blocking Action: Late Phase

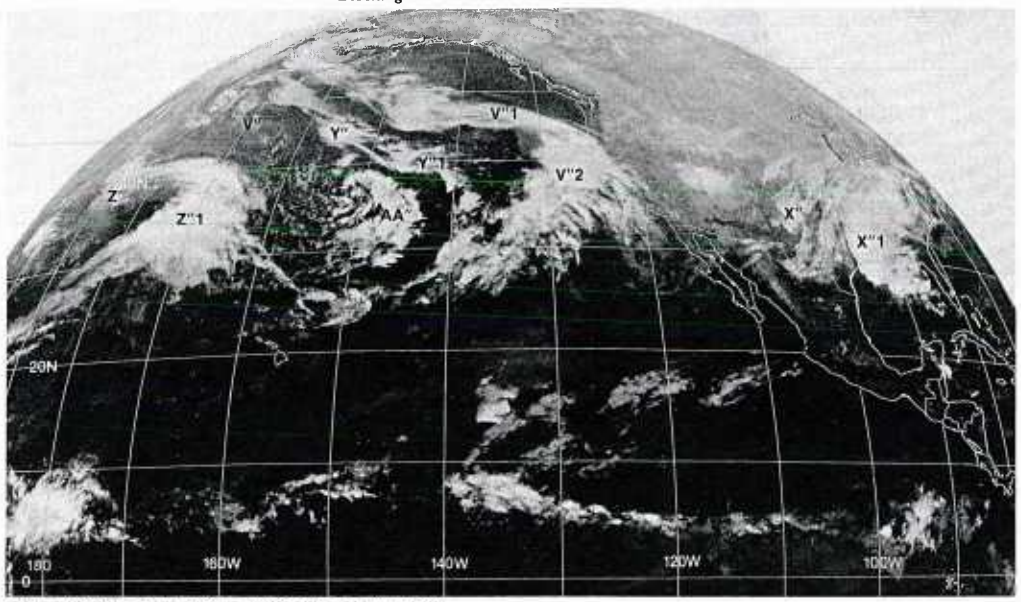

1B-47a. GOES-W. Infrared Picture. 0015 GMT 7 January 1979.

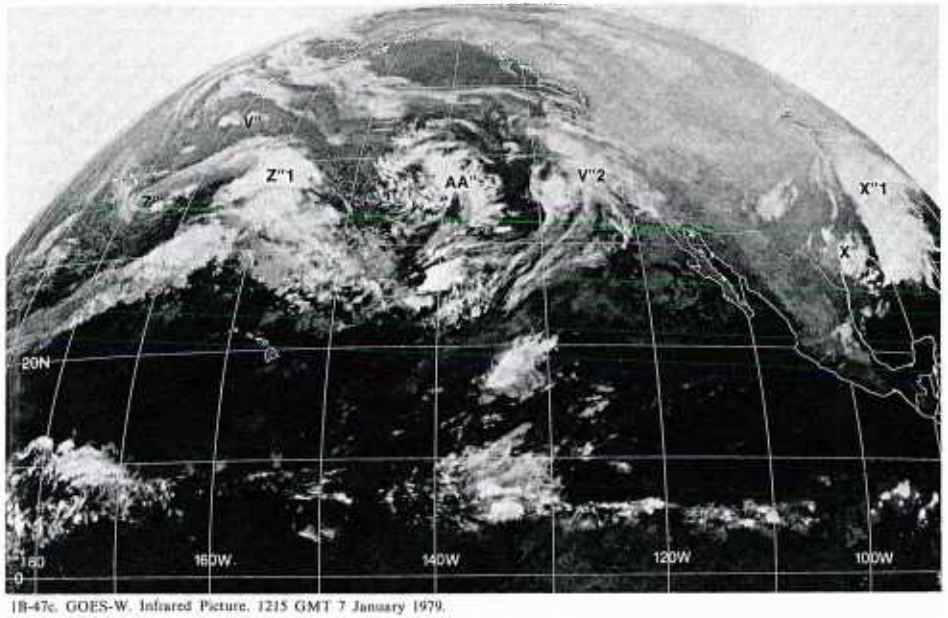

1B-47c. GOES-W. Infrared Picture. 1215 GMT 7 January 1979.

500 mb

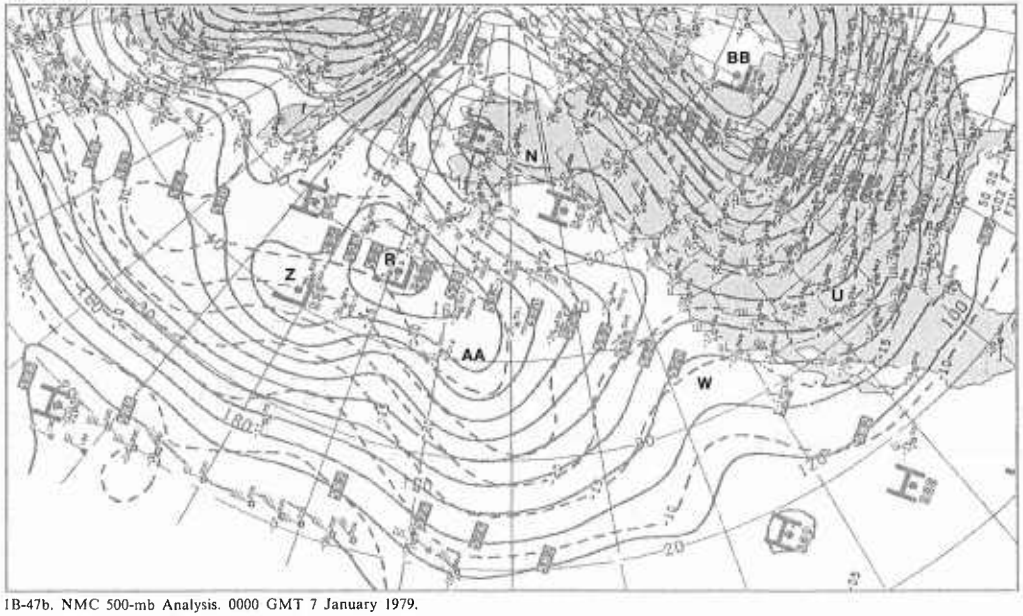

1B-47b. NMC 500-mb Analysis. 0000 GMT 7 January 1979.

500 mb

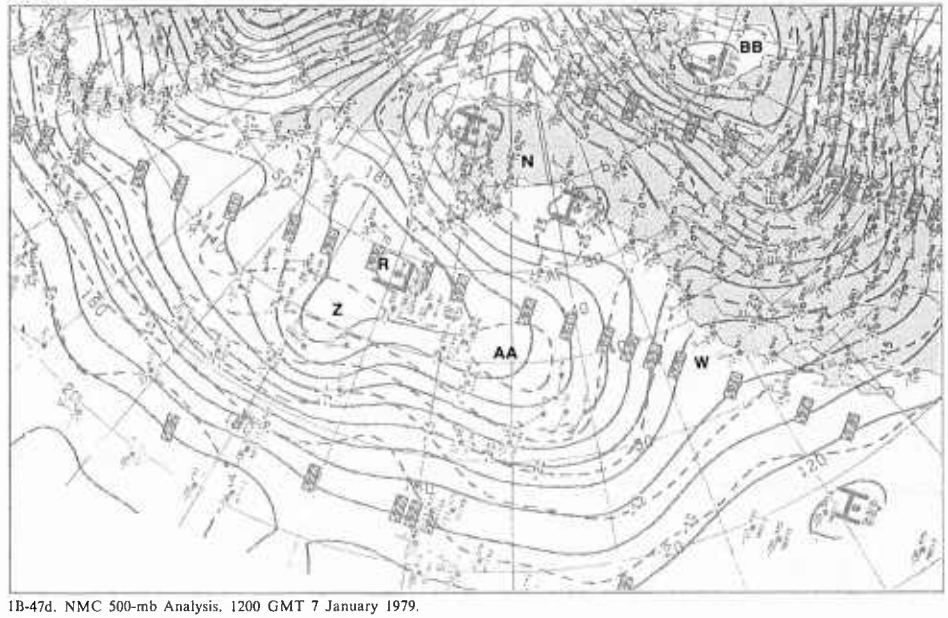

1B-47d. NMC 500-mb Analysis. 1200 GMT 7 January 1979.

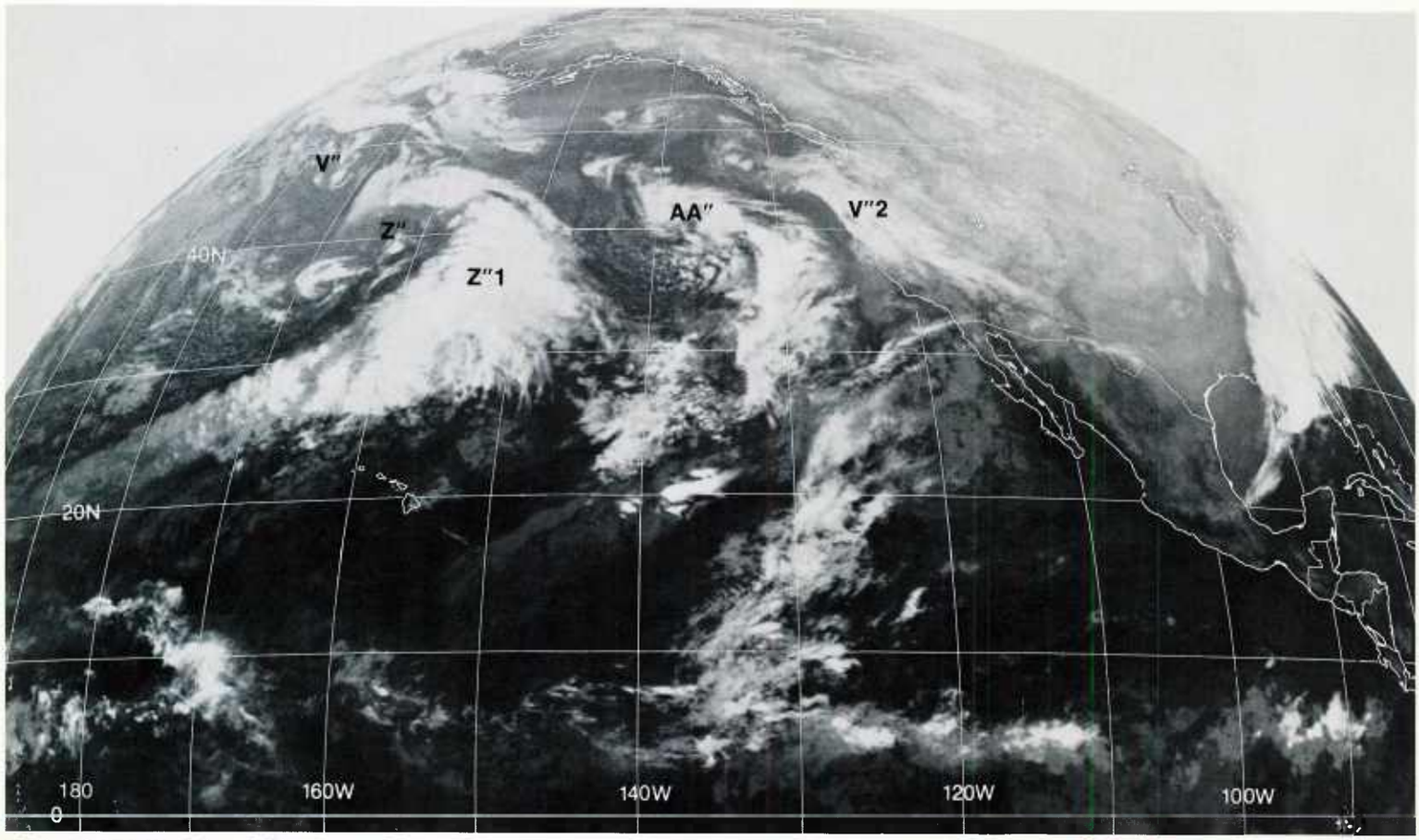

1B-48a. GOES-W. Infrared Picture. 0015 GMT 8 January 1979.

500 mb

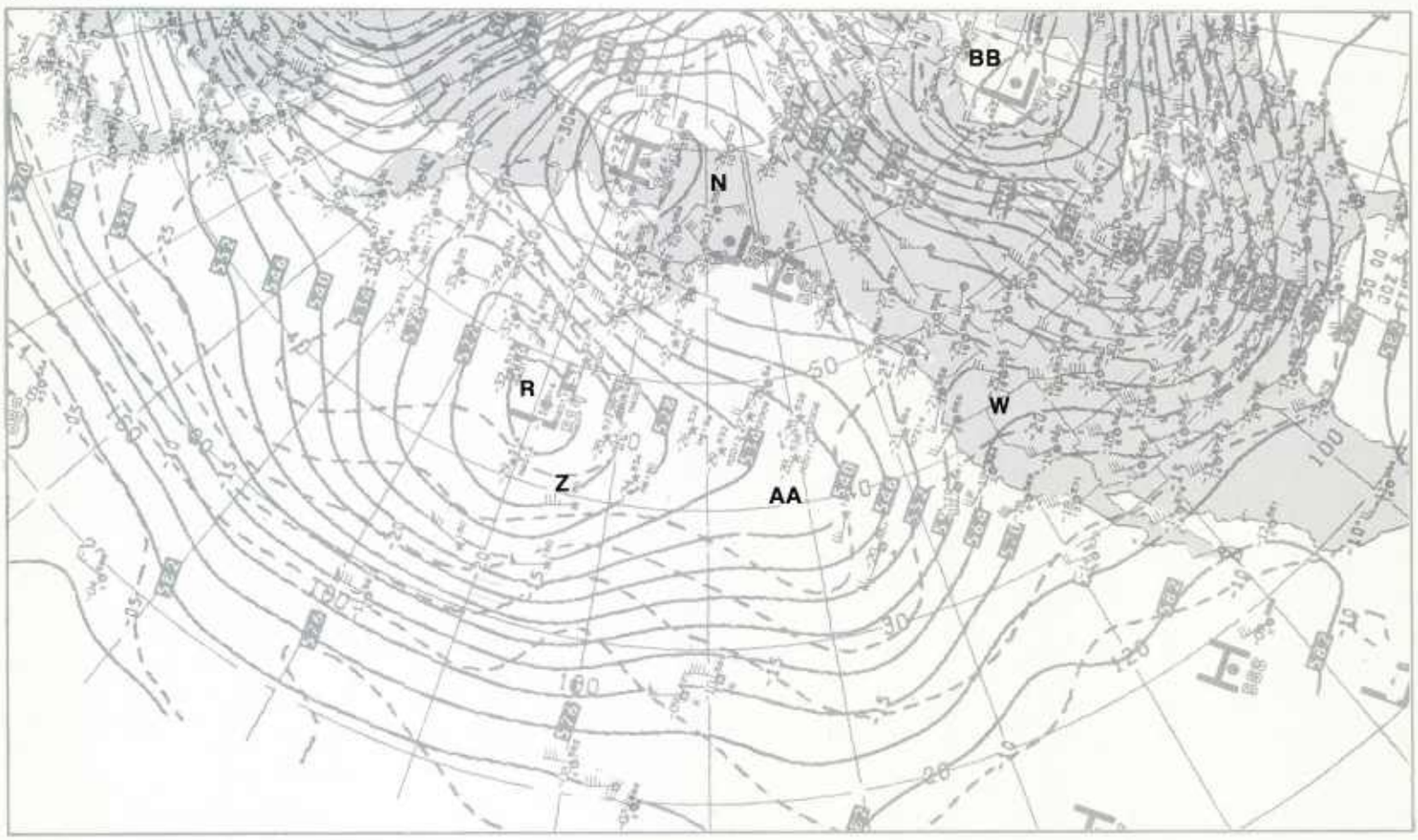

1B-48b. NMC 500-mb Analysis. 0000 GMT 8 January 1979.

Blocking Action: Late Phase

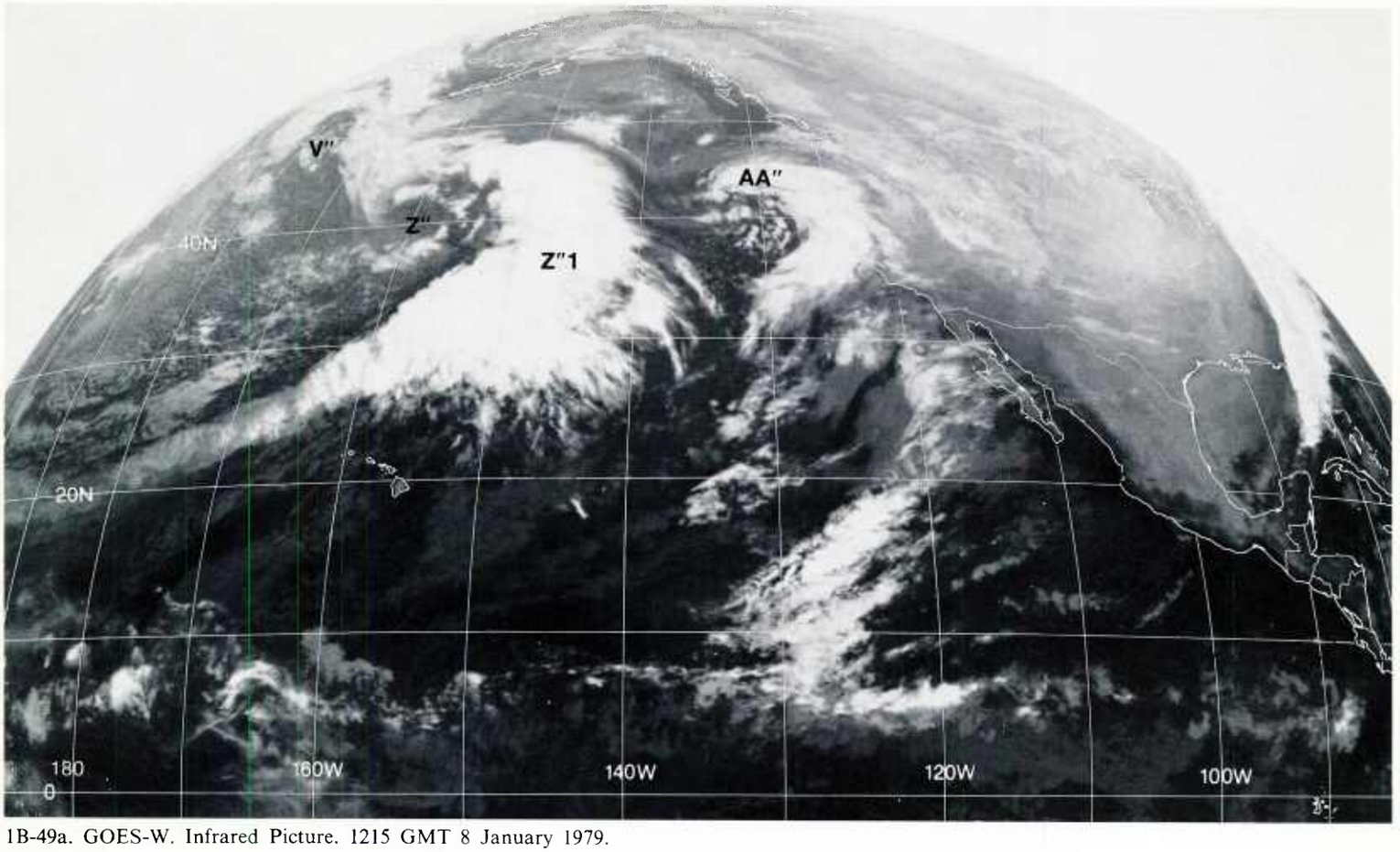

1B-49a. GOES-W. Infrared Picture. 1215 GMT 8 January 1979.

500 mb

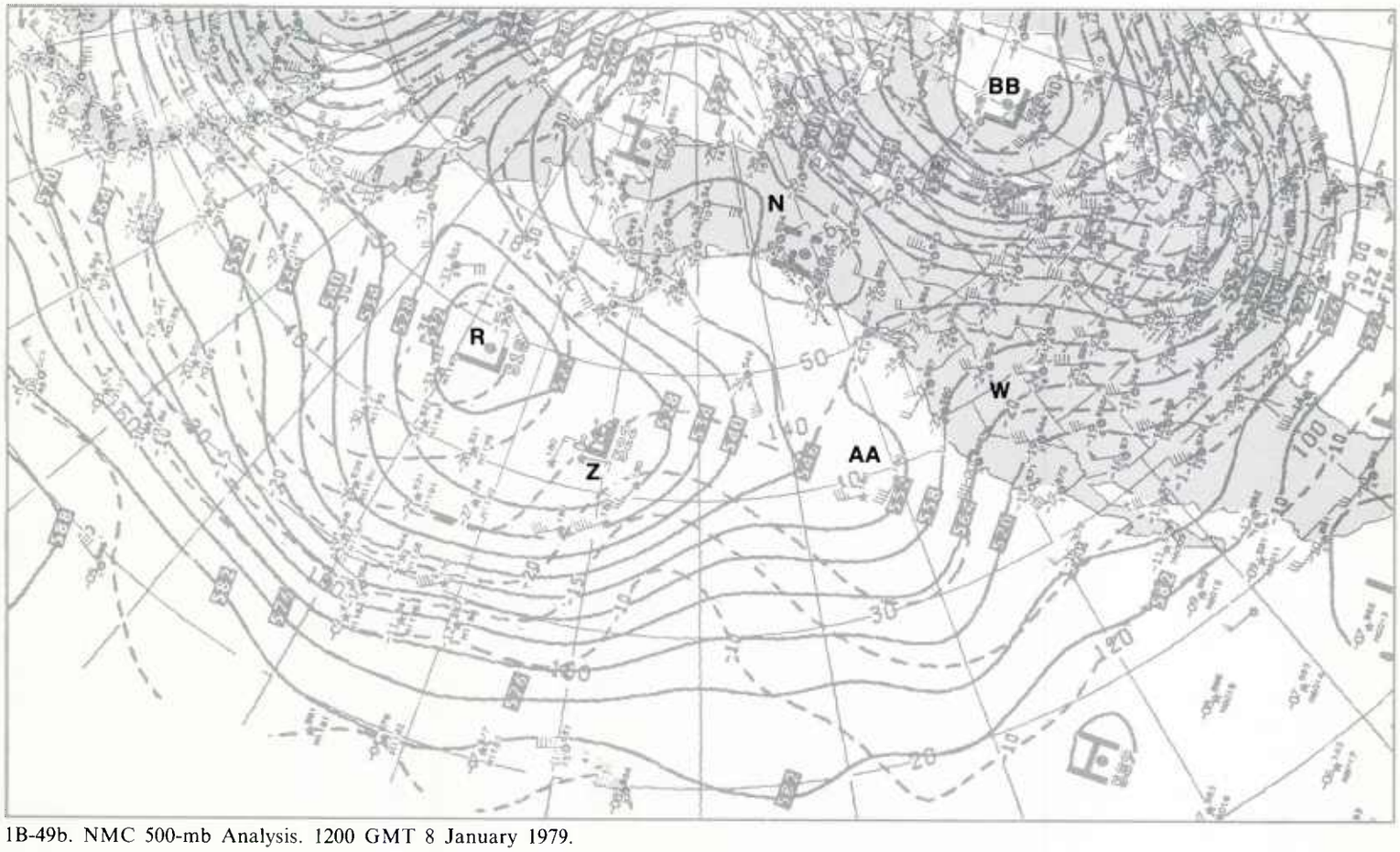

1B-49b. NMC 500-mb Analysis. 1200 GMT 8 January 1979.

Blocking Action: Final Phase

Blocking Action: Final Phase

Characteristic Features

1. *High-latitude block over Alaska retreats to the north over the Arctic Ocean.*
2. *Strong zonal westerlies are established at mid latitudes over the eastern Pacific.*
3. *Disturbances in the zonal flow at mid latitudes advance into the U.S.*
4. *Subtropical high-pressure cell is established over the eastern Pacific.*

9 January

An examination of the 500-mb analysis (1B-50b) shows that the location and pattern of the large synoptic-scale features compares satisfactorily with the 72-hour prognosis (1B-45a). The blocking high **N** is holding over Alaska; the major low **BB**, downstream of the block, has remained nearly stationary, as has the low upstream of the block which, however, shows two centers **R** and **Z** instead of the single forecast center **R**. The sharp ridge **W** along the U.S. west coast was not forecast. This ridge moved eastward more rapidly than was expected and has temporarily re-established a blocking ridge **W-N** along the Pacific coast. Strong zonal westerlies (closely-spaced height contour lines) are observed at mid latitudes over the Pacific, as forecast.

At 300 mb (1B-50a), the strong zonal westerlies show wind speeds in excess of 130 kt at mid latitudes over the Pacific. In particular, the jet streak **PJS-1** (110 kt) extends from 140° E to 160° W over the eastern Pacific. Downstream of the block, strong polar westerlies are located to the south of the major low **BB**, but the wind speeds have dropped off significantly in the northwest flow between this low and the high-latitude block (compare 1B-50a with 1B-42a). There has been a similar decrease in the wind speeds of the southerly flow upstream of the block. With this breakdown of the high-latitude polar jet moving around the block, the northern branch of the split in the zonal westerlies that was a main feature of the block has dissipated, and the blocking event over the eastern Pacific is in its final phase.

Note that there is a strong polar jet **PJS-2** at 300 mb associated with the deep 500-mb low **CC** located off the Asiatic mainland. This jet stream development is a significant feature in the changing flow pattern over the Pacific, and the jet is advancing to the south and to the rear of the major 500-mb low **R-Z** over the central Pacific. On the surface analysis (1B-51b), the mature storm **CC′** over the northwest Pacific confirms that the 500-mb low aloft is a major development. The cloud system accompanying the storm does not appear in the satellite picture (1B-51a), because it is not in the field-of-view of GOES-W.

The double-center 500-mb low **R-Z**, over the central Pacific, is reflected at the surface by an elongated surface pressure circulation system **R′-Z′**. The surface storm **Z′** is the major winter storm that developed in the western quadrant of the 500-mb low aloft. The satellite picture shows a distinct cloud vortex **Z″** and frontal cloud band **Z″1** curving to the southwest. The bright cloudiness along this frontal band is cirrus debris from deep convection produced in the baroclinic zone associated with the strong polar jet **PJS-1** paralleling the frontal zone. The cloud vortex **R″** in the satellite picture has developed as evolution of vortex **V″** (see 1B-49a) interacting with surrounding cloud vorticity features near the center of the 500-mb low **R**. Cloudiness from the vortex **Z″** has spread along the northern boundary of the 500-mb low to the vicinity of **R″**.

In the satellite picture (1B-51a), the comma cloud **AA″** is retaining its distinct features (see 1B-49a). There is only a weak low **AA′** and frontal system on the surface analysis (1B-51b). The absence of a prominent tail extending to the south from the comma cloud, such as observed with the cloud vortex **Z″** upstream, confirms that this system continues to be most intense aloft. At 500 mb, the short-wave trough **AA** associated with this storm is moving against the temporary blocking ridge **N-W**, and warm air advection is occurring to the west (rear) of the trough which would be expected to cause a filling of the trough. Note also that the closed vortex center of the disturbance **AA″** is located in the left rear quadrant of the jet streak **PJS-3**, at 300 mb. These conditions are unfavorable for the further development of this storm.

The 36-hour (1B-52a) and 72-hour (1B-53a) 500-mb prognoses show that the closed high center **N** over Alaska will move north over the Arctic Ocean, and strong polar westerlies will dominate at mid latitudes across the Pacific and the U.S. This indicates an end to the blocking event over the eastern Pacific. Disturbances in the polar westerlies should have a clear track into the U.S. by the end of the forecast period.

The new major low **CC** at high latitudes over the western Pacific is forecast to deepen and advance slowly eastward (1B-53a). This will maintain strong polar westerlies upstream of the major low **R** over the central Pacific. Cold air advection will occur to the rear of this low, which will result in a deep trough. As the trough deepens, warm air advection will increase downstream of the trough and a subtropical ridge of high pressure **DD** is forecast to develop over the eastern Pacific.

continued on page 1B-54

300 mb

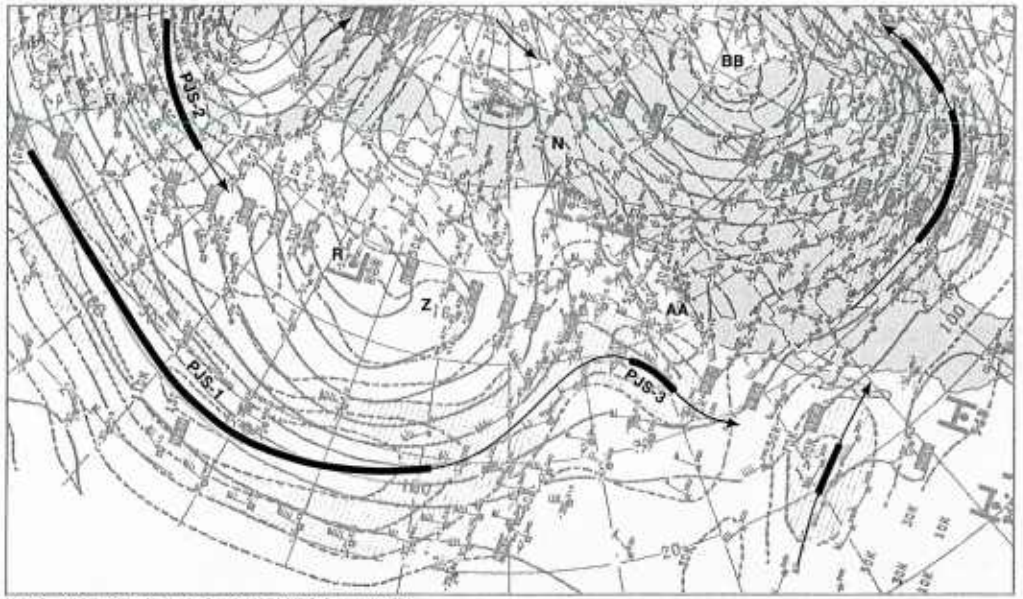

1B-50a. NMC 300-mb Analysis. 0000 GMT 9 January 1979.

500 mb

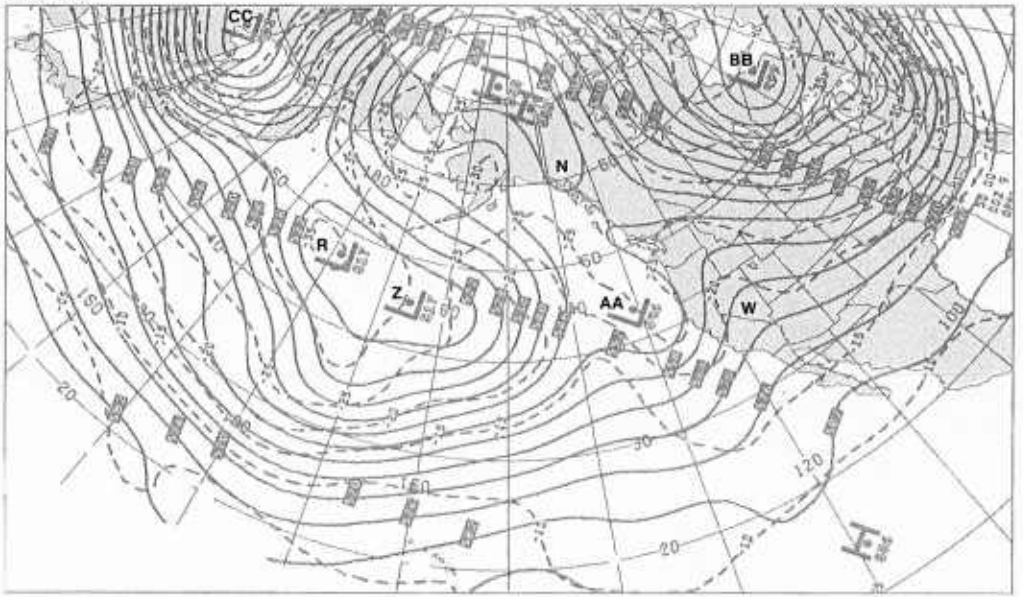

1B-50b. NMC 500-mb Analysis. 0000 GMT 9 January 1979.

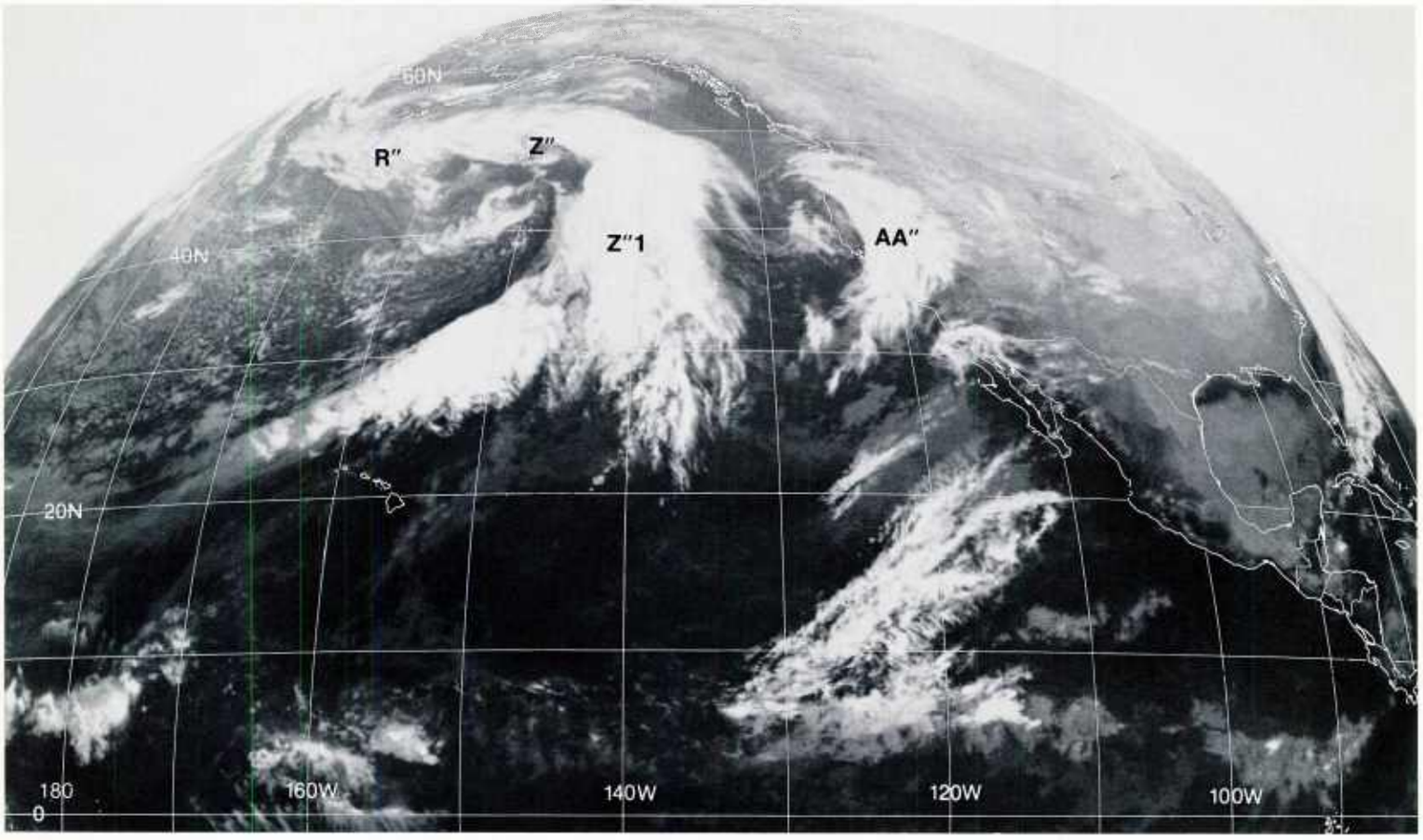

1B-51a. GOES-W. Infrared Picture. 0015 GMT 9 January 1979.

surface

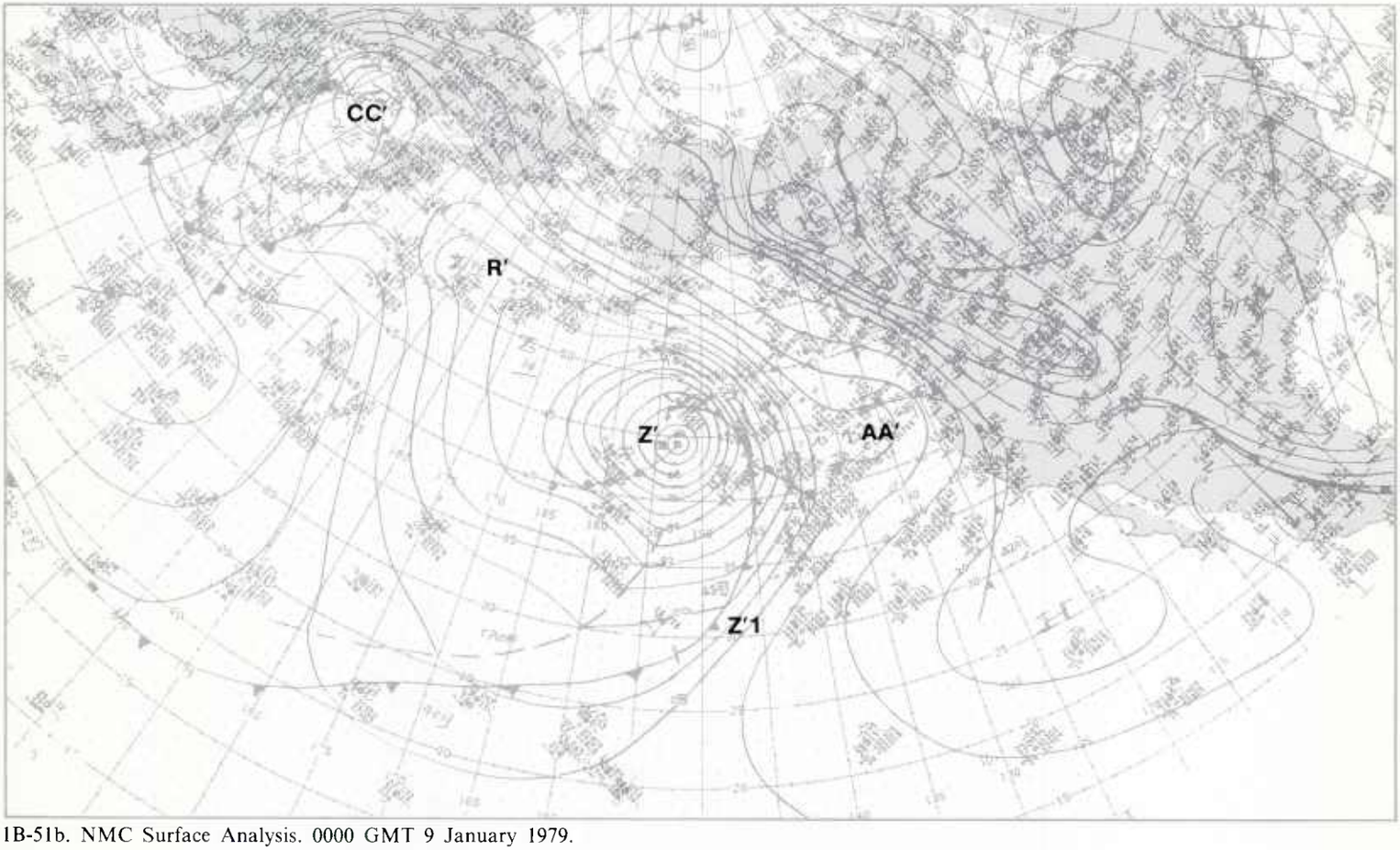

1B-51b. NMC Surface Analysis. 0000 GMT 9 January 1979.

The mean 700-mb contours for the first week of January (1B-53a) show the highly-amplified blocking ridge along the west coast of North America. This ridge moved from the eastern Pacific (1B-28b) to the west coast of North America forming a barrier to eastward moving disturbances in the westerlies, from low latitudes to the Arctic Ocean. The strong northwesterly flow downstream of the block blanketed the U.S. with repeated surges of Arctic air masses that resulted in record or near-record low temperatures over most of the U.S.

During the second week of January (1B-53b), the high-latitude portion of the block moved to the north over the Arctic Ocean. This allowed the westerlies to penetrate below the block into the continental U.S., and the mid-latitude block was eliminated. The movement of the deep low from Siberia (1B-53a) to the Asiatic coast (1B-53b) contributed significantly to the increased speed of the westerlies across the Pacific. In contrast to the first week of January, eastward moving disturbances in the westerlies, under the intensified zonal westerlies, had an open channel from the Pacific into the U.S.

Reference

Wagner, A.J., 1979: Weather and circulation of January 1979. *Mon. Wea. Rev.*, **107**, 354–360.

500 mb

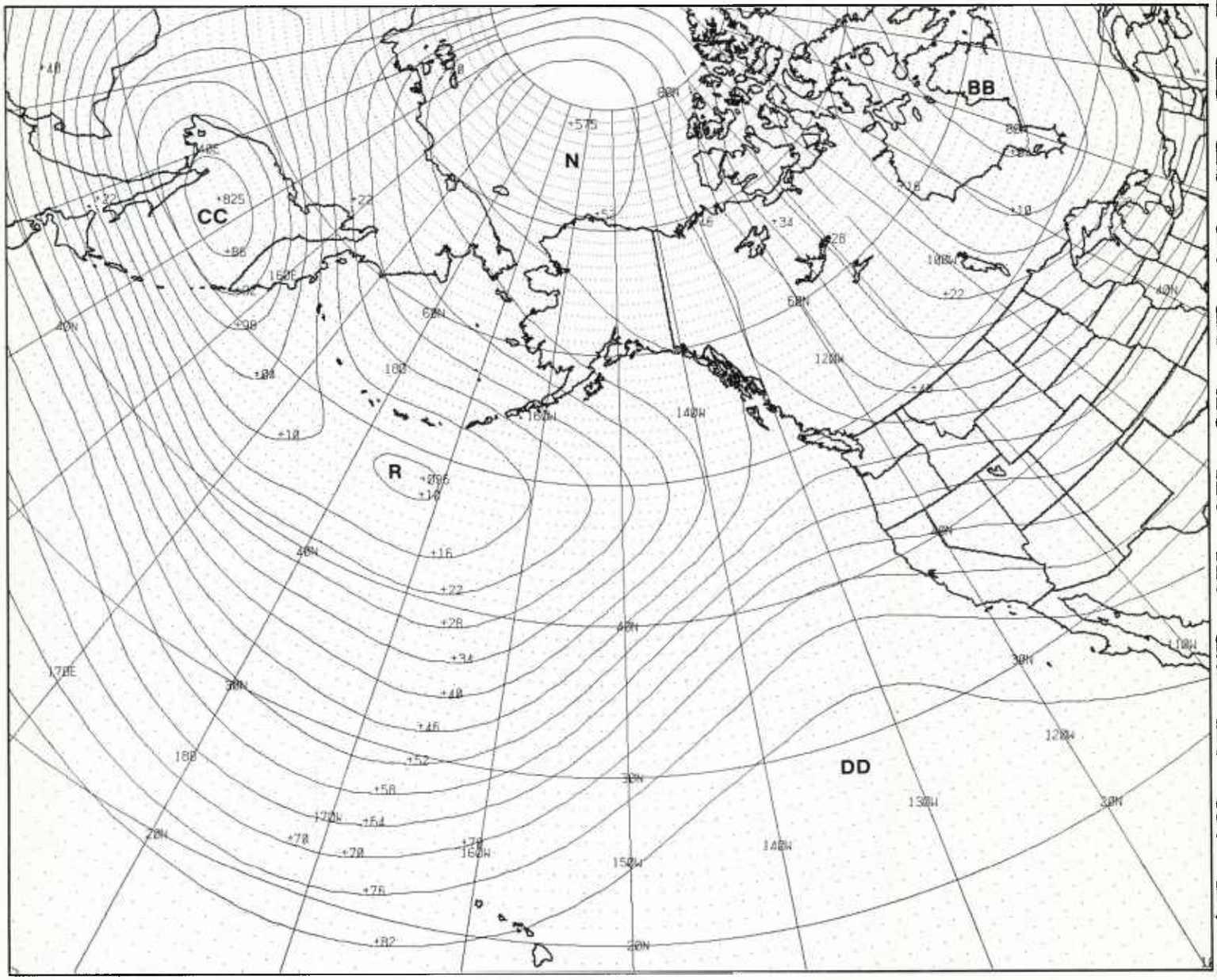

1B-52a. FNOC PE 36-hr 500-mb Prognosis. Valid 1200 GMT 10 January 1979.

Blocking Action: Final Phase

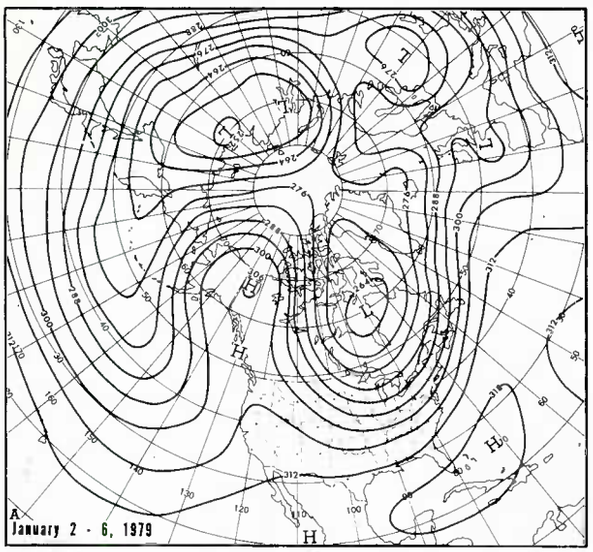

1B-53a. Mean 700-mb Contours for 2–6 January 1979. (After Wagner, 1979.)

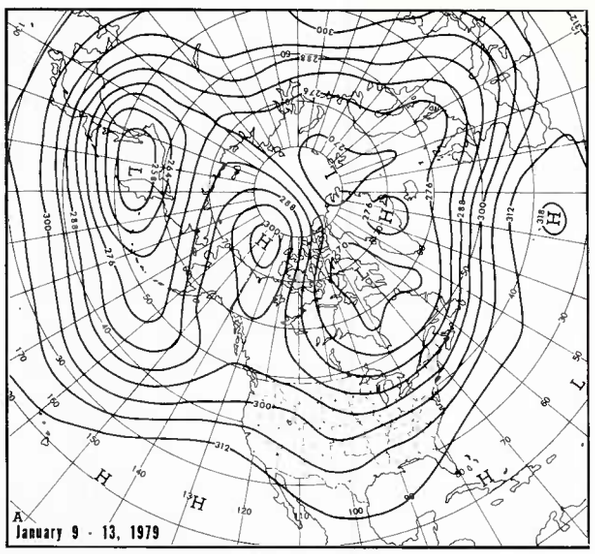

1B-53b. Mean 700-mb Contours for 9–13 January 1979. (After Wagner, 1979.)

500 mb

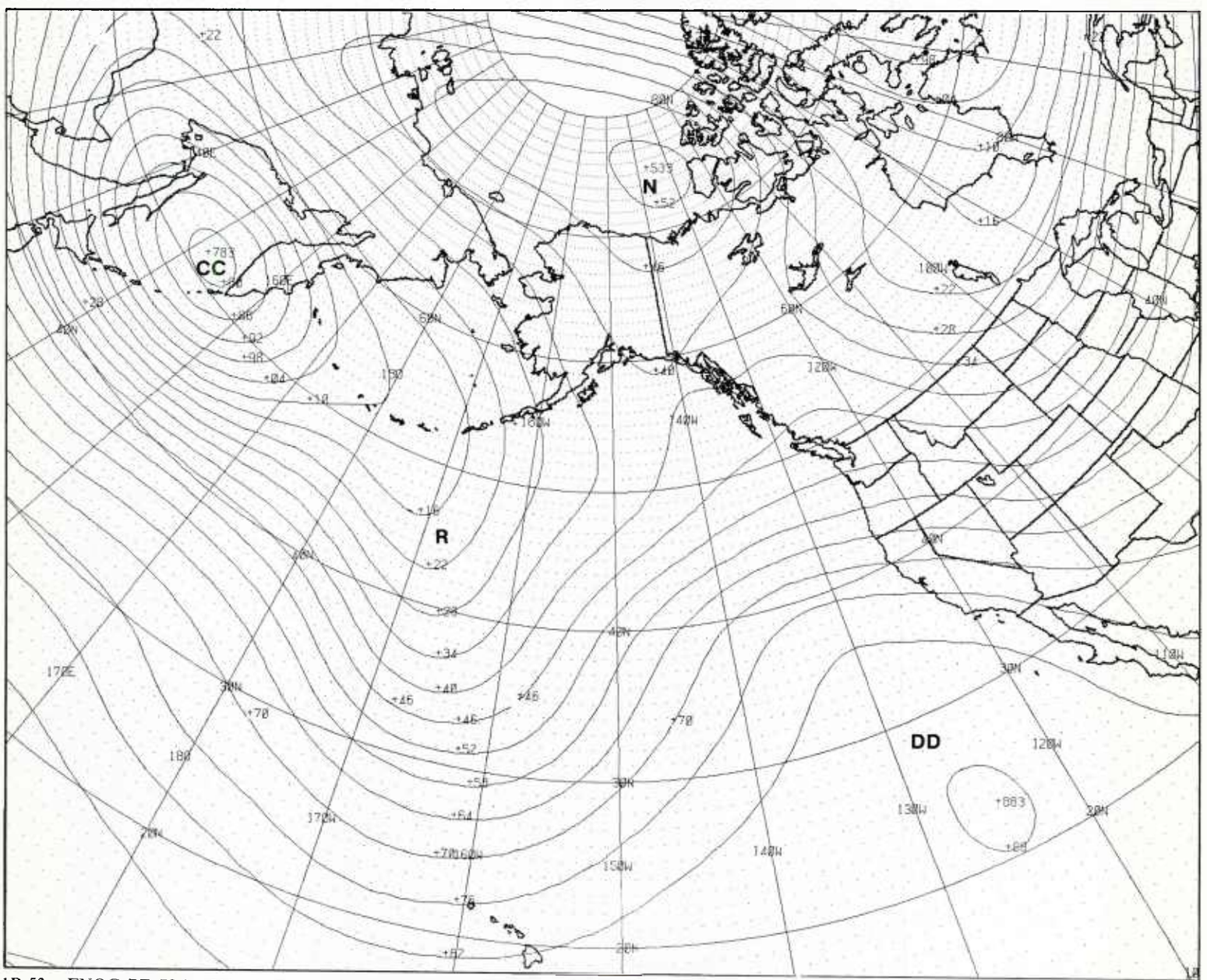

1B-53c. FNOC PE 72-hr 500-mb Prognosis. Valid 0000 GMT 12 January 1979.

10–11 January

During the first 36 hours of the forecast period, the large-scale features at 500 mb (1B-54b, 55b, and 55d) develop as forecast: the closed high center **N** over Alaska moves to the Arctic Ocean; the major low centers **CC**, **R**, and **Z** upstream of the high-latitude block and **BB** downstream of the block progress eastward; and strong polar westerlies (closely-spaced height contour lines) are observed over the central Pacific. Note that the vorticity comma **AA″** (1B-54a), which had shown a distinct cloud pattern (1B-51a), dissipates (1B-55c) as the subtropical ridge **DD** builds and forces the low **AA** eastward, where it merges with the northwesterly flow around the major low **BB**.

The cloud vortex **Z″** (1B-54a) is associated with the disturbance **Z** in the eastern periphery of the major low **R** (1B-54b). This disturbance is caught in the southerly flow in the eastern quadrant of the low **R** and is advected rapidly to the north where it dissipates against the temporary block **DD–N**. As the low **Z** dissipates against the block, the spiral cloud bands of the vortex **Z″** break up (1B-55c).

As the 500-mb low **Z** moves northward and dissipates against the block **DD–N**, the low **R** moves eastward toward the ridge **DD**. The pressure gradient tightens between these systems, and an increase in the speed of the mid-latitude westerlies (closely-spaced height contour lines) is observed between 160° W and 130° W (1B-55d). This process intensifies the baroclinic zone along the eastern periphery of the low, and a bright frontal cloud band **Z″1–Z″2–Z″3** (1B-55a), indicating an active frontal zone, is observed extending from the West Coast to south of Hawaii.

To the south of the cloudy area **R″** (1B-54a), an enhanced area of convection **EE″** has formed in the polar airflow, which is associated with a short-wave disturbance **EE** at 500 mb (1B-54b). This disturbance has developed in the westerlies to the south of the major low **R**. The bulge into the cold air **FF″** identifies another short-wave disturbance in the westerlies; however, this system has formed along the baroclinic frontal zone **Z″1–Z″3**. This storm develops slowly and does not show the typical spiral bands of a developing vortex (1B-55c). On the other hand, the storm **EE″** develops rapidly and remains entirely within the cold air north of the frontal cloud band. Still another cloud vortex system **GG″** is observed developing in the polar airstream upstream of the major low **R**.

Toward the end of this 72-hour forecast period (1B-56b and 57b), the strong southwesterlies (closely-spaced height contour lines) observed over the eastern Pacific (1B-55d) have become more zonally oriented, as the westerlies penetrate further inland over the continental U.S. The new storm **GG″** over the central Pacific shows signs of continued intensification, as new spiral cloud bands develop around the circulation center. The storm **EE″**, however, dissipates against the high-latitude block **N**, and the minor short-wave disturbances **FF″**, **HH″**, and **II″**, which have developed along the baroclinic zone **Z″1–Z″3**, move rapidly eastward in the strong zonal flow developing across the U.S.

continued on page 1B-58

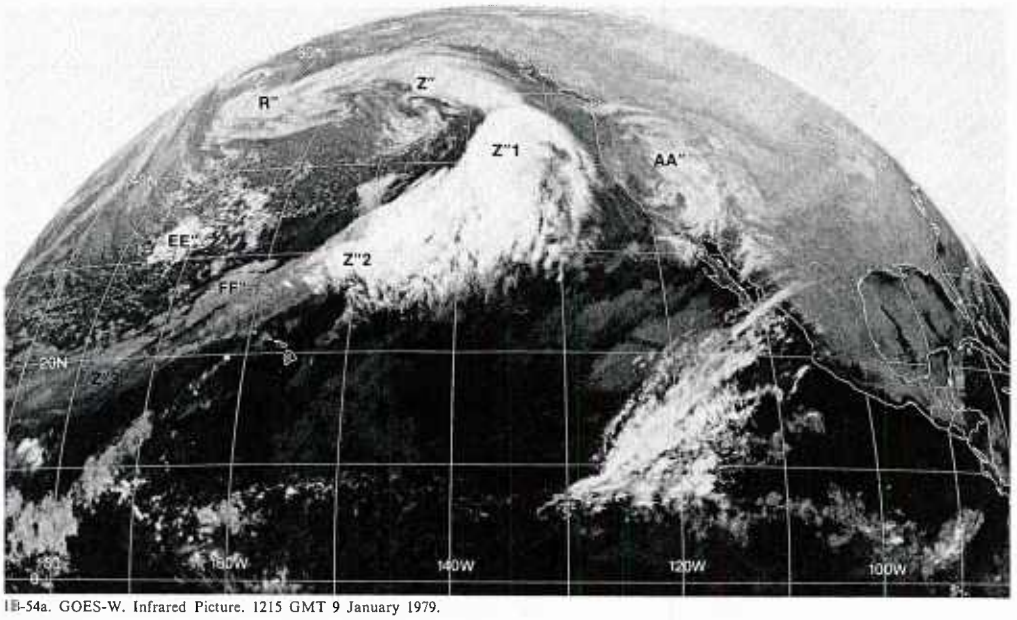

1B-54a. GOES-W. Infrared Picture. 1215 GMT 9 January 1979.

500 mb

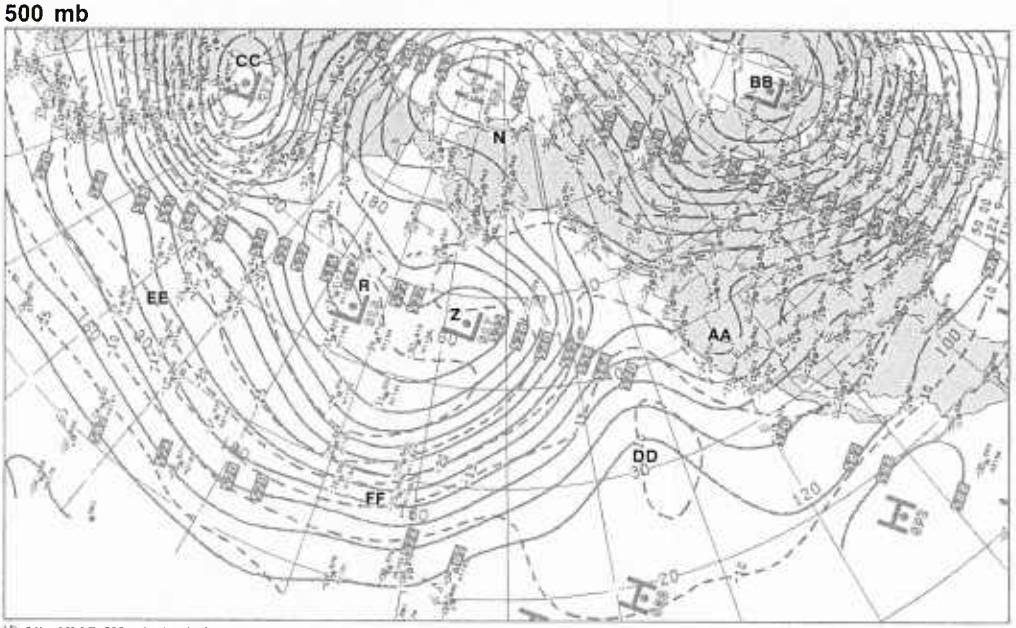

1B-54b. NMC 500-mb Analysis. 1200 GMT 9 January 1979.

Blocking Action: Final Phase

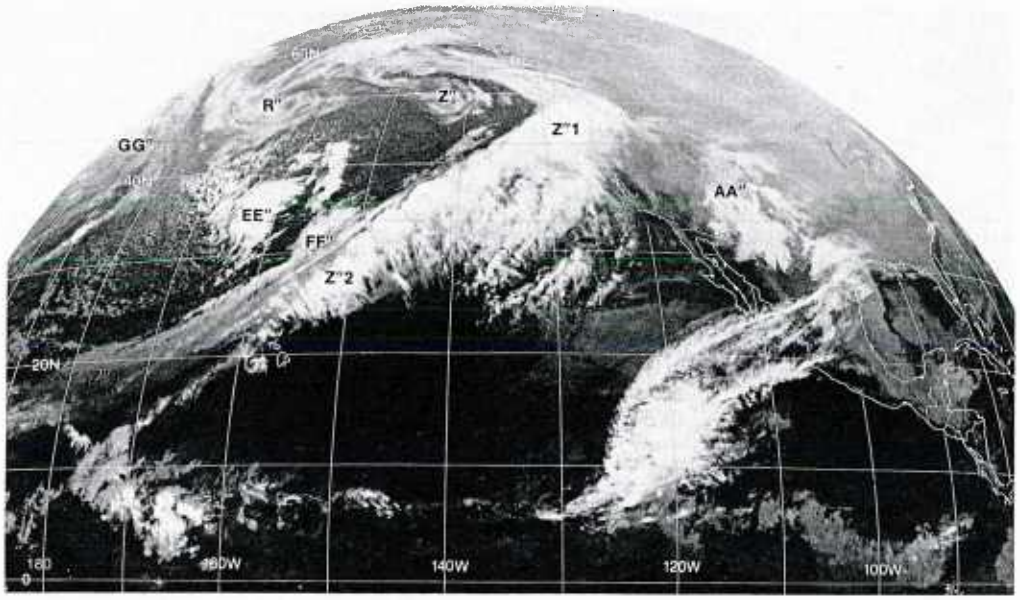

1B-55a. GOES-W. Infrared Picture. 0015 GMT 10 January 1979.

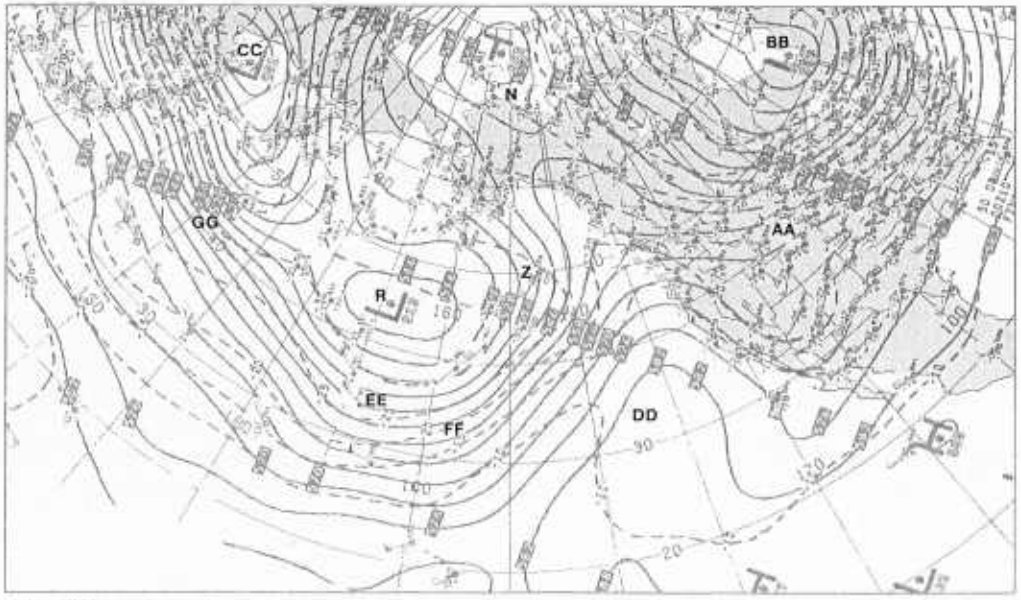

1B-55b. NMC 500-mb Analysis. 0000 GMT 10 January 1979.

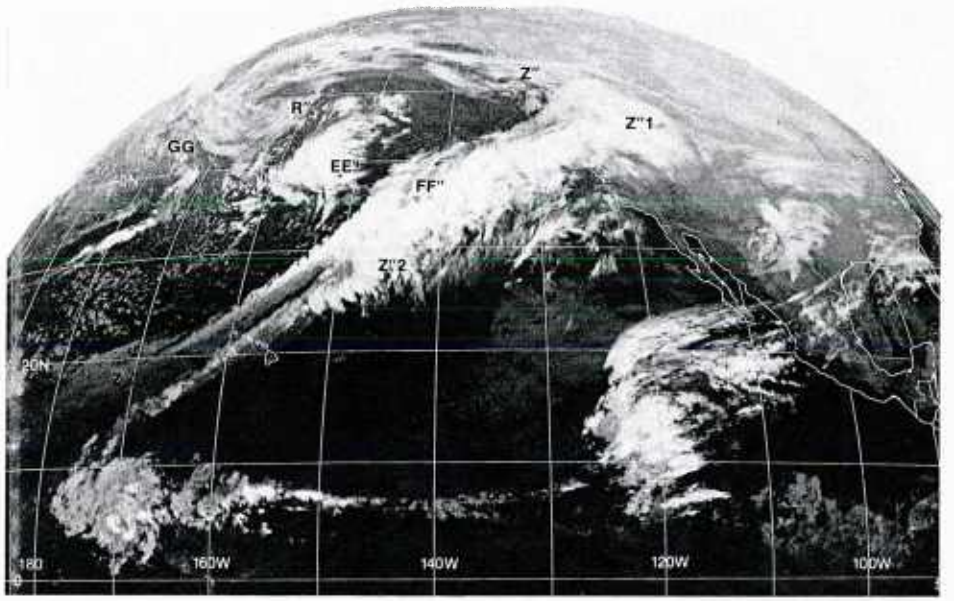

1B-55c. GOES-W. Infrared Picture. 1215 GMT 10 January 1979.

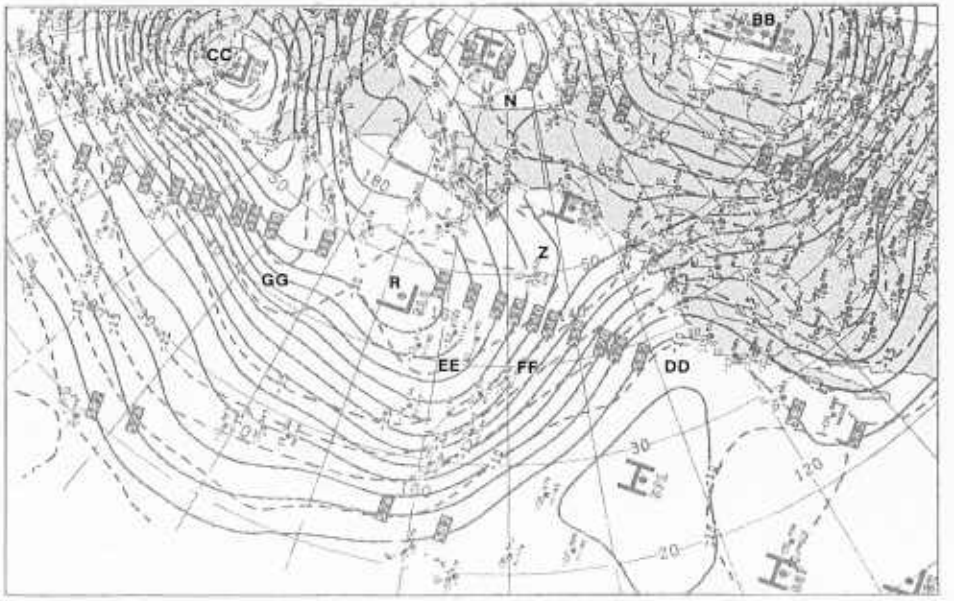

1B-55d. NMC 500-mb Analysis. 1200 GMT 10 January 1979.

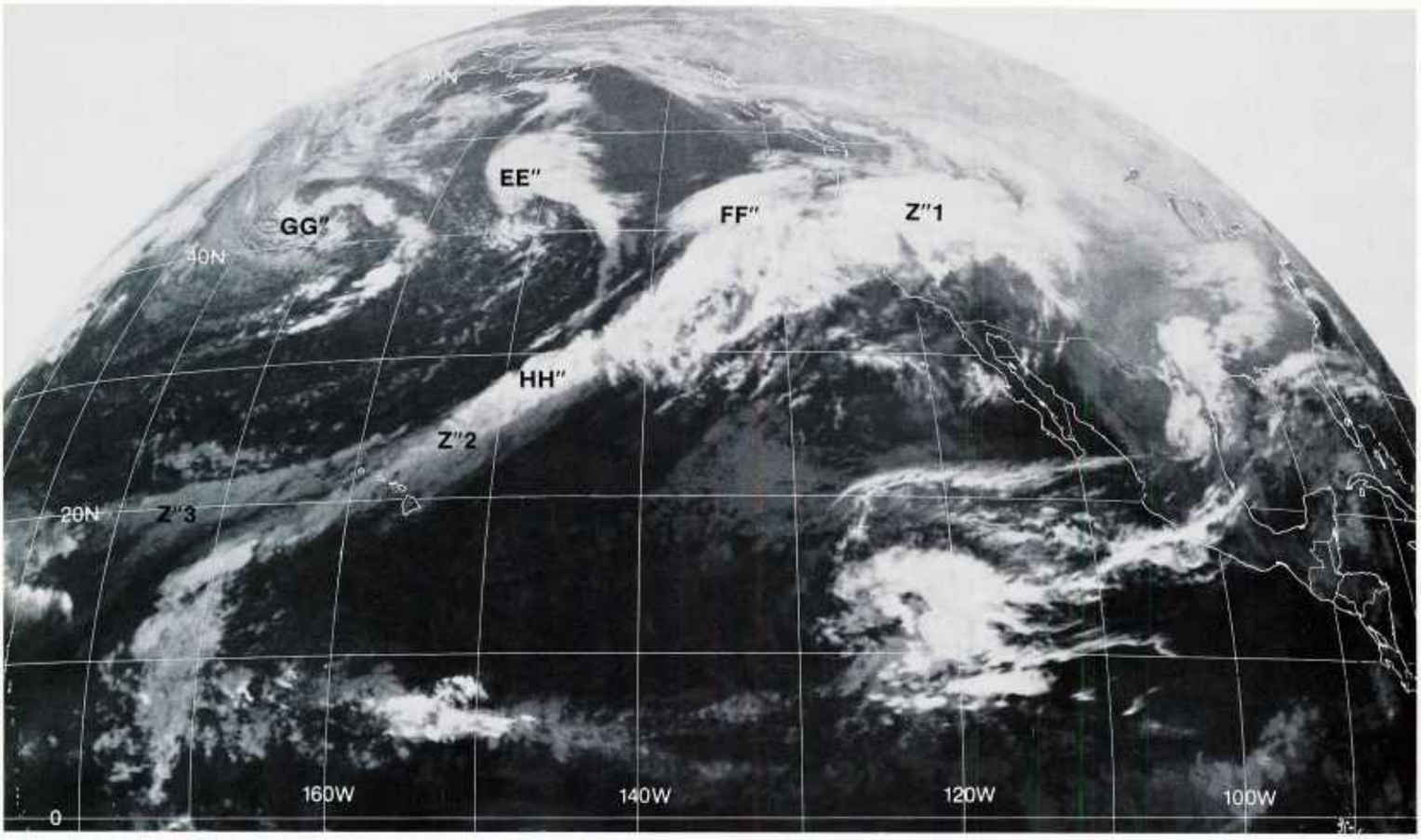

1B-56a. GOES-W. Infrared Picture. 0015 GMT 11 January 1979.

500 mb

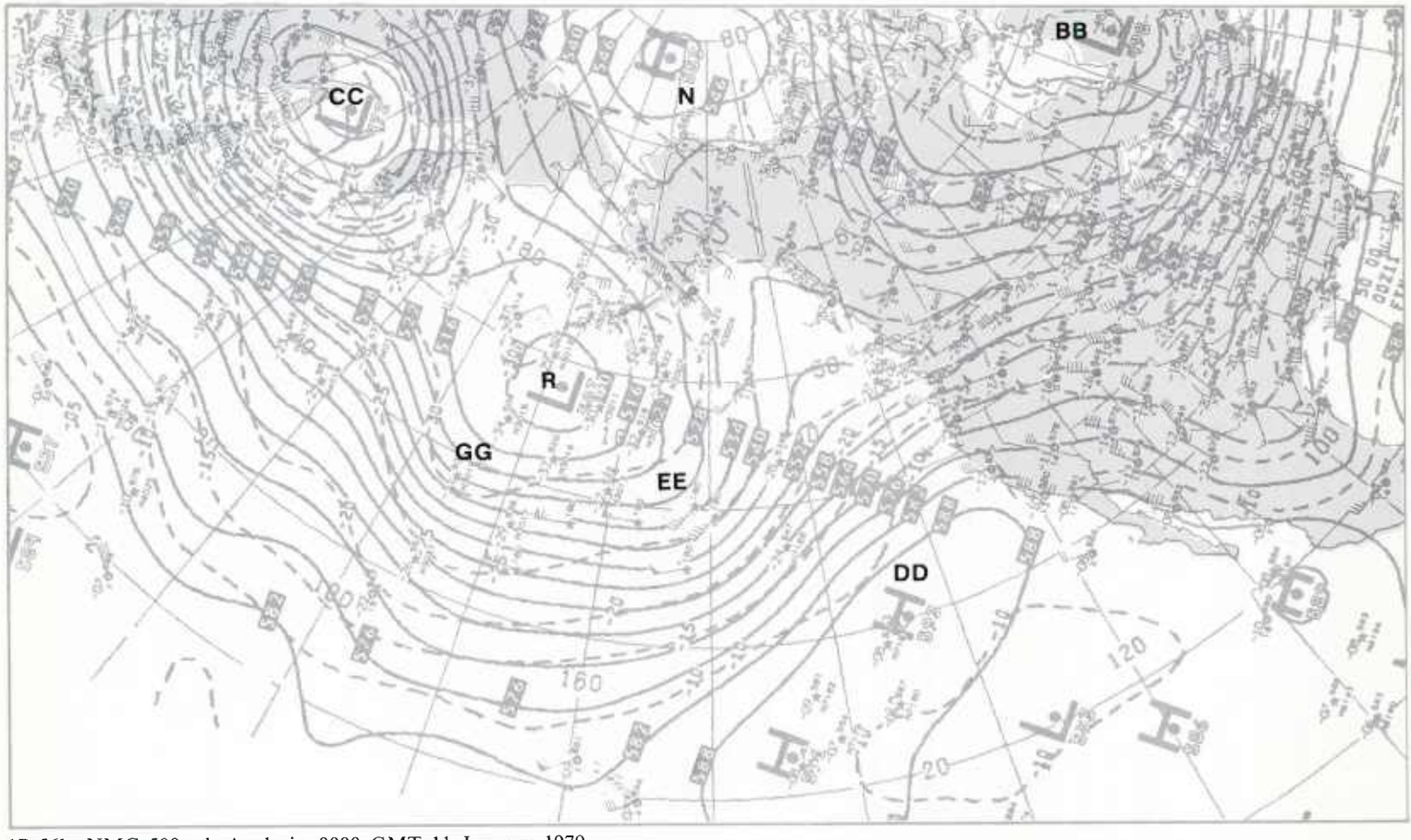

1B-56b. NMC 500-mb Analysis. 0000 GMT 11 January 1979.

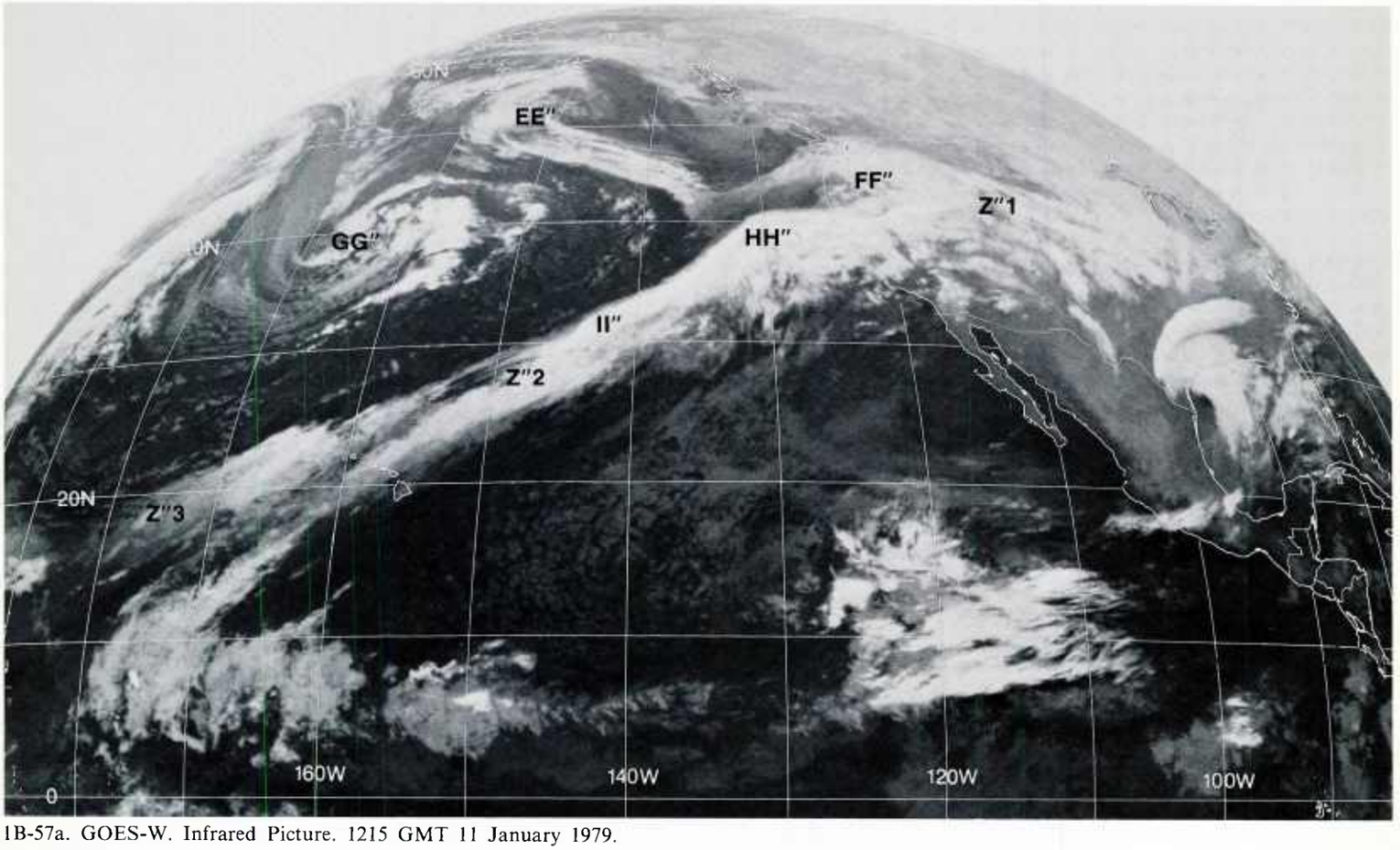

1B-57a. GOES-W. Infrared Picture. 1215 GMT 11 January 1979.

500 mb

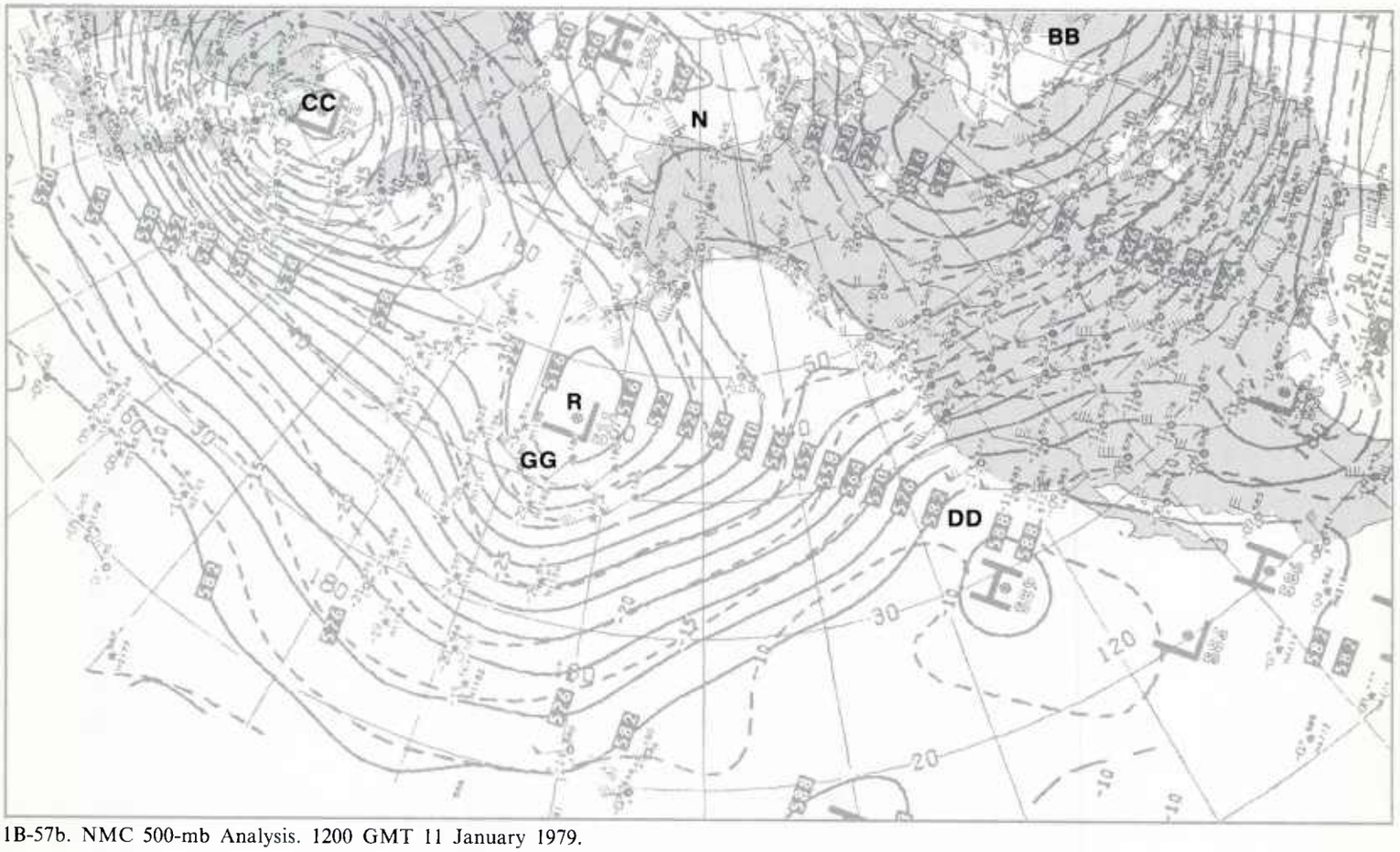

1B-57b. NMC 500-mb Analysis. 1200 GMT 11 January 1979.

Blocking Ends over the Eastern Pacific

Blocking Ends over the Eastern Pacific

Characteristic Features

1. *Strong zonal westerlies are established at mid latitudes across the eastern Pacific and the continental U.S.*
2. *The blocking ridge along the North America west coast at mid latitudes dissipates as the zonal westerlies over the eastern Pacific penetrate across the U.S. and break the connection between the subtropical high and the high-latitude block over the Arctic Ocean.*
3. *The major lows upstream and downstream of the high-latitude block weaken.*

12 January

The 500-mb analysis (1B-58b) shows that strong zonal westerlies (closely-spaced height contour lines) have developed at mid latitudes over the eastern Pacific and the continental U.S., as forecast (1B-53a). The major 500-mb lows **R** and **BB**, upstream and downstream of the block have weakened, however, the low **R** shows a closed circulation center instead of an open trough pattern and has advanced further east on a track taking it under the block **N**. The high-latitude block **N** still shows a vigorous, though less than jet-force, anticyclonic circulation pattern. At 300 mb (1B-58a), winds are still of moderate strength; however, there are no new jet streaks observed upstream or downstream of the block. This confirms that the high-latitude block is in the process of weakening.

Although the penetration of zonal westerlies at mid latitudes over the continental U.S. was forecast, the synoptic pattern attending the zonal westerlies did not develop as forecast. The most important difference is the development of the strong zonal westerlies which have completely broken the connection between the subtropical high **DD** and the high-latitude block **N**. This has eliminated any possibility of redevelopment of the blocking ridge along the West Coast, as long as the strong zonal westerlies are in place. At 300 mb (1B-58a), the isotach analysis reveals the strength and geographical extent of the mid-latitude westerlies—a series of closely-spaced 100-kt jet streaks, **PJS-1** to **PJS-4**, form a continuous polar jet stream from the central Pacific to the eastern Atlantic.

In the satellite picture (1B-59a), the frontal zone **Z″1–Z″3** continues to show short-wave disturbances (**FF″** and **HH″**) moving eastward along the northern boundary of the polar jet at 300 mb (1B-58a). These disturbances were previously observed developing along the frontal cloud band extending across the eastern Pacific (1B-56a and 57a). The strong zonal westerlies preclude any significant meridional circulation developments with these disturbances so that they do not grow into the typical mature cyclone, but remain as short-wave disturbances. This is confirmed on the surface analysis (1B-59b), where only frontal waves are observed along the surface frontal zone.

On the other hand, the storm **GG′** at the surface shows more development than the disturbances **FF′** and **HH′**. In the satellite picture, the storm **GG″** shows a distinct comma pattern. This storm developed from a disturbance (1B-55b) which has merged with the major low **R** at 500 mb (1B-58b) over the east-central Pacific. The slight anticyclonic curvature to the cirrus deck between **Z″2** and **Z″3** suggests that the storm **GG″** is beginning to interact with the baroclinic zone identified with the frontal cloud band **Z″2–Z″3**.

Upstream of the cloud vortex **GG″**, in the satellite picture, is a distinct frontal cloud band **JJ″1** and a barely visible cloud vortex **JJ″**. At the surface there is an intense, mature cyclone **JJ′** and a pronounced frontal system **JJ′1**. This storm is identified with the low **JJ** at 500 mb (1B-58b) moving out of the major low **CC** over the Asiatic coast. Note the strong polar jet **PJS-5** associated with this development at 300 mb (1B-58a). This jet has become more intense (see 1B-50b) and is digging to the southeast (**PJS-6**) to the rear of the major low **R** over the east-central Pacific.

With the breakdown of the mid-latitude block along the west coast of North America, the continued weakening of the high-latitude block, and the advance of the intense polar jet **PJS-5** at 300 mb, a return to more zonal flow conditions across the eastern Pacific is evident—in contrast to the strong meridional flow pattern observed during the blocking event.

300 mb

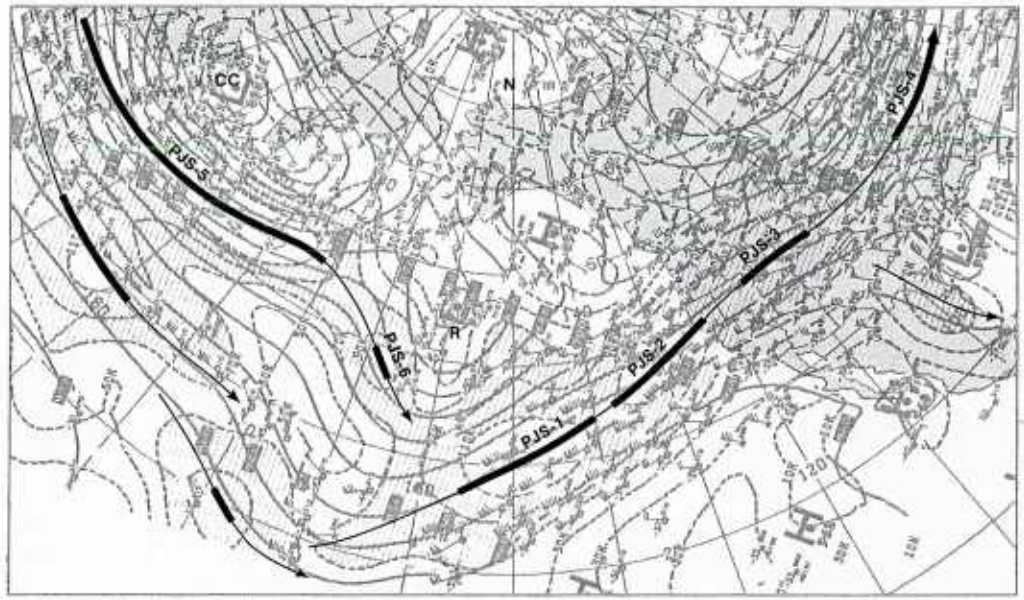

1B-58a. NMC 300-mb Analysis. 0000 GMT 12 January 1979.

500 mb

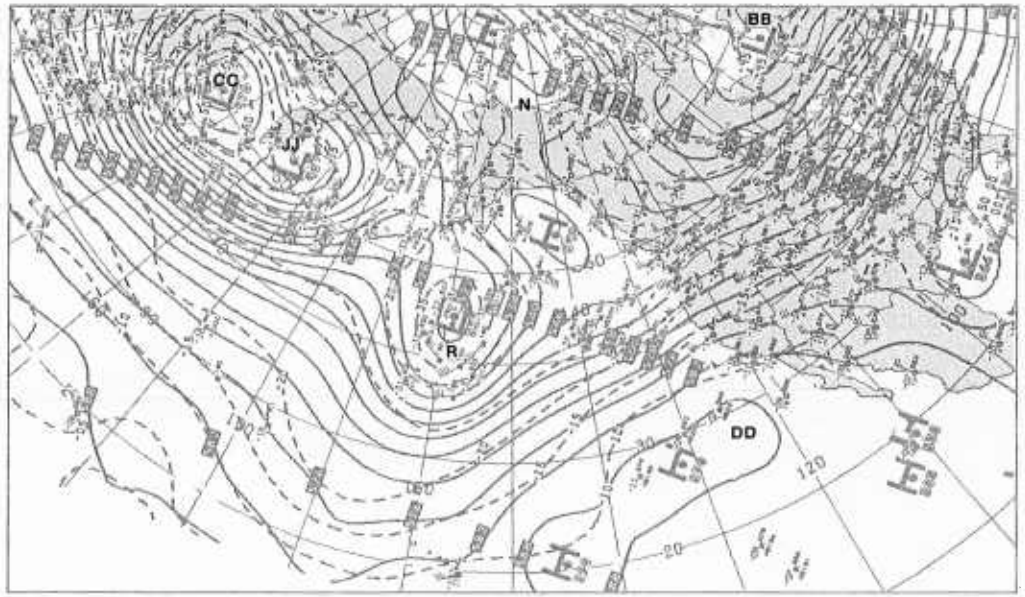

1B-58b. NMC 500-mb Analysis. 0000 GMT 12 January 1979.

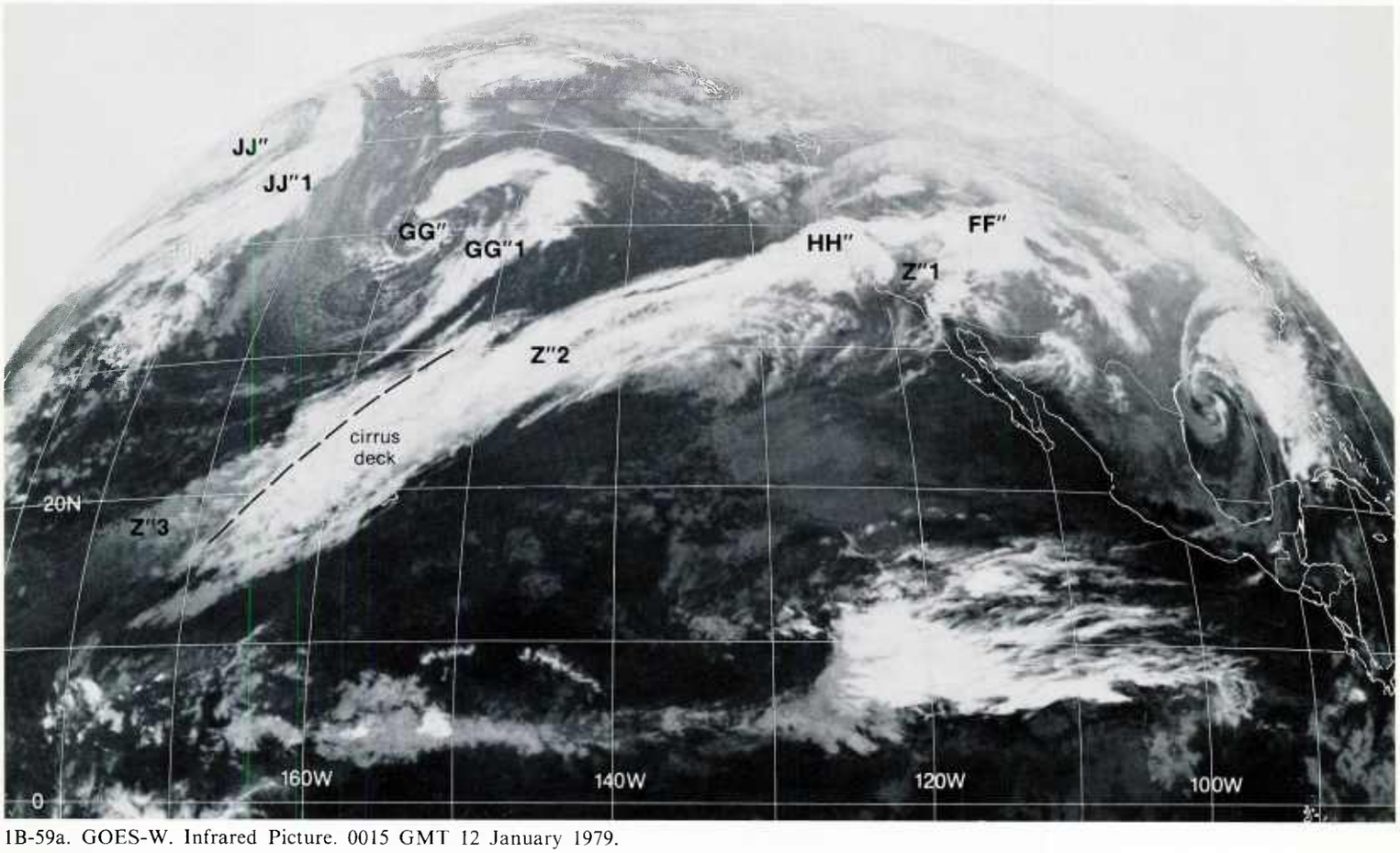

1B-59a. GOES-W. Infrared Picture. 0015 GMT 12 January 1979.

surface

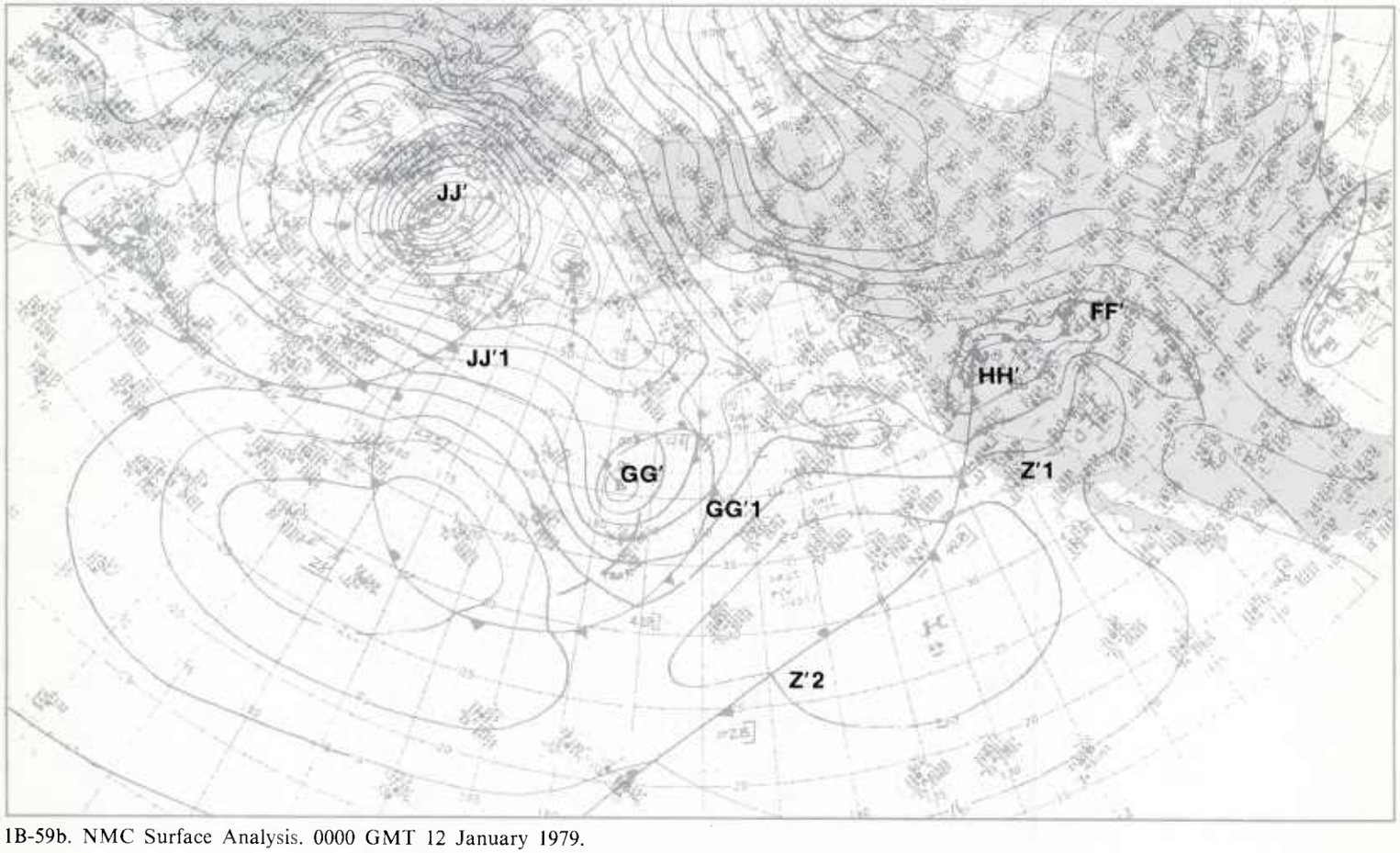

1B-59b. NMC Surface Analysis. 0000 GMT 12 January 1979.

Case 2 Blocking

Steering of Cyclonic Disturbances by Blocking Ridges

Large-amplitude, upper-air (500 mb) ridges over the eastern North Pacific can interrupt the advance of cyclonic disturbances in the westerlies. The ridges are slowly moving systems, and disturbances approaching from the west will be slowed and diverted northward. Frontal systems tend to become stationary along the western periphery of the blocking ridge and short-wave disturbances developing along these fronts move rapidly northeastward. The disturbances generally remain small and do not develop into major storms.

Blocking ridges also divert the tracks of cyclonic disturbances in the westerlies downstream of the ridge. This is most evident during the developing phase of a block. The north-south meandering of the westerlies is increased by the building ridge, and short waves are steered southward to lower latitudes along the east side of the amplifying ridge. In terms of operational significance, these disturbances are often accompanied by showers and gusty surface winds.

Southward displacement of a short-wave disturbance downstream of a building ridge
United States West Coast
January 1979

24 January

The NMC 300-mb analysis at 0000 GMT (1B-62a) shows a medium-amplitude, trough-ridge pattern **A-B-C-D** at midlatitudes across the North Pacific, the United States Pacific Northwest, and Canada. The north-south meandering of the polar westerlies in this pattern is clearly depicted by the superimposed jet stream analysis (jet streaks, or isotach maxima, are highlighted by heavier line segments). At 500 mb (1B-62b), the contour lines emphasize the sinusodial trough-ridge pattern, and the close spacing of these contour lines indicates a nearly uniform band of strong zonal polar westerlies (jet stream) extending across the eastern North Pacific. There is a cutoff low **E** at 500 mb, and a strong subtropical jet stream at 300 mb stretching from the vicinity of the Hawaiian Islands to Baja California.

The NMC surface analysis (1B-63b) at 0000 GMT shows two mature winter storms **A1** and **C1**. The nearly straight west to east displacement of the storms, indicated by the arrows along the past 6-hourly positions, reflects the steering effect of the strong zonal westerlies aloft on these disturbances. Disturbance **C2** is a recent development in the trough **C** at 500 mb.

In the GOES-W infrared picture (1B-63a) at 0015 GMT, the winter storm **A1** is identified by the small cloud vortex **A1** and the frontal cloud band **A1-A1**. The sharp protuberance **A2** indicates a frontal wave development. This evidence has been used to indicate an incipient wave on the surface front (1B-63b). The storm **C1** is located under predominately anticyclonic flow aloft and at the surface, and the satellite picture shows a diffuse cloud vortex **C1** and a weak, fragmented frontal cloud band **C1-C1**. It appears that the most intense development in the zonal westerlies is the distinct, bright vorticity comma **C2** located near the base of the trough **C** at 500 mb. There is also intense convective activity along the eastern quadrant of the 500-mb cutoff low **E** and to the south of the 300-mb subtropical jet stream (bright, globular cloud areas).

A comparison of the trough-ridge pattern on the FNOC 36-hour 500-mb prognosis (1B-63d) and the corresponding features on the FNOC initial 500-mb analysis (1B-63c) shows that the sinusodial trough-ridge pattern **A-B-C-D** and the strong zonal westerlies will persist over the region. The prognosis also indicates a well-defined ridge **B** extending from high latitudes to the tropics and the merging of the cutoff low **E** and the midlatitude trough **C**.

At 300 mb (1B-64a) and 500 mb (1B-64b), 12 hours later, the progressive trough-ridge pattern **A-B-C-D** and the surface winter storms **A1** and **C1** (1B-65b) have advanced eastward in the strong zonal westerlies at midlatitudes. However, the cyclonic disturbance **C2** (1B-65b) has not followed an eastward track; instead, the disturbance shows a displacement to the southeast. This movement suggests that the trough **C** at 500 mb is deepening as it moves in phase with the cutoff low to the south. It also indicates that the disturbance is more under the influence of the northerly flow along the east side of the ridge **B** at 500 mb than the southwesterly flow ahead of the trough **C**.

The GOES-W infrared picture at 1215 GMT (1B-65a) shows that the cloud patterns associated with the winter storms **A1** and **C1** have not changed markedly. Disturbance **A2** along the frontal cloud band **A1-A1** displays additional development and the frontal cloud system **C1-C1** continues to weaken. The major development is the appearance of the large, relatively cloud-free region **B**. This is due to the intensification of the surface high **B** (1B-65b) under the building ridge **B-B** at 500 mb (1B-64b). The vorticity comma **C2** in the satellite picture has increased in size and is accompanied by strong northerly winds (30 kt) at the surface (1B-65b).

During the following 36 hours (1B-65d), the northerly flow along the east side of the 500-mb ridge (1B-65c) is forecast to become increasingly northerly along the Pacific Northwest. This is due in part to the deepening of the trough **C**, and the slower eastward advance of the ridge **B** at low latitudes as compared to high latitudes, which causes a pronounced southwest to northeast tilt of the ridge. The stretching-out of the frontal cloud band **A1-A1** in the satellite picture (1B-65a), in a southwest to northeast orientation, indicates that the progressive ridge **B-B** is exhibiting the characteristics of a blocking ridge.

In the GOES-W infrared picture at 1815 GMT (1B-66a), six hours later, the comma cloud **C2** is losing its solid cloud cover and displays a narrow, spiral banded structure. The NMC surface analysis (1B-66b) shows that the disturbance has moved rapidly to the southeast, with strong winds (30 kt) continuing along the western periphery. Note that the location of the frontal cloud band **C1-C1** in the satellite picture indicates that the front is to the south of the analyzed position (1B-66b).

The surface high **B** (1B-66b) continues to intensify under the increased ridging aloft and is slowing the eastward advance of the front to the west. Notice that the disturbance **A2** has become a progressive wave and is moving rapidly northeastward along the front. The partly cloudy area **B** and the surrounding low clouds (medium gray shades) in the satellite picture (1B-66a) identify the location of the blocking surface high. A DMSP visible picture (1B-67a), about two hours later, provides a clear view of the central region of the surface high and the surrounding low clouds. The disturbance **C2** also appears in the picture.

continued on page 1B-68

300 mb

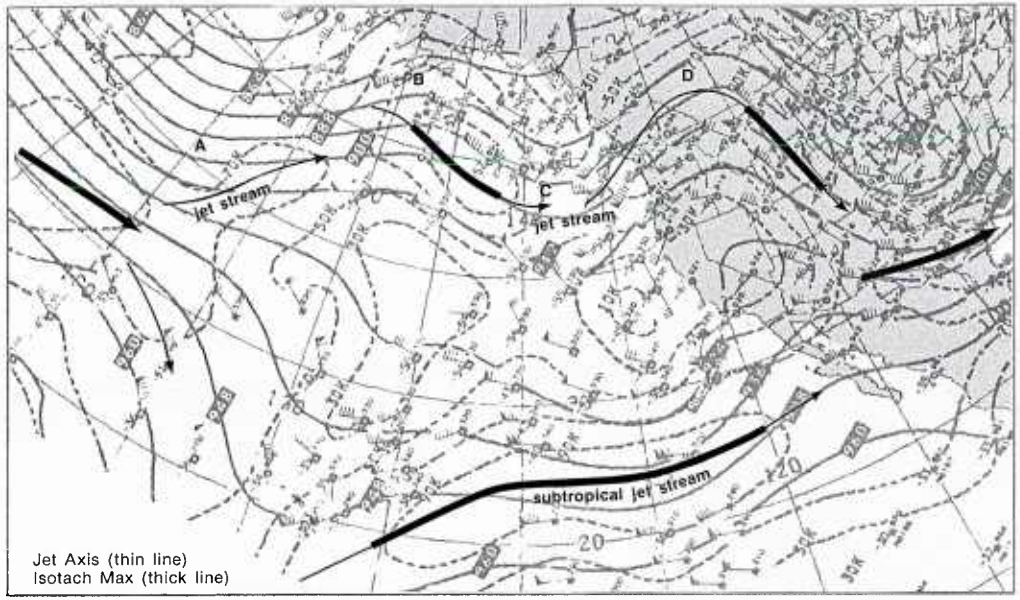

1B-62a. NMC 300-mb Analysis. 0000 GMT 24 January 1979.

500 mb

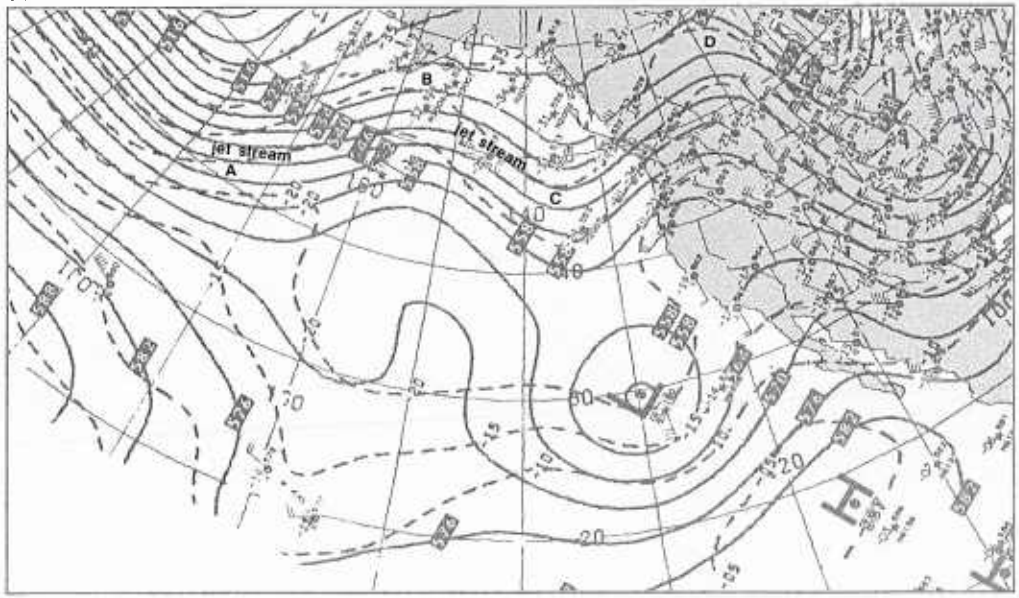

1B-62b. NMC 500-mb Analysis. 0000 GMT 24 January 1979.

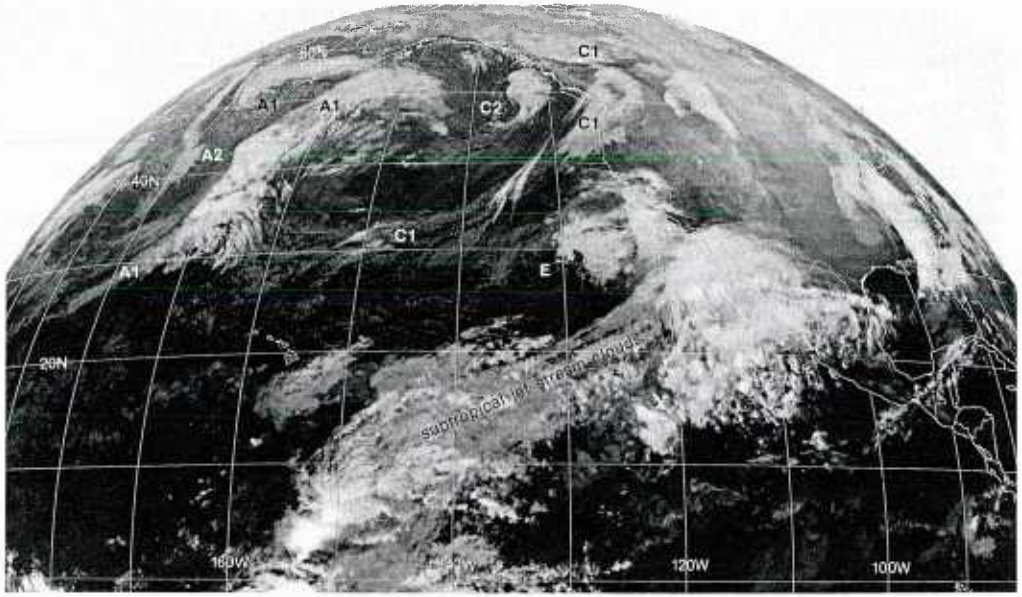

1B-63a. GOES-W. Infrared Picture. 0015 GMT 24 January 1979.

surface

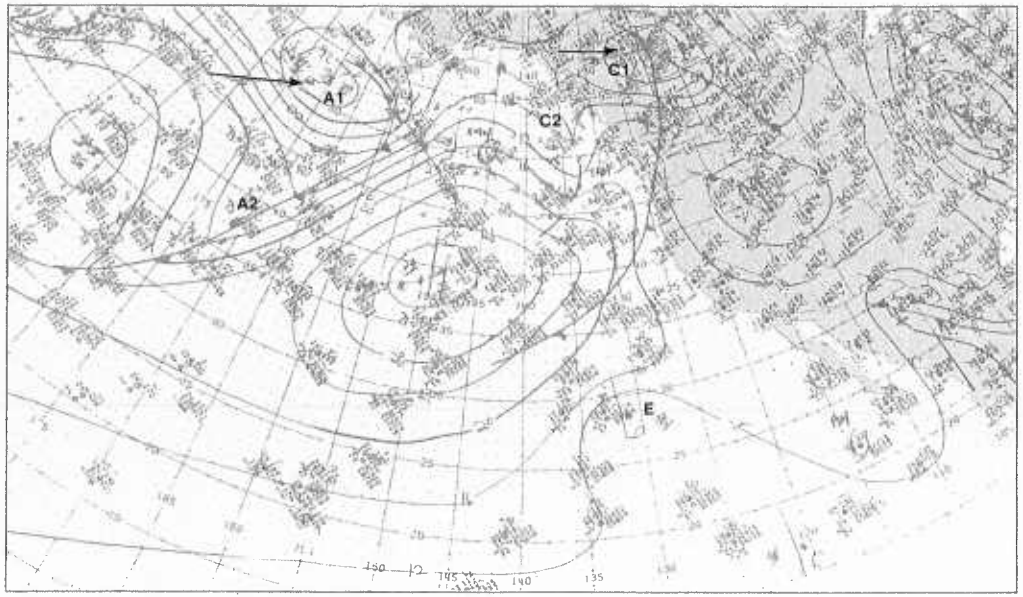

1B-63b. NMC Surface Analysis. 0000 GMT 24 January 1979.

500 mb

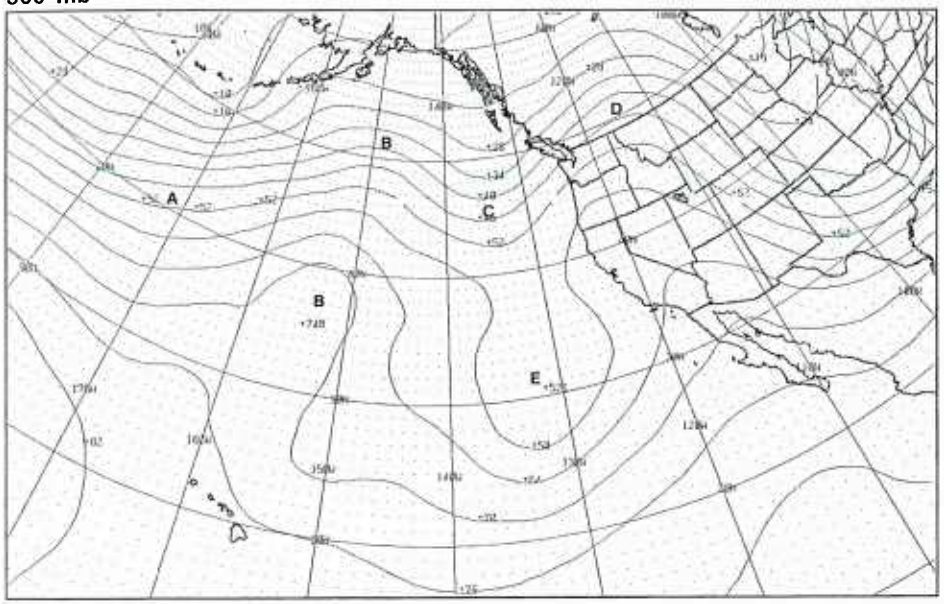

1B-63c. FNOC PE Initial 500-mb Analysis. 0000 GMT 24 January 1979.

500 mb

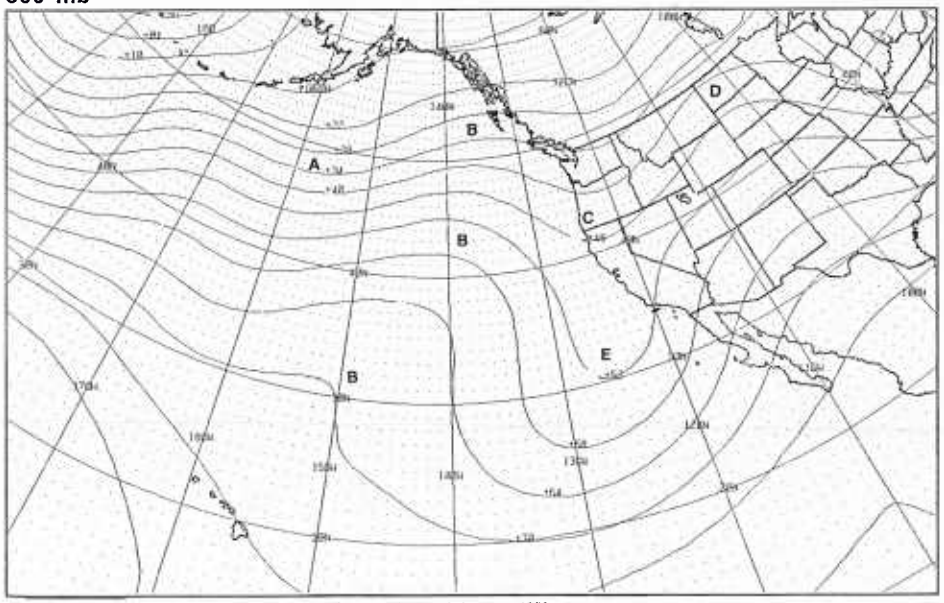

1B-63d. FNOC PE 36-hr 500-mb Prognosis. Valid 1200 GMT 25 January 1979.

300 mb

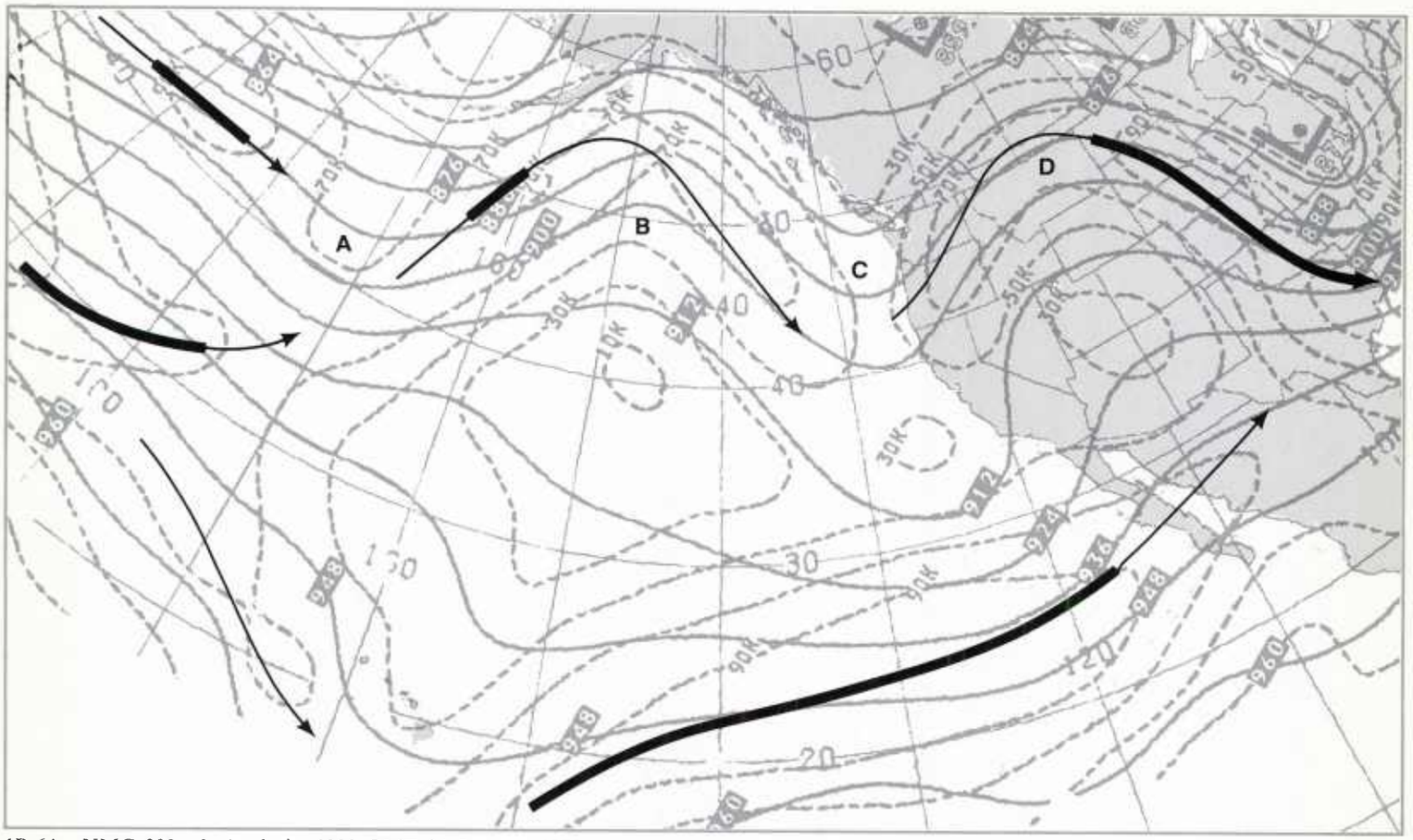

1B-64a. NMC 300-mb Analysis. 1200 GMT 24 January 1979.

500 mb

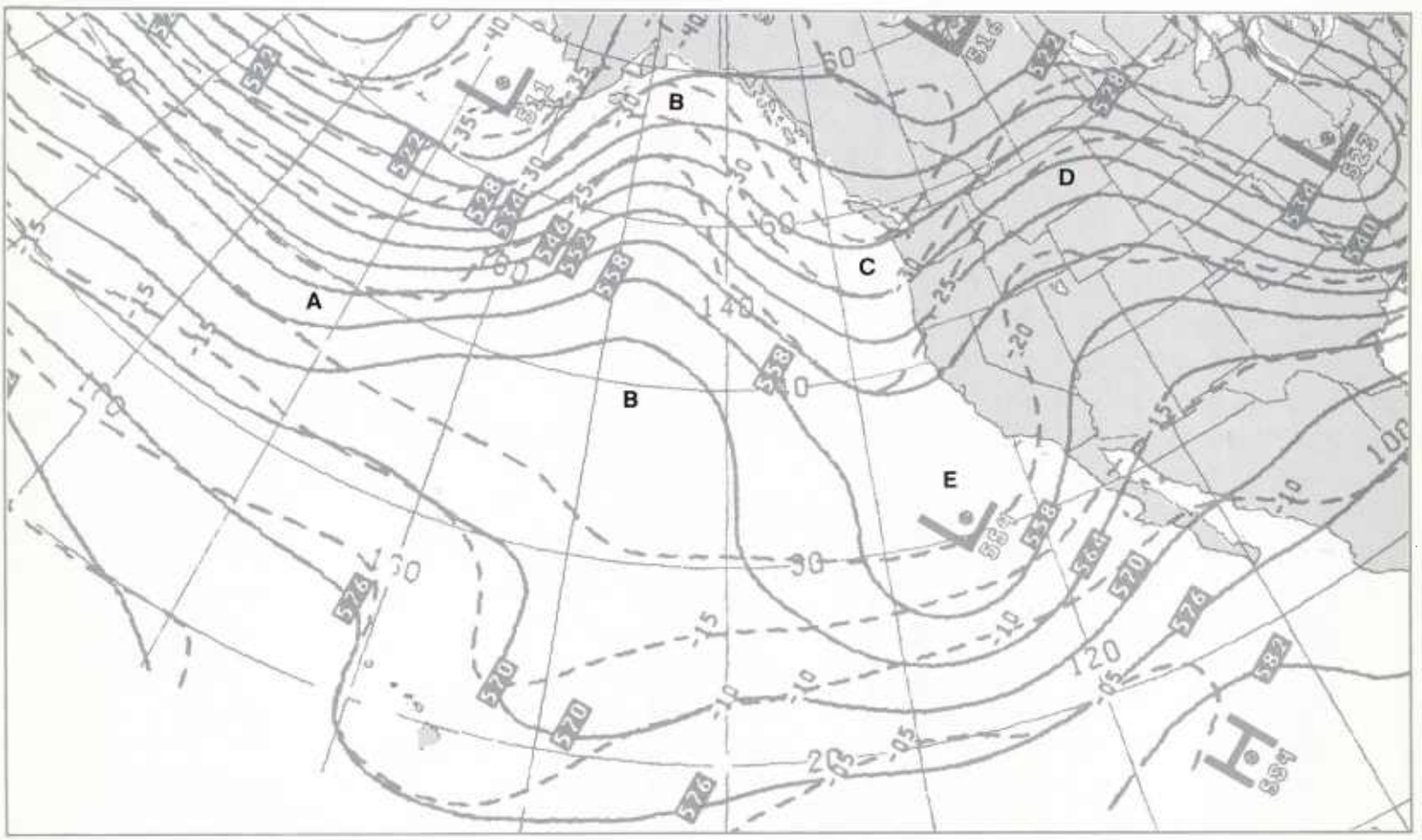

1B-64b. NMC 500-mb Analysis. 1200 GMT 24 January 1979.

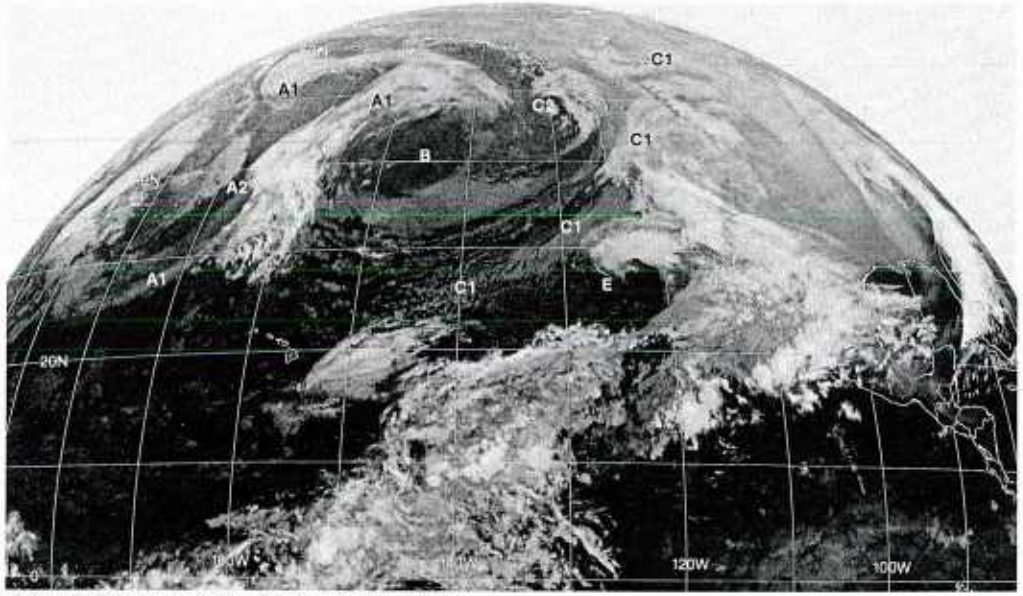

1B-65a. GOES-W. Infrared Picture. 1215 GMT 24 January 1979.

surface

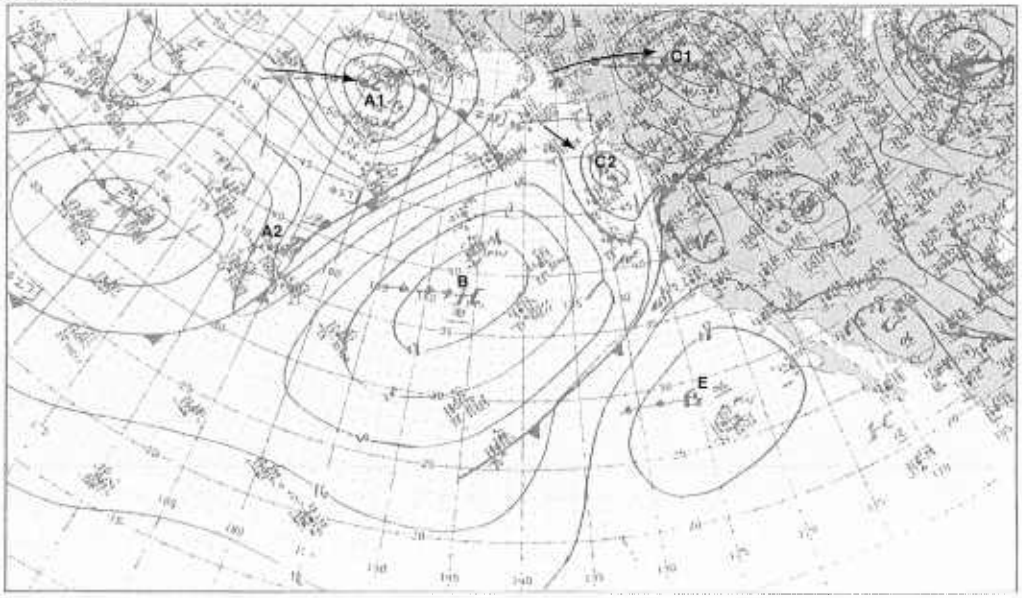

1B-65b. NMC Surface Analysis. 1200 GMT 24 January 1979.

500 mb

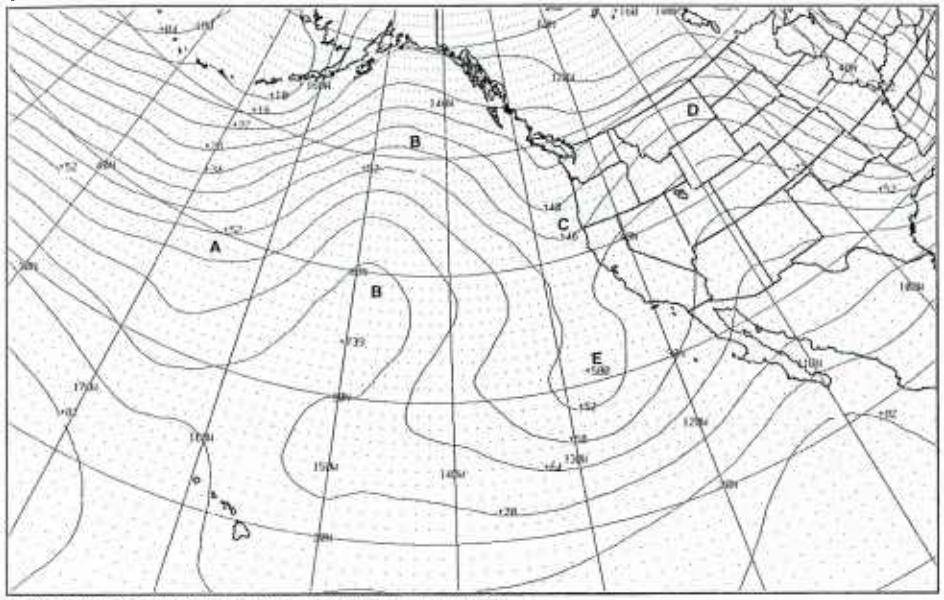

1B-65c. FNOC PE Initial 500-mb Analysis. 1200 GMT 24 January 1979.

500 mb

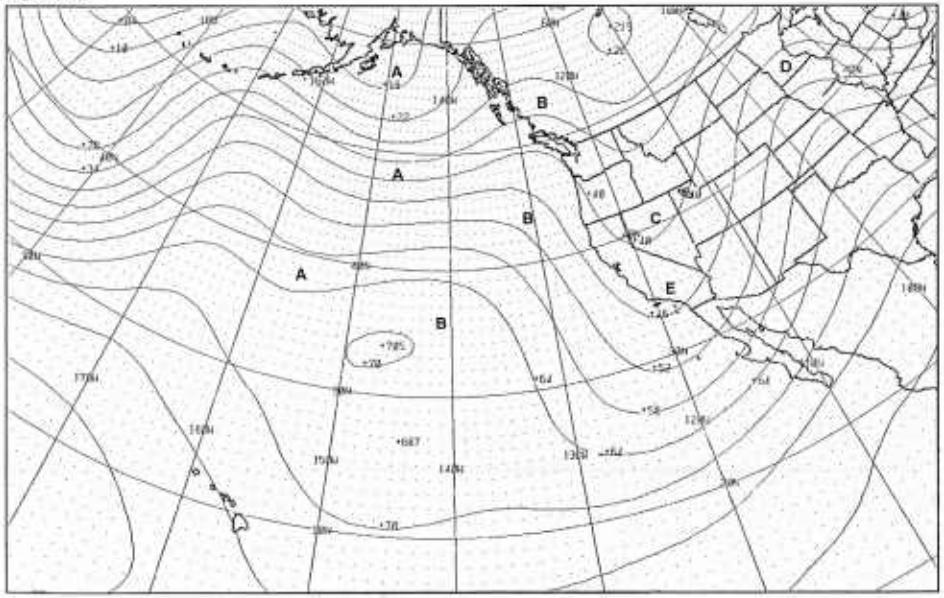

1B-65d. FNOC PE 36-hr 500-mb Prognosis. Valid 0000 GMT 26 January 1979.

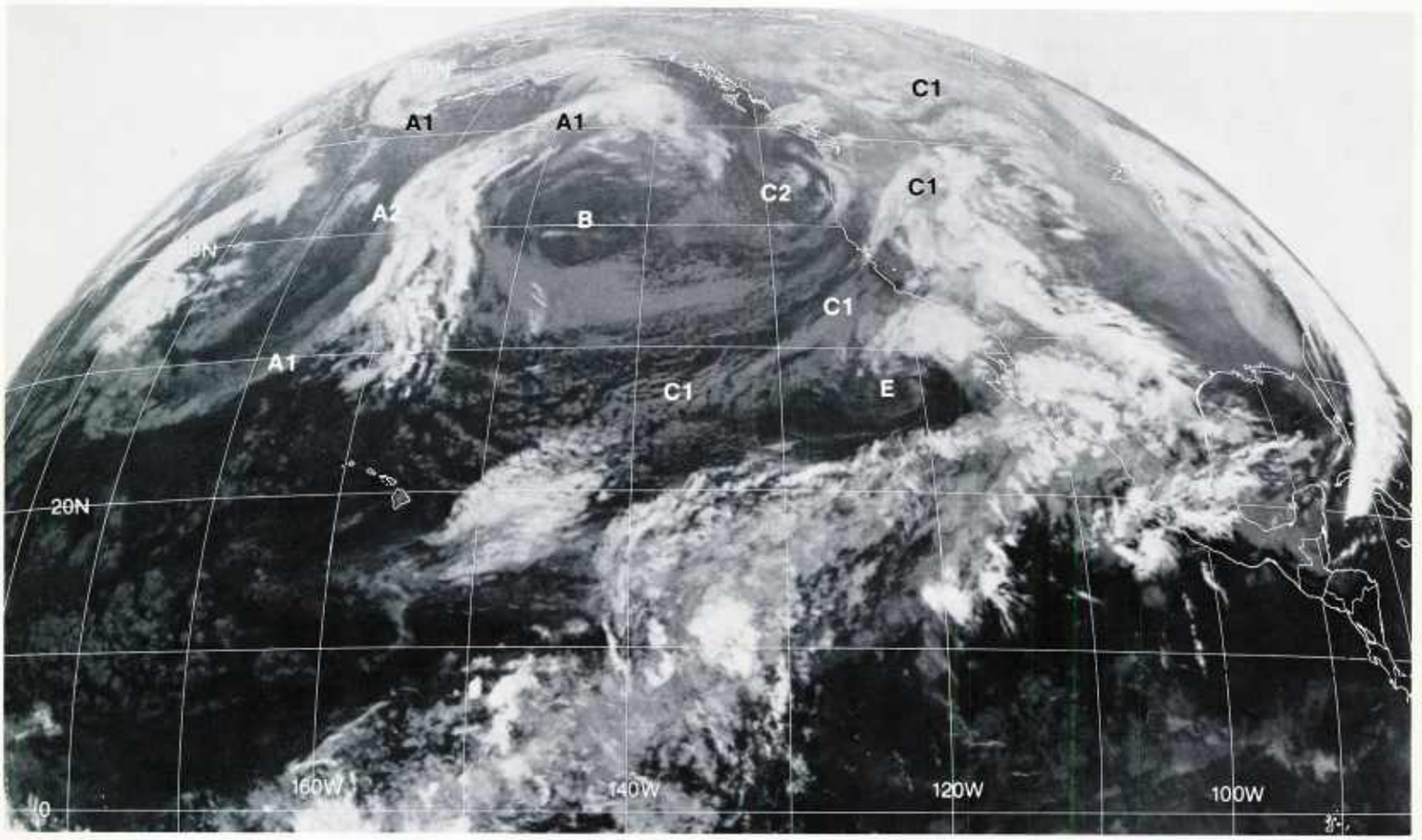

1B-66a. GOES-W. Infrared Picture. 1815 GMT 24 January 1979.

surface

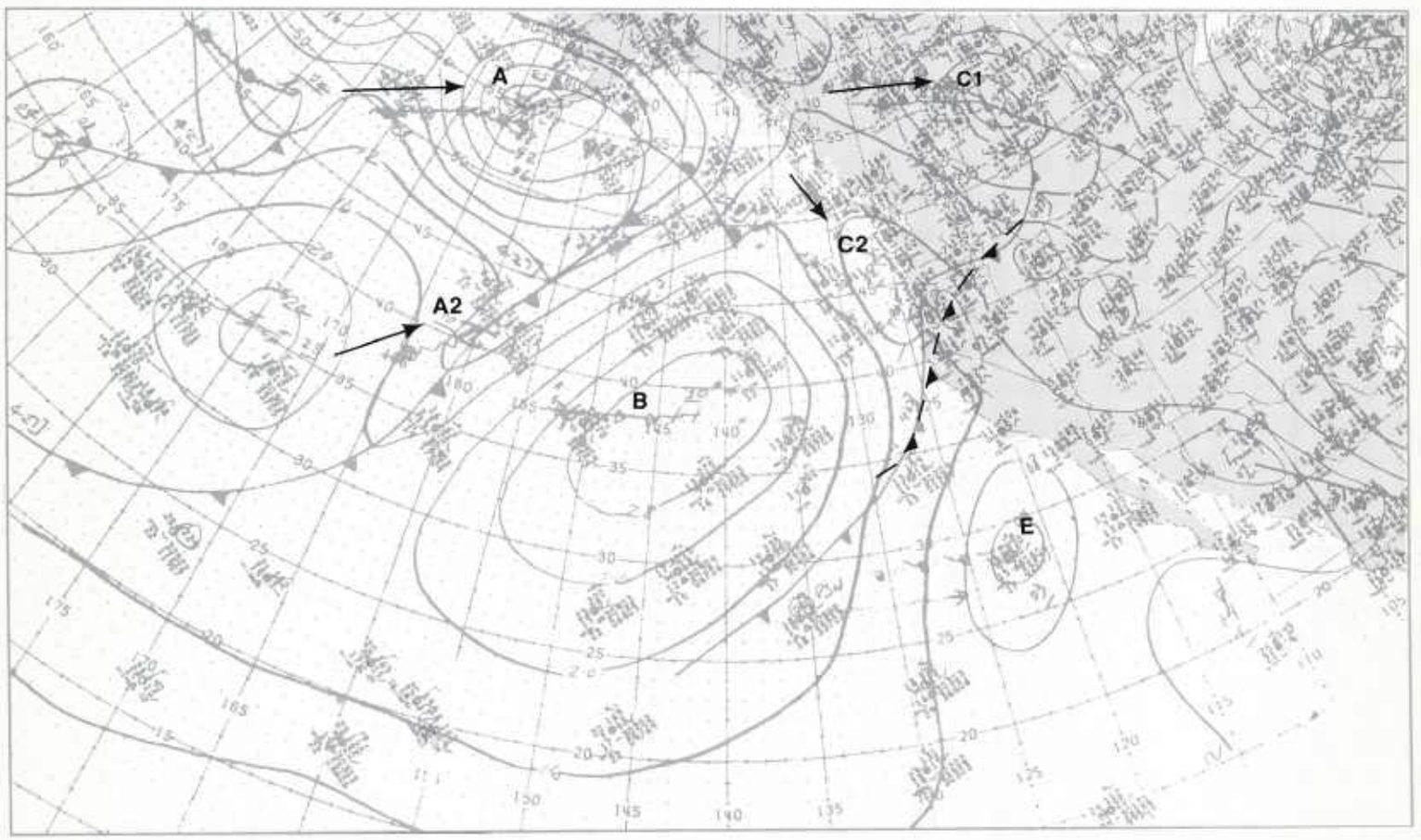

1B-66b. NMC Surface Analysis. 1800 GMT 24 January 1979.

1B-67a. F-1. DMSP LF Low Enhancement. 2005 GMT 24 January 1979.

25 January

A comparison of the 500-mb analyses at 0000 GMT (1B-68b) and 1200 GMT (1B-69c) with the corresponding 36-hour prognosis (refer to 1B-63d) shows that the progressive trough-ridge pattern **A-B-C-D** has advanced as forecast, with the ridge **B-B** intensifying and the midlatitude trough **C** merging with the low latitude cutoff low **E**. However, strong northerly flow which was forecast to develop later over the Pacific Northwest (refer to 1B-65d) is clearly observed by 1200 GMT (1B-69c). The satellite pictures 1B-68a and 1B-69b dramatically show the effects of the development of the strong northerly flow along the Pacific Northwest on the disturbance **C2**. The disturbance has been steered southward in contrast to the continued west to east advance of the winter storm centers **A1** and **C1**.

Although the ridge **B-B** at 500 mb is progressive, it is acting as a blocking ridge. The satellite picture (1B-68a) shows an almost north-south oriented frontal cloud band **A1-A1** which has been forced against the block. A close examination of the short-wave disturbance **A2** shows that it dissipates during the following 12 hours, and a new disturbance **A3** forms on the frontal cloud band **A1-A1** (1B-69b).

In the DMSP infrared picture (1B-69a), the extensive low cloud pattern (medium gray shades) over the eastern Pacific emphasizes the large areal extent of the surface blocking high. The oval-shaped, partly clear area **B** indicates that the blocking surface high has taken on a distinct north-south orientation. The small region of deep convection (bright, white globular cloud forms) observed over San Francisco Bay suggests that convection in the short-wave disturbance **C2** moving down the coast is rapidly decreasing.

During the next six hours, the short-wave disturbance **C2** advances across the Pacific Missile Southern California (SOCAL) Test Range. It is in a weakened state, as evidenced by the small convection area in the DMSP picture at 0847 GMT (1B-69a). By 1815 GMT, the disturbance has passed through the area and the satellite picture (1B-70a) shows only scattered low clouds remaining over the SOCAL Test Range. There is no evidence of the disturbance on the NMC surface analysis at 1800 GMT (1B-70b), except for some showers along the California/Mexico border coastal region. The GOES-W visible picture at 2016 GMT (1B-71a) shows a mostly clear southern California coastal region, with mesoscale cellular convection clouds offshore.

Important Conclusions

1. Short-wave disturbances located in strong northerly flow developing along the east side of a building 500-mb ridge will be steered to low latitudes.
2. The small size and rapid speed of the disturbances make them difficult to identify and track on conventional synoptic analyses.
3. Vorticity comma cloud patterns associated with these disturbances can be tracked in satellite imagery and convective weather identified for locating showers and gusty surface wind conditions.

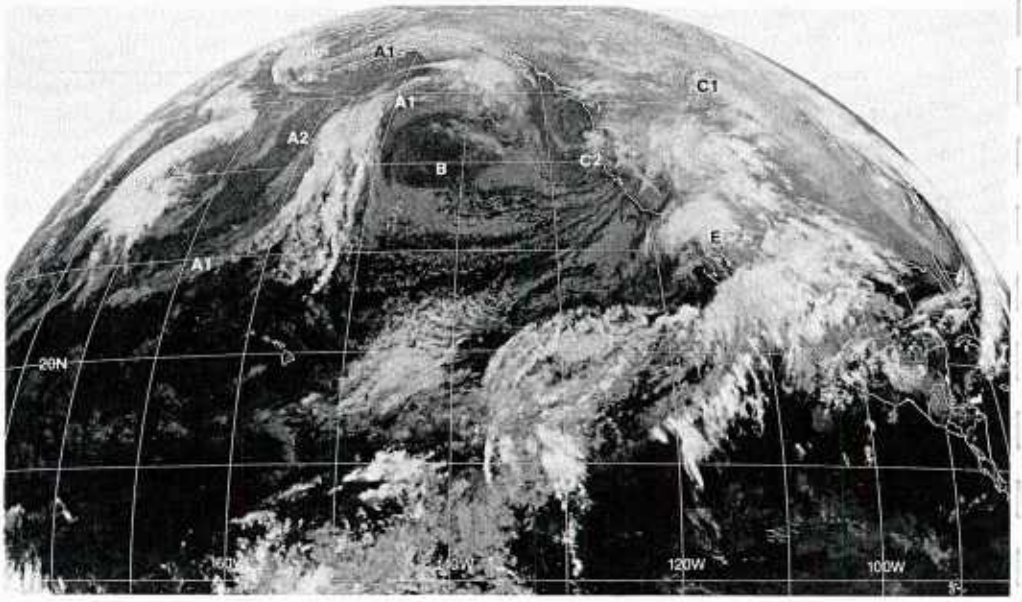

1B-68a. GOES-W. Infrared Picture. 0015 GMT 25 January 1979.

500 mb

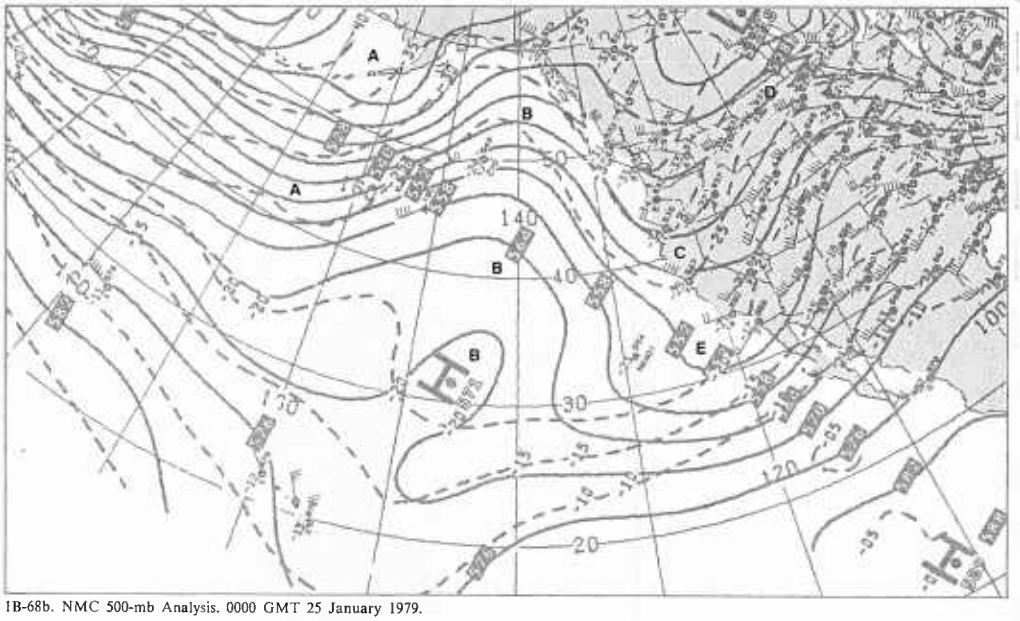

1B-68b. NMC 500-mb Analysis. 0000 GMT 25 January 1979.

Cutoff Low Development/Cyclone Formation

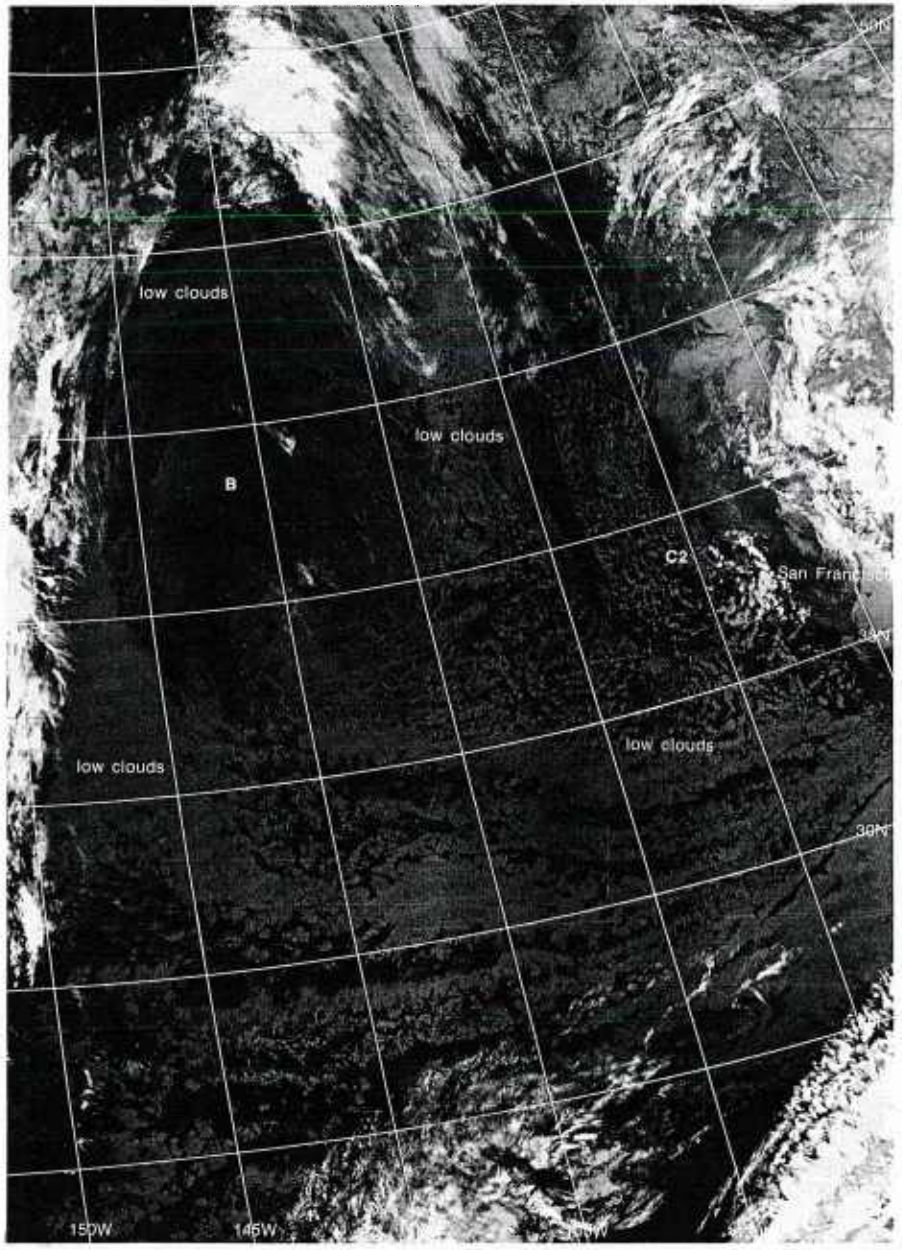

1B-69a. F-1. DMSP TF T-Expand Enhancement. 0847 GMT 25 January 1979.

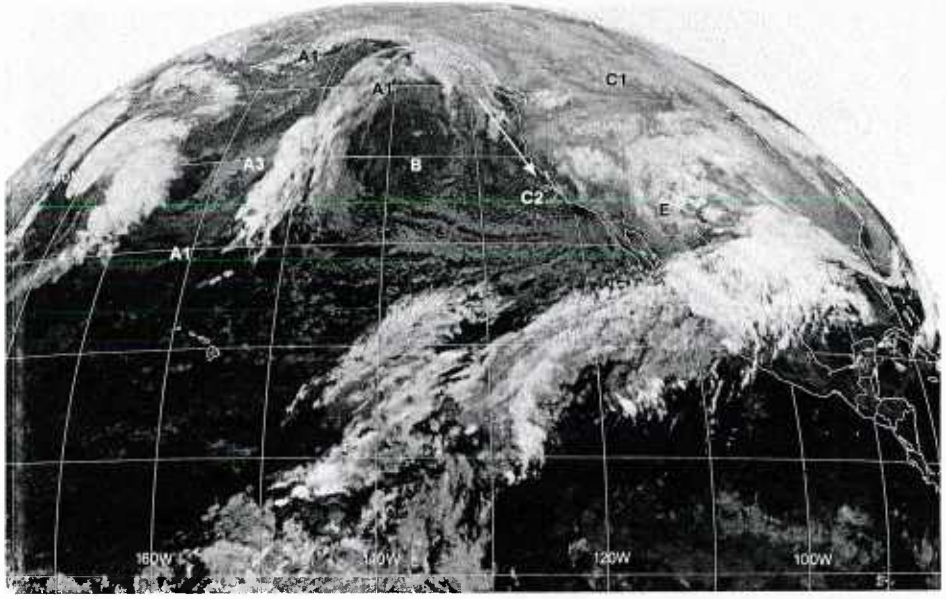

1B-69b. GOES-W. Infrared Picture. 1215 GMT 25 January 1979.

500 mb

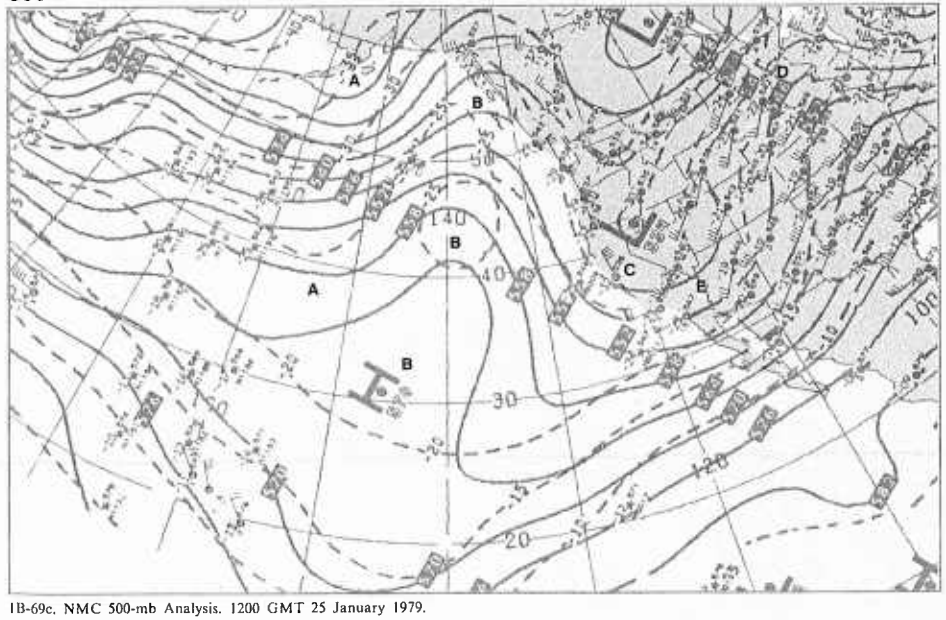

1B-69c. NMC 500-mb Analysis. 1200 GMT 25 January 1979.

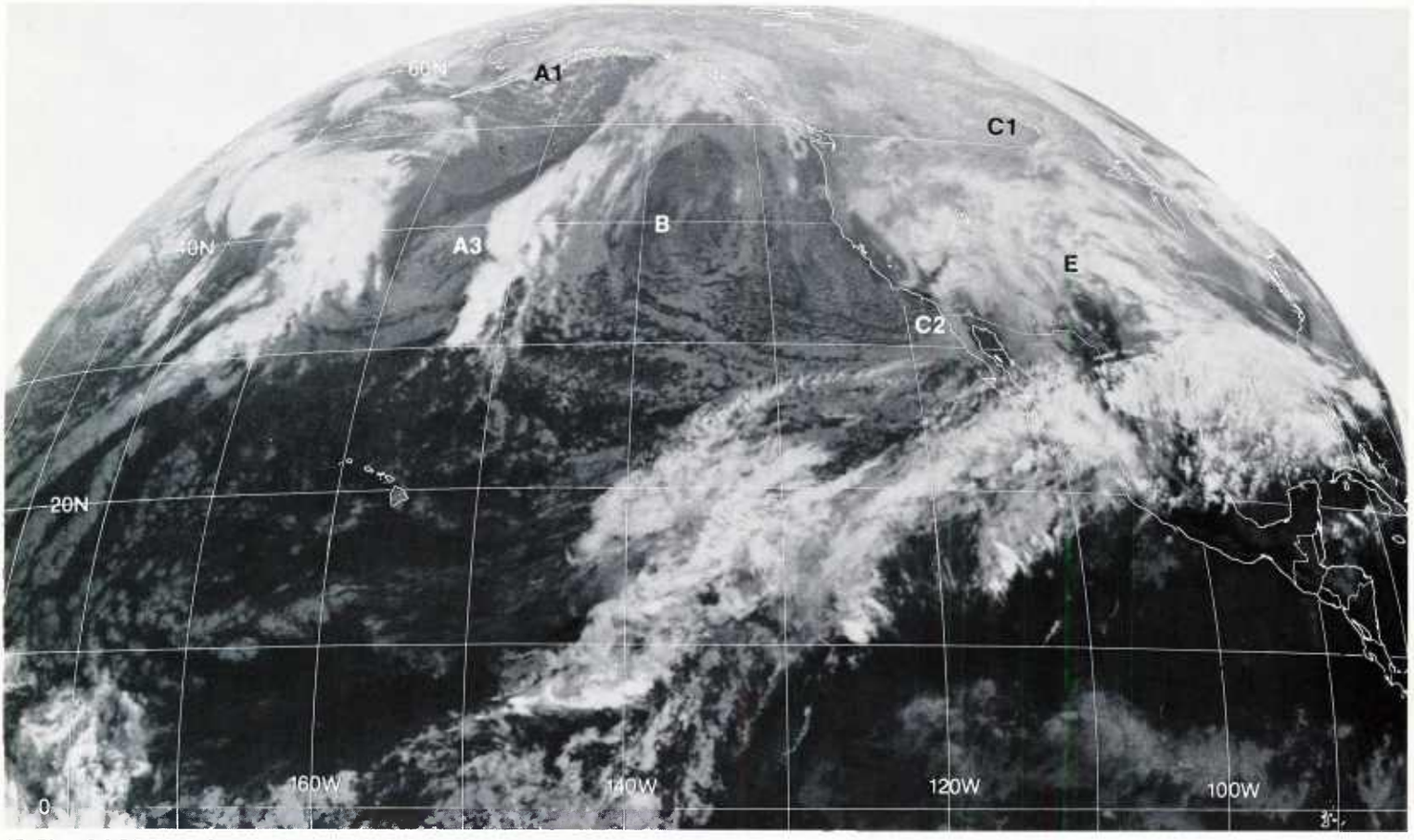

1B-70a. GOES-W. Infrared Picture. 1815 GMT 25 January 1979.

surface

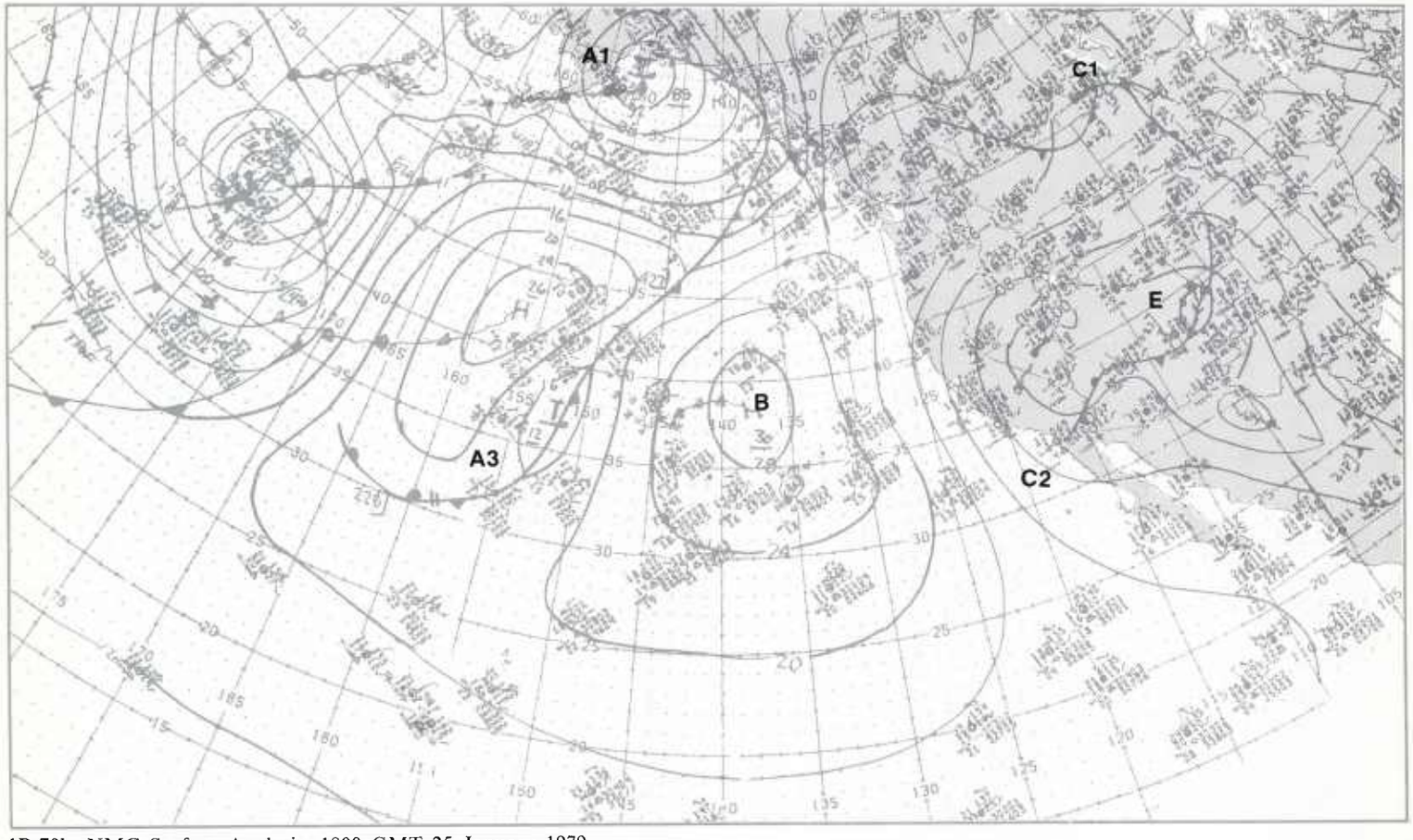

1B-70b. NMC Surface Analysis. 1800 GMT 25 January 1979.

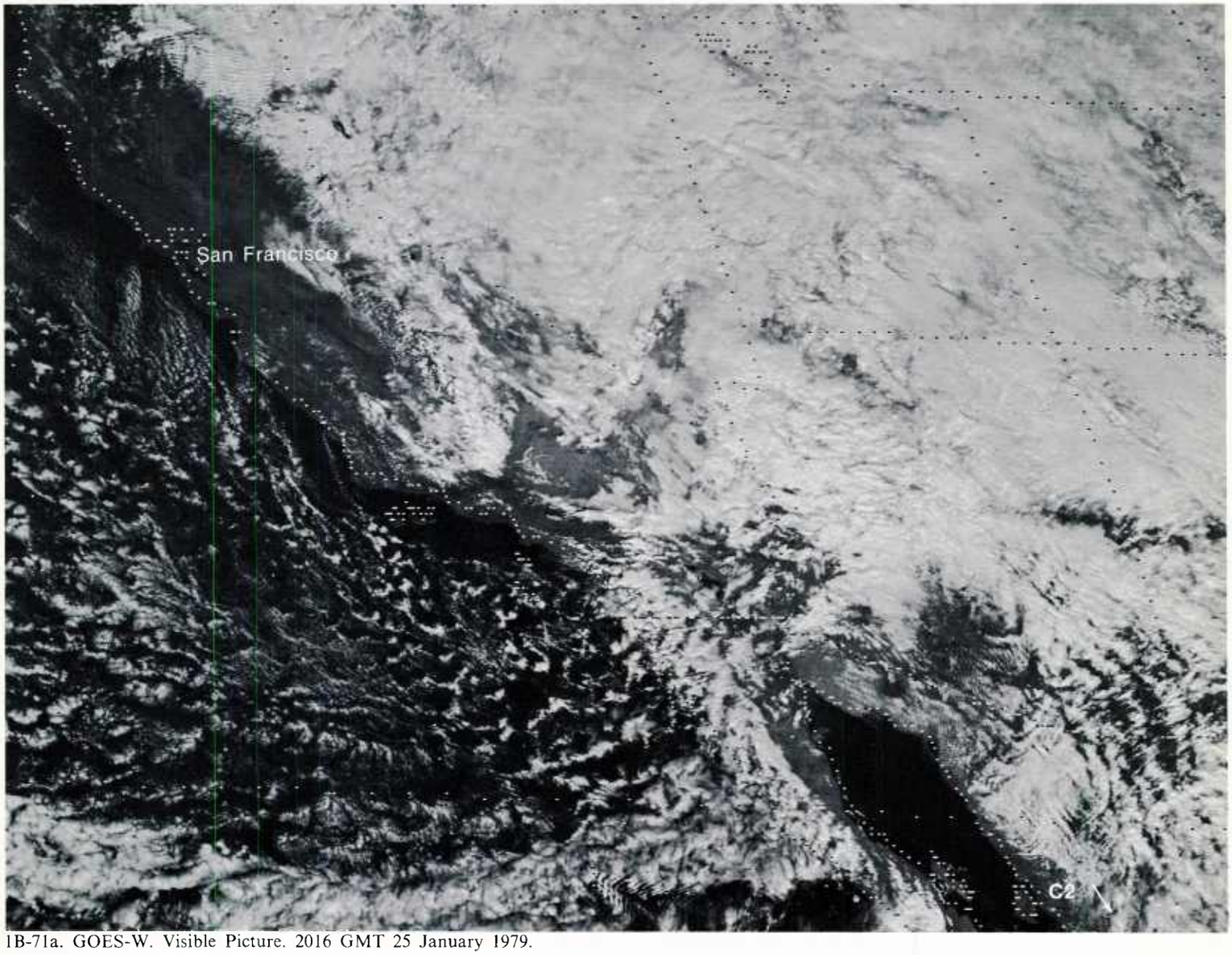

1B-71a. GOES-W. Visible Picture. 2016 GMT 25 January 1979.

The table below (1B-71b) provides hourly surface observations at San Nicholas Island, at the center of the test range, during the period the disturbance moved across the area. The observations reveal that even in a weakened state, the short-wave disturbance **C2** produced showers and strong northwest winds, gusting to 37 kt, and wind waves of 13 ft.

FEDERAL METEOROLOGICAL FORM 1 - 10 SURFACE WEATHER OBSERVATIONS (ABRIDGED FOR NAVAL WEATHER SERVICE USE)

SUNRISE 0658 | SUNSET 1723 | STATION ELEVATION (H_p) 568 Feet (MSL) | TIME CONVERSION (LST to GMT) 08 Hrs | MAG TO TRUE 15 Deg | DAY 25 | MONTH JAN | YEAR 19 79 | STATION

TYPE (1)	TIME (LST) (2)	SKY AND CEILING (HUNDREDS OF FEET) (3)	TIME (GMT)	VISIBILITY (STATUTE MILES) SURFACE (4)	VISIBILITY (STATUTE MILES) TOWER (4a)	WEATHER AND OBSTRUCTIONS TO VISION (5)	SEA LEVEL PRES (mb) (6)	TEMP (°F) (7)	DEW POINT (°F) (8)	WIND DIRECTION (9)	WIND SPEED (knots) (10)	WIND CHARACTER (11)	ALSTAG (inches) (12)	REMARKS AND SUPPLEMENTARY CODED DATA (DESIRED ORDER OF ENTRY: RVR, SPECIAL obstruction phenomena, visibility, wind shifts, radar reports of basis and tops, remarks elaborating on preceding coded data, 3- and 6-hourly additive data, radiosonde data, runway conditions, weather modification, PIREPS.) (13)	
R	0650	30 SCT	1450	20			088	48	35	31	18	G30	970	319 1200 (34)	SEAS 30908
S	0720	25 SCT E70BKN	1520	20						30	16	G24	972	RWU S-NW	
R	0750	25 SCT 40SCT E70BKN	1550	25			067	46	35	29	18	G30	973	CB SW-NW MOVG SE	SEAS 30908
S	0821	M21BKN 40BKN 70BKN	1621	25						30	15	G24	974	CB RWU S-N MOVG SE	
R	0850	M21BKN 40BKN 70BKN	1650	20		RW-	074	48	39	32	16	G27	975	CB ALQDS MOVG SE	SEAS 31108
S	0913	23SCT 70SCT	1713	25						31	15	G24	976	CB E-SW MOVG SE	
R	0950	23SCT 70SCT	1750	25			077	52	37	31	18	G30	976	CB E-SW MOVG SE / 11900 1360 46 (34)	
															SEAS 31108
S	1015	M23BKN 70BKN	1815	25						30	18	G27	976	CB E-W MOVG SE	
R	1050	M23BKN 70BKN	1850	25			078	52	36	30	18	G26	976	CB E-NW MOVG SE	SEAS 30808
R	1150	M21BKN 70BKN	1950	20		RW-	076	50	40	29	20	G30	976	CB E-NW MOVG SE	SEAS 30908
R	1250	M21BKN	2050	30			070	53	38	31	24	G32	974	CB NW MOVG SE BKN V SCT / 80500 1900 (36)	
														RADAT 64039	SEAS 30908
RS	1350	20 SCT 200 SCT	2150	30			074	52	39	31	21	G31	975		SEAS 30906
R	1450	20 SCT	2250	30			076	52	37	31	20	G33	976		SEAS 30807
R	1550	20 SCT	2350	30			083	52	31	31	24	G37	978	31200 1100 53 (31)	SEAS 30907
R	1650	20 SCT	0050	30			090	50	35	31	22	G32	980		SEAS 30907

1B-71b. Hourly Surface Observations for San Nicolas Island.

Case 3 Blocking

Formation of Cutoff Lows Downstream of Blocking Highs

A cyclonic circulation system in the upper-air wind field which has been cut off from its initially associated jet stream is referred to as a "cutoff low". In a given synoptic pattern which is favorable for cutoff low development it is important, therefore, to identify the location of the jet stream (axis of maximum wind) at upper levels and the position of jet streaks (wind speed maxima) along the jet stream.

Typically, cutoff lows are observed to form during the initial phase of a blocking high development. Weldon (1983) provides a description of the formation of cutoff lows downstream of slowly eastward moving building ridges showing a branch of a main jet stream located on the east side of the ridge. The jet stream configuration shown (1B-73a) is during the "closing" phase of the cutoff low formation. The main jet stream turns anticyclonically over the ridge, but does not cross the trough. The cutoff low that forms is located in the left front quadrant of the jet. Significant cloudiness usually forms at the base of the trough before the low closes, and persists after the low has cut off. In satellite imagery, the cloudiness can be used to monitor the movement and evolution of the cutoff low and for new cyclonic developments within the circulation system.

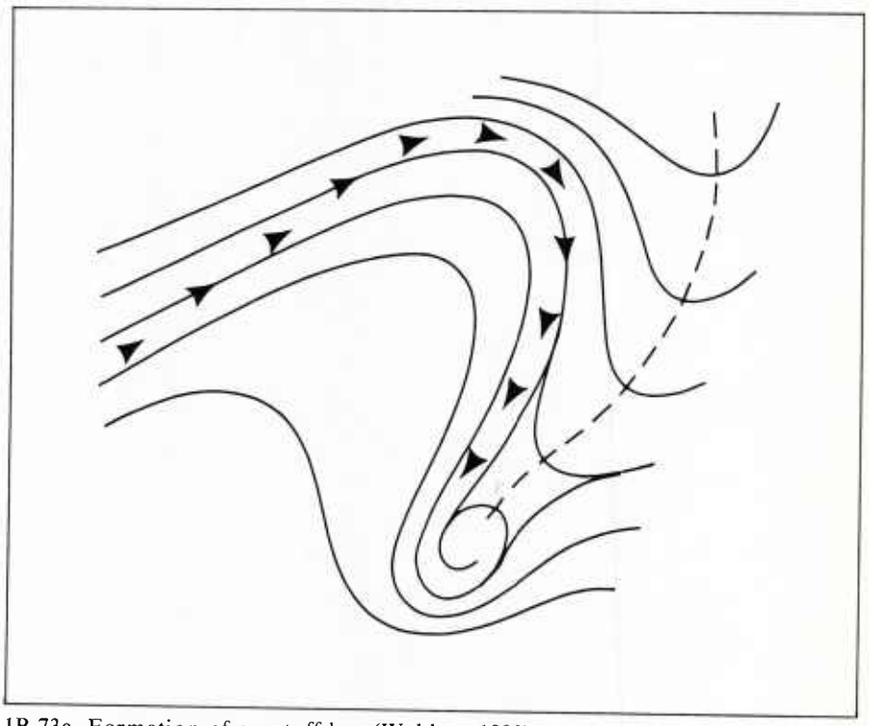

1B-73a. Formation of a cutoff low (Weldon, 1983).

Reference

Weldon, Roger A., 1983: Cutoff lows. Their cloud patterns, wind fields, and evolution. Unpublished notes. NOAA/NESDIS, Satellite Applications Laboratory. Washington, D.C.

Cutoff low development and subsequent deep cyclone formation in the cutoff low
Northeastern Pacific
March 1979

22 March

The upper-air wind field at 300 mb (1B-74a) shows a strong polar jet turning anticyclonically over a sharp ridge **B** in the Gulf of Alaska. Wind speeds of 195 kt and 95 kt, respectively, are located on the west side and east side of the ridge. The polar jet on the east side is digging toward the base of the elongated trough **C-C**. Along the southern border of the trough **C**, a subtropical jet is observed crossing Baja California into the United States. At 500 mb (1B-74b), the high-amplitude trough-ridge-trough pattern **A-B-C** suggests a slowly eastward-moving, synoptic system characteristic of a blocking situation.

In the GOES-W infrared picture at 0045 GMT (1B-75a), the bright, north-south oriented cloud band **A1-A1** is additional evidence that there is a block located over the northeastern Pacific. The NMC surface analysis (1B-75b) provides confirmation of the block: a strong surface high **B**, associated with the upper-air ridge at 500 mb, and a north-south cold front **A1-A1** forced against the western boundary of the surface high. A most important feature on the satellite picture is the vorticity comma cloud pattern **C1** north of cloud band **C1-C1** just off the United States Pacific Northwest. This disturbance has developed in the left front quadrant of the polar jet, on the east side of the ridge at 300 mb, and is the precursor to the development of a cutoff low in the trough **C-C**. This development proceeds according to Weldon's criteria that the cutoff low that forms is located in the left front quadrant of the jet.

An inspection of the FNOC 36- and 72-hour 500-mb prognoses (1B-75c and 1B-75d) reveals that the blocking ridge **B** will persist over the northeastern Pacific, and a cutoff low **C1** will develop and become a major upper-air circulation feature over the eastern Pacific by the end of the forecast period.

During the first 12 hours into the forecast period, the polar jet at 300 mb (1B-76a) has weakened somewhat on the west side of the blocking ridge **B**; however, it remains strong on the east side. At 500 mb (1B-76b), a cutoff low **C1** is developing in the elongated trough **C-C**. Notice that the cutoff low has formed in the left front quadrant of the 300-mb jet, as indicated by Weldon's model (refer to schematic 1B-73a). The cutoff low extends to the surface where it appears as a closed low **C1** on the NMC surface analysis (1B-77b).

In the satellite picture at 1245 GMT (1B-77a), the low **C1** also shows signs of intensifying, as evidenced by the appearance of a spiral pattern in the low-level clouds and a distinct crescent-shaped, middle-level cloud formation in the eastern sector.

23 March

The polar jet on the east side of the 300-mb ridge (1B-78a) has almost completed a full anticyclonic turn and has started to turn back cyclonically around the low **C1**. At 500 mb (1B-78b), the low **C1** is cut off as forecast. The combination of the low **C1**, the ridge **B**, and the upstream low **A** show the characteristic "Omega" blocking pattern typically observed over the eastern Pacific during the winter months.

The upper- and lower-level wind field associated with the cutoff low **C1** is strikingly outlined in the satellite picture (1B-79a). At upper levels, bright streaks of high clouds make a broad sweep around the cutoff low, and the tight, low-level spiral cloud pattern shows the location of the closed low at the surface (1B-79b). As the surface low **C1** has developed, the blocking surface high **B** has weakened. The frontal cloud band **A1-A1** has also weakened—this is because of the surface high **B1** moving eastward against the surface high **B**, in advance of the new major storm **D1**. Some enhanced convective activity **A2**, however, is occurring along the trailing section of the frontal band **A1-A1**, at the base of the 500-mb trough **A**.

The NMC 300-mb (1B-80a) and 500-mb (1B-80b) analyses display the synoptic situation over the northeastern Pacific at the end of the FNOC 36-hour guidance period. As forecast (refer to 1B-75c), a cutoff low **C1** is located off the Pacific Northwest, and the analyses show that a closed low extends from 300 mb (1B-80a) to the surface (1B-81b). Notice that the cutoff low **C1** has remained in the left front quadrant of the polar jet at 300 mb, and as the jet has turned westward the track of the low has followed, as indicated by the past position path of the cloud vortex **C1** in the satellite picture (1B-81a). According to Weldon, after the low closes, the branch of the main polar jet responsible for initiating the development decreases in intensity; however, wind speed maxima may persist in the wind field around the cutoff low.

The blocking high **B** at the surface (1B-81b) has slowed the eastward advance of the frontal system **A1-A1**. The satellite picture shows that this system has weakened considerably, particularly, as the surface high **B1**, in advance of the new storm **D1**, moves eastward and merges across the front with the high **B**.

continued on page 1B-82

300 mb

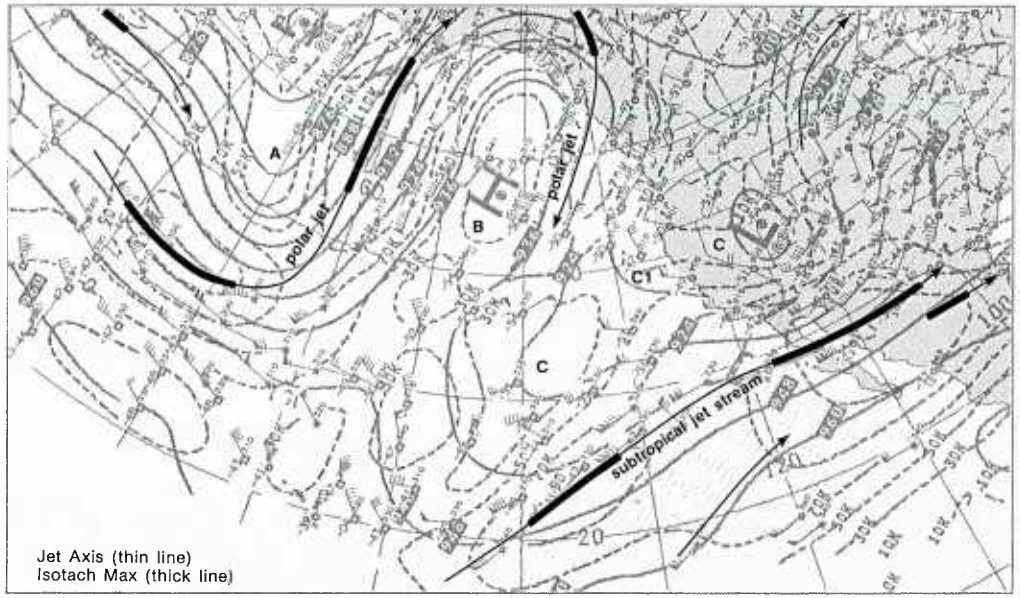

1B-74a. NMC 300-mb Analysis. 0000 GMT 22 March 1979.

500 mb

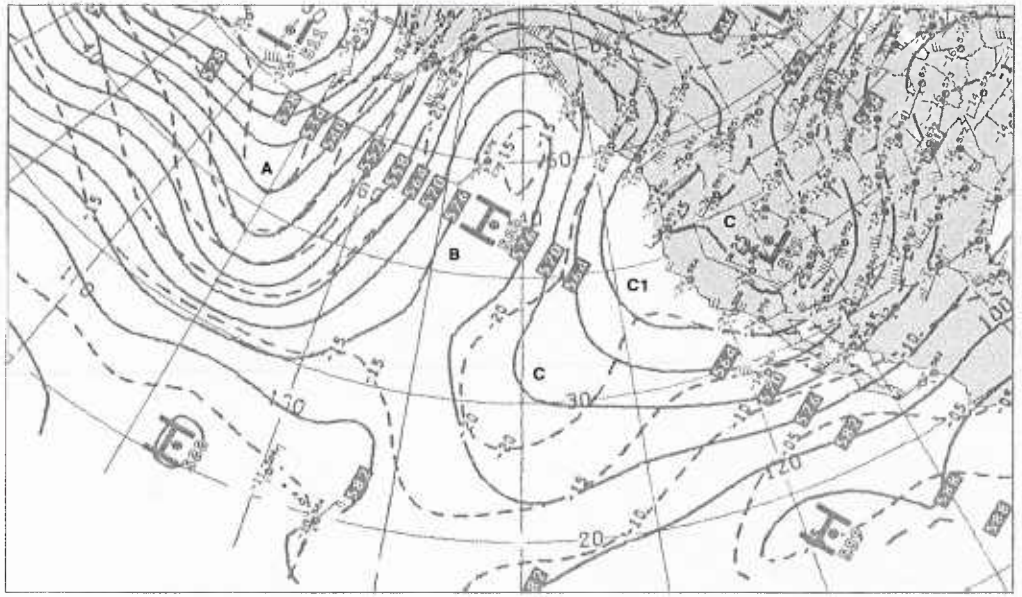

1B-74b. NMC 500-mb Analysis. 0000 GMT 22 March 1979.

Southward Displacement of a Short-wave Disturbance

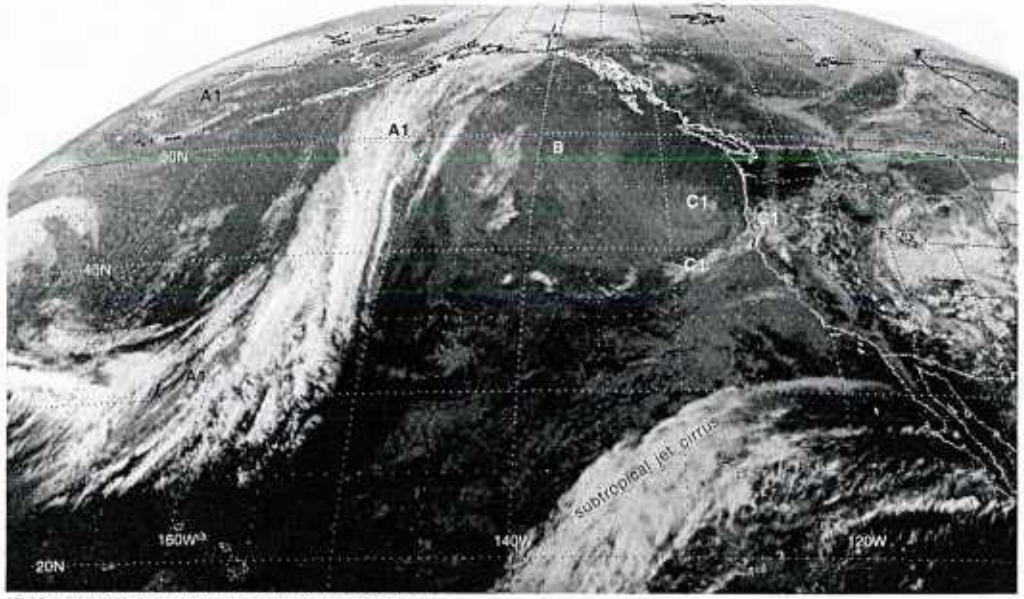

1B-75a. GOES-W. Infrared Picture. 0045 GMT 22 March 1979.

surface

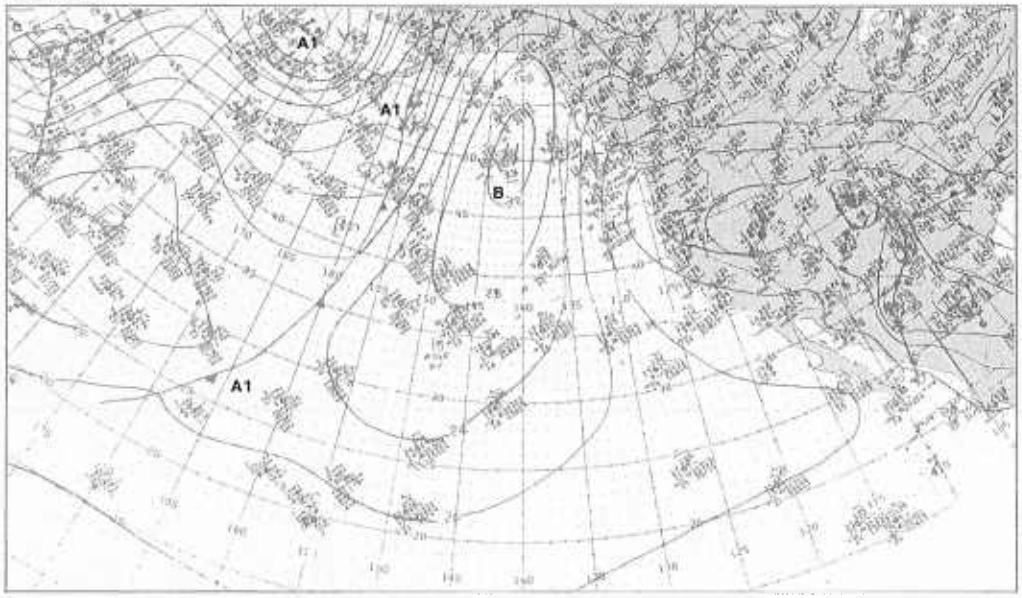

1B-75b. NMC Surface Analysis. 0000 GMT 22 March 1979.

500 mb

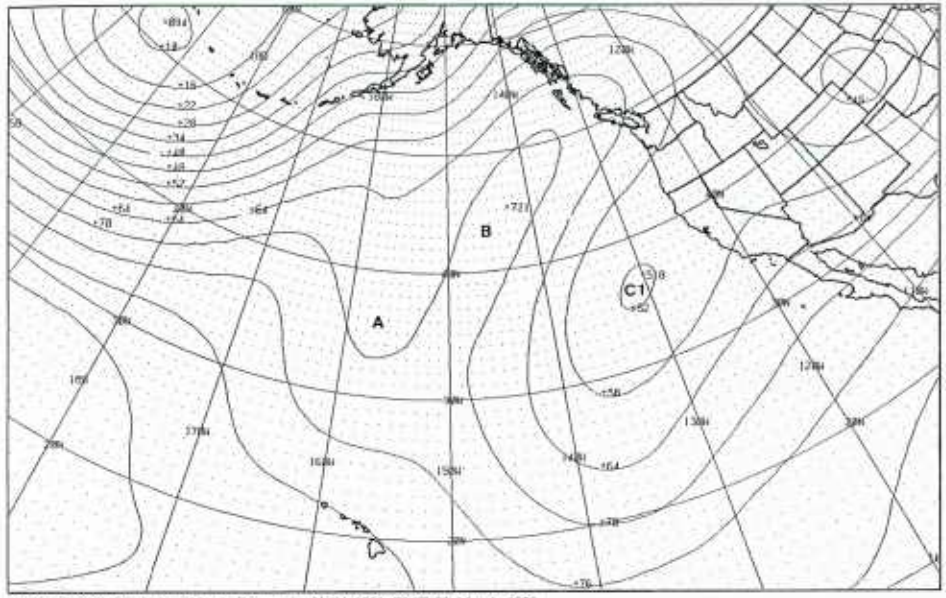

1B-75c. FNOC PE 36-hr 500-mb Prognosis. Valid 1200 GMT 23 March 1979.

500 mb

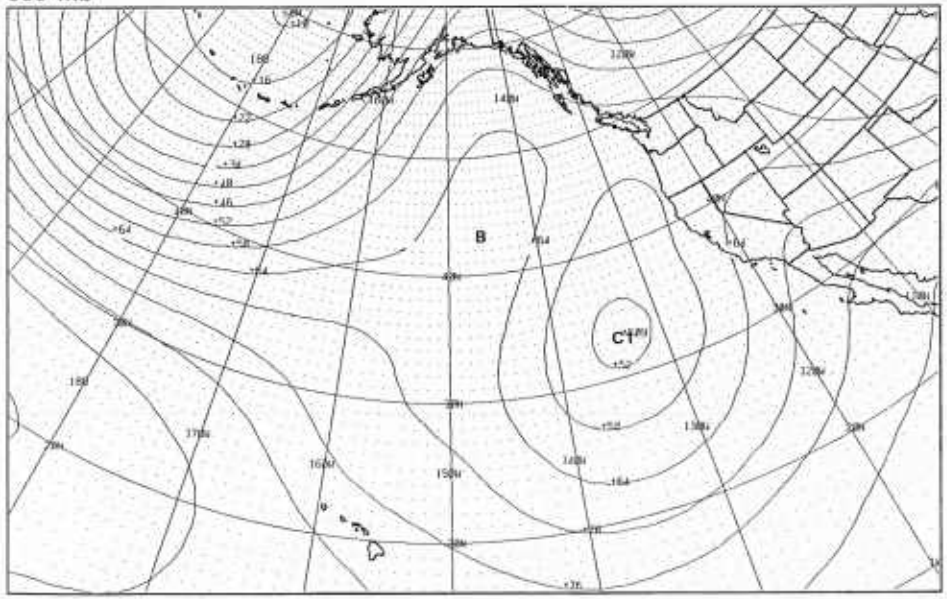

1B-75d. FNOC PE 72-hr 500-mb Prognosis. Valid 0000 GMT 25 March 1979.

300 mb

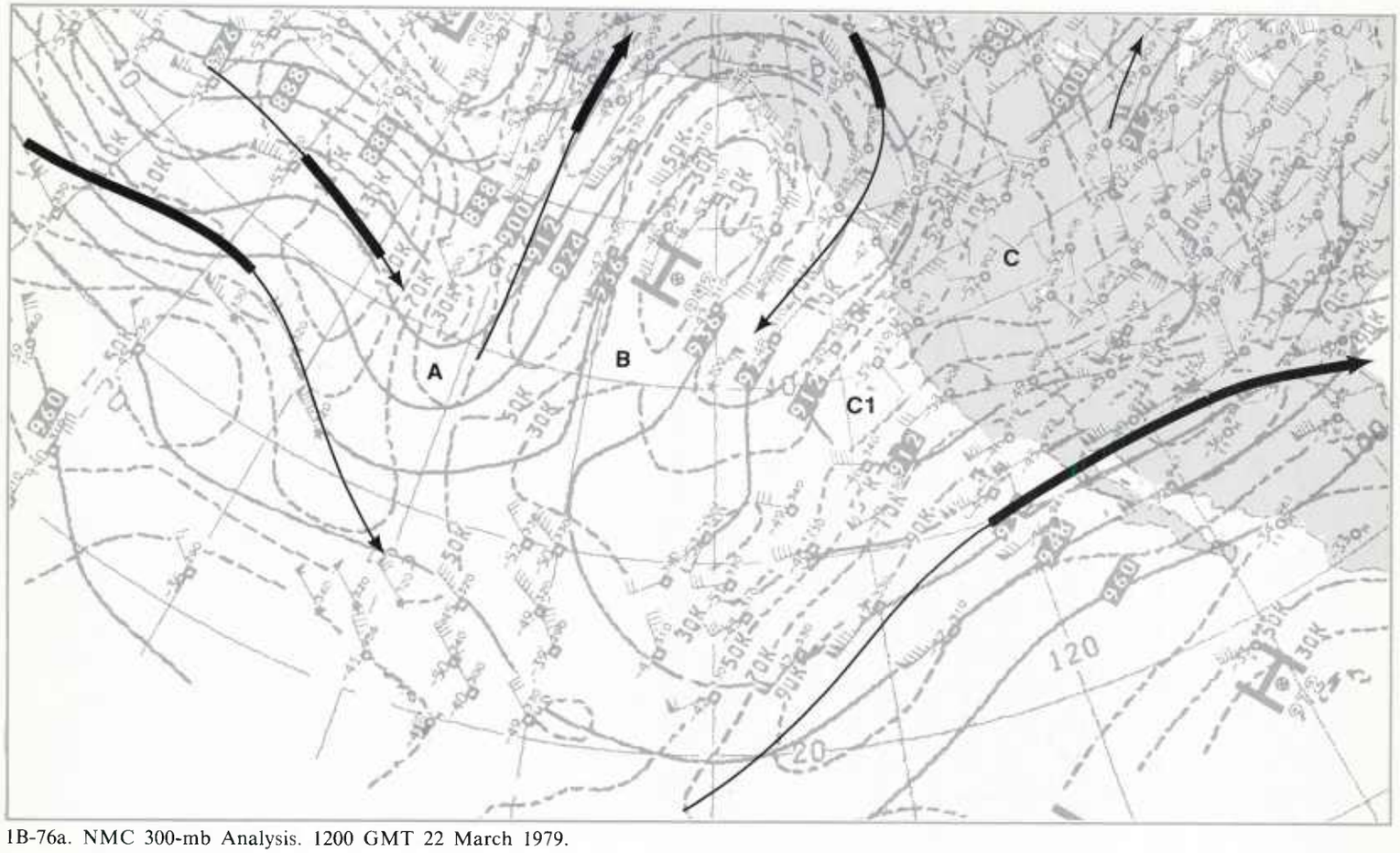

1B-76a. NMC 300-mb Analysis. 1200 GMT 22 March 1979.

500 mb

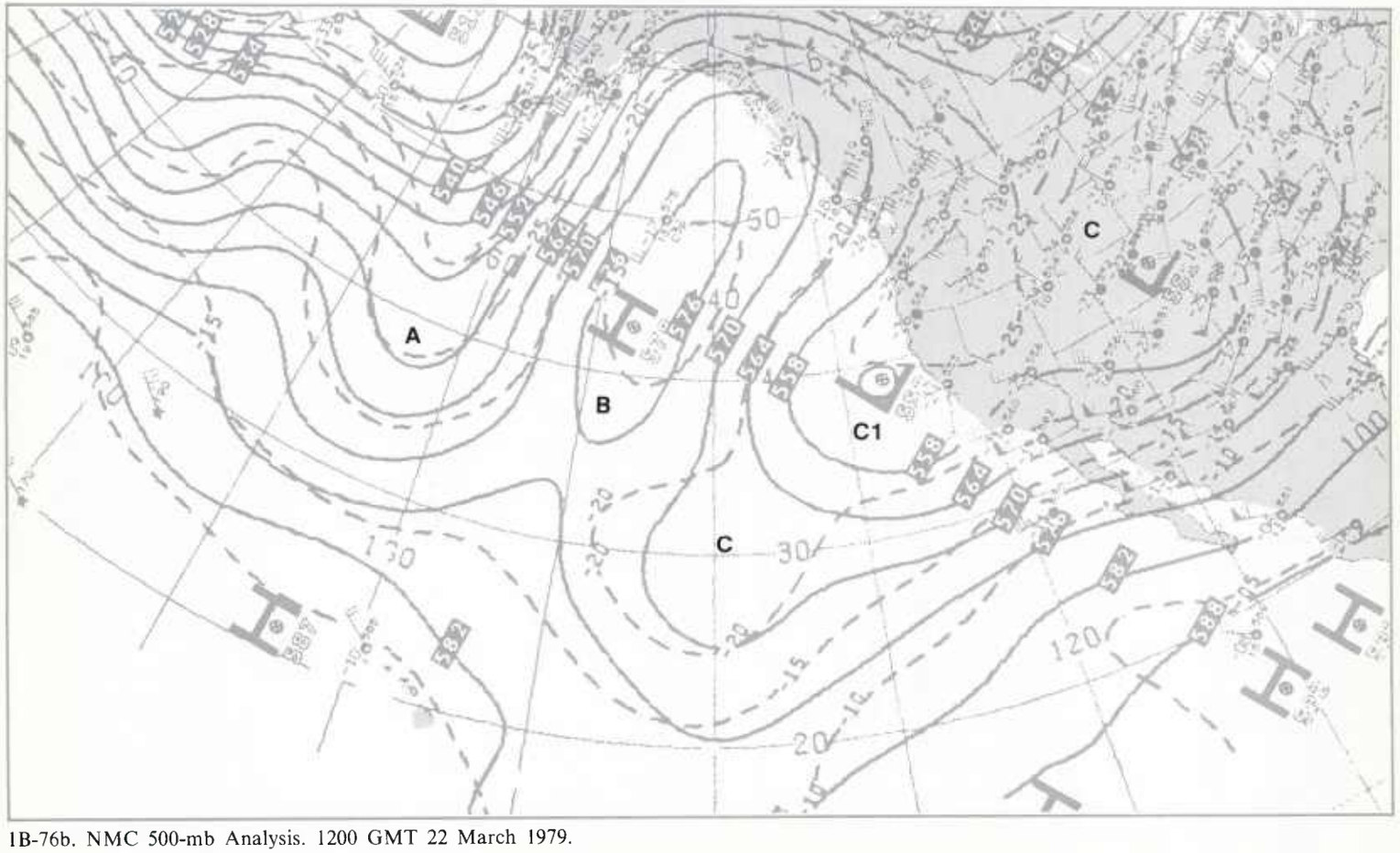

1B-76b. NMC 500-mb Analysis. 1200 GMT 22 March 1979.

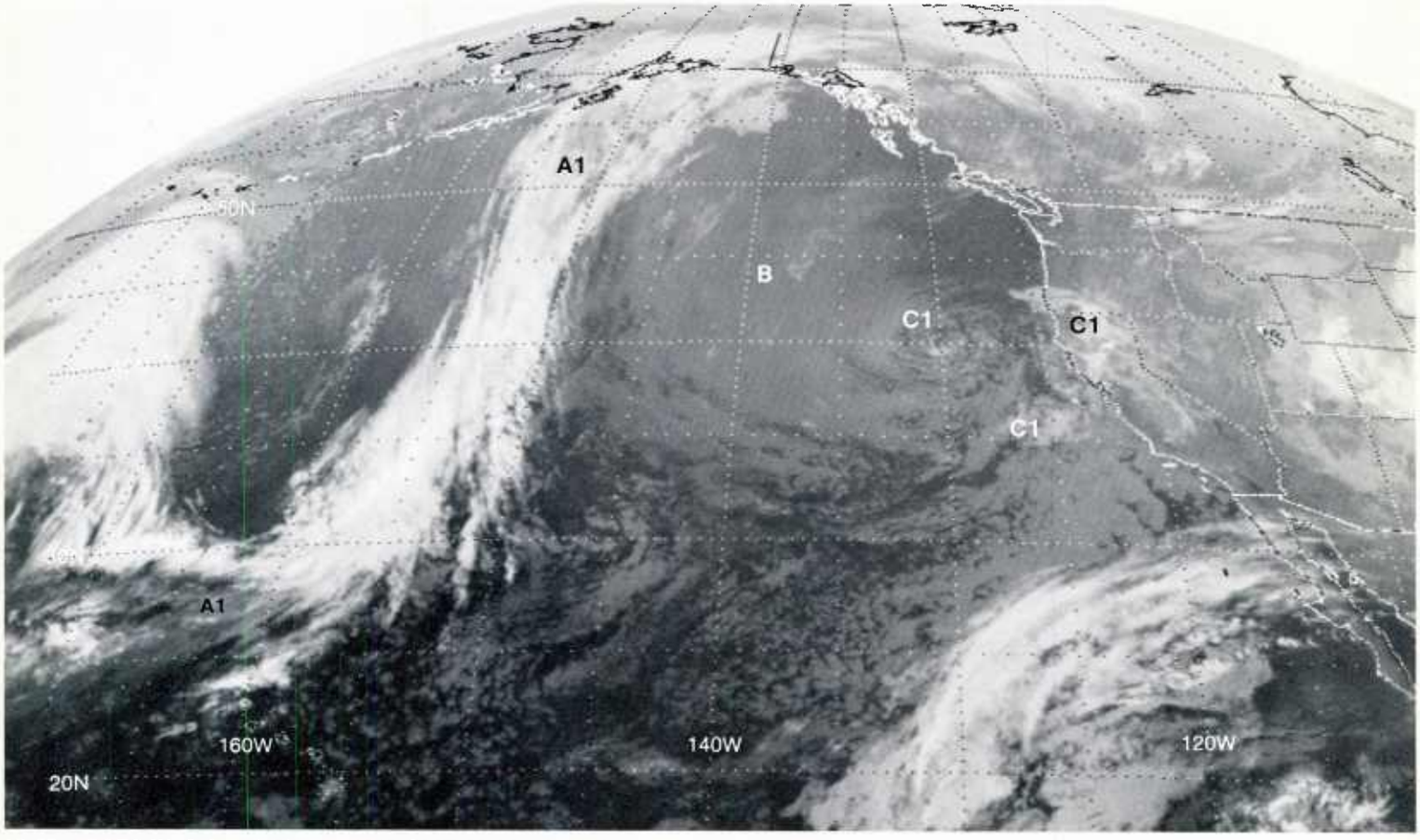

1B-77a. GOES-W. Infrared Picture. 1245 GMT 22 March 1979.

surface

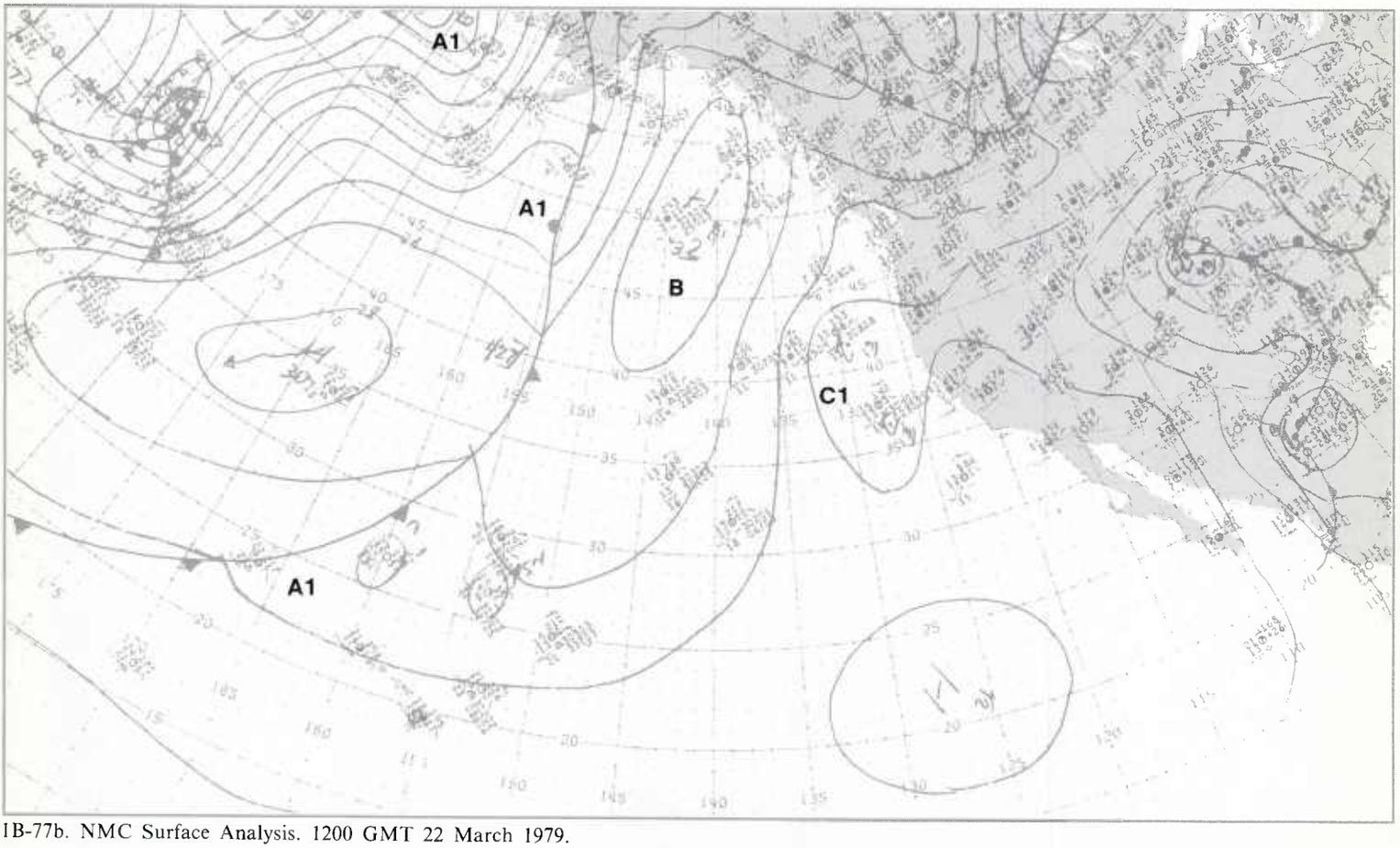

1B-77b. NMC Surface Analysis. 1200 GMT 22 March 1979.

300 mb

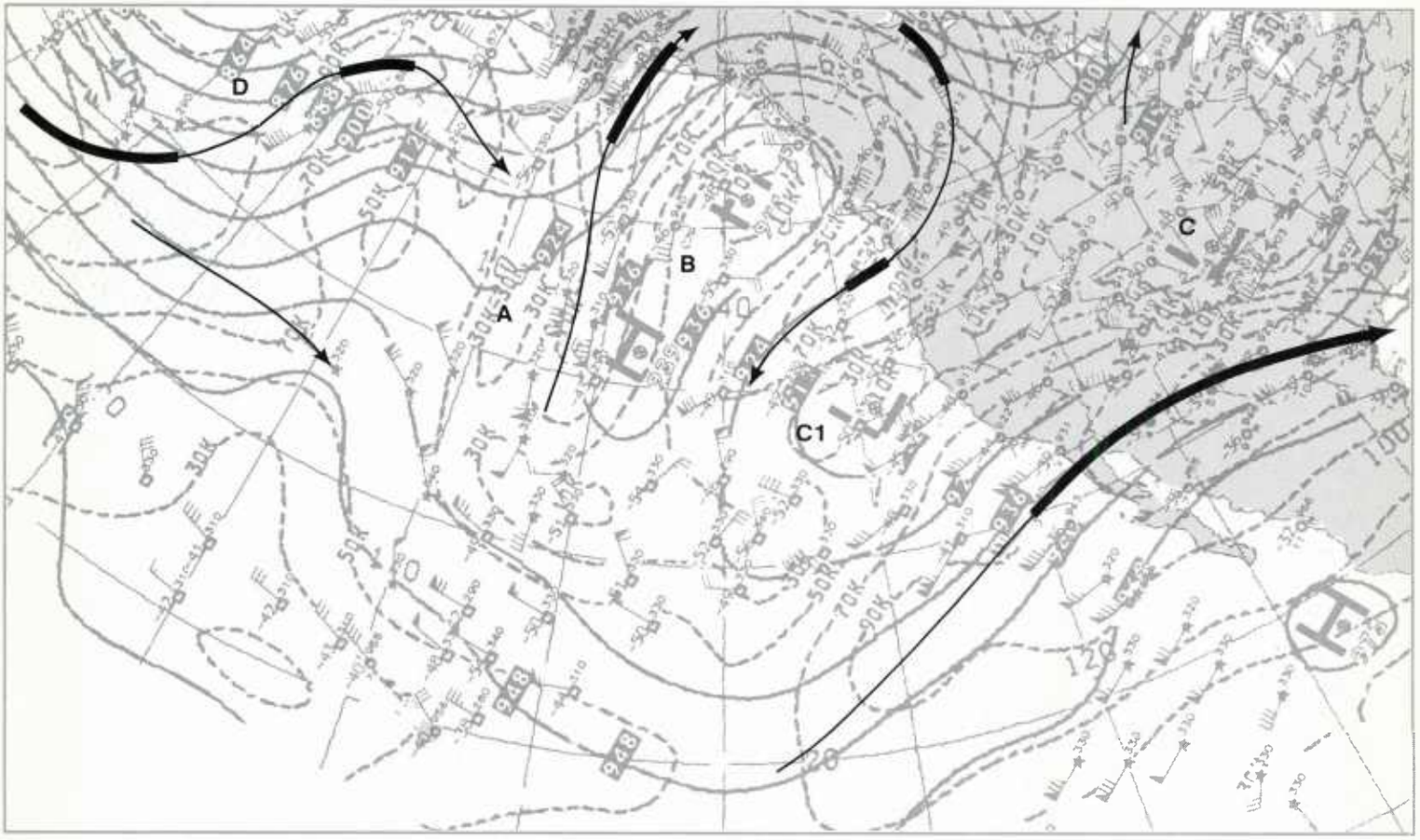

1B-78a. NMC 300-mb Analysis. 0000 GMT 23 March 1979.

500 mb

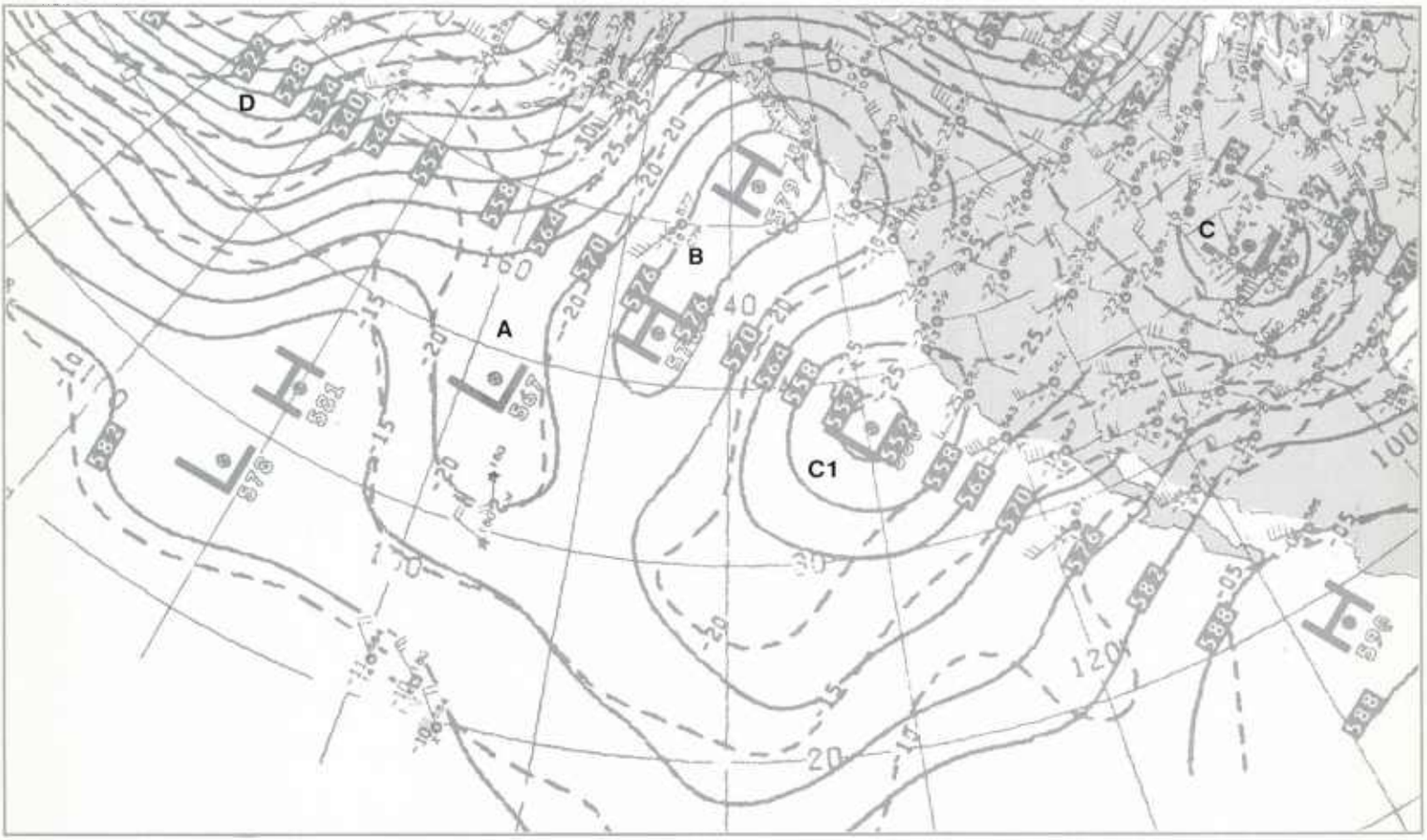

1B-78b. NMC 500-mb Analysis. 0000 GMT 23 March 1979.

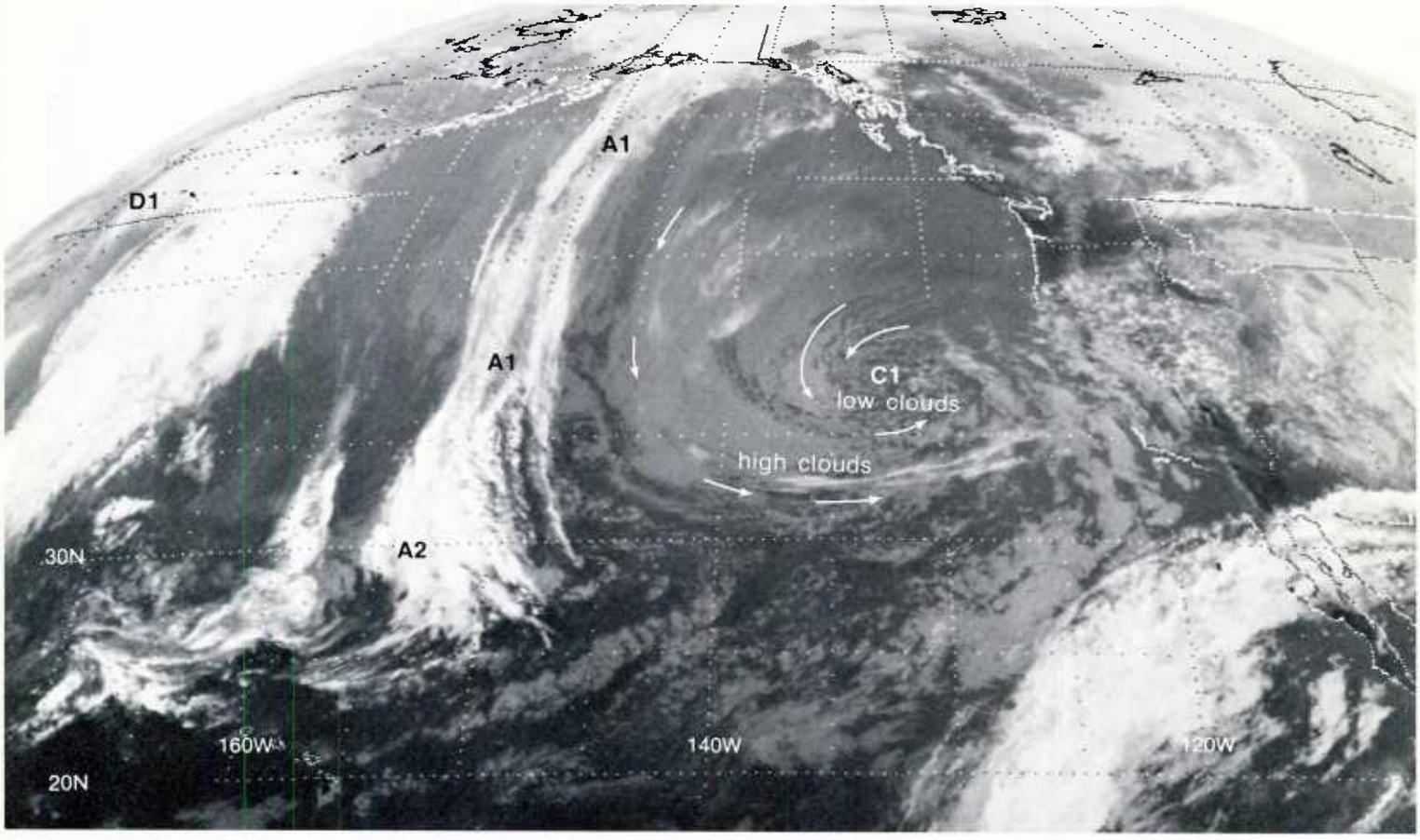

1B-79a. GOES-W. Infrared Picture. 0045 GMT 23 March 1979.

surface

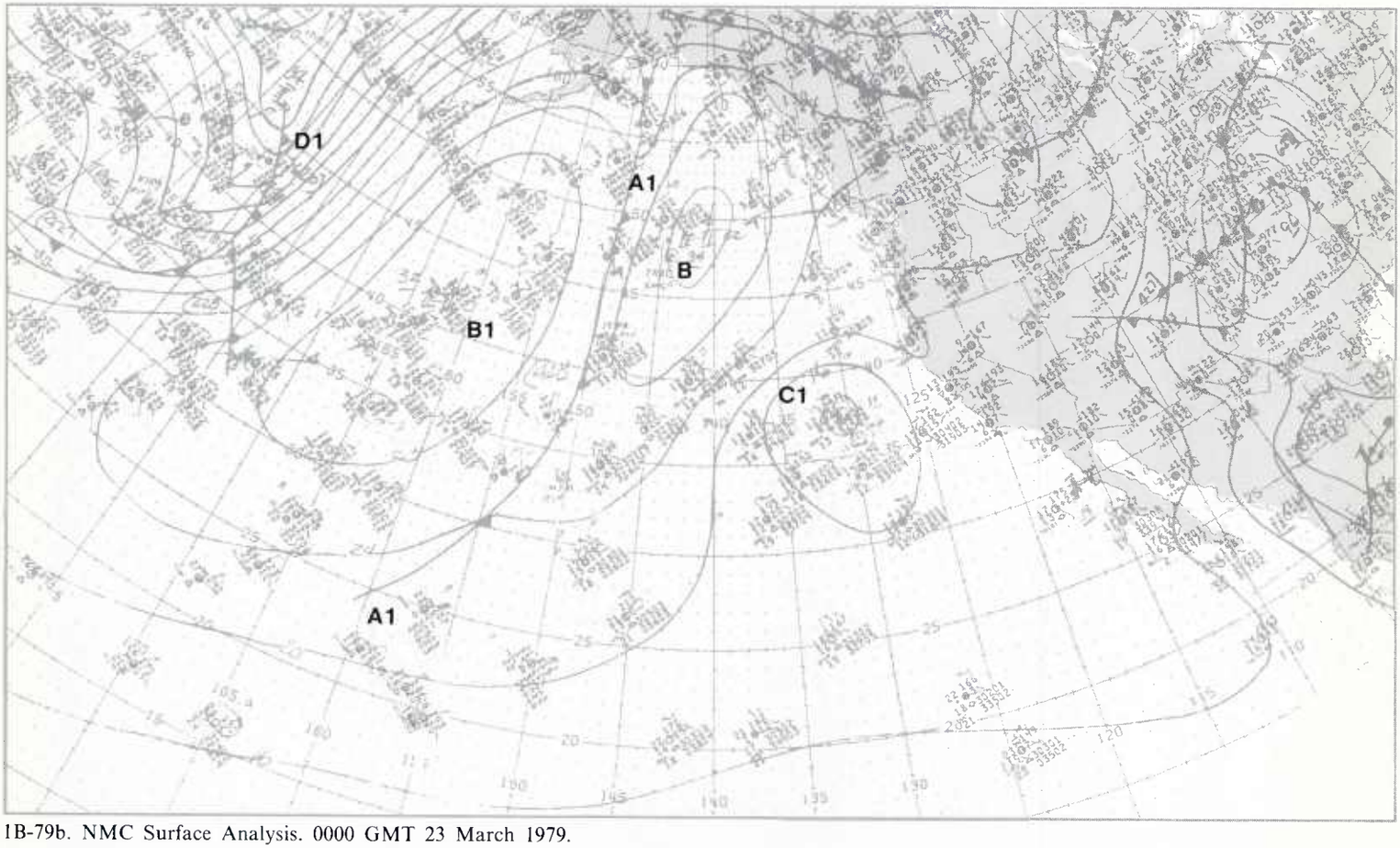

1B-79b. NMC Surface Analysis. 0000 GMT 23 March 1979.

300 mb

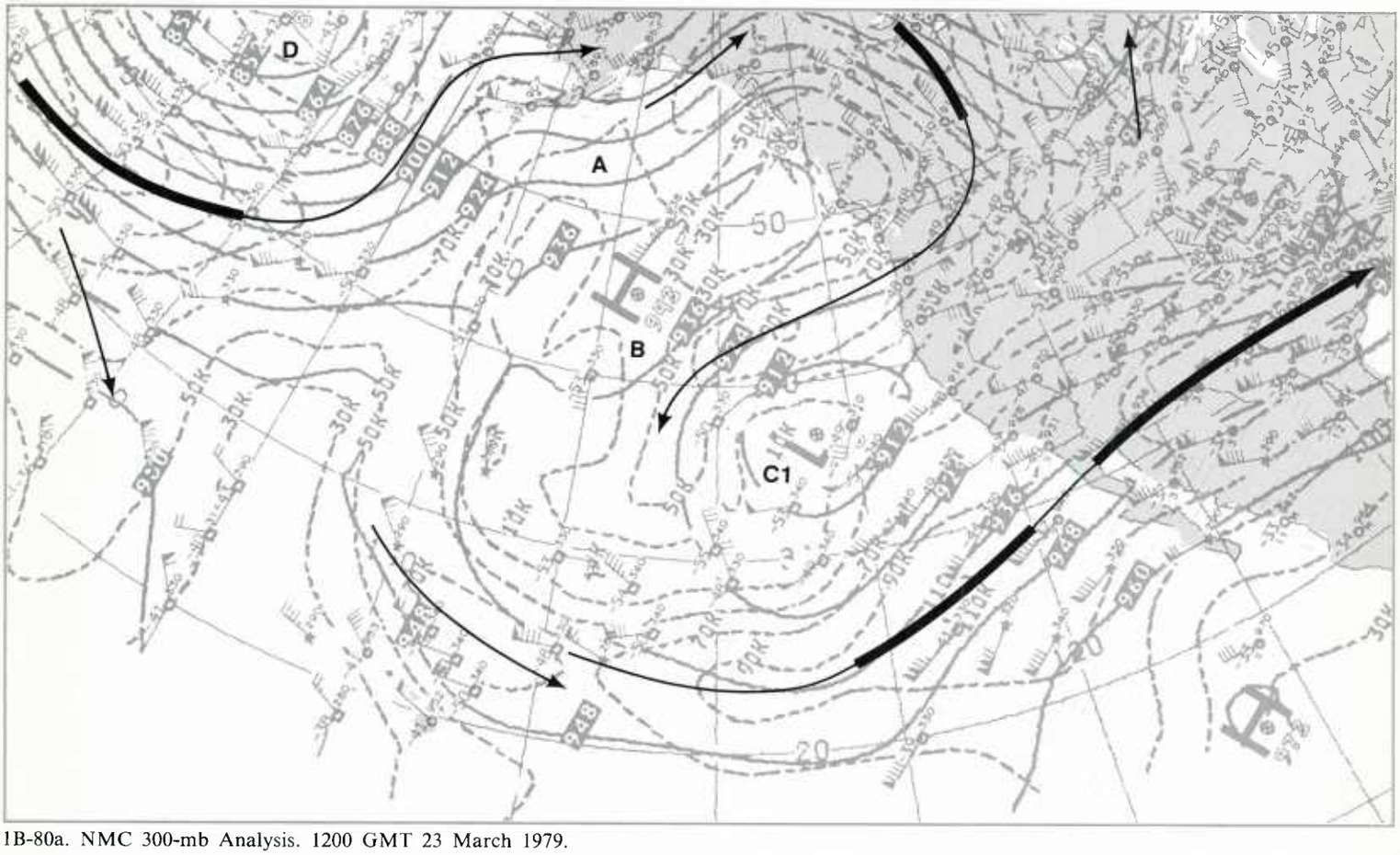

1B-80a. NMC 300-mb Analysis. 1200 GMT 23 March 1979.

500 mb

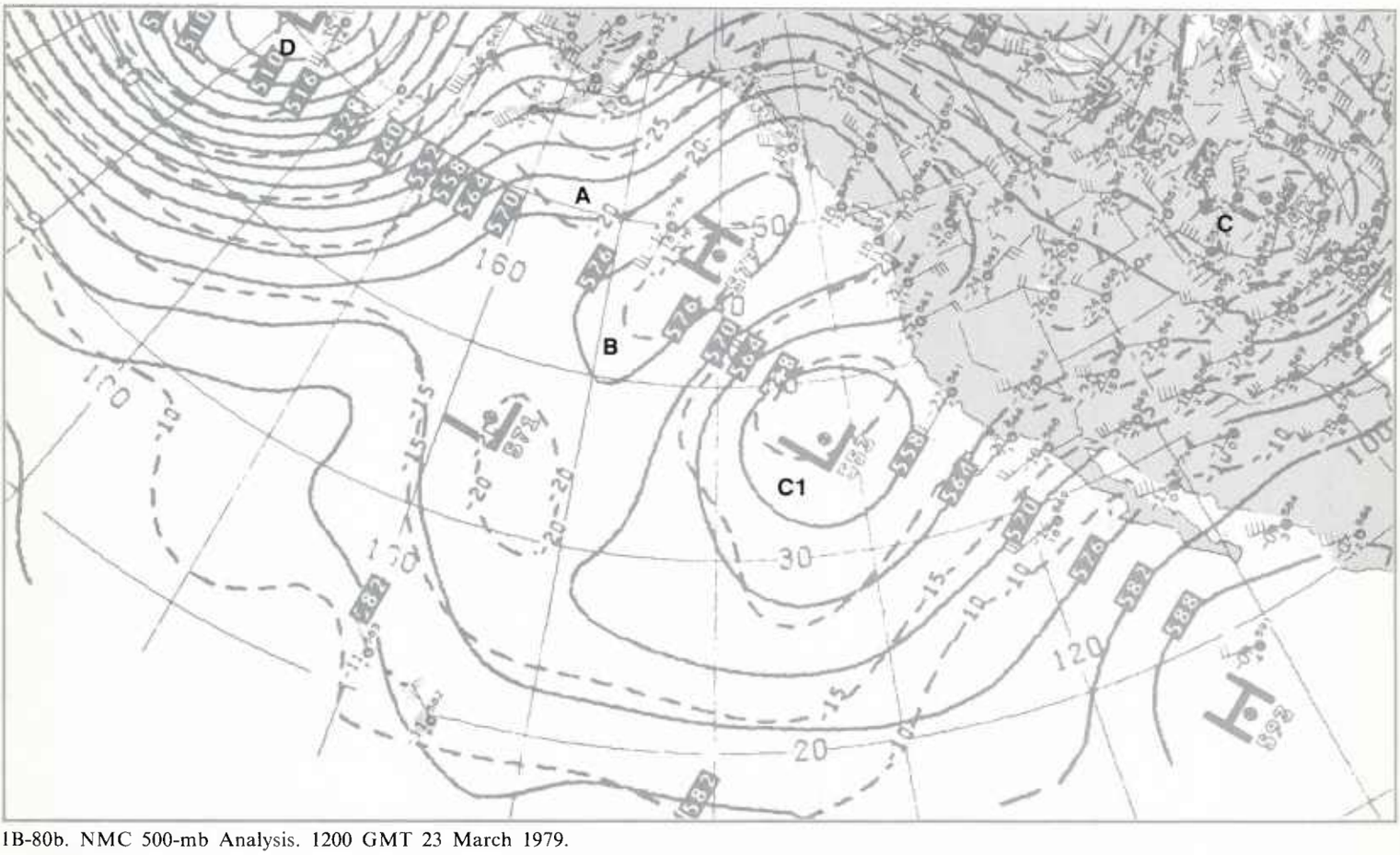

1B-80b. NMC 500-mb Analysis. 1200 GMT 23 March 1979.

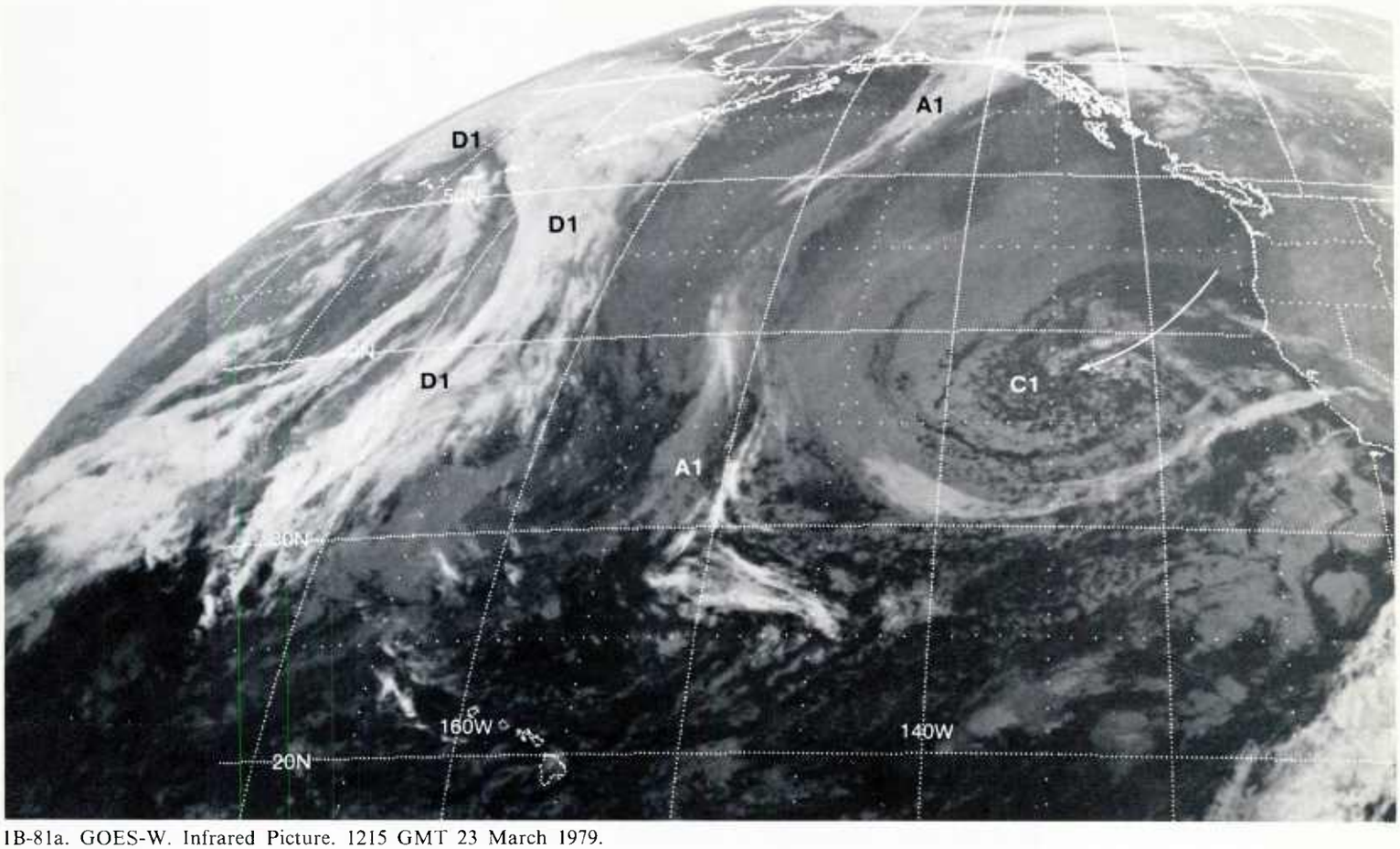

1B-81a. GOES-W. Infrared Picture. 1215 GMT 23 March 1979.

surface

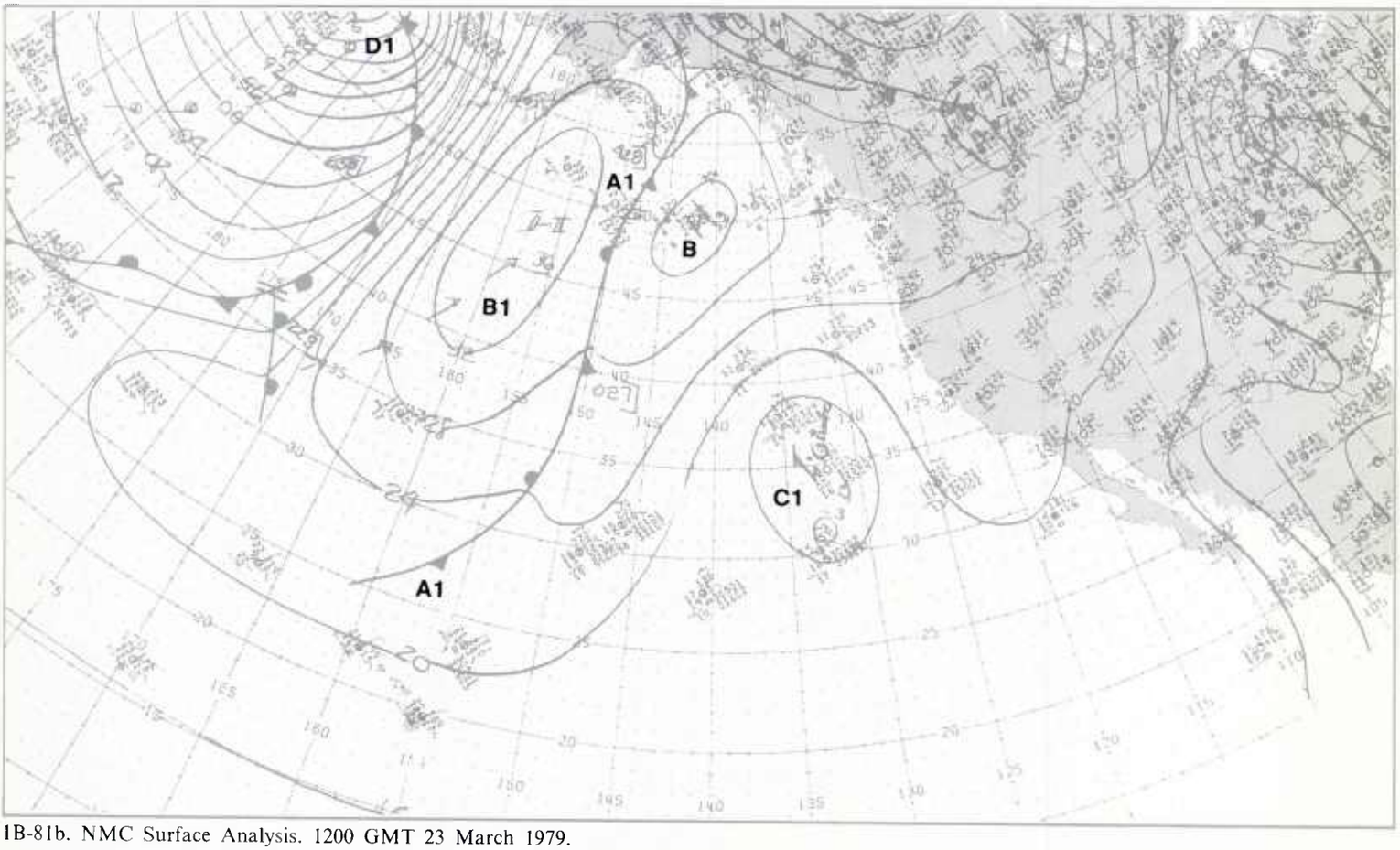

1B-81b. NMC Surface Analysis. 1200 GMT 23 March 1979.

24–25 March

On 24 March (data not shown), the cutoff low continued to track slowly westward and the polar jet on the east side of the blocking ridge diminished in intensity. By 0000 GMT 25 March, the cutoff low **C1** is vertically stacked from 300 mb (1B-82a), through 500 mb (1B-82b), to the surface (1B-83b). Notice that the polar jet on the back side of the cutoff low has weakened considerably and that a main branch of the polar jet coming over the block **B** is connected across the trough **A**, forming a band of westerlies at northern latitudes from the eastern Pacific to the northern United States.

A most significant feature at 300 mb (1B-82a) is the presence of polar jet streaks (**PJS**) in the wind field around the cutoff low **C1**. Such jet streaks are associated with short-wave disturbances, and the bright comma cloud **C2** in the satellite picture (1B-83a) pinpoints the location of one of these disturbances. The cloud vortex **C1** identifies the location of the cutoff low relative to the short-wave disturbance **C2**. The satellite picture also shows that the disturbance **D1** upstream of the blocking high **B** has become a major winter storm, with a deep surface low (1B-83b). At the surface, the high **B1** has replaced the previous blocking high **B**. The vorticity comma cloud **A3** (1B-83a) is a new development in the trough **A** which has moved over the block at high latitudes. The disturbance is located in a polar jet moving to the southeast along the east side of block **B**.

24–25 March continued on page 1B-84

300 mb

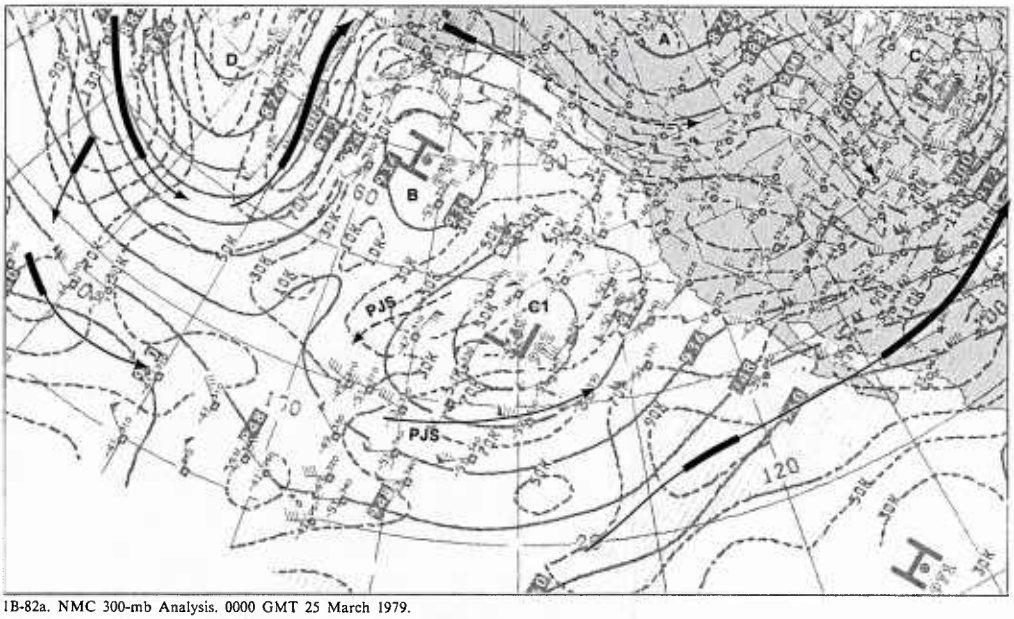

1B-82a. NMC 300-mb Analysis. 0000 GMT 25 March 1979.

500 mb

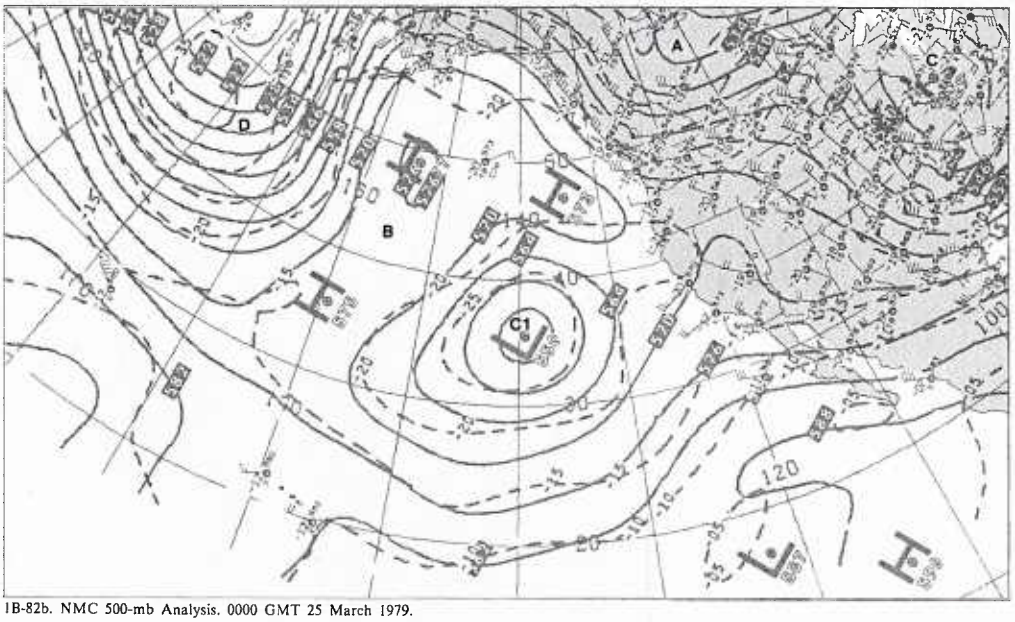

1B-82b. NMC 500-mb Analysis. 0000 GMT 25 March 1979.

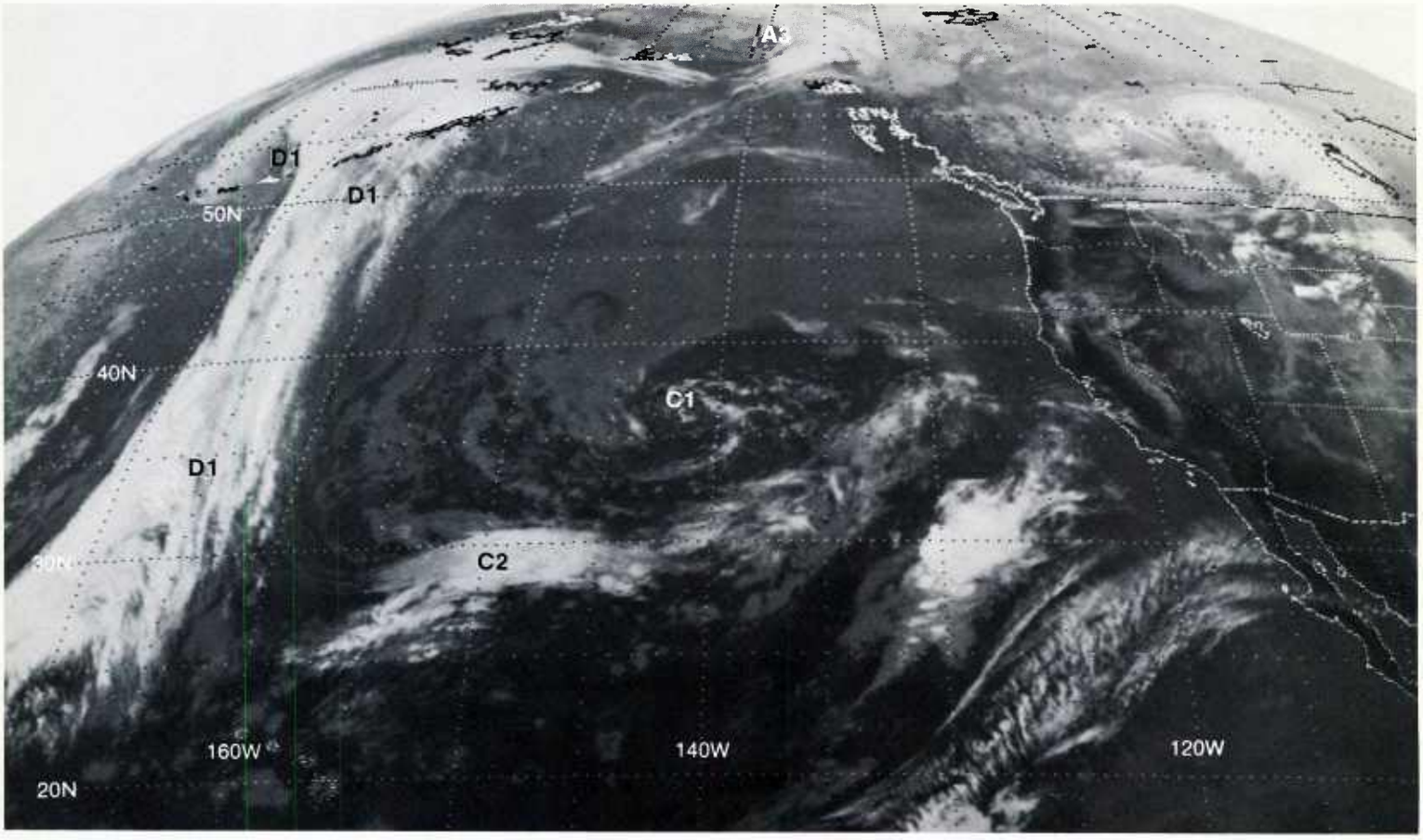

1B-83a. GOES-W. Infrared Picture. 0045 GMT 25 March 1979.

surface

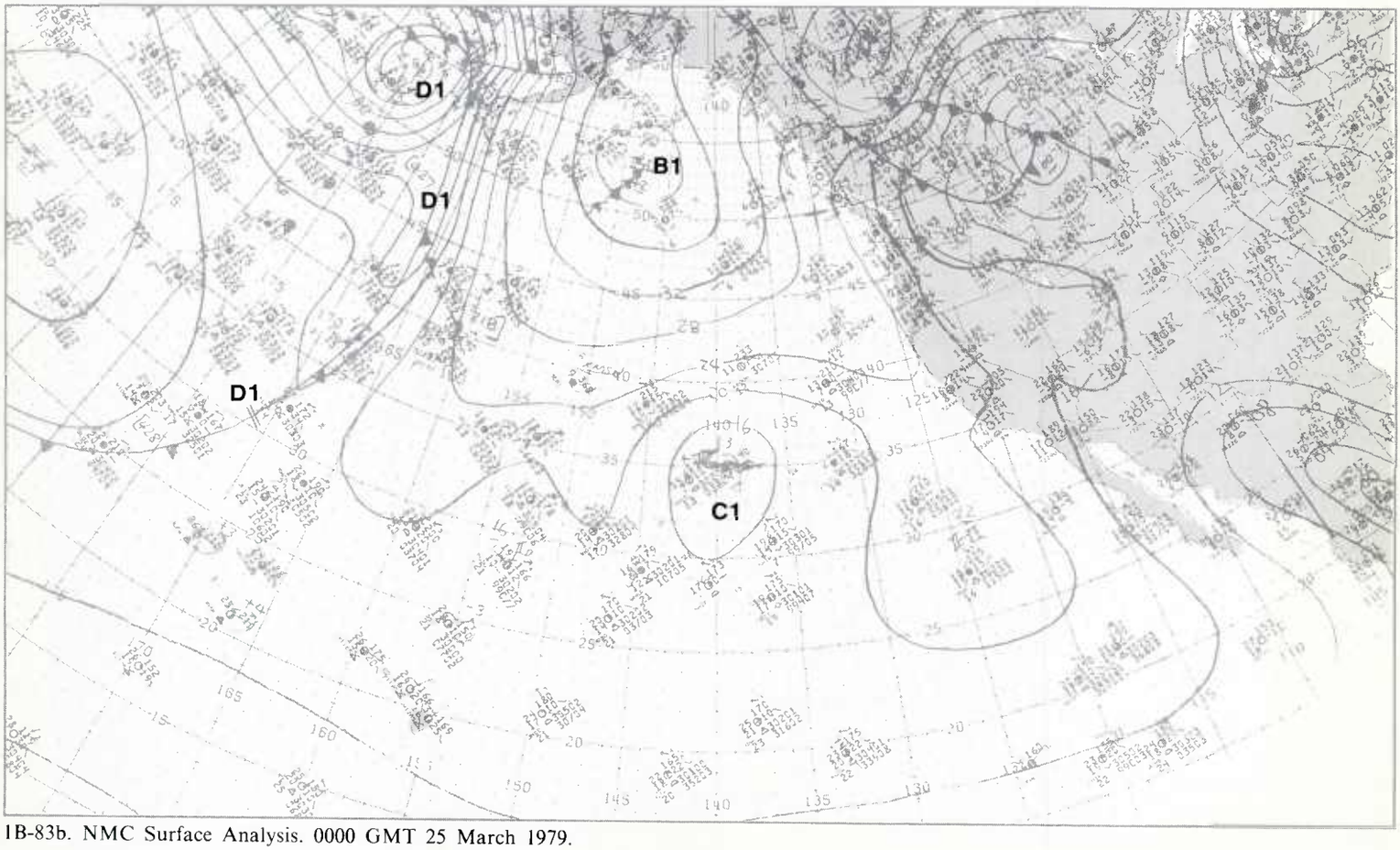

1B-83b. NMC Surface Analysis. 0000 GMT 25 March 1979.

The synoptic pattern over the northeastern Pacific, at 300 mb (1B-84a), 500 mb (1B-84b), and the surface (1B-85b), shows little change in the past 24 hours. In particular, the cutoff low **C1** has not moved from its location near 35° N, 140° W, or changed in intensity. An examination of the satellite picture (1B-85a), however, reveals a drastic change in the cloud pattern in the cutoff low. The cloud vortex **C1**, identifying the location of the cutoff low, from its initiation (1B-75a) to full development (1B-83a), has been replaced by the short-wave disturbance **C2**. The disturbance shows a very distinct comma cloud and cirrus shield characteristic of a developing storm. At 300 mb (1B-84a), note that a strong (90 kt) jet isotach maximum has formed to the south of the disturbance, and a branch of the main polar jet over the block is turning southward behind the cutoff low.

On the NMC surface analysis (1B-85b), the frontal system **D1-D1** has replaced the dissipated front **A1-A1** over the eastern Pacific. The strong frontal low **D2** which has formed on the front shows a bright, leading cloud band in the satellite picture (1B-85a). This is a squall line and indicates that the disturbance **D2** is an intense wave development. Note also in the satellite picture that the vorticity comma **A3** has moved to the southeast along the east side of the block **B** and a closed low appears at the surface.

By 0000 GMT 27 March, the cutoff low over the eastern Pacific has become a progressive trough with a major storm development. At 500 mb (1B-86b), the trough **C2** has moved eastward about 15° longitude and shows significant deepening in 24 hours (central height fall of 140 m). There is a strong (110 kt) polar jet streak (**PJS**) along the base of the trough **C2** and, at 300 mb (1B-86a), the main branch of the polar jet has plunged southward to the rear of the trough, causing strong cold air advection into the system.

In the satellite picture (1B-87a), a large, spiral cloud band has developed as the storm intensified during the past 24 hours. Note that the spiral vortex is located in the left front quadrant of the polar jet streak (**PJS**) at 300 mb—a most favorable position for rapid storm development. The NMC surface analysis (1B-87b) shows a deep surface low **C2** with an occluded frontal system. This is an excellent example of an "instant" occlusion since there were no surface fronts indicated with the low **C2**, 24 hours earlier (refer to surface analysis 1B-85b).

Important Conclusions

1. Cutoff lows are observed to form at the base of troughs to the east of slowly moving ridges that show a branch of the main polar jet stream curving anticyclonically over the ridge into the trough. The cutoff low forms in the left front quadrant of the jet streak.

2. Significant cloudiness forms at the base of the trough before the low closes, and persists after the low has cut off.

3. In satellite imagery, cloudiness can be used to monitor the movement and evolution of the cutoff low and to detect new cyclonic developments in the cutoff low circulation.

300 mb

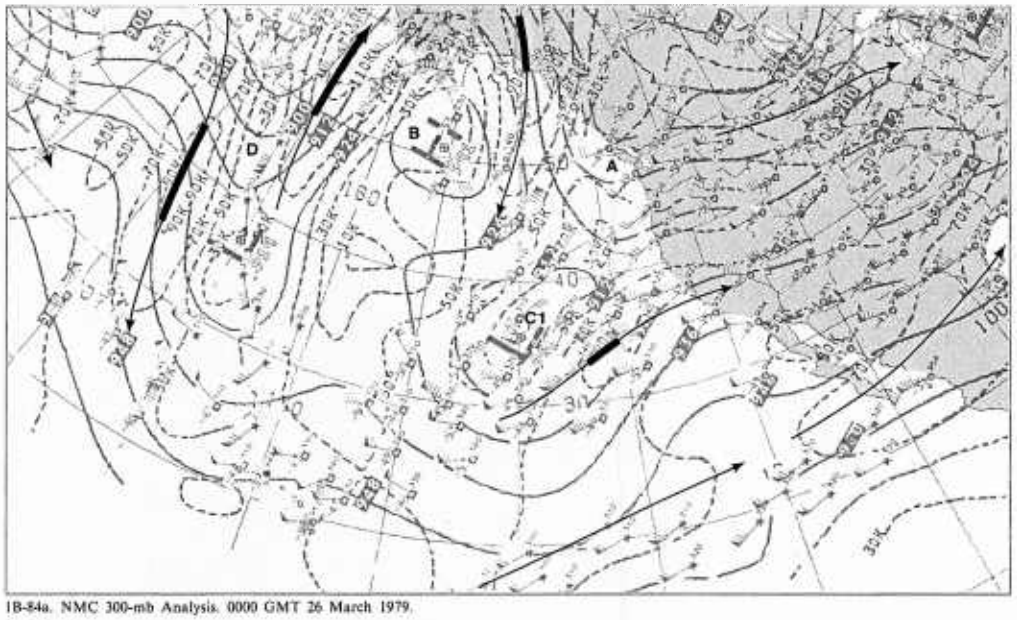

1B-84a. NMC 300-mb Analysis. 0000 GMT 26 March 1979.

500 mb

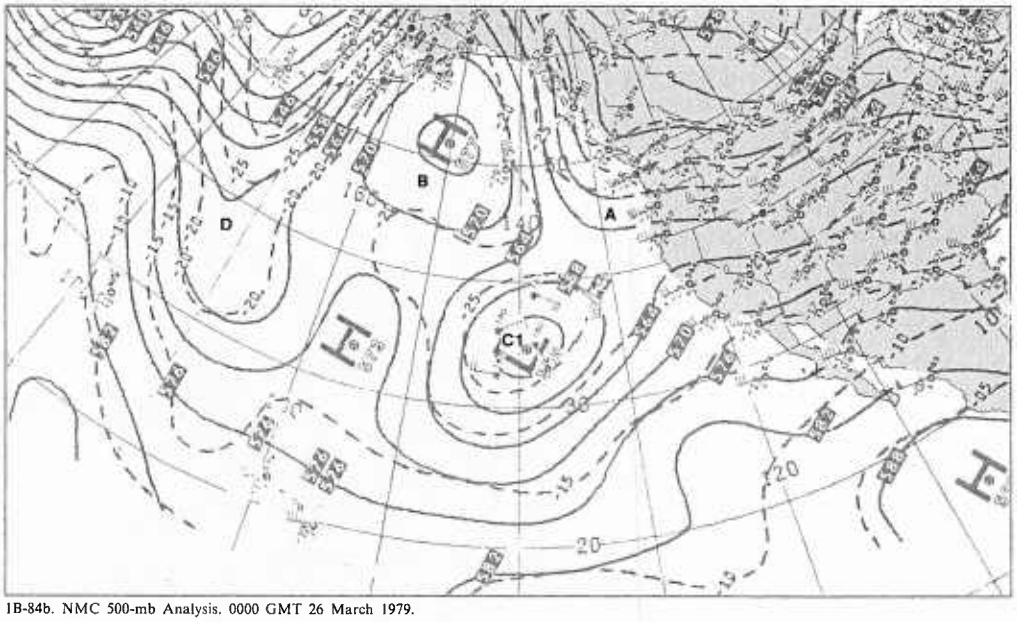

1B-84b. NMC 500-mb Analysis. 0000 GMT 26 March 1979.

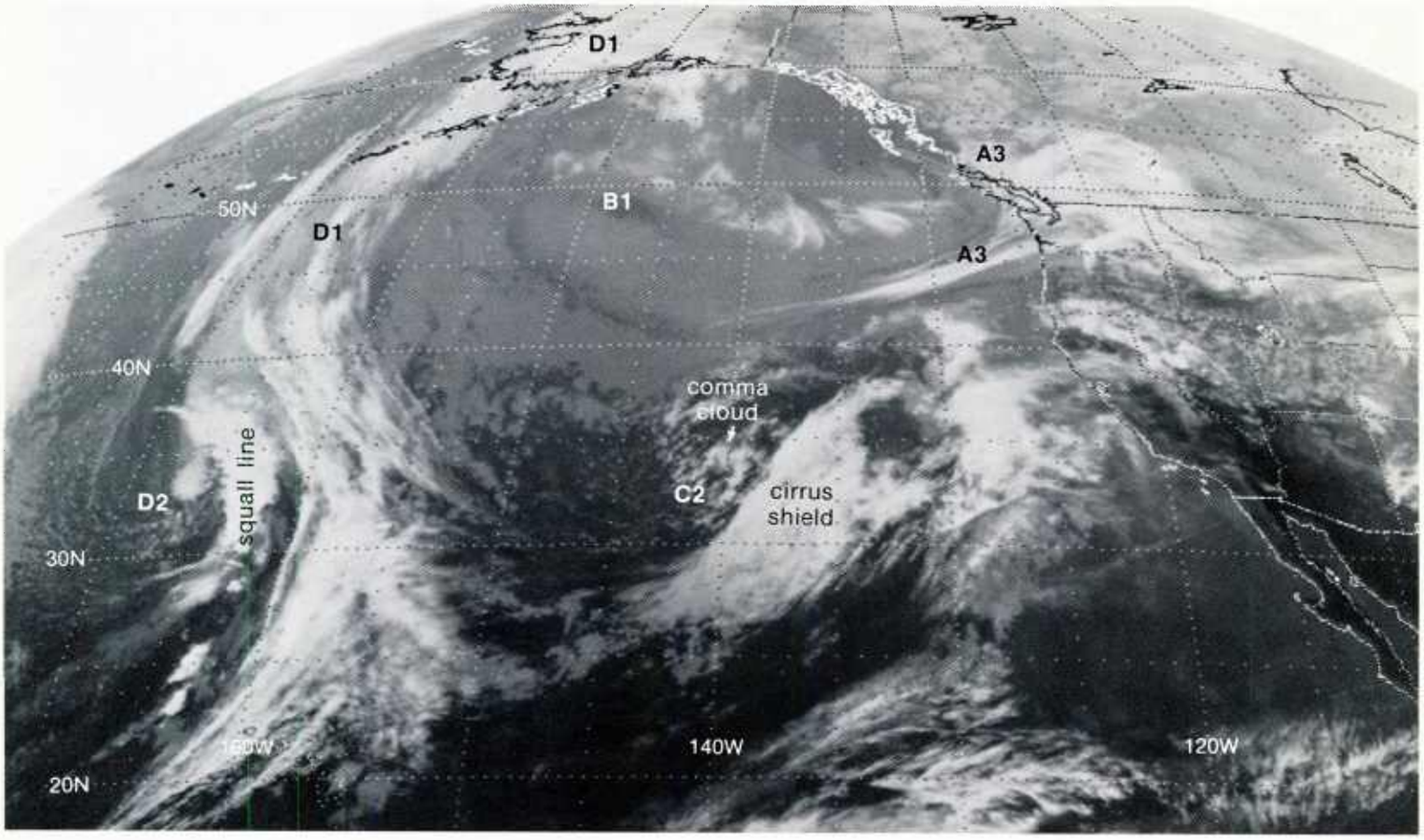

1B-85a. GOES-W. Infrared Picture. 0045 GMT 26 March 1979.

surface

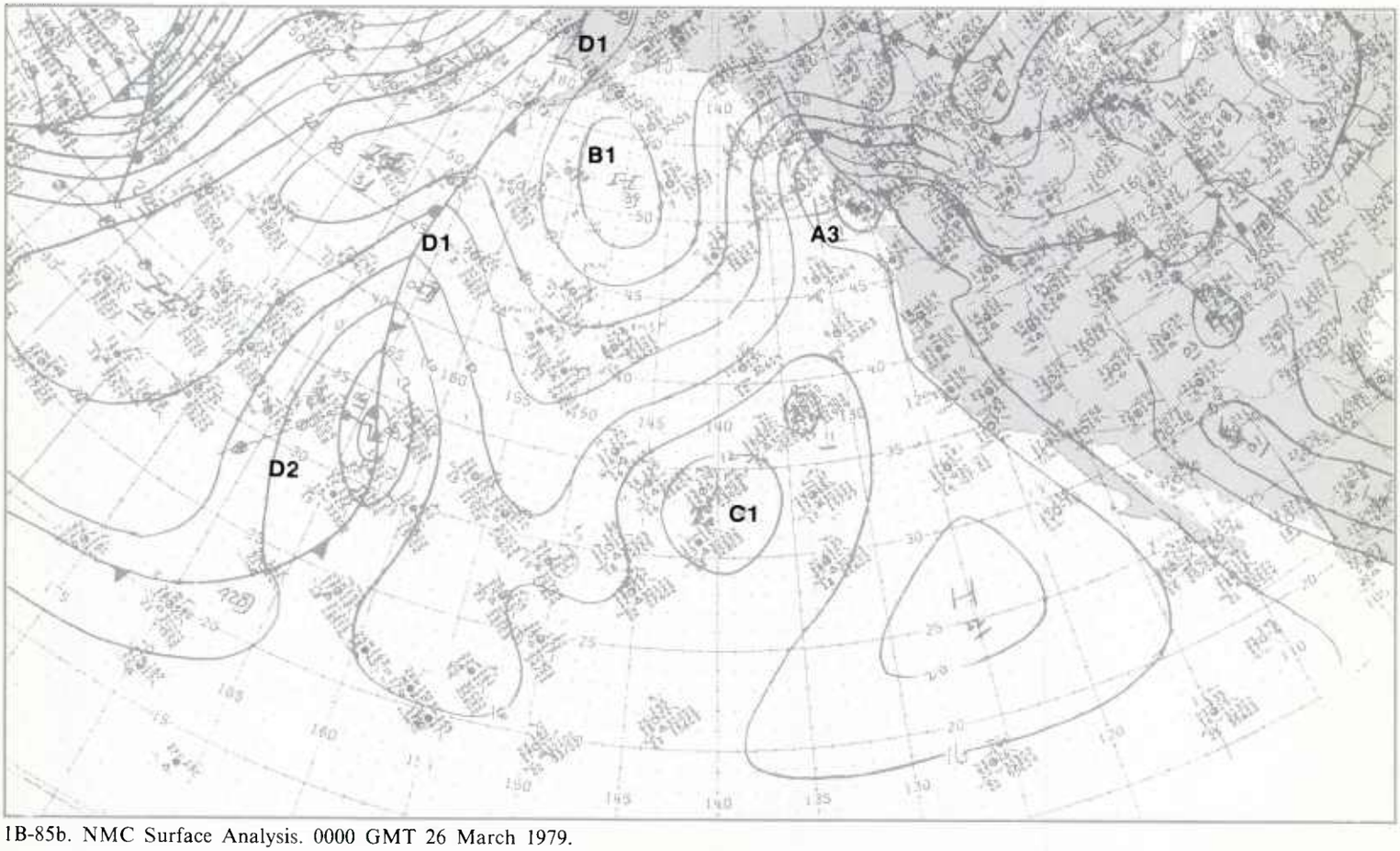

1B-85b. NMC Surface Analysis. 0000 GMT 26 March 1979.

300 mb

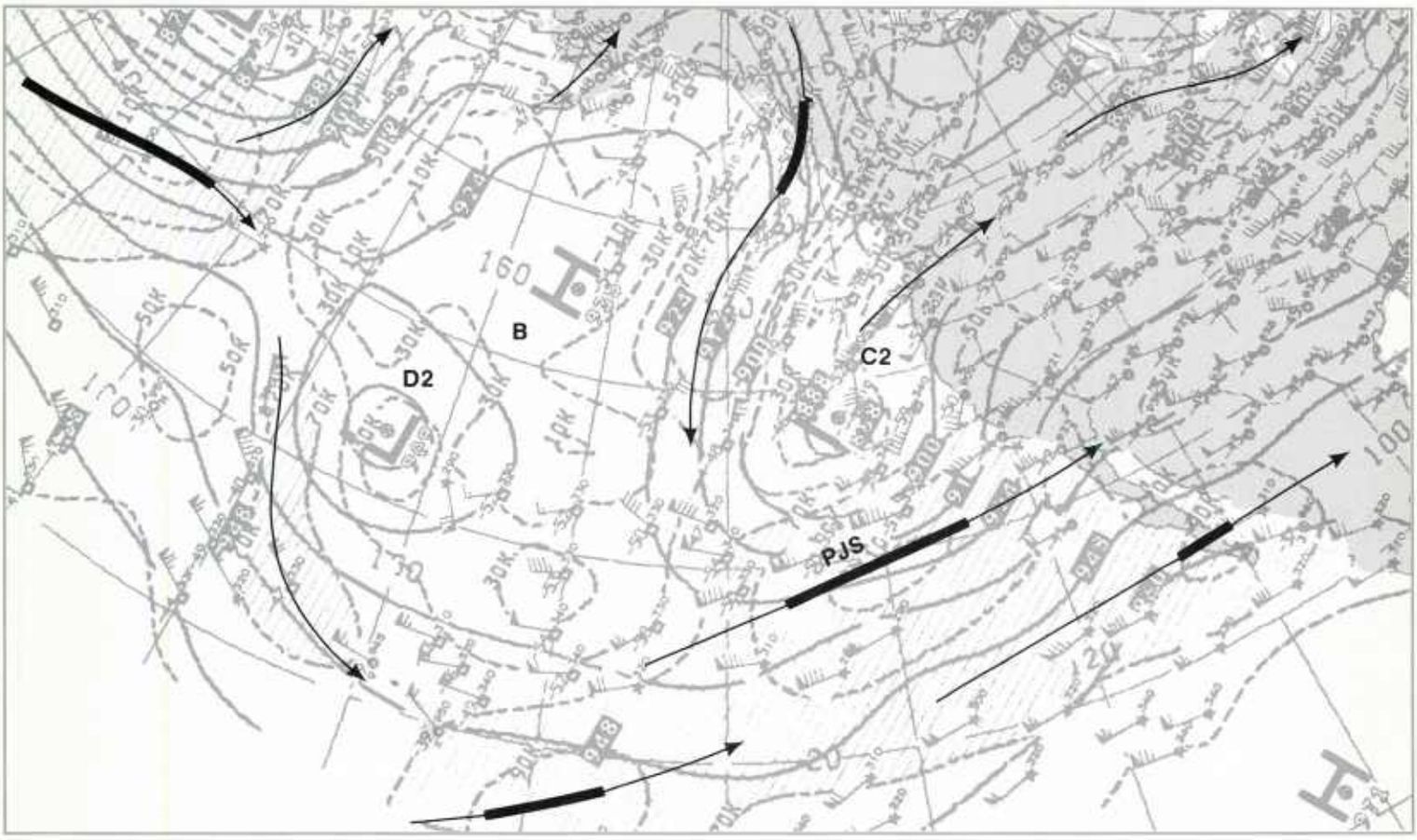

1B-86a. NMC 300-mb Analysis. 0000 GMT 27 March 1979.

500 mb

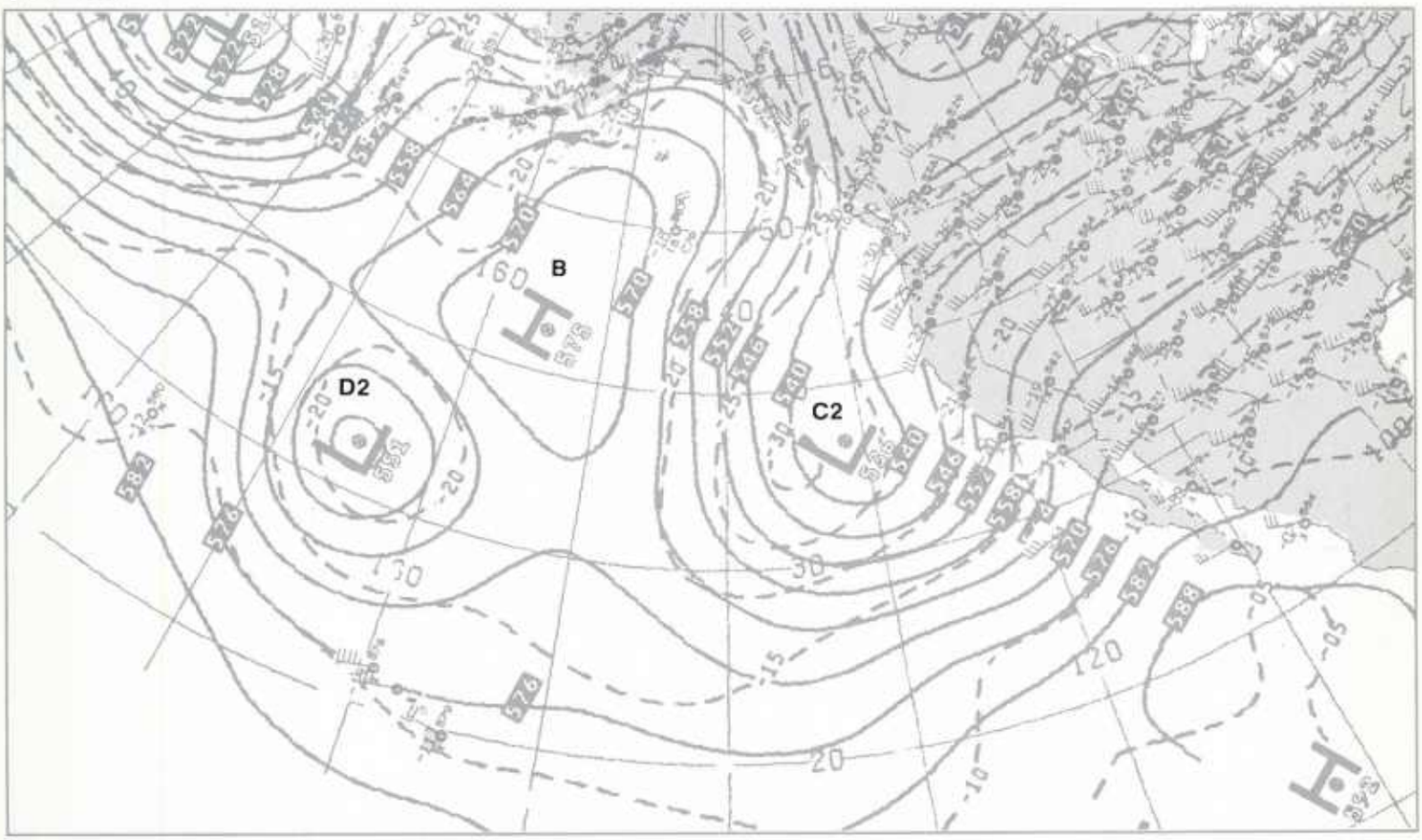

1B-86b. NMC 500-mb Analysis. 0000 GMT 27 March 1979.

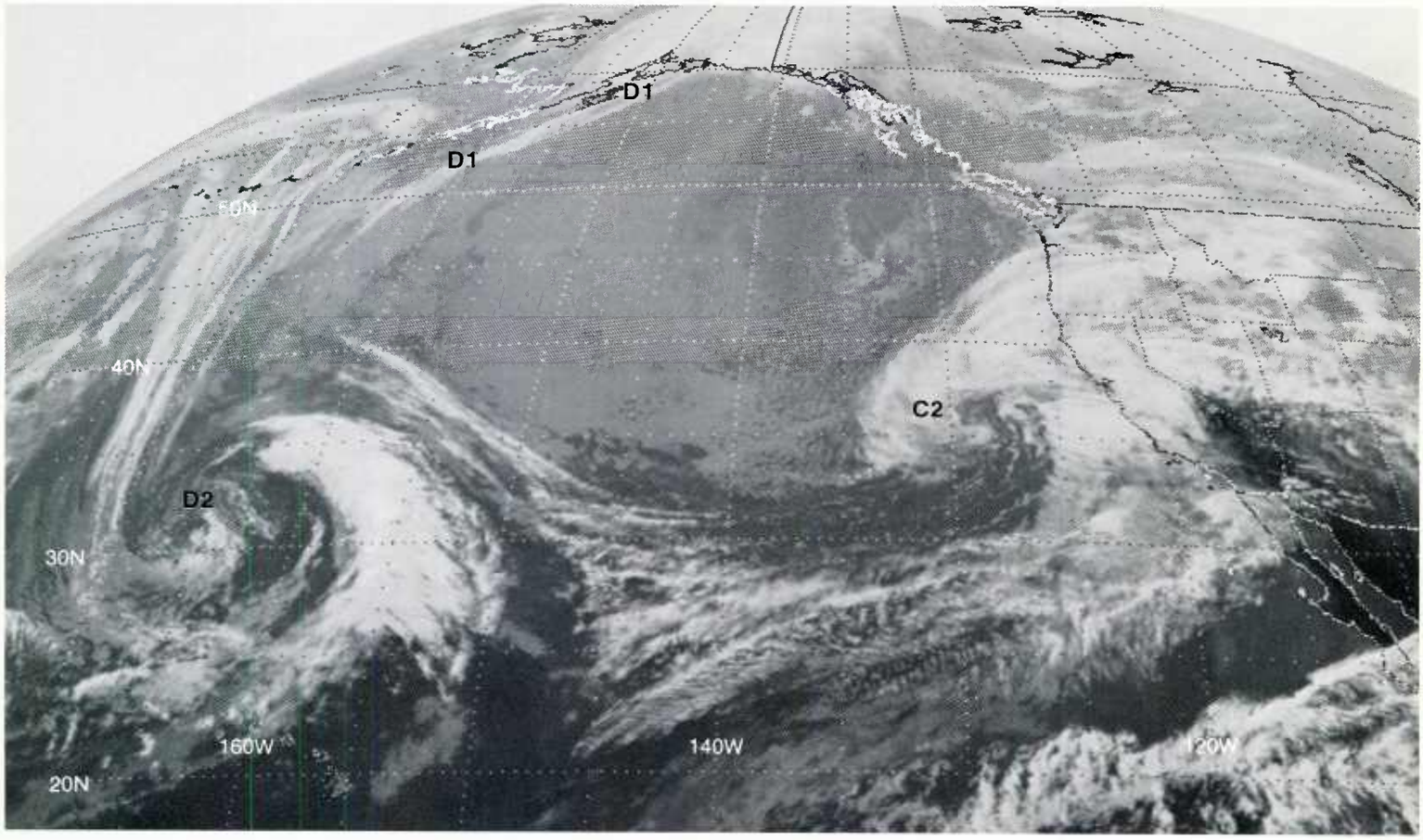

1B-87a. GOES-W. Infrared Picture. 0045 GMT 27 March 1979.

surface

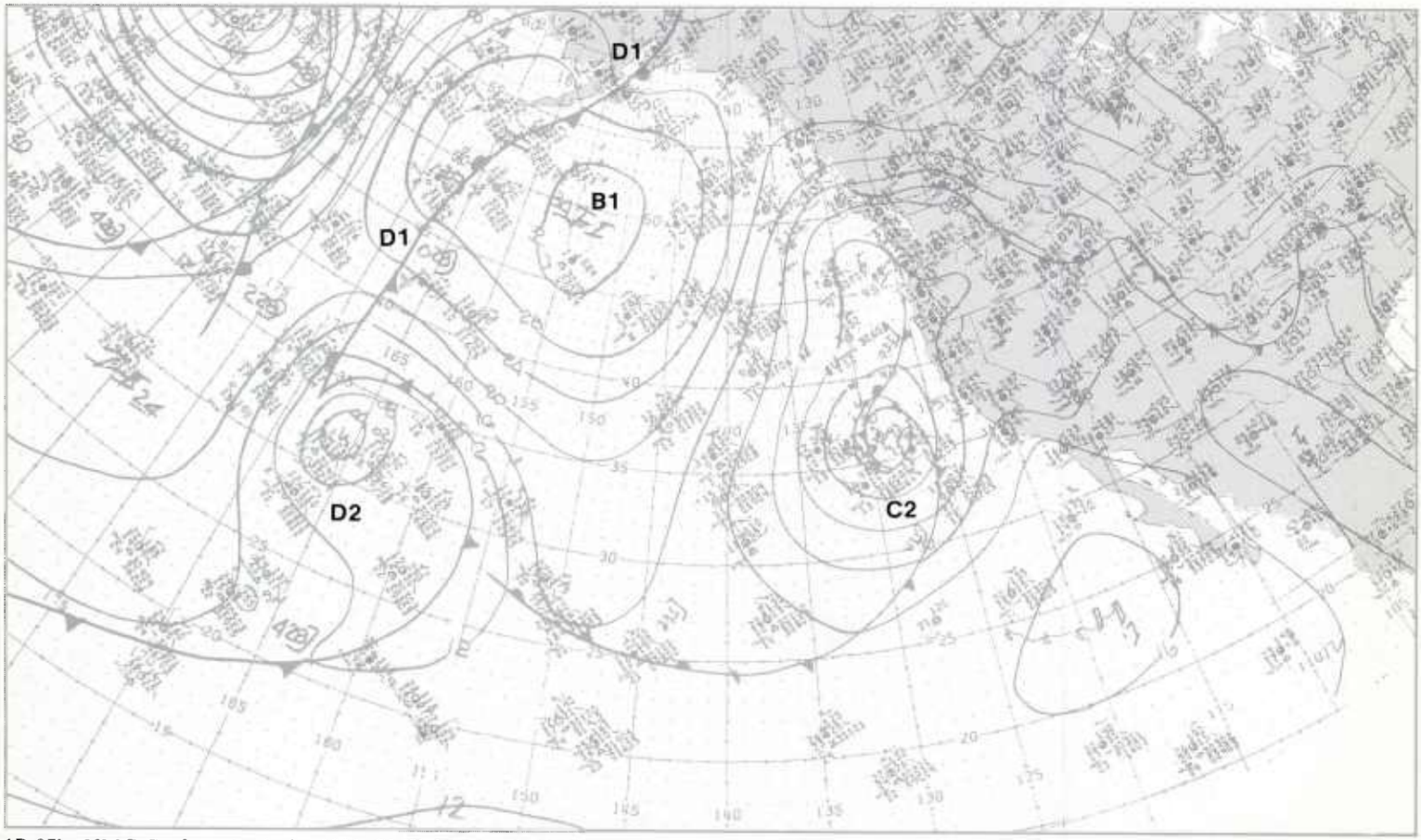

1B-87b. NMC Surface Analysis. 0000 GMT 27 March 1979.

Section 2

Cyclogenesis

2A Introduction

2B Case Studies

Cyclogenesis

2A Introduction

The Structure and Evolution of Winter Storms

Course Notes: National Weather Service Satellite Training

Roger B. Weldon
Satellite Applications Laboratory
National Environmental Satellite, Data, and Information Service/NOAA
Washington, D.C. 20233

Of the disturbances and weather systems of the jet-frontal zones, the most dominant are those usually referred to as winter storms—the major cyclones which form and move within the main belt of the westerlies. During the winter, the storms tend to be bigger, stronger, and more equatorward; otherwise most of the concepts to be discussed apply for all seasons.

Although the storms themselves are of synoptic scale—or at times even larger—their sub-structure is not. It is on these smaller-than-synoptic scales (related to the storm sub-structure), that much of the very significant weather occurs—both in time and space. Using infrared imagery at 30-minute intervals, the cloud pattern on such scales can now be observed. The problem is that of properly interpreting these patterns, and to understand their relation to the weather and to the dynamics of the weather system.

In the following discussion no intention is made to provide a set of rules or forecasting techniques. The intention is to provide some knowledge and understanding, the parts of which may then be combined to fit a specific situation as appropriate. In such an approach, pieces of knowledge are put together to construct a forecasting technique which is unique to each new atmospheric situation.

Note: For an abstract of the basic concepts of the evolution and structure of winter storms, as viewed in satellite infrared imagery, refer to the summary on page 2A-15.

The Cloud Patterns of Mature Winter Storms

Of the cloud patterns involved with winter storms, as observed in GOES and other satellite imagery, all are different. The reason for this is that each storm—at any given time—is made up of the sum of its parts. This may seem to be an elementary statement, but it cannot be overemphasized. It is the key to understanding the (quite often) complex cloud patterns associated with winter storms, and the differences between one storm and another.

Some storms begin with one short-wave scale disturbance and develop into a large mature storm pattern before any additional short waves enter the circulation pattern. These are the simplest, most clearly defined storms and are most likely to appear similar (on the satellite picture) to other storms of the same category (and phase of development).

Most mature winter storms, however, contain one or more short-wave disturbances, in addition to the primary one which was involved in the initial cyclogenesis. In fact, it is very common to have two or three short-wave disturbances at any given time within the circulation system of a large winter storm. It is the presence of these smaller scale systems (which may not all be of the same type or atmospheric level) which contributes largely to the variability in the cloud and weather patterns of the storms. This is the reason for the statement that a storm is made up of the sum of its parts.

Although the cloud and weather patterns are often complex and vary from one storm to the next (or within the same storm with time), the variety is not haphazard or random. It is governed by the characteristics and behavior of the short waves, their relation to each other, and their relation to the overall storm environment. It would be futile to try to categorize and understand the structure of storms merely upon their overall cloud patterns. Therefore, the approach to be presented is the following:

(1) Examine the cloud patterns of storms without multiple smaller scale disturbances within the circulation.
(2) Determine the nature and behavior of the smaller scale disturbances themselves.
(3) Integrate the information of parts (1) and (2) above to build the resulting cloud and weather pattern for a given storm at a given time.

Basically, there are two different typical mature storm cloud patterns, Type A (2A-3a) and Type B (2A-3c). The cloud patterns are intended to represent storms which have just about reached their lowest central pressure—if not at the surface, then in the middle troposphere (700 mb). Storms often evolve beyond this configuration by getting bigger. The central pressure does not get much lower, but the area of the low pressure expands, and the strong gradients retreat from the center. The drawings are intended to emphasize cloud systems with middle- and high-level tops, primarily. They represent models of cloud patterns that would be best observed in infrared imagery, not visible imagery.

Type A Cloud Pattern for a Mature Winter Storm

In the mature storm Type A (2A-3a), the portion of the cloud system labeled A represents a deck of cirrus. It is usually thick cirrostratus, often in multiple layers, and may include the tops (and the debris) of lower level based convection. It usually has a distinct, well-defined western and northern edge. This cirrus deck is best related to the upper-tropospheric baroclinic zone and associated jet stream. However, much of the clouds are often contributed by convection—either directly as debris, or indirectly by the deposit of moisture aloft.

The cloud system labeled B represents the later stage of a vorticity comma cloud pattern. This system is partially overlain by the baroclinic zone cirrus deck. Generally, the cloud tops of the vorticity comma system are at middle levels; however, the system is often highly convective with cirrus-level cumulus tops involved. The type and height (and amount) of the comma pattern clouds are much more variable than those labeled A. However, in almost all cases, where the back edge of the baroclinic zone cirrus deck crosses the comma, the comma clouds are at a distinct lower level.

The clouds labeled C are cirrus, usually lower and thinner than the cirrus labeled A. Often these are found in multiple bands and streaks. These clouds are called deformation zone cirrus. Usually they will exhibit a well-defined edge (on the western and northern side), and often a distinct brighter (probably thicker, not higher) band along the edge.

The dashed lines represent low-level cumulus or stratocumulus clouds mainly within the low-level cold air advection flow field. The cross-hatched area of clouds extending the tail of the vorticity comma are associated with the low-level cold frontal zone. This portion is generally not highly convective (no deep convection); the tops are often warmer than the cold advection cumulus just to the rear.

The Type A mature storm cloud pattern is shown again (2A-3b), but with other data superimposed. The streamlines represent the upper-tropospheric wind field (300 mb). The thick arrows represent the axis of the jet stream, which does not necessarily correspond to the same level as the streamlines. However, it can be interpreted as depicting the axis of maximum winds at the same level as the streamlines.

Note that the jet axis lies close to the edge of the baroclinic zone cirrus deck for most of the length of the edge. There is a tendency for the jet axis to be more and more west of the edge on its southern portion. That relation is not always so, but it is typical. The best agreement between the jet axis and the cloud edge is generally along the anticyclonic portion over the ridge.

The other well-defined cirrus edge, further to the west, lies along the convergent (or confluent) asymptote through the hyperbolic point in the streamlines, where the ridge and trough intersect. This is a common feature in mature storms. When viewed in motion on 30-minute interval time-lapse film loops, this deformation zone cirrus tends to deform with the southern parts moving southward, while the elements on the opposite end of the same band are moving northward or northeastward.

Note that the rear edges of the comma tail and the cirrus deck nearly coincide on their portions south of where the jet axis crosses the comma pattern. On a large scale, they do coincide in that area. However, note that the drawing shows the rear edge of the comma to be slightly in advance of the cirrus edge. Although there is variability in this relationship from storm to storm (or within one storm with time), it is

drawn this way as more representative of the particular model. In other words, south of the jet crossing point, the middle-level front is east of the high-level front in this model.

This brings up the idea of a front. Note on the drawing that a frontal symbol is depicted. This represents the position of the surface front. It is positioned along the rear edge of the comma cloud for a considerable distance. Note that it is not along the rear edge of the cirrus deck, although it is close to it along part of the route. The surface frontal position is better related to the rear edge of the comma pattern. Further south along the frontal zone, the surface front crosses under the end of the middle cloud comma and under the low-level frontal clouds—finally lying along the leading edge of the frontal cloud band in the southern part of the storm. The surface frontal position may cross under the edge of the middle- and low-level cloud edge further north than shown (or perhaps not at all). Often the surface front is further advanced in the area where it is furthest east on the drawing; thus, in that area it would be east of the rear edge of the comma cloud's rear edge—somewhere under the comma tail pattern.

Type B Cloud Pattern for a Mature Winter Storm

The cloud patterns for the second type of mature winter storm are shown in 2A-3c, and this pattern with other data superimposed is shown in 2A-3d.

The basic difference between the two types of storms is the configuration of the cirrostratus deck—the baroclinic zone cirrus pattern. Whereas, on Type A, the back edge of the cirrus deck crosses over the lower level comma pattern; on Type B it does not. Instead, it wraps around the circulation center (not completely around, but around to the northwest or west side), and merges with the deformation zone cirrus in the area of the hyperbolic region of the flow pattern.

Note the position of the jet axes in the Type B storm pattern (2A-3d). The ridge tends to wrap more around the low, and the jet does not cross over. Instead, the strong winds in the cyclonic portion form a wide zone just behind the cirrus edge. If a jet axis were drawn in this region, it would probably extend approximately through the heads of the thick arrows—thus, being at an oblique angle to the streamlines (and crossing the contours markedly from higher to lower pressure, or heights). The wind speeds drop off significantly over the ridge; and another jet is located along the cirrus cloud edge on the north side of the ridge.

The vorticity comma pattern, of generally lower tops than the cirrostratus deck and labeled B, is shown to be behind the cirrus edge. This is representative of many Type B storms, but the comma pattern need not be behind. In some cases, the rear edge of the comma and of the cirrostratus may coincide, or the comma edge may be slightly behind, with part of the comma pattern showing. During this phase of development of a Type B storm, the baroclinic zone cirrus pattern tends to move faster than the middle-level comma; thus, the comma emerges from under the rear edge of the cirrus with time. Quite typically the entire comma pattern will emerge, letting a gap or slot in the higher colder clouds between the two systems.

This trend for the higher level cloud edge to run out in advance of the middle-level comma continues even lower in the atmosphere; thus, the surface frontal position is even further behind, as depicted on the drawing. This is not always the case, but it is common enough to require emphasis by showing it that way.

In this regard, it is more common for the upper-tropospheric cloud edge to run out in advance of the middle-cloud comma, than it is for the middle-cloud comma to run out in advance of the surface front.

Usually heavy precipitation and embedded convection will be occurring under the cirrus deck even after the comma pattern emerges. Afterwards, convective precipitation will break out on (or in) the comma pattern. Even during the fall and winter, the convection here can cause heavy precipitation; and during the spring, severe thunderstorms may occur. Even more convective precipitation may break out at the position of the surface front.

Note that further southward along the frontal zone (2A-3d), the rear edge of the cirrus deck is progressively closer to the rear edge of the comma tail. In fact, the surface front crosses under both edges to be at the leading edge of the frontal cloud band at the bottom of the drawing. If a continuous baroclinic zone (or frontal interface) is observed in the vertical (to which the cloud edges are related), then the zone would slope forward with height in the northern part of the frontal zone, and reverse its slope in the southern portion. There is evidence that a significant baroclinic zone (density gradient) exists in the middle troposphere at the rear edge of the comma pattern, and in the upper troposphere at the rear edge of the cirrus deck. It is possible that these are parts of a continuous sloping baroclinic zone, or they are separated, discontinuous in the vertical. It appears that it is both: that, often, the system begins with a continuous zone which is then modified by localized vertical motions so that discontinuous parts are formed. When mountain barriers are involved, this kind of transformation can act in reverse. In either case, it is observed that the cloud edges involved in a storm frontal region often cross one another in the manner shown, and, although not as often, they sometimes cross the other way.

Why are there two different types of mature storm patterns?

The difference in the two patterns represents a measure of the degree of vertical development. In other words, the Type B pattern represents a storm which has developed deeper or higher into the atmosphere. The upper-tropospheric ridge and warm air has wrapped into the cyclonic circulation.

In this sense, the Type B can be considered to be a more mature phase of winter storm development than Type A. It is true that some big storms evolve from Type A to B configuration. Others do not, and these simply have not continued their development long enough. However, some storms routinely develop directly into Type B configurations. This fact does not rule out the idea of Type B indicating a deeper category of development.

Some Additional Comments on the Mature Winter Storm Patterns

Note that a surface warm front has not been depicted in either mature winter storm drawing. There are several reasons for this apparent oversight. On satellite pictures, surface warm fronts near storms are frequently difficult (or impossible) to locate, mainly because of the extensive thick cirrus over the area. Sometimes, the low-level clouds

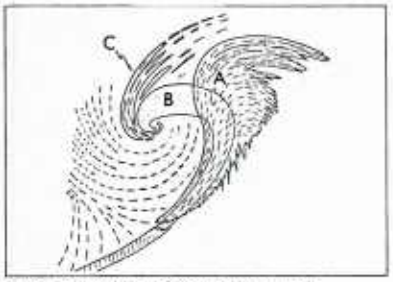

2A-3a. Type A Mature Storm Cloud Pattern.

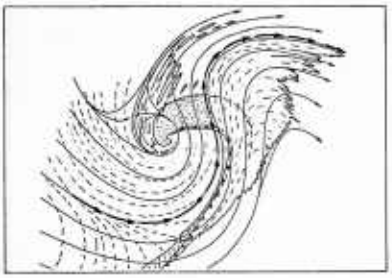
2A-3b. Type A Mature Storm Cloud Pattern with 300-mb Streamlines, Jet Axis and Surface Front.

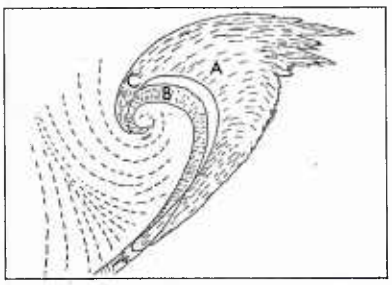

2A-3c. Type B Mature Storm Cloud Pattern.

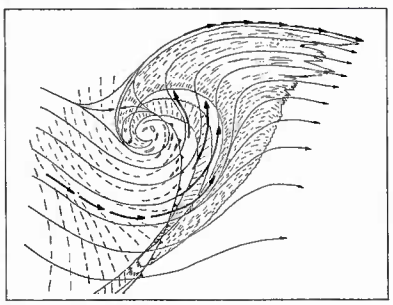
2A-3d. Type B Mature Storm Cloud Pattern with 300-mb Streamlines, Jet Axis and Surface Front.

associated with the warm front can be seen east of the storm and extrapolated inward toward the center. At other times, when the cirrus is thin enough, the low-level warm frontal clouds can be detected on the visible pictures close to the center of the storm. However, these cases are not typical.

Another reason for the omission is that, if the surface warm front is depicted, the subject of occluded fronts is introduced. It also brings up the subject of upglide or overrunning precipitation. Warm fronts are significant and the associated wind shifts, low cloud ceilings, and low visibilities are important. It is not possible, however, to relate satellite cloud imagery well to warm fronts in the vicinity of mature storms.

Storm Development and Cyclogenesis

There are as many kinds of storm development as there are storms. In this section, cyclogenesis will be discussed showing four types (or models) of storm development. Actually, there are three basic types, with the third being divided into two subcategories.

First, it should be emphasized that the models represent "clean" storms; that is, those without multiple smaller scale disturbances entering the circulation. Secondly, most real storms will not fit perfectly any of the four model patterns. The four types are not intended to be used to categorize storms. That, of course, could be done. The definition of each type could be widened so that all storms would fit into one of the categories; then, subcategorize further. One could then look at the cloud pattern of a developing storm, and categorize it as a II-B-5 or a I-A-3b, for example. However, the four types should be considered as models of development which can be used as a learning tool, to organize the knowledge. Armed with this generalized, but organized, knowledge of how storms behave, it can then be combined with a "model-of-the-day" approach for interpretation and forecasting. Thirdly, the choice of four types—not five or six or eight—is somewhat arbitrary and governed entirely by what appears to be most practical.

The four types of cyclogenesis are:

Type 1: Baroclinic Zone or Meridional Trough Cyclogenesis
Type 2: Split Flow Cyclogenesis
Type 3A: Cold Air Vortex Cyclogenesis
Type 3B: Induced Wave Cyclogenesis

The drawings 2A-5a, 2A-5b, and 2A-5c illustrate the kinds of upper-air flow patterns which are associated with the three basic types of cyclogenesis. (Note that Types 3A and 3B are subcategories and occur with a similar flow pattern). The drawings depict upper-tropospheric streamlines (thin lines) and jet stream axes (thick arrows). The streamlines represent the flow field at 300 mb; however, they are also representative of the 500-mb flow field in most cases. When more than one jet is present, the one directly associated with the cyclogenesis is shown as cross-hatched. The patterns represent conditions just before development begins or during the earliest identifiable phase.

Note that it is not the exact streamline or flow pattern itself that defines the type of development, but specific characteristics of the pattern.

The importance of the above categorization is that the cloud and weather patterns develop in a significantly different manner with each of the four types. Yet, within any one type, the cloud and weather development is similar from storm to storm; thus, changes as well as movement can be extrapolated with time to forecast the clouds and weather. In addition, the wind patterns forecast by the primitive equation models can be more closely related to the proper configuration of weather.

continued on page 2A-6

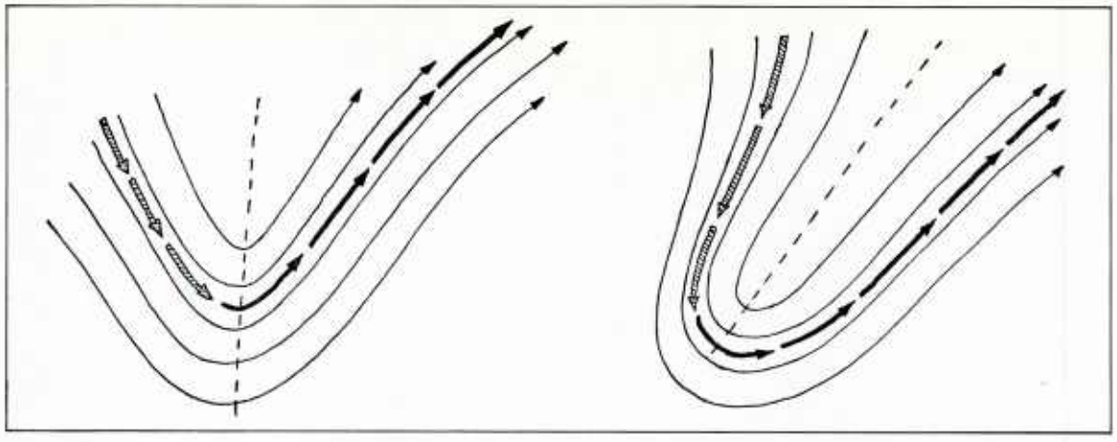

TYPE 1

2A-5a. Typical flow patterns for Meridional Trough Cyclogenesis.

The trough has a large meridional extent. The jet axis is located around the trough, without any significant branches either across the trough or outward into the adjacent ridges. The short-wave disturbances, including the one initiating the cyclogenesis, move around the major trough, within or under the jet baroclinic zone. They are not moving across the cold air in the central part of the trough. These disturbances or impulses are likely difficult or impossible to detect in the curvature of the streamlines and contours; they usually show best as maxima or perturbations in the 500-mb vorticity field, or as speed maxima moving within the jet zone.

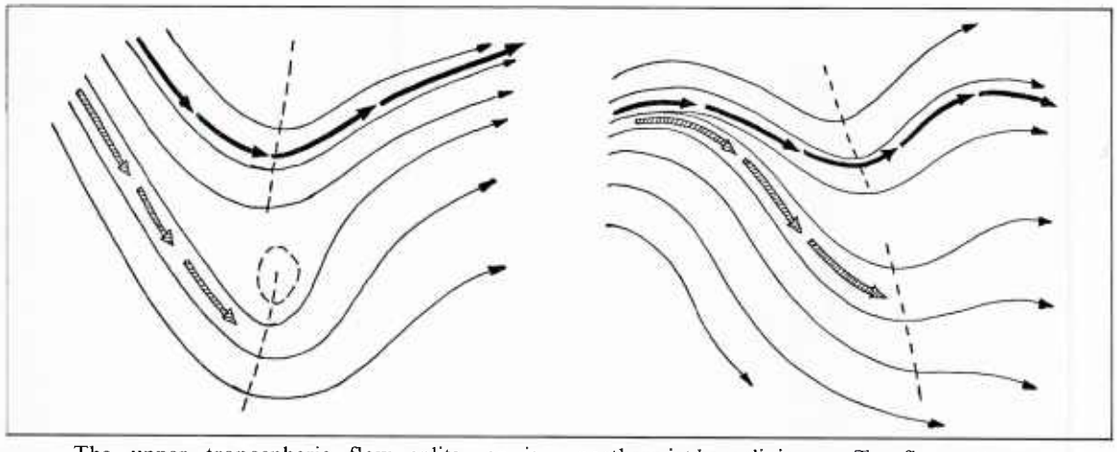

TYPE 2

2A-5b. Typical flow patterns for Split Flow Cyclogenesis.

The upper-tropospheric flow splits, or is diffluent. Often there are two branches of the westerlies forming, with the northern one being the older one. The new branch then forms further southward with the cyclogenesis occurring along the southern branch. Or, there may be two branches throughout the period, with the main energy transferring to the southern branch during cyclogenesis. In either case, the development occurs south (on the warm side) of the older northern jet baroclinic zone. Two flow patterns are illustrated. The first shows the northern trough about in phase (zonally) with the southern one; therefore, a distinct split is seen in the flow pattern. The second shows the northern trough further to the west; therefore, the split pattern is less distinct, and a diffluent appearance dominates. The short-wave disturbance initiating the cyclogenesis moves south of the older wave stream and jet zone.

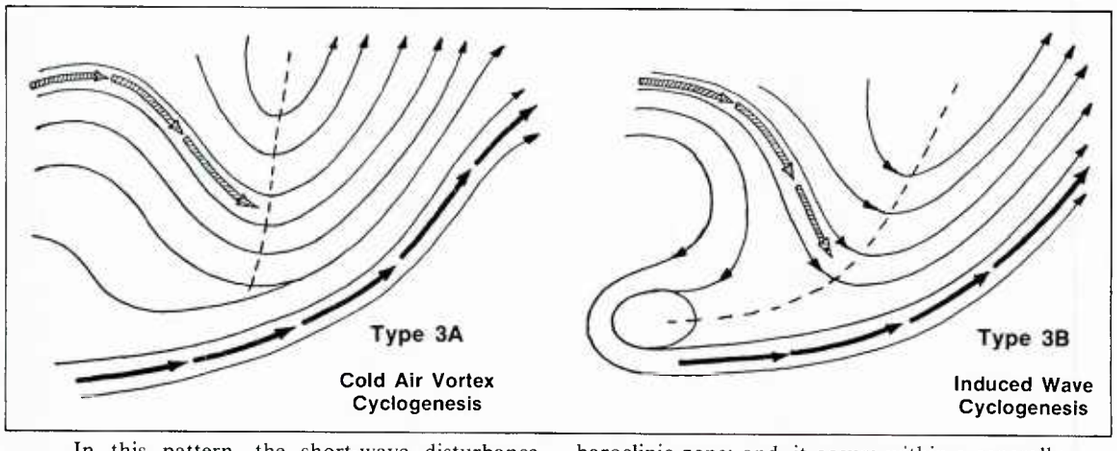

TYPE 3A, 3B

2A-5c. Typical flow patterns for Cold Air Vortex/ Induced Wave Cyclogenesis.

In this pattern, the short-wave disturbance initiating the cyclogenesis moves across the cold air in the central part of the trough behind the jet baroclinic zone, rather than within it as in Type 1. This type of development is opposite to that of Type 2 in two ways. The development occurs on the cold air side of the older or initially stronger jet baroclinic zone; and, it occurs within a generally confluent portion of the large scale flow pattern. Both subcategories of Type 3 development begin similarly; but in Type 3A, a complete new storm pattern develops on the cold air side of the old baroclinic zone. In Type 3B, the new development induces a wave on the old baroclinic zone.

Cloud Patterns of the Meridional Trough (Type 1) Cyclogenesis

This type of storm development is most prevalent along the east coast of North America and over the adjacent western Atlantic. It is also prevalent along the east coast of Asia. Although it is most prevalent in the areas described, this type occurs also over other parts of the U.S. and over the oceans as well. The cloud evolution is related to the type of flow pattern, not to the geography. Of the four types of cyclogenesis, the meridional trough type is the one which best fits the classical frontal wave model of cyclogenesis. Statistically, however, this type represents less than 25% of all storm developments.

The drawing 2A-6a illustrates the cloud pattern seen just before a meridional trough type development begins. The main cloud feature (labeled A) is the jet baroclinic zone cirrus deck. This is likely, even at this stage, to have a distinct western (or cyclonic side) edge which lies near the axis of the jet stream. The surface frontal position lies roughly along the east side of the cirrus.

At this stage, it is usually difficult to find, and maintain continuity on, any distinct surface low pressure centers. Rather, an elongated trough in the surface pressure extends along the frontal zone. Apparently, small low centers form and move rapidly along this frontal zone. This combined with diurnal changes and other problems adds to the difficulty of following the relatively weak centers.

When convective showers or CB's are occurring along and east of the low-level frontal zone, the more significant low centers will often be revealed by small comma-shaped areas of convection, or by upside-down comma-shaped clear areas in the general convection and debris cloud cover. If so, the surface low will be located in the clear part of the pattern very near the forward cloud edge. Two such patterns are shown on the drawing. Even at this stage, there is likely to be middle clouds and some precipitation under the cirrus deck. Note that the hatched cloud pattern on the drawings indicates low-level frontal related clouds—probably stratocumulus.

The problem at this stage is obviously that of determining if and when and exactly where significant cyclogenesis is beginning, or will begin. There will likely be weak vorticity maxima or mid-tropospheric disturbances moving northeastward along or within the baroclinic zone, which can be related to the middle clouds and precipitation under the cirrus deck. There may also be waves of relatively small scale running up the back edge of the cirrostratus deck. These disturbances are localized in the vertical at the cirrus level, and are fairly independent of the deeper disturbances which show on the 500-mb vorticity data, and do relate to the precipitation pattern. However, sometimes the waves will grow in size (wave length) and one of them—usually the southernmost—will be associated with development on the surface front. It is likely that as the wave grows horizontally, it also grows vertically and couples with the mid-tropospheric pattern.

When development does begin, it will be in response to one of the small- or short-wave scale vorticity maxima as it comes around onto the front side of the trough. The problem is: which one, and can it be detected in satellite imagery or other data. Usually the disturbances move very rapidly down the back side of the trough and are difficult to pinpoint in the spatial and especially time resolution of the upper-air network (even over the U.S.). Also, there are typically no clouds associated with the disturbance during the trip down the northwesterly branch of the trough. The clouds form when the disturbance reaches the east side of the major trough, and then it is likely under the cirrus. Sometimes it is possible to follow a band or piece of rapidly moving cirrus which is associated with the speed max over the middle-level system. However, this is not frequent enough to be generally useful.

The only real key to catching the development is to wait until it can be detected in satellite imagery. The exact time and location will then be known, and an estimate of the intensity can be made according to how fast things begin to happen. The first real hint of the development is a significant waving of the back edge of the cirrus deck.

During the second phase of development (2A-6b), the cirrus edge has formed a wave pattern which is matched by the jet axis and the streamlines. A short-wave trough has formed just east of the base of the major trough, and a short-wave ridge is growing in advance of the trough. On the satellite picture, the ridge is usually more obvious than the trough.

In the absence of good surface data (when the front is offshore), the low center can be located by drawing a line from the inflection point at the back edge of the cirrus, transverse to the major axis of the cloud band (or to the middle-level flow). Where the line intersects the surface front is a reliable estimate of the surface low position. If convection is occurring east of the frontal zone, it is likely to diminish significantly southward of the line.

The comma-shaped area labeled B would not be visible on the satellite data, since it is under the cirrus deck. It corresponds to the location of the vorticity comma which has now formed in the process of cyclogenesis. Aside from any thunderstorms that may be occurring east of the front, this area is likely to also be the area of heaviest precipitation.

In the third phase (2A-6c), the system begins to wrap up and form a closed circulation center into the middle troposphere, and the head of the vorticity comma begins to emerge from under the cirrus deck (see area labeled B). Note that the surface low center is now nearer to the back edge of the cirrus deck (it was near the eastern edge at the initial phase), but not quite out from under it yet. The surface cold front is under the cirrus near the back edge of the comma pattern. The comma head, although emerging, is not likely moving westward (or rearward) with respect to the ground; rather the cirrus edge is moving faster. The storm is developing very rapidly at this time, and the short-wave trough has increased in size and forms a negative tilt to the entire base of the major trough. The short-wave ridge has increased its amplitude.

In regard to the comma head now showing to the west of the cirrus, significant precipitation will be falling in that region as well as further east under the cirrus (in advance of the surface low). Although the tops of the clouds in the comma-head region are normally middle level, they do often reach cirrus level, but are lower than the cirrus deck to the right of the jet axis. Also, if the tops in the emerged portion are fairly uniform, they are likely to be higher and thicker on the west side and thinnest just beside the crossing

cirrostratus edge. It is likely that the effect of the downward vertical motion to the left of the cirrostratus edge is superimposed upon the lower-level upward vertical motion; or creates a lower stronger subsidence inversion there.

By the fourth phase (2A-6d), the closed circulation has deepened even more, an area of deformation cirrus (labeled C) has formed, and the overall pattern appears similar to the mature storm pattern (2A-3c), but not quite as advanced. By now the surface low is well west of the cirrostratus deck and north of the mid- and upper-tropospheric centers. There is a trend for the surface and upper centers to rotate cyclonically with respect to each other, getting closer together until the systems are vertically stacked. This usually happens before the surface low gets around to the southwest quadrant of the higher centers.

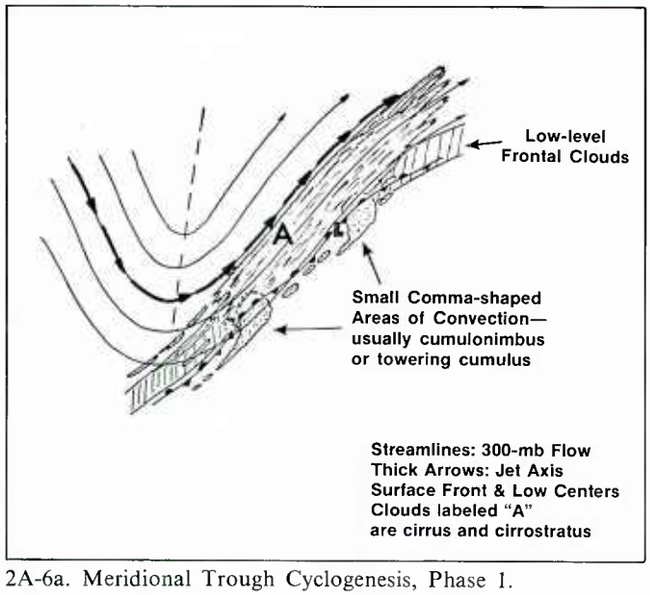

2A-6a. Meridional Trough Cyclogenesis, Phase 1.

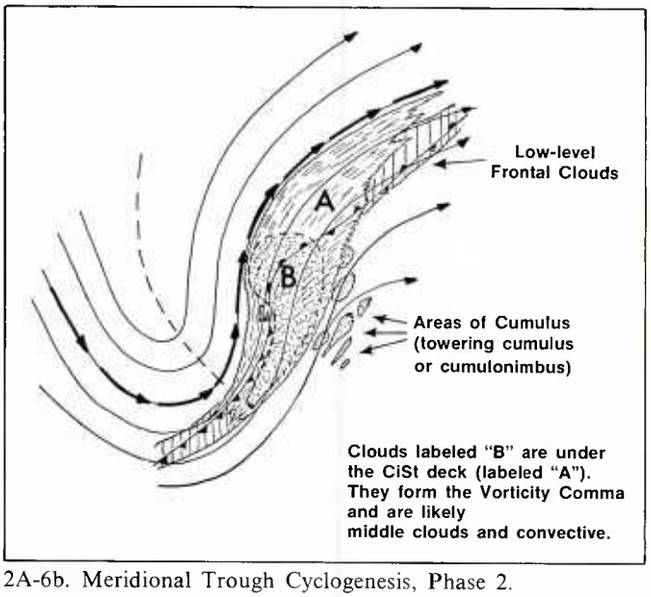

2A-6b. Meridional Trough Cyclogenesis, Phase 2.

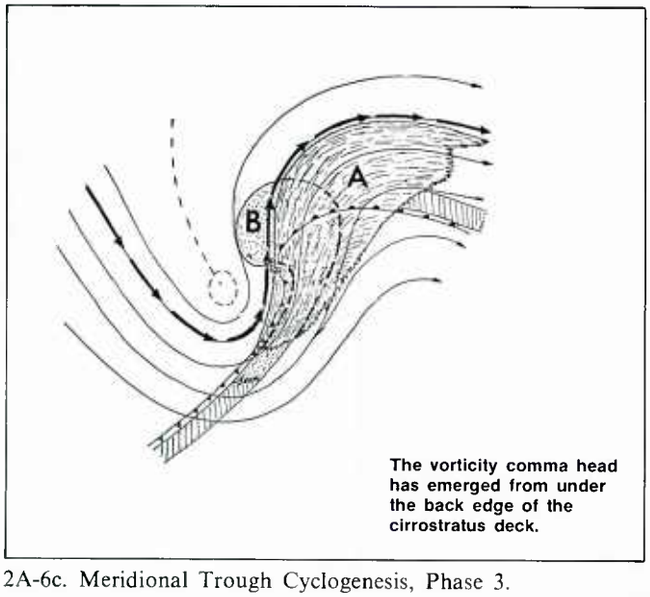

2A-6c. Meridional Trough Cyclogenesis, Phase 3.

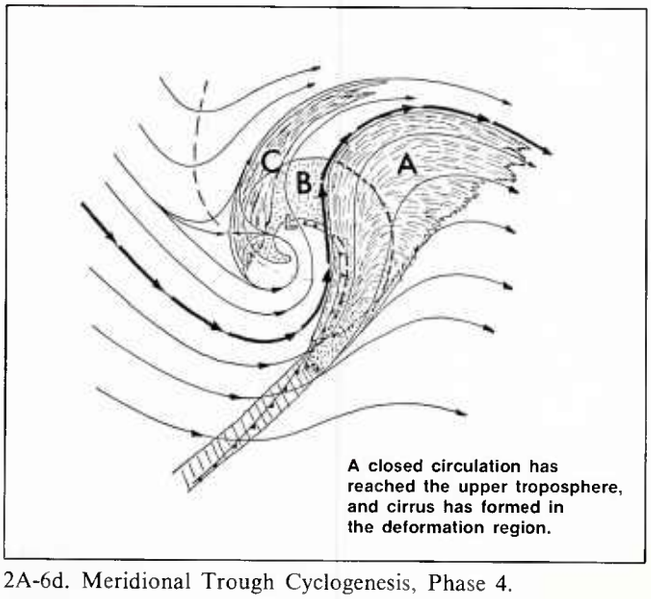

2A-6d. Meridional Trough Cyclogenesis, Phase 4.

Cloud Patterns of the Split Flow (Type 2) Cyclogenesis

This form of development is by far the most prevalent over the central U.S. just east of the Divide; in eastern Siberia east of the Ural mountain chain; and, less frequently, over the oceans. It is obvious that the flow pattern is most often induced by a major mountain chain. However, the mountains do not induce the cloud pattern evolution; they induce the flow pattern, and the cloud evolution is related to the flow. This is important, since the flow pattern can occur elsewhere although not as frequently. Also significant is the fact that mere split flow occurs frequently—such as on the west side of the common blocking pattern; but the development also requires a jet moving into the southern branch. Thus, split flow cyclogenesis is much less common than split flow. Although the split flow development of cloud patterns depends on the flow, the presence of mountains does directly influence the cloud patterns, especially in regard to some important details.

The cloud pattern of the split flow development (2A-9a) usually begins with an area of cirrus, and with perhaps middle clouds involved at times. This is labeled C on the drawing. It is usually curved anticyclonically, may be fairly straight, but is not cyclonically curved. The cirrus lies generally north and northwest of where the cyclogenesis is about to take place. Much of it is within a region of weak upper-level winds, but the winds usually increase in speed to the northeast or east end, where it lies along the jet axis of the northern flow regime.

If the systems are configured as a more diffluent flow pattern, such as shown on the second type (2A-5b), the cirrus is likely to be less well defined in shape, and will be entirely within weak flow. At this point in time, there may be a small area of convection or middle clouds southeast of the forming low.

By the very nature of the flow pattern, a closed circulation center appears in the middle troposphere very early in the development; and by the second phase (2A-9b), it is likely to appear at 300 mb. This is the most important single factor that influences the evolution of the cloud patterns (and the weather patterns). The circulation system develops higher in the atmosphere than the other types; it may be quite well developed aloft even before an organized system is consolidated at the surface.

To show the typical pattern of development, the northern short-wave trough is depicted moving on to the east over the ridge. The speed maximum along the northern branch of the jet also shifts eastward, and the cirrus edge is straightened out on its eastern end. Further west, the cirrus edge is better defined and slightly more anticyclonically curved. The most important change in the cloud pattern has been the development of the vorticity comma pattern which has formed very rapidly to the southeast of the closed circulation center. This has occurred as the southern branch of the jet advanced south of the center. The cloud types involved in the comma are highly dependent on the time of year (and the low-level stability). They are likely to be highly convective, but still consist primarily of middle cloud height tops at this stage.

By the third phase (2A-9c), the cloud patterns have become bigger and better defined. Usually by this phase, the comma pattern will have developed higher cloud tops with cirrus commonly present. Especially over the comma tail portion, the cirrus will appear thicker and striated, as the jet baroclinic zone develops aloft over that area. The older cirrus to the north has developed a well-defined edge and filled in to show a more uniform appearance. Along the eastern portion of that edge, a jet has formed—or the tail end (entrance region) of the jet previously there has not moved east and has increased in wind speeds.

No surface low or surface fronts have been included on the drawings. The reason for this is the large variability involved in the relation between these features and the cloud patterns for this type of cyclogenesis. There is a good relationship between the cloud patterns and the weather (precipitation), but a much poorer relationship between the cloud patterns and the surface pressure and temperature fields. A generalized rule for placing the surface low center would be the following: As the mid-tropospheric cyclogenesis proceeds, the surface low will usually consolidate at a location somewhere near the rear edge of the comma head, and on the cyclonic side of where the jet is shown crossing the rear edge. This relationship is valid for 2A-9b and 9c.

In the fourth phase (2A-9d), the area of thick cirrus has greatly increased. Cirrus has formed over the vorticity comma and merged with the northern cirrus. By this time, it is often difficult to distinguish between the cirrus deck associated with the jet baroclinic zones and the deformation zone cirrus to the north and rear of the closed circulation aloft.

The southern branch of the jet has significantly widened east and southeast of the low center. The streamlines cross the rear edge at an oblique angle, but the axis of maximum winds would be nearly parallel to the edge—drawn approximately through the heads of the thick arrows on the drawing. Wind speeds decrease significantly over the ridge with the southern speed maximum distinctly separated from the strong winds on the northern edge of the cirrus shield. That portion of the cirrus labeled C corresponds to the deformation area cirrus; the edge is distinct and through the hyperbolic point along the confluent asymptote, and the winds are light.

Usually, the cirrus deck that grows over the comma pattern does not constitute a simple upward extension of the middle clouds, but forms a higher deck with a vertical break in between. Quite often, then, the rear edge of the higher deck moves faster than that of the middle (or lower) deck which emerges at the rear (2A-9d).

The system may continue to evolve into a pattern such as that shown for the Type B mature storm pattern (2A-5b). The Type B mature storm pattern represents a more mature phase of development than the Type A pattern. To be more specific, the B pattern is considered a vertically deeper or higher phase of development, not necessarily a later one. If the storm developed in the manner of the meridional trough type—which involves a progressively upward development with time from the lower troposphere—then a Type B mature storm pattern would represent a later as well as higher phase. But, with the split flow type of cyclogenesis, the circulation tends to close in the middle and upper troposphere before it does at the surface. Therefore, it is a higher system to begin with; and the evolution directly into a Type B mature storm pattern is understandable.

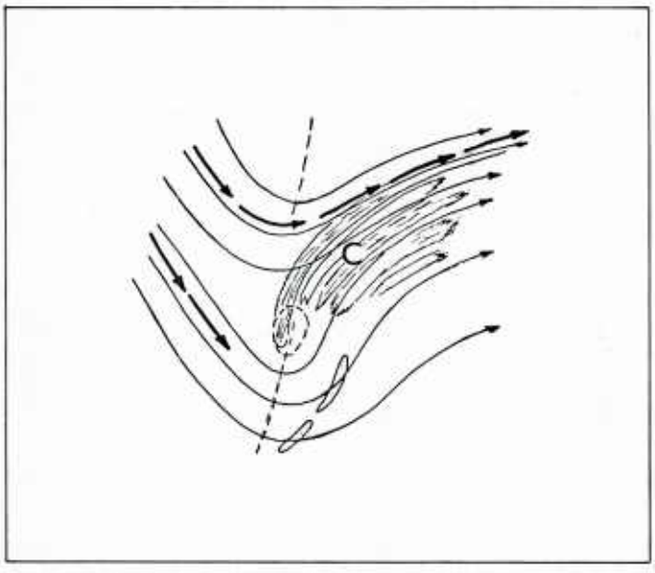

2A-9a. Split Flow Cyclogenesis, Phase 1.

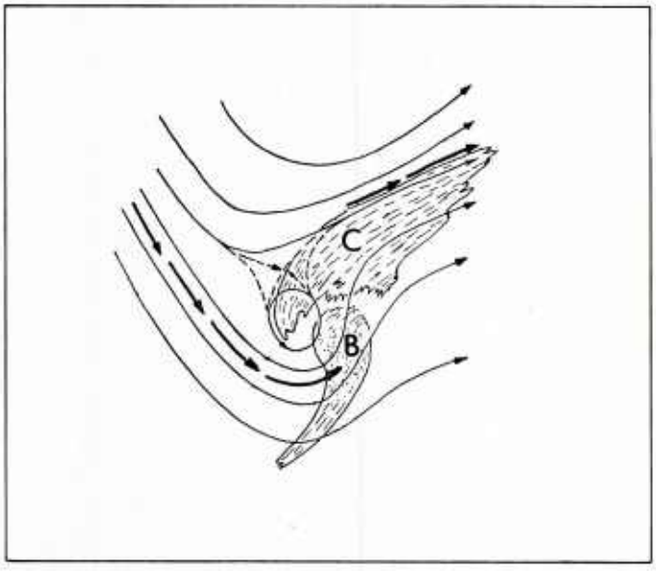

2A-9b. Split Flow Cyclogenesis, Phase 2.

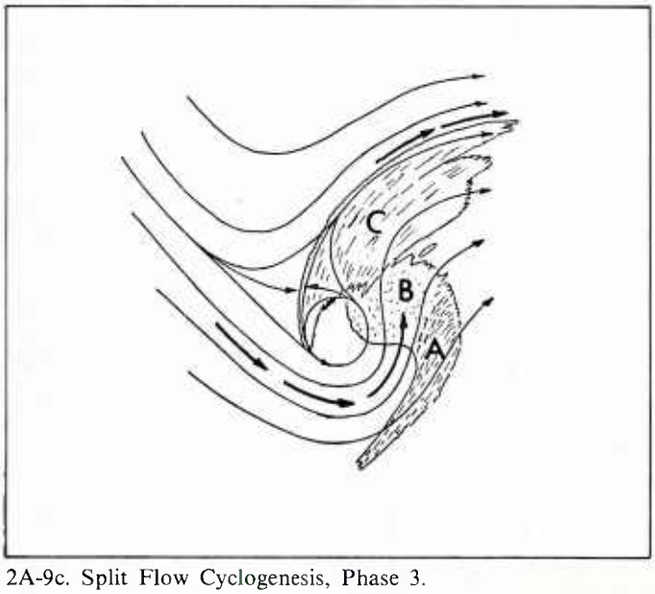

2A-9c. Split Flow Cyclogenesis, Phase 3.

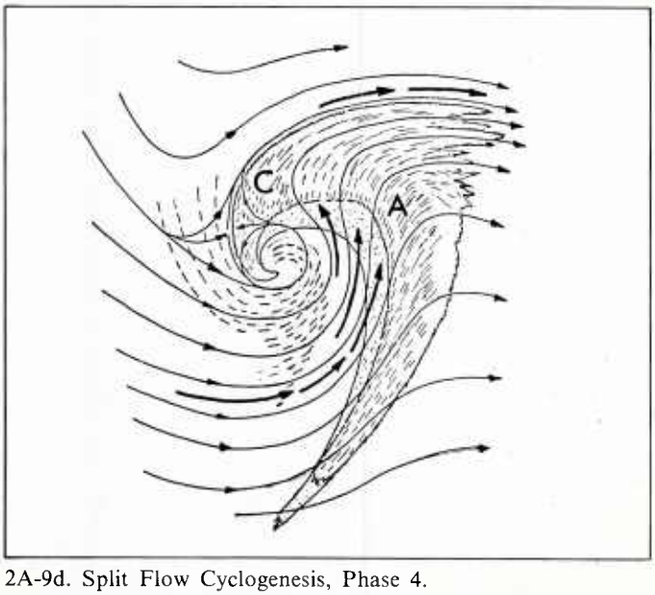

2A-9d. Split Flow Cyclogenesis, Phase 4.

Cold Air Regime Developments: Type 3 Cyclogenesis

This type of development has been subdivided into two kinds: Type 3A, Cold Air Vortex cyclogenesis; and Type 3B, Induced Wave cyclogenesis. Both types of cyclogenesis occur in response to a short-wave disturbance moving across the cold air to the rear of the original main baroclinic zone. With Type 3A, a complete new cyclone forms behind the older baroclinic zone, producing its own separate baroclinic zone with surface fronts and jet stream aloft. Whereas with Type 3B, the short-wave disturbance which initiates the cyclogenesis induces a wave on the original baroclinic zone. The main jet stream and frontal zone of the resulting mature cyclone are those of the original baroclinic zone which has responded to the disturbance crossing the cold air.

The Type 3 cyclogenesis occurs most frequently of the three basic types. However, the Type 3 forms of cyclogenesis are most prevalent over the oceans. This preference for the oceans is probably by default, since the geographic (mountain and coastal) influences of the North American continent frequently induce the flow patterns for meridional trough and split flow developments there. Even though Type 3 developments are more prevalent over the oceans, this geographical preference is not as strong as for the other types. Type 3B developments occur often east of the Rockies (over the rest of the continent), and Type 3A developments occur frequently just off the West Coast and over the eastern U.S.

Cloud and Weather Patterns of a Cold Air Vortex Cyclogenesis, Type 3A.

Prior to the development of the Type 3A storm (2A-11a), the dominent cloud pattern will be a baroclinic zone cloud system on the downstream or "anticyclonic" side of a major trough. This could be in the form of a long band of cirrus and middle clouds along the jet-frontal zone of an elongated SW–NE oriented trough, or with an E–W oriented zonal flow (especially at high latitudes over the ocean). Or, it may be less elongated and correspond to the jet-frontal zone of a major trough formed by a recent cyclogenesis.

In any of the above cases, the short-wave disturbance that will initiate new cyclogenesis will move toward the original baroclinic zone over the cold air. A pattern of confluence will be formed by the older jet zone and the speed maximum associated with the approaching disturbance.

It is important to note that the two speed maxima forming the confluence may not be at the same levels. Often the levels of maximum winds associated with the approaching short-wave disturbance will be near (or even below) 400 mb, while the jet axis of the older baroclinic zone in that vicinity will be well above 300 mb. Thus, the confluence of the speed maxima, although evident in the cloud patterns, may not show well on any single pressure level analysis.

The first phase of the Type 3A development (2A-11a) shows the clouds of the short-wave system on the back side of a major trough, with a pattern similar to those described above. With it is a new jet stream system entering the major trough circulation. The axis of maximum winds of that jet is shown beginning to bend around the trough axis instead of joining with the older jet system on the front side of the trough. The strongest winds are still well back, coming over the ridge at this time, but the behavior of the leading portion of the jet is a key or hint to whether the coming cyclogenesis will be Type 3A or 3B. When the new jet begins to curve around and become parallel to the old jet, with a zone of weaker winds between the two axes, it is an indication that the cyclogenesis will be Type 3A, and that the cyclone will form a complete new storm pattern behind the older baroclinic zone.

The surface low and front associated with the approaching short-wave disturbance is also shown. At this stage, the front is not moving much to the side—it is undergoing more of an extension southeastward. Also at this stage, the surface low is likely not to be well defined by displaying any exact center. The surface winds may not be forming a completely closed circulation on the northeast side. They are likely to appear as a vorticity center configuration instead—an open wave with strong flow and cyclonic shear.

Although the cloud pattern indicates a single short-wave feature of medium strength, this is not always the case during this critical time. Sometimes, there will be a series of smaller, less-defined cloud systems rushing down the back side of the trough. When the first one or two arrive onto the east side of the major trough axis, nothing much happens, except there seems to be an accumulation of middle clouds forming (without good pattern definition) just east of the trough axis. When the middle clouds associated with the approaching jet stream arrive at the trough axis, whether small short waves or bigger as in the figure, they tend to decelerate rapidly and rotate. This is important because it helps show by satellite imagery alone where the trough axis is. The track of the exact location can be lost with 12-hour upper air network time steps. As these smaller scale cloud systems arrive on the east side of the axis, each seems to add more energy to the development, until finally after several arrive, a well-defined comma pattern begins to form.

In the second phase (2A-11b), the short-wave middle cloud pattern has just arrived on the east side of the major trough axis (it will also be affecting that axis by making it sharper and better defined as increased curvature forms there). The pattern begins to take the vorticity comma shape with convection increasing over the comma and resulting in higher cloud tops. Although light precipitation may have been occurring previously, the precipitation will now be heavier and extend over the portion of the dotted portion of the cloud pattern on the drawing. Even at this time, a single surface low center may not have consolidated. There may be an elongated surface trough north of the jet crossing and under the comma head, with more than one center evident.

Cirrus will be developing rapidly along the jet baroclinic zone associated with the new system. Sometimes this baroclinic zone cirrus will form earlier. When it does, a band will extend along the new jet axis partly up the front side of the major trough before the middle cloud comma is well defined. That kind of cirrus development often happens when the cyclogenesis is initiated by a series of smaller impulses rather than a single larger one as shown.

During the third phase (2A-11c), the new storm has begun to form the comma pattern. Considerably more cirrus and cirrostratus has formed along the newer jet axis on the east side of the major trough, but the older jet axis and its cirrus deck remain further to the east. As the new storm intensifies

and sharpens the amplitude of the upper-level trough, the edge of the older cirrus deck will tend to become generally parallel to the newer cirrus, especially along the cyclonically curved portion. However, there may still be smaller scale waves along the older cirrus edge that are out of phase with the new system at this stage.

By the fourth phase (2A-11d), a completely new storm cloud pattern has formed behind (or on the cold side) of the old baroclinic zone. Usually, as the new system develops, the older jet baroclinic zone and its cloud system weakens—in effect becoming partly isolated from its previous cold air supply, and with the development of warm moist air aloft in advance of the new system.

If the new cyclone continues to develop beyond this stage, it is likely that the new frontal zone will catch up to the old one in the south quadrant of the low, and the frontal zones will merge into one in that area. The double jet and cirrus structure in the northeast quadrant are likely to continue for a longer period of time; but even there, the eastern jet will often weaken with the newer jet zone becoming dominant.

continued on page 2A-12

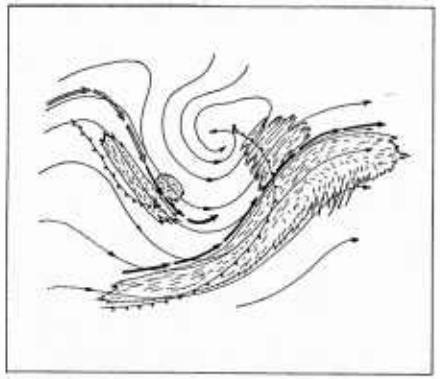

2A-11a. Cold Air Vortex Cyclogenesis, Phase 1.

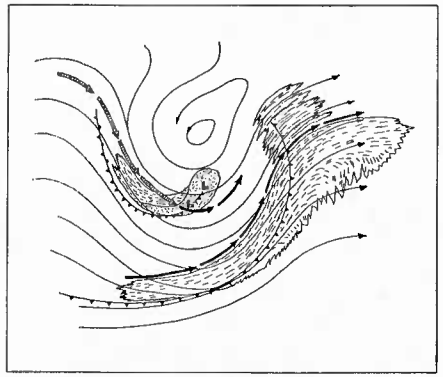

2A-11b. Cold Air Vortex Cyclogenesis. Phase 2.

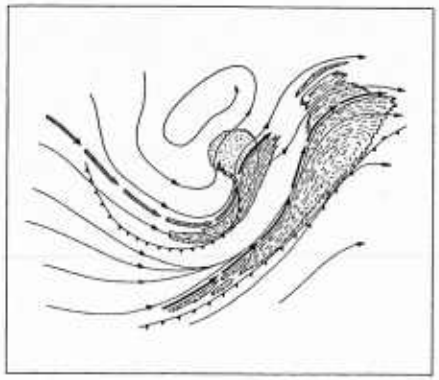

2A-11c. Cold Air Vortex Cyclogenesis, Phase 3.

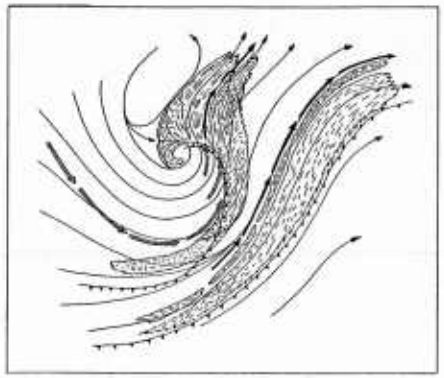

2A-11d. Cold Air Vortex Cyclogenesis, Phase 4.

2A-11e. Characteristic Cloud and Flow Patterns of Type 3 Cyclogenesis.

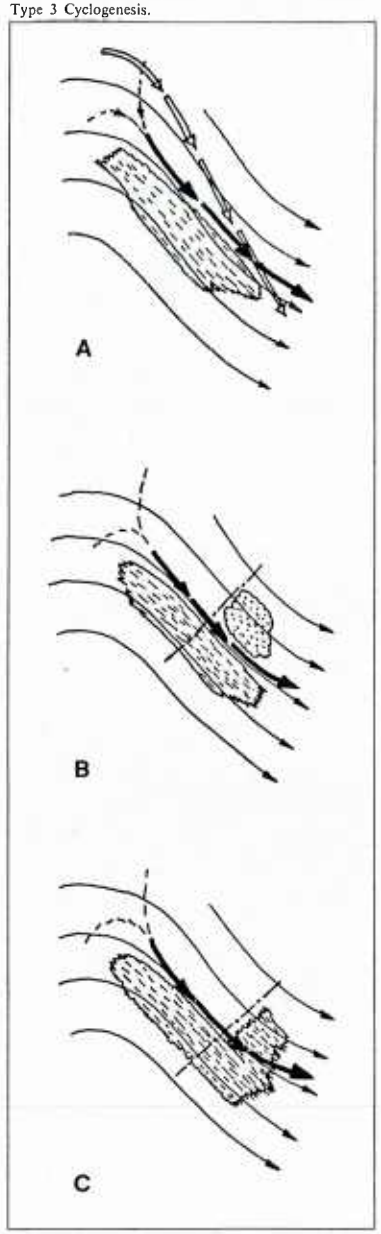

Unlike the case of Type 1 cyclogenesis, in which the short-wave disturbance coming around the periphery of the trough does not usually have clouds associated while on the back side of the trough, the initiating disturbance of the Type 3 developments does show in the clouds. The drawings 2A-11e (A, B, and C), illustrate some of the characteristics of the clouds associated with the short-wave disturbance which are approaching the axis of the major trough from the upstream ridge.

In the drawings, the streamlines correspond to 300 mb. The solid thick arrows correspond to the axis of maximum winds at cloud level. The open thick arrows (A) correspond to the jet axis (a higher level than the solid arrows). The drawings do not represent a sequence of patterns; they represent a variation of cloud patterns likely to be seen on different occasions.

When the short-wave disturbance that will initiate cyclogenesis is approaching the major trough axis, it will usually be evident in infrared imagery as a pattern of middle clouds. Often they will form merely an elongated zone of clouds (A). They will be moving rapidly (propagating). Often there will be additional clouds, usually of warmer tops and even less well defined along the left forward portion of the band (B). The two areas then form a rough "L" shape together. At times the "L" pattern is better defined, and the clouds forming the base of the "L" are nearly as cold as the rest (C). Often these middle clouds will have a distinct well-defined northern edge which will be just to the right of the axis of maximum winds at cloud top level.

The jet axis (A), depicted by thick open arrows, is shown as crossing the cloud level max wind axis at an angle, where the middle cloud edge is related best to the wind speed max at that level. Such differences between the cloud level axis of maximum winds and the jet axis aloft, both in horizontal displacement and in orientation, are common during this phase of the development.

Conditions at the middle cloud levels (700 mb is often the best standard level chart to compare) can be summarized as follows: The often distinct northern (or northeastern) edge is in a region of strong baroclinity. The temperature gradient will be almost transverse to the wind direction and cloud edge; it will be strong but not as sharply defined as the dew point front near the cloud edge. The dew point front slopes toward the southwest with decreasing height, below the cloud top level at the edge location.

The dash-dot lines (B and C) represent the axis of maximum vorticity at the cloud level. The NMC 500-mb vorticity analyses often do not show such a distinct relationship. After the system gains in strength, or on systems that are stronger to begin with, it will. In the stage represented by the drawings, most of the vorticity is contributed by the shear term; little curvature can be seen in the winds. Also, it is common to have a series of small disturbances (speed maxima, vorticity maxima) coming down the front side of the ridge. During those cases, because of the resolution of the upper-air network, the systems are most easily followed on infrared imagery.

With the cloud systems as shown in the drawings, there may not be a well-defined surface front. When there is, it will normally be near the southern or southwestern edge of the cloud band. At times, it may also be several degrees of latitude further to the south, which implies a very large slope. In those cases the surface front may not be a part of the same baroclinic zone that corresponds to the middle cloud edge (north side of clouds). On the surface analysis, there is likely to be an elongated ridge of high pressure with its axis near the northern edge of the middle cloud system. In the surface winds, under the cloud edge, there may be a diffluent asymptote. The winds to the left of the asymptote will be generally parallel to the winds aloft, and those to the right will be curving off anticyclonically toward the surface front which is further to the right.

Cloud and Weather Patterns of an Induced Wave Cyclogenesis, Type 3B.

With this type of storm formation, the initiating short-wave disturbance moves across the major trough over the cold air, as in the Type 3A. However, before development has progressed very far, the jet and baroclinic zone accompanying the new system merge with the older zone on the east side of the major trough. As the middle-level comma cloud pattern forms and approaches the older jet cirrus zone, it appears to induce a wave on the older baroclinic zone and its cirrus deck. If the four types of cyclogenesis are considered separately, the Type 3B is the most frequent form of development among the four. This type of cyclogenesis has the least geographical preference.

In the first phase of development (2A-13a), the pattern will be very similar to that of the Type 3A. The older jet-zone cirrus is likely to be closer to the major trough axis, especially at the point where the new speed max and short-wave disturbance is approaching. The leading portion of the jet maximum coming over the ridge may appear to merge with the older jet axis in asymptotic manner, such that no double jet structure can be seen east of the trough axis.

In some cases, the leading part of the new jet will turn the corner and move up the east side of the major trough, with two parallel jet axes present. When this kind of jet structure evolves, it is common to have a series of smaller scale disturbances moving along both jet zones. One series, showing as middle clouds (mainly) will move down the newer jet branch, and the other showing as perturbations in the older jet cirrus deck will be moving from the southwest. As the two streams merge closer together, the small-scale disturbances of the two streams will usually be out of phase. As they are out of phase, development is deterred. When a pair of systems arrive in phase, development begins. At other times, a single larger scale disturbance approaches the older baroclinic zone.

During the second phase (2A-13b), the disturbance and the leading portion of the strong winds arrive at the major trough axis and a comma-shaped middle cloud pattern develops, often with convection and precipitation forming rapidly. Some higher cloud tops will likely form over the comma and form a plume where the axis of maximum winds crosses the comma surge region. The rear edge of the older baroclinic zone cirrus deck immediately begins to deform (or conform) to the pattern of the developing comma.

By the third phase (2A-13c), the comma has become better defined and grown larger, and the jets have merged into a single upper-level baroclinic zone. The region of strong winds is likely to be wider in this area, but no double jet structure can usually be found—either in the upper air network or in evidence of the cirrus.

Whereas the comma tail was parallel to the cirrus deck cloud edge on the third phase, the comma rotates and the tail moves under the cirrus deck during the fourth phase (2A-13d). More cirrus has formed over the head of the comma—especially at the deformation region, and a typical mature storm pattern has formed. The clouds over the comma head near where the jet axis and cirrus edge cross are likely to be lower than on the rest of the comma head. There is often a slot in the middle and high cloud deck just to the left of the cirrostratus edge where it crosses.

The comma tail is shown swinging around under the cirrus with only the "head" of the comma showing. This would be most likely when the storm continues to develop well to maturity. With many developments which do not go full cycle (and most don't), the comma tail may remain nearly parallel to the cirrus edge, and still out in the open (not under the cirrus). Similarly, in many cases, a well-defined comma pattern does not form, but a region of irregular-shaped middle clouds shows at the position where the comma head appears on the drawings.

Some General Comments on Type 3A and 3B Developments

Shallow-amplitude long-wave trough:

When the major long-wave trough involved is of shallow amplitude, with smaller than average meridional wind components, the following differences are likely to be seen in the cloud patterns: The short-wave disturbances moving across the cold air are likely to have a better defined comma shape (with more curvature vorticity) before they arrive at the trough axis. Their development is likely to be slower and more uniform, and there will usually be two or three well-defined comma patterns moving nearly in tandem within the trough flow pattern.

Enhanced cumulus cloud patterns:

Often, over the oceans, and especially with a Type 3B development, the short-wave disturbance crossing the cold air will appear as an area of deeper convection embedded within the general cold air advection cumulus field. The convection involved, in addition to being deeper in the vertical, will usually include cells or elements of larger horizontal dimensions than the general convection around it. These patterns are often referred to as enhanced cumulus.

The short waves with this type of cloud pattern tend to move more slowly and show more rotation on the time-lapse movie loops of satellite imagery. Also, the development seems to proceed more slowly. The rotation, however, is usually not as well implied on still pictures; the comma shape or vortical characteristics are not well defined in the pattern shape, although at this phase very heavy precipitation and showers will likely be occurring within the area.

As the system develops, the area will begin to fill in with debris and develop a cirrus overcast. If a comma or vortical shape begins to emerge at the same time, the development will probably be Type 3A; if not, Type 3B is more likely, and a waving of the baroclinic zone should be underway. This form of short-wave pattern also occurs over land—it is probably the availability of moisture that causes the higher prevalence over the ocean. It should be pointed out that, when the enhanced cumulus systems are very small, much of the vorticity will be contributed by shear.

Instant occlusion process:

The Type 3B cyclogenesis is best related to the instant occlusion kind of development. It will usually be analyzed that way, especially when the surface low consolidates early in the development.

At times, Type 2 cyclogenesis will also be analyzed as an instant occlusion. A typical case of this is when a split-flow development occurs over the High Plains of the U.S., with cool stable air at the low levels. In those conditions, the

surface low and temperature field consolidation will lag the middle-level development significantly; and, there is likely to be an old surface front trailing back near the Gulf Coast. An instant occlusion will be analyzed from the developing system to the old frontal zone. In this kind of case, the satellite imagery is a very useful aid for interpretation of the weather patterns. This can be a difficult situation for explaining the precipitation pattern to non-meteorologists. Another way to handle it is to bend the tail end of the old surface front northward on the analysis, and call it a warm front with overrunning precipitation.

The cyclogenesis models vs. the real atmosphere

The four types of cyclogenesis show clean storms. One short-wave disturbance—the one that initiated the development—is depicted. The addition of secondary or even tertiary disturbances within the storm circulation will alter the storm structure and complicate the real cloud pattern. Other factors, such as the vertical structure of the frontal zones, will also change the cloud pattern of a given storm. In regard to these differences, the more typical structure or substructure is depicted on the drawings.

Another factor that contributes to real cloud patterns different from the models is that many storms are hybrids relative to the four types. For example, if a short-wave disturbance moves around a major trough circulation so that it arrives on the east side similar to that of a Type 1 meridional trough case, but slightly further west toward the cold side of the baroclinic zone, the middle cloud comma may form already partially west of the edge of the cirrus deck. Thus, the storm cloud development will proceed as a hybrid between the Type 1 and Type 3B forms or models. Another difficulty often occurs with storms being a hybrid type between Types 3A and 3B—this can involve the change with time as well as the spatial characteristics.

Satellite Training Course notes
edited for NTAG Volume 4 by
Walter A. Bohan

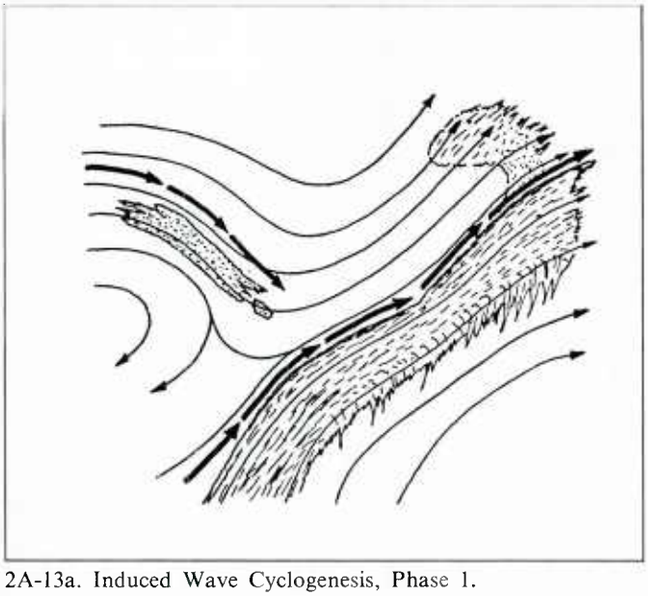

2A-13a. Induced Wave Cyclogenesis, Phase 1.

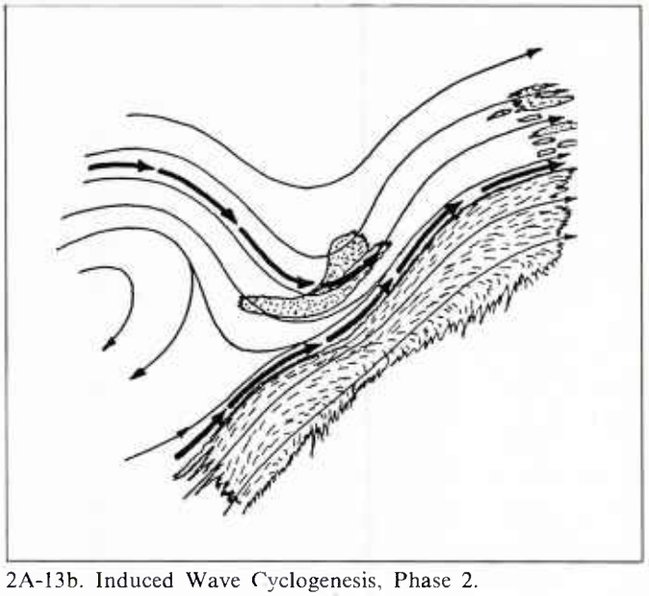

2A-13b. Induced Wave Cyclogenesis, Phase 2.

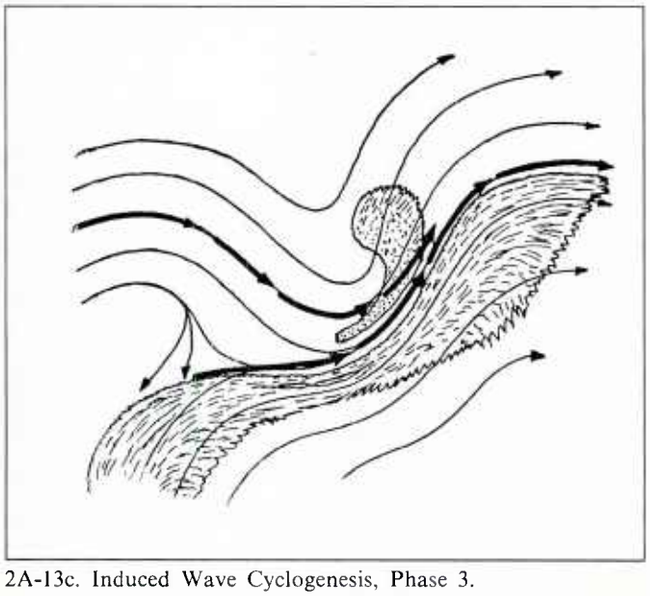

2A-13c. Induced Wave Cyclogenesis, Phase 3.

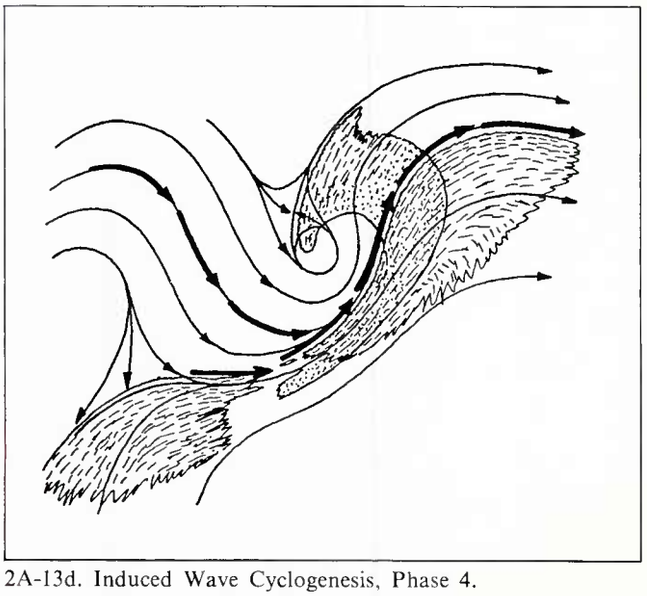

2A-13d. Induced Wave Cyclogenesis, Phase 4.

SUMMARY

The Evolution and Structure of Winter Storms

Abstract by Jay Rosenthal

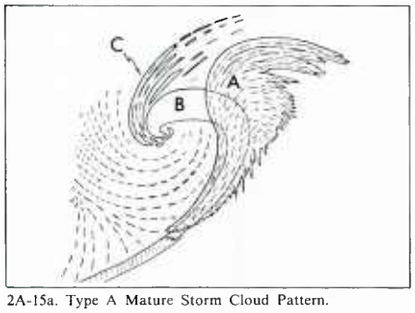

2A-15a. Type A Mature Storm Cloud Pattern.

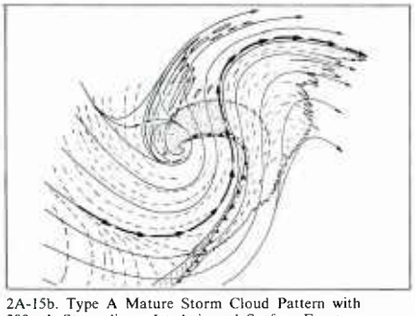

2A-15b. Type A Mature Storm Cloud Pattern with 300-mb Streamlines, Jet Axis and Surface Front.

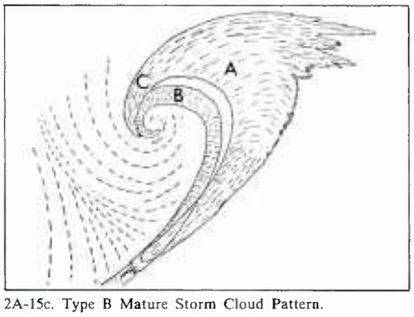

2A-15c. Type B Mature Storm Cloud Pattern.

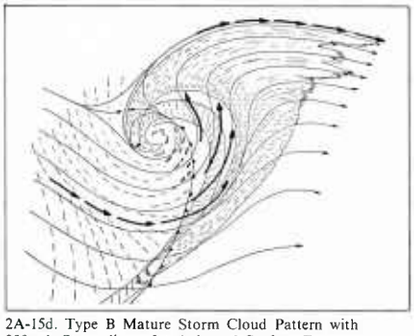

2A-15d. Type B Mature Storm Cloud Pattern with 300-mb Streamlines, Jet Axis and Surface Front.

Winter Storms

Winter storms are major cyclones which form and move within the main belt of the westerlies and are associated with fronts and jet streams. Much of their significant weather occurs with small short wave features embedded within the overall larger synoptic system. These are in addition to the initial disturbance which started the cyclones in the first place. Moreover, the associated short waves may not have the same origin, characteristics or even height of the original disturbance. Infrared imagery at 30-minute intervals is the best way to observe, monitor and predict the often fast evolution of these significant weather features and the relationship between the whole storm and its parts.

Just like two fingerprints are never exactly alike, cloud patterns in winter storms also differ from each other in detail because of the various weather elements embedded within them. Nevertheless, certain characteristic patterns and evolutionary changes do appear and these are summarized below to serve as a reference for forecasters.

Typical Mature Storms

Figures 2A-15a through 15d show schematic models of two types (A & B) of mature winter cyclones. For each type is a diagram showing typical cloud patterns as they appear on infrared imagery. In these figures, Type A shows upper-level baroclinic zone cirrus related to jet streams, Type B shows the convective comma or frontal band, and Type C shows deformation zone cirrus frequently observed to the north of low centers.

In Type A, the jet crosses the front, and the cirrus shield **A** often moves out ahead of the lower frontal band. The surface front itself is located mainly at the rear edge of the frontal cloud band except at its southern fringe where it leads the band. As in most mature systems, western and northern cloud edges are distinct. Precipitation is moderate or heavy under the cirrus shield **A** but also in zones within the front or comma cloud **B**.

In Type B, there is much less separation between cloud systems **A** and **B**. The jet does not cross over and the ridge preceding the trough wraps more around the low center. The main difference between Types A and B is the degree of vertical development. Type B is deeper and usually produces more precipitation.

Storm Development and Cyclogenesis

There are as many kinds of storm development as there are storms. These real storms can be made to fit into three or four models although the fit isn't always perfect. The upper-air pattern that accompanies each type of development is shown in figures 2A-16a through 16c. In Meridional Trough Cyclogenesis (Type 1), the trough has a large meridional extent. There is typically a single jet that moves around the trough and short waves which initiate the cyclogenesis likewise move around the major trough, being most easily observed as vorticity maxima or speed maxima. In Split Flow Cyclogenesis (Type 2), there are two branches of westerlies with the main energy and development taking place in the southern branch. Sometimes, the split into two jets takes place in the stronger part of a diffluent flow. Cold Air Vortex Cyclogenesis (Type 3A) involves development in the cold air behind an existing baroclinic zone. If the cold air development begins relatively close to the baroclinic zone, it may induce a wave on an existing front and the resultant development becomes Induced Wave Cyclogenesis (Type 3B).

Meridional Trough Cyclogenesis

The first real sign of Meridional Trough Cyclogenesis (figures 2A-16d through 16g) may be waving of the back edge of the sharply defined cirrus deck which covers the baroclinic zone ahead of the trough. This occurs as small shallow waves that are otherwise hard to follow move rapidly along the front. As development proceeds, a comma cloud **B** grows under the cirrus, eventually emerging since the jet associated cirrus **A** moves faster than the comma **B**. In the final stages of development, the deep comma may reach the cirrus level producing heavy precipitation. Also, the surface and upper low centers rotate around until the system is vertically stacked. Deformation cirrus **C** also appears.

Split Flow Cyclogenesis

This type of development (figures 2A-17a through 17d) requires a jet moving into a southern branch of the westerlies associated with a diffluent flow pattern. Development usually starts with an area of cirrus and mid-clouds as a mid-troposphere low forms and works its way upward. In fact, this upper low may be very developed before organization even takes place at the surface. When the convective vorticity comma does form to the southeast of the closed circulation, it develops fast. As it grows, the comma's dense cirrus merges with the deformation cirrus **C** ahead of the trough.

Cold Air Vortex Cyclogenesis

This is one of the most frequent types of cyclogenesis, especially over the oceans. In the cold air behind an existing baroclinic zone (figures 2A-17e through 17h), a complete new cyclone forms producing its own separate baroclinic zone complete with fronts and jet stream. In the beginning of the development, several short waves move toward the trough axis in the region between the old jet zone and a new speed maximum. These short waves decelerate and rotate at the trough line, and are much more easily seen on satellite imagery than on analyses and prognoses. Finally, a well-defined comma forms from the short waves and grows. As this new baroclinic zone intensifies, the old one ahead of the trough weakens. Eventually, the new one catches up and they merge.

2A-16a. Typical flow patterns for Meridional Trough Cyclogenesis.

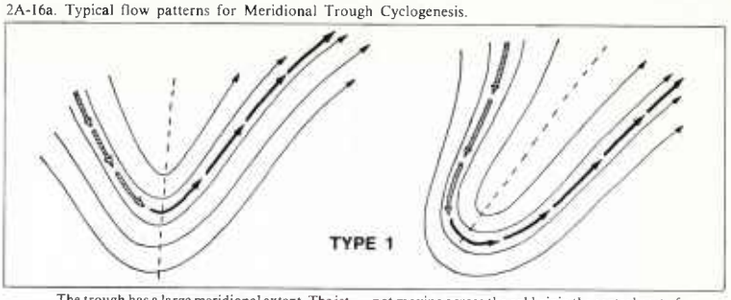

The trough has a large meridional extent. The jet axis is located around the trough, without any significant branches either across the trough or outward into the adjacent ridges. The short-wave disturbances, including the one initiating the cyclogenesis, move around the major trough, within or under the jet baroclinic zone. They are not moving across the cold air in the central part of the trough. These disturbances or impulses are likely difficult or impossible to detect in the curvature of the streamlines and contours; they usually show best as maxima or perturbations in the 500-mb vorticity field, or as speed maxima moving within the jet zone.

2A-16b. Typical flow patterns for Split Flow Cyclogenesis.

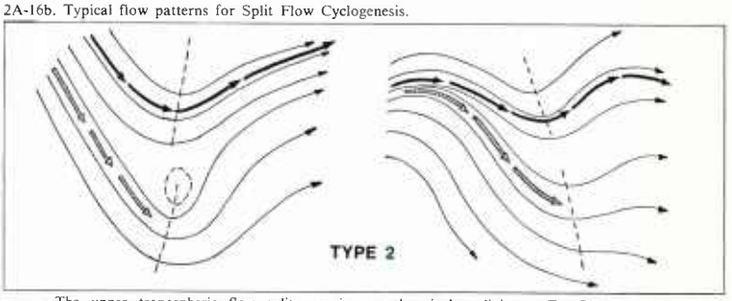

The upper-tropospheric flow splits, or is diffluent. Often there are two branches of the westerlies forming, with the northern one being the older one. The new branch then forms further southward with the cyclogenesis occurring along the southern branch. Or, there may be two branches throughout the period, with the main energy transferring to the southern branch during cyclogenesis. In either case, the development occurs south (on the warm side) of the older northern jet baroclinic zone. Two flow patterns are illustrated. The first shows the northern trough about in phase (zonally) with the southern one; therefore, a distinct split is seen in the flow pattern. The second shows the northern trough further to the west; therefore, the split pattern is less distinct, and a diffluent appearance dominates. The short-wave disturbance initiating the cyclogenesis moves south of the older wave stream and jet zone.

2A-16c. Typical flow patterns for Cold Air Vortex/Induced Wave Cyclogenesis.

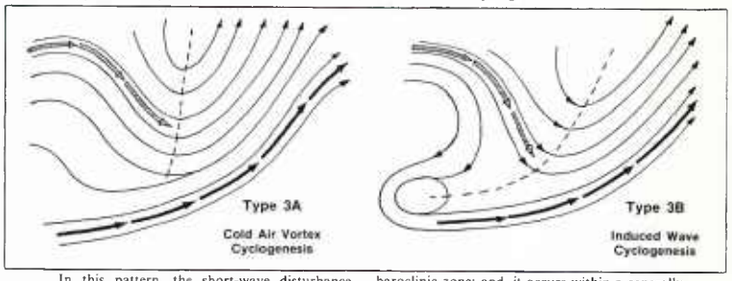

In this pattern, the short-wave disturbance initiating the cyclogenesis moves across the cold air in the central part of the trough behind the jet baroclinic zone, rather than within it as in Type 1. This type of development is opposite to that of Type 2 in two ways. The development occurs on the cold air side of the older or initially stronger jet baroclinic zone; and, it occurs within a generally confluent portion of the large scale flow pattern. Both subcategories of Type 3 development begin similarly; but in Type 3A, a complete new storm pattern develops on the cold air side of the old baroclinic zone. In Type 3B, the new development induces a wave on the old baroclinic zone.

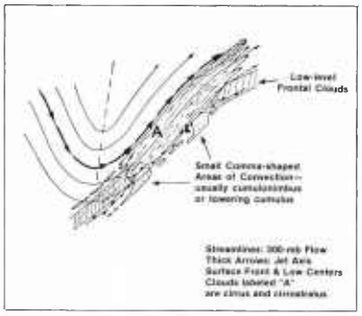

2A-16d. Meridional Trough Cyclogenesis, Phase 1.

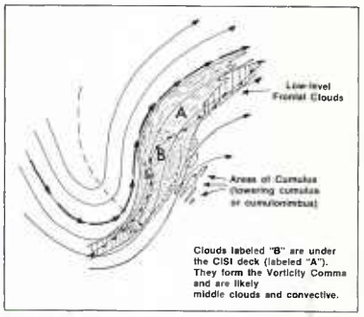

2A-16e. Meridional Trough Cyclogenesis, Phase 2.

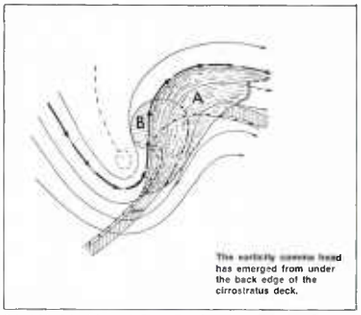

2A-16f. Meridional Trough Cyclogenesis, Phase 3.

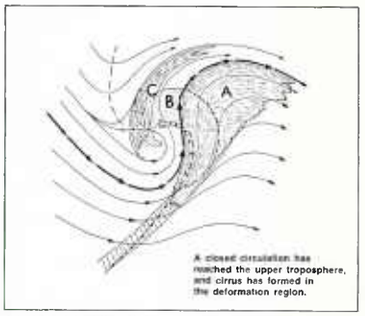

2A-16g. Meridional Trough Cyclogenesis, Phase 4.

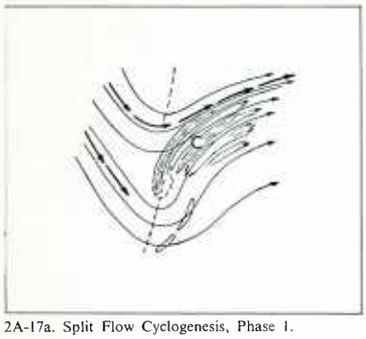

2A-17a. Split Flow Cyclogenesis, Phase 1.

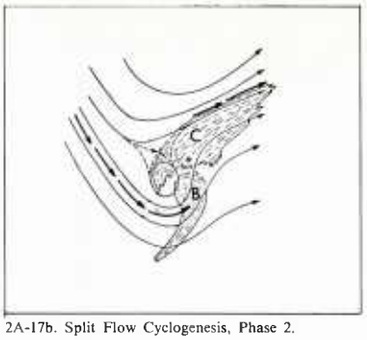

2A-17b. Split Flow Cyclogenesis, Phase 2.

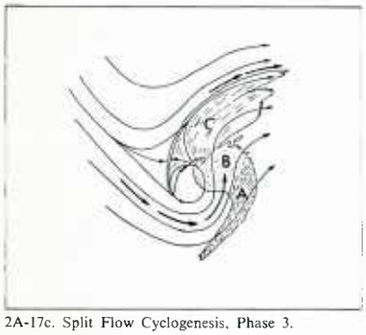

2A-17c. Split Flow Cyclogenesis, Phase 3.

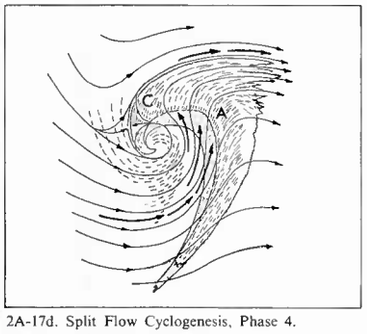

2A-17d. Split Flow Cyclogenesis, Phase 4.

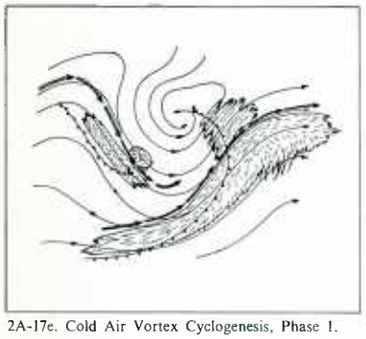

2A-17e. Cold Air Vortex Cyclogenesis, Phase 1.

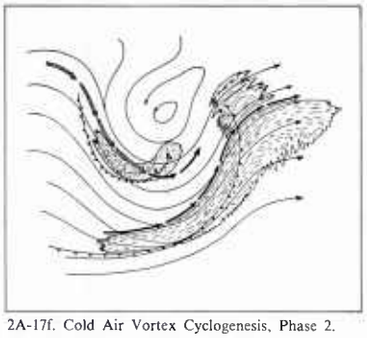

2A-17f. Cold Air Vortex Cyclogenesis, Phase 2.

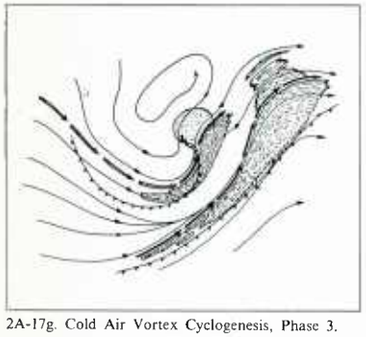

2A-17g. Cold Air Vortex Cyclogenesis, Phase 3.

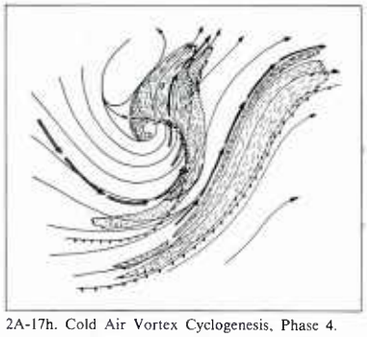

2A-17h. Cold Air Vortex Cyclogenesis, Phase 4.

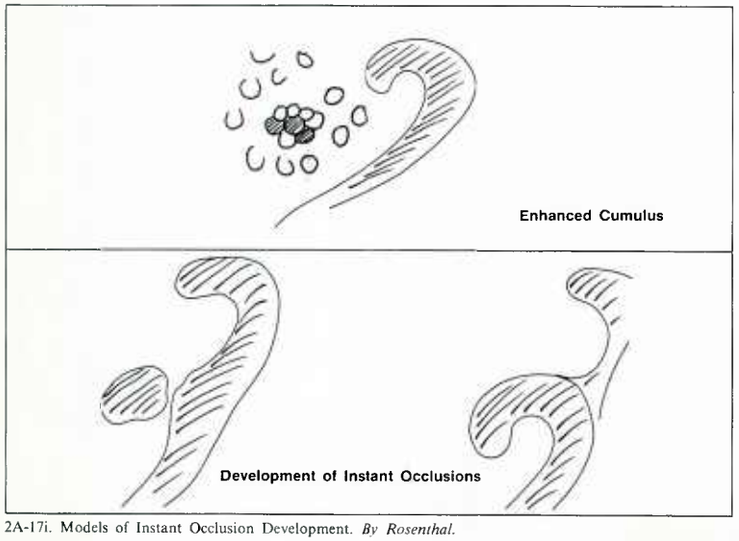

2A-17i. Models of Instant Occlusion Development. *By Rosenthal.*

Induced Wave Cyclogenesis

In this type of cyclogenesis, systems coming down the new baroclinic zone in the cold air eventually come in phase with short waves moving up the old one. They are so close that a new comma grows on the old front. As it grows, the two jets merge into one. If the trough is shallow, multiple well-formed commas may occur.

Enhanced Cumulus

Over the oceans, short waves are sometimes identifiable as areas of brighter, deeper convection within the post-frontal, open-celled advection cumulus. They often rotate and move slowly, producing heavy showers. As they develop, cloud elements fill in and cirrus forms.

Instant Occlusions

Instant Occlusions frequently form over the oceans when eastward-moving short waves catch up with waves induced on pre-existing fronts. The joining of the cloud features and vorticity (figure 2A-17i) results in a new hook-shaped cloud system which rapidly evolves into a spiral "occlusion". Explosive Deepeners in the Pacific Ocean are often of this type.

Cyclogenesis Models vs. Reality

The four cyclogenesis models previously discussed are seldom exactly reproduced in nature. Real storms are often complicated by secondary cloud systems and many storms are hybrids.

Case 1 Cyclogenesis

Cyclogenesis in Meridional Troughs

Winter storms are major cyclones that form and move within the main belt of the westerlies. Some storms begin as a wave perturbation on a polar front separating tropical and polar air masses and then develop into large mature storms. This is the most familiar type of winter storm development. Recently, it has been recognized (Reed, 1979) that major cyclones can originate in the polar air stream behind or poleward of a polar front. These cyclones form in short-wave scale disturbances associated with the jet stream, and, in general, they can be detected in the cloud patterns in infrared imagery just before development begins. Weldon (1975) has examined such disturbances in detail and has classified them as cold air vortex or induced wave developments, depending on whether or not they interact with nearby baroclinic zones (frontal systems) as they evolve to maturity.

During the winter, when a block is in place at high latitudes over the eastern North Pacific, there is generally a quasi-stationary closed low over the central North Pacific upstream of the block. Sometimes, as the block breaks down, the low begins to move slowly eastward and becomes a progressive long-wave trough. If a branch of the polar jet stream extends over the upstream ridge and digs southward toward the base of the trough, repeated cyclogenesis events may occur in the polar air stream behind the trough. The cyclones that form are short-wave disturbances that are steered by the flow field of the meridional trough as it advances eastward.

References

Reed, Richard J., 1979: Cyclogenesis in polar air streams. *Mon. Wea. Rev.*, **107**, 38-52.

Weldon, Roger A., 1975: The structure and evolution of winter storms. Satellite Training Notes. Satellite Applications Laboratory (NESDIS), Washington, D.C., 37 pp.

Cyclogenesis events in a progressive meridional trough
Eastern North Pacific
January 1979

The satellite imagery and weather analyses for the first three days of this case are a repetition of the last three days of Blocking Case 1 (Sec. 1B). The blocking action over the eastern North Pacific is in its final phase, and disturbances in the westerlies upstream of the block are observed to dissipate as they move against the block. It is during this period that the major low over the central Pacific, which had been quasi-stationary between 160° W and 180° W, begins to advance slowly eastward as a major meridional trough. Three distinct cold air cyclogenesis events occur in the trough during the period 9–14 January. Each storm is followed in the satellite imagery throughout its life cycle: initiation, growth to maturity, and dissipation in the flow field of the trough.

9–11 January

The NMC 500-mb analysis for 0000 GMT 9 January (2B-2b) shows the block **B–B**, which extends from Alaska to the western states along the North American west coast, and the major, quasi-stationary low **A** upstream of the block over the central Pacific; these features are also observed at 300 mb (2B-2a). The corresponding surface analysis (2B-3b) shows a major low and frontal system **A1–A1** and the remnants of two earlier disturbances **A2** and **A3**, to the west and east, respectively.

The potential for cold air cyclogenesis is suggested by the appearance of a small area of enhanced convection **A4** in the satellite picture (2B-3a). This cloudiness is located in a field of cold air advection cumulus, in the polar air stream behind the surface low **A1**. Aloft, the enhanced convection **A4** is located in northwesterly flow at 500 mb and, at 300 mb, there is a strong polar jet **PJS** upstream of the low **A**. The height contour lines (flow field) indicate that the disturbance **A4** will be advected southward behind the low **A**, toward the polar jet **PJS** at low latitudes and the corresponding strong baroclinic zone **A1–A1** in the satellite picture. The distinct poleward cloud edge of the frontal band **A1–A1** clearly identifies the location of the low-latitude polar jet **PJS** along the frontal zone.

The FNOC 36-hour (2B-3c) and 72-hour (2B-3d) 500-mb prognoses show that the closed high **B** over Alaska will move north over the Arctic Ocean, and strong polar westerlies (closely-spaced height contour lines) will dominate at mid latitudes across the Pacific. The low **A** is forecast to advance slowly eastward with north-south flow increasing and forming a pronounced meridional trough in 72 hours. The presence of closely-spaced height contour lines upstream of the low **A** indicates polar westerlies digging southward to the rear of the meridional trough throughout the period.

The new major low **C** at high latitudes over the western Pacific is forecast to deepen and advance eastward. This will maintain strong polar westerlies upstream and provide strong cold air advection to the rear of the low **A**. The cold air advection will result in deepening of the low and, as the system intensifies, warm air advection will increase downstream and a subtropical ridge of high pressure **B1** is forecast to develop over the eastern Pacific.

During the first 24 hours of the forecast period, the large-scale features at 500 mb (2B-4b and 5b) develop as forecast. The closed high **B** moves over the Arctic Ocean; the major low center **A** consolidates into a single center and moves slowly eastward; and strong polar westerlies (closely-spaced height contour lines) are observed over the central Pacific. Warm air advection ahead of the low **A** has resulted in a more rapid buildup of a subtropical ridge **B1** over the eastern Pacific than forecast (2B-3c).

An examination of the satellite picture (2B-4a) shows that the enhanced cumulus area **A4** has increased in size and, as it advances toward the frontal cloud band (baroclinic zone) **A1–A1**, it develops the vorticity comma shape (2B-5a) characteristic of a short-wave disturbance in the westerlies. This is cold air cyclogenesis Event No. 1 in the 500-mb low **A**. The cloud bulge **A5** into the cold air identifies another short-wave development; however, this disturbance has formed on the baroclinic zone **A1–A1** and is moving rapidly to the northeast.

The surface analysis (2B-4c) depicts a surface front **A1–A1** curving into the central area of an elongated low pressure with two centers, **A1** and **A2**. There is also an elongated 500-mb low **A** aloft (2B-4b). As the 500-mb low **A** consolidates into a single center (2B-5b), the surface low also displays a single center **A2** (2B-5c). During this period, the surface low **A1** dissipates as it moves against the surface block **B** and, in the satellite picture (2B-5a), only a faint, detached cloud vortex **A1** is observed south of the cloud band lying along the border of the block **B** from the frontal band **A1** to the vortex **A2**.

The satellite picture twelve hours later (2B-7a) shows that the vorticity comma **A4** has reached the mature stage. There is a distinct, dense cirrus deck, and a spiral comma head has emerged to indicate a deep vertical development. Notice, however, that there is only a short, narrow comma tail extending to the south from the cirrus deck. Thus, although a low **A4** has formed at the surface (in the location of the emerged comma head), the absence of a prominent comma tail has led the analyst to depict only a trough line (TROF, 2B-7b) instead of a front extending to the south from the surface low **A**.

9–11 January continued on page 2B-6

300 mb

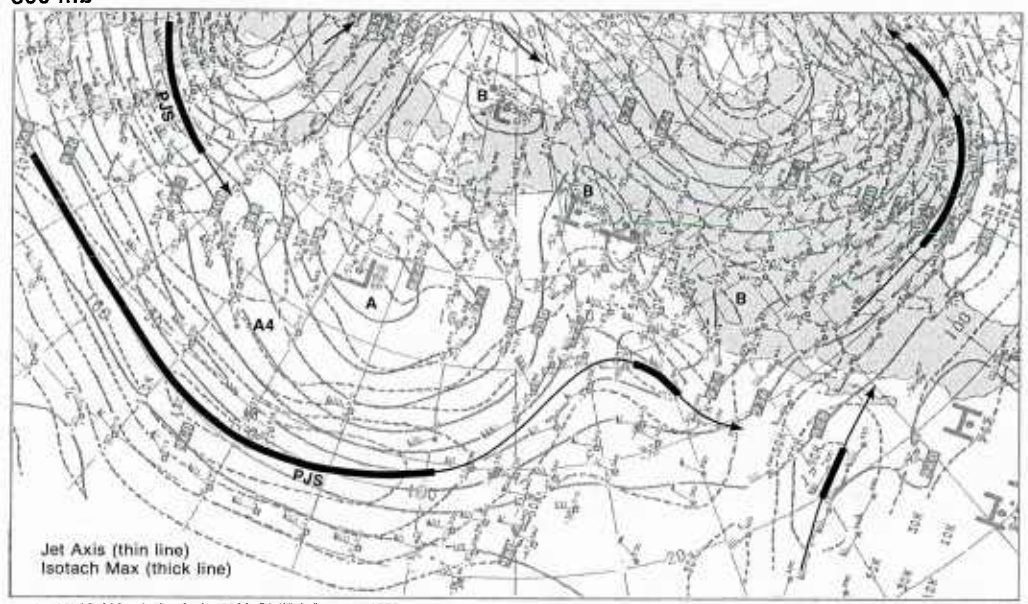

2B-2a. NMC 300-mb Analysis. 0000 GMT 9 January 1979.

500 mb

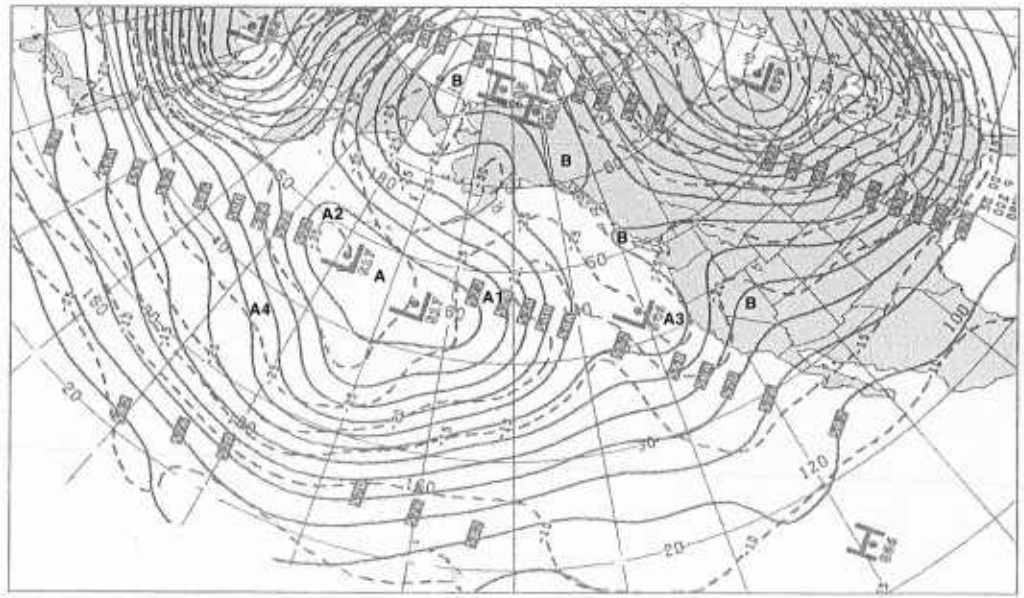

2B-2b. NMC 500-mb Analysis. 0000 GMT 9 January 1979.

Cyclogenesis in a Progressive Meridional Trough

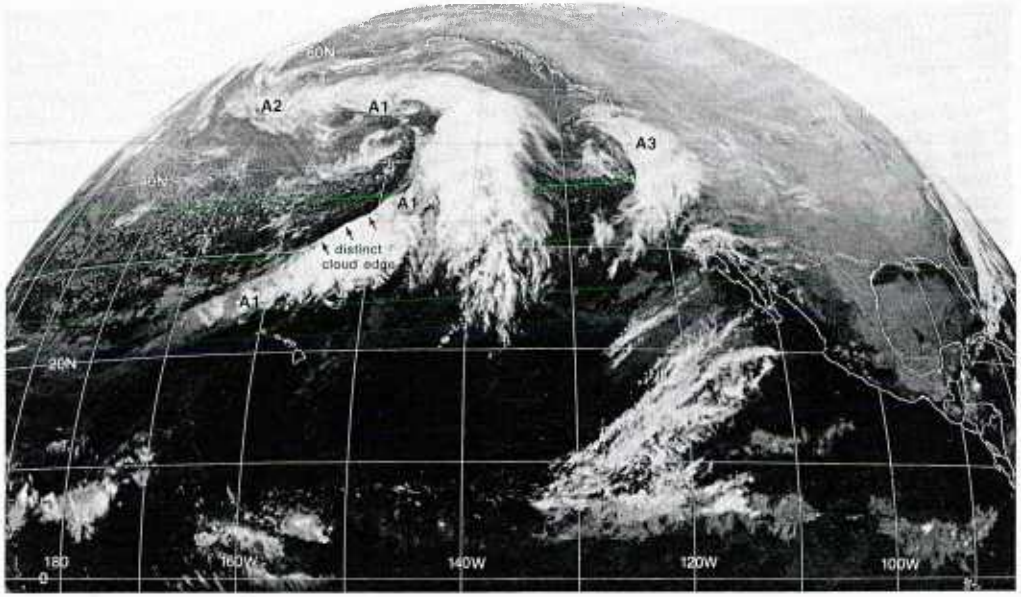

2B-3a. GOES-W. Infrared Picture. 0015 GMT 9 January 1979.

surface

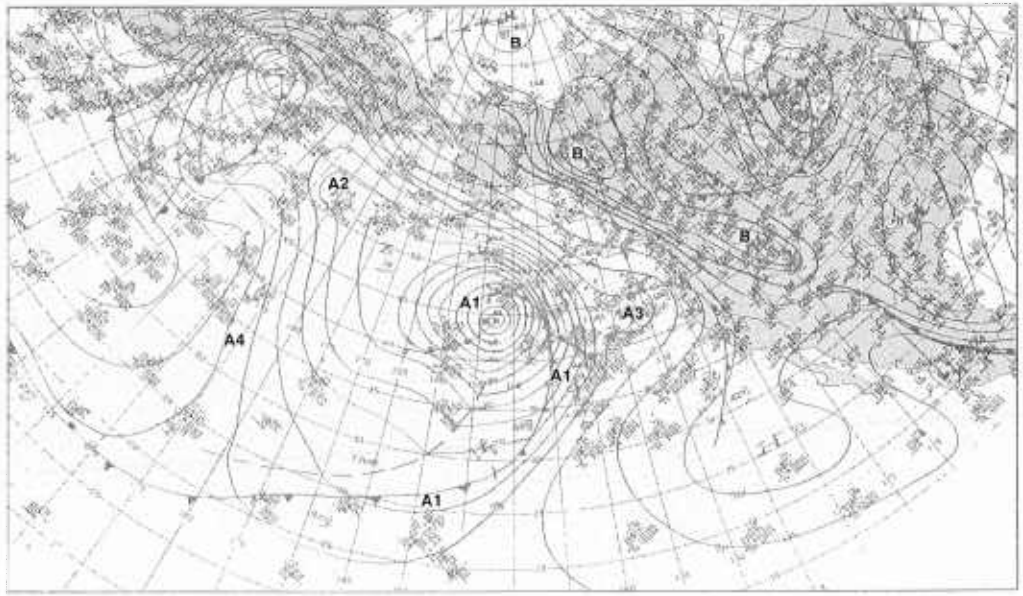

2B-3b. NMC Surface Analysis. 0000 GMT 9 January 1979.

500 mb

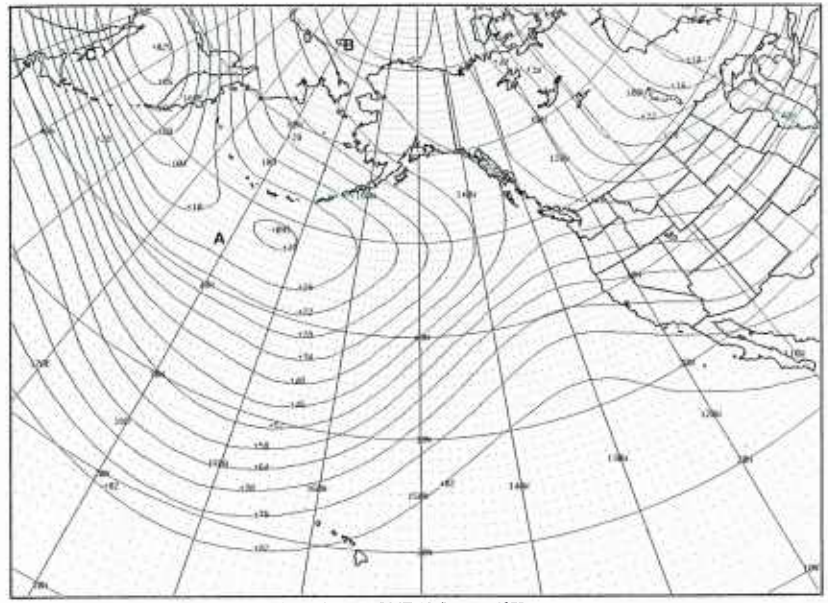

2B-3c. FNOC PE 36-hr 500-mb Prognosis. Valid 1200 GMT 10 January 1979.

500 mb

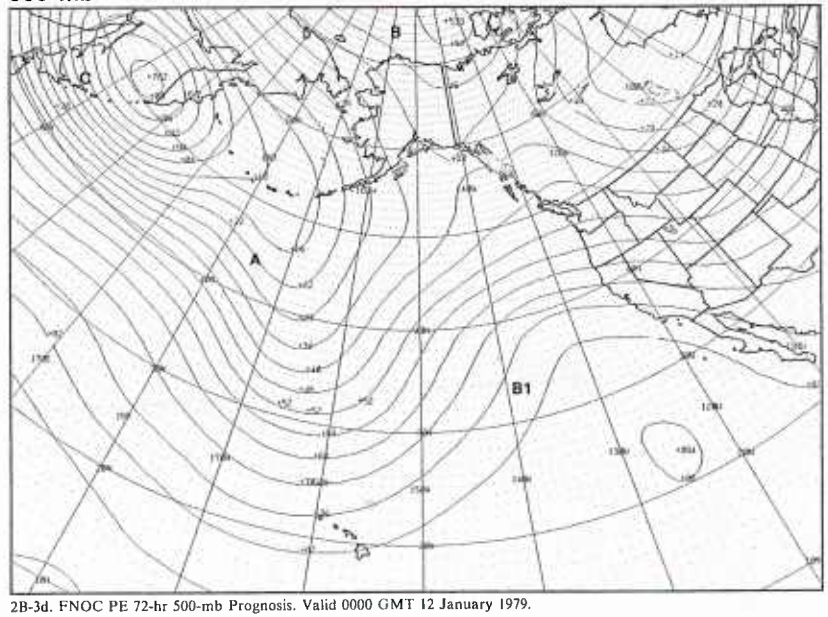

2B-3d. FNOC PE 72-hr 500-mb Prognosis. Valid 0000 GMT 12 January 1979.

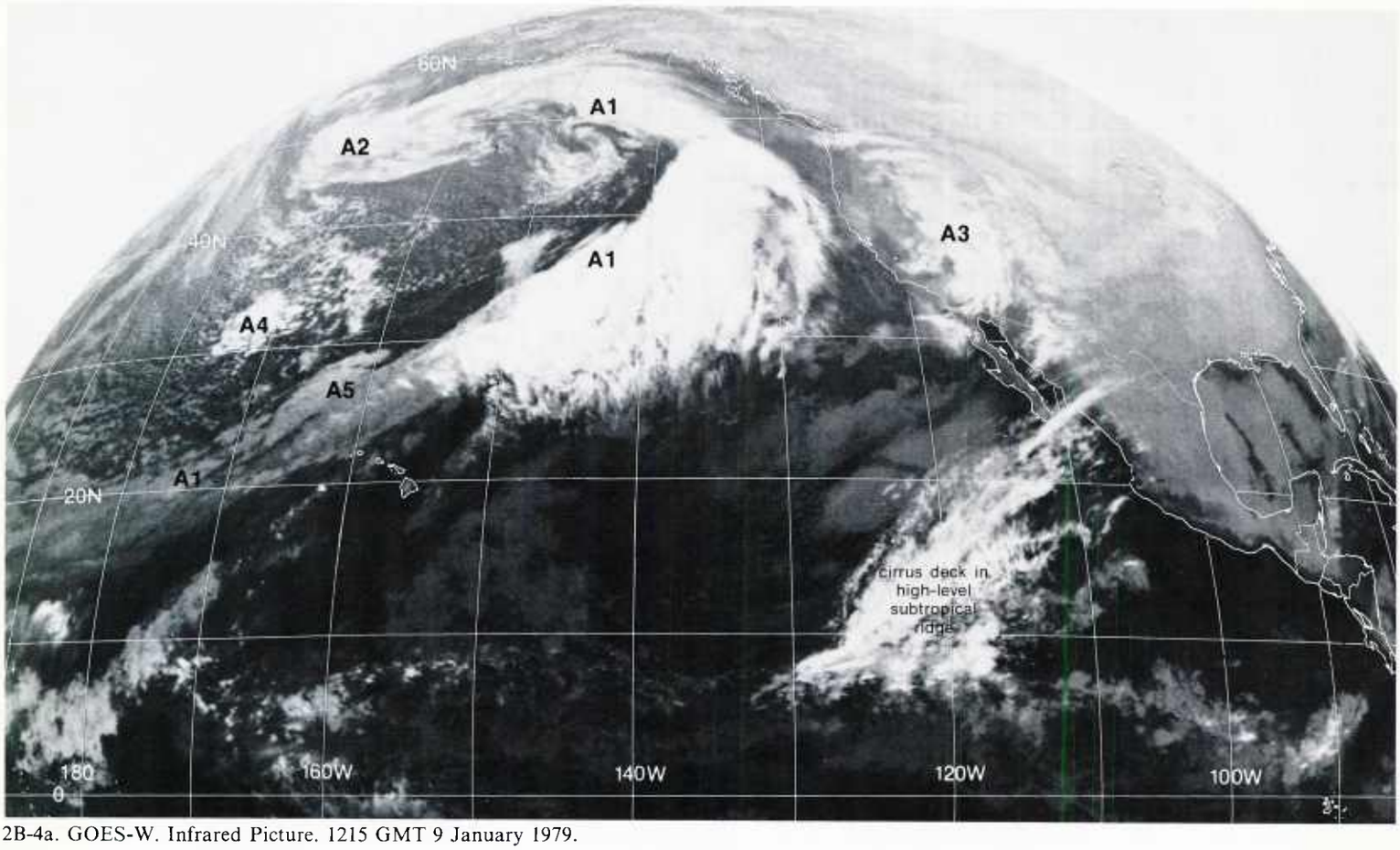

2B-4a. GOES-W. Infrared Picture. 1215 GMT 9 January 1979.

500 mb

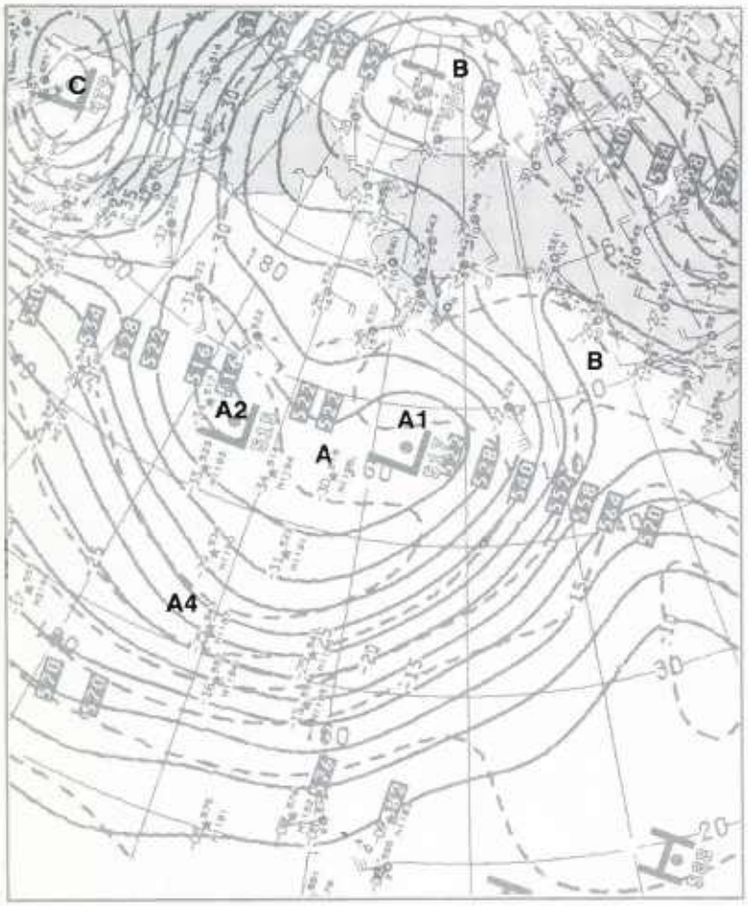

2B-4b. NMC 500-mb Analysis. 1200 GMT 9 January 1979.

surface

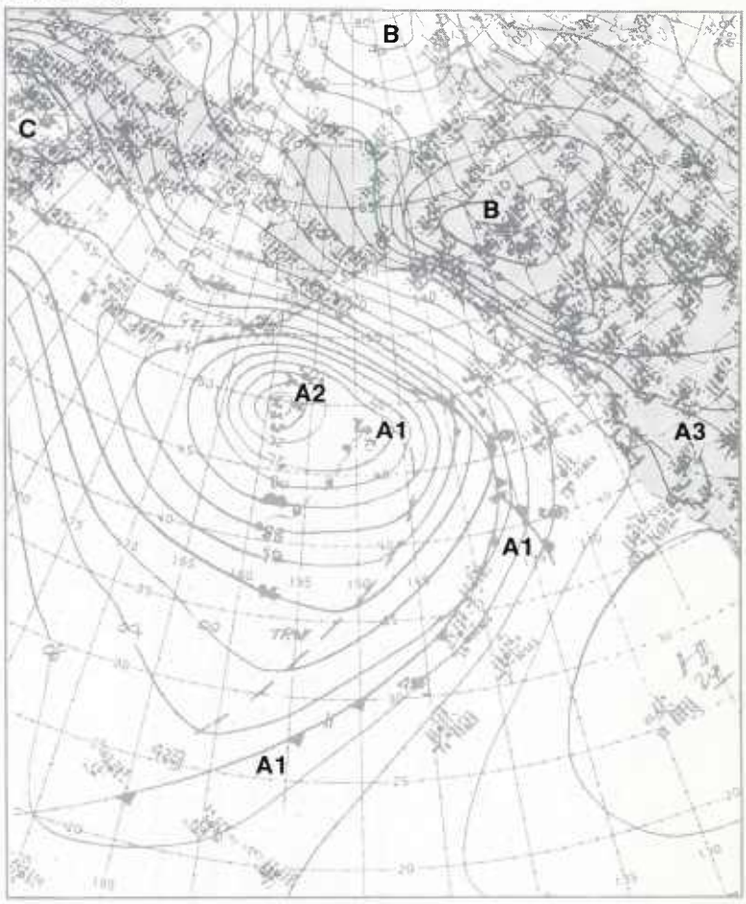

2B-4c. NMC Surface Analysis. 1200 GMT 9 January 1979.

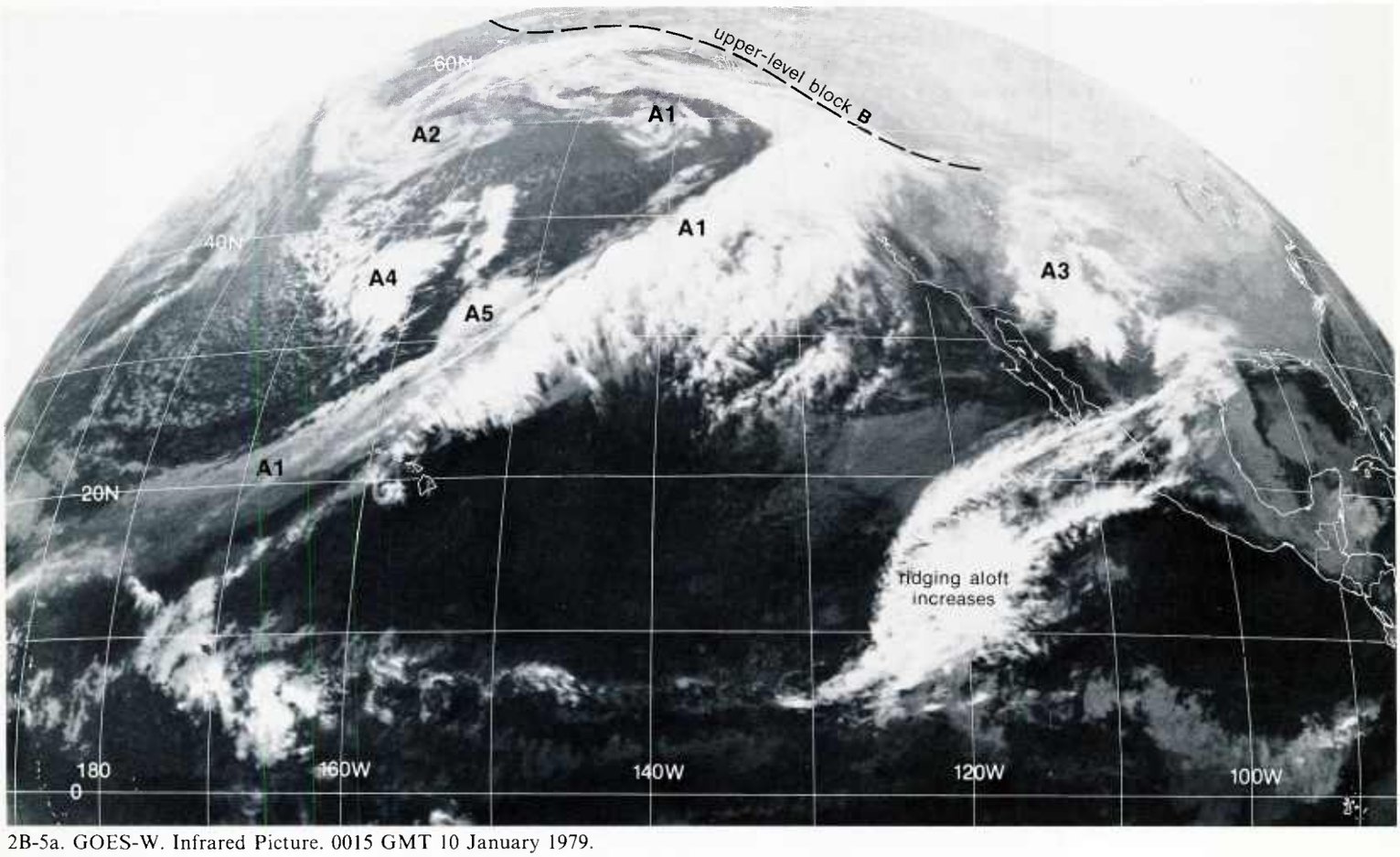

2B-5a. GOES-W. Infrared Picture. 0015 GMT 10 January 1979.

500 mb

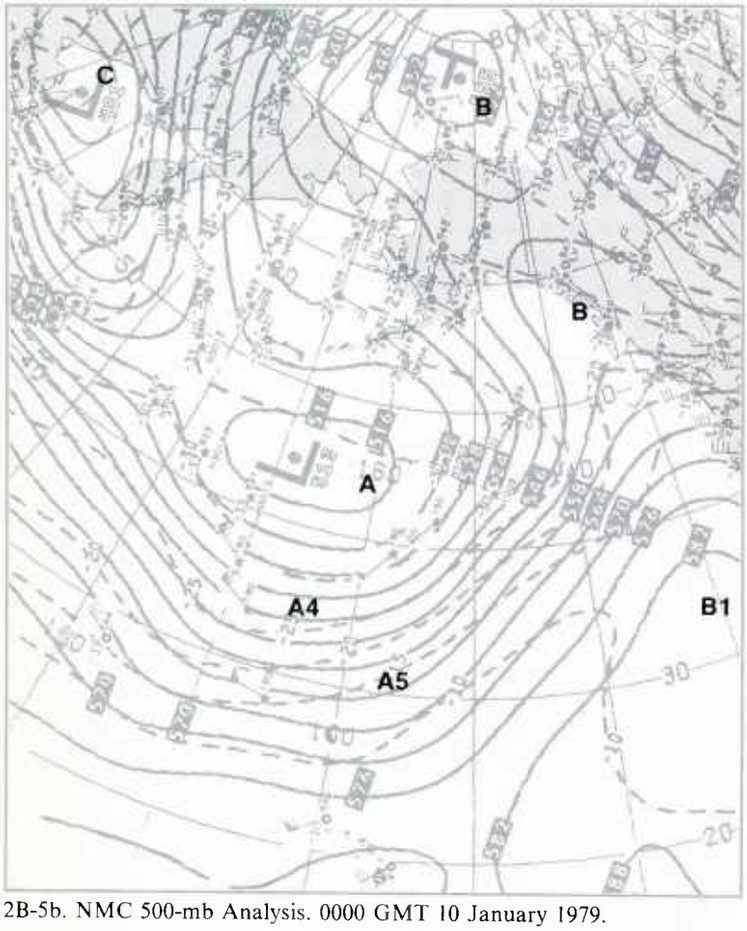

2B-5b. NMC 500-mb Analysis. 0000 GMT 10 January 1979.

surface

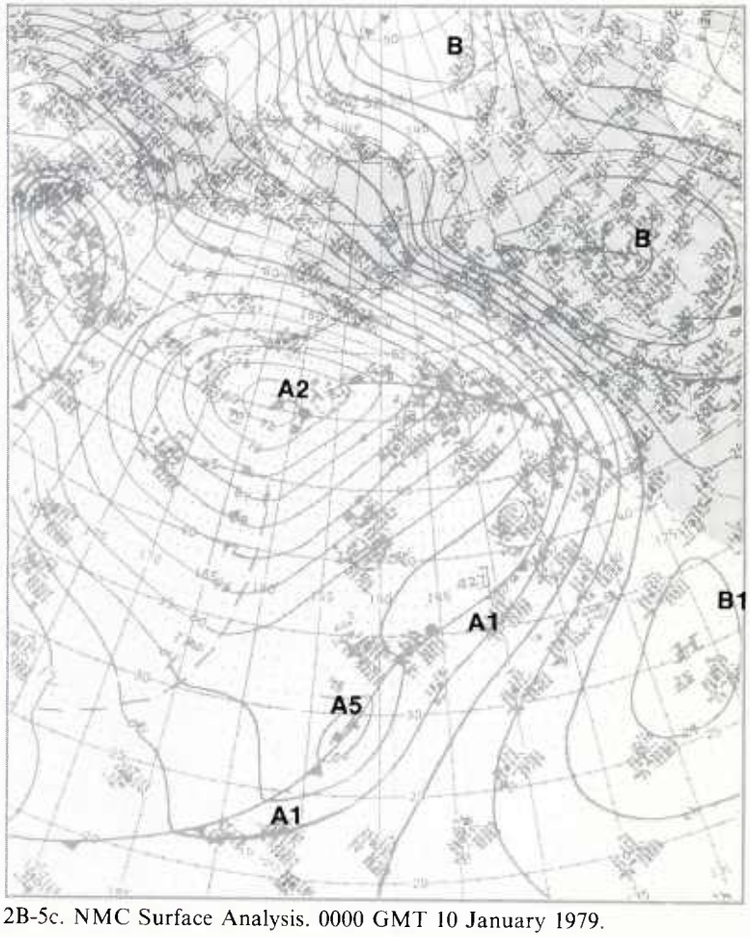

2B-5c. NMC Surface Analysis. 0000 GMT 10 January 1979.

At 300 mb (2B-6a), the polar westerlies **PJS** have penetrated to the West Coast, between the high latitude block **B** and the subtropical high **B1**, providing a channel for the disturbances in the westerlies to advance across the Pacific Northwest. The disturbance **A4**, which was located in northwesterly flow earlier, has moved around the base of the trough **A** at 300 mb (2B-6a) and 500 mb (2B-6b) into the southwesterly flow ahead of the trough. Thus, it appears that the comma cloud **A4** (2B-7a) may be steered by the southwesterly flow aloft toward the frontal band **A1–A1** and merge with it to form a wave development on the front. At the western edge of the satellite picture, there is a spiral cloud formation **A6** which suggests that another cold air advection cyclogenesis is occurring in the polar air stream behind the upper low **A**.

By 48 hours into the forecast period, the satellite picture (2B-8a) shows that the vorticity comma **A4** has not merged with the baroclinic zone **A1–A1** and is located entirely on the cold air side to the north. At the surface (2B-8c), there is a closed low **A4** (984 mb), but no surface front which indicates that the disturbance remains primarily an upper-air system. Since the cyclogenesis develops and remains entirely on the cold air side of the baroclinic zone **A1–A1**, this identifies cyclogenesis Event No. 1 as a cold air cyclogenesis Type 3A, according to Weldon's classification (see 2A Introduction). It is important to note, therefore, that not every vorticity comma approaching a frontal zone on the cold air side will induce a wave development on the front.

The disturbance **A4** is short lived. By 1215 GMT 11 January (2B-9a), the vorticity comma cloud pattern is no longer recognizable and only an elongated cloud band remains, as the disturbance dissipates against the block **B** (most clearly evident at 500 mb, 2B-9b). The surface analysis (2B-9c) shows the remains of this system: a weak low **A4** and a trough (TROF) extending to the southeast.

To the west, over the central Pacific, the spiral cloud pattern **A6** has increased in size and become more organized (2B-9a) as it advances around the base of the 500-mb low **A** (2B-9b) toward the baroclinic zone **A1–A1**. The surface analysis (2B-9c) shows a strong surface front associated with this new cold air disturbance, which did not occur with cyclogenesis Event No. 1. This is cold air cyclogenesis Event No. 2 in the polar air stream surges behind the 500-mb low **A**, as it moves slowly eastward.

continued on page 2B-10

300 mb

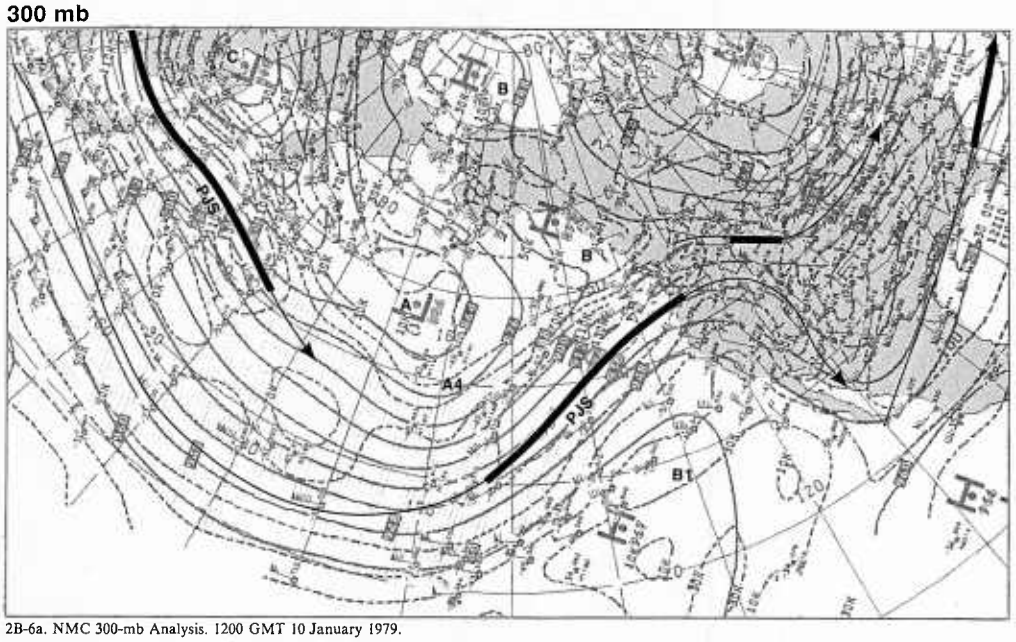

2B-6a. NMC 300-mb Analysis. 1200 GMT 10 January 1979.

500 mb

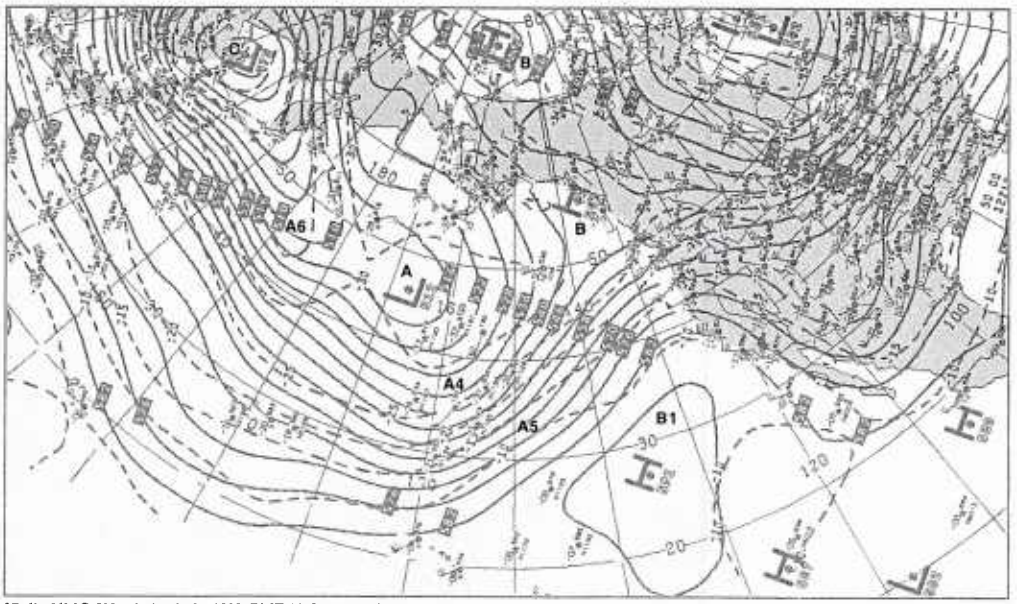

2B-6b. NMC 500-mb Analysis. 1200 GMT 10 January 1979.

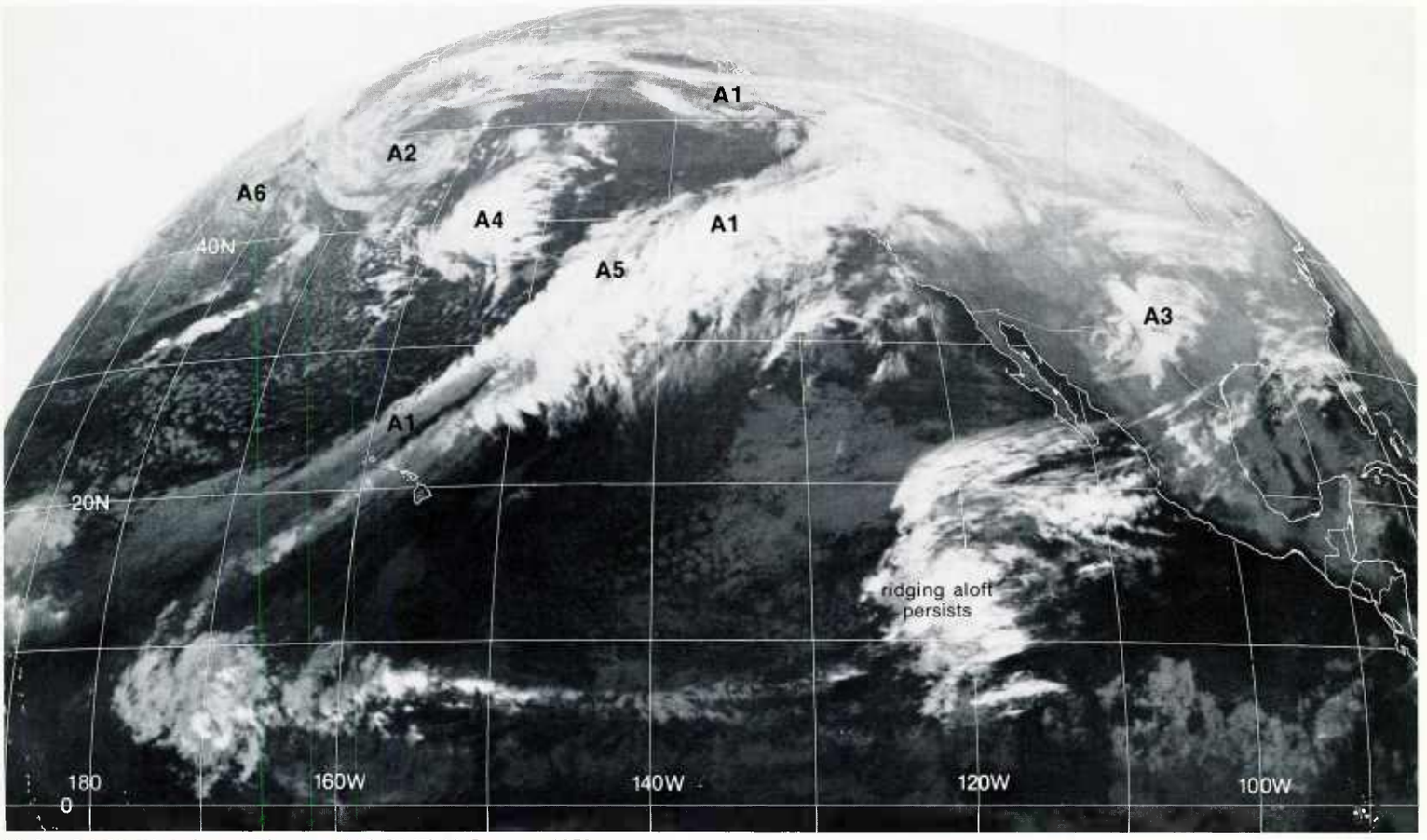

2B-7a. GOES-W. Infrared Picture. 1215 GMT 10 January 1979.

surface

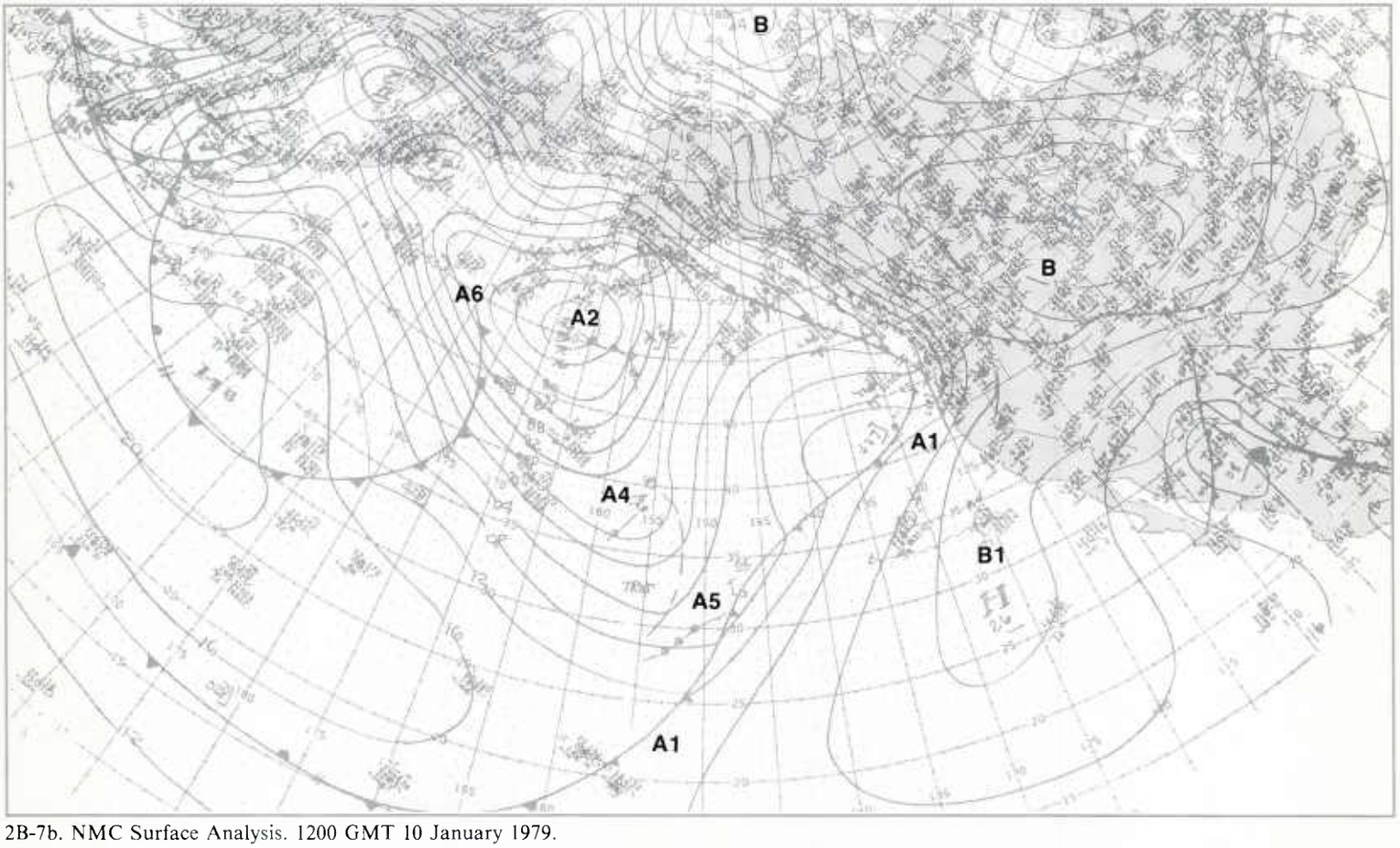

2B-7b. NMC Surface Analysis. 1200 GMT 10 January 1979.

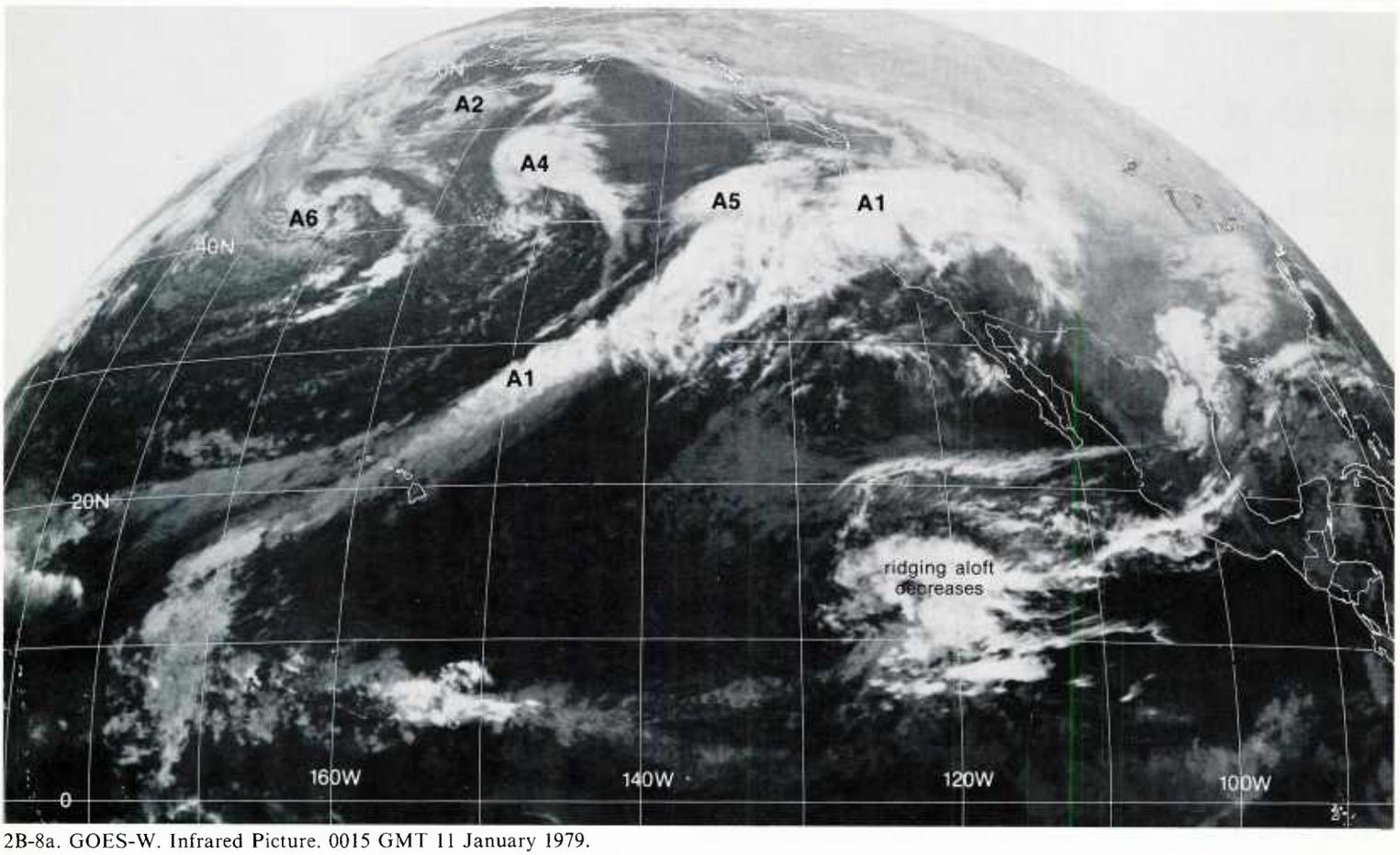

2B-8a. GOES-W. Infrared Picture. 0015 GMT 11 January 1979.

500 mb

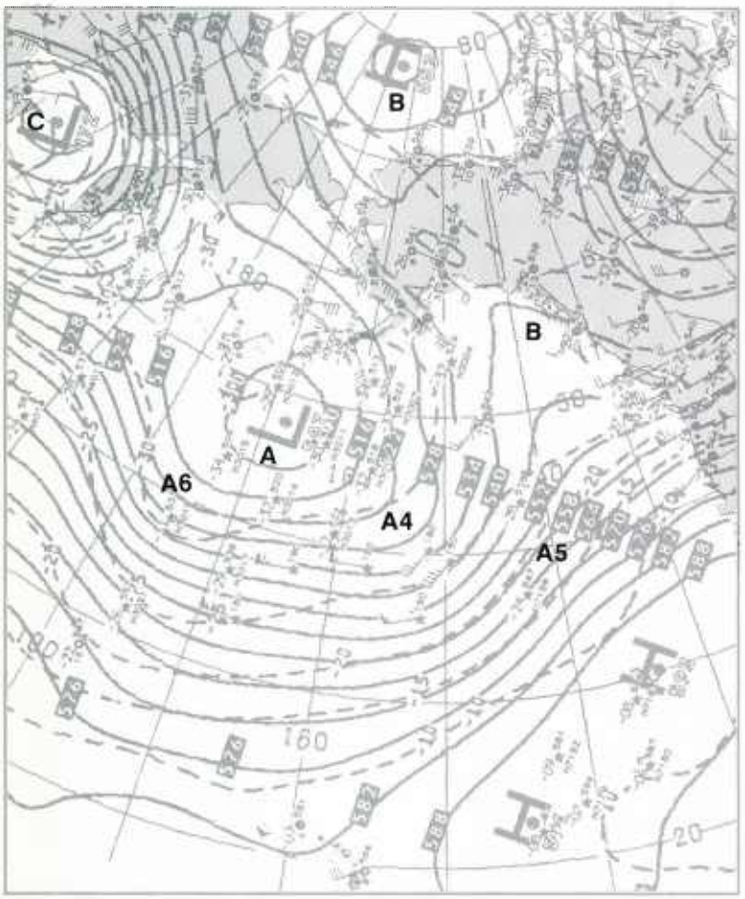

2B-8b. NMC 500-mb Analysis. 0000 GMT 11 January 1979.

surface

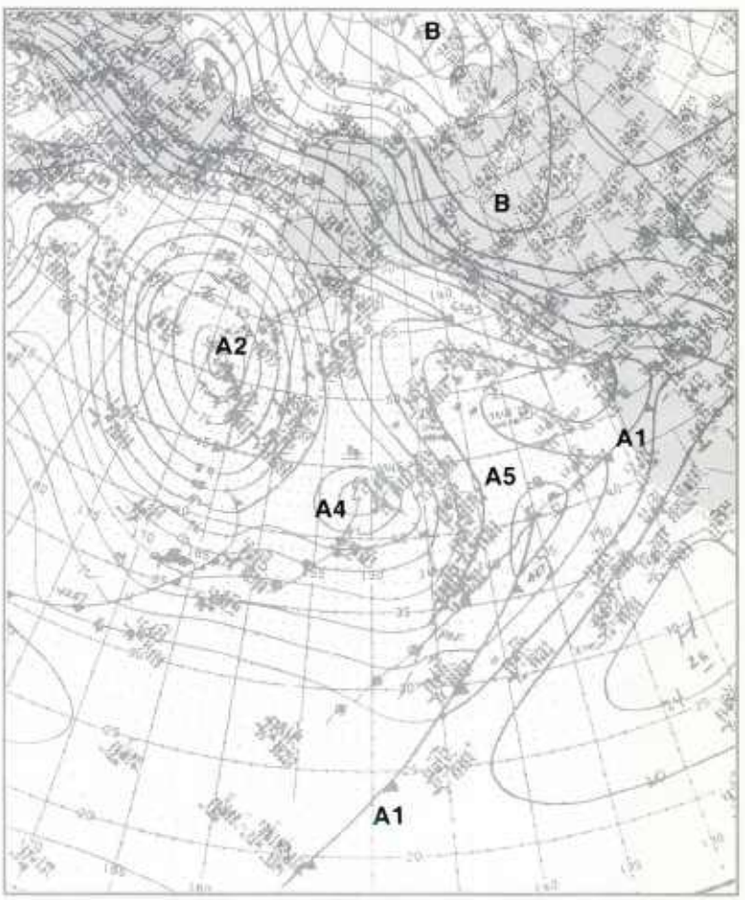

2B-8c. NMC Surface Analysis. 0000 GMT 11 January 1979.

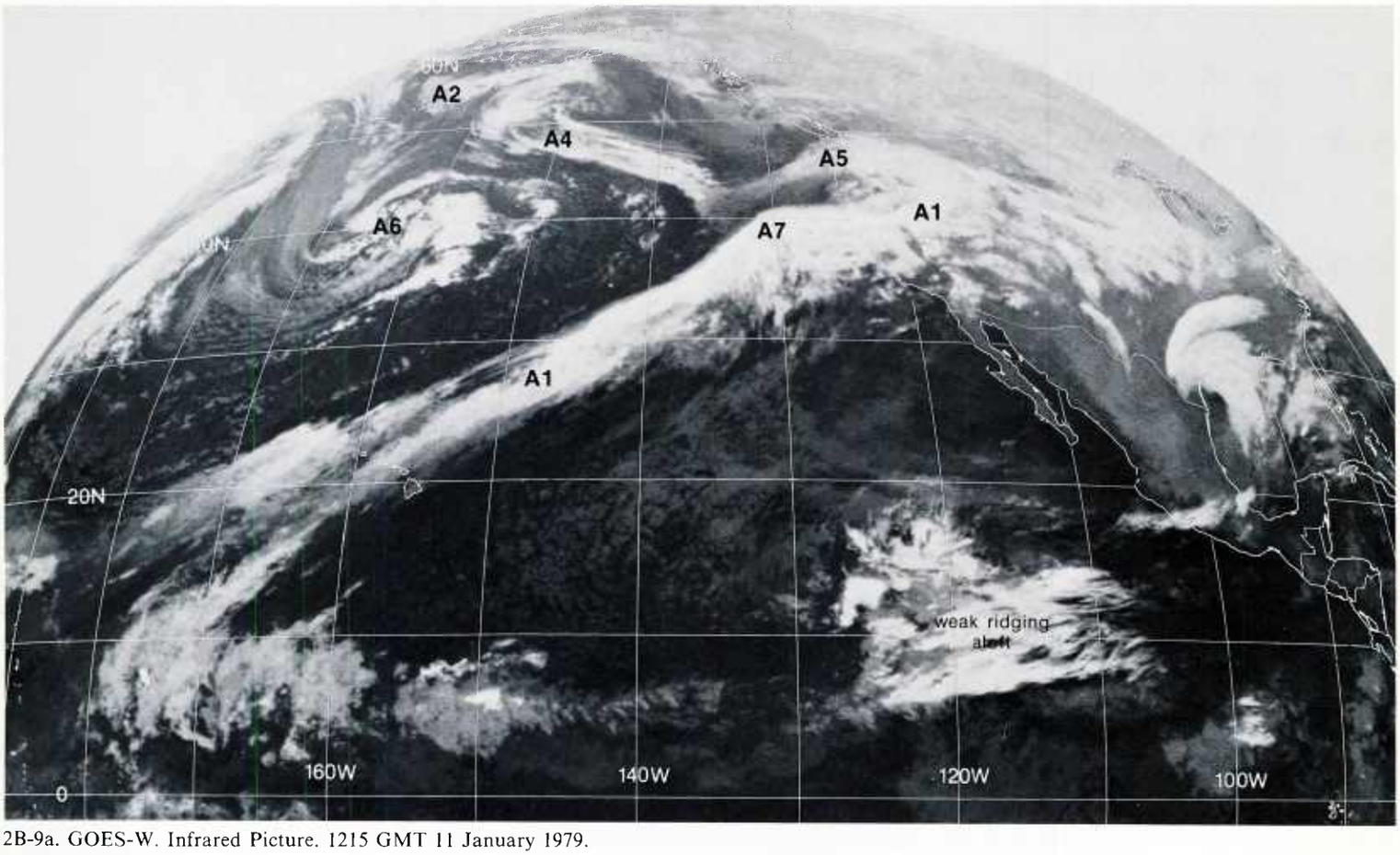

2B-9a. GOES-W. Infrared Picture. 1215 GMT 11 January 1979.

500 mb

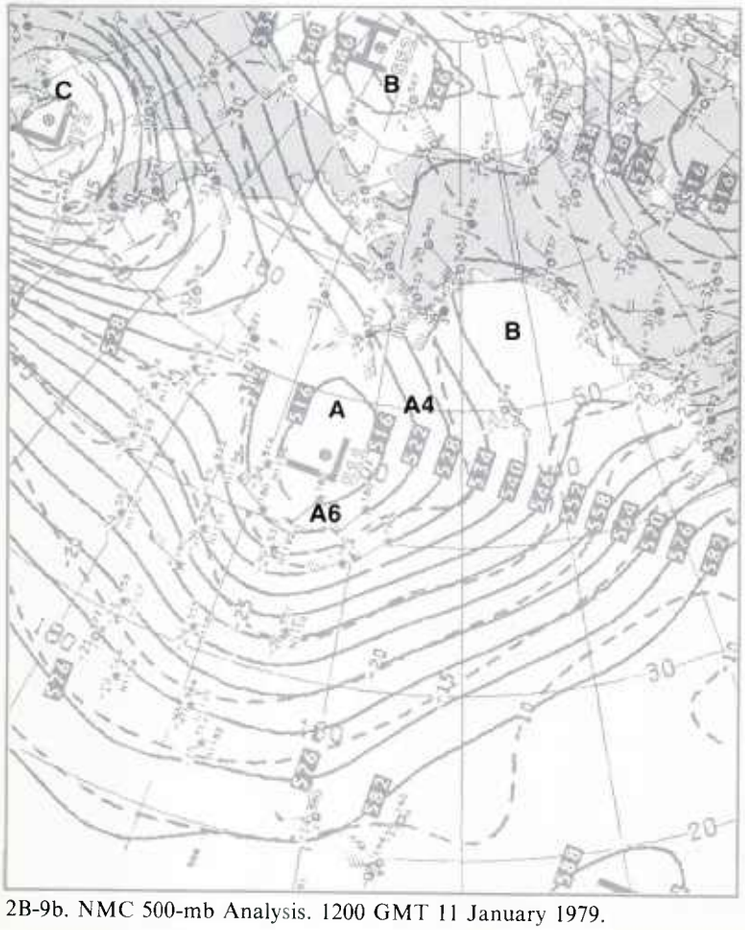

2B-9b. NMC 500-mb Analysis. 1200 GMT 11 January 1979.

surface

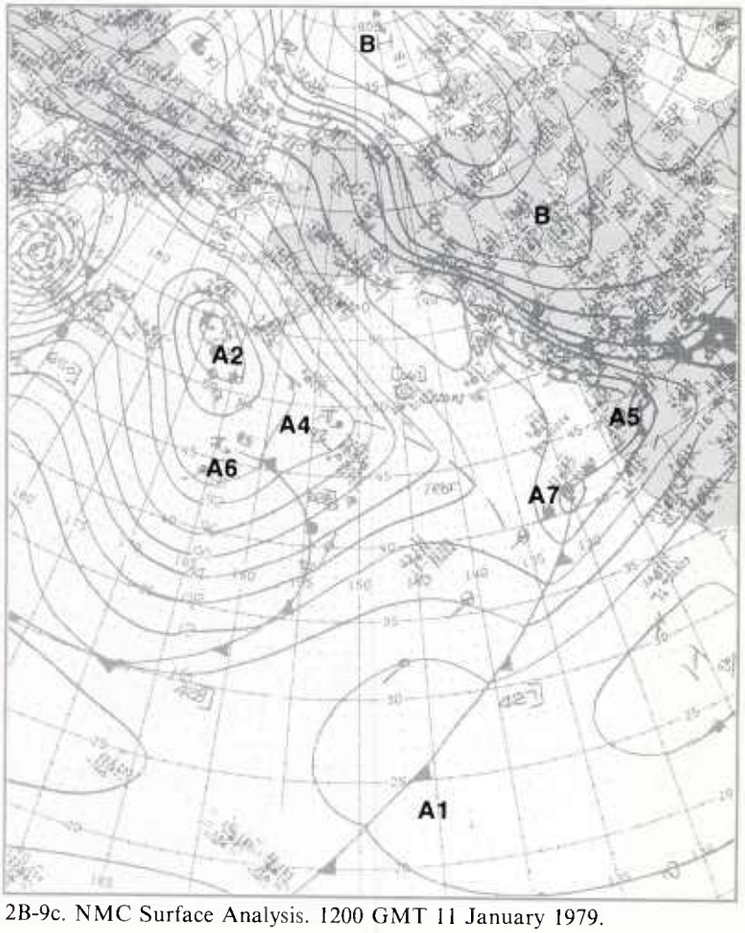

2B-9c. NMC Surface Analysis. 1200 GMT 11 January 1979.

12-13 January

A comparison of the 500-mb analysis (2B-10b) and the 500-mb analysis 72 hours earlier (2B-2b) shows that the low **A**, upstream of the block along the west coast of North America, has advanced eastward as forecast. It is an intense, closed low instead of an open trough due to the cold air advection associated with the strong polar jet stream **PJS** at 300 mb (2B-10a) digging southward along the southern periphery of the deep low **C**. At 300 mb, there is also a strong (140 kt) jet stream extending across the eastern Pacific into the Pacific Northwest, where the mid-latitude block **B–B** was located 72 hours earlier.

In the satellite picture at 0015 GMT 12 January (2B-11a), the baroclinic zone **A1–A1** has intensified and extends in a broad band across the eastern Pacific. This baroclinic zone developed with the earlier storm **A1** (2B-3a) that moved eastward and dissipated over North America. The cirrus band has a very distinct poleward edge along its entire length which identifies the location of the strong polar jet stream at 300 mb.

The trailing comma tail from the cloud vortex **A6** has almost merged with the baroclinic zone to the south. Notice the slight anticyclonic curvature and the bright, white density of the cirrus deck **AA** where the tail is nearest the baroclinic zone—this indicates an area of enhanced vertical motions and the potential for wave development on the baroclinic zone. However, the area is located in the left rear quadrant of the 300-mb polar jet streak **PJS-1**, which is a zone of subsidence at upper levels, so that wave development is not favorable at this time.

The surface analysis (2B-11b) shows a deep low **A6** and a front which connects to the new frontal system **C1** moving into the central Pacific at high latitudes. The position of the short-wave disturbance associated with the low **A6** is indicated by the trough line (TROF). The location of the front **A1–A1** in the center of the subtropical high **B1** suggests that it is very weak at the surface; any new cyclogenetic activity associated with the disturbance **A6** will, therefore, be initiated along the baroclinic zone aloft (identified by the cirrus cloud band **A1–A1** in the satellite picture).

During the following 36-hour period, the 500-mb low **A** is forecast to advance eastward (2B-11c), passing to the south of the high-latitude block **B**. Strong meridional flow will continue upstream and downstream of the low, and southerly flow ahead of the trough will produce warm air advection and a buildup of the subtropical high **B2**. In 72 hours (2B-11d), the low **A** is forecast to deepen as it moves to the east of the high-latitude block **B**. However, the base of the meridional trough will lag behind, resulting in a southwest to northeast oriented trough.

In the satellite picture (2B-12a), the tail of the vorticity comma **A6** has merged with the baroclinic zone **A1–A1**. During the same period, the baroclinic zone cirrus deck **AA** has increased in amplitude and appears as a single, pronounced anticyclonically curved arch extending over the eastern Pacific. Note that the inflection point (where the curvature of the cirrus deck changes from cyclonic to anticyclonic) is well to the southwest of the intersection of the vorticity comma **A6** and the cirrus deck **AA**. This is the location of any potential new wave development along the baroclinic zone.

At 500 mb (2B-12b), the subtropical high **B2** has amplified rapidly northward ahead of the low **A**, which shows a pronounced meridional trough extending to the south. On the surface analysis (2B-12c), the track of the deep low **A6** is turning to the north, in response to the building ridge **B2** aloft; and the old surface front **A1** also shows a bend to the north along the western portion.

The satellite picture (2B-13a), 24 hours into the forecast period, shows that the baroclinic zone cirrus arch **AA** has increased further in amplitude. The inflection point to the southwest is barely noticeable along the poleward boundary of the cirrus deck; however, the short-wave disturbance indicated by the inflection point is moving northeastward—this is the first indication of the formation of cyclogenesis Event No. 3 in the low **A** at 500 mb.

The 500-mb analysis (2B-13b) shows that the trough to the south of the low **A** is beginning to lag behind as the main center advances to the east. The low **A6** at the surface (2B-13c) has deepened and is forced to move on a continued northeasterly track due to the building of the surface high **B2**, in advance of the low and the sharp ridge at 500 mb.

Since it appears that cyclogenesis Event No. 3 is in the formative stage, it is appropriate to examine the FNOC 36-hour 500-mb prognosis (2B-13d) for guidance on the upper-air pattern to be expected with the development. A comparison of this prognosis with the earlier 72-hour forecast (2B-11d), valid 12 hours later, indicates a significant change in the forecast flow pattern of the low **A**. Instead of a weak ridge upstream, the 36-hour prognosis (2B-13d) shows a pronounced ridge over the eastern Pacific which suggests a significant winter storm development in the upper low **A**. This is confirmed by the FNOC 36-hour surface prognosis (2B-13e) which displays a large, moderately deep surface low **A** over the Pacific Northwest. It is instructive to follow the evolution of this disturbance in the satellite imagery which follows.

The 500-mb trough extending to the southwest from the low **A** (2B-14b) is showing the characteristics of a meridional trough; at 300 mb (2B-14a) there is a strong (120 kt) polar jet streak **PJS-1** located in the southwest flow ahead of the trough; and, in the satellite picture (2B-15a), the inflection point on the poleward side of the baroclinic cirrus arch **AA** is located precisely in the left front quadrant of this jet streak—a most favorable position for rapid cyclogenesis to be initiated.

The cloud vortex **A6** shows the mature stage of development, with several enhanced areas of convection (potential vorticity comma developments) in the circulation around the low. The weakening center at the surface (2B-15b, as compared to 2B-13c) indicates that this disturbance is beginning to dissipate.

12-13 January continued on page 2B-16

300 mb

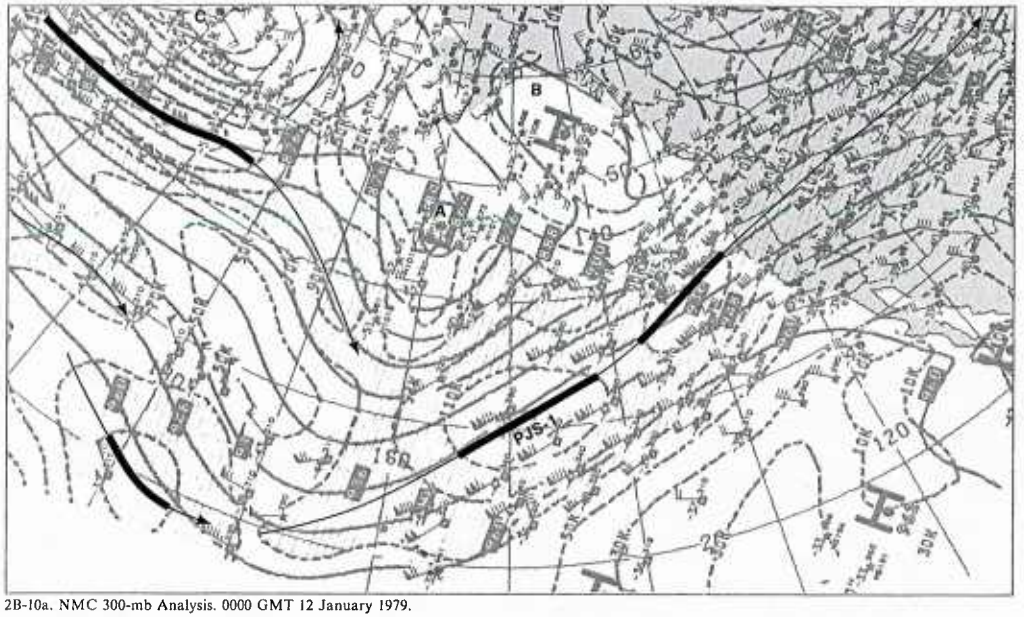

2B-10a. NMC 300-mb Analysis. 0000 GMT 12 January 1979.

500 mb

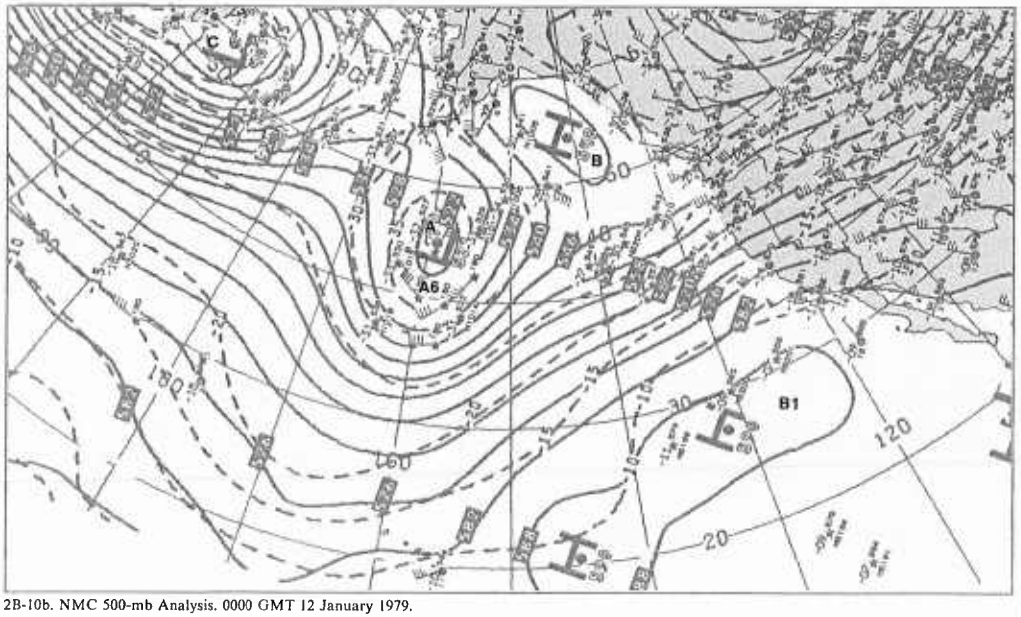

2B-10b. NMC 500-mb Analysis. 0000 GMT 12 January 1979.

Cyclogenesis in a Progressive Meridional Trough

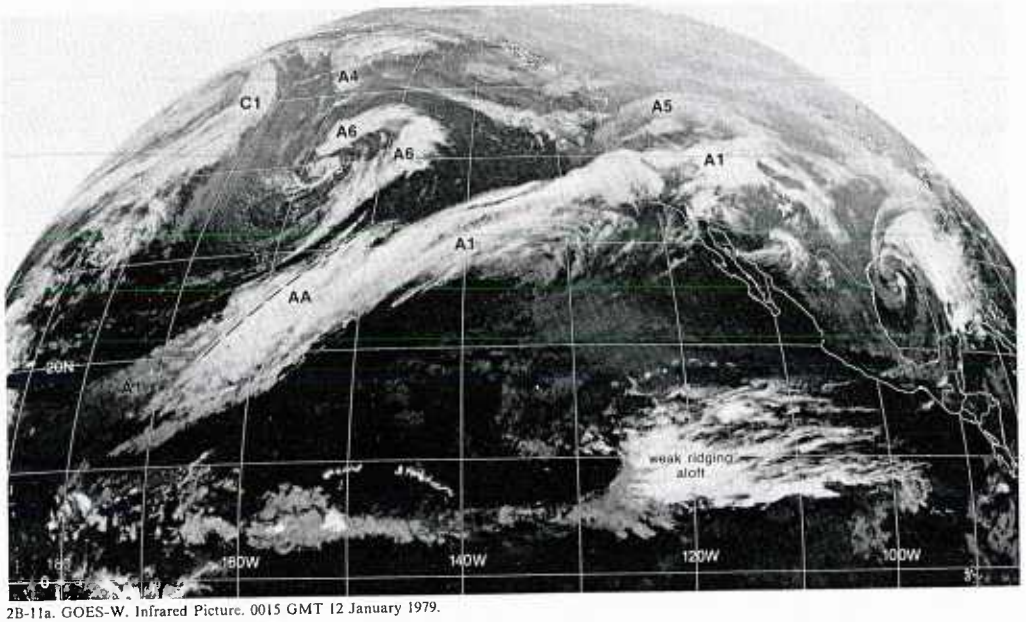

2B-11a. GOES-W. Infrared Picture. 0015 GMT 12 January 1979.

surface

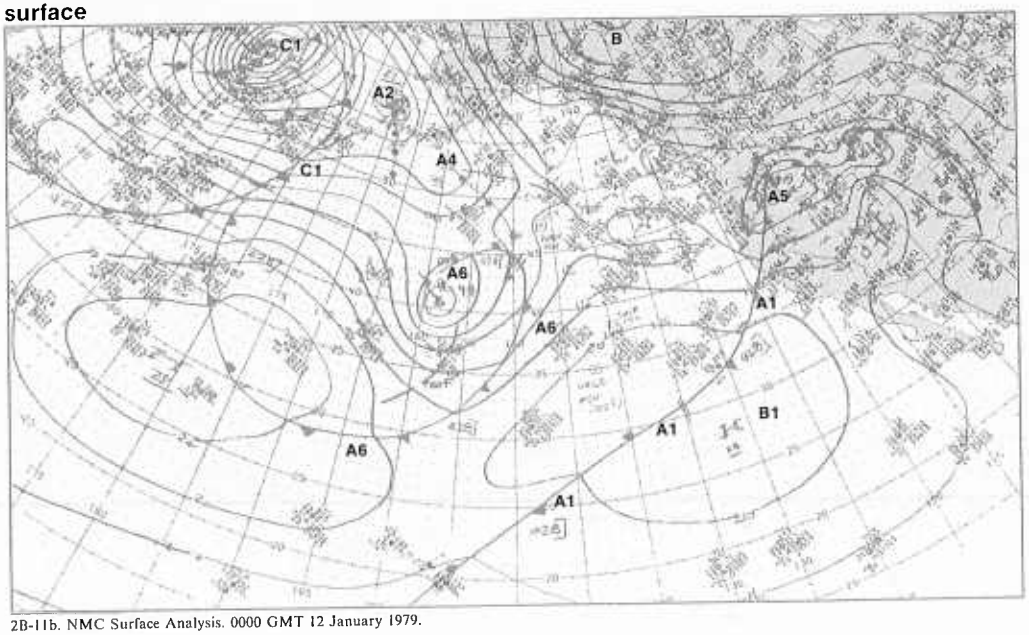

2B-11b. NMC Surface Analysis. 0000 GMT 12 January 1979.

500 mb

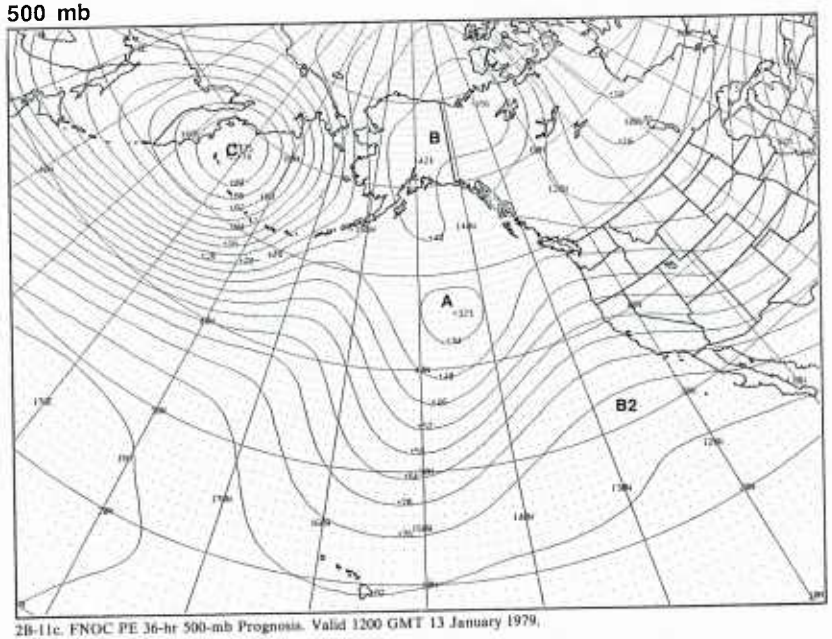

2B-11c. FNOC PE 36-hr 500-mb Prognosis. Valid 1200 GMT 13 January 1979.

500 mb

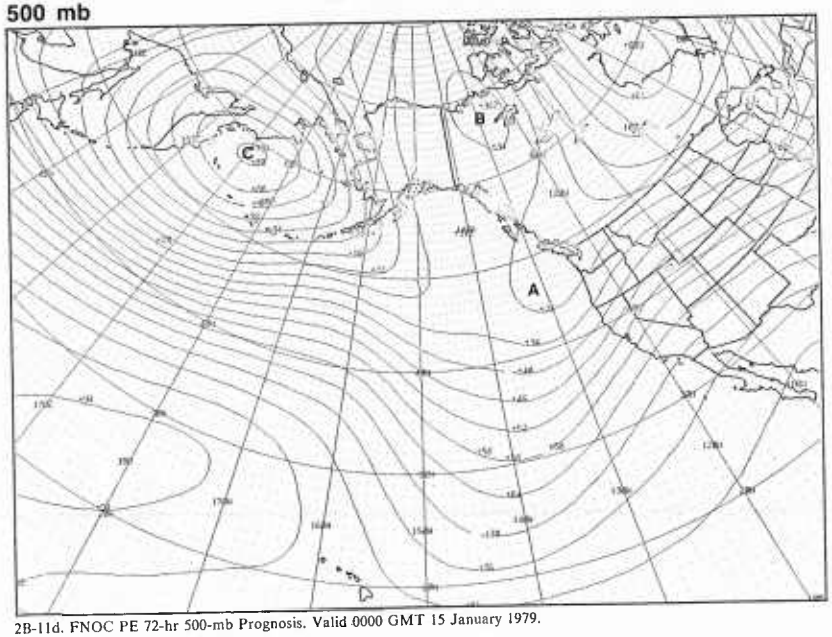

2B-11d. FNOC PE 72-hr 500-mb Prognosis. Valid 0000 GMT 15 January 1979.

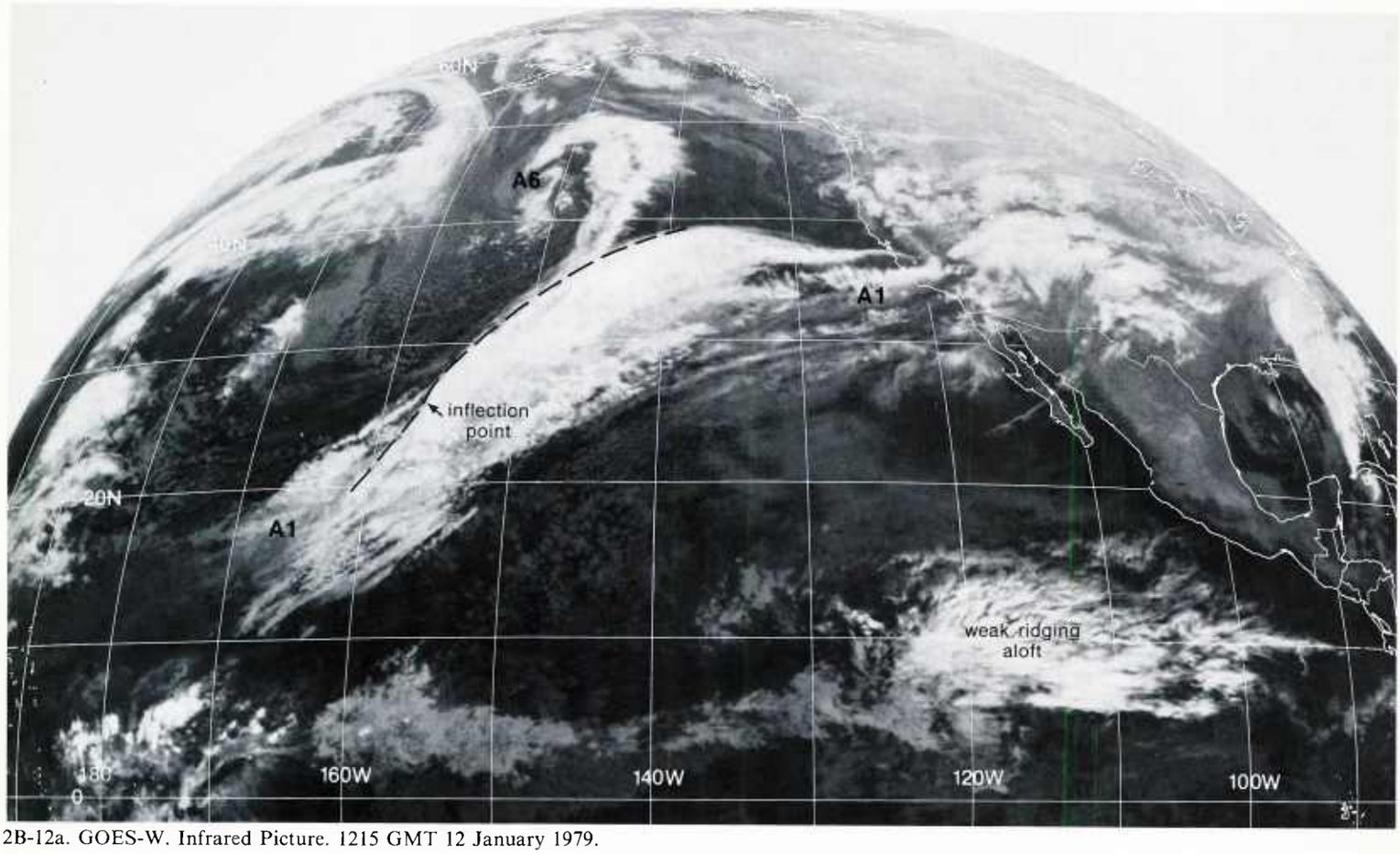

2B-12a. GOES-W. Infrared Picture. 1215 GMT 12 January 1979.

500 mb

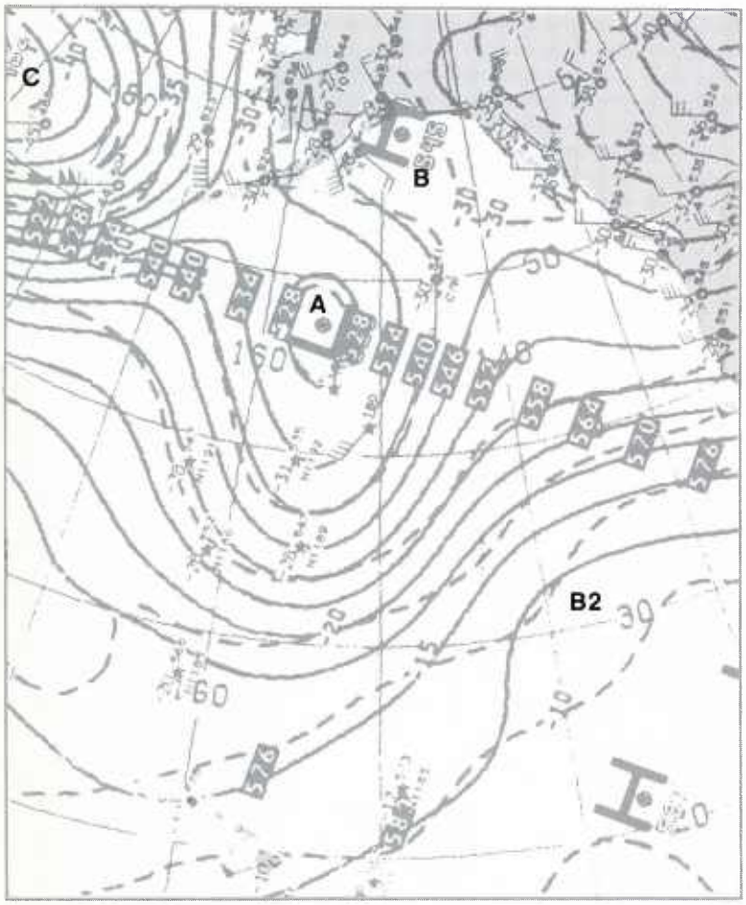

2B-12b. NMC 500-mb Analysis. 1200 GMT 12 January 1979.

surface

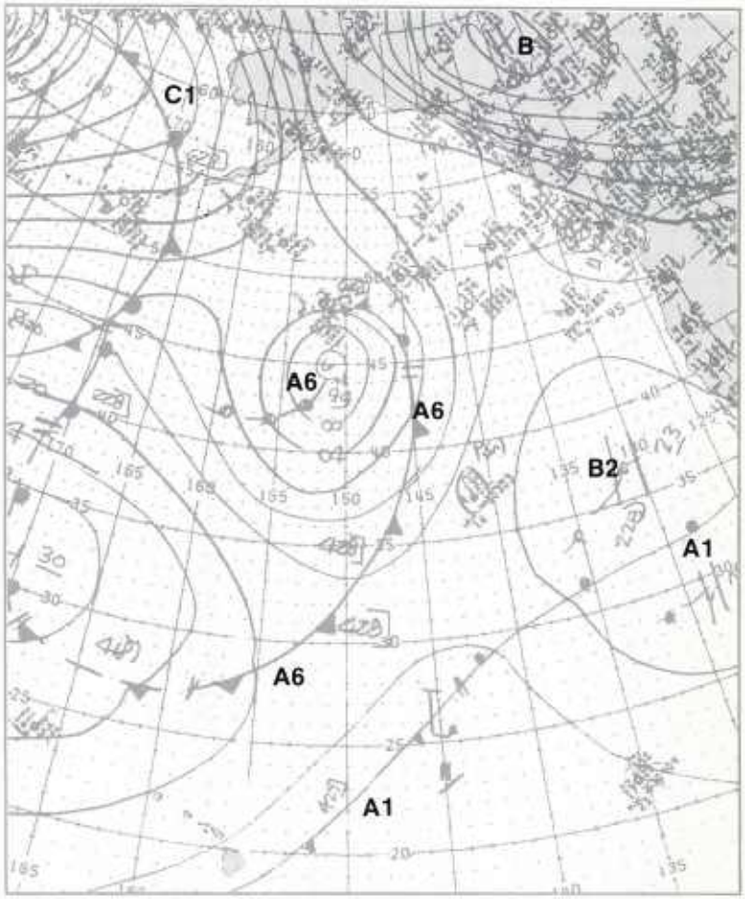

2B-12c. NMC Surface Analysis. 1200 GMT 12 January 1979.

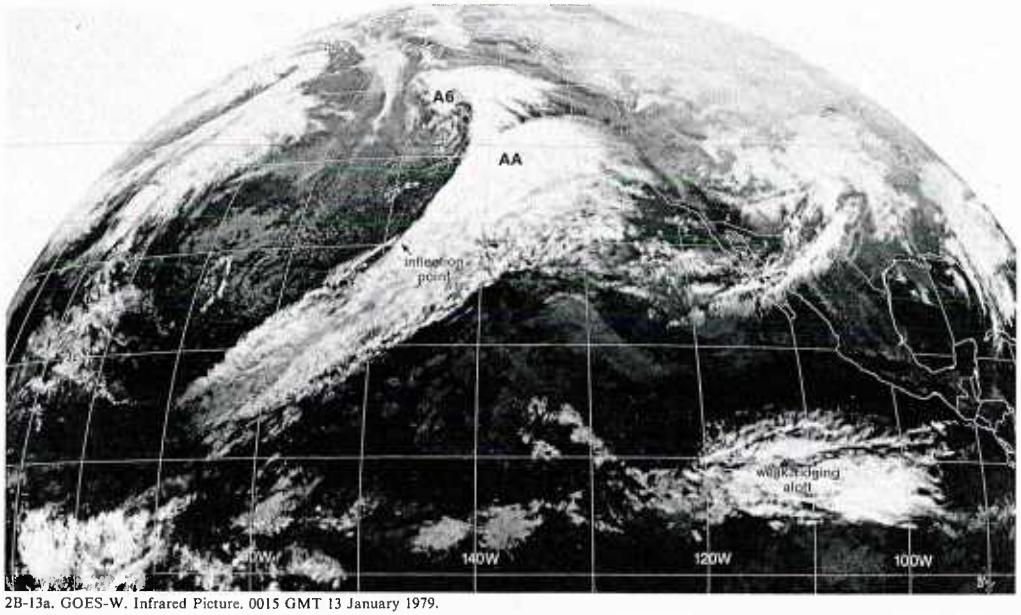

2B-13a. GOES-W. Infrared Picture. 0015 GMT 13 January 1979.

500 mb

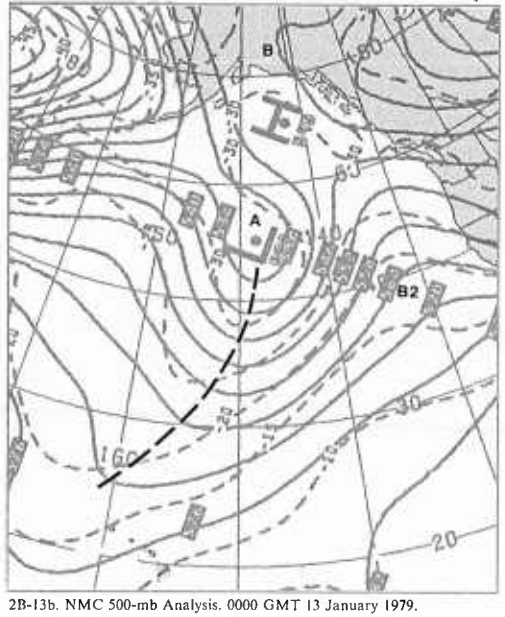

2B-13b. NMC 500-mb Analysis. 0000 GMT 13 January 1979.

surface

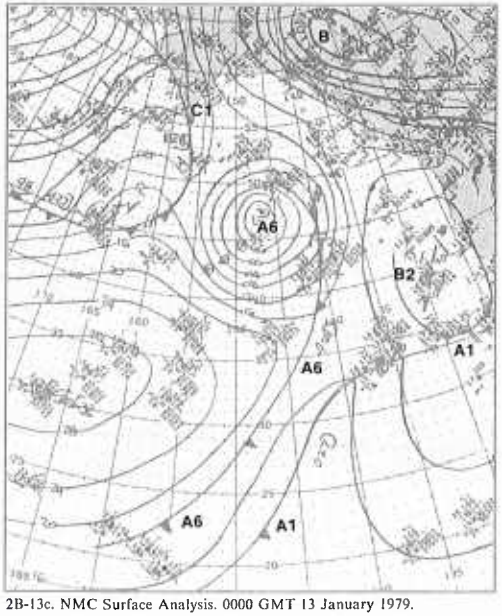

2B-13c. NMC Surface Analysis. 0000 GMT 13 January 1979.

500 mb

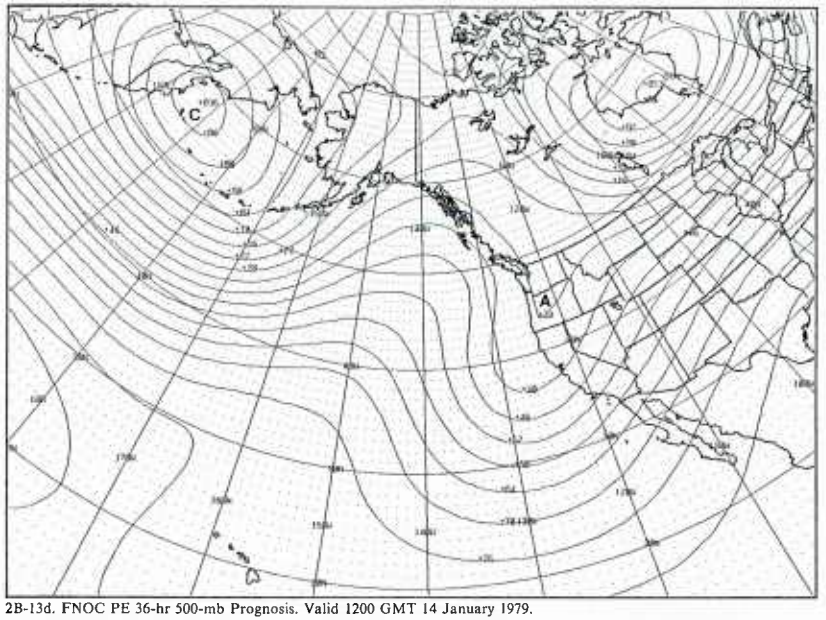

2B-13d. FNOC PE 36-hr 500-mb Prognosis. Valid 1200 GMT 14 January 1979.

surface

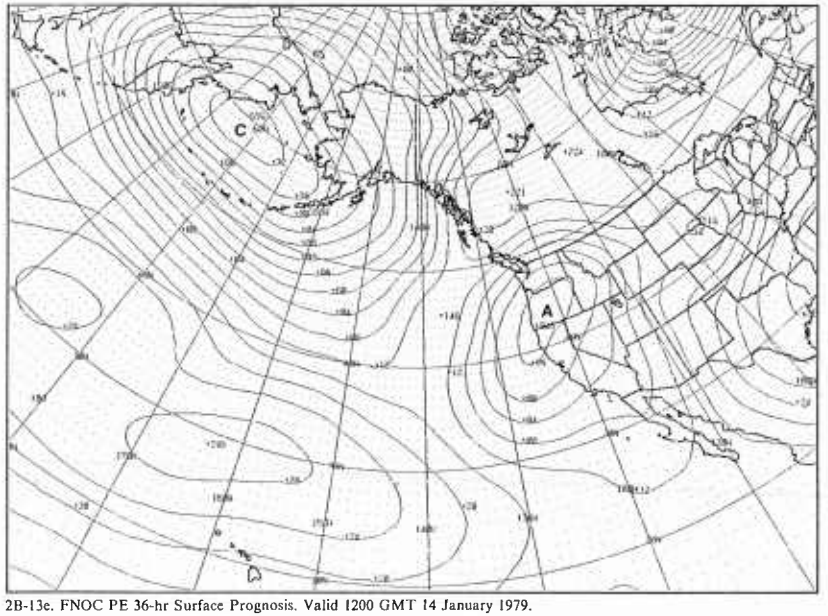

2B-13e. FNOC PE 36-hr Surface Prognosis. Valid 1200 GMT 14 January 1979.

300 mb

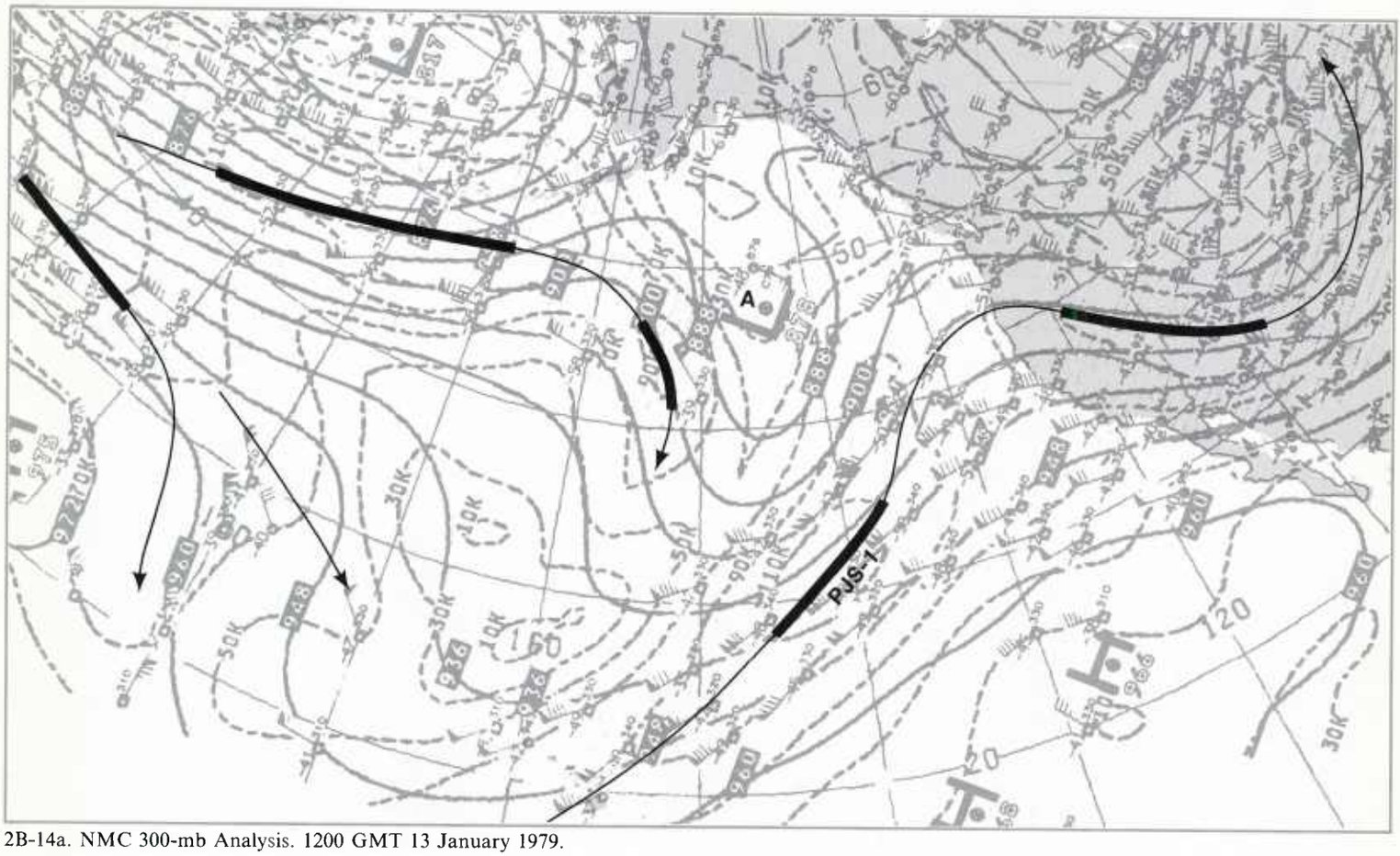

2B-14a. NMC 300-mb Analysis. 1200 GMT 13 January 1979.

500 mb

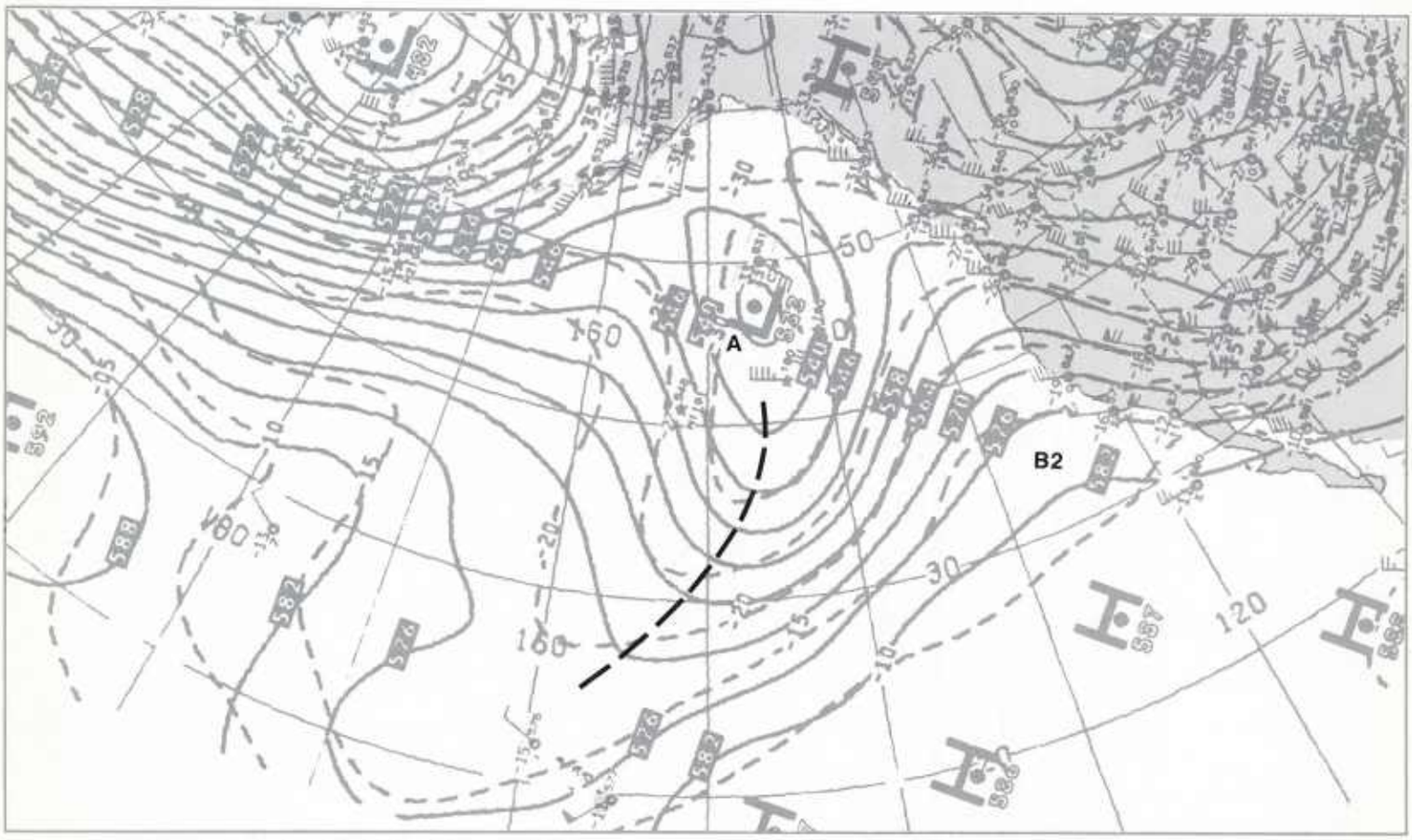

2B-14b. NMC 500-mb Analysis. 1200 GMT 13 January 1979.

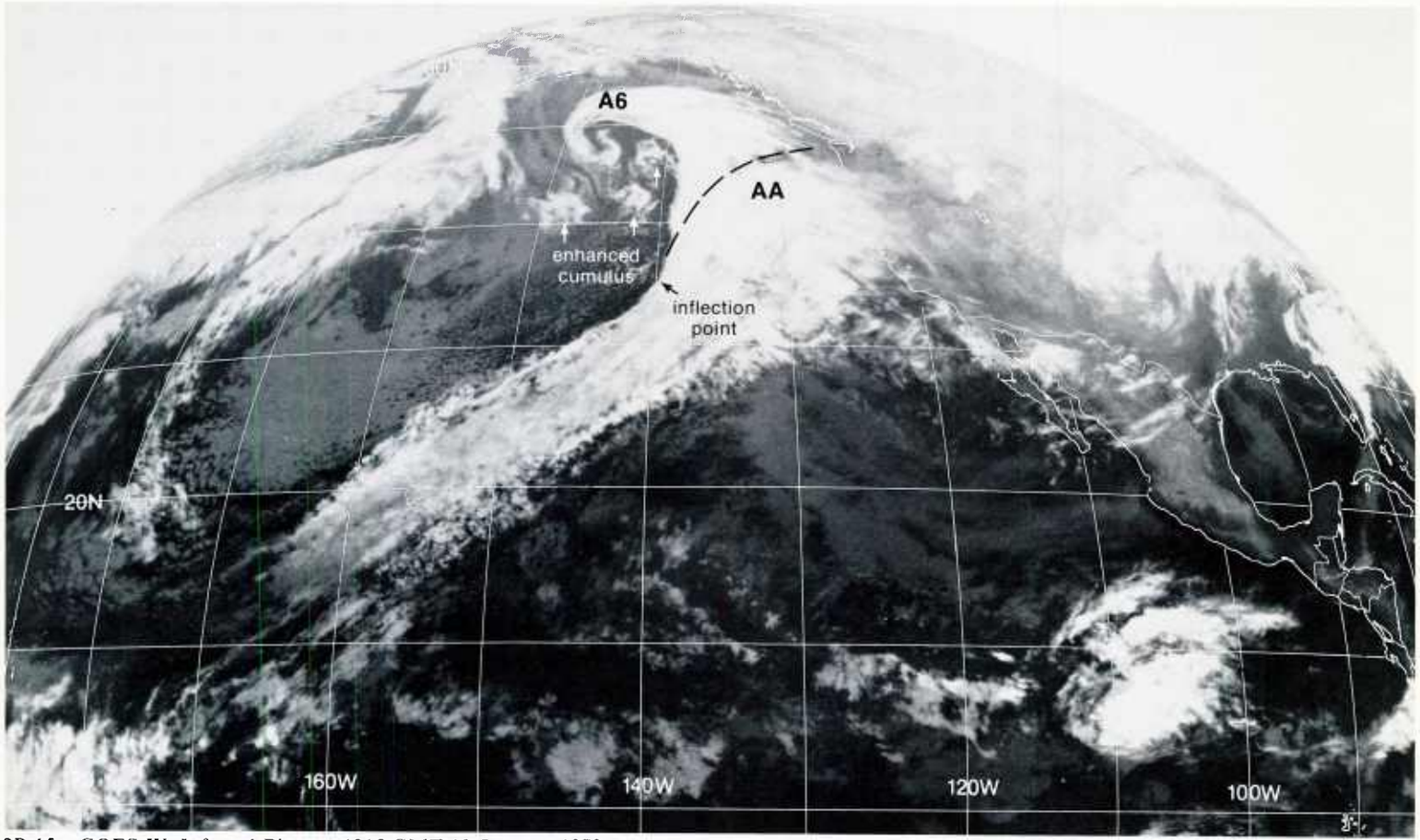

2B-15a. GOES-W. Infrared Picture. 1215 GMT 13 January 1979.

surface

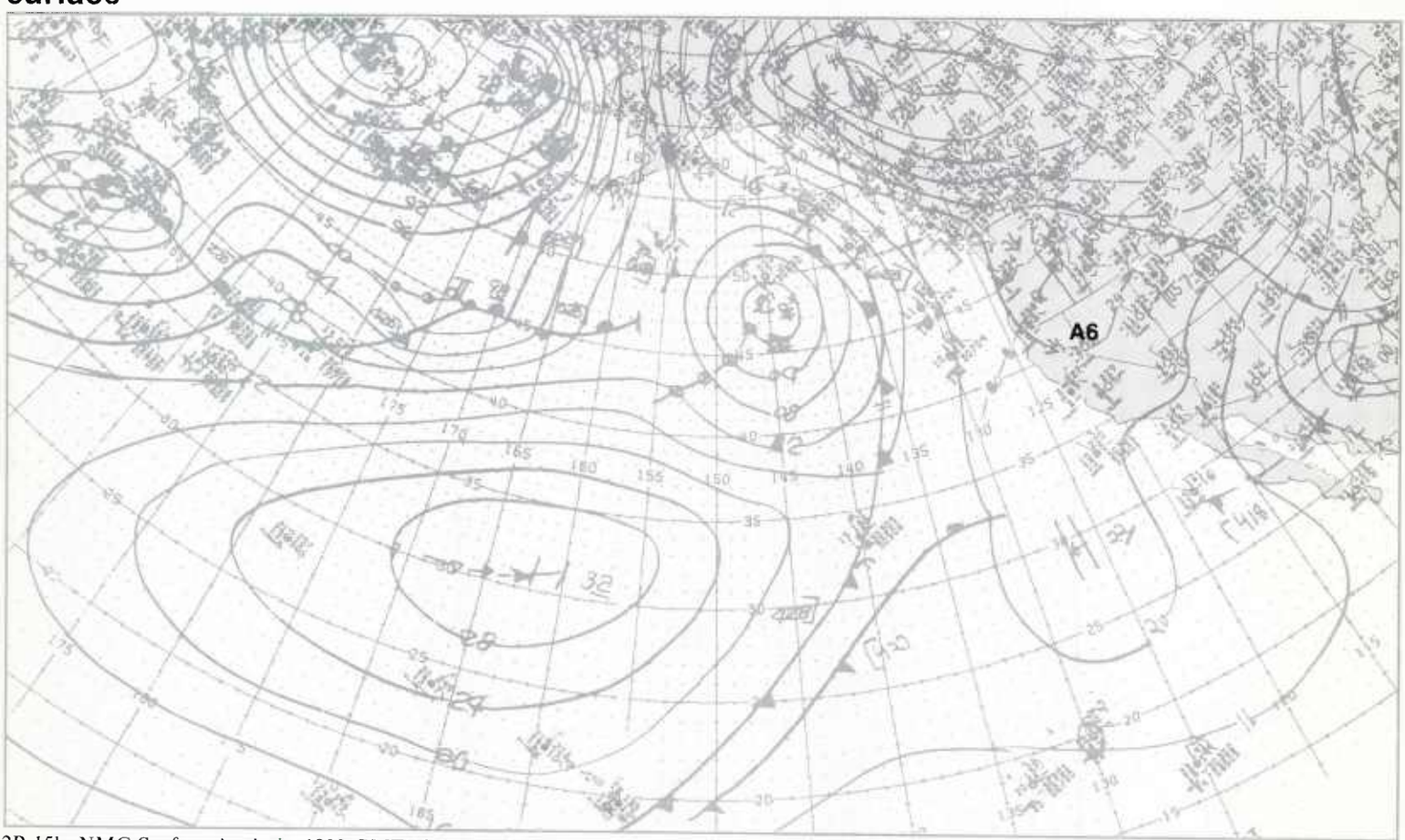

2B-15b. NMC Surface Analysis. 1200 GMT 13 January 1979.

A review of the evolution of the cold air cyclogenesis Event No. 2 shows the following: The vorticity comma **A6** advances around the base of the 500-mb low **A** (2B-8b, 9b, and 10b). It is caught in the strong southerly flow ahead of the 500-mb low **A** (2B-12b) and is steered to the north (2B-13b and 14b). During this time, the vorticity comma **A6** merges with the old baroclinic zone **A1-A1** (2B-12a and 13a) and development of the surface low **A6** accelerates (2B-13c); however, the storm is short lived since the surface low **A6** weakens rapidly (2B-15b) even as the vorticity comma displays the mature spiral vortex pattern (2B-15a). The old baroclinic zone **A1-A1** (2B-11a) is being reinforced with a pronounced cirrus arch **AA** (2B-15a) developing in the southwesterly flow ahead of the meridional trough extending to the south of the 500-mb low **A** (2B-14b). This evolutionary process (vorticity comma merging with an old baroclinic zone, intensifying to a mature spiral vortex, and forming a new baroclinic zone) identifies this disturbance as a Type 3B cold air cyclogenesis, according to Weldon's classification (see 2A Introduction).

The development of cyclogenesis Event No. 3 is clearly revealed in the following sequence of GOES-West infrared imagery at 2-hour intervals. At 1815 GMT (2B-16a), the distinct cloud bulge **A7** into the cold air identifies the incipient short wave. The wave is located near the inflection point along the baroclinic zone cirrus where the curvature changes from cyclonic to anticyclonic over the cirrus deck **AA**. A clear slot is just beginning to appear between the wave and the baroclinic zone cirrus. The disturbance continues to develop (2B-17a) and, by 2215 GMT (2B-17b), a comma head has emerged to the west of the baroclinic zone cirrus deck **AA**.

In contrast to the developing wave **A7**, the vortex **A6** has lost most of its spiral cloud pattern (2B-16a), and shows no signs of further intensification (2B-17a and 17b). At the surface (2B-16b), there is only a weak low **A6** which has also continued to fill in. Instability is evident at upper levels, however, and, in the satellite picture at 1815 GMT (2B-16a), one of the enhanced areas of convection **VC** displays a typical vorticity comma cloud pattern. This vorticity comma is the remnant breakaway from **A6** (see 2B-15a). This is how new frontal systems sometimes form—from breakoffs of old occluded centers—and they represent a new understanding of cyclogenesis based on satellite data which differs in many ways from classical concepts.

continued on page 2B-18

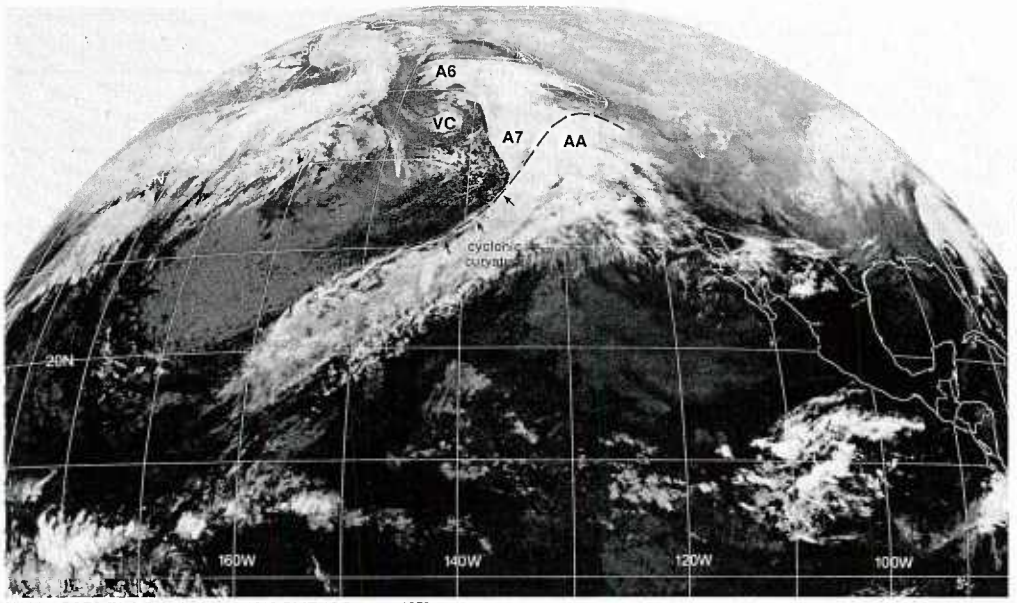

2B-16a. GOES-W. Infrared Picture. 1815 GMT 13 January 1979.

surface

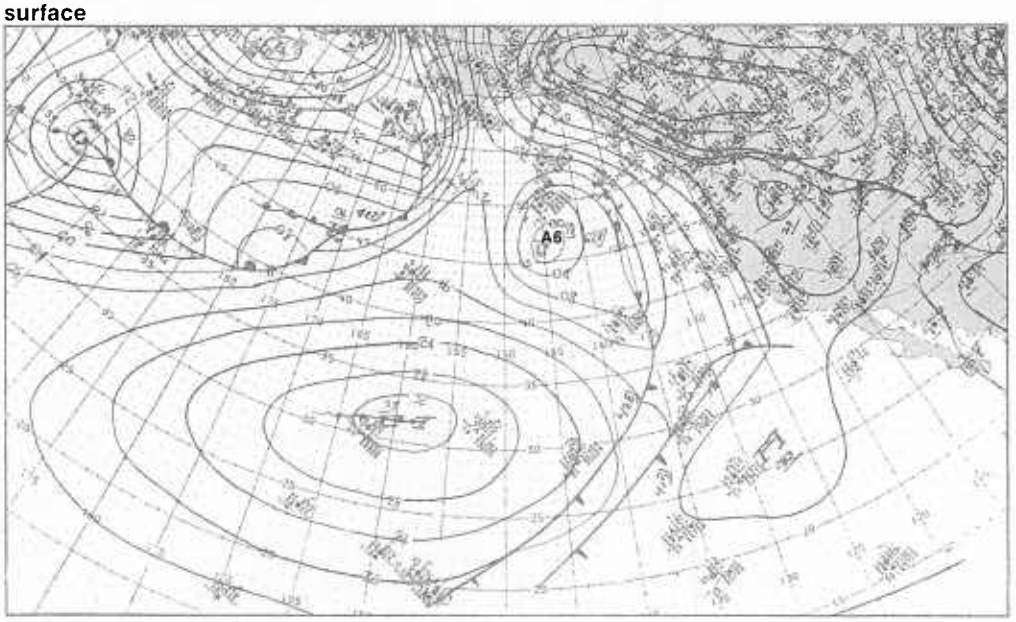

2B-16b. NMC Surface Analysis. 1800 GMT 13 January 1979

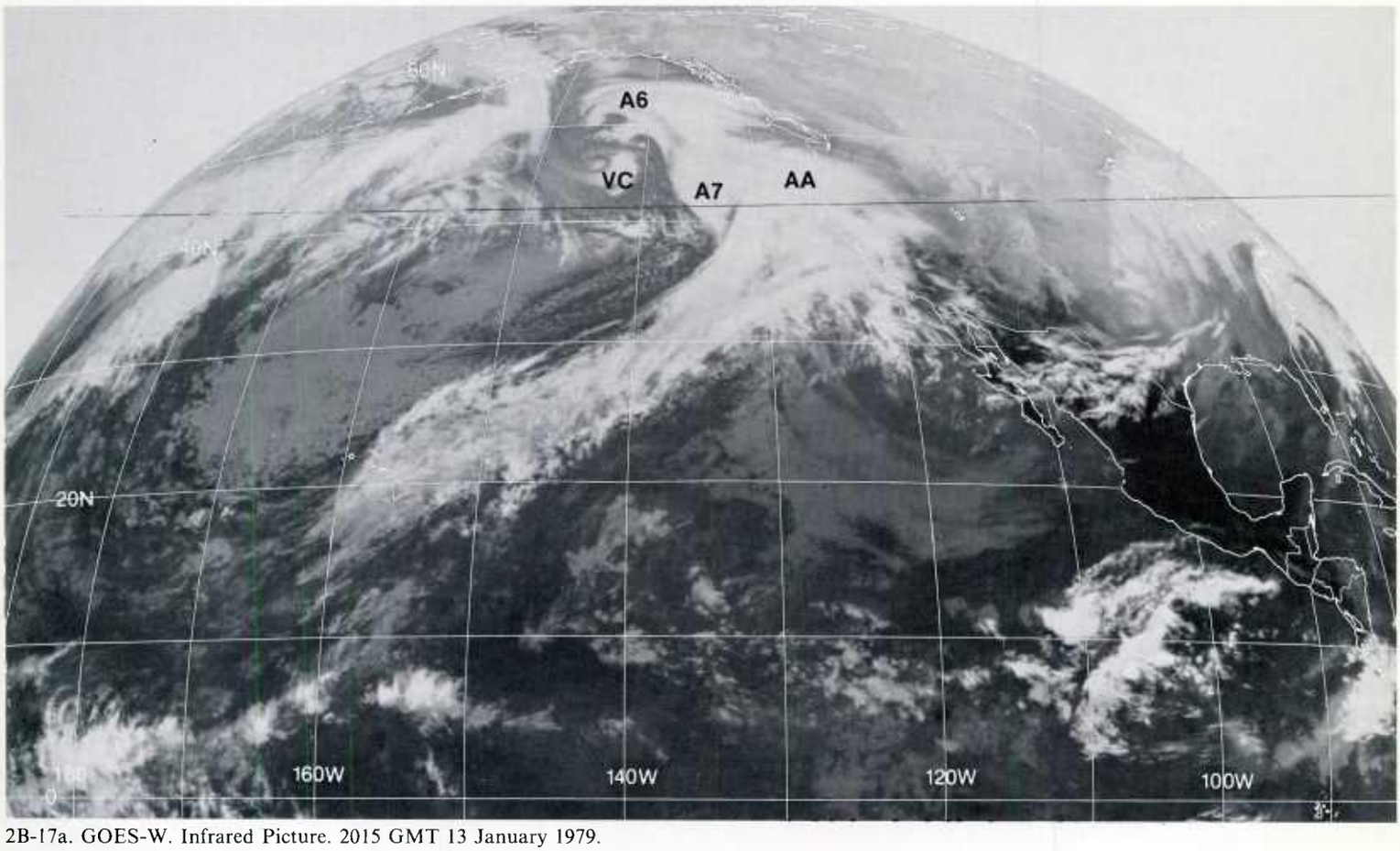

2B-17a. GOES-W. Infrared Picture. 2015 GMT 13 January 1979.

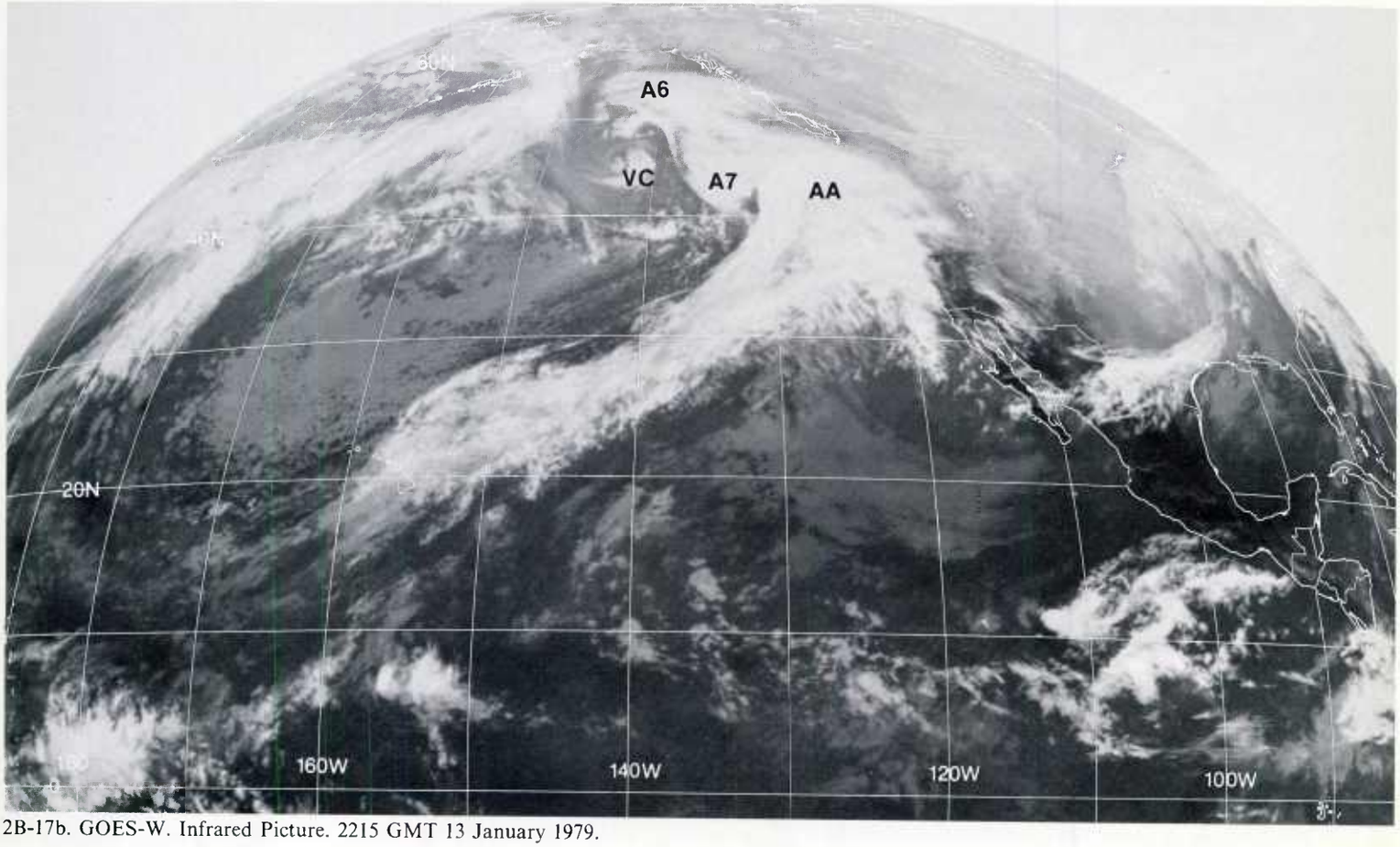

2B-17b. GOES-W. Infrared Picture. 2215 GMT 13 January 1979.

14 January

In the GOES-West infrared picture at 0015 GMT (2B-19a), a well-defined comma pattern **A7** is visible to the northwest of the cirrus deck **AA**. At this stage, a surface low is located in the clear area of the tight cloud spiral at the tip of the comma; the surface analysis (2B-19b) shows a 990-mb closed low at this location. A comparison of the configuration of the comma pattern **A7** and the cloud patterns used for estimating surface pressures of developing mid-latitude winter storms (see NTAG Vol. 3, Sec. 3A, Cyclogenesis) indicates a surface pressure of about 990 mb, as depicted on the surface analysis. This development has occurred in just six hours. The wave **A7** was first identified in the satellite imagery at 1800 GMT (2B-16a) when it was located in an elongated trough extending from the weak surface low **A6** (2B-16b).

An examination of the storm **A7** in relation to the upper-level flow field shows that it is in the left front quadrant of the polar jet streak **PJS-1**, on the east side of the low **A** at 300 mb (2B-18a). This polar jet streak was observed on the east side of the low **A** at 0000 GMT 12 January (2B-10a) and at 1200 GMT 13 January (2B-14a). The conditions favorable for cyclogenesis in the area are now emphasized. At 500 mb (2B-18b), the closely-spaced height contour lines on the west side of the low **A** indicate strong cold air advection which should further intensify the storm **A7**. In the satellite picture (2B-19a), there is an area of enhanced convection **EC** and the vorticity comma **VC** (remnant of the breakaway from **A6**) in the polar air stream behind the 500-mb low **A**.

By 1200 GMT 14 January, rapid deepening has occurred at the surface (2B-21b), where the surface pressure in the low **A7** has dropped about 10 mb in six hours. The tight, spiral cloud pattern of this storm indicates that the surface pressure should be about 970 mb, based on the technique of surface pressure estimates from cloud patterns (see NTAG Vol. 3, Sec. 3B, Cyclogenesis). This classifies the storm as an "explosive" cyclogenesis event (pressure fall of at least 1 mb/hr), according to Sanders (1980). The low **A** has also intensified aloft, with strong closed lows at 300 mb (2B-20a) and 500 mb (2B-20b).

The satellite picture at 1215 GMT (2B-21a) shows a spectacular closed spiral cloud vortex **A7**, which has developed from the comma cloud pattern 12 hours earlier (2B-19a). The poleward edge of the cirrus deck **AA** identifies the location of the polar jet streak **PJS-1**, as it curves anticyclonically over the storm.

As indicated on the 500-mb numerical guidance chart (2B-13d), a significant upper-air low **A** was forecast off the Pacific Northwest, with a moderately deep surface low. The 500-mb low **A** intensified, as forecast; however, as shown on the surface analysis (2B-21b), explosive cyclogenesis occurred at the surface. From a forecast viewpoint, it is important to note that the surface low **A6** (2B-12c) did not deepen, but a disturbance that formed well to the south on the old baroclinic zone **A1–A1** (2B-12a) was the origin of the explosive cyclogenesis event over the eastern Pacific. This development occurred because the disturbance occupied the most favorable location for cyclogenesis—the left front quadrant of the newly formed polar jet streak **PJS-1** at 300 mb (2B-13b).

Weldon classifies winter storm cyclogenesis into three basic types based on satellite infrared imagery and the jet stream configuration at 300 mb: (1) Meridional trough or baroclinic zone cyclogenesis; (2) Split flow cyclogenesis; and (3) Cold air regime cyclogenesis. It is interesting to note that the three cyclogenesis events occurred in the same progressive 500-mb low A, as it advanced on an easterly track from the central Pacific to the U.S. West Coast. Without satellite imagery at frequent time intervals, it would have been difficult to identify and classify these storms, especially over the conventional data-void region of the eastern Pacific.

Important Conclusions

1. Successive cyclogenesis events can occur in a progressive 500-mb low over the eastern Pacific—each going through a full life cycle: initiation, maturity, and dissipation. These events are produced by short-wave disturbances moving in the flow field of the 500-mb low, and are associated with the polar jet stream.

2. Numerical guidance products (500 mb and surface) are useful for tracking the progressive 500-mb low, and satellite imagery can provide details on the initiation and development of the cyclogenesis events.

3. Cloud forms are specified for each type of development which are useful for identifying precursor winter storm cyclogenesis conditions in satellite imagery.

Reference

Sanders, F., and J. R. Gyakum, 1980: Synoptic-dynamic climatology of the "Bomb". *Mon. Wea. Rev.*, **108**, 1589-1606.

300 mb

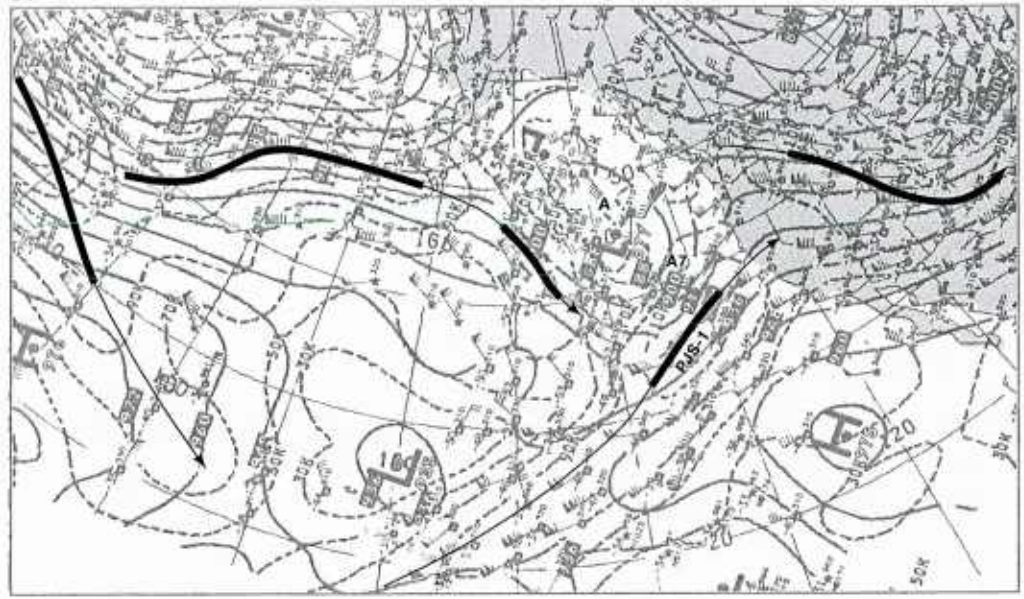

2B-18a. NMC 300-mb Analysis. 0000 GMT 14 January 1979.

500 mb

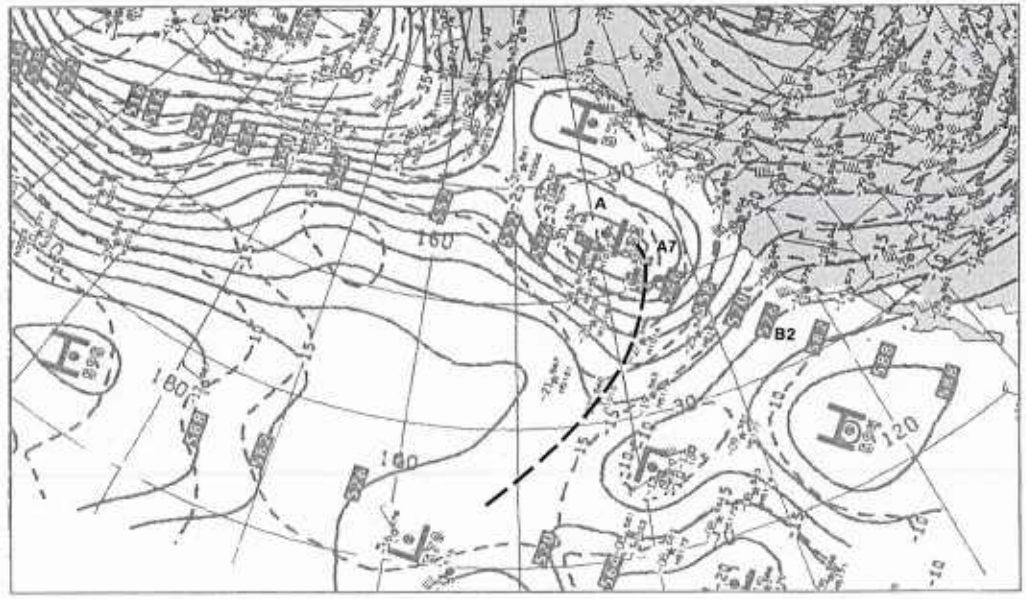

2B-18b. NMC 500-mb Analysis. 0000 GMT 14 January 1979.

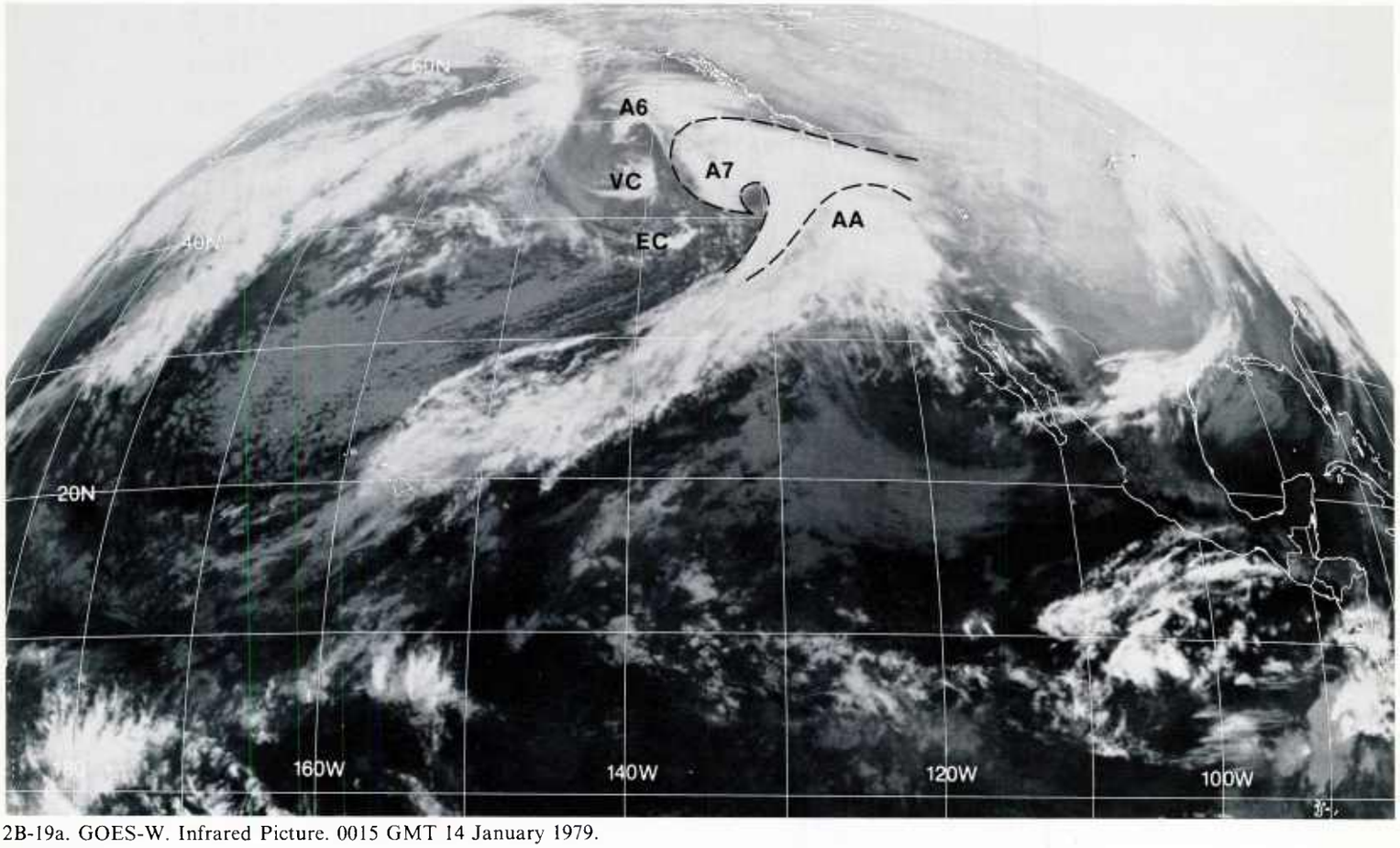

2B-19a. GOES-W. Infrared Picture. 0015 GMT 14 January 1979.

surface

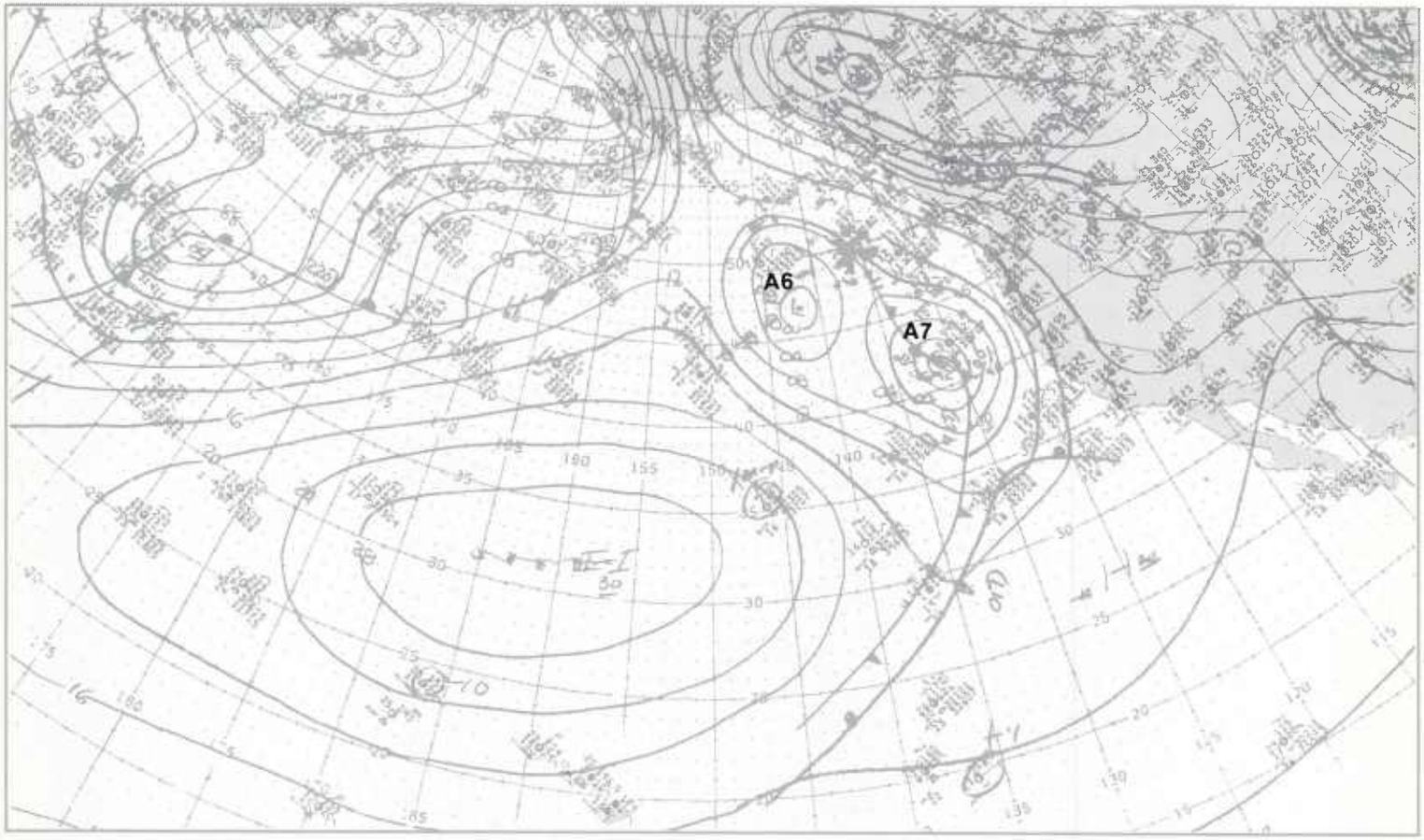

2B-19b. NMC Surface Analysis. 0000 GMT 14 January 1979.

300 mb

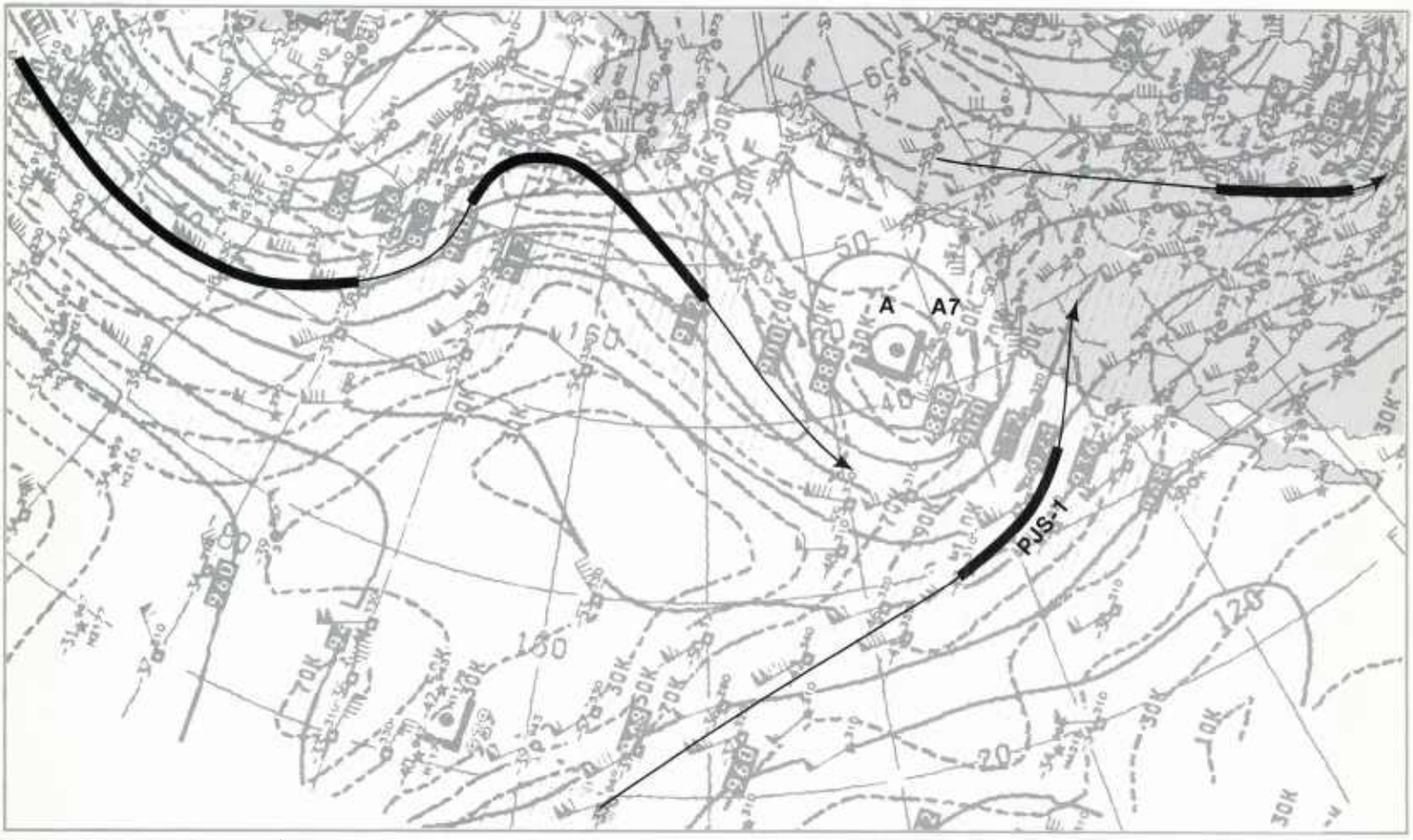

2B-20a. NMC 300-mb Analysis. 1200 GMT 14 January 1979.

500 mb

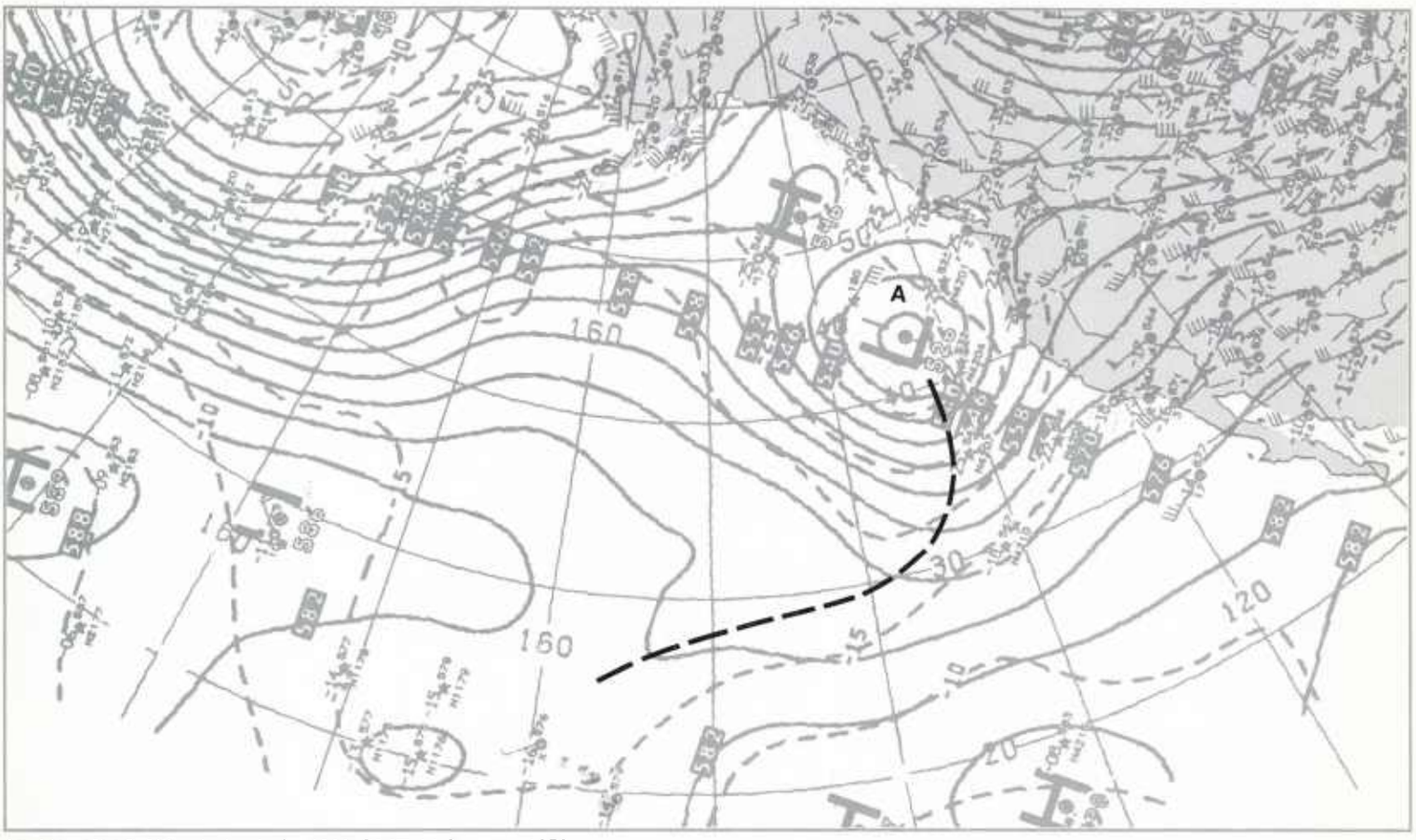

2B-20b. NMC 500-mb Analysis. 1200 GMT 14 January 1979.

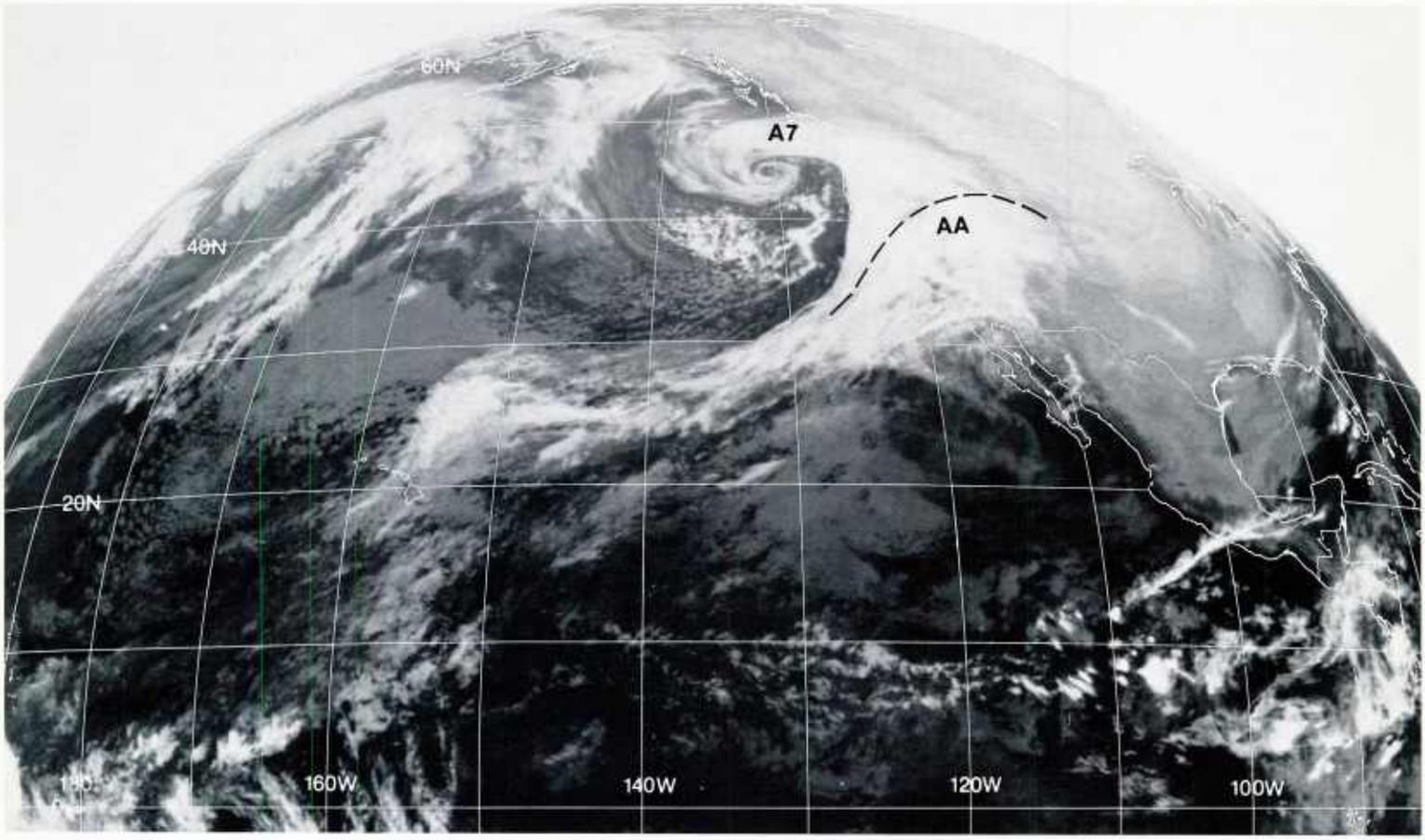

2B-21a. GOES-W. Infrared Picture. 1215 GMT 14 January 1979.

surface

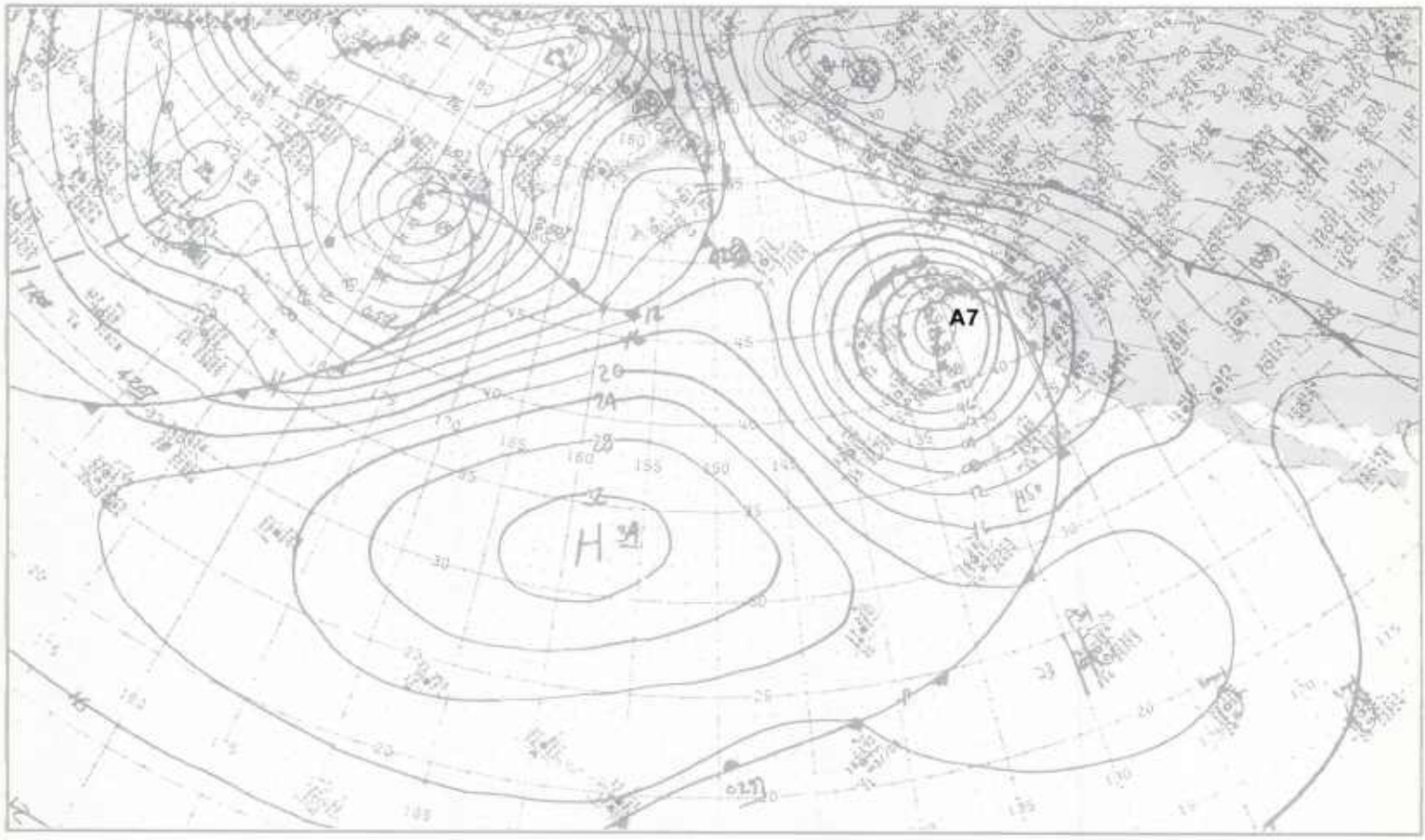

2B-21b. NMC Surface Analysis. 1200 GMT 14 January 1979.

Case 2 Cyclogenesis

The Identification of the Tropical Upper-Tropospheric Trough (TUTT) in Water Vapor Imagery

Atmospheric sensing by satellites in the water vapor absorption band (5.7–7.1 micrometers) has generated a new dimension in detecting the formation, development, and dissipation of middle- and upper-tropospheric disturbances. Of particular interest are those disturbances which form in low latitudes over the oceans, near the boundary between the polar westerlies and the tropics. Sadler (1976) described how one such feature, the Tropical Upper-Tropospheric Trough (TUTT), can be an important outflow mechanism to the westerlies for the development of tropical cyclones. The TUTT is also associated with other weather developments and undoubtedly plays a key role in the general circulation of the atmosphere from a global perspective.

The particular value of water vapor imagery is that it reveals circulation features associated with the TUTT and other middle- and high-level circulations even when such features are not apparent in visible or infrared satellite imagery.

Reference

Sadler, James C., 1976: Tropical cyclone initiation by the Tropical Upper-Tropospheric Trough. NAVENVPREDRSCHFAC Tech. Paper 2-76.

In Sadler's (1972) mean mid-summer (July) positions of Northern Hemisphere ridges and troughs at 200 mb over the Pacific Ocean (2B-24a), two upper-level ridges are indicated with the southern one designated the subequatorial ridge and the northern one termed the subtropical ridge. The two upper-level ridges are separated by a trough which is termed the Tropical Upper-Tropospheric Trough (TUTT). This feature is sometimes also referred to as the Mid-Pacific Trough. In the mean, the mid-summer position of the TUTT extends from about 20° N in the western Pacific to about 45° N in the eastern Pacific. The alternating belts of westerly and easterly winds which result from the TUTT and upper-level ridges are the temperate westerlies, subtropical easterlies, subtropical westerlies, and the equatorial easterlies.

Sadler's mean Pacific 200-mb streamline and wind patterns for the month of August (2B-25a), with TUTT and ridge positions superimposed, show that the TUTT extends northeastward across the North Pacific to about 50° N. A confluent zone (subtropical westerlies) is located south of the TUTT extending to the U.S. West Coast. When this confluent zone is also characterized by upper-level convergence, subsidence, low-level divergence, and drying would be expected. At the trough line (TUTT), formation of cyclonic circulations is also likely.

26 August

The GOES-West infrared picture at 2345 GMT on 25 August (2B-26a) shows the following large-scale circulation features: (1) Hurricane Hilary; (2) A spiral cloud vortex **A** associated with an upper-level low **A** (2B-27b); (3) A disturbance **B** and frontal cloud band over the central Pacific; and (4) A large field of suppressed stratocumulus between Hawaii and the U.S. The NMC surface analysis for 0000 GMT 26 August (2B-26b) shows the locations of these features, including the large surface high pressure area **C** overlying the suppressed stratocumulus cloudiness over the eastern Pacific.

The GOES-W water vapor picture (2B-27a) shows some additional details not apparent in the infrared picture or the surface analysis. The outflow region of moisture (light gray shade) surrounding Hurricane Hilary is quite evident; a dry slot (dark gray shade) is very prominent extending from the area just north of Los Angeles southwest to the Hawaiian Islands; and there appears to be a wave development and possible vortex formation **D** north of the Hawaiian Islands. A protuberance of moisture **E** is also evident to the east-northeast of the apparent wave development. Neither the FNOC 200- or 500-mb analyses (2B-27c and 27d) provide information useful in explaining the presence of the dry slot, wave and vortex development, and moisture protuberance north of Hawaii.

The NMC tropical mercator 250-mb analysis (2B-27b), however, shows aircraft and satellite-derived wind reports which do yield some information useful in evaluating the water vapor imagery. In this analysis, the subequatorial ridge is apparent stretching from the Baja Peninsula westward toward the Hawaiian Islands. The position of the dry region, shown in the water vapor picture (2B-27a), has been superimposed on the 250-mb analysis. It can be seen that this region lies generally north of the subequatorial ridge where westerly winds to the north converge with southwesterly winds from the subequatorial ridge. This holds true except in the Hawaiian Island region where the dry slot merges with the axis of the subequatorial ridge.

The center of the wave-like feature **D** north of the Hawaiian Islands is in a region of vorticity advection aloft, but shows no evidence of a closed circulation on the 250-mb analysis.

Water vapor imagery at 1215 GMT (2B-28a) shows features previously observed at 0000 GMT, which appear equally prominent at this time. Hurricane Hilary has developed a human-like facial appearance and the moisture outflow continues to appear well-defined. The dry slot (dark gray shade) is relatively unchanged and the moisture vortex **D** and moisture protuberance **E** north and northeast of Hawaii have become more pronounced.

The NMC tropical mercator 250-mb analysis (2B-28b) now shows evidence of the vortex formation **D** and moisture protuberance **E** through a cyclonic turning of the winds, indicating a trough development which is maximizing vorticity at each of those locations.

These short-wave trough features occur near the southwest extremity of the trough associated with the low pressure system **A** off the Washington coast. This trough and its extension, in fact, occupy the climatological position of the TUTT. The subequatorial ridge remains well-defined on this analysis and, again, the dry slot is found in the confluent zone on the north side of the subequatorial ridge.

The FNOC 24-hour 500-mb and surface prognoses, valid 1200 GMT 27 August (2B-29a and 29b), retain the large high pressure cell northeast of Hawaii, which acts as a block to the progression of the meridional trough northwest of Hawaii. There is no suggestion of the wave formation noted in the water vapor imagery on these prognoses.

continued on page 2B-30

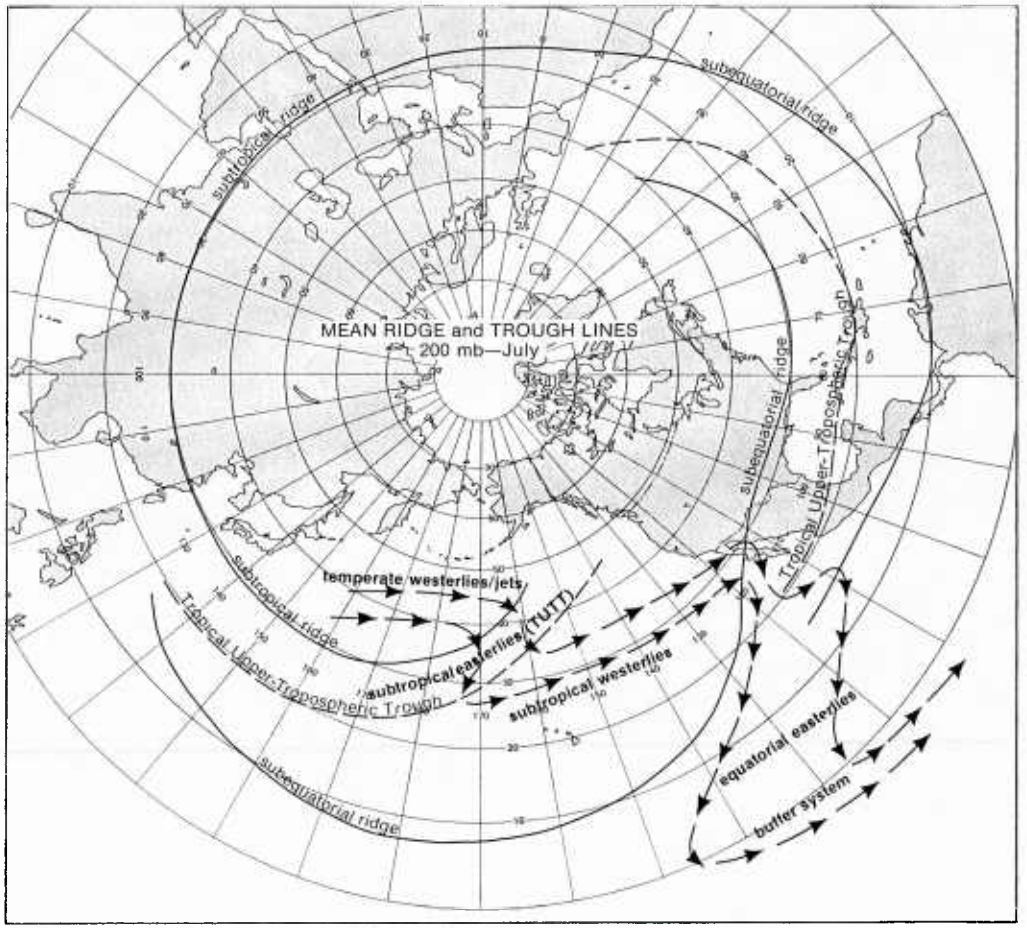

2B-24a. Mean Mid-Summer (July) Positions of Ridges and Troughs at 200 mb (Sadler, 1972).

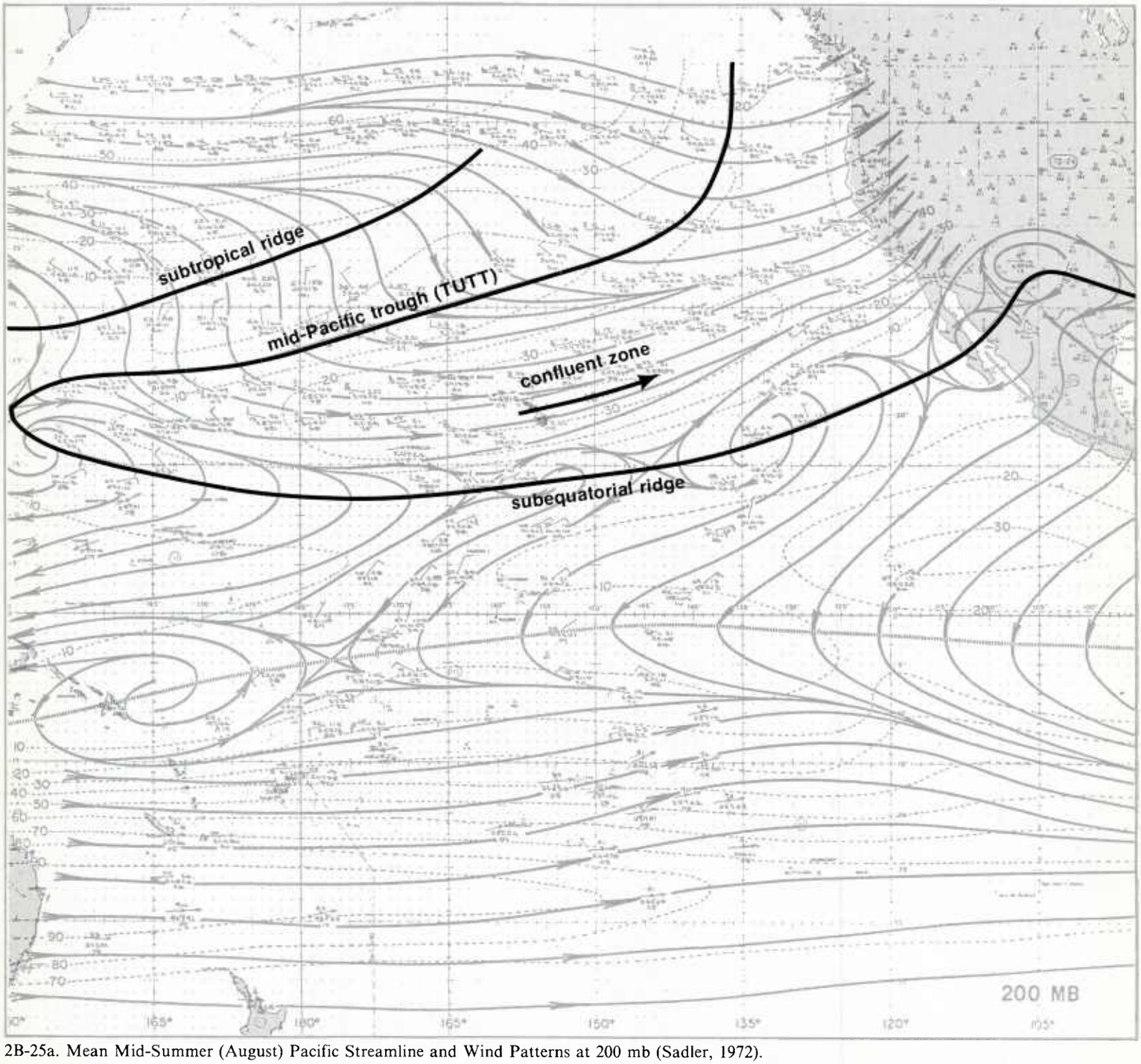

2B-25a. Mean Mid-Summer (August) Pacific Streamline and Wind Patterns at 200 mb (Sadler, 1972).

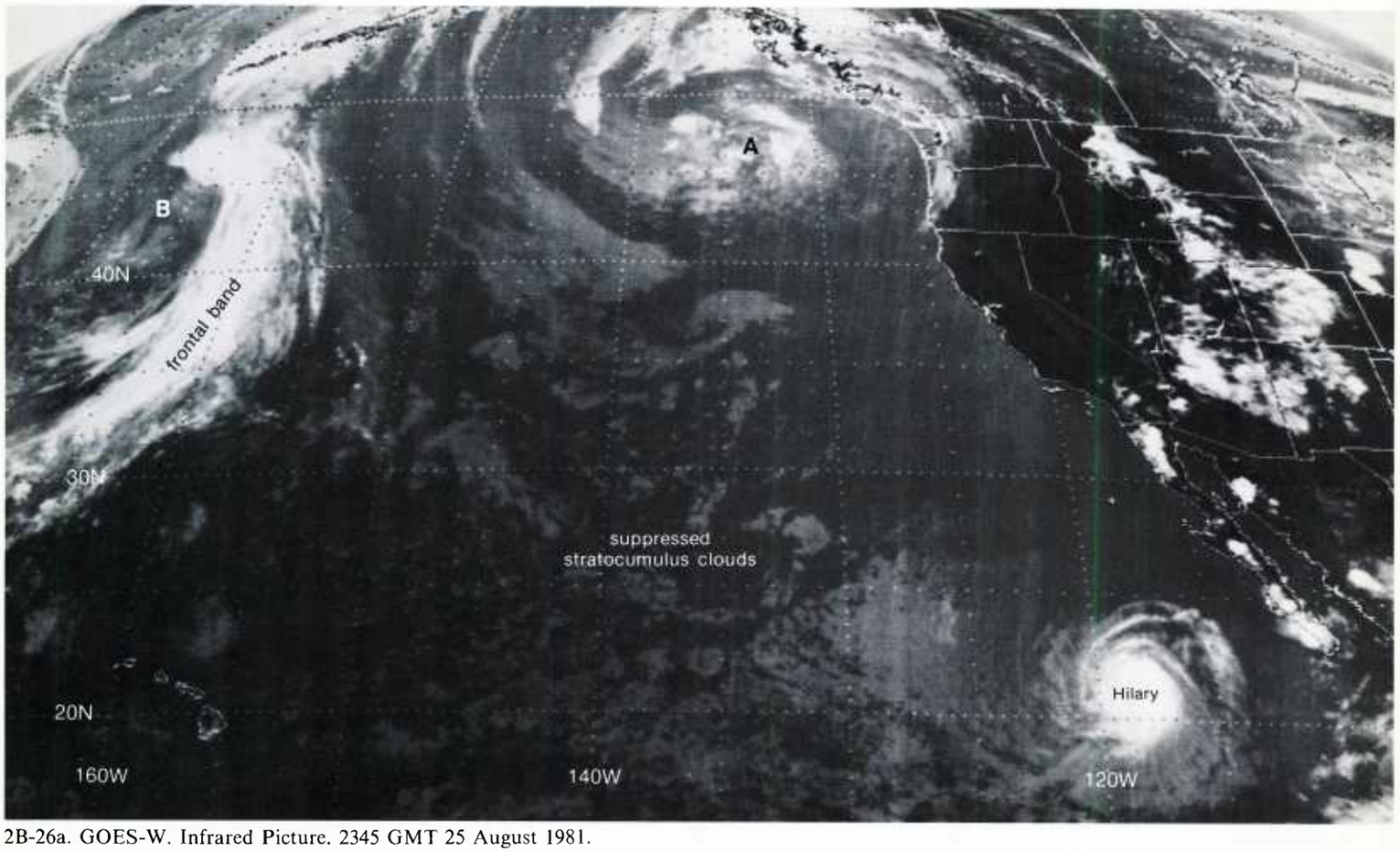

2B-26a. GOES-W. Infrared Picture. 2345 GMT 25 August 1981.

surface

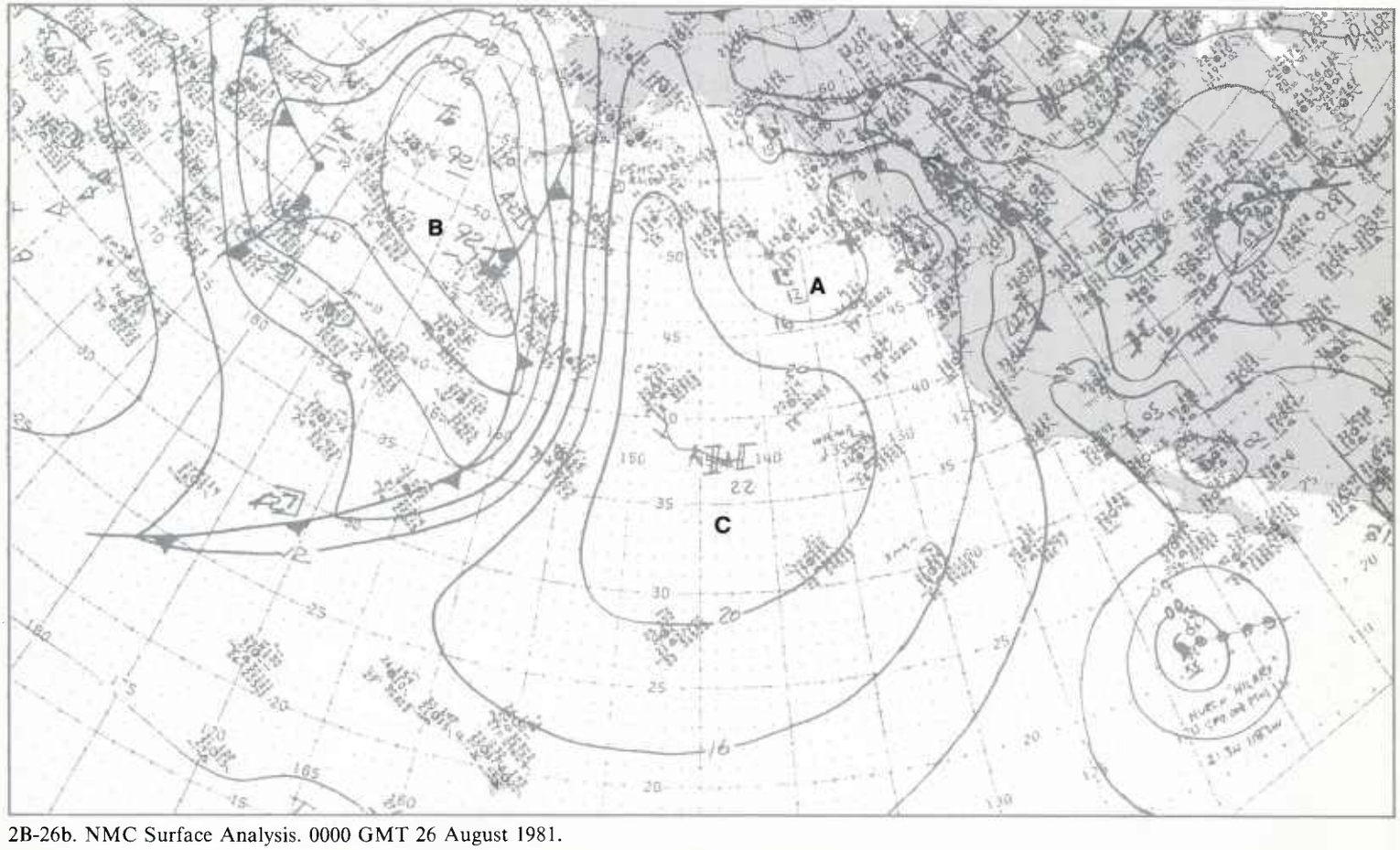

2B-26b. NMC Surface Analysis. 0000 GMT 26 August 1981.

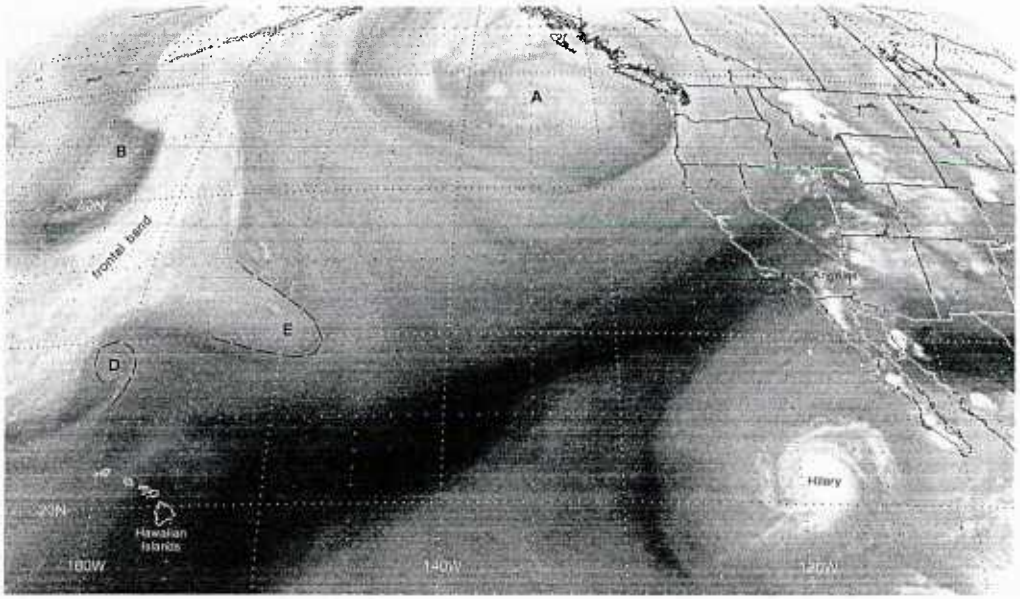

2B-27a. GOES-W. Water Vapor Picture. 0015 GMT 26 August 1981.

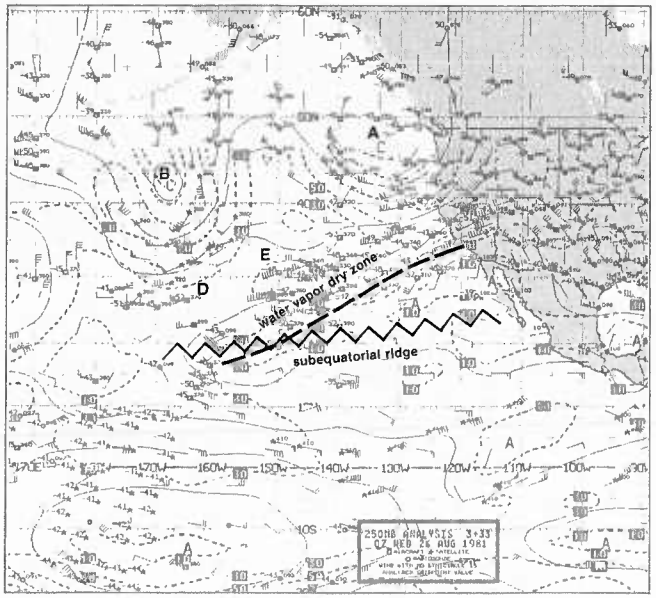

2B-27b. NMC Tropical Mercator 250-mb Analysis. 0000 GMT 26 August 1981.

200 mb

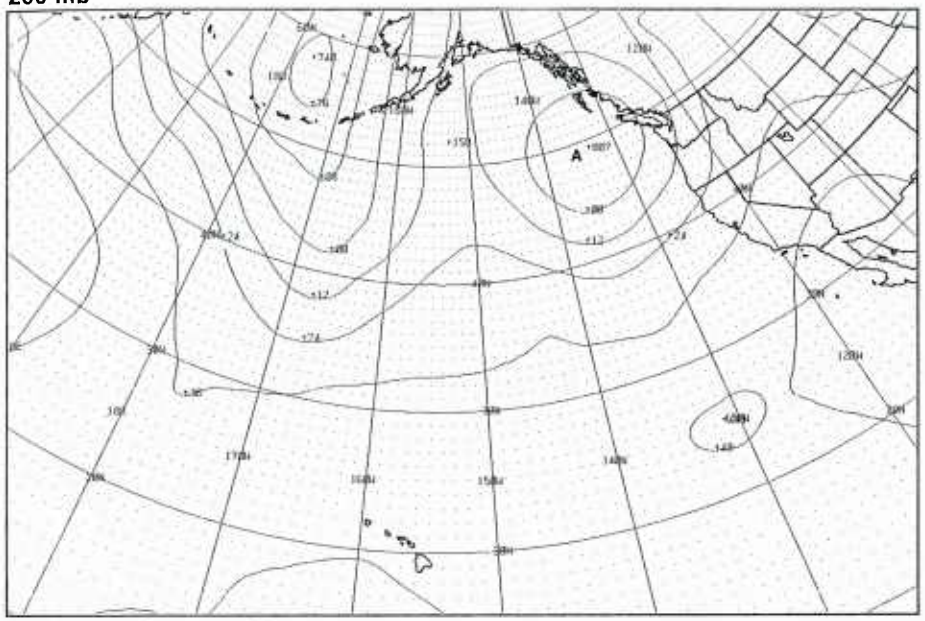

2B-27c. FNOC PE 200-mb Analysis. 0000 GMT 26 August 1981.

500 mb

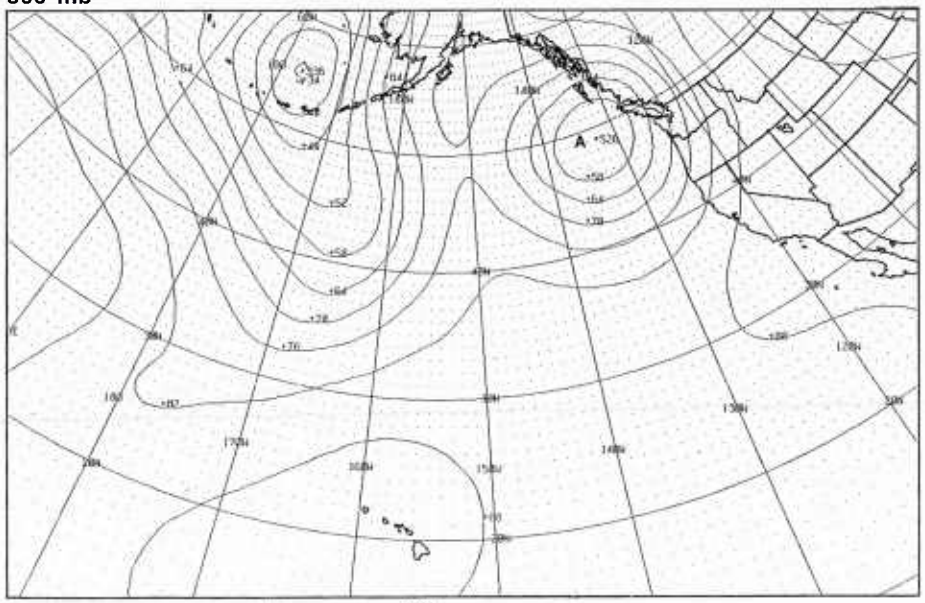

2B-27d. FNOC PE 500-mb Analysis. 0000 GMT 26 August 1981.

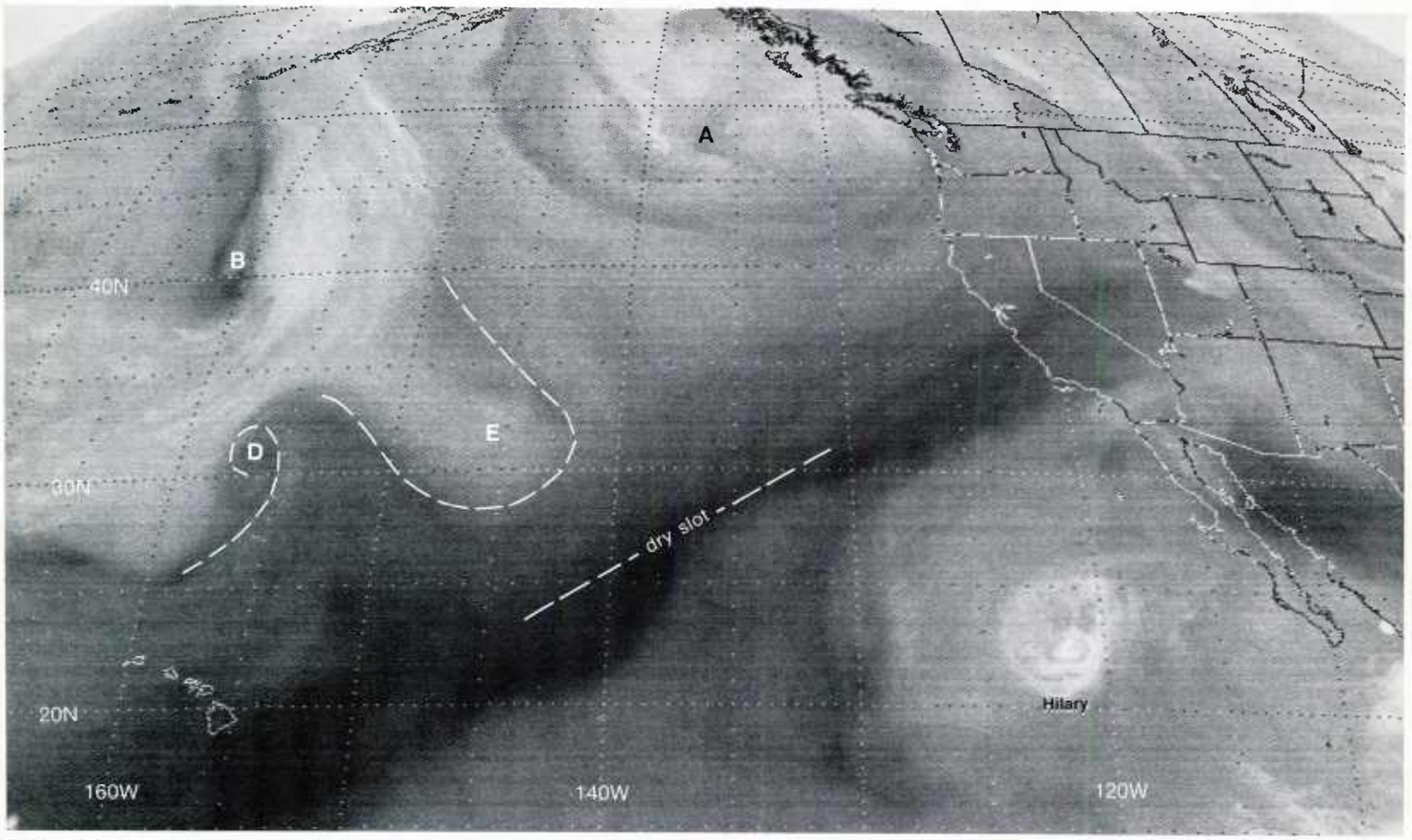

2B-28a. GOES-W. Water Vapor Picture. 1215 GMT 26 August 1981.

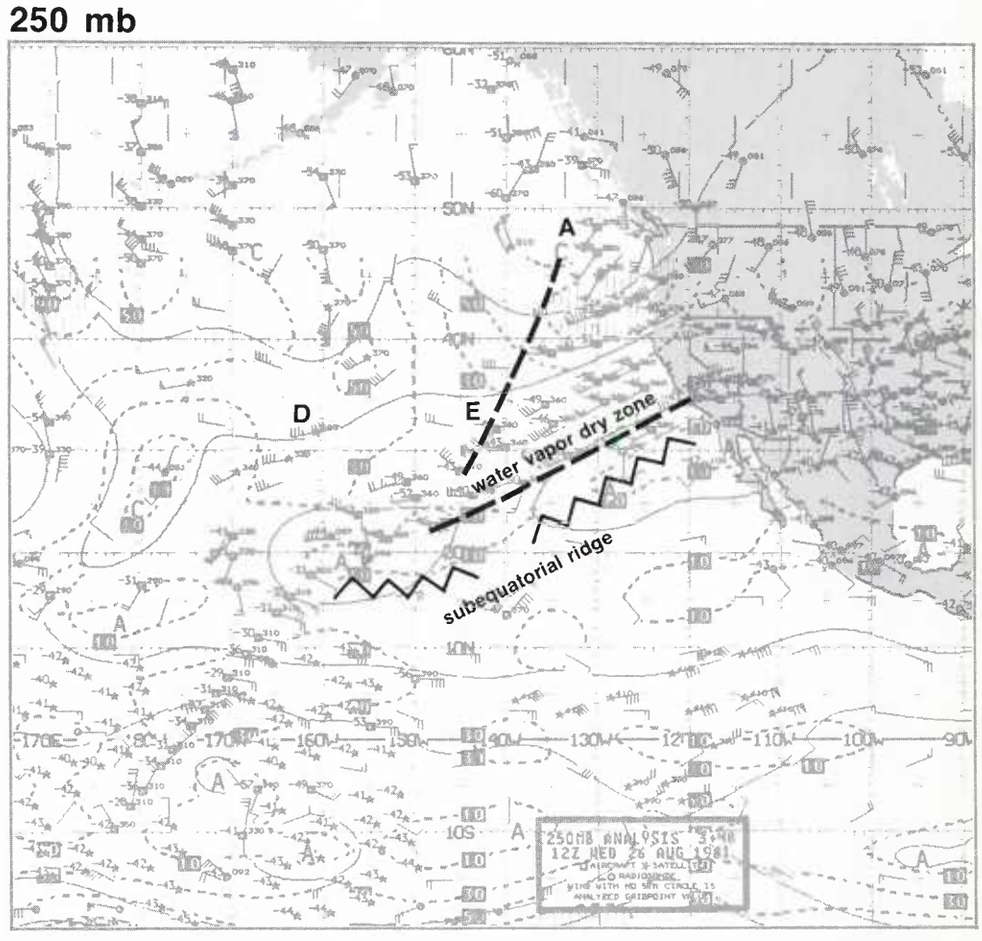

2B-28b. NMC Tropical Mercator 250-mb Analysis. 1200 GMT 26 August 1981.

500 mb

Vortex Development within the TUTT

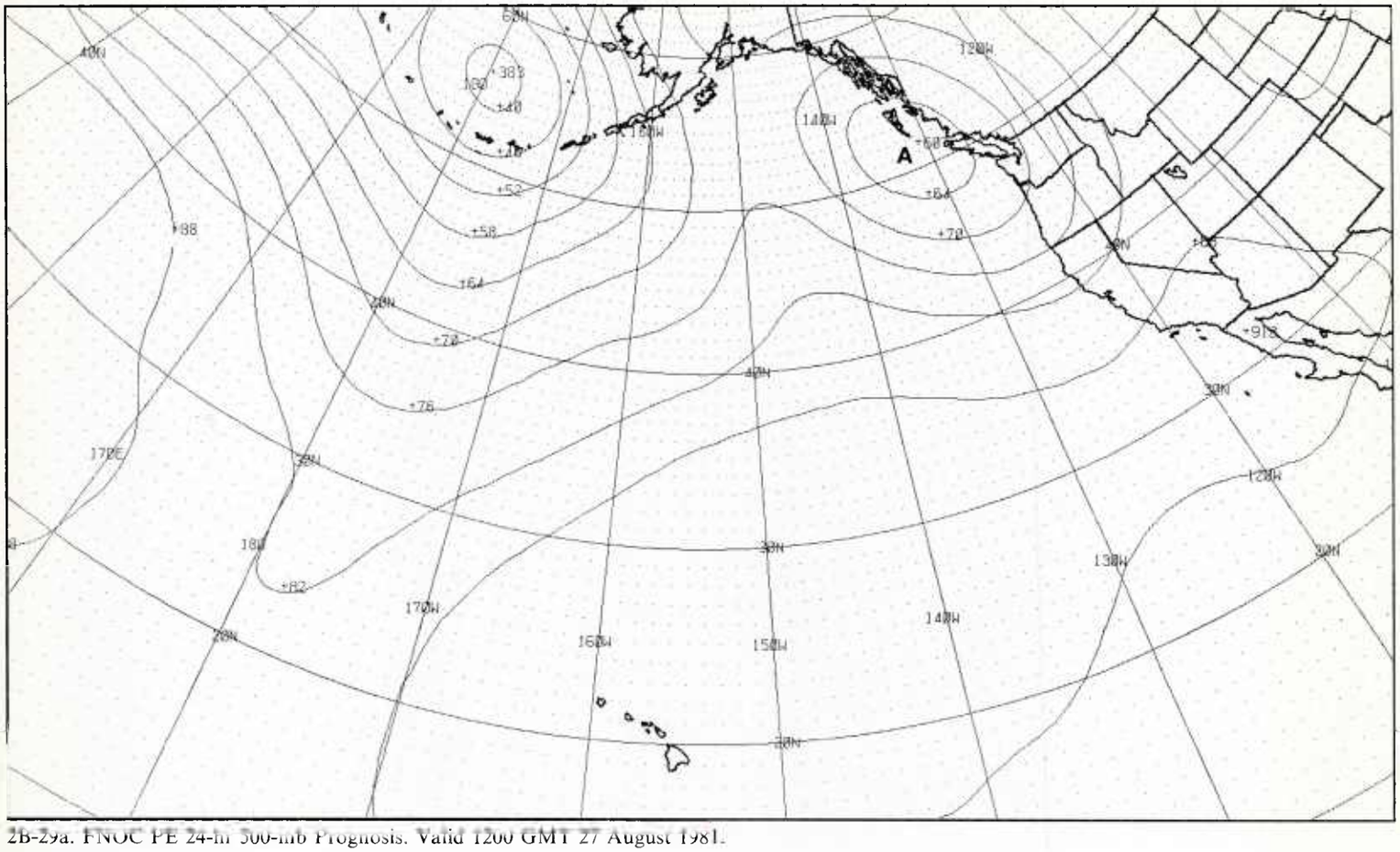

2B-29a. FNOC PE 24-hr 500-mb Prognosis. Valid 1200 GMT 27 August 1981.

surface

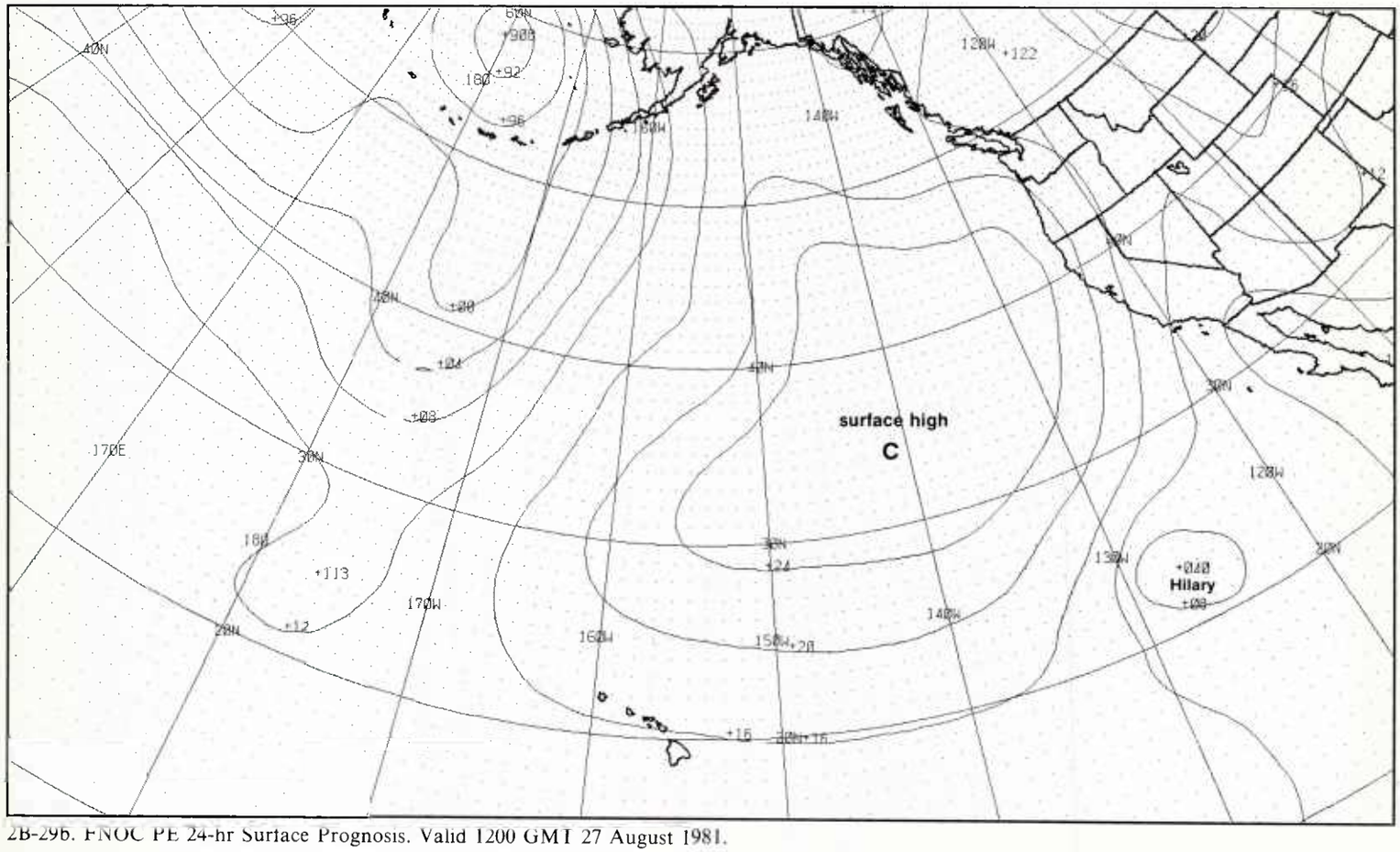

2B-29b. FNOC PE 24-hr Surface Prognosis. Valid 1200 GMT 27 August 1981.

27 August

The GOES-W water vapor picture at 0015 GMT (2B-30a) shows that major features which were observed on the earlier water vapor pictures are still recognizable at this time. One noticeable change is the development of a vortex **F** on the northeast side of the moisture protuberance **E**.

This development continues to be evident, as shown in the GOES-W picture at 1215 GMT (2B-30b). At this time, the vortex **D** north of the Hawaiian Islands is defined by a band of moisture that has almost completely cut off a dry pocket coincident with the center of the cyclonic system.

The NMC surface analysis (2B-31b) shows no evidence of cyclonic circulation to correlate with the water vapor vortex **D**. In fact, the water vapor vortex **D** center, near 29° N, 153° W, is almost coincident with the surface ridge-line axis emanating from a high pressure system **C**. The protuberant vortex feature **F** also overlies the surface region of high pressure. The 700-mb analysis (2B-31a) similarly reveals that these water vapor features are over or close to a closed high **C** ridge-line axis at this level. At 500 mb (2B-32b) evidence of low pressure is indicated near the protuberance **F**; however, the vortex north-northeast of Hawaii is still located in an analyzed region of high pressure.

The tropical mercator 250-mb analysis (2B-32a), however, with superimposed water vapor features, provides evidence consistent with vortex formation at both locations. The trough extending from a low center **A** off the coast of British Columbia connects with both of the water vapor features in the climatological position of the TUTT.

Notice again on this analysis that the dry slot still remains in the confluent region on the north side of the subequatorial ridge. Moisture in the outflow region of Hurricane Hilary is located in a high pressure cell of the subequatorial ridge and is limited in its northward extent by the confluent zone of the dry slot where subsidence presumably takes place. FNOC 24-hour 500-mb and surface prognoses (2B-33a and 33b) continue to predict no effect of the upper circulations down to those levels.

28 August

The GOES-W infrared picture at 2345 GMT on 27 August (2B-34a) reveals that Hurricane Hilary has largely dissipated. A frontal band extends from the region north of the Hawaiian Islands to a vortex **G** off the coast of British Columbia. It would stretch the imagination to believe from this depiction that a vigorous upper-level circulation was positioned just northeast of the Hawaiian Islands, over the relatively cloud-free region south of the frontal band. The GOES-W water vapor picture at 0015 GMT (2B-34b), however, shows that this is true. This imagery still reveals moisture aloft remaining from the outflow of Hurricane Hilary, the dry slot extending from the San Francisco area to Hawaii, and the apparently weakened circulation of the moisture protuberance **F**.

By 1215 GMT, the water vapor imagery (2B-35a) shows that a dry pocket has been cut off, as moisture has completely encircled the vortex **D** northwest of Hawaii. The easternmost vortex **F** appears to have further weakened at this time. The FNOC 200-mb analysis (2B-35c) yields no information concerning these significant upper-level features. The NMC tropical mercator 250-mb analysis (2B-35b), however, shows a closed circulation associated with this vortex **D** and reveals that the weaker system **F** to the east is located on the axis of the trough extending up to the low **A** off the coast of British Columbia. The trough and embedded vortices revealed by the water vapor imagery lie very close to the climatological position expected of the TUTT during August (2B-25a).

The dry slot, again, is found in the region of confluence between the equatorial ridge and the TUTT (2B-35b). The vortex **D** north of Hawaii appears in an analyzed high pressure region at 500 mb (2B-35d), while the easternmost vortex **F** is positioned in the col area between two highs.

Important Conclusions

1. Water vapor data in the 6.7 micrometer wave band provides new information concerning the structure of the middle and upper atmosphere, often not apparent in visible and infrared satellite imagery.

2. Water vapor imagery appears to be particularly useful in defining the location and development of vortices within the Tropical Upper-Tropospheric Trough (TUTT).

3. The downward extension of such upper-level features, in general, appears limited.

4. The dry slot in the eastern North Pacific, as it appears in water vapor imagery during summer months, seems to coincide with the confluent region where mid-latitude westerlies converge with air turning anticyclonically around the subequatorial ridge. It separates and aids in positioning the subequatorial ridge to the south and the TUTT to the north.

5. Circulations indicating closed circulations in water vapor imagery appear to reflect the presence of cyclonic vorticity but may or may not actually represent closed circulations in the atmosphere, particularly in their early development.

6. The anticyclonic outflow region associated with a hurricane appears to be well depicted in water vapor imagery and is a feature of the subequatorial ridge in the eastern North Pacific.

Reference

Sadler, James C., 1972: The mean winds of the upper troposphere over the central and eastern Pacific. NAVENVPREDRSCHFAC Tech. Paper 8-72.

2B-30a. GOES-W. Water Vapor Picture. 0015 GMT 27 August 1981.

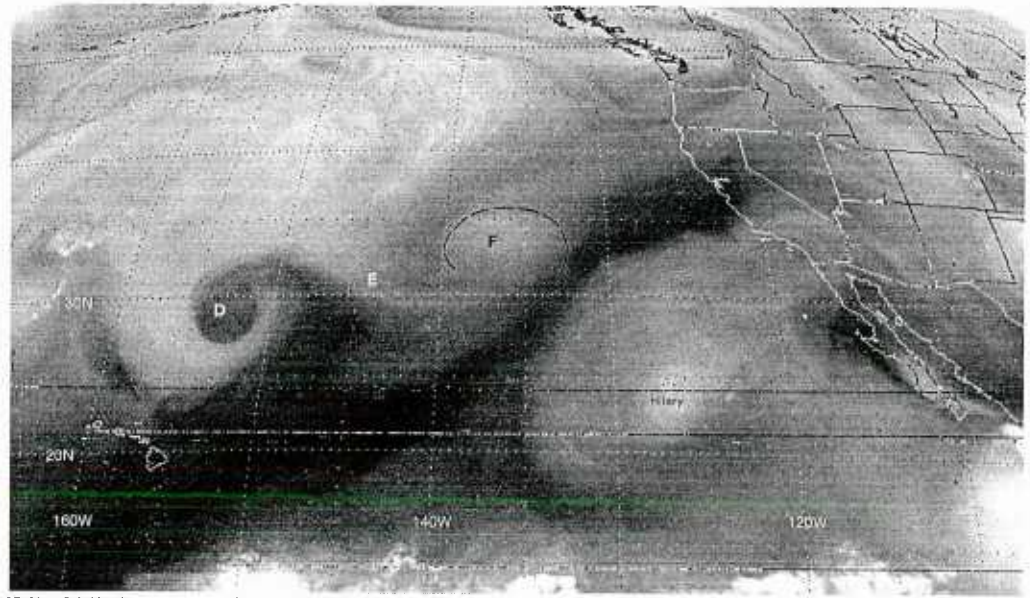

2B-30b. GOES-W. Water Vapor Picture. 1215 GMT 27 August 1981.

700 mb

Vortex Development within the TUTT

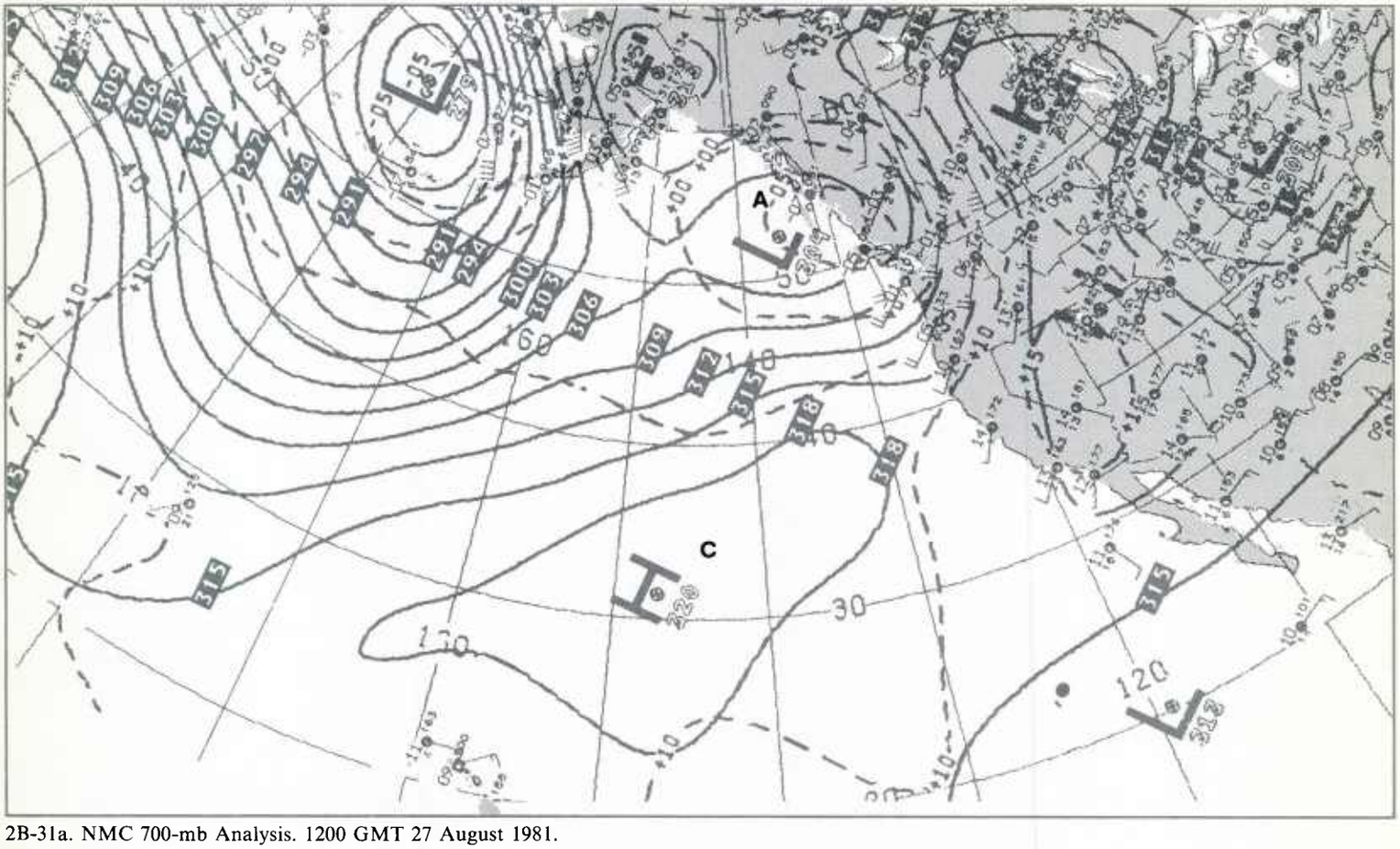

2B-31a. NMC 700-mb Analysis. 1200 GMT 27 August 1981.

surface

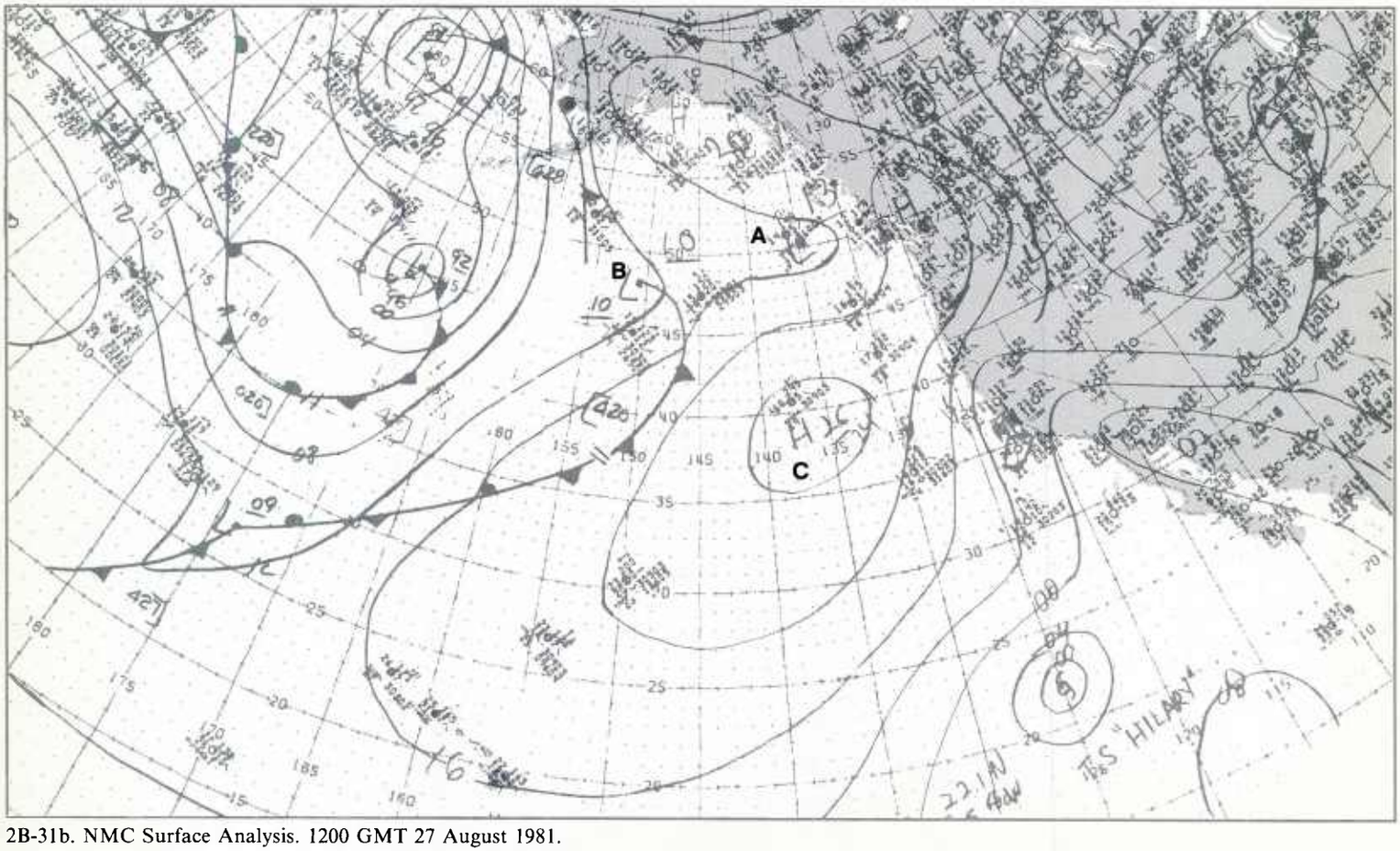

2B-31b. NMC Surface Analysis. 1200 GMT 27 August 1981.

250 mb

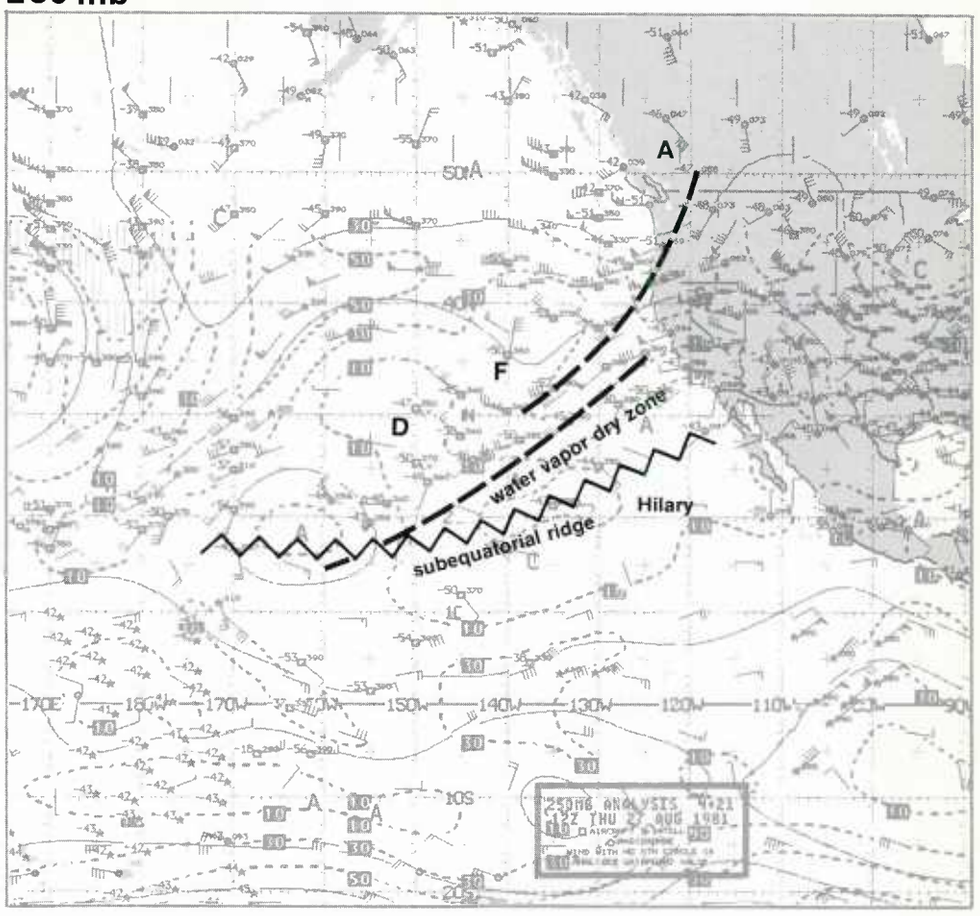

2B-32a. NMC Tropical Mercator 250-mb Analysis. 1200 GMT 27 August 1981.

500 mb

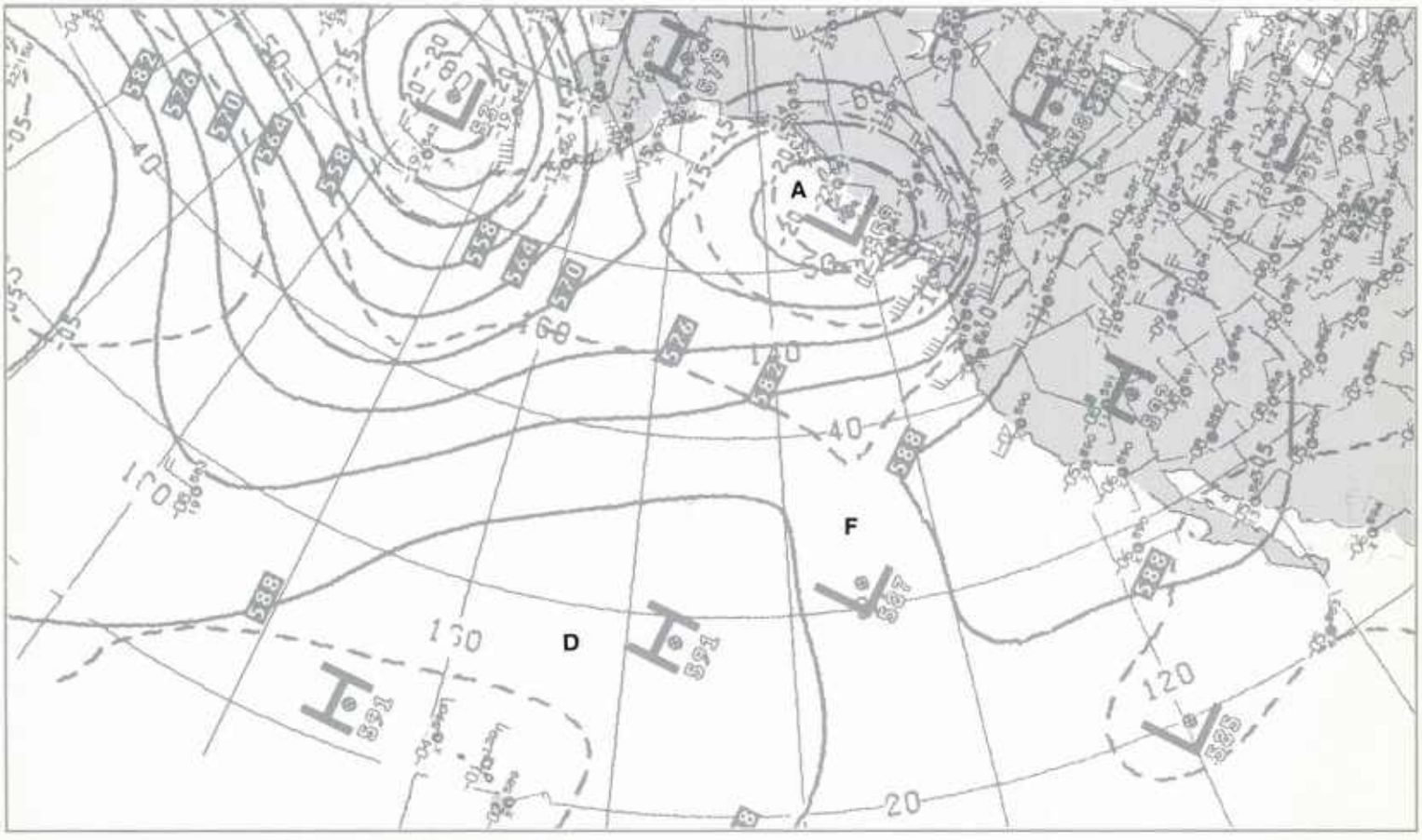

2B-32b. NMC 500-mb Analysis. 1200 GMT 27 August 1981.

500 mb

Vortex Development within the TUTT

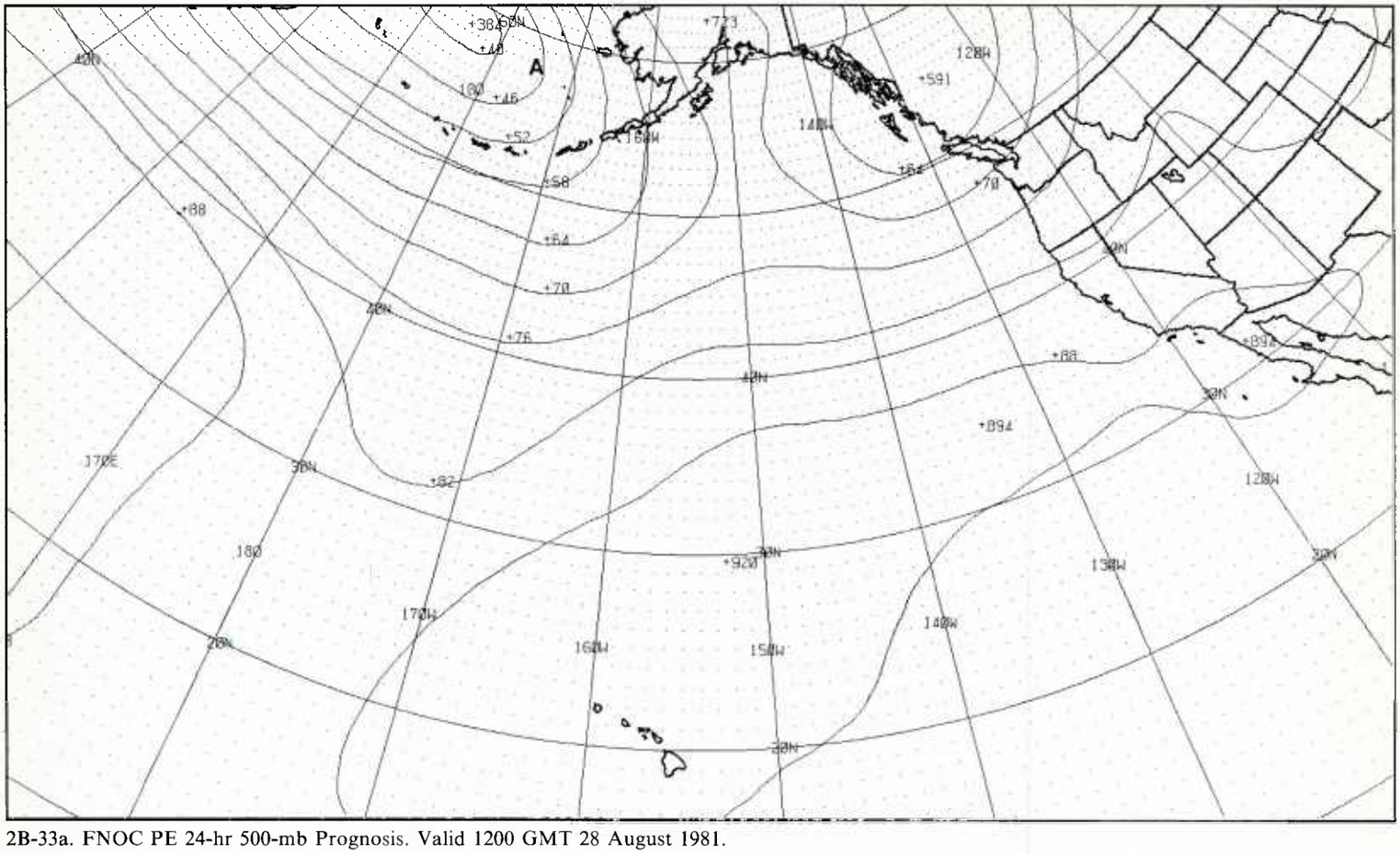

2B-33a. FNOC PE 24-hr 500-mb Prognosis. Valid 1200 GMT 28 August 1981.

surface

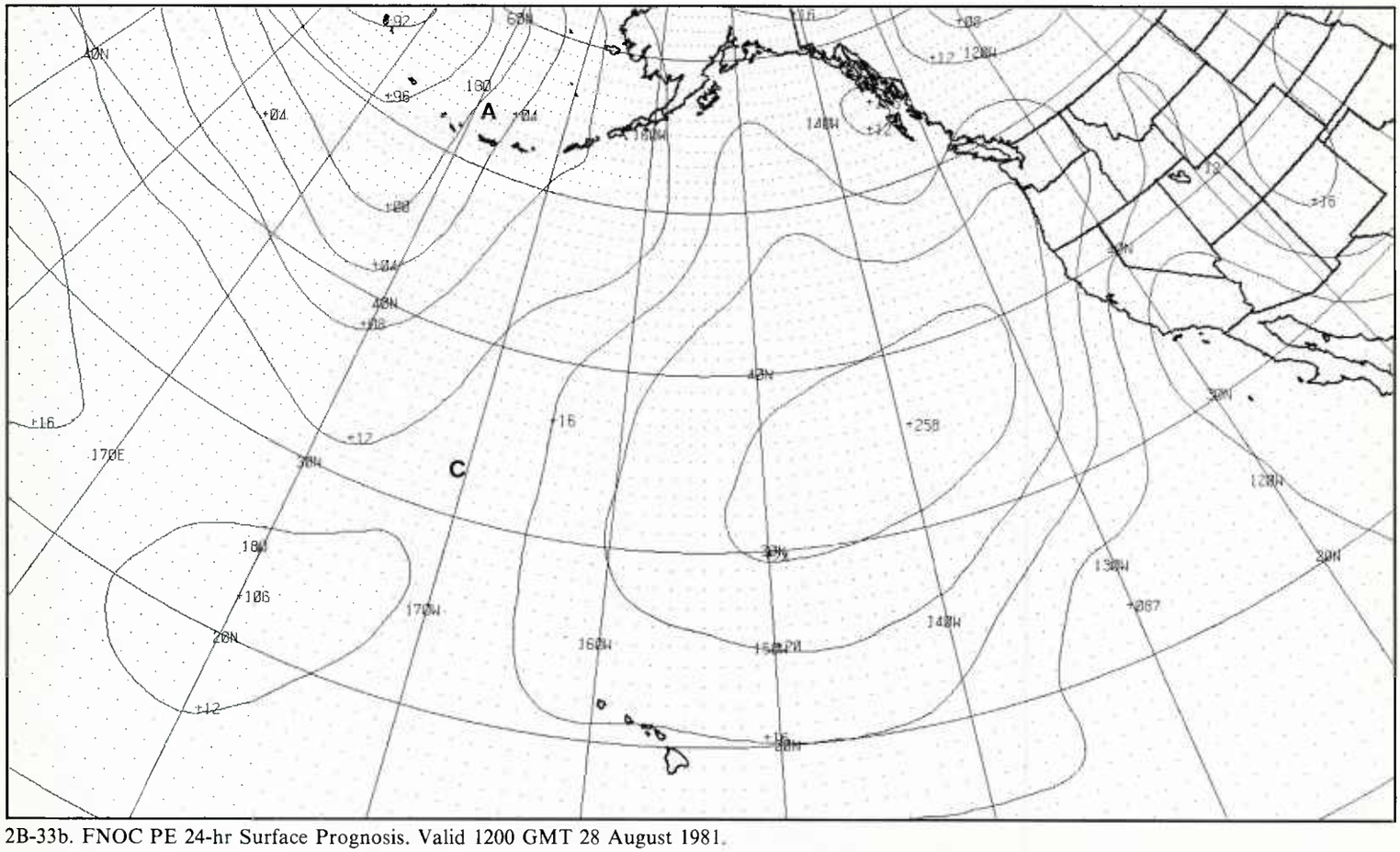

2B-33b. FNOC PE 24-hr Surface Prognosis. Valid 1200 GMT 28 August 1981.

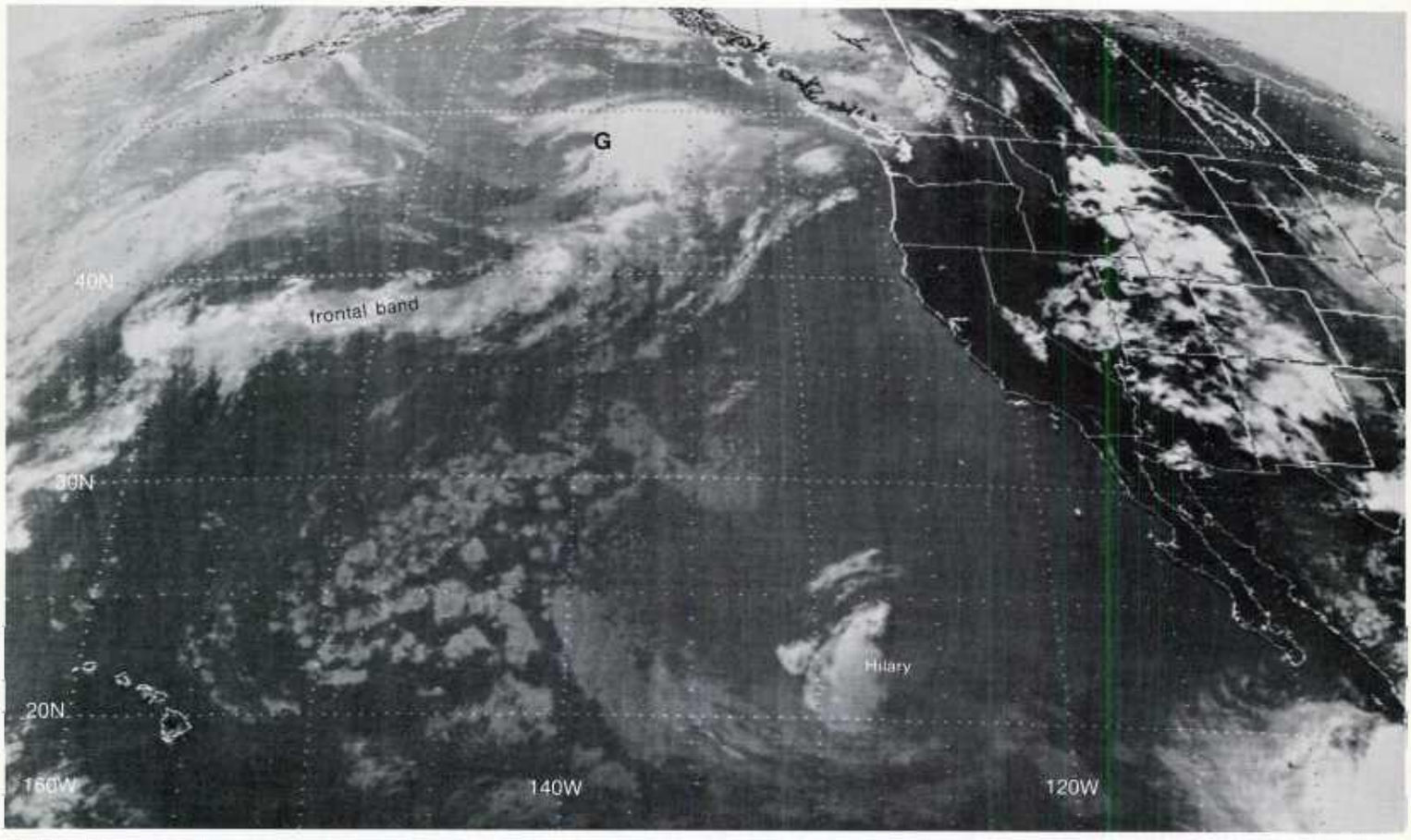

2B-34a. GOES-W. Infrared Picture. 2345 GMT 27 August 1981.

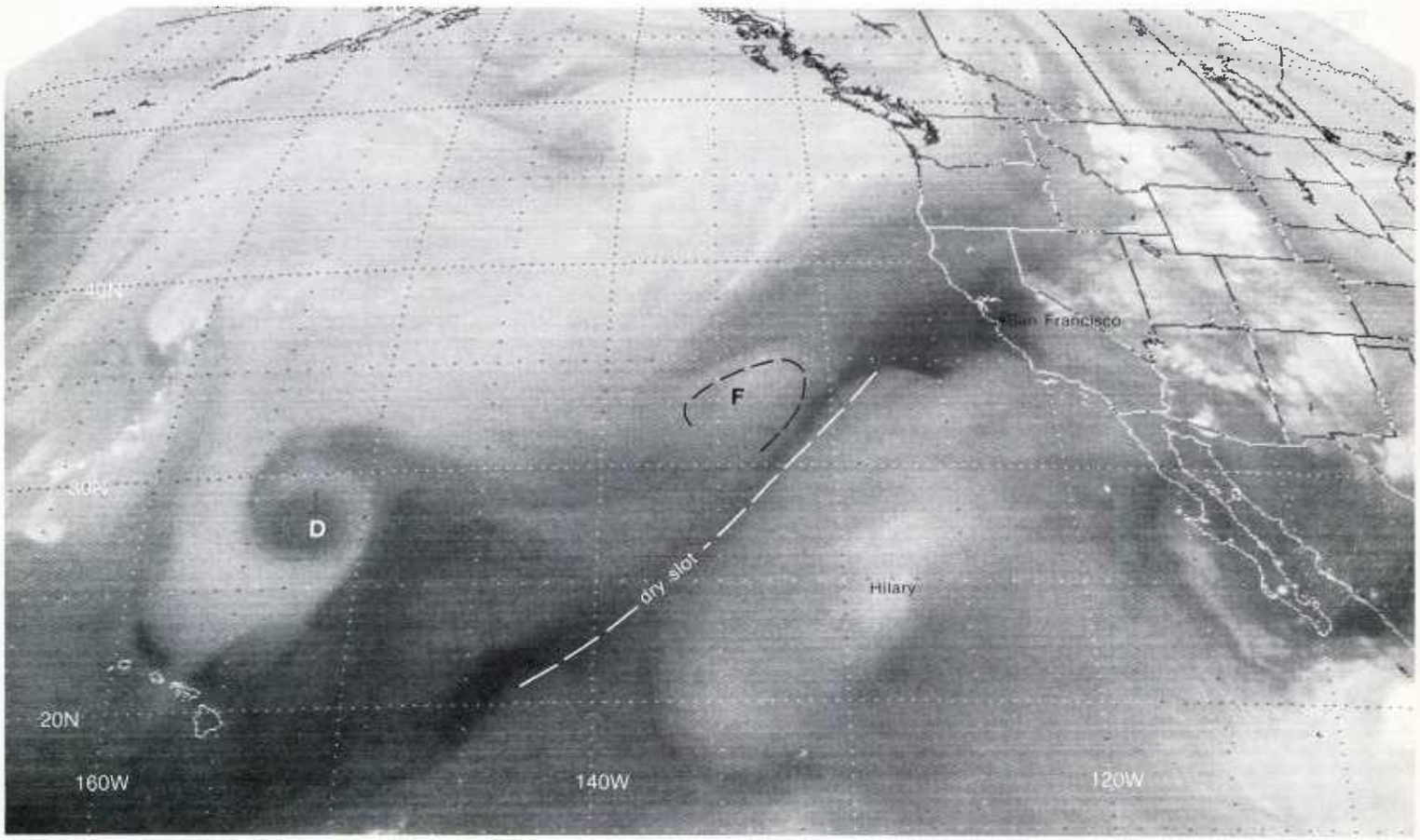

2B-34b. GOES-W. Water Vapor Picture. 0015 GMT 28 August 1981.

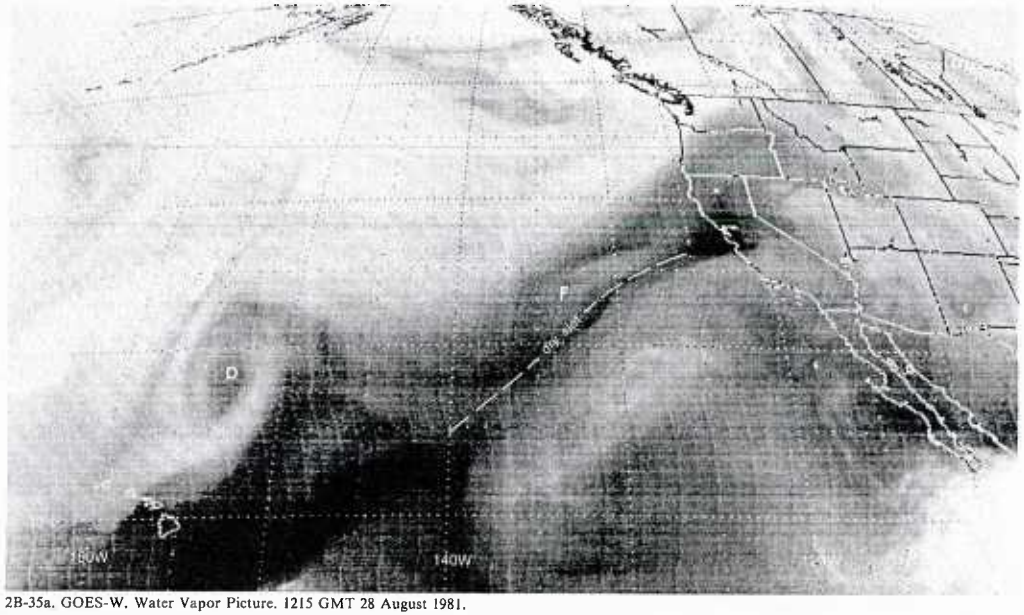

2B-35a. GOES-W. Water Vapor Picture. 1215 GMT 28 August 1981.

250 mb

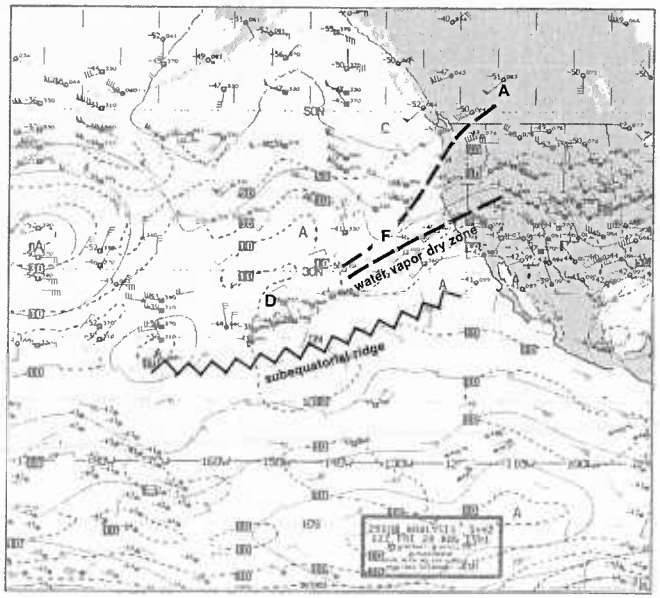

2B-35b. NMC Tropical Mercator 250-mb Analysis. 1200 GMT 28 August 1981.

200 mb

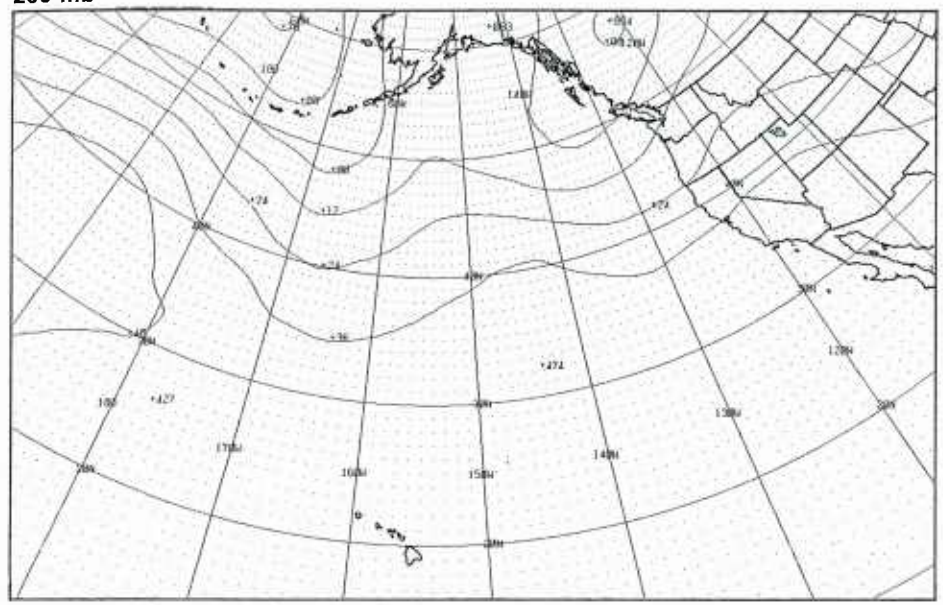

2B-35c. FNOC PE 200-mb Analysis. 1200 GMT 28 August 1981.

500 mb

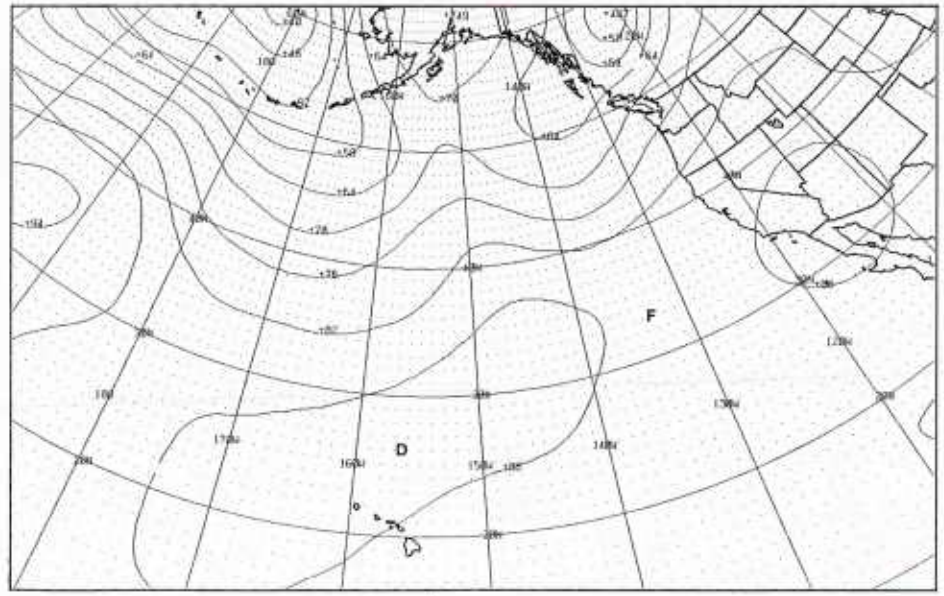

2B-35d. FNOC PE 500-mb Analysis. 1200 GMT 28 August 1981.

Section 3

Coastal Zone Phenomena

3A Introduction

3B Case Studies

Coastal Zone Phenomena

3A Introduction

Coastal Stratus in the Marine Layer

The widespread occurrence of stratus along the California coast is most pronounced during the warm months, May through September. There is a diurnal oscillation of the landward edge of the stratus: it advances inland at night and in the early morning, and retreats seaward in the afternoon. Over the southern California bight, the seaward extent of the diurnal dissipation is greater than over the coastal areas further north and south. This is attributed to increased offshore subsidence in the marine layer associated with divergence in the daytime sea breeze circulation.

The southern California bight coastline has a concave shape which curves inland and, as the sea breeze crosses the coastline, the onshore flow undergoes horizontal divergence. Under fair weather conditions, strong sea breezes can develop so that the divergence in the surface flow results in a pronounced decrease in the height of the marine layer along the coast and out to sea. The rapid lowering of the height of the marine layer causes dissipation of the stratus much further out to sea than along the coastlines to the north and south, where the divergence effect is not observed.

Another phenomenon which disrupts the normal diurnal oscillation of the stratus along the southern California coast is a small-scale vortex in the marine layer in the southern California bight. The vortex is called the Catalina Eddy, and it derives its name from the fact that the circulation center is usually located just southwest of Catalina Island. The Catalina Eddy forms when an eastward-moving upper trough nears southern California, with strong northerly surface winds prevailing along the California coast.

If the eddy is strong, the marine layer will deepen rapidly, obscuring the coastal region and blanketing Los Angeles and nearby valleys. In these cases, the normal daytime diurnal dissipation of coastal stratus over the southern California bight is disrupted because of the increased depth of the marine layer. This is in contrast to the lowering of the marine layer under fair weather conditions, which favors a strong sea breeze development, divergent flow across the coastline, and dissipation of the stratus far out to sea.

Case 1 Coastal Zone Phenomena

Coastal Stratus

From May through November, extensive low-level cloudiness (stratus and stratocumulus) is observed along the U.S. West Coast. This cloudiness is due to a combination of oceanographic and atmospheric factors. The primary oceanic factor is the California Current—a broad, cold current in the eastern Pacific that flows southward along the West Coast. The atmospheric factor is the persistent northerly winds blowing around the semi-permanent anticyclonic circulation over the eastern Pacific during the summer. These winds produce pockets of coastal zone upwelling that bring cold subsurface waters to the surface which extend out into the California Current. The extensive areas of coastal stratus are formed when warm, moist maritime Pacific air moves southward, around the eastern periphery of an offshore anticyclone, and is cooled from below by the cold water masses of the California Current and the upwelled coastal waters. As the air moves south over progressively warmer waters, the marine layer and associated stratus become deeper, higher and more unstable on the average. The marine layer in the stratus area is capped by a dry, stable layer (temperature inversion) aloft, due to subsidence of the air at upper levels in the eastern periphery of the anticyclone. The stratus forms below the base of the inversion which is typically between 1,000 and 2,000 feet.

During the summer months, coastal stratus is observed along the California coastline. GOES satellite visible pictures reveal that the early morning coastal stratus dissipates quickly out to sea, leaving a cloud-free strip just offshore by afternoon. When there are no synoptic-scale disturbances over the ocean moving toward the California coast, a marked diurnal cycle in the stratus cloud cover occurs along the coastal zone.

Diurnal dissipation of coastal stratus
California Coastal Zone
July 1977

12 July

The 1200 GMT (0400 Pacific Standard Time) NMC surface analysis (3B-2a) shows a large anticyclone over the eastern Pacific. This is a typical summer Pacific high pressure system in which surface air flows from north and northwest along the California coast, as indicated by the surface isobars. Stratus forms in this flow as the air moves southward over the cold water masses of the California Current and upwelled coastal waters.

The 1615 GMT (0815 PST) GOES visible picture (3B-2b), about 4 hours after the surface analysis, is the earliest morning picture on this day that clearly shows the southern California region. Note the dense area of offshore stratus and stratocumulus from central California to Baja California. This is the typical summer coastal stratus that forms in this region.

By 1945 GMT (1145 PST) the stratus along the southern California coast (3B-3a) has already dissipated, and a nearly cloud-free offshore area is observed from Point Conception to Baja California. Note that the clouds north of Point Conception continue to hug the coastline. Later in the afternoon at 2315 GMT (1515 PST), the stratus forms a well-defined offshore boundary (3B-3b), and the clear coastal area extends out to sea, about 60 n mi off southern California, and then narrows sharply to the south along Baja California. This sequence of events represents a diurnal cycle in the coastal stratus, and is a striking summer feature along the California coast.

The GOES pictures on this day were used as part of a comprehensive southern California coastal stratus dissipation investigation by Lee (1979), for the month of July 1977 and 1978. Measurements of the stratus inland penetration and seaward retreat were made at several latitudes along the coast three times during the day: morning (0745–0845 PST), midday (1115–1215 PST), and afternoon (1445–1545 PST). The results are shown in 3B-4a. They reveal a distinct diurnal change in the location of the eastern edge of the stratus from morning to afternoon.

Notice that in the morning, along 35° N (central California), the onshore penetration of the coastal stratus is observed to be limited by the terrain to small distances (25 n mi)—the 600-m elevation contour in the figure marks the approximate eastward penetration of the coastal stratus. Through midday the stratus edge retreats rapidly westward toward the shore; yet by afternoon the stratus edge is only a few miles out to sea. This limited off-shore dissipation is due to the inhibiting effects of the cold coastal waters. To the south, along Baja California (31°–32° N), a similar pattern is observed. In the morning the inland penetration is again limited by the 600-m elevation contour, at midday the stratus edge is most frequently between 0 and 10 n mi offshore, and in the afternoon only slightly more than 15 n mi.

Along latitudes 33° N and 34° N, the southern California bight, morning stratus is observed to often extend well inland—up to 40 n mi. This onshore penetration occurs along the broad coastal plain and the east–west oriented San Gabriel Valley that extends inland about 80 n mi. By midday it is most often found between 30 and 70 n mi offshore, and by afternoon it is between 50 and 100 n mi offshore. Thus, the greatest inland penetration and seaward retreat of the coastal stratus occurs in this region.

Studies show that fluctuations in the marine layer depth is one of the most important processes by which dissipation of coastal stratus occurs. The diurnal changes in the depth of the marine layer in the southern California bight are closely related to the normal sea breeze regime in this region. The broad, deep coastal plain inland of the bight favors the development of a strong sea breeze/land breeze regime. After the onset of the sea breeze, a sinking zone (3B-5a) appears offshore as part of the return sea breeze circulation. This produces subsidence over the marine inversion, and it begins to weaken. As the sea breeze moves across the concave shaped coastline of the bight, it diverges as it spreads inland; this contributes to the vertical shrinking of the marine layer along the coast and results in the dissipation of the coastal stratus. At night, after the initiation of the land breeze, the convergence of the flow as it spreads offshore deepens the marine layer in the coastal region and the stratus reforms. This diurnal cycle repeats on successive days as long as the weather situation remains undisturbed along the coast and the sea breeze/land breeze regime continues. Along the Baja California and central California coast, the retreat of the coastal stratus is less pronounced because of the inhibiting effects of cold coastal sea surface water temperatures.

Important Conclusions

1. Persistent coastal stratus penetrates inland in coastal valleys and is restricted to the coastal strip by hilly terrain.

2. Under fair weather conditions, onshore coastal stratus dissipates rapidly during daytime surface heating, and the onshore edge retreats to the shore and then offshore, leaving a clear area along the coast.

3. Daytime offshore coastal stratus dissipation distances are greatest in regions where sea breeze circulations develop along curved coastlines with inland coastal plains, such as the southern California bight.

Reference

Lee, T. F., 1979: Diurnal variations of coastal stratus. PMTC Tech. Pub. TP80-02, Pacific Missile Test Center, Point Mugu, CA, 59 pp.

surface

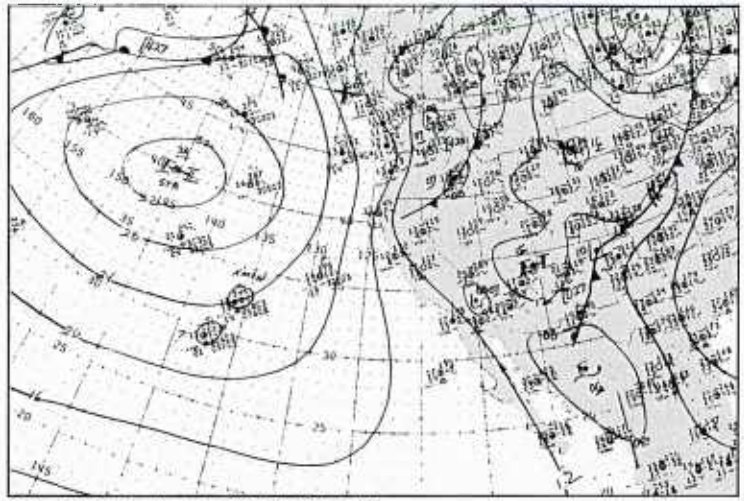

3B-2a. NMC Surface Analysis. 1200 GMT 12 July 1977.

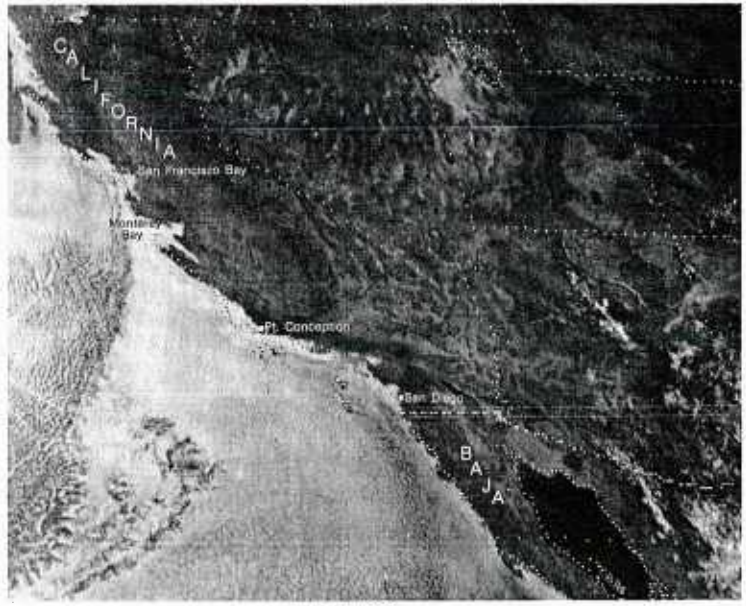

3B-2b. GOES-W. Visible Picture. 1615 GMT 12 July 1977.

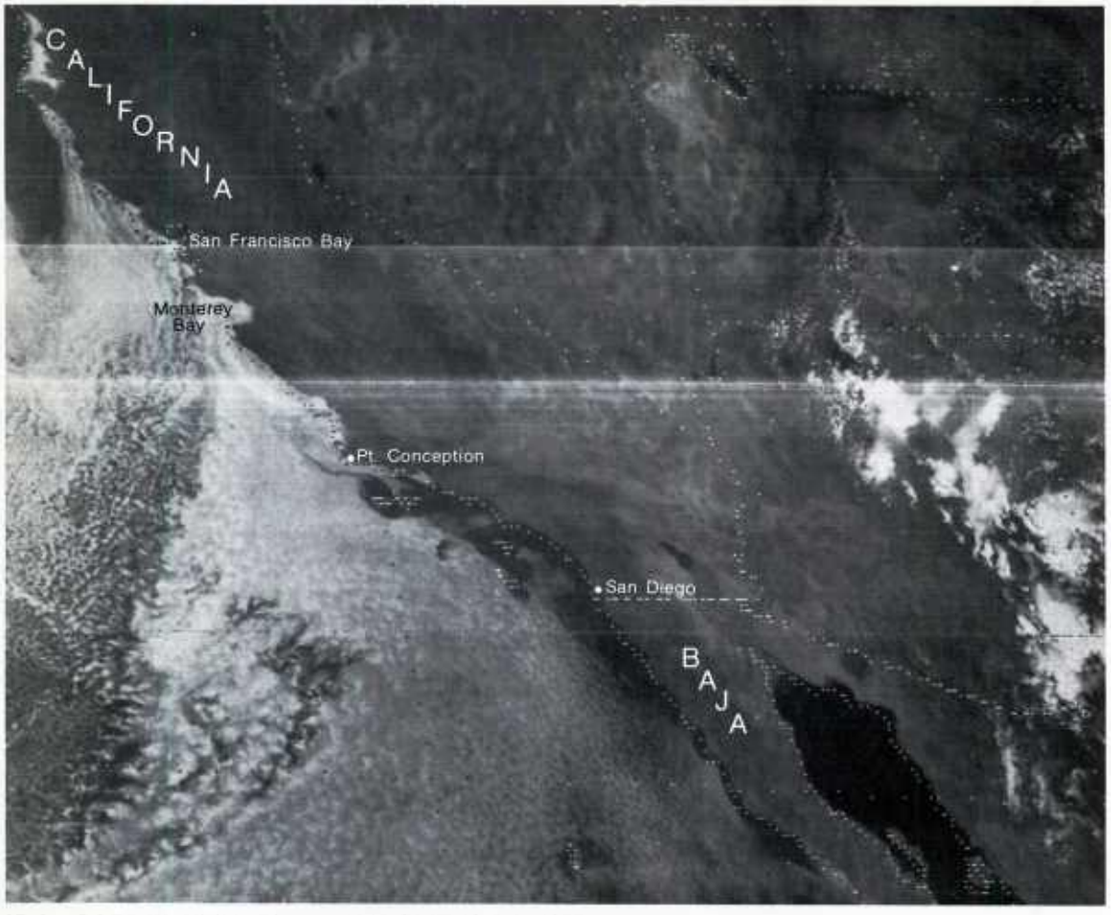

3B-3a. GOES-W. Visible Picture. 1945 GMT 12 July 1977.

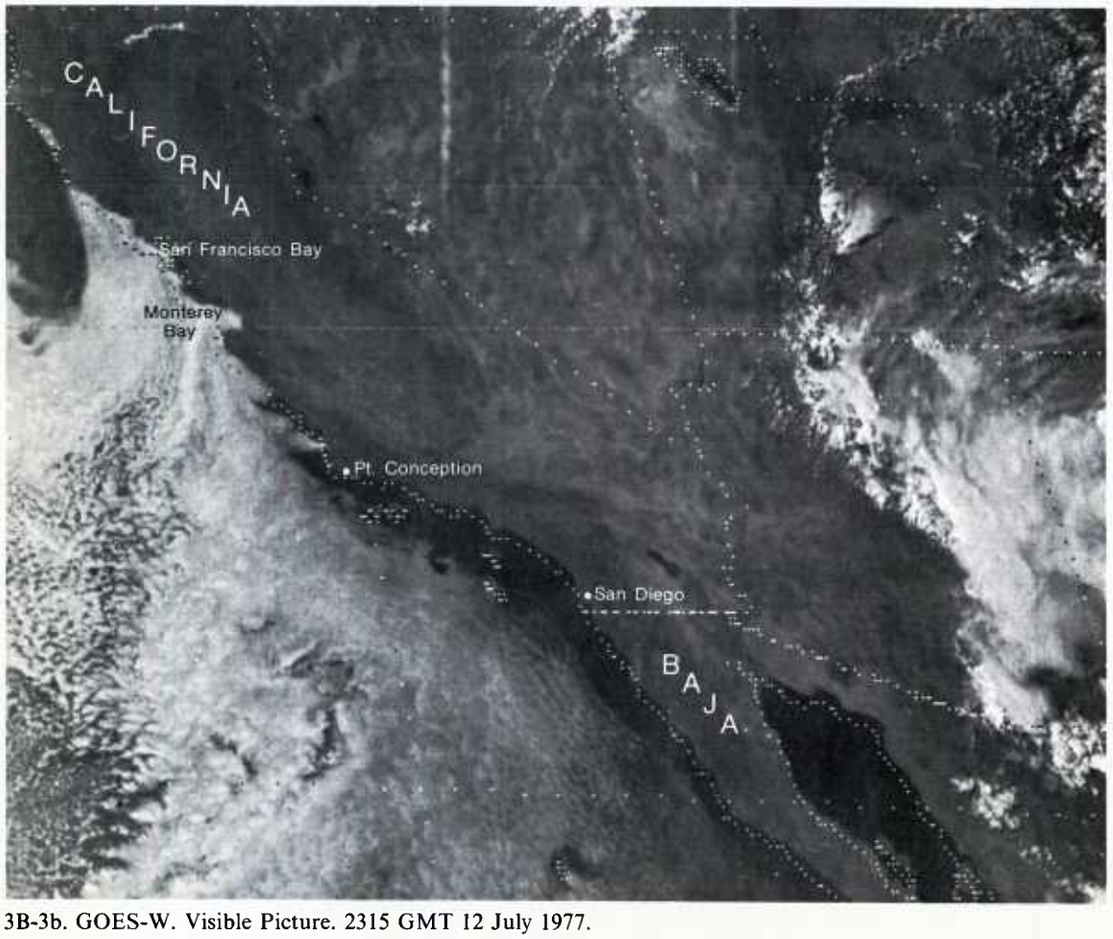

3B-3b. GOES-W. Visible Picture. 2315 GMT 12 July 1977.

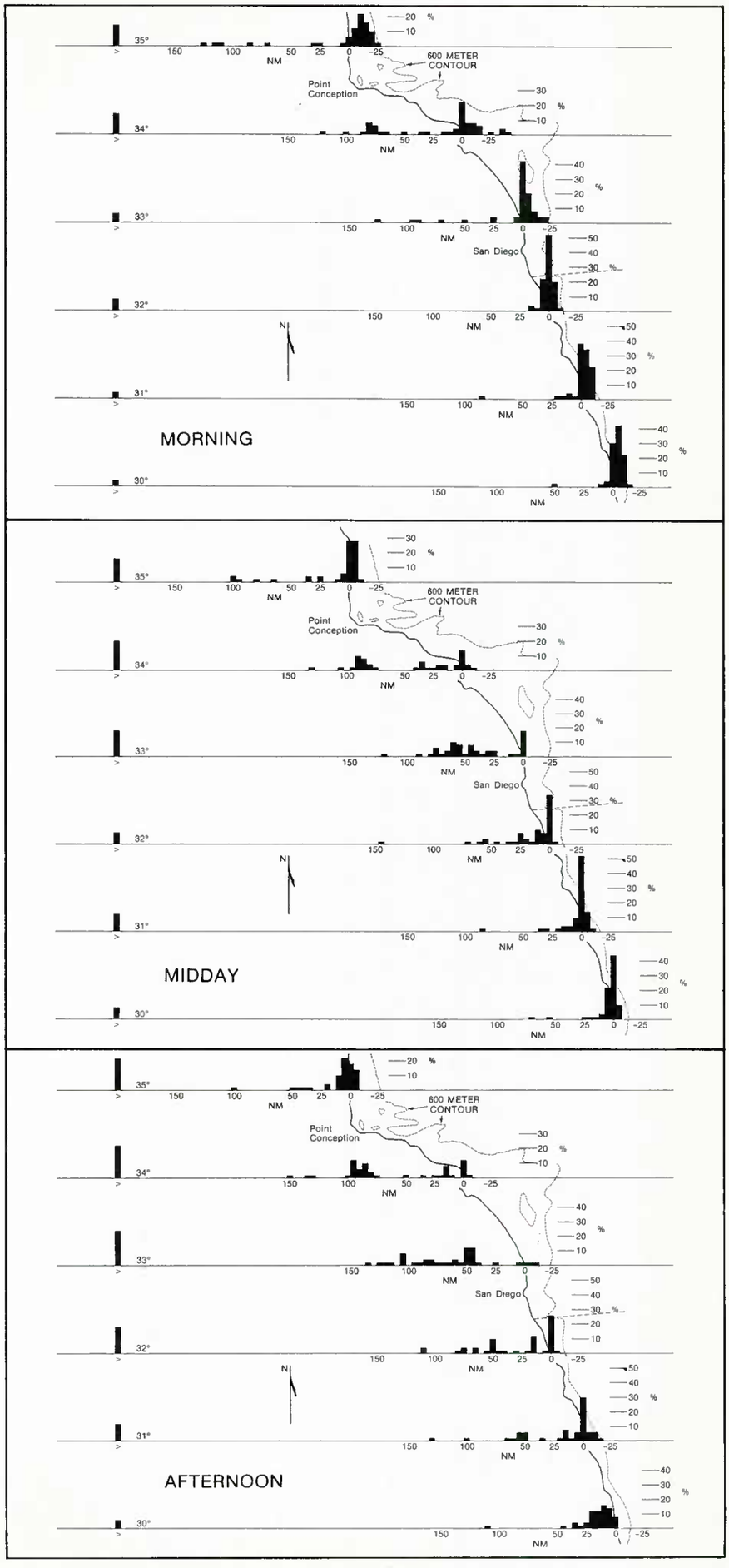

3B-4a. Stratus Margin Frequency. The diurnal behavior of coastal stratus at various locations along the coast is shown at three times during the day: morning, midday, and afternoon. Along each parallel, frequency of stratus occurrence is plotted versus distance from the shore in nautical miles. Along a given parallel, offshore distances to a stratus edge are recorded as positive, onshore distances as negative, and stratus at the shoreline as zero distance. The 600-m contour shown marks the approximate limit of eastward penetration of the morning stratus edge. (After Lee, 1979).

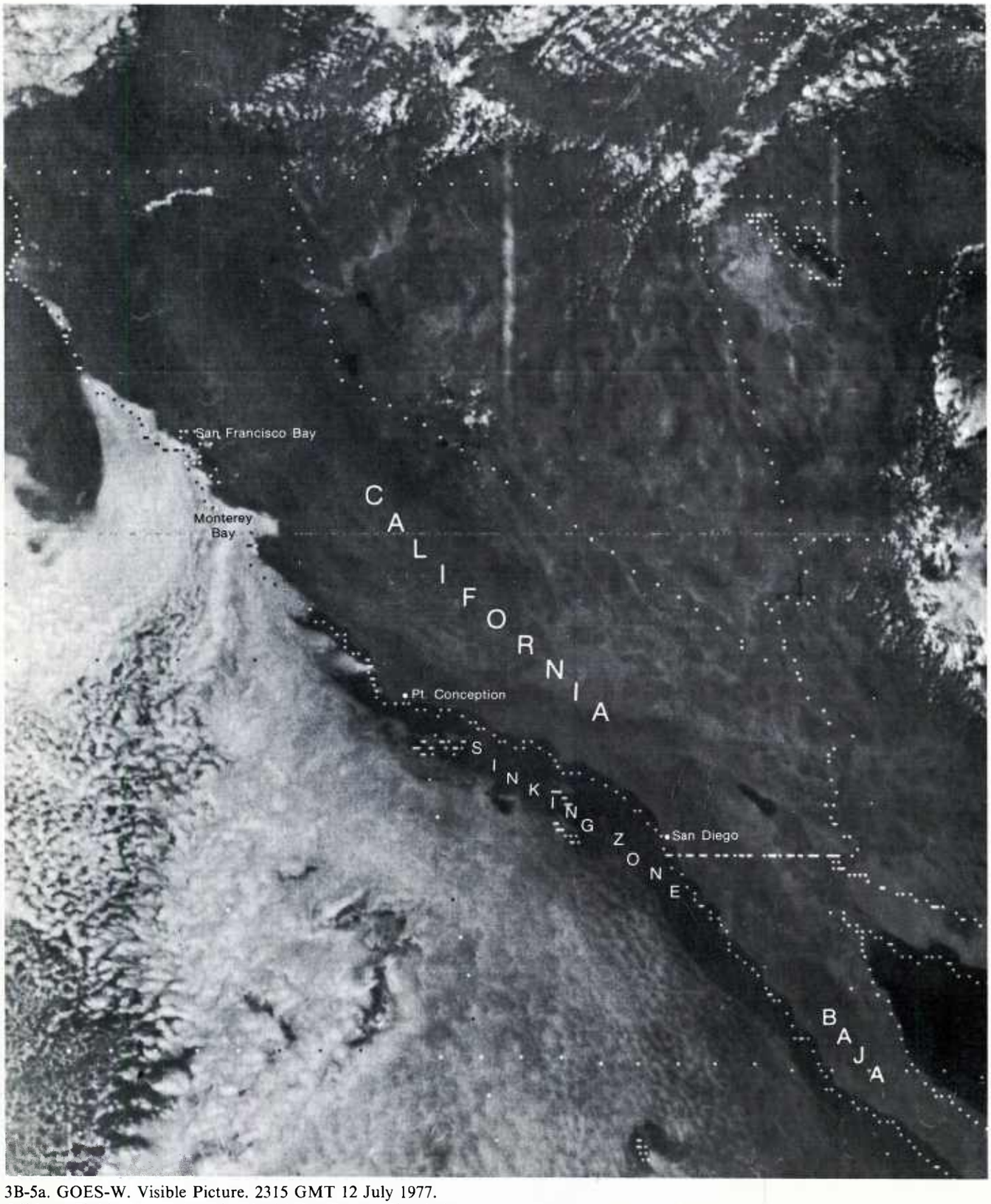

3B-5a. GOES-W. Visible Picture. 2315 GMT 12 July 1977.
Offshore Sinking Zone Associated with Sea Breeze Circulation.

Case 2 Coastal Zone Phenonema

Mesoscale Cloud Eddies in the Marine Layer

Mesoscale cyclonic eddies are observed off the southern coast of California during all months of the year. The most vigorous eddies, however, are a warm season phenomenon, occurring from May to September. Since the circulation center of these eddies is frequently located near Catalina Island, they are called Catalina Eddies. The eddies are identified in satellite imagery by a characteristic spiral-shaped stratus cloud pattern that forms in the offshore marine layer.

The typical Catalina Eddy is observed to develop simultaneously with the movement of a maritime cold front from the North Pacific through the Pacific Northwest (3B-7a). To the rear of the front, a wedge of high pressure builds inland so that strong, dry, northerly flow develops offshore along the California coast. The east-west oriented Arguello headlands, east of Point Conception, act as a barrier to the northerly flow, and the winds spiral cyclonically into the California bight. The mechanism for initiating the Catalina Eddy, however, is the eastward movement of an upper-level trough, associated with the cold frontal system, providing positive vorticity advection into the southern California coastal area. The most intense deepening of the marine layer and the strongest onset of a Catalina Eddy occurs when the frontal system decelerates as it moves into central California and Nevada, and is accompanied aloft by positive vorticity advection into southern Nevada and the Los Angeles area. The dotted line (3B-7a) delineates the zone in which stratus cloud development is exceptionally pronounced as a result of local wind shear and convergence. A change in marine layer depth occurs in this area, creating a wall-like boundary separating cloudy from mostly clear conditions.

The Catalina Eddy and similar coastal eddies are of considerable interest to marine operations because of the much deeper, cloud-filled marine layer associated with these eddies, which slopes upward from the

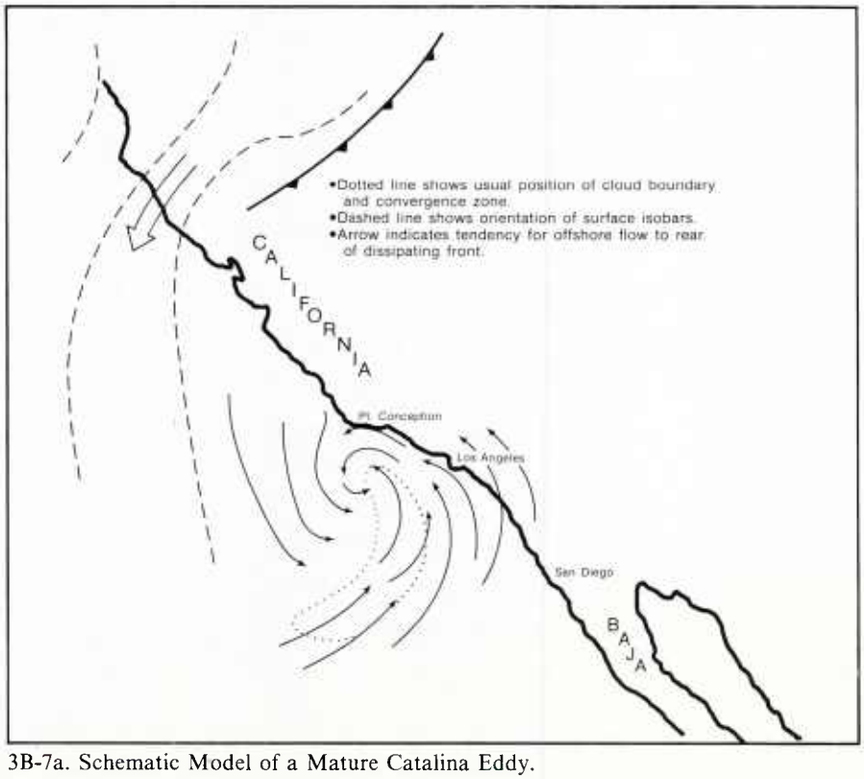

3B-7a. Schematic Model of a Mature Catalina Eddy.

sea to the coastline. The deeper, coastal cloud-filled marine layer can result in a significant delay of the normal diurnal dissipation of low clouds. On some occasions the low clouds may persist throughout the day. The sharp, sloping marine layer associated with the eddies also affects radar and radio signal propagation. Models used for assessing or predicting propagation paths generally assume a horizontally-stratified lower atmosphere, and the anomalous marine layer structure can result in inaccurate predictions which are not useful and may sometimes be detrimental to naval operations.

Although generally considered to be strictly a mesoscale phenomenon, recent studies show eddy circulations that apparently extend far seaward from the cloud vortex center, providing evidence that these features extend into the near-synoptic scale (Rosenthal, 1968).

Forecasting the Catalina Eddy

Eichelberger (1971) has developed a useful objective forecasting aid for predicting the onset of Catalina Eddies. The vorticity value at Los Angeles LAX, obtained from the initial NMC barotropic 500-mb height and vorticity prognoses, is related to the sea level pressure difference between LAX and an offshore position at 35° N, 125° W (3B-9a). Although developed for the Los Angeles area, the basic concept is applicable to other coastline areas of similar topographic features.

Once formed, the Catalina Eddy will persist until either a frontal passage occurs; the vorticity maximum aloft passes over the area; the marine layer deepens to 5,000 ft, spilling over the coastal mountain range; or general onshore flow develops east of the California bight, in response to unusually strong vorticity values over the coastal waters.

References

Rosenthal, J., 1968: A Catalina Eddy. Picture of the Month. *Mon. Wea. Rev.*, **96**, 742–743.

Eichelberger, Arthur L., 1971: Forecasting the Catalina Eddy. U.S. Department of Commerce, NOAA Technical Memorandum NWSTMWR 62, p. 15.

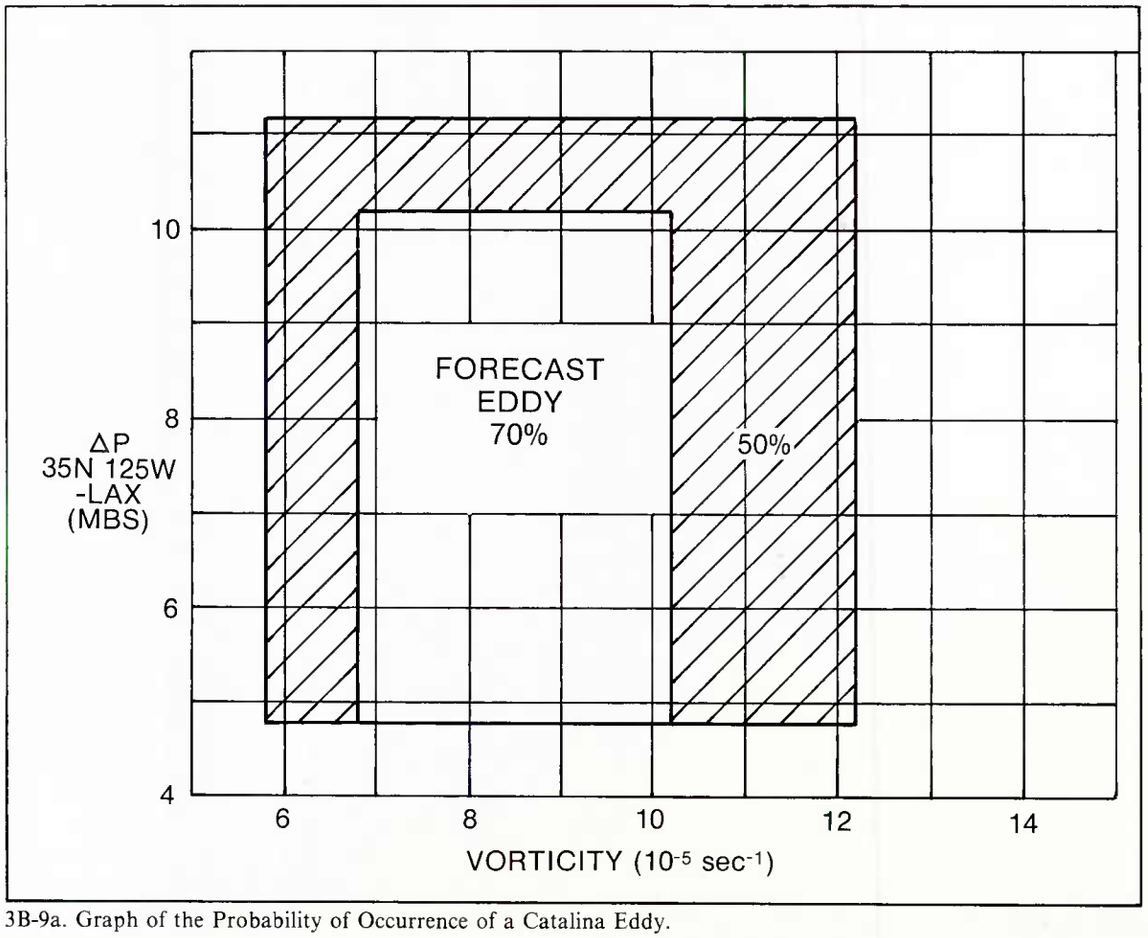

3B-9a. Graph of the Probability of Occurrence of a Catalina Eddy.

Catalina Eddy development
California bight
August 1977

29-30 August

A particularly well-defined Catalina Eddy is observed in the GOES-West picture at 1915 GMT 29 August (3B-10a). Onshore stratus from San Diego to the Los Angeles area indicates westerly or southwesterly flow over the region. Lee clearing east of Guadalupe Island provides further evidence of southwesterly low-level flow over the region. This evidence, together with the offshore cloud vortex, suggests a low-level circulation approaching synoptic-scale size. Since the marine layer is relatively shallow at this time, the tops of offshore islands are protruding through the stratus.

The surface analysis at 1800 GMT (3B-10b), shortly before the GOES-W picture, shows the synoptic pattern associated with the eddy development. A weak, dissipating cold front is observed over northern California, with a high pressure cell extending inland behind the front. This produces a moderate northerly offshore flow immediately south of the front along the coast. A pressure difference of about 5 mb exists between Los Angeles and 35° N, 125° W.

The 500-mb analysis at 1200 GMT (3B-11a) shows a cyclonic turning of the winds over the Los Angeles area, and a low pressure center just to the east of San Diego. This indicates that conditions aloft are also favorable (upper-level cyclonic vorticity) for Catalina Eddy development. The NMC barotropic 12-hour 500-mb height and vorticity prognosis valid at 1200 GMT 29 August (3B-11b) and the 24-hour prognosis valid at 0000 GMT 30 August (3B-11c) show vorticity values of 8 x 10^{-5} sec^{-1} over the Los Angeles bight. These values, together with the 5 mb pressure difference between LAX and 35° N, 125° W, are consistent with a 70% probability of Catalina Eddy development, according to Eichelberger (1971).

The GOES-W picture at 2245 GMT (3B-12a) reveals that the eddy circulation has spiraled around and isolated a small cloud-free area in the center. Thus, in only 3½ hours from the previous picture (3B-10a), an important change in cloud distribution has occurred which emphasizes the rather rapid development near the eddy center. On the other hand, the outer edge of the eddy circulation remains as a quasi-stationary sharp boundary separating marine stratus from cloudless (drier) air to the north and west. The GOES-W picture at 1915 GMT (3B-12b) shows isochrones of the sharp boundary separating marine stratus from the cloud-free area to the north and west. The isochrones reveal that there is little movement of much of the cloud boundary during the daylight hours.

The eddy, in fact, persisted throughout the following day with major dense overcast remaining in much the same configuration (3B-13a). After the isolation and filling in of drier air within the initial eddy center on the previous day, a new surge of cyclonically turning marine stratus created the hook-shaped cloud pattern west of Los Angeles. The new surge of cyclonically turning marine stratus was accompanied by increases in the depth of the marine layer from 1,500 to 3,000 ft at various locations. The development of the small eddy to the north, south of Point Sur, emphasizes the fact that such eddy formations are not uniquely confined to the Los Angeles area.

Important Conclusions

1. Catalina Eddies and similar coastal eddies may be rather consistently forecast based on recognition of a model surface and upper-level pattern.
2. Anomalous propagation of radio and radar can be anticipated over the region of such eddy formations.
3. NMC barotropic 500-mb vorticity forecasts are useful in determining the timing of eddy formation and dissipation.

Reference

Eichelberger, Arthur L., 1971: Forecasting the Catalina Eddy. U.S. Department of Commerce, NOAA Tech. Memorandum NWSTMWR 62, p. 15.

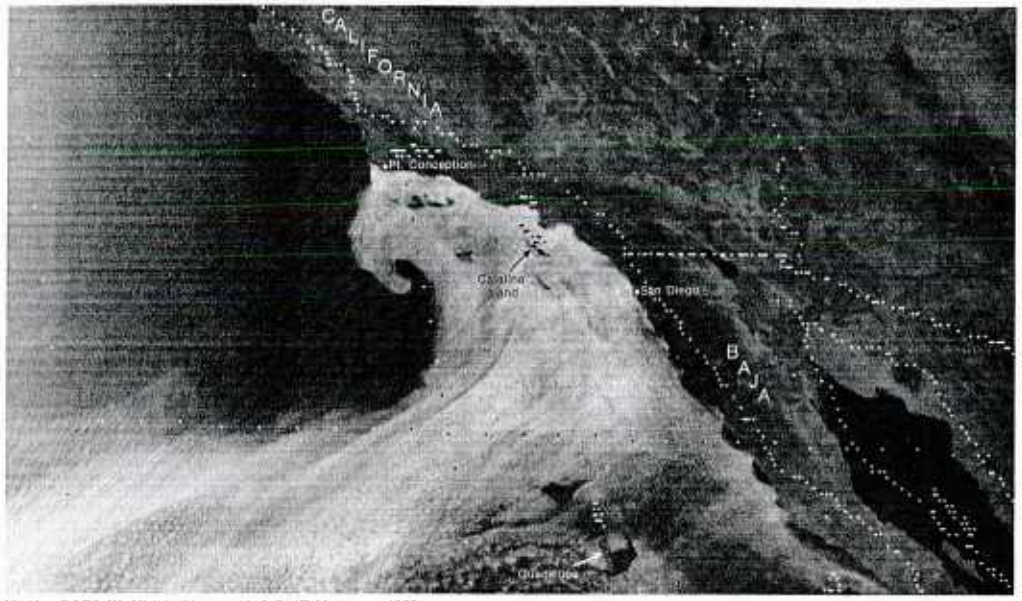

3B-10a. GOES-W. Visible Picture. 1915 GMT 29 August 1977.

surface

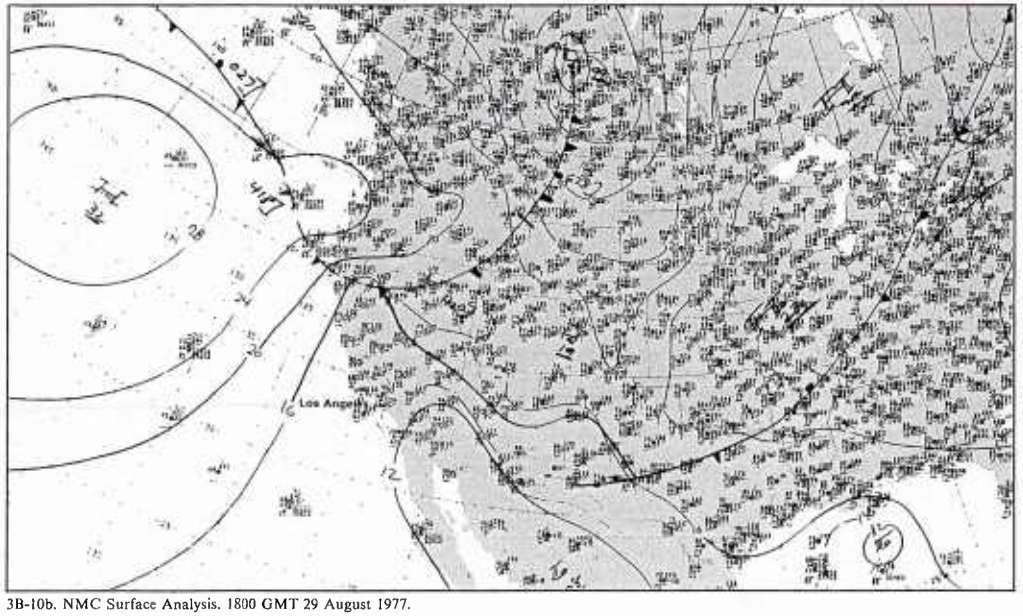

3B-10b. NMC Surface Analysis. 1800 GMT 29 August 1977.

500 mb *Catalina Eddy Development*

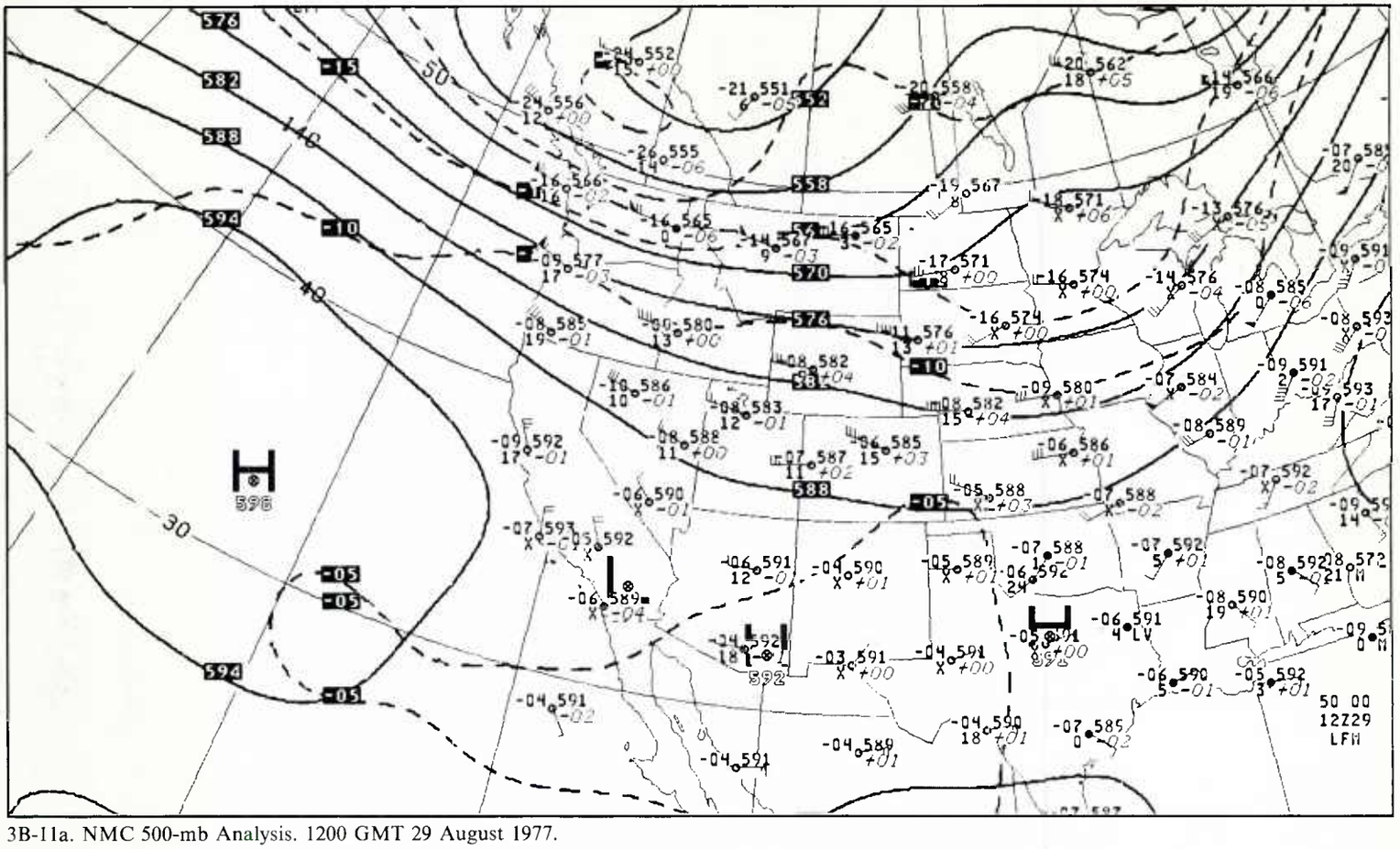

3B-11a. NMC 500-mb Analysis. 1200 GMT 29 August 1977.

500 mb

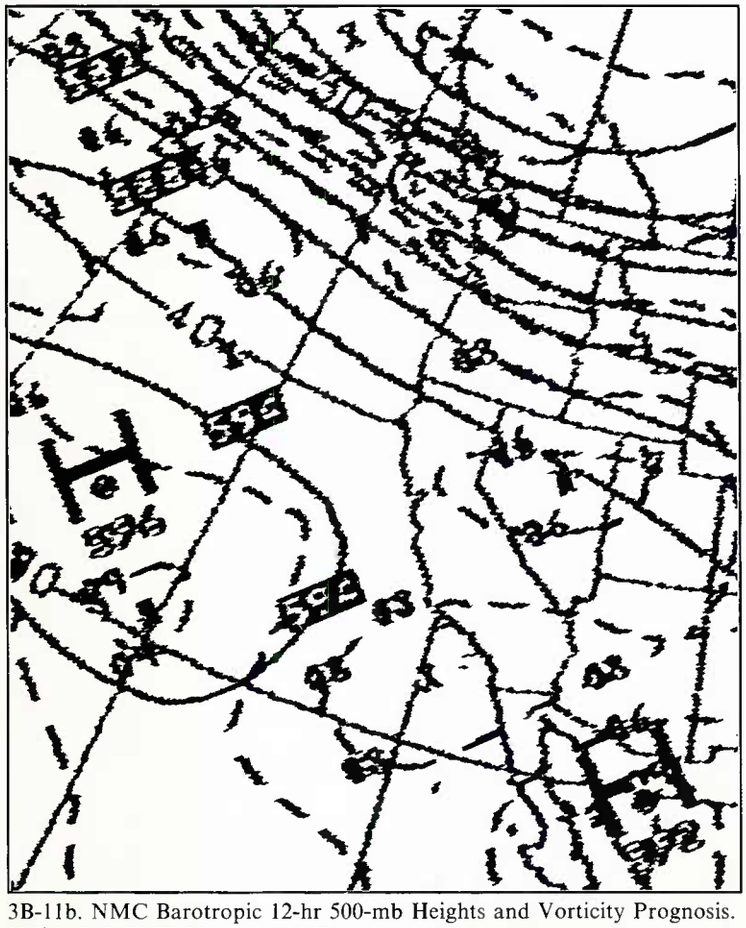

3B-11b. NMC Barotropic 12-hr 500-mb Heights and Vorticity Prognosis. Valid 1200 GMT 29 August 1977.

500 mb

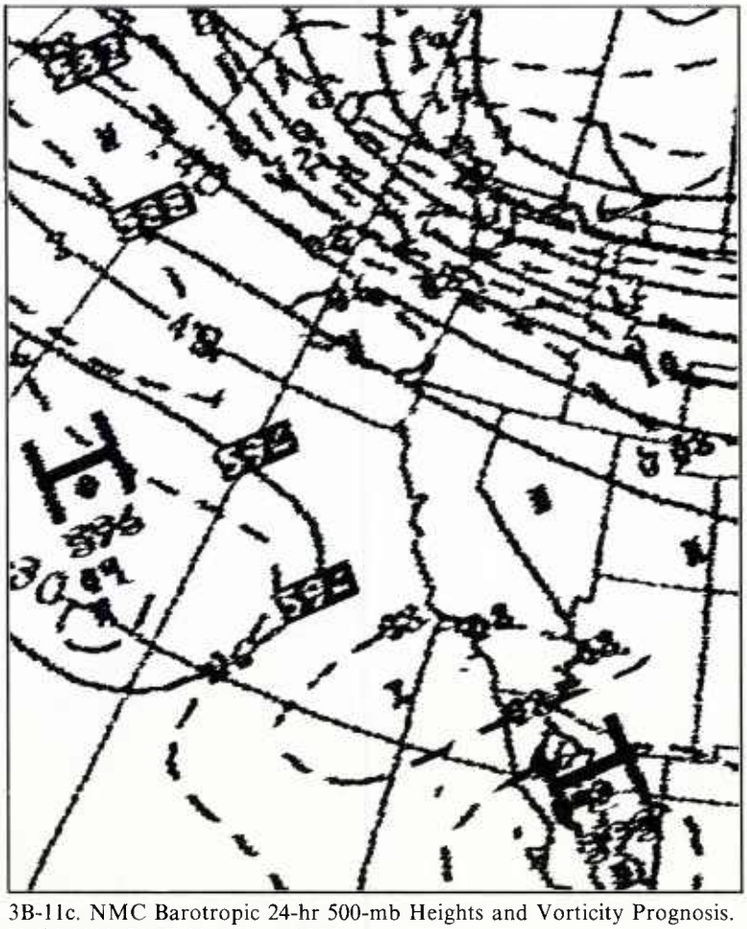

3B-11c. NMC Barotropic 24-hr 500-mb Heights and Vorticity Prognosis. Valid 0000 GMT 30 August 1977.

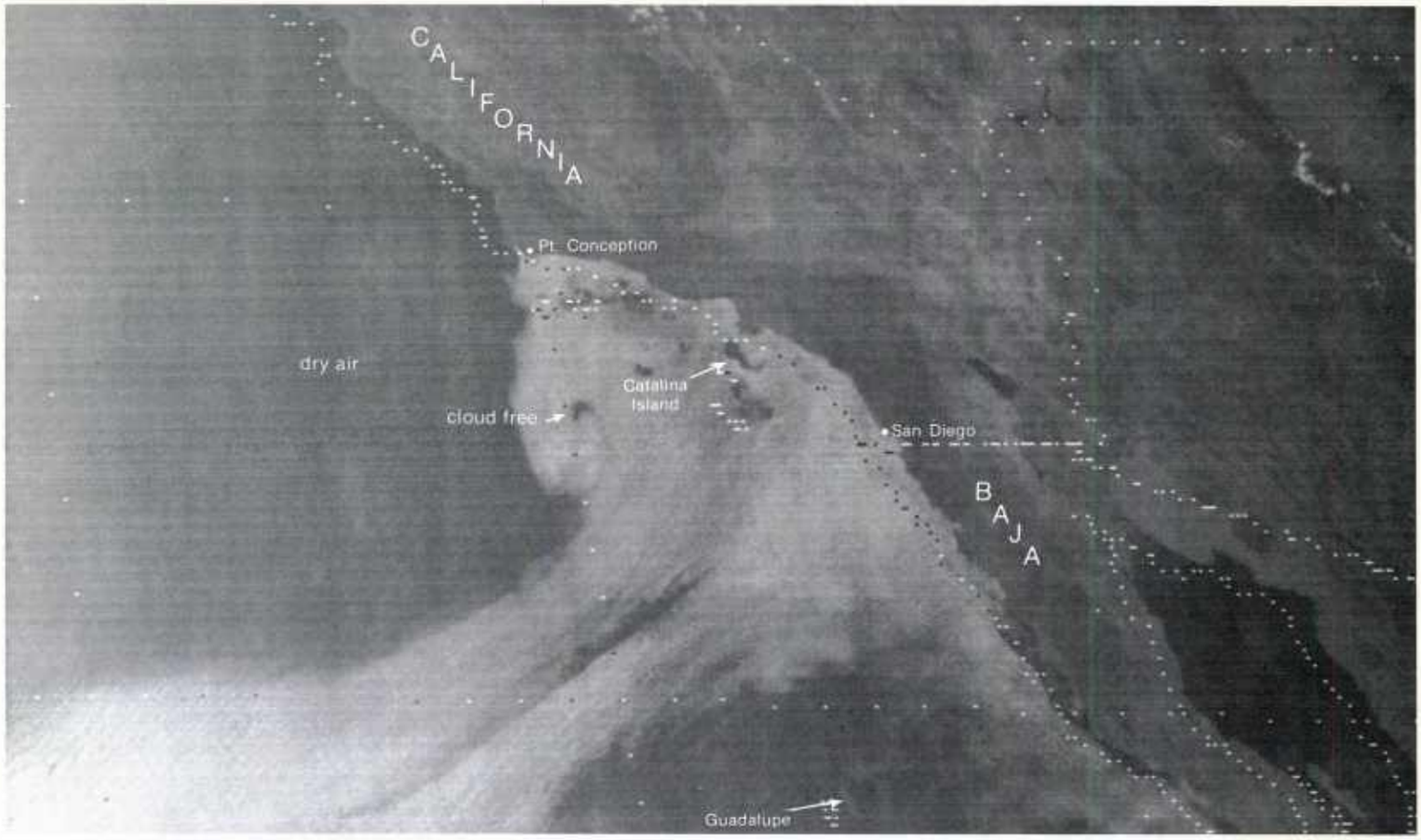

3B-12a. GOES-W. Visible Picture. 2245 GMT 29 August 1977.

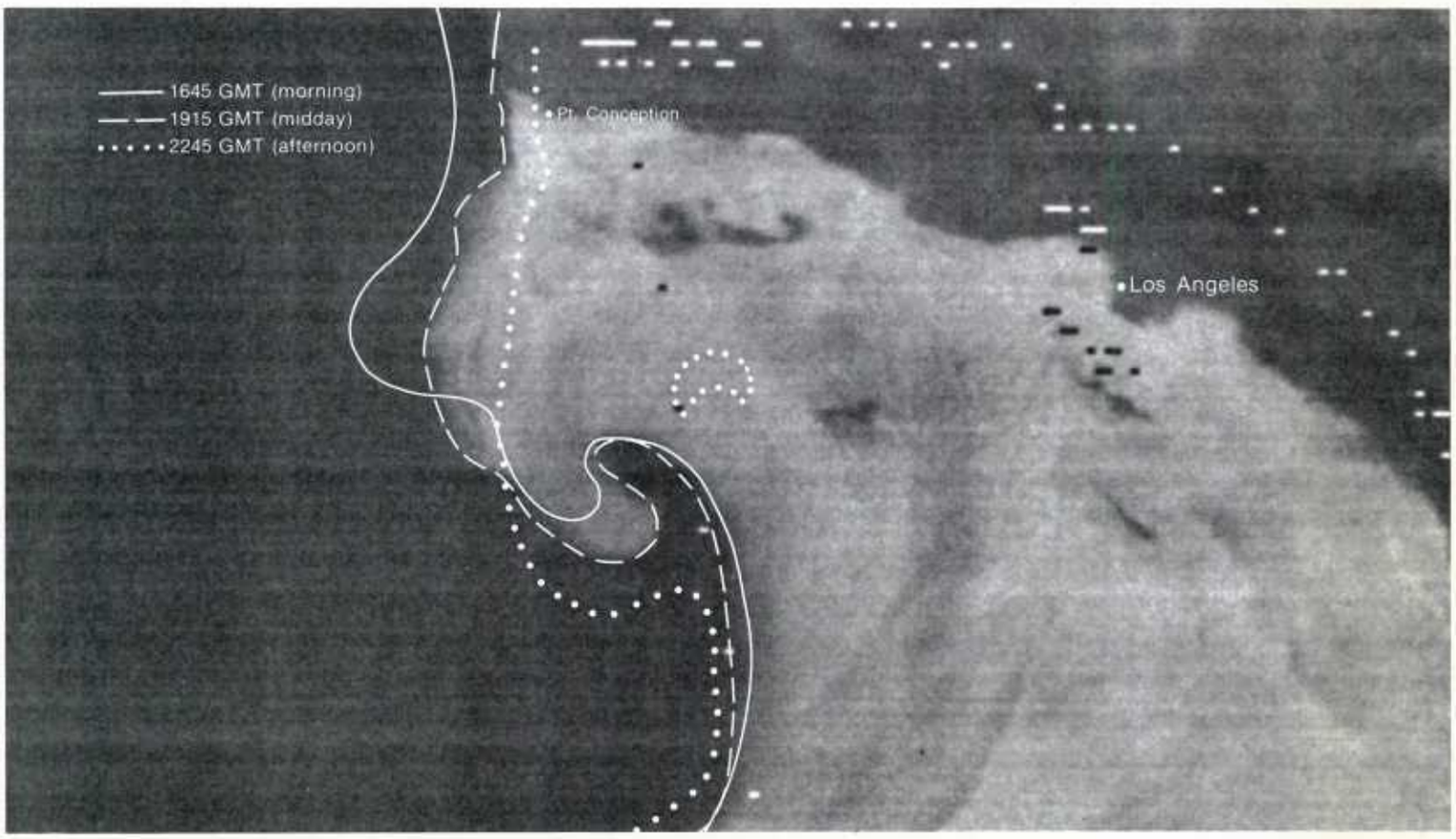

3B-12b. GOES-W. Enlarged View. Visible Picture. 1915 GMT 29 August 1977.
Isochrones of the Cloud Boundary of the Catalina Eddy from Previous GOES Visible Pictures.

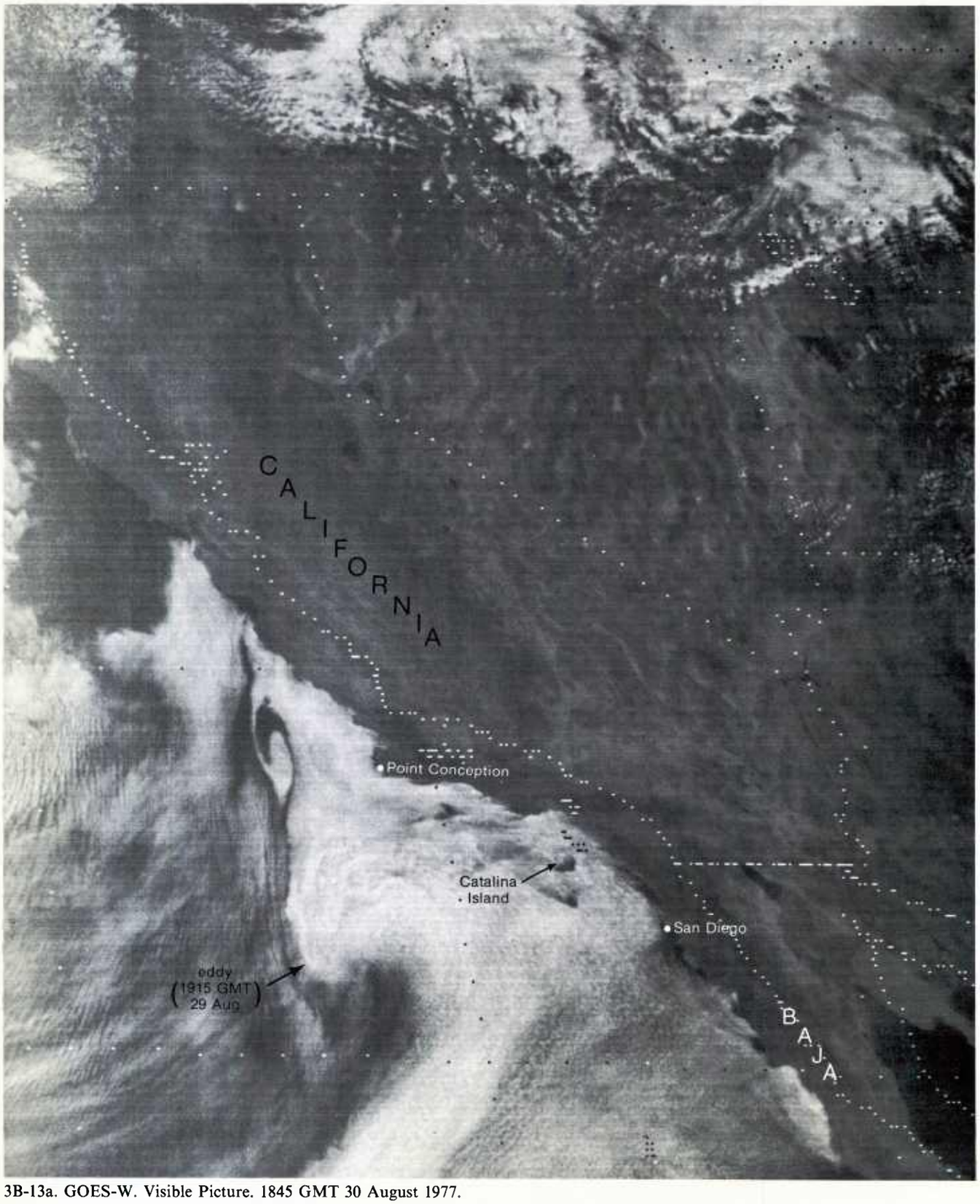

3B-13a. GOES-W. Visible Picture. 1845 GMT 30 August 1977.